Biochemical investigations on bacterial and fungal dimethylallyltryptophan synthases

Biochemische Untersuchungen zu bakteriellen und pilzlichen Dimethylallyltryptophan-Synthasen

Dissertation
zur Erlangung des Doktorgrades
der Naturwissenschaften
(Dr. rer. nat.)

dem
Fachbereich Pharmazie
der Philipps-Universität Marburg

vorgelegt von

Julia Winkelblech
aus Bad Bergzabern

Marburg an der Lahn, 2016

Erstgutachter: **Prof. Dr. Shu-Ming Li**

Zweitgutachter: **Prof. Dr. Peter Kolb**

Eingereicht am **6. Oktober 2016**

Tag der mündlichen Prüfung: **23. November 2016**

Hochschulkennziffer: **1180**

Dedicated to my family

Table of contents

List of publications

Winkelblech, J. & Li, S.-M. (2014). Biochemical investigations of two 6-DMATS enzymes from *Streptomyces* revealing novel features of L-tryptophan prenyltransferases. *Chembiochem.* **15**, 1030-1039.

Winkelblech, J.,* Liebhold, M.,* Gunera, J., Xie, X., Kolb, P. & Li, S.-M. (2015). Tryptophan *C5*-, *C6*- and *C7*-prenylating enzymes displaying a preference for C-6 of the indole ring in the presence of unnatural dimethylallyl diphosphate analogues. *Adv. Synth. Catal.* **357**, 975-986.

Winkelblech, J., Xie, X., Li, S.-M. (2016). Characterisation of 6-DMATS$_{Mo}$ from *Micromonospora olivasterospora* leading to identification of divergence in enantioselectivity, regioselectivity and multiple prenylation of tryptophan prenyltransferases. *Org. Biomol. Chem.,* DOI: 10.1039/C6OB01803C.

Winkelblech, J., Fan, A. & Li, S.-M. (2015). Prenyltransferases as key enzymes in primary and secondary metabolism. *Appl. Microbiol. Biotechnol.* **99**, 7379-7397.

Fan, A., Winkelblech, J. & Li, S.-M. (2015). Impacts and perspectives of prenyltransferases of the DMATS superfamily for use in biotechnology. *Appl. Microbiol. Biotechnol.* **99**, 7399-7415.

*these authors contributed equally to this work

Share of author contributions

Publication (status)	Authors	Estimated equity ratio [%]
Biochemical investigations of two 6-DMATS enzymes from *Streptomyces* revealing novel features of L-tryptophan prenyltransferases. *Chembiochem.* (published)	Winkelblech, J. & Li, S.-M.	75
Tryptophan *C5*-, *C6*- and *C7*-prenylating enzymes displaying a preference for C-6 of the indole ring in the presence of unnatural dimethylallyl diphosphate analogues. *Adv. Synth. Catal.* (published)	Winkelblech, J., Liebhold, M., Gunera, J., Xie, X., Kolb, P. & Li, S.-M.	40
Characterisation of 6-DMATS$_{Mo}$ from *Micromonospora olivasterospora* leading to identification of divergence in enantioselectivity, regioselectivity and multiple prenylation of tryptophan prenyltransferases. *Org. Biomol. Chem.* (online published)	Winkelblech, J., Xie, X. & Li, S.-M.	65
Prenyltransferases as key enzymes in primary and secondary metabolism. *Appl. Microbiol. Biotechnol.* (published)	Winkelblech, J., Fan, A. & Li, S.-M.	65
Impacts and perspectives of prenyltransferases of the DMATS superfamily for use in biotechnology. *Appl. Microbiol. Biotechnol.* (published)	Fan, A., Winkelblech, J. & Li, S.-M.	10

…… ……

Signature candidate **Signature supervisor**

Poster and oral presentations

Mundt K., Wunsch,C., **Winkelblech, J.** & Li, S.-M

Nichtribosomale Peptidsynthetasen und Prenyltransferasen als Instrument zur Herstellung neuer Wirkstoffe, poster presentation,

Evaluation of the LOEWE programs (Synmikro), August 15, 2012, Marburg (MPI)

Winkelblech, J. & Li, S.-M.

New Biochemical Features of Indole Prenyltransferases from *Streptomyces*
poster presentation,
DPhG-Jahrestagung 2014, September 24 – 29, 2014, Frankfurt

Winkelblech, J., Liebhold, M., Gunera, J., Xie, X., Kolb, P. & Li, S.-M

Tryptophan *C5*-, *C6*- and *C7*-Prenylating Enzymes revealed a clear Preference for C-6 Alkylation/Benzylation in presence of unnatural DMAPP analogues, poster presentation,

Annual Conference of the Association for General and Applied Microbiology (VAAM), March 1-4, 2015, Marburg/Lahn

Winkelblech, J., Backhaus, K., Mundt, K., Wusch C, Li, S.-M

Entwicklung potenzieller Wirkstoffe durch Konstruktion neuer Synthesewege basierend auf Peptid bildenden und modifizierenden Enzymen, poster presentation,

Evaluation of the LOEWE programs (Synmikro), August 6-7, 2015, Marburg (MPI)

Winkelblech, J. & Li, S.-M

Prenyltransferasen in der chemischen Synthese, short lecture

Fachbereichstag Chemie 2016, July 1, 2016, Phillips-Universität Marburg

Abbreviations

For units of measurements the international system of units (SI; Le Système international d'unités) and units derived thereof have been used.

$[M]^+$	molecular ion
$[M+H]^+$	molecular ion plus hydrogen
$[M+Na]^+$	molecular ion plus sodium
× g	gravitational acceleration
2-pentenyl-PP	2-pentenyl diphosphate
4HB	4-hydroxybenzoate
5-DMATS	5-dimethylallyltryptophan synthase
5-$DMATS_{Sc}$	5-dimethylallyltryptophan synthase from *S. coelicolor*
6-$DMATS_{Mo}$	6-dimethylallyltryptophan synthase from *M. olivasterospora*
6-$DMATS_{Sa}$	6-dimethylallyltryptophan synthase from *S. ambofaciens*
6-$DMATS_{Sv}$	6-dimethylallyltryptophan synthase from *S. violaceusniger*
7-DMATS	7-dimethylallyltryptophan synthase
A. flavus	*Aspergillus flavus*
A. fumigatus	*Aspergillus fumigatus*
A. nidulans	*Aspergillus nidulans*
A. oryzae	*Aspergillus oryzae*
A. terreus	*Aspergillus terreus*
A. thaliana	*Arabidopsis thaliana*
A. versicolor	*Aspergillus versicolor*
Ar	aromatic residue
benzyl-PP	benzyl diphosphate
BLAST	basic local alignment search tool
bp	base pairs
C. purpurea	*Claviceps purpurea*
CD	circular dichroism
CD_3OD	deuterated methanol
Co	coenzyme
COSY	correlation spectroscopy
cyclo-L-Trp-Gly	*cyclo*-L-tryptophanyl-glycinyl
cyclo-L-Trp-L-Ala	*cyclo*-L-tryptophanyl-L-alaninyl
cyclo-L-Trp-L-Leu	*cyclo*-L-tryptophanyl-L-leucinyl
cyclo-L-Trp-L-Phe	*cyclo*-L-tryptophanyl-L-phenylalaninyl
cyclo-L-Trp-L-Pro	*cyclo*-L-tryptophanyl-L-prolinyl
cyclo-L-Trp-L-Trp	*cyclo*-L-tryptophanyl-L- tryptophanyl

cyclo-L-Trp-L-Tyr	*cyclo*-L-tryptophanyl-L-tyrosinyl
cyclo-L-Tyr-L-Tyr	*cyclo*-L- tyrosinyl-L-tyrosinyl
d	doublet
DA	Dalton
dd	double doublet
DMAI	dimethylallylindole
DMAPP	dimethylallyl diphosphate
DMATS	dimethylallyltryptophan synthase
DMSO	dimethyl sulfoxide
DNA	deoxyribonucleic acid
DOPE	Discrete Optimized Protein Energy
E. coli	*Escherichia coli*
e. g.	*exempli gratia*
EDTA	ethylenediamine tetraacetic acid
EI-MS	electron impact mass spectrometry
ESI-MS	electrospray ionization spectrometry
FPP	farnesyl diphosphate
FPPase	FPP synthase
gDNA	genomic DNA
GGPP	geranylgeranyl diphosphate
GGTase	geranylgeranyltransferase
GPP	geranyl diphosphate
His_6	hexahistidine
His_8	octahistidine
HPLC	high performance liquid chromatography
HR	high resolution
Hz	hertz
i. e.	*id est*
IPP	isopentenyl diphosphate
IPTG	isopropyl *β*-thiogalactopyranoside
J	coupling constant
k_{cat}	turnover number
K_M	Michaelis-Menten constant
LB	Luria-Bertani or lysogeny broth
L-Trp	L-tryptophan
m	multiplet
M. olivasterospora	*Micromonospora olivasterospora*
MAPP	methylallyldiphosphate
MD	molecular dynamics
MOE	Operating Environment

MS	mass spectrometry
N. fischeri	*Neosartorya fischeri*
Ni-NTA	nickel-nitrilotriacetic acid
NMR	nuclear magnetic resonance
NOESY	nuclear Overhauser effect spectroscopy
NRPS	non-ribosomal peptide synthetase
OD_{600}	optical density at 600 nm
OPPS	octaprenyl diphosphate synthase
P. aeruginosa	*Pseudomonas aeruginosa*
P. roqueforti	*Penicillium roqueforti*
PCR	polymerase chain reaction
PPi	inorganic pyrophosphate
ppm	parts per million
RMSD	root-mean-square deviation
RP	reverse phase
rpm	revolutions per minute
s	singlet
S. ambofaciens	*Streptomyces ambofaciens*
S. arenicola	*Salinispora arenicola*
S. coelicolor	*Streptomyces coelicolor*
S. violaceusniger	*Streptomyces violaceusniger*
SDS	sodium dodecyl sulfate
SDS-PAGE	sodium dodecyl sulfate polyacrylamide gel electrophoresis
sp.	species
t	triplet
tRNA	transfer ribonucleic acid
UV	ultraviolet
v/v	volume per volume
w/v	weight per volume
YMG	yeast, malt, glucose (medium)
δ_C	chemical shift of ^{13}C
δ_H	chemical shift of ^{1}H

Summary

Prenyl transfer reactions occur ubiquitously in nature and play an important role in primary and secondary metabolism in all domains of life. Prenylated secondary metabolites including indole alkaloids usually demonstrate improved biological and pharmacological activities and thus makes them to promising candidates for drug discovery and development. Important producers of such bioactive compounds are fungi of ascomycetes and bacteria of actinomycetes. The transfer reactions of a prenyl moiety from prenyl diphosphate, primarily dimethylallyl diphosphate (DMAPP), onto indole derivatives including tryptophan are mainly catalyzed in nature by the members of the dimethylallyltryptophan synthase (DMATS) superfamily. In the last years, remarkable progress has been achieved in their biochemical, molecular biological, and structural characterization, especially for DMATS enzymes from fungi.

The major challenge of this thesis is to provide a better understanding of the catalytic features of these enzymes from different origins. Several putative genes for new tryptophan prenyltransferases were identified in diverse actinomycetes *via* blast search by using two known *Streptomyces* prenyltransferases (SCO7467 and IptA). Cloning and expression of these genes as well as the subsequent biochemical investigations of the three novel tryptophan prenyltransferases provided several new intriguing features. Initially, two tryptophan *C6*-prenyltransferases were identified, *i.e.* 6-DMATS$_{Sa}$ from *Streptomyces ambofaciens* and 6-DMATS$_{Sv}$ from *Streptomyces violaceusniger*. Biochemical investigation on these enzymes revealed a remarkable broad substrate specificity. In addition to a number of indole derivatives also several hydroxynaphthalenes were accepted by 6-DMATS$_{Sa}$ and 6-DMATS$_{Sv}$. Interestingly, they catalyze the prenylation at the unsubstituted benzene rings of the tested hydroxynaphthalenes. Moreover, they represent the first examples of tryptophan prenyltransferases that accept both DMAPP and geranyl diphosphate (GPP) as prenyl donors and catalyze the same prenylation positions.

Consequently, the studied 6-DMATSs were used for further investigations on the acceptance of unnatural alkyl or benzyl donors. Prior to this study, investigations on this issue are limited to fungal *C4*- and *C5*- prenyltransferases. The L-tyrosine prenyltransferase TyrPT with a tryptophan *C7*-prenyltransferase activity, the two mentioned 6-DMATSs as well as the bacterial 5-DMATS$_{Sc}$ (SCO7467) were included in this project. In total, five *C5*-, *C6*- and *C7*-prenytransferases (5-DMATS, 5-DMATS$_{Sc}$, 6-DMATS$_{Sa}$, 6-DMATS$_{Sv}$, TyrPT) were investigated in the presence of the DMAPP analogs methylallyl (MAPP), 2-pentenyl (2-

pentenyl-PP) and benzyl diphosphate (benzyl-PP). The unnatural donors were accepted by all tested enzymes with different relative activities and regioselectivities. *C6*-alkylated or benzylated derivatives were identified in all the reactions, as unique product of the two 6-DMATSs or as one of the main products of the other enzymes. These results demonstrated a clear preference of the five enzymes for alkylation/benzylation at C-6 of the indole ring in the presence of the unnatural DMAPP derivatives. Furthermore, homology modeling of the 5-DMATS and subsequent docking as well as molecular dynamics studies with DMAPP, MAPP and 2-pentenyl-PP, led to a distance-based explanation of the observed reaction results.

Later on, a third tryptophan *C6*-prenyltransferase 6-DMATS$_{Mo}$ from *Micromonospora olivasterospora* was identified and characterized. Similar to the previously characterized 6-DMATSs, 6-DMATS$_{Mo}$ uses indole derivatives, cyclic dipeptides and naphthalenes as prenyl acceptors and DMAPP as well as GPP as prenyl donors. The most notable feature of 6-DMATS$_{Mo}$ is the high relative activity toward D-tryptophan. This result led to the comparative study on enantioselectivity of the seven DMATS enzymes from fungi and bacteria. The tested prenyltransferases displayed different substrate preferences as well as different regioselectivities toward the L- and D-enantiomers of tryptophan and their methylated derivatives. Interestingly, the bacterial 5-DMATS$_{Sc}$ and 6-DMATS$_{Mo}$ highly preferred the D-enantiomer of 5-methyltryptophan to the L-enantiomer, although that was the better substrate in all other reactions. In the presence of the racemate, the D-enantiomer reaction was strongly inhibited, which could be explained by the high affinity to the respective L-form as the main reason. Another interesting output of this project is the reduced or even completely changed regioselectivity for the reactions of FgaPT2, 5-DMATS$_{Sc}$, and 7-DMATS with the D-enantiomers of tryptophan or 5-methyltryptophan. Moreover, the observed diprenylation by 5-DMATS$_{Sc}$ was the first report on a tryptophan prenyltransferase which catalyzes two successive prenylation steps.

In conclusion, identification and characterization of the three new 6-DMATSs from actinomycetes expand our knowledge on bacterial tryptophan prenyltransferases. Furthermore, prenyltransferases including the three 6-DMATSs could serve as valuable biocatalysts in chemoenzymatic synthesis for alkylated compounds with potential biological activities.

Zusammenfassung

Prenylierungsreaktionen sind in der Natur weit verbreitet und spielen eine wichtige Rolle in dem Primär- und Sekundärmetabolismus aller Lebensformen. Prenylierte Sekundärmetabolite einschließlich Indolalkaloide weisen häufig eine verstärkte biologische und pharmakologische Aktivität auf, wodurch sie vielversprechende Kandidaten für die Arzneistoff-Findung und Entwicklung darstellen. Wichtige Produzenten solcher bioaktiver Substanzen sind Pilze der Askomyzeten und Bakterien der Aktinomyzeten. Die Übertragung eines Prenylrestes von Prenyldiphosphat, meistens Dimethylallyldiphosphat (DMAPP), auf Indolderivate mitunter Tryptophan werden in der Natur durch Enzyme der Dimethylallyltryptophan-Synthase (DMATS)-Superfamilie katalysiert. Bemerkenswerte Fortschritte wurden in den letzten Jahren in der biochemischen, molekularbiologischen und strukturellen Charakterisierung dieser Enzyme, insbesondere solcher aus Pilzen, erzielt.

Die größte Herausforderung dieser Arbeit besteht darin, ein besseres Verständnis über die katalytischen Eigenschaften dieser Enzyme unterschiedlicher Herkunft zu erlangen. Mittels einer „Blast"-Suche zweier bekannter *Streptomyces*-Prenyltransferasen (SCO7467 und IptA), wurden mehrere potenzielle Gene neuer Tryptophan-Prenyltransferasen in verschiedenen Aktinomyzeten identifiziert. Die Klonierung, Expression und die anschließenden biochemischen Untersuchungen drei neuer Tryptophan-Prenyltransferasen offenbarten neue, interessante Eigenschaften.

Zunächst wurden mit 6-DMATS$_{Sa}$ aus *Streptomyces ambofaciens* und 6-DMATS$_{Sv}$ aus *Streptomyces violaceusniger* zwei Tryptophan-*C6*-Prenyltransferasen identifiziert. Die biochemischen Untersuchungen dieser Enzyme ergaben eine breite Substratspezifität. Neben einer Vielzahl an Indolderivaten wurden auch mehrere Hydroxynaphthaline von 6-DMATS$_{Sa}$ und 6-DMATS$_{Sv}$ akzeptiert. Interessanterweise katalysieren diese eine Prenylierung an nicht substituierten Benzolringen der getesteten Hydroxynaphthaline. Zudem handelt es sich um die erstmalige Beschreibung für Tryptophan-Prenyltransferasen, die sowohl DMAPP als auch GPP als Prenyldonor akzeptieren und die Prenylierung an derselben Position katalysieren. Folglich stellen die untersuchten 6-DMATS Enzyme interessante Kandidaten für weitere Untersuchungen bezüglich der Akzeptanz von unnatürlichen Alkyl- oder Benzyldonoren dar. Bisherige Studien zu diesem Thema beschränken sich auf die pilzlichen *C4*- und *C5*-Prenyltransferasen. Im Rahmen dieses Projektes wurden daher die L-Tyrosin-Prenyltransferase TyrPT mit Tryptophan-*C7*-Prenyltransferase Aktivität, zwei 6-DMATS sowie die bakterielle

5-DMATS$_{Sc}$ (SCO7467) analysiert. Hierzu wurde das Verhalten der *C5*-, *C6*- und *C7*-Prenytransferasen (5-DMATS, 5-DMATS$_{Sc}$, 6-DMATS$_{Sa}$, 6-DMATS$_{Sv}$, TyrPT) in Gegenwart der unnatürlichen Prenyldonoren Methylallyl- (MAPP), 2-Pentenyl (2-Pentenyl-PP) oder Benzyldiphosphat (Benzyl-PP) untersucht. Diese DMAPP-Analoga wurden von allen getesteten Enzymen mit unterschiedlichen, relativen Aktivitäten und Regioselektivitäten akzeptiert. *C6*-alkylierte/benzylierte Derivate wurden in allen Reaktionen identifiziert, entweder als einzelnes Produkt der beiden 6-DMATS oder als eines der Hauptprodukte der anderen Enzyme. Diese Ergebnisse weisen auf eine deutliche Präferenz der fünf Enzyme für die Alkylierung/Benzylierung an C-6 des Indolrings in Gegenwart der unnatürlichen DMAPP-Derivate hin. Des Weiteren führte das „homology modeling" der 5-DMATS und anschließende „docking"- sowie „molecular dynamics"-Studien mit DMAPP, MAPP und 2-Pentenyl-PP zu einer distanzbasierten Erklärung für die beobachteten Reaktionsergebnisse.

Später wurde mit 6-DMATS$_{Mo}$ aus *Micromonospora olivasterospora* eine dritte Tryptophan-*C6*-Prenyltransferase identifiziert und charakterisiert. Ähnlich wie die zuvor untersuchten 6-DMATS-Enzyme, verwendet 6-DMATS$_{Mo}$ Indolderivate, zyklische Dipeptide und Naphthaline als Prenylakzeptoren sowie DMAPP und GPP als Prenyldonoren. Das auffälligste Merkmal der 6-DMATS$_{Mo}$ ist die hohe relative Aktivität gegenüber D-Tryptophan. Dieses Resultat führte zu der vergleichenden Studie über die Enantioselektivität von sieben DMATS-Enzymen aus Pilzen und Bakterien. Für die verschiedenen Prenyltransferasen wurden unterschiedliche Substratpräferenzen sowie eine unterschiedliche Regioselektivität bezüglich der L- und D-Enantiomere von Tryptophan und deren methylierten Derivaten festgestellt. Interessanterweise bevorzugten die bakteriellen 5-DMATS$_{Sc}$ und 6-DMATS$_{Mo}$ das D-Enantiomer von 5-Methyltryptophan gegenüber dem L-Enantiomer, was in allen anderen Reaktionen das bessere Substrat darstellte. In Gegenwart des Racemats, führt die hohe Affinität zur L-Form zur Hemmung der D-Enantiomer-Reaktion. Weiterhin konnte eine reduzierte oder sogar grundlegend veränderte Regioselektivität der Reaktion von FgaPT2, 5-DMATS$_{Sc}$ und 7-DMATS mit dem D-Enantiomer von Tryptophan und 5-Methyltryptophan beobachtet werden. Außerdem konnte mit 5-DMATS$_{Sc}$ erstmals eine Tryptophan-Prenyltransferase beschrieben werden, die eine Diprenylierung in einem sukzessiven Reaktionsmechanismus katalysiert.

Zusammenfassend lässt sich sagen, dass die Identifizierung und Charakterisierung drei neuer 6-DMATS-Enzyme aus Aktinomyzeten zu einem besseren Verständnis bakterieller Tryptophan-Prenyltransferasen führen. Auf Grund der besonderen Eigenschaften untersuchter Prenyltransferasen ergibt sich schließlich die Möglichkeit, mittels neuer Biokatalysatoren das Repertoire alkylierter, potenziell aktiver Substanzen zu erweitern.

Introduction

1.1. Ascomycota

Ascomycota or colloquially called ascomycetes represent the largest phylum of fungi including more than 64,000 species, whereas it is assumed that the majority is still not discovered (Kirk *et al.,* 2008). Their characteristic feature is the sac-like reproductive structure called ascus containing the sexual produced ascospores. The asci can form a macroscopic fruiting body, the ascocarp, which is clearly obvious in many species including the familiar truffels (James *et al.,* 2006). Compared to sexual reproduction, the ascomycetes reproduce also asexually via budding or production of conidiospores formed by conidiophores. Ascomycota are spread ubiquitous in nature and occur in various lifestyles as saprotrophs, necrotrophic or biotrophic parasites of plants and animals (Webster & Weber 2007). Members of this phylum can also pose risks for human's health. For example, the yeast *Candida albicans* infects mouth and vagina, while *Aspergilllus fumigatus* (*A. fumigatus)* causes chronic pulmonary aspergillosis in immunocomprised individuals (Latge 1999). Each year more than 200,000 cases of invasive aspergillosis were estimated (Brown *et al.,* 2012). Also plant pathogens cause harm in agriculture and affect humans directly via mycotoxins or indirectly via harvest losses or food spoilage. For instance, mycotoxins such as the cancerogenic aflatoxins and cytotoxic gliotoxin are produced by *Aspergillus flavus* (*A. flavus*) and by both *A. flavus* and *Aspergillus terreus* (*A. terreus*), respectively (Amaike & Keller 2011; Stanzani et al., 2005). The plant pathogen and ergot fungus *Claviceps purpurea* (*C. purpurea*) grows on cereal grains and produces ergot alkaloids, which causes ergotism in human. Nevertheless, research on these mycotoxins revealed that ergot alkaloids are potent drugs *e.g.* in obstetrics or for treatment of migraines (Gerhards *et al.,* 2015). This example demonstrates also the beneficial effects of ascomycetes *i.e.* their usage as sources for drugs. The important antibiotic penicillin G is produced by *Penicillium chrysogenum* (Flemming 1929) and *Aspergillus nidulans* (*A. nidulans*) (Brakhage *et al.,* 2004; MacCabe *et al.,* 1990). Another example is the immunosuppressant agent cyclosporine isolated at first from *Tolypocladium inflatum* (Dittmann *et al.,* 1994). A further important medicinal agent is the cholesterol-lowering lovastatin produced by *A. terreus* (Manzoni & Rollini 2002). Beside the pharmaceutical function of secondary metabolites derived from ascomycetes, which will be described more detailed in the following sections in this thesis, several species are important in food industry. Yeast has been used for centuries in production of bread, beer and wine, whereas some *Penicillum* species produces different mold

cheeses (Ropars *et al.,* 2012). *Aspergillus oryzae* (*A. oryzae*) is used as efficient producer of α-amylase, glucoamylase, and α-glucosidase (Hata *et al.,* 1991; Minetoki *et al.,* 1995; Yin *et al.,* 2015). Moreover, baker's yeast (*Saccharomyces cerevisiae*) as well as *Neurospora crassa* are common model organisms with great scientific significance (Cherry *et al.,* 1997; Davis & Perkins 2002; Galagan *et al.,* 2003; Webster & Weber 2007). In addition, genetic manipulation can be easily carried out with several ascomycetes like yeast or several *Aspergillus* species (Punt *et al.,* 2002; Webster & Weber 2007). Therefore they also play an important biotechnological role for example in production of peptides and proteins such as insulin (Kjeldsen 2000).

1.2. Actinobacteria

The phylum of actinobacteria constitutes the largest group of the Gram-positive bacteria. Most members belong to the order actinomycetales and are distinguished by their high genomic guanine-cytosine (GC) content. As fungi of ascomycetes also the actinobacteria were wide spread in nature as terrestrial but also marine or freshwater bacteria. In soil, they are important ecological decomposer and therefore also economically significant in agriculture for human. Similar to fungi, they usually reproduce *via* spores and also growth as hyphae. Two third of the known microbial antibiotics are produced by actinobacteria and the main part by the genus of *Streptomyces* (Kieser *et al.,* 2000). Intensive research on antibacterial agents from *Streptomyces* began in 1940 with the discovery of actinomycin from *Actinomyces antibioticus,* followed by streptomycin, chloramphenicol, tetracyclines, erythromycin from diverse actinomycetes, and countless more (Mahajan & Balachandran 2012). A recent example is the discovery of the antimicrobial prenylated isatin antibiotic from *Streptomyces* sp. MBT28. Thereby an indole prenyltransferase play the key role in the conversion of tryptophan to 7-prenylisatin (Wu *et al.,* 2015). In addition, *Streptomyces* are also producers of antifungal agents (Gupte, 2001) or compounds with other important properties including anticancer (Shah *et al.,* 2016; Shan *et al.,* 2005), antiviral (Kohno *et al.,* 1996; Zhang *et al.,* 2016), and anti-inflammatory immunosuppressive activities (Hassan *et al.,* 2016). The search for novel metabolites based on the identification and analyses of new biosynthetic gene clusters. Genome mining is required due to the common occurrence of cryptic gene clusters among actinomycetes with unknown natural products. Activation of silent genes could be achieved either by genetic manipulation of the host strain or by heterologous expression of the cryptic genes in a related host.

Streptomyces coelicolor (*S. coelicolor*) A3(2), the most studied species, is a very suitable heterologous host for production of secondary metabolites derived from actinomycetes (Gomez-Escribano & Bibb 2014). Its chromosome was completely sequenced and annotated by Bentley *et al.* in 2002. The more efficient and cheaper sequencing technics including advanced computational tools led to an increased number of sequenced genomes of *Streptomyces* and related species (Gomez-Escribano & Bibb 2014; Harrison & Studholme 2014). Therefore significant progress in elucidation of actinomycetous genetics and metabolisms was achieved in the last decade. The availability of the genome sequences of *Streptomyces ambofaciens* (*S. ambofaciens*) (Choulet *et al.,* 2006; Thibessard *et al.,* 2015), *Streptomyces violaceusniger* (*S. violaceusniger*) and *Micromonospora olivasterospora* (*M. olivasterospora*) apart from numerous other species is the basis for a major part of this thesis.

1.3 Prenylated aromatic secondary metabolites

Aromatic natural products bearing an isoprenoid residue or moiety derived thereof are widely distributed in nature. These compounds show a vast structurally diversity regarding their aromatic scaffolds such as indoles, xanthones, flavonoids, hydroxynaphthalenes and so on. In addition, the chain length and the number of the attached prenyl moieties as well as their position on the scaffold can varied. The prenylation reactions take place either in regular or reverse manner. The regular prenylation implies the connection of the prenyl moieties via their C-1 to an acceptor and the reverse prenylation via their C-3 atoms (Fig 1.1) (Heide 2009a; Yu & Li 2012).

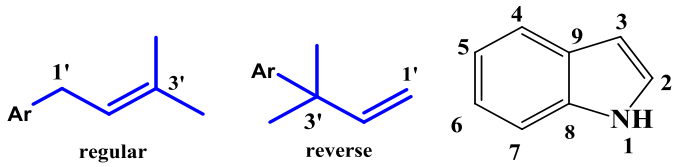

Fig. 1.1 Regular and reverse prenyl pattern and numbering of the indole. Ar: aromatic residue.

The broad variety could be further extended by other modifications such as rearrangement, cyclization or oxidation (Raju *et al.,* 2011; Tagami *et al.,* 2013). Producers of such compounds include several families of plants, fungi of ascomycetes and bacteria of actinomycetes, where the latter two received the most attention in this thesis. Several studies demonstrated that the presence of the prenyl group gives the aromatic secondary metabolites improved biological and

pharmacological activity (Alhassan A.M. *et al.,* 2014; Botta *et al.,* 2005a; El-Seedi *et al.,* 2010; Heide 2009b; Li 2010; Sunassee & Davies-Coleman 2012). For instance, the plant prenylflavonoid 8-prenyl-quercetin has a stronger anti-inflammatory effect than its non-prenylated derivative (Hisanaga *et al.,* 2016). 6-prenylindole as another example from *Streptomyces* revealed antifungal activity affected by its substituted allyl-side-chain (Sasaki *et al.,* 2002). The influence of the prenyl group on pharmaceutical activity of aromatic molecules was attributed to an enhanced affinity and access to lipophilic membranes or interactions with proteins by their increased lipophilicity (Alhassan A.M. *et al.,* 2014; Botta *et al.,* 2005a).

1.3.1. Prenylated indole alkaloids

Prenylated indole alkaloids contain an indole core, derived from L-tryptophan, its precursors or derivatives thereof, and isoprenoid moieties. These hybrid natural products exhibit a wide diversity of chemical structures and bioactivities and thus they fulfill an important role in pharmaceutical research and drug development. Prenylated indole alkaloids can be classified according to their backbones, *inter alia*, into simple indole derivatives, tryptophan-containing cyclic dipeptides, and indole terpenes (Li 2010). Such compounds are found in ascomycetes but also in several bacteria and plants. Beside the aforementioned toxic and pharmaceutical effects of the ergot alkaloids from *Claviceps*, further prenylated indole alkaloids with important pharmacological and biological activities were isolated and identified (Li 2010). For example, neoechinulin B from *Eurotium rubrum*, semicochliodinols A, B, and isocochliodinol from *Chrysosporium merdarium* show antiviral activities (Fig. 1.2) (Chen *et al.,* 2015; Debbab *et al.,* 2009; Fredenhagen *et al.,* 1997). Other biologically active compounds of this group are fumitremorgin C (Fig. 1.2) from *A. fumigatus*, which inhibits the breast cancer resistance protein, and the anti-inflammatory cyclomarin A and B from the actinomycete *Salinispora arenicola* (*S. arenicola*) CNS-205 (Allen *et al.,* 2002; Rabindran *et al.,* 2000; Schultz *et al.,* 2008; Yamazaki *et al.,* 1980).

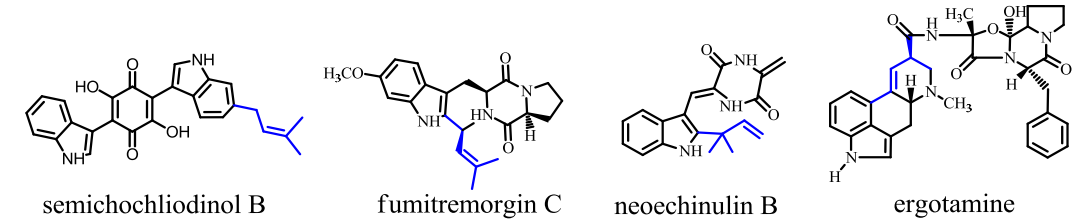

Fig. 1.2 Examples of bioactive prenylated indole alkaloids from distinct ascomycetes.

1.3.1.1. Prenylated simple indole derivatives derived from L-tryptophan

This thesis deals with the enzyme group of the indole prenyltransferases catalyzing the formation of prenylated tryptophan and simple indole derivatives with the prenyl moiety attached at C-4, C-5, C-6, and C-7 of the indole ring. For instance, *C4*-prenylated L-tryptophan represents the first precursor in the biosynthesis of the prominent ergot alkaloids isolated from *Claviceps, Aspergillus, Penicillium* and even plants (Gerhards *et al.,* 2014). Further representatives with *C4*-prenylation are the cytotoxic α-cyclopiazonic acid, rugulovasines A, B and 8-chloro-rugulovasines A and B from diverse *Penicillium* species (Cole *et al.,* 1976; Holzapfel 1968; Hymery *et al.,* 2014). The *C5*-prenylated simple indole alkaloid 5-dimethylallylindole (DMAI)-3-acetonitrile, several *C6*-prenylated indole derivatives such as 6-DMAI-3-carbaldehyde and 6-DMAI, as well as the *C7*-prenylated antibiotic 7-DMA-isatin were identified in diverse *Streptomyces* spp. (Fig. 1.3) (Ozaki *et al.,* 2013; Sasaki *et al.,* 2002; Takahashi *et al.,* 2010; Wu *et al.,* 2015). In addition, *N1*-prenylated indole derivatives such as the antibacterial cyclomarazines were found in actinomycetes (Schultz *et al.,* 2010). Simple indole derivatives were also produced by plants *e.g. C5*- and *C7*-prenylindole or the diprenylated hexalobines (Fig. 1.3) (Achenbach *et al.,* 1995; Vougogiannopoulou *et al.,* 2011). Furthermore, the prenylated tryptamine derivative deformylflustrabromine with anti-cancer activity was isolated from the marine bryozoan *Flustra foliacea* (Adla *et al.,* 2013).

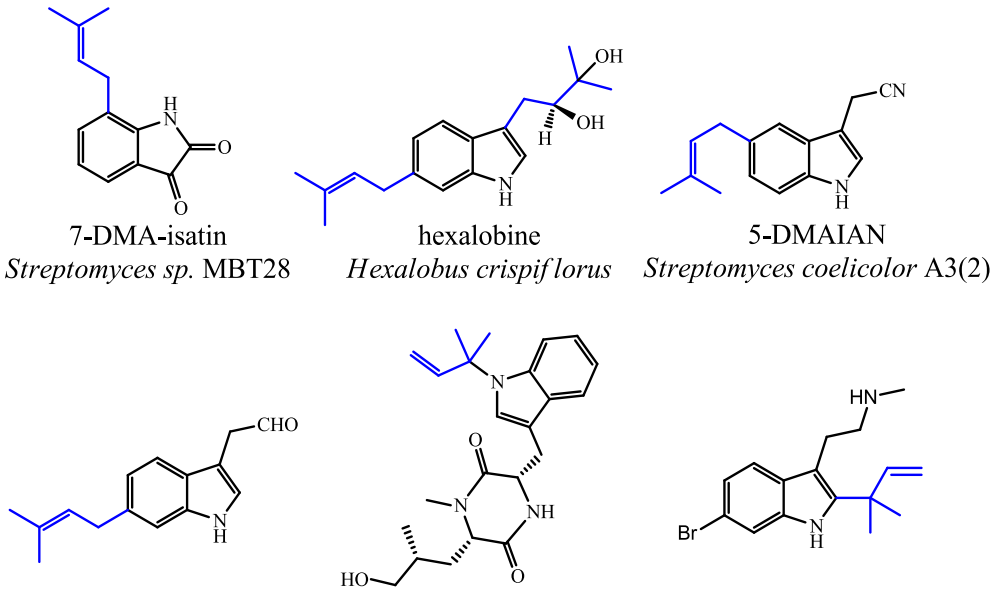

Fig. 1.3 Examples of prenylated indole alkaloids derived from L-tryptophan with prenyl moiety attached on different positions.

1.3.1.2. Prenylated tryptophan-containing cyclic dipeptides

Prenylated cyclic dipeptides form a major and diverse group of prenylated indole alkaloids with important pharmaceutical significance. Cyclic dipeptides usually contain a 2,5-diketopiperazine scaffold, emerged from the double condensation of two α-amino acids, or a benzodiazepindine scaffold (Giessen & Marahiel 2015; Li 2010). The assembly of usually L-tryptophan and a second amino acid is catalyzed mainly by non-ribosomal peptide synthetases (NRPSs), but also by the recently identified tRNA-dependent cyclic dipeptide synthetases CDPSs (Giessen & Marahiel 2014; Koglin & Walsh 2009). Cyclic dipeptides synthesized by NRPSs were found in fungi and in bacteria mostly in the phylum of ascomycota and actinobacteria, whereas the biosynthetic system including CDPSs is almost limited to bacteria *e.g. Streptomyces* (Giessen & Marahiel 2015). The most common prenylated cyclic dipeptides are *C2*-prenylated derivatives derived from the precursor *cyclo*-L-tryptophanyl-L-prolinyl (*cyclo*-L-Trp-L-Pro) also known as brevianamide F (Williams *et al.,* 2000). Diverse tremorgenic mycotoxins with genotoxic effects *e.g.* fumitremorgines and verruculogen, result from the conversion of the regularly *C2*-prenylated brevianamide F *i.e.* trypostatin B (Fig. 1.4). These prenylated natural products were identified in several *Aspergillus* and *Penicillium* strains and display diverse biological activities *e.g.* the antitumor activity of trypostatin B and its methoxylated derivative trypostatin A (Borthwick 2012; Gallagher & Latch 1977; Kosalec *et al.,* 2005; Yamazaki *et al.,* 1974; Yamazaki & Suzuki 1986). Beside the aforementioned regularly prenylated cyclic dipeptides, the family of brevianamides, notoamides, stephacidins, and other related structures are derived from the reversely *C2*-prenylated brevianamide F (deoxybrevianamide E) (Li 2010). The antibacterial brevianamide S isolated from *Aspergillus versicolor* (*A. versicolor*) was reported to represent a potential antitubercular drug (Song *et al.,* 2012). Another group of prenylated cyclic dipeptides consist of two L-tryptophan molecules *e.g.* the okaramines with insectidal activities or the fellutanines derived from *Penicillium* (Fig. 1.4) (Hayashi *et al.,* 1989; Hayashi *et al.,* 1991; Kozlovsky *et al.,* 2001). A famous example of the reversely *C3*-prenylated *cyclo*-L-tryptophanyl-L-histidinyl is roquefortine C from *Penicillium roqueforti* (Fig. 1.4) (Scott & Kennedy 1976). Moreover, acetylaszonalenin derived from L-tryptophan and anthranilic acid was isolated from diverse ascomycetes (Fig. 1.4) (Li *et al.,* 2009). Further examples for the great diversity of prenylated cyclic dipeptide are echinulin and its analogs representing *cyclo*-tryptophanyl-alaninyl (*cyclo*-L-Trp-L-Ala) derivatives substituted by three prenyl moieties (Chen *et al.,* 2015; Zou *et al.,* 2014).

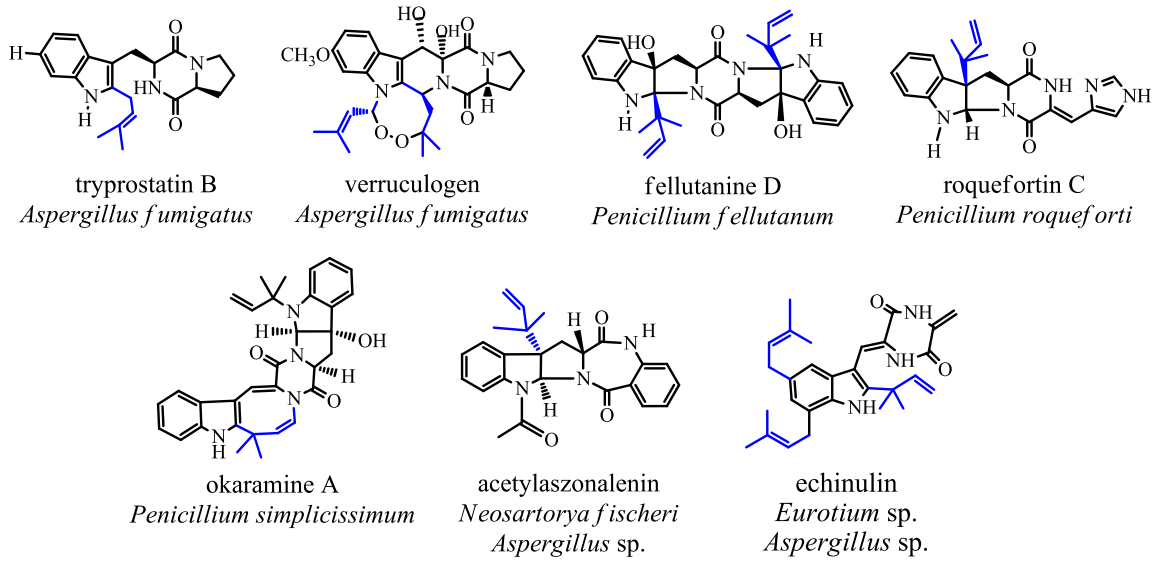

Fig. 1.4 Examples of prenylated cyclic dipeptide derivatives.

1.3.2. Prenylated naphthalenes and quinones

Prenylated naphthalenes are a less abundant class of prenylated secondary metabolites, which were isolated from plants and bacteria (Hussein *et al.,* 2004; Monache *et al.,* 1985). Examples for prenylated naphthalenes from plants are the cytotoxic two- or threefold prenylated adenoforins A-D (Fig. 1.5) from *Adenaria floribunda* as well as the potential anti-malarial vismione B from *Cratoxylum* and *Psorospermum* (Botta *et al.,* 1983; Hussein *et al.,* 2004; Laphookhieo *et al.,* 2009). The antibiotic merochlorin A was identified with the naphthoquinones merochlorin B-D from *Streptomyces* (Kaysser *et al.,* 2012). The more common prenylated naphthoquinones and quinones are distributed throughout various marine and terrestrial organisms including plants, fungi, bacteria as well as algae and sponges (Hussain *et al.,* 2007; Sedmera *et al.,* 1991; Sunassee & Davies-Coleman 2012; Suzuki *et al.,* 2014). These compounds received pharmaceutical interest, particularly due to their anti-inflammatory and antitumor activities (de los Reyes *et al.,* 2013; Sunassee & Davies-Coleman 2012). Moreover, a potential agent for treatment of malaria was obtained within the *C*-diprenylated quinone scabellone B from the sea squirt *Aplidium scabellum* (Andersen et al., 2011). The highly oxygenated and cytotoxic terreumol C (Fig. 1.5) was isolated from *Tricholoma terreum* (Yin *et al.,* 2013a). The antioxidant naphterpin is a prenylated naphthoquinone derived from the polyketide 1,3,6,8-tetrahydroxynaphthalene and produced by some *Streptomyces* species (Shin-Ya *et al.,* 1990a; Shin-Ya *et al.,* 1990b).

1.3.3. Prenylated flavonoids

Prenylated flavonoids are a large class of naturally occurring products, urgently distributed in the plant kingdom and in particular in the families of Fabaceae (Leguminosae) and Moraceae (Botta *et al.,* 2005a). These polyphenolic compounds with a C_6-C_3-C_6 carbon skeleton and one or more prenyl side chains, usually C_5 or C_{10} units, exhibit a wide range of bioactivities including anti-inflammatory, antibacterial, antioxidant, cytotoxic as well as estrogenic activities (Hosek *et al.,* 2011; Kim *et al.,* 2013; Urmann *et al.,* 2015; Vogel *et al.,* 2008). The structure diversity includes mainly the subclasses of flavones, isoflavones, chalcones and flavanoles (Barron & Ibrahim 1996; Botta *et al.,* 2005b). For example, the most abundant prenylated chalcone from hop, the xanthohumol (Fig. 1.5), display pharmaceutical important properties such as antiviral (Lou *et al.,* 2014), anti-angiogenic and anti-inflammatory activities (Gallo *et al.,* 2016). A further example for a prenylated flavonoid is the isoflavone isowighteone isolated from *Lupinus albus* (Fig. 1.5) (Shen *et al.,* 2012).

1.3.4. Prenylated xanthones

Prenylated xanthones or dibenzo-γ-pyrones are produced in higher plants, fungi and lichens. As natural secondary metabolites, these compounds has drawn attention from diverse scientists (El-Seedi *et al.,* 2009; Pinto *et al.,* 2005). For example, the HIV-inhibitory macluraxanthone B was found in the extract of *Maclura tinctoria* (Fig. 1.5) (Groweiss *et al.,* 2000). Further multiple *C*-prenylated xanthones such as α- and γ-mangostin as well as garcinone C were extracted from *Garcinia* species. These compounds inhibit acetylcholinesterase and thus makes them to potent agents for treatment of Alzheimer's disease (Khaw *et al.,* 2014; Wang *et al.,* 2012). Moreover, cytotoxic activities were reported for γ-mangostin and garcinone C (Xu *et al.,* 2014), while α-mangostin was evaluated as a potential anticancer agent (Kwak *et al.,* 2016) and also exhibit anti-inflammatory activity (Gutierrez-Orozco *et al.,* 2013). Beside the reported *C*-prenylated xanthones in plants, both *C*- and *O*-prenylated derivatives were found in fungi *e.g.* variecoxanthones from *Aspergillus* species (Fig. 1.5) (Simpson 2012).

1.3.5. Prenylated coumarins

The major producer of prenylated coumarins are plants, but also several species of fungi and bacteria. The structures based on a 1,2-benzopyron scaffold are modified at C- or O-atom by an isoprenoid moiety (Venugopala *et al.,* 2013). Whereas coumarins are distributed throughout all families of plant kingdom, many prenylated coumarins were found in the family of Apiaceae (Gliszczynska & Brodelius 2012; Venugopala *et al.,* 2013). For instance, several genera of Apiaceae produce the bioactive secondary metabolite umbelliprenin (Fig. 1.5) displaying anti-bacterial (Rosselli *et al.,* 2007), anti-inflammatory (Zamani Taghizadeh *et al.,* 2016), cytotoxic/anti-cancer (Barthomeuf *et al.,* 2008) and anti-leishmanial activities (Iranshahi *et al.,* 2007). Another example for this class of natural products with various bioactivities is the *O*-prenylated imperatorin (Venugopala *et al.,* 2013). Furthermore, novobiocin from the actinobacterium *Streptomyces sphaeroides* belong to the family of aminocoumarin antibiotics featured with a 3-amino-4,7-dihydroxycoumarin moiety and act as gyrase inhibitor (Fig. 1.5). One related structure of this family is clorobiocin and also derived from *Streptomyces*. The biosynthesic pathways of these two antibiotics have been completely understood by genetic and biochemical investigations on the corresponding gene clusters (Heide 2009b).

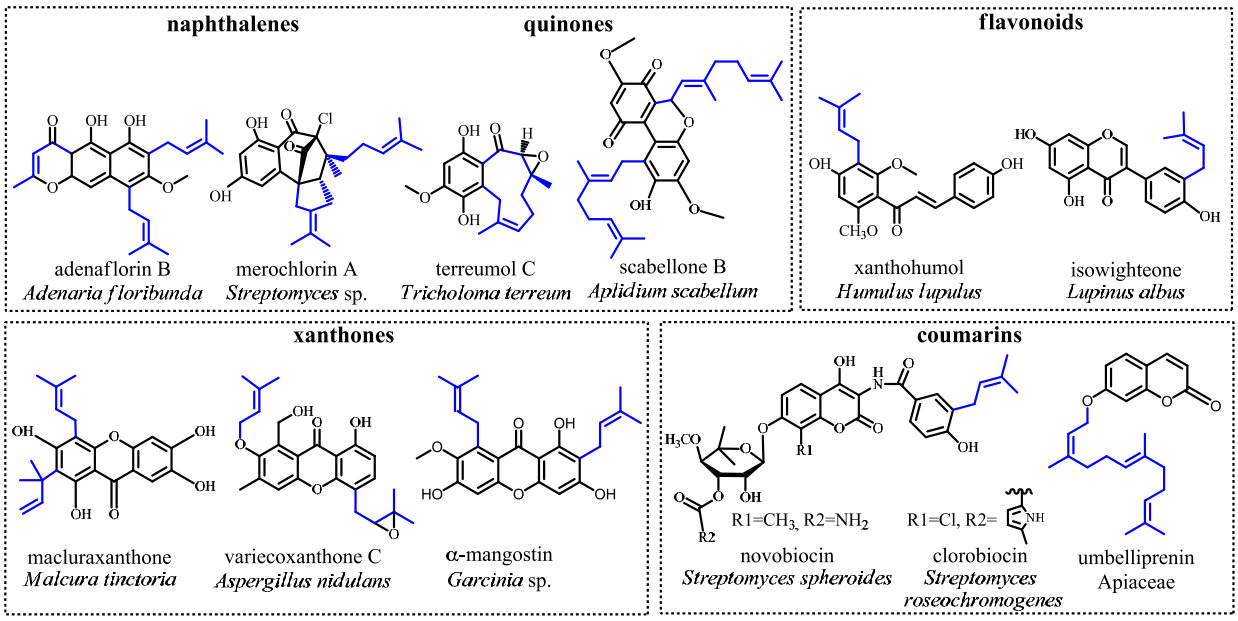

Fig. 1.5 Examples of prenylated aromatic compounds.

1.4. Prenyltransferases

The manifold enzyme family of prenyltransferases and their catalyzed prenylation reactions are found in all living organisms and are crucial in primary and secondary metabolism. They catalyze the transfer reactions of prenyl moieties from different prenyl donors to various aliphatic or aromatic acceptors of both low and high molecular substances including proteins and nucleic acids (Dumelin *et al.,* 2012; Heide 2009a; Li 2009a; Oldfield & Lin 2012; Palsuledesai & Distefano 2015; Xie *et al.,* 2007; Yazaki *et al.,* 2009). The prenyl donors consisting of n × C_5 units are derived from the terpenoid biosynthetic pathways *e.g.* dimethylallyl (DMAPP with a branched C_5-chain), geranyl (GPP, C_{10}), farnesyl (FPP, C_{15}) or geranylgeranyl (GGPP, C_{20}) diphosphate. Prenyltransferases are classified into different subgroups based on their primary amino acid sequences, biochemical and structural characteristics. In the last years, remarkable progress has been achieved in research on this enzyme group, especially on the members of the dimethylallyltryptophan synthase (DMATS) superfamily. These enzymes are the main focus of research in this thesis. Therefore they will be discussed in more detail.

1.4.1. Prenyl diphosphate synthases: *trans*- and *cis*-prenyltransferases

Prenyl diphosphate synthases using prenyl diphosphate as donor *e.g.* DMAPP and isopentenyl diphosphate (IPP) as acceptor are involved in the biosynthesis of over 63,000 isoprenoid natural products including terpenoids, steroids and membrane components (Liang *et al.,* 2002; Oldfield & Lin 2012; Ramamoorthy *et al.,* 2015). Sequential condensation of the donor and a given number IPP lead to the formation of the carbon backbone with a certain chain length. Depending on the formed double bond configuration (*trans* (*E*) and *cis* (*Z*)) in the resulting prenyl units, these chain elongating enzymes can be classified into two major groups, *i.e. trans*- and *cis*-prenyltransferases. For instance, the formation of the all-*trans* C_{15} precursor FPP was catalyzed by FPP synthases (FPPase) which belongs to the first group (Poulter 2006). In contrast, *cis*-prenyltransferases, *e.g.* undecaprenyl diphosphate synthase, produce prenyl diphosphates containing both *Z*- and *E*-configured double bonds. *Trans*- and *cis*-prenyltransferases are both Mg^{2+}-dependent enzymes but their amino acid sequence as well as their tertiary structures are completely different from each other (Guo *et al.,* 2004; Guo *et al.,* 2005; Winkelblech *et al.,* 2015a).

1.4.2. Protein, peptide and tRNA prenyltransferases

Protein prenylation including farnesylation or geranylgeranylation is a post-translational modification which is found in all eukaryotic cells (Palsuledesai & Distefano 2015). The isoprenoid moieties derived from FPP and GPP were attached by farnesyltransferase (FTase) and geranylgeranyltransferase type 1 (GGTase-I), respectively, to the cysteine residue in the C-terminal consensus sequence CaaX. In contrast, geranylgeranyltransferase type 2 (GGTase-II or Rab geranylgeranyltransferase) catalyzes the transfer reaction of two geranylgeranyl moieties to special sequence motifs like CXC or CCXX. Protein prenyltransferases play an important role in cellular protein localization, protein-protein interactions and protein activity. This makes them to interesting drug targets *e.g.* in tumor therapy (Palsuledesai & Distefano 2015).

Modification of large molecules by prenylation are not limited to proteins, but were also found for peptides or even nucleic acids. The peptide prenyltransferase ComQ from *Bacillus subtilis* was suggested to catalyze a regular *C3*-geranylation of tryptophan in a heptapeptide resulting in the ComX pheromone (Tsuji *et al.,* 2012). SelU is a tRNA prenyltransferase from *Escherichia coli* (*E. coli*) which catalyze *S*-geranylation of 5-methylaminomethyl-2-thiouridyl residue in tRNA (Dumelin *et al.,* 2012).

1.4.3. Aromatic prenyltransferases

Aromatic prenyltransferases contribute significantly to the large diversity of prenylated secondary metabolites in plants, fungi and bacteria (Heide 2009b; Li 2009b; Yazaki *et al.,* 2009). They catalyze the attachment of the prenyl moiety to C-, O- or N-atom of a wide range of aromatic substances, such as phenols, phenolic acids, flavonoids, coumarins, naphthalenes, phenazines or indole derivatives. For classification of these enzymes, several aspects for discrimination could be considered such as structural fold, substrate binding motifs, metal ion dependency, and soluble or membrane-bound form.

1.4.3.1. Membrane-bound prenyltransferases for aromatic substrates

In contrast to the soluble aromatic prenyltransferases, the membrane-bound prenyltransferases are not only involved in secondary metabolism, but also in primary metabolism. They play an important role in the biosynthesis of ubiquinones and menaquinones (Boronat & Rodriguez-Concepcion 2015; Meganathan & Kwon 2009) or diverse secondary metabolites from fungi,

bacteria and plants (Holm *et al.,* 2014; Wang *et al.,* 2014; Yazaki *et al.,* 2009; Zeyhle *et al.,* 2014a; Zeyhle *et al.,* 2014b). Enzymes of this family contain characteristic aspartate-rich motifs, *e.g.* NDxxDxxxD and their catalyzed reactions are dependent on the presence of divalent ions. Natural substrates of membrane-bound prenyltransferase include 4-hydroxybenzoate (4HB), homogentisic acid, coumarins, flavonoids, 1,4-dihydroxy-2-naphthoate or phenazines (Heide 2009a; Karamat *et al.,* 2014; Yazaki *et al.,* 2009; Zeyhle *et al.,* 2014a; Zeyhle *et al.,* 2014b). The most famous representative of this group is UbiA from *E. coli*, which catalyze the transfer of an all-*trans* octaprenyl moiety onto 4HB. Furthermore, a high flexibility of UbiA toward prenyl donors lead to formation of ubiquinones CoQ_6 to CoQ_{10} in different species (Cheng & Li 2014). The crystal structure of an archeal UbiA was solved and reported in 2014 (Cheng & Li 2014). Recently, two membrane-bound prenyltransferases from *Humulus lupulus* were reported to catalyze three sequential prenylation steps in the biosynthetic pathway of bitter acid in hop (Li *et al.,* 2015). Two examples for membrane-bound prenyltransferases from bacteria were identified in *Streptomyces* catalyzing phenazine prenylations (Zeyhle *et al.,* 2014a; Zeyhle *et al.,* 2014b).

1.4.3.2. Soluble prenyltransferases

Compared to the aforementioned membrane-bound enzymes, metal ions are not essential for the enzyme activity of the soluble PTs in most cases and they usually contain no aspartate-rich motif (Bonitz *et al.,* 2011; Heide 2009a). This enzyme group of soluble aromatic prenyltransferases includes the CloQ/NphB group and the extensively investigated DMATS superfamily (Winkelblech *et al.,* 2015a). Enzymes of both subgroups comprise a PT-barrel, termed *aββa*-fold (ABBA). Firstly, this structure was observed for the naphthalene geranyltransferase NphB (Kumano *et al.,* 2008; Kuzuyama *et al.,* 2005) and later for four fungal indole prenyltransferases.

1.4.3.2.1. Prenyltransferases of the CloQ/NphB group

The name of the CloQ/NphB group derived from the first identified members from *Streptomyces*. CloQ and its orthologue NovQ catalyze the prenylation of 4-hydroxyphenylpyruvic acid in the biosynthesis of clorobiocin and novobiocin, respectively (Pojer *et al.,* 2003; Steffensky *et al.,* 2000). Afterwards, NphB involved in the biosynthesis of naphterpin (Kuzuyama *et al.,* 2005) was found in *Streptomyces* sp. (Kuzuyama *et al.,* 2005; Pojer *et al.,* 2003). In general, the known enzymes of this group use naphthalenes, quinones,

phenols and phenazines as substrates (Heide 2009a). In the last years, a number of further enzymes of the CloQ/NphB group have been identified (Winkelblech *et al.,* 2015a).

1.4.3.2.2. Enzymes of the DMATS superfamily

The DMATS superfamily is the most investigated group among the prenyltransferases. Enormous progress has been made in the last years, concerning the great number of newly identified and biochemically characterized enzymes as well as the availability of novel crystal structures. So far, more than 40 members of the DMATS superfamily were identified and investigated by mining of fungal and bacterial genomes. A detailed summary comprising all known studied DMATSs up to 2015, was provided in the overview article (Chapter 4.4) (Winkelblech *et al.,* 2015a). In Fig. 1.6 several examples of DMATSs and their distinct functions are illustrated. Generally, a broad substrate promiscuity and a high regioselectivity regarding the prenylation position are characteristics for the DMATS superfamily. The common prenyl donor is DMAPP, while a few DMATSs use GPP. Most enzymes of this group catalyze the prenylation of indole derivatives including tryptophan and tryptophan-containing cyclic dipeptides. In the following, bacterial and fungal tryptophan prenyltransferases will be discussed more detailed.

The first enzyme of the DMATS superfamily, DmaW, was identified in the ascomycete and ergot alkaloid producer *C. purpurea* in 1995 (Gebler & Poulter 1992; Tsai *et al.,* 1995). DmaW and its orthologue FgaPT2 from *A. fumigatus* catalyze the *C4*-prenylation of L-tryptophan with DMAPP as prenyl donor and are involved in the biosynthesis of ergot alkaloids. Thus, these enzymes function as 4-dimethylallyltryptophan synthases (Tudzynski *et al.,* 1999; Unsöld & Li 2005). Later on, the two fungal prenyltransferases 7-DMATS from *A. fumigatus* and 5-DMATS from *Aspergillus clavatus* were identified, which acting as *C7*- and *C5*-prenylating enzymes, respectively (Kremer & Li 2010; Yu *et al.,* 2012). At least eight fungal DMATSs were identified until now, which act as *C4-, C5-,* and *C7*-prenylating enzymes (Winkelblech *et al.,* 2015a). CymD identified in *S. arenicola* was the first bacterial tryptophan prenyltransferase. CymD is involved in the biosynthesis of the abovementioned cyclomarin A and cyclomarazine A by catalyzing the reverse *N1*-prenylation at the indole ring (Schultz *et al.,* 2010). Only two further bacterial tryptophan prenyltransferases with *C5*- and *C6*-tryptophan prenylating activities were known at the beginning of this thesis. The *C5*-prenyltransferase SCO7467 and the flavin-dependent monooxygenase SCO7468 from *S. coelicolor* were found to be involved in the biosynthesis of 5-DMAI-3-acetonitrile (Ozaki *et al.,* 2013; Subramanian *et al.,* 2012).

IptA functions as 6-DMATS in the biosynthesis of 6-DMAI-3-carbaldehyde in *Streptomyces sp.* SN-593 (Takahashi *et al.,* 2010). In the present work, the knowledge on bacterial tryptophan prenyltransferases was expanded by identification and characterization of three new outstanding 6-DMATS from different actinomycetes. Moreover, within the last two years, the IptA orthologue, $IptA_{Am}$ from *Actinoplanis missouriensis* (*A. missouriensis*) (Satou *et al.,* 2014) and the *C7*-prenyltransferase IsaA from *Streptomyces* MBT28-91, which catalyzes the formation of the new antibiotic 7-prenylisatin (Wu *et al.,* 2015), were reported.

Tryptophan-containing cyclic dipeptides were regiospecific prenylated, especially at N-1, C-2, C-3, and C-7 position at the indole ring by diverse prenyltransferases (Winkelblech *et al.,* 2015a). A regular *C2*-prenylation was catalyzed by FtmPT1 from *A. fumigatus* in the biosynthesis of the previously reported fumitremorgines/verruculogen (Grundmann & Li 2005; Li 2011), while NotF from an *Aspergillus* sp. and BrePT from *A. versicolor* catalyze the reverse *C2*-prenylation in the biosynthesis of notoamides (Ding *et al.,* 2010; Yin *et al.,* 2013b). In addition, the cyclic dipeptide reverse *C2*- prenyltransferase CdpC2PT from *Neosartorya fischeri* (*N. fischeri*) was suggested to be involved in the biosynthesis of fellutanine (Mundt & Li 2013). Furthermore, AnaPT from *N. fischeri* catalyzes a reverse *C3α*-prenylation of (R)-benzodiazepinedinone in the biosynthesis of acetylaszonalenin (Yin *et al.,* 2009). In contrast, the reverse *C3ß*-prenylation of cyclic dipeptides was catalyzed by CdpNPT from *A. fumigatus* and CdpC3PT from *N. fischeri* (Schuller *et al.,* 2012; Yin *et al.,* 2010). After identification of the cyclic dipeptide *C7*- and simultaneous *N1*- prenyltransferase CTrpPT from *A. oryzae* (Zou *et al.,* 2010), the *C7*-prenylating CdpC7PT, revealing a much higher regioselectivity and substrate flexibility toward cyclic dipeptides, was identified in *A. terreus* (Wunsch *et al.,* 2015).

Some bacterial cyclic dipeptide prenyltransferases including LtxC from *Lyngbya majuscula*, TleC from *Streptomyces blastmyceticus* and MpnD from *Marinactinospora thermotolerans* catalyze the reverse prenylation of (-)-indolactam V at position C-7 in the biosynthesis of lyngbyatoxins, teleocidin B, and methylpendolmycin, respectively (Awakawa *et al.,* 2014; Edwards & Gerwick 2004; Ma *et al.,* 2012; Mori *et al.,* 2016). In contrast to the first two geranyltransferases, MpnD uses DMAPP as prenyl donor. Recent studies on TleC and MpnD revealed a high flexibility toward prenyl donors with different chain length. Furthermore, enzyme engineering based on their crystal structures led to an altered donor specificity, regio- and stereoselectivities of the prenylation reactions (Mori *et al.,* 2016).

In addition to tryptophan and tryptophan-containing cyclic dipeptides, other indole derivatives were used as prenyl acceptor by several members of the DMATS family such as the indole

diterpene prenyltransferases AtmD and PaxD from *A. flavus* and *Penicillium paxilli,* respectively (Liu *et al.,* 2013a; Liu *et al.,* 2014). TdiB from *A. nidulans* and AstPT from *A. terreus* are involved in the biosynthesis of prenylated bisindolyl benzoquinones (Balibar *et al.,* 2007; Schneider *et al.,* 2008; Tarcz *et al.,* 2014a).

Beside the numerous indole prenyltransferases, several prenyltransferases use non-indole substrates *e.g.* the tyrosine *O*-prenyltransferase SirD from *Leptosphaeria maculans* and TyrPT from *Aspergillus niger* (*A. niger*) (Fan *et al.,* 2014; Kremer & Li 2010). One example for a prenyltransferases from DMATS superfamily, PAPT from *Phomopsis amygdali* uses a non-aromatic derivative for *O*-prenylation in the glucose moiety (Noike *et al.,* 2012).

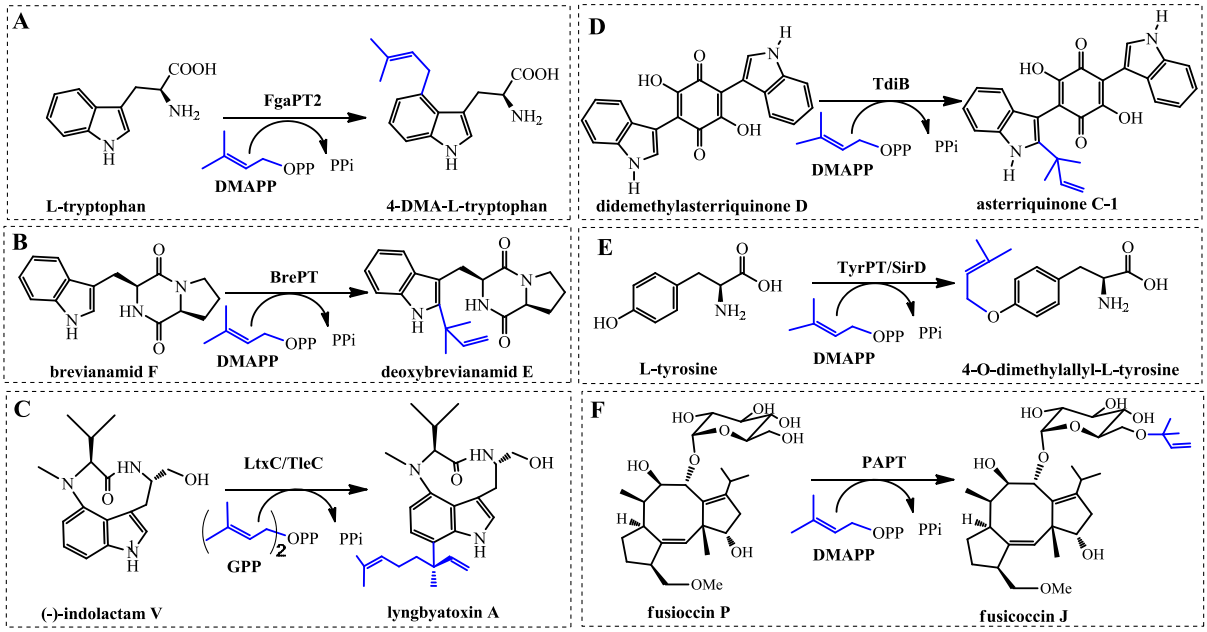

Fig. 1.6 Selected prenyltransferases of distinct subgroups (A-F) belonging to the DMATS superfamily. A: tryptophan prenyltransferase, B/C: tryptophan-containing cyclic dipeptide prenyltransferase, D: prenyltransferases of other indole derivatives, E: tyrosine prenyltransferases, F: prenyltransferases of non-aromatic derivatives.

To understand the mechanisms of the DMATS reactions, structural analyses based on the crystal structures were essential. The first structure was obtained for the tryptophan prenyltransferase FgaPT2 (Metzger *et al.,* 2009), followed by the crystal structures for FtmPT1, CdpNPT and AnaPT (Jost *et al.,* 2010; Schuller *et al.,* 2012; Yu *et al.,* 2013). All four structures contain the PT-barrel, formed by five repetitive αββα-elements (ABBA), which is similar to the tertiary structure of the bacterial prenyltransferase NphB, although the primary and secondary amino acid sequences including the active site strongly differ between these two enzyme groups. Recently, the crystal structures of the bacterial indolactam prenyltransferases TleC and

MpnD were determined, sharing the ABBA barrel fold (Mori *et al.,* 2016). The binding sites are located in the hydrophobic pocket inside the PT-barrel. The amino acids in the binding site for the prenyl donor DMAPP are strictly conserved in these structures, whereas the binding sites for the aromatic substrates are different. This makes molecular modeling or functional predictions for specific amino acids more difficult. Nevertheless, the gained structural information provide substantial insights into the reaction mechanism (Jost *et al.,* 2010). The first step of a proposed three step reaction is the cleavage of the pyrophosphate from the isoprenoid chain, resulting in a dimethylallyl cation, proved by a positional isotope exchange with O^{18}-labeled DMAPP (Luk & Tanner 2009; Metzger *et al.,* 2009; Shibuya *et al.,* 1990). Subsequent electrophilic substitution on the indole nucleus leads to the formation of an areniumion, which is deprotonated in the third step. The second step have been strongly disputed, whether the described substitution take place directly at the prenylation site or initially at C-3, followed by rearrangement to the final position (Luk *et al.,* 2011; Mahmoodi *et al.,* 2013; Mahmoodi & Tanner 2013; Tanner 2014).These results could be further used in molecular modeling and site-directed mutagenesis experiments in order to get deeper insights into the function of DMATSs and to create new enzymes with modified features for application in chemoenzymatic synthesis.

1.5. DMATSs as biocatalysts in chemoenzymatic synthesis of prenylated compounds

The above presented biochemical properties of the DMATSs such as the high substrate specificity facilitated an enzyme-driven regiospecific production of various prenylated products. These products in turn could provide potential drug candidates with biological activities due to the attached prenyl moieties. As aforementioned, the presence of a prenyl group has strong effects on bioactivity due to the increased lipophilicity of prenylated compounds. Therefore, the enzymes of the DMATS superfamily serve as valuable biocatalysts for usage in biotechnology and pharmacy. The advantage of using this simple method is the easy-handling and the high efficiency compared to the more complicated chemical synthesis. Targeted production of tryptophan and derivatives substituted by a dimethylallyl residue at N-1, C-4, C-5, C-6 or C-7 was achieved by the usage of regiospecific prenyltransferases of the DMATS superfamily. Regiospecific synthesis of *C4,C7*-diprenylated tryptophan was reported for FgaPT2 and 7-DMATS (Ruan *et al.,* 2009). The tyrosine prenyltransferases SirD and TyrPT

can be also used for the synthesis of 7-DMA-L-tryptophan, while the tryptophan prenyltransferases FgaPT2 and 7-DMATS also accepted L-tyrosine and 4-amino-L-phenylalanine as substrates (Fan *et al.,* 2015a; Fan & Li 2014). Cyclic dipeptide prenyltransferases catalyze prenylation of diverse peptides with distinct prenylation positions and different stereochemistry. For instance, the regular *C2*-prenyltransferase FtmPT1 and the two reverse *C2*-prenylating enzymes BrePT and CdpC2PT produce in total 30 regularly or reversely *C2*-prenylated products (Fan *et al.,* 2015b). Ten prenylated cyclic dipeptides were obtained from the CdpC7PT reactions with six substrates. CdpC7PT even catalyze a O-prenylation of *cyclo*-L-Tyr-L-Tyr, which was not observed prior to that study (Wunsch *et al.,* 2015). The *C4*-prenyltransferase FgaPT2 is also applicable for production of *C4*-prenylated cyclic dipeptides (Steffan & Li 2009). Mutation on R244 of FgaPT2 increased its activity toward cyclic dipeptides (Fan & Li 2016). Beside the natural substrates also unnatural compounds were accepted by DMATS *e.g.* the unnatural cyclic dipeptide *cyclo*-L-homotryptophan-D-valine was accepted by cyclic dipeptide prenyltransferases as well as by tryptophan prenyltransferases (Fan & Li 2013). Further prenylated aromatic compounds comprises xanthones reported for XptB (Pockrandt *et al.,* 2012) and naphthalenes reported for 7-DMATS, AnaPT, CdpNPT as well as CdpC3PT (Kremer *et al.,* 2007; Schuller *et al.,* 2012; Yin *et al.,* 2009; Yin *et al.,* 2010). Membrane-bound prenyltransferases in plants are natural biocatalysts for prenylated flavonoids, but their potential use in chemoenzymatic synthesis is impaired due to difficult protein isolation and low catalytic efficiency. Therefore 7-DMATS and AnaPT, accepting several flavonoids, represent alternative biocatalysts (Yu & Li 2011; Zhou *et al.,* 2015). In addition, indolocarbazoles and acylphloroglucinols, which are natural bacterial and plant metabolites, can also be prenylated by DMATS enzymes (Fan *et al.,* 2015b).

Previously, the usage of DMATSs in biotechnology was discussed based on the large pool of aromatic substrates, but another possibility to expand the product range of alkylated compounds affect the used prenyl donor. Although DMATSs are often high regiospecific toward their natural donor, recent studies have demonstrated the acceptance of other prenyl donors like GPP, FPP or even unnatural alkyl and benzyl donors (Liebhold *et al.,* 2012; Liebhold *et al.,* 2013; Liebhold & Li 2013). The identification of the geranyltransferase VrtC from *Penicillium aethiopicum* initiated further investigations on the acceptance of different prenyl donors. Over the last three years, GPP was reported to be used as prenyl donor by AnaPT (Pockrandt & Li 2013), while GPP and FPP were used by AstPT in the presence of hydroxyxanthones (Tarcz *et al.,* 2014b) as well as by BAE61387 for prenylation of hydroxynaphthalenes (Pockrandt *et al.,* 2014).

To get deeper insights into the donor promiscuity of DMATSs and for production of novel unnatural prenylated indole derivatives, five unnatural DMAPP analogs were synthesized and tested as alternative donors (Liebhold *et al.,* 2012). The results demonstrated that the double bond at *ß*-position to pyrophosphate is essential for the enzyme activity. One methyl group can be deleted as in the case of MAPP or shifted to the *δ*-position as in the case of 2-pentenyl-PP. For FgaPT2 and 5-DMATS, the alkylation positions of tryptophan were shifted partially or completely to the neighboring position in the presence of the unnatural donors MAPP and 2-pentenyl-PP (Liebhold *et al.,* 2012). FgaPT2 even used the more space-demanding substrate benzyl-PP as donor and produced regiospecifically *C5*-benzylated tryptophan (Liebhold & Li 2013). In addition, the acceptance of unnatural DMAPP analogs was proven for several cyclic dipeptide prenyltransferases, resulting in a mixture of *C2*- and *C3*-reversely alkylated diastereomers, contrary to the natural reactions (Liebhold *et al.,* 2013).

In this thesis, the investigations on unnatural alkylation of L-tryptophan by further DMATSs including *C6*- and *C7*-prenyltransferases should be extended. Recently, the acceptance of unnatural DMAPP analogs was also reported for the two tyrosine *O*-PTs TyrPT and SirD with L-tyrosine as substrate (Yu *et al.,* 2015).

An approach in synthetic biology for the production of prenylated metabolites in high amounts with a minimum cost represents the development of whole cell biocatalyst *e.g*. coexpression of NRPS and prenyltransferase genes in the same organism. For instance, the NRPS gene *ftmPS* was expressed together with the cyclic dipeptide prenyltransferase genes *cdpC2PT*, *cdpNPT* or *cdpC3PT* resulting in the NRPS produced brevianamide F and subsequently the corresponding prenylated derivatives thereof (Mundt & Li 2013; Yin *et al.,* 2010; Yu *et al.,* 2013). Furthermore, the "Autodisplay" technique reported for the *C4*-prenyltransferase FgaPT2, which was displayed on the surface of *E. coli* cells, is a further example for an advanced technique in chemoenzymatic synthesis.

A further important point for chemoenzymatic synthesis is the creation of new biocatalysts by site-directed mutagenesis based on structural analyses including the availability of crystal structures or modeling experiments. Thereby enzymes with changed substrate specificity and regioselectivity or enzymes with optimized catalytic efficiency could be generated. One example for successful mutant design was shown for the intensively studied FgaPT2. Modeling-guided site-directed mutagenesis of FgaPT2 resulted in a changed substrate preference from a tryptophan *C4*- to a tyrosine *C3*-prenylating enzyme (Fan *et al.,* 2015a).

2. Aims of this thesis

The following issues have been addressed in this thesis:

Identification and biochemical investigations of tryptophan prenyltransferases from actinomycetes

The DMATS superfamily represents the largest and most investigated subgroup among aromatic prenyltransferases. Whereas the recent research was primarily focussed on prenyltransferases from fungi, this study should offer more insights into the function of bacterial DMATSs. The known bacterial tryptophan prenyltransferases are all from actinomycetes and involved in the biosynthesis of prenylated indole derivatives. In order to identify and characterize further bacterial indole prenyltransferases, following experiments were carried out:

- Sequence homology search with known bacterial tryptophan prenyltransferases to identify putative indole prenyltransferases.
- Amplifying and cloning of the putative prenyltransferase genes *SAML0654, Strvi8510*, and *MolI14.36* from gDNA of *S. ambofaciens* ATCC2387, *S. violaceusniger* Tü 4113, and *M. olivasterospora* DSM 43868, respectively.
- Overproduction and purification of the recombinant proteins SAML0654, Strvi8510 and MolI14.36.
- Proving enzyme activity with several indole derivatives and other substances by enzyme assays and HPLC analysis.
- Proving acceptance of different prenyl donors.
- Isolation of enzyme products for structure elucidation by NMR and mass analyses.
- Biochemical characterization of the recombinant enzymes by proving the ion dependency and determination of kinetic parameters for several substrates.
- Comparison of the biochemical properties of the newly identified prenyltransferases with those of other DMATSs.

Investigations on the acceptance of unnatural allyl and benzyl diphosphates by tryptophan *C5*-, *C*6-, and *C7*-prenylating enzymes

Members of DMATS superfamily show a remarkably high flexibility toward aromatic substrates and are usually more specific toward their prenyl donor. Nevertheless prenyl diphosphates like GPP and FPP were also accepted with lower activity by few DMATS *e.g.* 6-DMATS$_{Sa}$ and 6-DMATS$_{Sv}$ identified within this work. These two enzymes accepted both DMAPP and GPP as prenyl donor. Previous investigations with tryptophan *C4*- and *C5*-prenyltransferases showed that they also used the unnatural MAPP, 2-pentenyl-PP or benzyl-PP as alkyl/benzyl donors (Liebhold *et al.,* 2012; Liebhold & Li 2013). Due to the availability of the two 6-DMATSs from *Streptomyces* and the L-tyrosine prenyltransferase TyrPT with a tryptophan *C7*-prenyltransferase activity in our laboratory, these studies could be expanded by investigations with tryptophan *C-6*- and *C-7*-prenylating enzymes. The aim of this project was to analyze the behaviors of the DMATSs in the presence of unnatural DMAPP analogs and to expand their potential usage in chemoenzymatic synthesis.

- Overexpression and subsequent purification of the recombinant proteins of two *C5*-prenyltransferases 5-DMATS and 5-DMATS$_{Sc}$, two *C6*-prenyltransferases 6-DMATS$_{Sa}$ and 6-DMATS$_{Sv}$ as well as the L-tryptophan *C7*-prenylating TyrPT.

- Preparation of enzyme assays containing the recombinant proteins, DMAPP analogs and L-tryptophan.

- Evaluation of the assays on HPLC and determination of enzyme activities.

- Isolation of enzymatic products for structure elucidation by NMR spectroscopy and MS analysis.

- Determination of the kinetic parameters for the three DMAPP analogs.

Investigation on DMATSs regarding their substrate specificity and regioselectivity for mono- and diprenylation of enantiomers of tryptophan and methylated derivatives thereof

As mentioned in the previous project, the tryptophan prenyltransferase 6-DMATS$_{Mo}$ from *M. olivasterospora* was identified and characterized. The finding of the unusually high acceptance of D-tryptophan by 6-DMATS$_{Mo}$ prompted us to study the enantioselectivity of several DMATSs toward L- and D-isomers of tryptophan and analogs. In addition, the regioselectivity and the capability for diprenylation of the enzymes were analyzed and compared to each other. For this propose the following experiments were carried out:

- Overproduction and purification of the recombinant proteins FgaPT2, 5-DMATS, 5-DMATS$_{Sc}$, 6-DMATS$_{Sv}$, 6-DMATS$_{Sa}$ and 7-DMATS.
- Enzyme assays with L- and D-tryptophan and subsequent HPLC analysis.
- Determination of kinetic parameters of DMATSs toward L- and D-tryptophan.
- NMR analysis of the enzyme products of D-tryptophan with 5-DMATS$_{Sc}$.
- LC-MS and HPLC analyses for detection and identification of prenylated tryptophan products.
- Isolation of L- and D-enantiomers of 5-methyltryptophan, 6-methyltryptophan, and 7-methyltryptophan from their racemates by using chiral column on HPLC.
- Enzyme assays with isolated enantiomers of methylated tryptophan derivatives.
- HPLC and LC-MS analyses for enzyme activities and prenylation of methylated tryptophan derivatives.
- Isolation of enzyme products for 5-methyl-D-tryptophan with 6-DMATS$_{Mo}$ and 5-DMATS$_{Sc}$ and structure elucidation by NMR analysis.

3. Results and Discussion

3.1. Identification and biochemical investigations of tryptophan prenyltransferases from actinomycetes

Previous studies on prenyltransferases were mainly focused on the DMATS enzymes, especially on those with fungal origin. Tryptophan prenyltransferases from fungi and bacteria have different polypeptide lengths, 420 to 470 amino acids of those from fungi versa 370 to 390 amino acids from bacteria. They share practically no homology on the amino acid level, but catalyze independent of their origins the regiospecific prenylation of tryptophan in the presence of DMAPP, in some cases even the same reaction (Winkelblech *et al.,* 2015a). In contrast to the extensively investigated DMATS enzymes from fungi, only few members of the bacterial tryptophan prenyltransferases were characterized biochemically. Therefore, biochemical characterization of new tryptophan prenyltransferases from bacteria will contribute to our understanding on these enzymes from different origins.

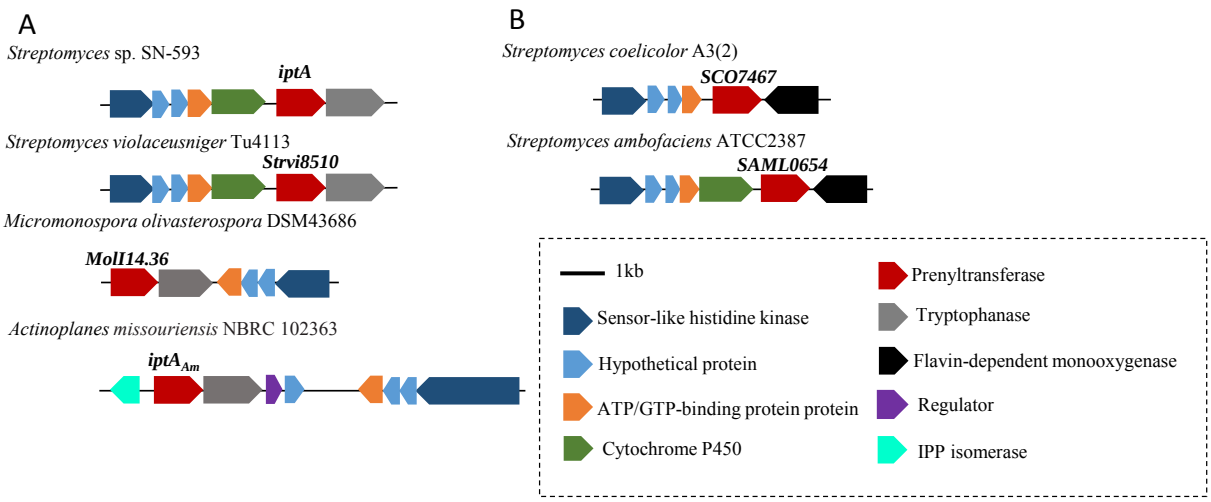

Fig. 3.1 Gene clusters containing selected tryptophan prenyltransferase genes from actinomycetes (modified from Ozaki *et al.,* 2013 and Satou *et al.,* 2014).

The identified bacterial tryptophan prenyltransferases involved in the biosynthesis of prenylated indole derivatives are all from actinomycetes. Two gene clusters containing *iptA* for a 6-DMATS and *SCO7467* for a 5-DMATS (5-DMATS$_{Sc}$) were identified in the biosynthesis of 6- DMAI-3-carbaldehyde in *Streptomyces* sp. SN-593 and 5-DMAI-3-acetonitrile in *S. coelicolor* A3(2), respectively (Ozaki *et al.,* 2013; Subramanian *et al.,* 2012; Takahashi *et al.,* 2010). BLAST searching with these two enzymes led to identification of several homologues

in bacterial genomes, including SAML0654 from *S. ambofaciens* ATCC2387, Strvi8510 from *S. violaceusniger* Tü 4113 and MolI14.36 from *M. olivasterospora* (Fig. 3.1) (Ozaki *et al.*, 2013; Subramanian *et al.*, 2012; Takahashi *et al.*, 2010).

3.1.1. Identification and characterization of the two 6-DMATSs SAML0654 and Strvi8510 from *Streptomyces*

The deduced proteins of SAML0654 and Strvi8510 with 375 (39.9 kDa) and 380 (40.9 kDa) amino acids, respectively, share a sequence identity of 63 % on the amino acid level. The coding gene *Strvi8510* was found in a gene cluster accompanied by a tryptophanase gene (type A gene cluster). Such gene clusters consist of four further genes encoding for a sensor-like histidine kinase, two hypothetical proteins and an ATP/GTP-binding protein (Satou *et al.*, 2014) (Fig. 3.1). Type A gene clusters with corresponding prenyltransferase genes have been identified in several actinomycetes, *e.g. Streptomyces* sp. SN-593 with the gene for IptA, *A. missouriensis* with $IptA_{Am}$, *Streptomyces* sp MBT28 with IsaA and *M. olivasterospora* with MolI14.36, which was part of the present study (Ozaki *et al.*, 2013; Satou *et al.*, 2014; Wu *et al.*, 2015). In comparison, the tryptophan prenyltransferase gene *SAML0654* is associated with genes coding for a flavin-dependent monooxygenase and a cytochrome P450. This gene cluster belongs to so-called type B gene clusters similar to that with SCO7467 (5-$DMATS_{Sc}$) from *S. coelicolor* (Fig. 3.1).

For heterologous expression in *E. coli*, *SAML0654* and *Strvi8510* were cloned into the expression vector pQE60 (pJW12) and $pHIS_8$ (pJW18), respectively. The recombinant His-tagged proteins were purified to near homogeneity and analyzed by SDS-PAGE. Monomeric characteristics were suggested for 6-$DMATS_{Sa}$ with a molecular mass at 36.9 kDa and for 6-$DMATS_{Sv}$ with a molecular mass at 46.0 kDa determined by size exclusion chromatography.

Evaluation of the respective enzyme assays on HPLC revealed a high flexibility toward indole derivatives for both enzymes with almost similar conversion yields. Structure elucidation of the isolated enzyme products led to identification of SAML0654 and Strvi8510 as *C6*-prenylating enzymes referred to as 6-$DMATS_{Sa}$ and 6-$DMATS_{Sv}$, respectively. These results were somewhat surprising due to the higher sequence identity of SAML0654 to 5-$DMATS_{Sc}$ (75 %) than to the 6-DMATS IptA (60 %). Therefore, it provided a good example that the function of enzymes cannot be predicted with accuracy by protein sequence alignments and thus illustrates the necessity of experimental proof. Their functions as L-tryptophan prenyltransferase were

further confirmed by determination of the kinetic parameters. Detailed biochemical investigations of the two 6-DMATSs and especially of 6-DMATS$_{Sa}$ revealed several interesting features for tryptophan prenyltransferases (Fig. 3.2). For instance, these enzymes show a high promiscuity not only toward the prenyl acceptor, as characteristic feature of most DMATS enzymes, but also toward the prenyl donor. So far, the most of the known tryptophan prenyltransferases utilize solely DMAPP as prenyl donor (Ozaki *et al.,* 2013; Schultz *et al.,* 2008; Subramanian *et al.,* 2012; Takahashi *et al.,* 2010; Yu & Li 2012). 6-DMATS$_{Sa}$ and 6-DMATS$_{Sv}$ are the first examples that also accept GPP as prenyl donor with the same regiospecific prenylation as for DMAPP.

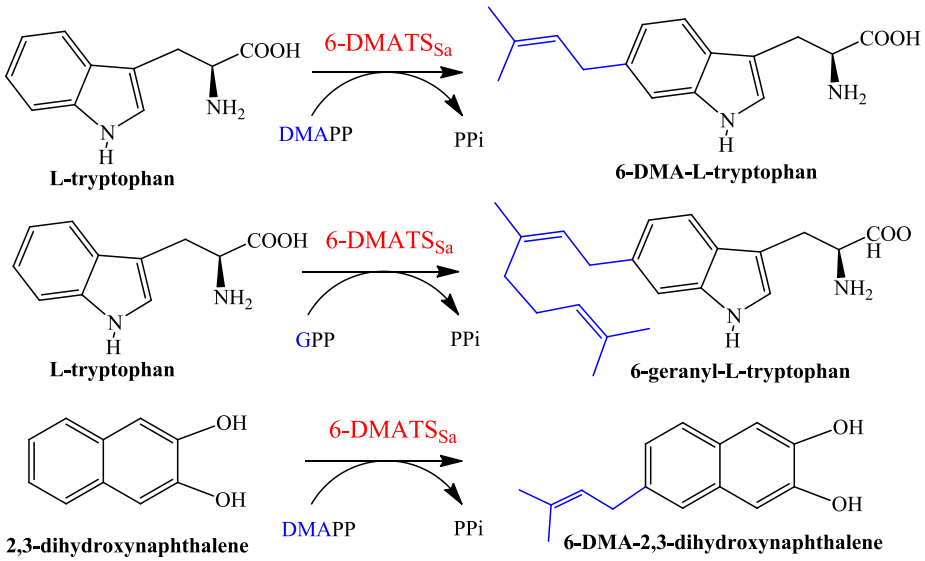

Fig. 3.2 Substrate specificity and regioselectivity of 6-DMATS$_{Sa}$. 6-DMATS$_{Sa}$ catalyzes a regiospecific *C6*-prenylation of tryptophan and derivatives in the presence of DMAPP and GPP. Dihydroxynaphthalenes are prenylated at the unsubstituted ring by 6-DMATS$_{Sa}$ (modified graphical content of Winkelblech *et al.*, 2014).

Moreover, their broad substrate specificity was demonstrated by the acceptance of several hydroxynaphthalenes, which are the natural substrates of some prenyltransferases of the CloQ/NphB group. Several DMATSs from fungi including FgaPT2 and 7-DMATS also catalyze the prenylation of several hydroxynaphthalenes (Yu *et al.,* 2011), but no report for an acceptance of hydroxynaphthalenes by bacterial tryptophan prenyltransferases was found prior to this study. The substrate preferences of 6-DMATS$_{Sa}$ and 6-DMATS$_{Sv}$ toward the naphthalene derivatives differ from those of fungal indole prenyltransferases. For example, 1,3- and 2,3-hydroxynaphthalenes were better accepted by 6-DMATS$_{Sa}$, while 1-naphthol was a better substrate for fungal DMATSs. More interestingly, 1,3- and 2,3-dihydroxynaphthalenes were

prenylated at their unsubstituted benzene rings, which has not been reported previously for an enzymatic prenylation (Fig. 3.2).

In summary, two new bacterial 6-DMATS were identified and characterized. Their special characteristics including the broad flexibility toward prenyl donor and acceptor as well as their high regioselectivity makes them good candidates for chemoenzymatic synthesis. Furthermore, crystal structures of these enzymes would provide new insights for understanding the reaction mechanism of bacterial prenyltransferases.

For details of this work, please see the publication (section 4.1)

Winkelblech, J. & Li, S.-M. (2014). Biochemical investigations of two 6-DMATS enzymes from *Streptomyces* revealing novel features of L-tryptophan prenyltransferases. *Chembiochem.* **15**, 1030-1039.

3.1.2. Biochemical investigations on MolI14.36 from *Micromonospora olivasterospora*

After identification of 6-DMATS$_{Sa}$ and 6-DMATS$_{Sv}$, the putative homologous bacterial tryptophan prenyltransferase MolI14.36 from *M. olivasterospora* was successfully overproduced in *E. coli*. MolI14.36 shares a sequence identity of 68 % with IptA$_{Am}$ from *A. missouriensis* (Satou *et al.,* 2014), 44 % with IptA from *Streptomyces* sp. SN-593 (Takahashi *et al.,* 2010), 42 % with 6-DMATS$_{Sv}$ from *S. violaceusniger* (Winkelblech & Li 2014), and 38 % with 6-DMATS$_{Sa}$ from *S. ambofaciens* (Winkelblech & Li 2014) (Table 1). Due to these differences in the amino acid sequences we proved the function of MolI14.36 by biochemical investigations in order to expand our knowledge on tryptophan prenyltransferases with bacterial origin. Similar to *Strvi8510* and several other genes of bacterial tryptophan prenyltransferases, the coding gene *MolI14.36* belong to type A gene cluster (Fig. 3.1).

The corresponding coding gene sequence was cloned into pHIS$_8$ resulting in the expression construct pJW32. The His$_8$-tagged protein with a calculated molecular mass of 43.5 kDa was purified to near homogeneity with a protein yield of 16 mg per liter of culture for comprehensive investigations. The molecular mass of the recombinant protein was determined by size exclusion chromatography to be 46 kDa as in the case of 6-DMATS$_{Sv}$, indicating that MolI14.36 presumably acts as a monomer.

Table 1 Comparison of protein identities of selected bacterial tryptophan prenyltransferases.

	SAML0654 (6-DMATS$_{Sa}$)	Strvi8510 (6-DMATS$_{Sv}$)	MolI14.36 (6-DMATS$_{Mo}$)	IptA	AMIS_22580 (IptA$_{Am}$)
Strvi8510 (6-DMATS$_{Sv}$)	63 %				
MolI14.36 (6-DMATS$_{Mo}$)	38 %	42 %			
IptA	60 %	64 %	44 %		
AMIS_22580 (IptA$_{Am}$)	38 %	39 %	68 %	39 %	
SCO7467 (5-DMATS$_{Sc}$)	75 %	60 %	40 %	59 %	38 %

MolI14.36 was assayed with L-tryptophan, its enantiomer and eight analogs thereof, which were all well accepted with conversion yields of higher than 15 %. These results demonstrate its high substrate flexibility for indole derivatives. Structure elucidation of the isolated enzyme products by MS and NMR analyses revealed that MolI14.36 catalyzes a unique or predominant *C6*-prenylation at the indole ring of tryptophan and analogs. As in the case of IptA and 6-DMATS$_{Sa}$

a switch of the prenylation site to C-7 was detected for 6-methyl-DL-tryptophan which is blocked at position C-6 (Takahashi *et al.,* 2010; Winkelblech & Li 2014). In conclusion, MolI14.36 was identified as a L-tryptophan *C6*-prenyltransferase and therefore termed 6-DMATS$_{Mo}$. Moreover, the enzyme also accepted several cyclic dipeptides as well as naphthalene derivatives. Thereby the preferences of the orthologues 6-DMATS$_{Mo}$, 6-DMATS$_{Sa}$, and 6-DMATS$_{Sv}$ differ from each other (Fig 3.3). In addition, GPP was also used as a prenyl donor by 6-DMATS$_{Mo}$, which is similar to the two other 6-DMATSs. Investigations on biochemical properties revealed that metal ions are not essential for the enzyme activity as observed for other members of the DMATS superfamily (Takahashi *et al.,* 2010; Winkelblech & Li 2014; Yu *et al.,* 2012).

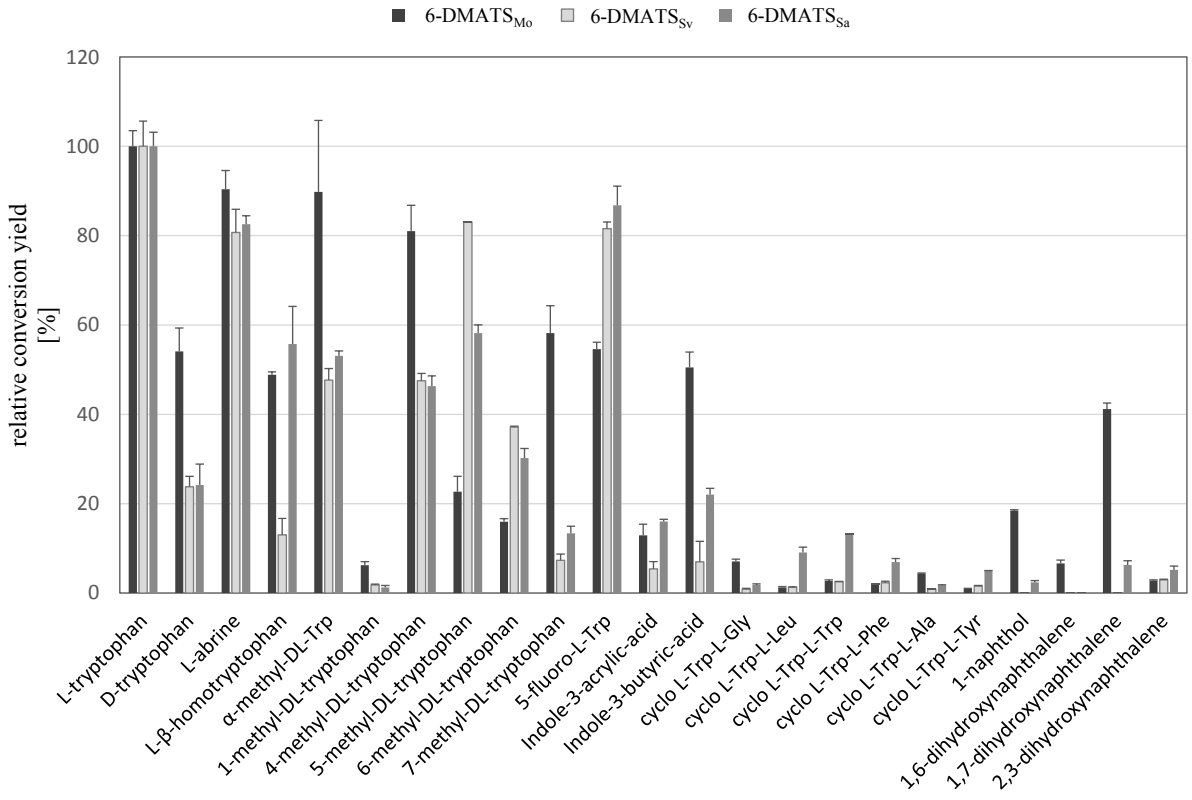

Fig. 3.3 Comparison of the substrate preferences of the three 6-DMATS enzymes 6-DMATS$_{Mo}$, 6-DMATS$_{Sv}$, and 6-DMATS$_{Sa}$. The conversion yields toward several indole derivatives, cyclic dipeptides as well naphthalene derivatives were determined relative to L-tryptophan.

The high affinities to L-tryptophan and DMAPP demonstrated by kinetic parameters are in the same range of those of other tryptophan prenyltransferases (Ozaki *et al.,* 2013; Takahashi *et al.,* 2010; Unsöld & Li 2005; Winkelblech *et al.,* 2015b; Yu *et al.,* 2012), justifying its function as a tryptophan prenyltransferase. The K_M value for L-tryptophan is nearly the same as that of 6-DMATS$_{Sa}$, but the calculated k_{cat} value of 6-DMATS$_{Mo}$ is much smaller than those of other

DMATS enzymes. Comparison of the enzyme activities for tryptophan and analogs revealed that the newly identified 6-DMATS$_{Mo}$ showed clearly different preferences from those of 6-DMATS$_{Sa}$ and 6-DMATS$_{Sv}$. Therefore, these enzymes can be complementarily used as biocatalysts for specific prenylation of a given tryptophan analog. Interestingly, unusually high relative activity of approximately 50 % of that of L-tryptophan was found toward D-tryptophan. To the best of our knowledge, such high conversion for D-tryptophan has not been reported prior to this study. In contrast, relative activities of less than 25 % were observed for 6-DMATS$_{Sa}$ and 6-DMATS$_{Sv}$ with D-tryptophan, respectively. These values are already relative high in comparison to other DMATS enzymes (Kremer & Li 2008; Steffan *et al.,* 2007; Winkelblech & Li 2014).

The natural function of MolI14.36 is unknown and no prenylated aromatic derivatives have been isolated from the fortimicin producer *M. olivasterospora.* Due to the high sequence similarity between 6-DMATS$_{Mo}$ and IptA$_{Am}$ and genes in their neighbourhood, it can be speculated that both enzymes are involved in a very similar or the same biosynthetic pathway. IptA$_{Am}$ was proven to be responsible for the formation of 6-dimethylallyltryptophan, which was converted to 6-DMAI by the tryptophanase TnaA$_{Am}$. 6-DMAI then serves as precursor for the biosynthesis of 3-hydroxy-6-DMAIN-2-one (Satou *et al.,* 2014). Together with 6-DMATS$_{Mo}$, five 6-DMATSs, one 5-DMATS, and recently one 7-DMATS have been identified from actinomycetes (Winkelblech *et al.,* 2015a; Wu *et al.,* 2015). The increased number of known 6-DMATS enzymes strengths the importance of *C6*-prenylated indole derivatives in actinomycetes, which should be explored in the future. In comparison, 6-DMATS enzyme was reported neither for fungi nor plant, although several indole derivatives with a dimethylallyl moiety at C-6 have been identified in these organisms (Achenbach *et al.,* 1995; Fredenhagen *et al.,* 1997).

For details of this work, please see the publication (section 4.3)

Winkelblech, J., Xie, X., Li, S.-M. (2016). Characterisation of 6-DMATS$_{Mo}$ from *Micromonospora olivasterospora* leading to identification of divergence in enantioselectivity, regioselectivity and multiple prenylation of tryptophan prenyltransferases. *Org. Biomol. Chem.* DOI: 10.1039/C6OB01803C.

3.2. Investigations on the acceptance of unnatural allyl and benzyl diphosphates by tryptophan *C5*-, *C*6-, and *C7*-prenylating enzymes

Due to the importance of bioactive prenylated secondary metabolites for medicinal research and drug development (Clardy & Walsh 2004; Newman & Cragg 2012), research on DMATSs has been enhanced regarding their potential application as biocatalysts for production of such compounds. Their remarkable broad substrate specificity and high regioselectivity toward aromatic prenyl acceptors provide an useful tool for increasing the diversity of desired prenylated products. DMAPP is the mostly used prenyl donor for the prenylation of a wide range of substrates catalyzed by DMATSs. Their potential usage in chemoenzymatic synthesis could be strongly widen by the acceptance of various donors. Therefore, investigations on the acceptance of different natural and also unnatural donors have been focussed in the recent years. Previous studies by Liebhold *et al.* demonstrated that the unnatural DMAPP analogs MAPP and 2-pentenyl-PP were accepted by tryptophan *C4*-, *C5*- as well as cyclic dipeptide *C2*- and *C3*-prenyltransferases (Liebhold *et al.,* 2012; Liebhold & Li 2013). Furthermore, the more space-demanding benzyl-PP was accepted by the tryptophan *C4*-prenyltransferase FgaPT2 (Liebhold & Li 2013). In the presence of these unnatural donors, the alkylation position of the enzyme products could be changed compared to the natural donor DMAPP. The finding of the high flexibility of 6-DMATS$_{Sa}$ and 6-DMATS$_{Sv}$ toward their prenyl donor and acceptor makes them interesting candidates for further investigations on the acceptance of unnatural alkyl or benzyl donors (Winkelblech & Li 2014). With identification of these two bacterial *C6*-prenyltransferases as well as the L-tyrosine prenyltransferase TyrPT with a tryptophan *C7*-prenyltransferase activity, we were able to expand the previous studies which were limited to the fungal *C4*- and *C5*-prenylating enzymes. Moreover, the studies on tryptophan alkylation or benzylation by 5-DMATS$_{Sc}$ from *S. coelicolor* completed the elucidation on the distinct behaviors of bacterial tryptophan prenyltransferases.

The recombinant proteins of 5-DMATS, 5-DMATS$_{Sc}$, 6-DMATS$_{Sa}$, 6-DMATS$_{Sv}$ and TyrPT were overproduced in *E. coli*, purified, and assayed with L-tryptophan and the aforementioned unnatural DMAPP analogs. MAPP, 2-pentenyl-PP as well as benzyl-PP were accepted by all the tested enzymes with different relative activities. More importantly, the selected enzymes showed different regioselectivities toward the unnatural donors. The unique enzyme products of 6-DMATS$_{Sa}$ and 6-DMATS$_{Sv}$ were identified as *C6*-alkylated or benzylated L-tryptophan by NMR and MS analyses. These findings are consistent with the previously reported data for GPP (see Chapter 3.1.1) and demonstrated that the two 6-DMATSs catalyze a very regiospecific reaction independent on the used donors. In comparison, the regioselectivity of 5-DMATS and

FgaPT2 was partially or completely shifted in the presence of the DMAPP analogs (Liebhold *et al.,* 2012; Liebhold & Li 2013). In the case of the *C7*-prenylating enzyme TyrPT, *C6*-alkylated or benzylated L-tryptophan was found as main or one of two predominant products. To compare alkylation or benzylation reactions catalyzed by bacterial and fungal enzymes, the regioselectivity of 5-DMATS and 5-DMATS$_{Sc}$ were investigated. For 5-DMATS, the previous data were reproduced with MAPP and 2-pentenyl-PP, which revealed a shift of the prenylation from C-5 to C-6 of the indole ring (Liebhold *et al.,* 2012). *C6*-alkylated tryptophan was the sole product of 2-pentenyl-PP and the main product of MAPP. In the assays with benzyl-PP, *C5*- and *C6*-benzylated products were detected, with the latter one as main product, Similar to the TyrPT reactions with 2-pentenyl-PP and benzyl-PP, 5-DMATS$_{Sc}$ produced *C5*-, *C6*- and *C7*-alkylated or benzylated derivatives, confirming the preference for an alkylation at C-6 of the indole ring in the presence of the unnatural DMAPP analogs. Furthermore, the reduced regioselectivity of 5-DMATS$_{Sc}$ disproved the bacterial origin as reason for a high regioselectivity as observed for the 6-DMATSs.

To explain the observed phenomenon of divergence in regioselectivity, a homology model for 5-DMATS was generated, using the structure of FgaPT2 as template. Docking studies and MD simulations with the 5-DMATS homology model and DMAPP, MAPP or 2-pentenyl-PP resulted in a distance-based explanation for the observed regioselectivities. Therefore, the donor-acceptor distance was speculated as major factor for the regioselectivity of the prenyltransferases. MD simulation with benzyl-PP was not successful, because it became unstable.

In conclusion, we completed the study on the acceptance of unnatural DMAPP analogs by comprehensive investigations on the regioselectivity of two *C5*-prenyltransferases 5-DMATS and 5-DMATS$_{Sc}$, two *C6*-prenyltransferases 6-DMATS$_{Sa}$ and 6-DMATS$_{Sv}$ as well as one *C7*-prenyltransferase TyrPT. The results demonstrated a clear preference of the five enzymes for alkylation or benzylation at C-6 of the indole ring in the presence of unnatural DMAPP analogs (Fig. 3.4).

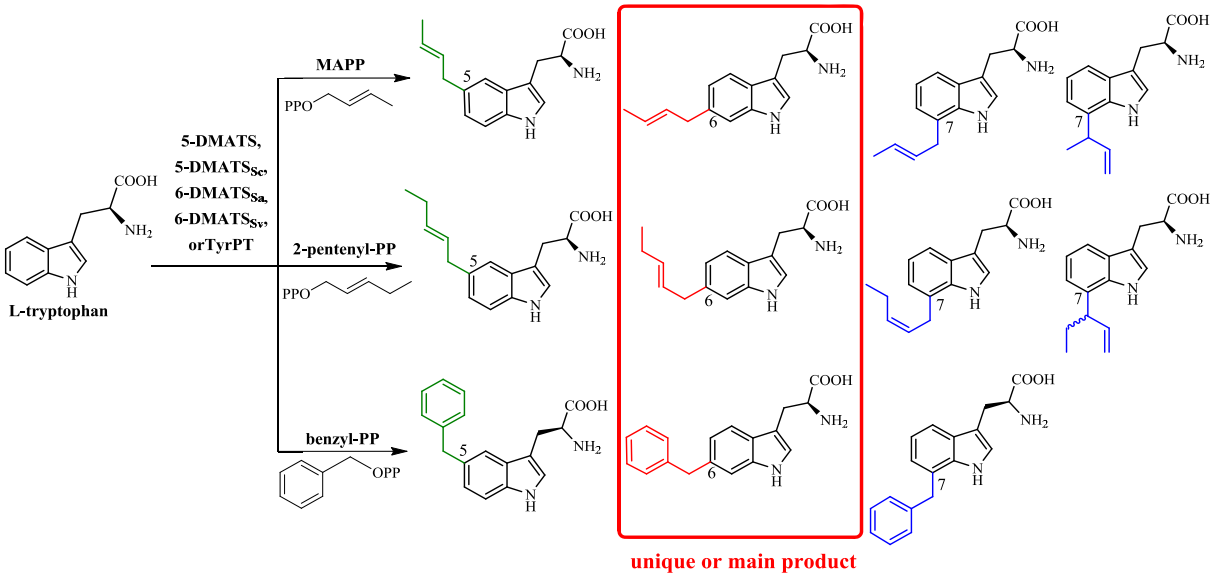

Fig. 3.4 Tryptophan *C5*-, *C6*- and *C7*-prenylating enzymes preffered *C6*-prenylation of the indole ring in the presence of the indicated unnatural dimethylallyl diphosphate analogs.

This study provides new opportunities for the production of new alkylated or even benzylated indole derivatives. New insights into the substrate binding sites of such enzymes and a more accurate explanation for their differences in regioselectivity could be obtained by further analyses on protein structures in complex with unnatural DMAPP analogs.

This project was a cooperation with Dr. Mike Liebhold. Homology modeling, docking experiments, and MD simulation were done in cooperation with Jakub Gunera and Prof. Dr. Peter Kolb from Philipps-Universität in Marburg.

For details of this work, please see the publication (section 4.2)

Winkelblech, J., Liebhold, M., Gunera, J., Xie, X., Kolb, P. & Li, S.-M. (2015). Tryptophan *C5*-, *C6*- and *C7*-prenylating enzymes displaying a preference for C-6 of the indole ring in the presence of unnatural dimethylallyl diphosphate analogs. *Adv. Synth. Catal.* **357**, 975-98.

3.3. Investigation on DMATSs regarding their substrate specificity and regioselectivity for mono- and diprenylation of enantiomers of tryptophan and methylated derivatives thereof

Chiral molecules such as amino acids can occur as L- and D-isomers and fulfill essential roles in biological and chemical processes of life (Shimada & Ozaki 2012). In nature, the occurrence of α-amino acids is strongly predominated by the L-enantiomer, but the less abundant D-form is also widely spread in nature and play an important role in biological systems (Gao *et al.,* 2015). For instance, D-amino acids provide protease resistance in cell walls of bacteria, function as neurotransmitter in nervous system of animals or contained fungal and bacterial peptide antibiotics (Cava *et al.,* 2011; D'Aniello *et al.,* 2011; Gao *et al.,* 2015; Strauch *et al.,* 2015). Such compounds are also interesting candidates for diverse industrial applications. For example, D-amino acids were used in pharmaceutical industry for semi-synthetic antibiotics or as potential agents for treatment of several disease such as Alzheimer's diseases, HIV and cancers (Gao *et al.,* 2015; Kumar & Sim 2014; Veine *et al.,* 2014; Welch *et al.,* 2007). In this thesis, the amino acid tryptophan and derivatives thereof play a significant role. L-tryptophan serves a key precursor for various secondary metabolites including prenylated indole derivatives (Li 2010).

The transfer reaction of the isoprenoid moiety onto the aromatic substrate is catalyzed by prenyltransferases, comprising *C4*-, *C5*-, *C6*- and C7- prenyltransferases and usually improve their biological activity (Botta *et al.,* 2005a; Li 2010; Liu *et al.,* 2013b; Oya *et al.,* 2015; Winkelblech *et al.,* 2015a; Wollinsky *et al.,* 2012). In previous reports on substrate specificity of DMATSs, a much lower enzyme activity toward D-tryptophan than to L-tryptophan were reported (Fan *et al.,* 2015b). More substrate flexibility toward the D-form was observed for 6-$DMATS_{Sa}$ and 6-$DMATS_{Sv}$ and a remarkably high acceptance was found for the recently identified 6-$DMATS_{Mo}$. This result prompted us to carry out comparative investigation on the divergence of microbial DMATSs regarding their preferences and regioselectivities for enantiomers. Therefore, we evaluated the acceptance of L- and D-tryptophan and their methylated derivatives 5-, 6-, and 7-methyltryptophan by seven DMATSs. The corresponding enzyme assays with FgaPT2, 5-DMATS, and 7-DMATS from fungi and 5-$DMATS_{Sc,}$ 6-$DMATS_{Sa}$, 6-$DMATS_{Sv}$, and 6-$DMATS_{Mo}$ from bacteria were elucidated by HPLC on a chiral column as well as by LC-MS analysis. The results displayed different preferences for the tested recombinant enzymes toward L- and D-enantiomers of tryptophan and methylated derivatives.

In most cases, the L-form of the tested substrates was accepted with significantly higher conversion yields than the D-form by the DMATSs. In contrast, 5-DMATS$_{Sc}$ and 6-DMATS$_{Mo}$ revealed a very high flexible enantioselectivity. Both enzymes accepted all of the tested D-enantiomers. More interestingly 5-DMATS$_{Sc}$ and 6-DMATS$_{Mo}$ accepted the D-enantiomer of 5-methyltryptophan much better than the respective L-enantiomer, confirmed by determination of the kinetic parameters. In the presence of the racemate conversion yields of the D-enantiomer were reduced or even completely disabled. Corresponding kinetic studies with the enantiomers of 5-methyltryptophan explained the repression of the D-enantiomer reaction by the high affinities toward the L-enantiomers. However, the strong inhibition of the D-tryptophan reaction in the presence of the racemate cannot be attributed solely to the high affinity to the L-form, due to the fact that the L-form was almost completely converted at the end of incubation. Therefore, we speculated that the products of L-tryptophan could also function as inhibitors.

As already mentioned, the tested enzymes all catalyze a highly regiospecific prenylation on L-tryptophan by using DMAPP as donor. In contrast, the L-tryptophan *C4*-prenyltransferase FgaPT2 and *C5*-prenyltransferase 5-DMATS$_{Sc}$ displayed a reduced regioselectivity toward D-tryptophan with *C5*- and *C6*-prenylated derivatives as main products, respectively. Clearly different regioselectivities were also identified for enantiomers of 5-methyltryptophan with FgaPT2, 5-DMATS$_{Sc}$ and 7-DMATS.

An additional interesting output of this study is the capability for diprenylation observed for the bacterial 5-DMATS$_{Sc}$. For L-tryptophan, the two diprenylated products 5,6- and 5,7-di-dimethylallyl-L-tryptophan were identified in a ratio of 1:1 by NMR analysis. In comparison, 5,6-di-dimethylallyl-D-tryptophan was detected as main diprenylated product in the reaction mixture with D-tryptophan. Diprenylation of tryptophan by 5-DMATS$_{Sc}$ was the first example for a tryptophan prenyltransferase, which catalyzes two successive prenylation steps. The presented results pointed out the different biochemical behaviors of the tryptophan prenyltransferases in many respects and therefore expand significantly our knowledge in this field. For instance, this was the first comprehensive study on enantioselectivity of prenyltransferases which supplied interestingly new features.

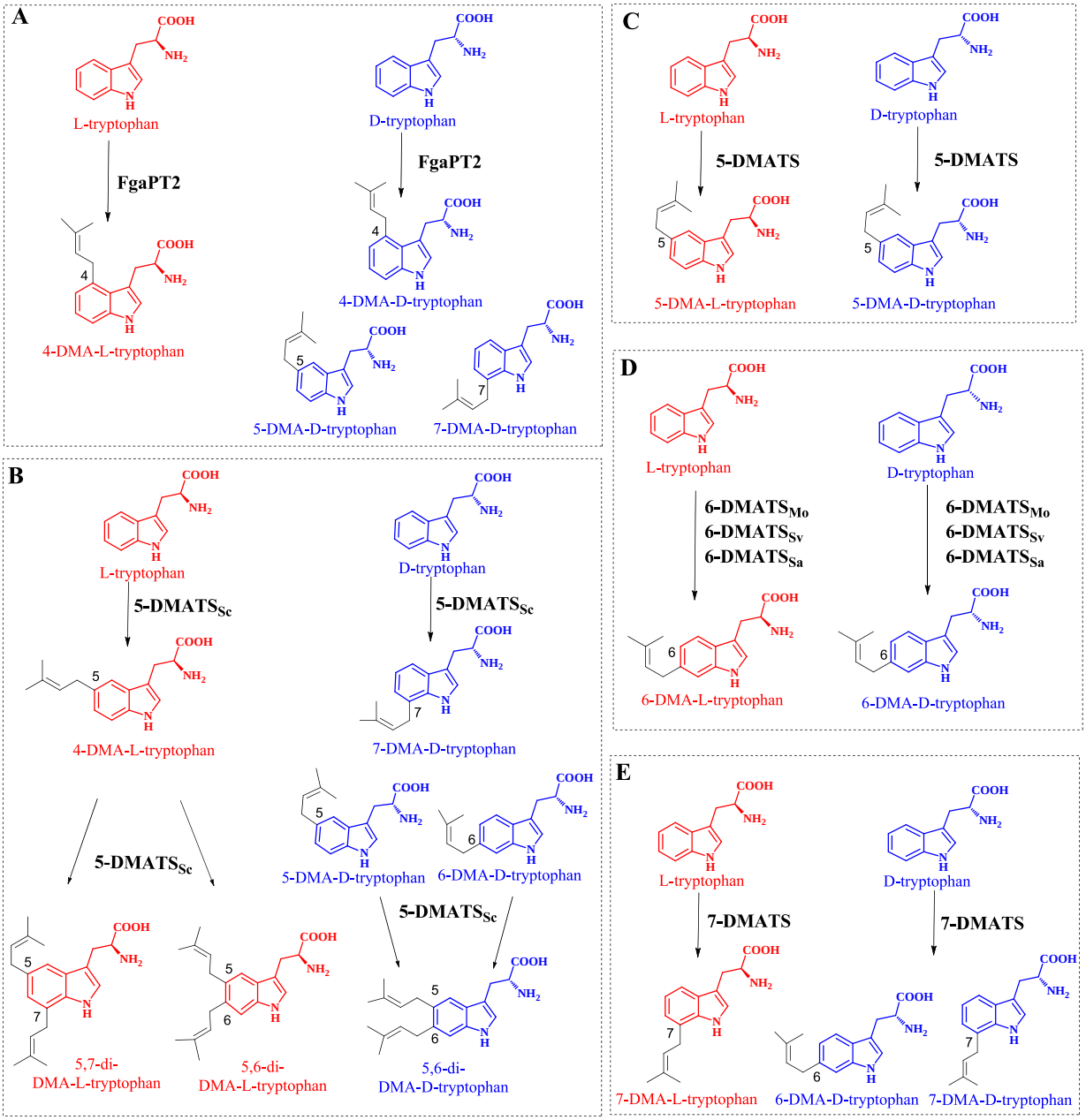

Fig. 3.5 Microbial tryptophan *C4*-,*C5*-, *C6*- and *C7*-prenyltransferases catalyze prenylation of L- and D-tryptophan (A-E). FgaPT2 (A), 5-DMATS$_{Sc}$ (B), and 5-DMATS (C) differ in their reactions toward L- (red) and D- enantiomer (blue). 6-DMATSs (D) and 7-DMATS (E) catalyze the same reaction with both enantiomers.

Moreover D-amino acids and also monosubstituted tryptophan derivatives are of great medicinal value. For instance, D-Phe or D-Pro derivatives can be used for treatment of several disease such as Alzheimer's disease, diabetes mellitus, familial amyloid polyneuropathy, scrapie, and Kreuzfeld-Jacob disease or depression and Parkinson's disease, respectively (Gao *et al.,* 2015; Heller 1982). Furthermore, the monosubstituted tryptophan derivatives 6-chlorotryptophan, 1-methyl-L- and 1-methyl-D-tryptophan were found as inhibitors of indoleamine 2,3-dioxygenase, which is involved in several disorders such as cataracts,

Alzheimer's disease and cancer (Di *et al.,* 2010; Fukushima *et al.,* 2015; Jia *et al.,* 2008; Saito *et al.,* 1993; Tanaka *et al.,* 2013). Therefore the presented biochemical properties of these enzymes make them potential biocatalyst in chemical synthesis for prenylated indole derivatives, which represent promising candidates for drug development. Testing the bioactivity of these compounds is intended in near future.

For details of this work, please see the publication (section 4.3)

Winkelblech, J., Xie, X., Li, S.-M. (2016). Characterisation of 6-DMATS$_{Mo}$ from *Micromonospora olivasterospora* leading to identification of divergence in enantioselectivity, regioselectivity and multiple prenylation of tryptophan prenyltransferases. *Org. Biomol. Chem.* DOI: 10.1039/C6OB01803C.

4. Publications

4.1. Biochemical investigations of two 6-DMATS enzymes from *Streptomyces* revealing novel features of L-tryptophan prenyltransferases

DOI: 10.1002/cbic.201400046

Biochemical Investigations of Two 6-DMATS Enzymes from *Streptomyces* Reveal New Features of L-Tryptophan Prenyltransferases

Julia Winkelblech[a, b] and Shu-Ming Li*[a, b]

Two putative prenyltransferase genes, *SAML0654* and *Strvi8510*, were identified in *Streptomyces ambofaciens* and *Streptomyces violaceusniger*, respectively. Their deduced products share 63% sequence identity. Biochemical investigations with recombinant proteins demonstrated that L-tryptophan and derivatives, including D-tryptophan, 4-, 5-, 6- and 7-methyl-DL-tryptophan, were well accepted by both enzymes in the presence of DMAPP. Structural elucidation of the isolated products revealed regiospecific prenylation at C-6 of the indole ring and proved unequivocally the identification of two very similar 6-dimethylallyltryptophan synthases (6-DMATS). Detailed biochemical investigations with SAML0654 proved L-tryptophan to be the best substrate (K_m 18 μM, turnover 0.3 s^{-1}). Incubation with different prenyl donors showed that they also accepted GPP and catalyzed the same specific prenylation. Utilizing GPP as a prenyl donor has not been reported for tryptophan prenyltransferases previously. Both enzymes also catalyzed prenylation of some hydroxynaphthalenes; this has not previously been described for bacterial indole prenyltransferases. Interestingly, SAML0654 transferred prenyl moieties onto the unsubstituted ring of hydroxynaphthalenes.

Introduction

Natural products and their derivatives are important resources for drug discovery and development.[1] Prenylated aromatic compounds, including prenylated indole derivatives, represent a large group of secondary metabolites and are widely distributed across bacteria, fungi, and plants. Prenylation (transfer reactions of nxC5-units) contributes largely to structural diversity and often significantly increases the biological and pharmacological activity of the resulting compounds. These prenylation reactions and the responsible enzymes are of interest not only to biologists but also to scientists from other disciplines.[2–6] The transfer reactions of prenyl moieties from prenyl donors (usually dimethylallyl diphosphate, DMAPP) onto indole nuclei are catalyzed in nature by indole prenyltransferases. A large number of such enzymes of the dimethylallyltryptophan synthase (DMATS) superfamily have been identified in recent years in bacteria and fungi, and these have been studied biochemically.[7–10] They mainly accept tryptophan and tryptophan-containing cyclic dipeptides as substrates and catalyze regiospecific prenylation at the indole ring.[8] Three DMATS enzymes that use L-tryptophan and DMAPP as substrates have been identified in *Aspergillus fumigatus* and *Aspergillus clavatus*: FgaPT2, 5-DMATS, and 7-DMATS. They were shown to catalyze prenylation of L-tryptophan at C-4, C-5, and C-7, respectively.[11–13] Three bacterial DMATSs have shown prenylation at positions N1, C-5, and C-6: CymD (*Salinispora arenicola*), SCO7467 (*Streptomyces coelicolor*), and IptA (*Streptomyces* sp. SN-593), respectively.[7,9,10,14] Fungal DMATS enzymes share very little sequence similarity with those from bacteria.

Similarly to most known indole prenyltransferases, FgaPT2, 5-DMATS, IptA, and 7-DMATS exhibit high specificity for their prenyl donor DMAPP and do not accept geranyl diphosphate (GPP) as a substrate.[9,11,13,15] In contrast, they show high promiscuity for the aromatic substrate and accept a large number of tryptophan derivatives.[9,11,16,17] FgaPT2 and 7-DMATS even used hydroxynaphthalenes as prenyl acceptors;[18] these are natural substrates of prenyltransferases of the CloQ/NphB group, from both bacteria and fungi.[19,20] The acceptance of hydroxynaphthalenes by FgaPT2 and 7-DMATS encouraged us to compare the biochemical properties and substrate specificities of DMATSs from bacteria and fungi. BLAST searching with the 6-DMATS IptA from *Streptomyces* sp. SN-593 and the 5-DMATS SCO7467 from *S. coelicolor* revealed several homologues in bacterial genomes, including SAML0654 from *Streptomyces ambofaciens* ATCC2387[7,21] and Strvi8510 from *Streptomyces violaceusniger* Tü 4113. SAML0654 shares 75% amino acid sequence identity with SCO7467, 60% with IptA, and 63% with Strvi8510, thus it was speculated that SAML0654 functions as a 5-DMATS. Strvi8510 showed 60 and 64% identity with SCO7467 and IptA, respectively, so the specific reaction catalyzed by this enzyme could not be predicted from sequence analysis. Here, we report the cloning and expression of SAML0654 and Strvi8510 and their identification as 6-DMATSs.

[a] J. Winkelblech, Prof. Dr. S.-M. Li
Philipps-Universität Marburg
Institut für Pharmazeutische Biologie und Biotechnologie
Deutschhausstrasse 17A, 35037 Marburg (Germany)
E-mail: shuming.li@staff.uni-marburg.de

[b] J. Winkelblech, Prof. Dr. S.-M. Li
Zentrum für Synthetische Mikrobiologie, Philipps-Universität Marburg
Hans-Meerwein-Strasse, 35032 Marburg (Germany)

Supporting information for this article is available on the WWW under http://dx.doi.org/10.1002/cbic.201400046.

Biochemical characterization of the recombinant proteins revealed several new features for the tryptophan prenyltransferases in terms of substrate specificity towards both prenyl donor and acceptor as well as the unusual prenylation position of hydroxynaphthalenes.

Results

Sequence analysis

SAML0654 is a member of a small gene cluster (type B) found in several actinomycetes strains, for example, *S. coelicolor* and *Streptomyces lividans*; it contains genes for a prenyltransferase and for a flavin-dependent monooxygenase.[7,9] Heterologous expression of the prenyltransferase gene SCO7467 and the flavin-dependent monooxygenase gene SCO7468 from *S. coelicolor* A3(2) in *S. lividans* TK23 resulted in the formation of 5-dimethylallylindole-3-acetonitrile.[7] It was speculated that similar clusters in other strains including *S. ambofaciens* would also be responsible for the biosynthesis of 5-dimethylallylindole-3-acetonitrile.[7] In comparison to those in *S. coelicolor* A3(2) and *S. lividans*, the *SAML0654*-containing gene cluster in *S. ambofaciens* has an additional gene coding for a cytochrome P450, but its end product is unknown.[7] *Strvi8510* from *S. violaceusniger* and *IptA* from *Streptomyces* sp. SN-593 belong to type A gene clusters found in different actinomycetes.[7] Although no gene coding for a flavin-dependent monooxygenase is found in these clusters, there is a gene for tryptophanase. These clusters were speculated to be responsible for the formation of 6-dimethylallylindole-carbardehyde.[7]

The deduced product of *SAML0654* has 375 amino acids and a calculated mass of 39.9 kDa. The deduced product of *Strvi8510* has 380 amino acids and a calculated mass of 40.9 kDa.

Cloning and purification of overexpressed His-tagged SAML0654 and Strvi8510

To prove its function biochemically, *SAML0654* was amplified by PCR from genomic DNA of *S. ambofaciens* DSM40053. The PCR product (1133 bp) was cloned into pGEM-T Easy and then subcloned into vector pQE-60, thereby resulting in the expression construct pJW12. The C-terminal His_6-tagged protein was overproduced in *Escherichia coli* M15 (induction with 0.5 mM IPTG) at 30 °C for 16 h and purified by Ni-NTA affinity chromatography.

For the overproduction of Strvi8510, expression plasmid pJW13 was constructed by PCR amplifying the gene from genomic DNA of *S. violaceusniger* Tü 4113 and subcloning into pQE-70. After unsuccessful expression attempts with pJW13, the gene was again amplified, and the product (1155 bp) was cloned into pGEM-T Easy and subcloned into vector $pHIS_8$, thereby resulting in the expression construct pJW18. The N-terminal His_8-tagged protein was overproduced in *E. coli BL21 (DE3) pLysS* cells (induction with 0.5 mM IPTG) at 22 °C for 16 h and purified by Ni-NTA affinity chromatography.

SDS-PAGE analysis of the purified proteins showed significant bands just below the 45 kDa size marker (Figure S1 in the Supporting Information); these correspond well to the calculated masses of the His_6- and His_8-tagged proteins (41.1 and 43.3 kDa, respectively). Protein yields of 3.5 mg purified protein per liter of culture were obtained for both enzymes.

Acceptance of tryptophan and derivatives by SAML0654 and Strvi8510

Because of their high sequence similarity to tryptophan prenyltransferases, such as SCO7467 from *S. coelicolor* and IptA from *Streptomyces* sp. SN-593, SAML0654 and Strvi8150 were firstly assayed with L-tryptophan (**1a**) in the presence of DMAPP. HPLC analysis clearly revealed the presence of one significant product peak each in the incubation mixtures (Figure 1); this was dependent on the presence of prenyl donor and active protein (data not shown). Incubation of 1 mM **1a** with 1 mM DMAPP and 2.4 or 2.3 μM recombinant enzyme for 16 h at 37 °C achieved product yields of 59.4 and 42.2% for SAML0654 and Strvi8510, respectively.

D-tryptophan and 12 tryptophan derivatives (modifications on the indole ring and at the side chain) were assayed subsequently with the purified proteins in the presence of DMAPP. One product for each was detected in the incubation mixtures of the tested tryptophan derivatives (Table S1). HPLC analysis showed that D-tryptophan was well accepted by SAML0654 and Strvi8510, respectively (activities of 73.5 and 60.7% relative to those for L-tryptophan; Table S1). Such high relative activity for D-tryptophan by an L-tryptophan prenyltransferase has not been reported previously. The known DMATS enzymes FgaPT2, IptA, and 7-DMATS showed activities of 1.8, 4.3, and 15.5%, respectively, relative to those with L-tryptophan.[9,12,13]

High conversion yields were also achieved for tryptophan derivatives. In the incubation mixtures of SAML0654, conversion yields for L-abrine (**2a**) and L-β-homotryptophan (**3a**) were nearly the same as for L-tryptophan. Some of the incubation mixtures contained racemic substrates, and the conversion yields of each enantiomer could not be determined. However, the sum of their conversion yields was estimated from the total amount of substrates. Relative activities of 96.4, 87.9, 72.2, and 51.3% (relative to L-tryptophan) were calculated for 4- (**4a**), 5- (**5a**), 6- (**6a**), and 7-methyl-DL-tryptophan (**7a**), respectively (Figure 1, Table S1), thus proving high conversion of D-configured tryptophan derivatives. In comparison, low product formation was observed for 1-methyl-DL-tryptophan under the same conditions.

HPLC analysis of the incubation mixtures of Strvi8510 showed that it, too, accepted well the tested tryptophan derivatives. The relative activities of tryptophan derivatives with Strvi8510 were in the same range as for SAML0654 (Table S1). One significant exception was **3a** (product yield 36.7%, relative to that of **1a**; Table S1). Remarkably, for a given substrate the products of Strvi8510 and SAML0654 had the same retention times in the HPLC chromatograms, thus indicating the presence of same product. On the basis of substrate specificity towards methylated tryptophan derivatives, one would conclude

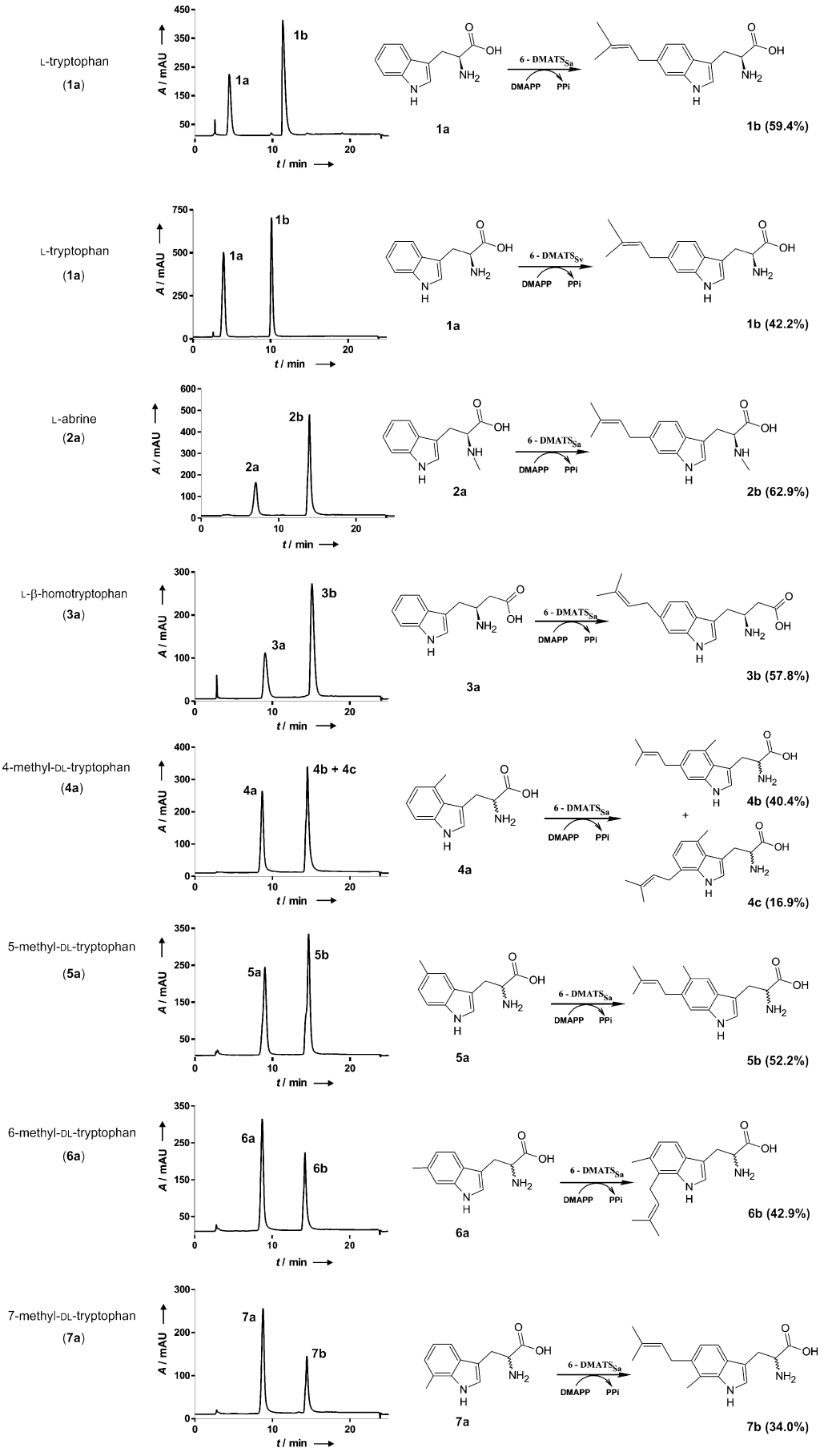

prenylation at position N1 by the tested enzymes. This conflicts with the high sequence similarity of SAML0654 and Strvi8510 with the C5-prenyltransferase SCO7467 and C6-prenyltransferase IptA.

Confirmation of the prenylation position of the enzyme products

Based on the high sequence similarity with SCO7467, we speculated that 5-DMAT could be the enzyme product of SAML0654 with L-tryptophan and DMAPP. In the HPLC chromatogram of the incubation mixture with **1a**, the enzyme peak showed nearly the same retention time as C5-prenylated tryptophan produced by 5-DMATS from *A. clavatus* (data not shown). To confirm prenylation and determine the prenylation position, seven enzyme products (**1b**–**7b**) were isolated by HPLC from incubation mixtures of SAML0654 with **1a**–**7a** in the presence of DMAPP and subjected to MS and NMR analyses (Tables S3–S4.1 and Figures S3.1–S3.7). High resolution EI-MS (HR-EI-MS) revealed molecular masses 68 Da larger than those of the respective substrates, thus verifying the attachment of one dimethylallyl moiety to the substrates. The signals in the ^{1}H NMR spectra of the isolated enzyme products at $\delta_H =$ 3.37–3.56 (d, 2H-1′), 5.09–5.35 (t sept, H-2′), 1.74–1.83 (s, 3H-4′), 1.68–1.75 ppm (s, 3H-5′) confirmed the attachment of a regular dimethylallyl moiety to a C atom.[9,11,16,17] Comparison of the NMR spectra of **1b**–**7b** with those of **1a**–**7a** revealed the disappearance of signals for one aromatic proton, thus proving the attachment of the prenyl moiety at the indole ring. The singlet at $\delta_H =$ 7.08–7.15 ppm for H-2 in all the spectra indicated that prenylation did not take place at C-2.

In the ^{1}H NMR spectra of the enzyme products of **1a**–**3a**, the ABM coupling systems of three protons with coupling constants of 8.2 and 1.2–1.5 Hz indicated attachment of a prenyl moiety to C-5 or C-6. The ^{1}H NMR spectra of **1b**–**3b** clearly differed from those of the enzyme products of 5-DMATS with **1a**–**3a** (coupling pattern and chemical shifts),[11] thus indicating prenylation at C-6. Furthermore, the ^{1}H NMR spectra of **1b** and **2b** corresponded well to those of the enzyme products of IptA with **1a** and **2a**.[9] These findings unequivocally prove C6-prenylation in **1b**–**3b** (Figure 1).

The NMR spectrum of the product peak of **4a** represents a mixture of two products, **4b** and **4c** (2.4:1). Unfortunately, **4b** and **4c** could not be separated. However, it was possible to assign the prenylation positions as C-6 in **4b** and C-7 in **4c**. The presence of three singlets for aromatic protons in the spectra of **4b** and **5b** unambiguously confirmed prenylation at C-6. The two doublets at 7.4 and 6.9 ppm with a coupling constant of 8.1 Hz in **6b** and **7b** proved prenylation at C-7 and C-6, respectively. The structure of **4c** was elucidated by interpretation of the NMR spectrum and by comparison with those of C5- and C7-prenylated derivative of **4a**.[11,22]

In conclusion, SAML0654 from *S. ambofaciens* catalyzed the prenylation of L-tryptophan and derivatives at C-6 of the indole ring; it therefore functions as a 6-DMATS, (hereafter termed 6-DMATS$_{Sa}$). If this position is blocked, for example by a methyl group as in the case of **6a**, the prenylation is shifted to C-7, as observed for another 6-DMATS, IptA. Interestingly, blocking of the C-6 by the methyl group did not significantly reduce the enzyme activity of 6-DMATS$_{Sa}$. For **6a** the activity was 72.2% relative to that of **1a**. In the case of IptA, for **6a** the activity was only 9.3% relative to that of **1a**.

The enzyme product of Strvi8510 with **1a** and DMAPP was also isolated, and its structure was elucidated by NMR analysis: the product (**1b)** was the same as for the incubation mixture with SAML0654. This demonstrates clearly that Strvi8510 from *S. violaceusniger* also functions as a tryptophan C6-prenyltransferase (hereafter termed 6-DMATS$_{Sv}$). As mentioned, the product with 6-DMATS$_{Sv}$ for a given tryptophan derivative showed the same HPLC retention time as that with 6-DMATS$_{Sa}$. We concluded that it produces the same products and decided not to isolate these peaks.

GPP also serves as a prenyl donor for 6-DMATS$_{Sa}$ and 6-DMATS$_{Sv}$

HPLC analysis of the DMATS$_{Sa}$ reaction with **1a** and GPP or farnesyl diphosphate (FPP) indicated product formation in the reaction mixture of GPP, but not in that of FPP (data not shown). Therefore, **1a** and six derivatives (**2a**–**7a**) with high conversion yields in the presence of DMAPP were incubated with GPP and 6-DMATS$_{Sa}$ or 6-DMATS$_{Sv}$. Product formation was detected in five cases with 6-DMATS$_{Sa}$ (Table S1). In the assays with GPP under the condition used for DMAPP, **1a**, **2a**, and **5a** were accepted by 6-DMATS$_{Sa}$ with conversion yields of 26.45, 10.8, and 21.6%, respectively (Figure 2), that is, with activities of 46.2, 18.8, and 37.8% relative to that of **1a** with DMAPP (Table S1). With 9.6 μM 6-DMATS$_{Sa}$ in the reaction mixtures of L-tryptophan and GPP, an absolute conversion yield of 40% was achieved. In comparison, GPP was a poor prenyl donor for 6-DMATS$_{Sv}$: low product formation was only detected with **1a** and **5a** (activities of 3.7 and 6.2%, respectively, relative that for DMAPP with **1a**). For structure elucidation, **1a**, **2a**, and **5a** were incubated with 6-DMATS$_{Sa}$ in large scale (10 mL) at 37 °C for 16 h. The enzyme products **1c**, **2c**, and **5c** with GPP were isolated on HPLC and subjected to MS and NMR analyses.

MS analysis showed that the molecular masses of **1c**, **2c**, and **5c** were 136 Da larger than those of **1a**, **2a**, and **5a**, respectively, thus proving attachment of a geranyl moiety. Detailed inspection of the ^{1}H NMR spectra revealed signals for a regular geranyl residue attached at a C atom.[15] The chemical

Figure 1. HPLC analysis of enzyme assays with **1a**–**7a** in the presence of DMAPP (left), and prenyl transfer reactions catalyzed by 6-DMATS$_{Sa}$ and 6-DMATS$_{Sv}$ (right). Reaction mixtures (100 μL) contained 50 mM Tris·HCl (pH 7.5), 5 mM $MgCl_2$, 1 mM aromatic substrate, 1 mM DMAPP, 0.15–5% (*v/v*) glycerol, 0–5% (*v/v*) DMSO, and 2.4 or 2.3 μM purified recombinant protein, and were incubated at 37 °C for 16 h. Detection was carried out with a photodiode array detector (absorption at 277 nm). Conversion yields are shown in parentheses (mean of two independent measurements).

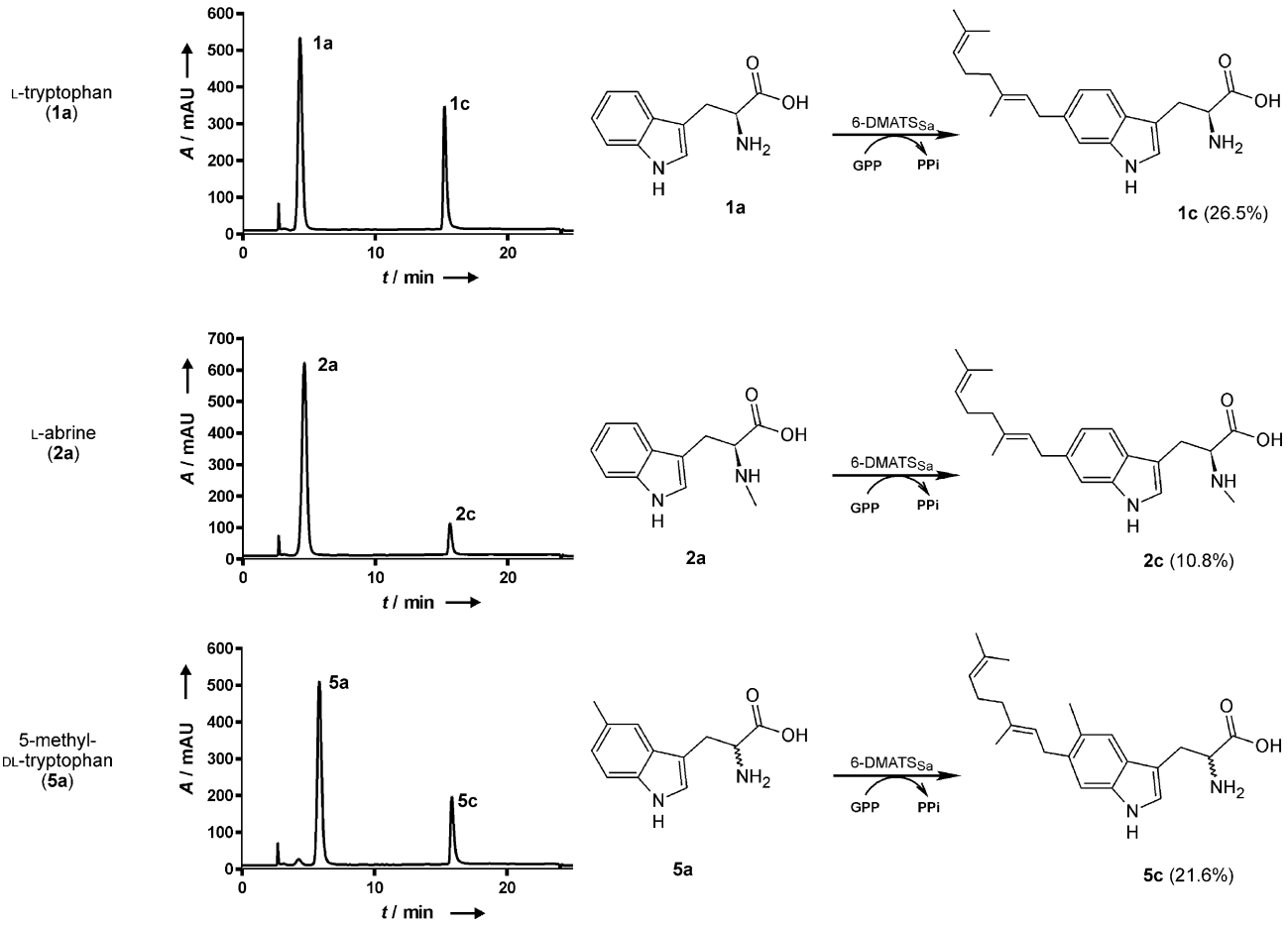

Figure 2. HPLC analysis of enzyme assays with **1a**, **2a**, and **5a** in the presence of GPP (left), and prenyl transfer reactions catalyzed by 6-DMATS$_{Sa}$ (right). Reaction mixtures (100 μL) contained 50 mM Tris·HCl (pH 7.5), 5 mM $MgCl_2$, 1 mM aromatic substrate, 1 mM GPP, 0.15–5% (*v*/*v*) glycerol, 0–5% (*v*/*v*) DMSO and 2.4 μM purified recombinant protein, and were incubated at 37 °C for 16 h. Detection was carried out with a photodiode array detector (absorption at 277 nm). Conversion yields are shown in parentheses (mean of two independent measurements).

shifts and coupling patterns for aromatic protons in the NMR spectra of **1c**, **2c**, and **5c**, respectively, were nearly early identical to those of **1b**, **2b** and **5b**, thus unequivocally proving the same prenylation position for **1c**, **2c**, and **5c** as for **1b**, **2b**, and **5b**. In other words, 6-DMATS$_{Sa}$ also catalyzed C6-prenylation of L-tryptophan and derivatives in the presence of GPP (Figure 2).

Acceptance of dihydroxynaphthalenes by 6-DMATS$_{Sa}$ and C-prenylation on the unsubstituted benzene ring

As mentioned above, hydroxynaphthalenes are natural substrates of some prenyltransferases of the CloQ/NphB group from bacteria and fungi.[19,20] These enzymes share no sequence similarity with members of the DMATS superfamily, but do share structural similarity.[23] It has been demonstrated that several enzymes of the DMATS superfamily from fungi (including FgaPT2 and 7-DMATS) also catalyze prenylation of several hydroxynaphthalenes.[18] There are no reports of acceptance of hydroxynaphthalenes by bacterial indole prenyltransferases.

For naphthalene derivatives with 9.6 μM 6-DMATS$_{Sa}$ in the presence of DMAPP, HPLC analysis revealed clear product formation in 9 of 15 incubation mixtures (Table S2). Product yields of more than 10% were achieved for five substrates after incubation at 37 °C for 16 h. For 6-DMATS$_{Sv}$, product formation was found for four hydroxynaphthalenes (Table S2). As observed for fungal indole prenyltransferases,[18] activation of the naphthalene ring was necessary for acceptance. The substrate preferences among hydroxynaphthalenes by 6-DMATS$_{Sa}$ and 6-DMATS$_{Sv}$ differed, however, from those of fungal indole prenyltransferases. For example, 1-naphthol was very well accepted by fungal indole prenyltransferases, but only poorly accepted by 6-DMATS$_{Sa}$ and 6-DMATS$_{Sv}$ (total conversion yield of 3 and $\leq$0.2%, respectively). Compounds 1,3- (**8a**), 1,7- (**9a**), and 2,3-dihydroxynaphthalene (**10a**) were very well accepted by 6-DMATS$_{Sa}$ (conversion yields 61.5, 33.7, and 43.8%, respectively; Figure 3). Compounds **8a** and **10a** were also good substrates for 6-DMATS$_{Sv}$ (conversion yields 66 and 14%, respectively; Table S2). Again, the retention times on HPLC of products of 6-DMATS$_{Sa}$ and 6-DMATS$_{Sv}$ for a given hydroxynaphthalene were the same, although 2,7-dihydroxynaphthalene was not accepted by DMATS$_{Sa}$ but was well accepted by DMATS$_{Sv}$ (conversion yield 42.1%). Other dihydroxynaphthalenes, such as 1,4-, 1,5-, 1,6-, and 2,6-dihydroxynaphthalene, were poor substrates for

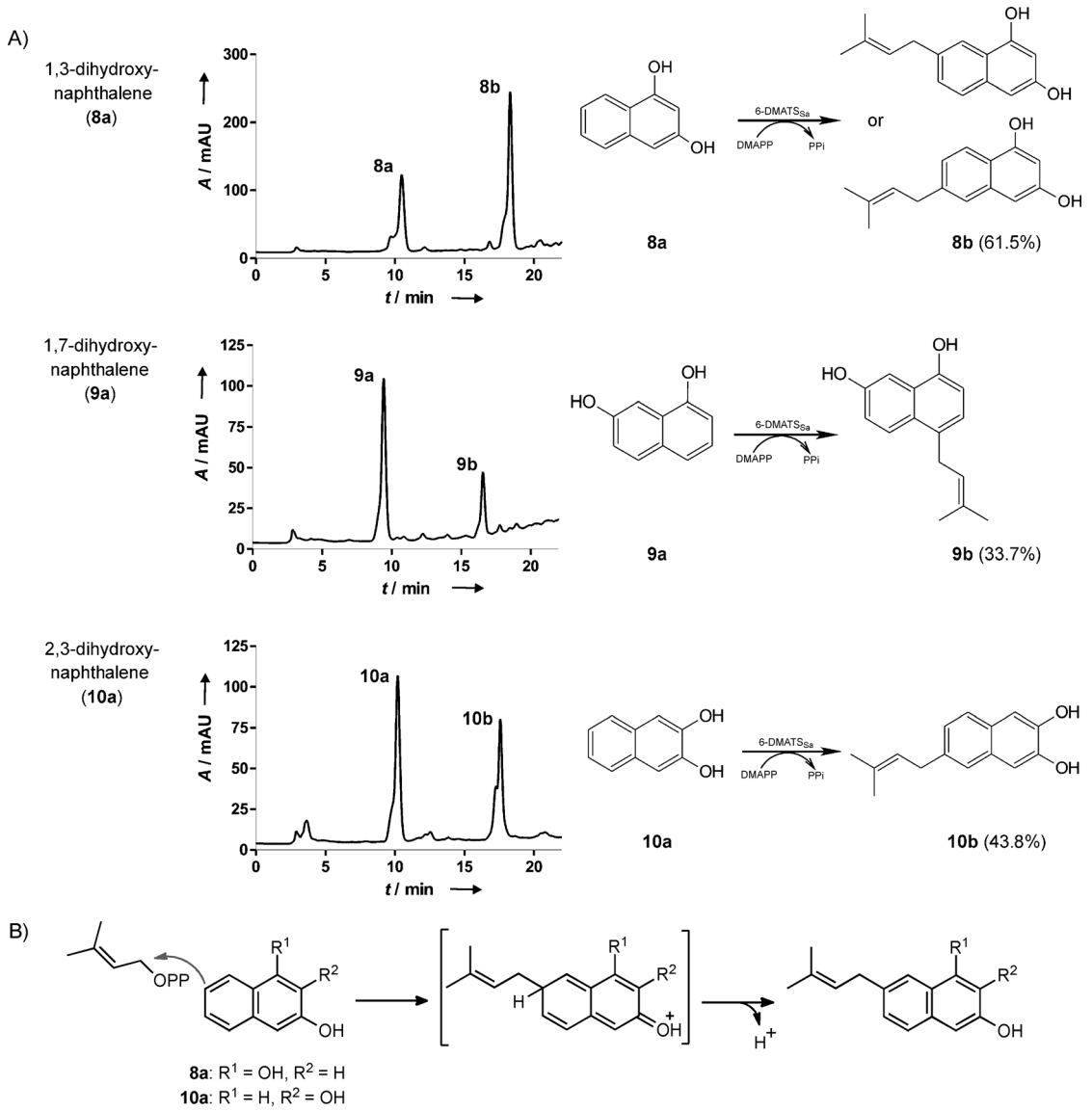

Figure 3. A) HPLC analysis of enzyme assays with **8a**–**10a** in the presence of DMAPP (left) and prenyl transfer reactions catalyzed by 6-DMATS$_{Sa}$ (right). Reaction mixtures (100 μL) contained 50 mM Tris·HCl (pH 7.5), 5 mM $MgCl_2$, 1 mM aromatic substrate, 2 mM DMAPP, 0.15–5% (*v*/*v*) glycerol, 0–5% (*v*/*v*) DMSO and 9.6 μM purified recombinant protein, and were incubated at 37 °C for 16 h. Detection of the compounds was carried out with a photodiode array detector (absorption at 296 nm). Conversion yields are shown in parentheses. B) Proposed reaction mechanism for **8a** and **10a**.

both 6-DMATS$_{Sa}$ and 6-DMATS$_{Sv}$ (Table S2). For structure elucidation, **8b**–**10b** were isolated from the incubation mixtures of the three best accepted naphthalene derivatives (**8a**–**10a**) with 6-DMATS$_{Sa}$ in the presence of DMAPP (Figure 3) and subjected to MS and NMR analyses (Table S3 and Figure S3.8–S3.10). HR-EI-MS analysis confirmed a prenyl moiety in each of **8b**–**10b** by their molecular masses (68 Da larger than for the respective substrates; Table S3). The ^{1}H NMR spectra of **8b**–**10b** show clear signals for a regular dimethylallyl moiety attached to a C atom at δ_H = 3.40–3.59 (d, 2H-1′), 5.31–5.37 (t sept, H-2′), 1.76 or 1.78 (s, 3H-4′), 1.76 or 1.73 (s, 3H-5′; Table S5, Figure S3.8–S3.10). Comparison of the spectra of **9b** with those of **9a** proved prenylation at C-4 of 1,7-dihydroxynaphthalene, that is, at a *para*-position of a hydroxyl group. Compound **9b** has also been identified as an enzyme product of fungal prenyltransferases.[18]

Surprisingly, inspection of the NMR spectra of **8b** and **10b** revealed prenylation in both cases at the unsubstituted benzene ring. The structure of **10b** was easily identified as 6-dimethylallyl-2,3-dihydroxynaphthalene by the presence of one new three spin system with coupling constants at 8.4 and 1.8 Hz. The ^{1}H NMR spectrum of **8b** indicated the presence of three coupling protons at δ_H = 7.80 (br s), 7.44 (d, 8.4 Hz), and 7.15 (dd, 8.4 and 1.8 Hz) ppm, caused by prenylation at C-6 or C-7 of 1,3-dihydroxynaphthalene (this cannot be confirmed or excluded from the obtained spectrum). Even with additional spectroscopic analyses, such as HSQC, HMBC, NOE or NOESY, it would be difficult to distinguish the two possibilities. We favor

C7-prenylated 1,3-dihydroxynaphthalene as a plausible structure for **8b**, because the prenylation position is at the *para*-position of a hydroxyl group, although they are located on two benzene rings. Previously, prenylation of hydroxynaphthalenes at the unsubstituted benzene ring (as in the case of **8b** and **10b**) has not been reported for either indole prenyltransferases of the DMATS superfamily, or enzymes of the NphB/CloQ group. The bacterial prenyltransferase Fnq26 of NphB/CloQ group catalyzed O-prenylation of **8a**.[24]

Biochemical characterization and kinetic parameters of 6-DMATS$_{Sa}$

The dependency of the 6-DMATS$_{Sa}$ reaction on metal ions was examined by incubation of DMAPP with **1a** and different metal ions (5 mM). Reaction mixtures without additives (or with the chelating agent EDTA) served as controls (Figure S2). Addition of Mg^{2+}, Ca^{2+}, or EDTA did not have any influence on the enzyme activity, thus indicating that the 6-DMATS$_{Sa}$ reaction is likely independent of the presence of divalent ions. $CuCl_2$, $ZnCl_2$, and $NiSO_4$ strongly inhibited enzyme activity.

To better understand the 6-DMATS$_{Sa}$ reaction, kinetic parameters (Michaelis–Menten constant K_m, turnover number k_{cat}) were determined for tryptophan (**1a**), six derivatives (**2a**–**7a**), three hydroxynaphthalenes (**8a**–**10a**), DMAPP, and GPP. The reactions with all tested substrates were consistent with Michaelis–Menten kinetics. For calculation of the kinetic parameters (Table 1), data processing was carried out by constructing Hanes–Woolf, Lineweaver–Burk, and Eadie–Hofstee plots (Figure S4.1–S4.7). High affinities (K_m 0.018 to 0.092 mM) were determined for **1a**–**7a**, with **1a** as the best aromatic substrate (K_m 0.018 mM, k_{cat} 0.3 s^{-1}, thus catalytic efficiency 16.7 s^{-1} mM^{-1}). 1,7-Dihydroxynaphthalene (**9a**, K_m 0.059 mM) showed affinity similar to those of the indole derivatives. The other two hydroxynaphthalenes showed much lower affinity. Consistent with the high conversion yields for **2a**–**5a** (Figure 1), high turnover numbers (0.19–0.43 s^{-1}) were determined for these substrates. Consequently, 6-DMATS$_{Sa}$ had higher catalytic efficiency with **1a**–**5a** (Table 1). The kinetic parameter of 6-DMATS$_{Sa}$ towards L-tryptophan and derivatives are comparable with those of the C6-prenyltransferase IptA (Takahashi et al).[9] GPP (K_m 0.070 mM) showed a slightly higher affinity to 6-DMATS$_{Sa}$ than did DMAPP (K_m 0.095 mM). However, GPP turnover (k_{cat} 0.043 s^{-1}) was much slower than for DMAPP (k_{cat} 0.63 s^{-1}).

Table 1. Kinetic parameters of 6-DMATS$_{Sa}$ for selected substrates.

Substrate	K_m [mM]	k_{cat} [s^{-1}]	k_{cat}/K_m [s^{-1} mM^{-1}]	Relative catalytic efficiency [%]
L-tryptophan (**1a**)	0.018	0.30	16.67	100
L-abrine (**2a**)	0.023	0.27	11.74	69
L-β-homotryptophan (**3a**)	0.092	0.23	2.50	15
4-methyl-DL-tryptophan (**4a**)	0.063	0.19	3.02	18
5-methyl-DL-tryptophan (**5a**)	0.074	0.43	5.81	35
6-methyl-DL-tryptophan (**6a**)	0.030	0.028	0.93	5.6
7-methyl-DL-tryptophan (**7a**)	0.072	0.013	0.18	1.1
1,3-dihydroxynaphthalene (**8a**)	0.29	0.43	1.47	8.8
1,7-dihydroxynaphthalene (**9a**)	0.059	0.088	1.49	8.9
2,3-dihydroxynaphthalene (**10a**)	0.28	0.13	0.46	2.7
DMAPP[a]	0.095	0.63	6.63	40
GPP[a]	0.070	0.043	0.61	3.7

[a] L-tryptophan (**1a**) as prenyl acceptor.

Discussion

Indole prenyltransferases catalyze the transfer of prenyl moieties onto different positions of indole rings; they have been identified mainly in fungi (ascomycetes)[8] and occasionally in bacteria (actinomycetes).[7,9,10] These enzymes belong to the DMATS superfamily and accept tryptophan, tryptophan-containing cyclic dipeptides, or more-complex indole derivatives as prenyl acceptors. The important features of these enzymes are high promiscuity with the aromatic substrate, high regioselectivity of the prenylation position, and high substrate specificity towards the prenyl donor. The known tryptophan prenyltransferases use solely DMAPP as the prenyl donor.[7–10,14]

In this study, we successfully identified two putative prenyltransferases, SAML0654 from *S. ambofaciens* and Strvi8510 from *S. violaceusniger*, as indole prenyltransferases with broad substrate specificity. Determination of the kinetic parameters with diverse aromatic substrates showed that L-tryptophan was best accepted as a substrate, and that the enzymes function as a 6-DMATS. Detailed biochemical characterization of the enzymes (especially of 6-DMATS$_{Sa}$) revealed a number of new features of these indole prenyltransferases:

1) The identification of SAML0654 as a 6-DMATS was somewhat surprising, because amino acid sequence alignment revealed much higher similarity to the 5-DMATS SCO7467 (75%) from *S. coelicolor*[10] than to the 6-DMATS IptA (60%) from *Streptomyces* sp. SN-593.[9] Our results highlight that the functions of enzymes should be proven experimentally, not just inferred from sequence comparison with known proteins.
2) 6-DMATS$_{Sa}$ and 6-DMATS$_{Sv}$ accepted well a number of indole derivatives, including D-tryptophan and 6-methyl-DL-tryptophan (**6a**; Figure 1 and Table S1). Conversion yields of 73.5 and 60.7% of that of L-tryptophan were calculated for D-tryptophan. The conversion yields for 6-methyl-DL-tryptophan were 72.2 and 82%. These values are unusually high for L-tryptophan C6-prenyltransferases. Other known DMATSs, such as IptA (*Streptomyces* sp. SN-593), FgaPT2, and 7-DMATS (both from *A. fumigatus*), accepted D-tryptophan with activities of only 4.3, 1.8, and 15.5%, respectively, relative to that for L-tryptophan.[9,12,13] IptA also accepted 6-methyl-DL-tryptophan as a substrate, but with activity of only 9.33% relative of that of L-tryptophan. As in the case of IptA, highly regiospecific C7-prenylation of 6-methyl-DL-tryptophan (**6a**) was observed with 6-DMATS from *S. ambofaciens*.

3) 6-DMATS$_{Sa}$ showed relatively high promiscuity towards the prenyl donor. In the presence of L-tryptophan and several tryptophan derivatives, GPP was accepted by 6-DMATS$_{Sa}$ as the prenyl donor (activities of up to 46.2% relative of that for DMAPP); 6-DMATS$_{Sv}$ also accepted GPP, but with lower conversion yields. In contrast, no known DMATS (including *A. fumigatus* FgaPT2, *A. clavatus* 5-DMATS, *Streptomyces* sp. SN-593 IptA, and *A. fumigatus* 7-DMATS) have been reported to use GPP or other prenyl donors.[9,11–13] Therefore, 6-DMATS$_{Sa}$ from *S. ambofaciens* and 6-DMATS$_{Sv}$ from *S. violaceusniger* represent the first examples of tryptophan prenyltransferases that accept both DMAPP and GPP as prenyl donors.
4) Isolation and structure elucidation of the enzyme products from L-tryptophan (**1a**) and two derivatives (**2a** and **5a**) with GPP led to the identification of C6-geranylated derivatives, that is, the same prenylation position as for the products from DMAPP. This differs from the situation for some fungal indole prenyltransferases in the presence of DMAPP analogues, GPP, or benzyl diphosphate. In those cases, complete or partial shifts of the prenylation position were observed.[25–27]
5) 6-DMATS$_{Sa}$ and 6-DMATS$_{Sv}$ also accepted several hydroxynaphthalenes as prenyl acceptors; these are natural substrates of prenyltransferases of the bacterial and fungal CloQ/NphB group.[19,20,24] It has been demonstrated that some members of the fungal DMATS superfamily can also use these compounds as substrates.[18] However, there is no report on the behavior of bacterial indole prenyltransferase like IptA or SCO7467 towards hydroxynaphthalenes.[7,9,10] Interestingly, all fungal indole prenyltransferases accept 1-naphthol as one of the best substrates. In contrast, 1-naphthol was not accepted by 6-DMATS$_{Sv}$, and it was barely accepted by 6-DMATS$_{Sa}$ (<3%, Table S2). In contrast 1,3- and 2,3-dihydroxynaphthalenes were better accepted by 6-DMATS$_{Sa}$ than by fungal indole prenyltransferases. 1,7-Dihydroxynaphthalene was accepted by both bacterial and fungal enzymes.
6) Structure elucidation of the enzyme products of 1,3- (**8a**) and 2,3-dihydroxynaphthalenes (**10a**) identified the prenylation position at the unsubstituted benzene ring. This clearly differs from fungal indole prenyltransferases and prenyltransferases of the NphB/CloQ group; these attached prenyl moieties to *para*- or *ortho*-position of a hydroxyl group at the same benzene ring, or onto a hydroxyl group.[18–20,28] The structure of **10b** was unequivocally proven to be 6-dimethylallyl-2,3-dihydroxynaphthalene. In the case of **8b**, we favor 7-dimethylallyl-1,3-dihydroxynaphthalene as the more likely of the two possible structures. This means that prenyl moieties in both structures are *para* to a hydroxy group on the second benzene ring. It could be speculated that activation by a hydroxyl group (although at another benzene ring) is important for the stabilization of an intermediate cation (Figure 3B).

Conclusion

In summary, the identified and characterized 6-DMATS$_{Sa}$ and 6-DMATS$_{Sv}$ showed several new intriguing biochemical features, and greatly expand our knowledge of bacterial indole prenyltransferases. These enzymes are very good candidates for further investigations, such as protein crystallization and structural analysis of the active sites, to understand their broad substrate specificity towards prenyl donor and acceptor, as well as their reaction mechanisms.

Experimental Section

Computer-assisted sequence analysis: Sequence identities were obtained by alignments of amino acid sequences with the program BLASTP (http://www.ncbi.nlm.nih.gov).

Chemicals: DMAPP, GPP, and FPP were prepared according to the method described for GPP by Woodside et al.[29] Indole and hydroxynaphthalene derivatives of the highest available purity were purchased from TCI, Acros Organics, Sigma–Aldrich, Bachem, and Alfa Aesar.

Bacterial strains, plasmids, and culture conditions: pGEM-T Easy and pQE-60/70 were purchased from Promega and Qiagen, respectively. pHIS$_8$[30] was a kind gift from Prof John Noel (Salk Institute for Biological Studies). *E. coli* strains XL1 Blue MRF′ (Stratagene/Agilent Technologies), M15 [pREP4] (Qiagen), and BL21 (DE3) pLysS (AMS Biotechnology, Abingdon, UK) were used for cloning and expression. They were grown in liquid lysogeny broth (LB) or on solid LB medium (with agar (1.5% *w/v*)) at 37 or 30 °C. Carbenicillin (50 μg mL^{-1}) or kanamycin (25 μg mL^{-1}) were used for selection of recombinant *E. coli* XL1 Blue MRF′ strains containing pQE-60 or pHIS$_8$ constructs, respectively. Kanamycin (25 μg mL^{-1}) with carbenicillin (50 μg mL^{-1}) or chloramphenicol (12.5 μg mL^{-1}) was used for selection of recombinant *E. coli* M15 [pREP4] or BL21 (DE3), respectively. *S. ambofaciens* DSM40053 (ATCC 23877) was purchased from Deutsche Sammlung von Mikroorganismen und Zellkulturen (Braunschweig, Germany). *S. violaceusniger* Tü 4113 was obtained from Prof. Wolfgang Wohlleben (Tübingen University). For genomic DNA isolation, these were cultivated in a 300 mL cylindrical flask containing liquid YMG medium (50 mL; yeast extract (0.4% *w/v*), malt extract (1% *w/v*), glucose (0.4% *w/v*)) at 28 °C on a rotary shaker (160 rpm) for 3 days.

DNA manipulation and PCR amplification: DNA propagation in *E. coli* was carried out by standard methods.[31] DNA isolation from *Streptomyces* strains was carried out by phenol-chloroform extraction.[32] PCR amplification was performed on an iCycler (Bio-Rad). PCR products containing the coding sequence of SAML0654 and Strvi8510 were obtained by using Expand High Fidelity kit (Roche Diagnostic) with genomic DNA as template. The primers for SAML0654 were SAML0654_fw (5′-CCATGG CCACCG TACGGA CCGGCG CGG-3′) and SAML0654_r (5′-GGATCC GCGCAC CGCCAC CGGGCG G-3′), and for Strvi8510 they were Strvi_bam_fw (5′-GGATCC ATGAAC GGTTTC CATTCG GGTG-3′) and Strvi_hind3_r (5′-AAGCTT TCACAG CCCTGC CCGCAC C-3′). Underlined letters represent the restriction sites for NcoI, BamHI, and HindIII, located at the predicted start and stop codon in the primer sequences. The PCR products for SAML0654 (1133 bp) and Strvi8510 (1155 bp) were cloned into pGEM-T Easy to create plasmids pJW09 and pJW16, and then subcloned into pQE-60 and pHIS$_8$ to produce the expres-

sion plasmids pJW12 (SAML0654) and pJW18 (Strvi8510), respectively.

Gene expression and purification of recombinant 6-DMATS$_{Sa}$ and 6-DMATS$_{Sv}$: For expression of *SAML0654*, an overnight culture of *E. coli* M15 [pREP4] harboring pJW12 was inoculated into LB medium (1 L) supplemented with carbenicillin (50 μg mL^{-1}) and kanamycin (25 μg mL^{-1}), and cultivated at 37 °C and 220 rpm to A_{600} = 0.6. For induction of gene expression, isopropyl thiogalactosid (IPTG, 0.5 mM) was added. After further cultivation for 16 h at 30 °C, cells were harvested by centrifugation and the pellet was resuspended in lysis buffer (NaH_2PO_4 (50 mM, pH 8.0), imidazole (10 mM), NaCl (300 mM)) at 2–5 mL per gram wet weight. After addition of lysozyme (1 mg mL^{-1}), the cell suspension was incubated on ice for 30 min then sonicated (×6, 10 s, 200 W). Cellular debris was separated from the soluble proteins by centrifugation (20000 *g*, 30 min, 4 °C). Recombinant His$_6$-tagged fusion protein was isolated by affinity chromatography with Ni-NTA agarose resin (Qiagen) according to the manufacturer's instructions. The protein was eluted with imidazole (250 mM) in NaH_2PO_4 (50 mM, pH 8.0) with NaCl (300 mM). In order to change the buffer, the protein fraction was passed through a PD-10 column (GE Healthcare), previously equilibrated with Tris·HCl (50 mM, pH 7.5) containing glycerol (15% *v/v*). Purified 6-DMATS-His$_6$ was used immediately for enzyme assays or stored at −80 °C. The proteins were analyzed by 12% (*w/v*) SDS-PAGE gels according to the method of Laemmli[33] and stained with Coomassie Brilliant Blue G-250.

For overproduction of His$_8$-Strvi8510, *E. coli* BL21 (DE3) pLysS cells harboring pJW18 were cultivated in LB medium (1 L) supplemented with chloramphenicol (12.5 μg mL^{-1}) and kanamycin (25 μg mL^{-1}) at 37 °C to A_{600} = 0.6. Gene expression was induced by addition of IPTG (0.5 mM). Cells were cultivated for a further 16 h at 22 °C and then centrifuged to harvest the cells. Protein purification was carried out as described above.

Enzyme assays for 6-DMATS$_{Sa}$ and 6-DMATS$_{Sv}$: To determine the relative activities of 6-DMATS$_{Sa}$ for different substrates, enzyme assay mixtures (100 μL) contained Tris·HCl (50 mM, pH 7.5), $MgCl_2$ (5 mM), aromatic substrate (1 mM), DMAPP or GPP (1 or 2 mM), glycerol (0.15–5% *v/v*), DMSO (0–5% *v/v*), and purified recombinant protein (10 or 40 μg; 2.4 or 9.6 μM). Mixtures were incubated at 37 °C for 16 h, before reaction termination by addition of methanol (100 μL). For determination of the kinetic parameters of L-tryptophan and derivatives, DMAPP (1 mM) and aromatic substrate (up to 2 mM) were used. Protein concentrations: 61 nM (for **1a** and **2a**), 122 nM (**3a**, **4a**, and **5a**), 244 nM (**6a**), 732 nM (**7a**). Incubation times were 15 min (**1a**–**5a**), 30 min (**6a**), or 60 min (**7a**). For determination of the kinetic parameters of DMAPP, **1a** (1 mM) was used as prenyl acceptor. DMAPP (up to 2 mM) and protein (122 nM) were incubated for 15 min. For determination of the kinetic parameters of GPP, the reaction mixtures contained GPP (up to 1 mM) and protein (732 nM) and were incubated for 30 min. For determination of the kinetic parameters of dihydroxynaphthalenes, the assays contained aromatic substrate (up to 5 mM), DMAPP (1 mM), and protein (0.5 μM for **8a** and **10a**, 0.73 μM for **9a**) and were incubated at 37 °C for 30 min (**8a**, **10a**) or 45 min (**9a**).

For determination of 6-DMATS$_{Sv}$ substrate specificity, the enzyme assays were carried out as for 6-DMATS$_{Sa}$. The reaction mixtures of simple indole derivatives and naphthalene derivatives contained DMAPP (1 mM) and recombinant protein (10 μg (2.3 μM) or 20 μg (4.6 μM), respectively).

Preparation and isolation of enzyme products for structure elucidation: For isolation of the enzyme products, large-scale enzyme reactions (10 mL) were carried out. The reaction mixtures contained substrate **1a**–**10a** (1 mM), DMAPP (2 mM), $MgCl_2$ (5 mM), Tris·HCl (50 mM, pH 7.5) and 6-DMATS$_{Sa}$ (2.4 μM for **1a**–**7a**, 4.8 μM for **8a**–**10a**). The reaction mixture with 6-DMATS$_{Sv}$ and **1a** was carried out as described above for 6-DMATS$_{Sa}$ (2.3 μM). For isolation of geranylated products, **1a**, **2a**, and **5a** (1 mM) were also incubated with GPP (2 mM), $MgCl_2$ (5 mM), Tris·HCl (50 mM, pH 7.5), and 6-DMATS (2.4–10 μM) at 37 °C for 16 h. For **1a**–**7a** reactions were terminated by addition of methanol (10 mL). The precipitated protein was removed by centrifugation, and the obtained supernatants were concentrated on a rotating vacuum evaporator at 30 °C to 0.5–1 mL for HPLC purification. For **8a**–**10a** the mixtures were extracted three times with ethyl acetate immediately after incubation. The ethyl acetate phases were concentrated on a rotating vacuum evaporator at 30 °C to dryness and dissolved in methanol (0.5–1 mL) for HPLC purification.

HPLC conditions for analysis and isolation of enzyme products: The enzyme products of the incubation mixtures were analyzed on an series 1200 HPLC device (Agilent Technologies) with a Multospher 120 RP-18 column (250×4 mm, 5 μm; C+S Chromatography Service, Langenfeld, Germany) at a flow rate of 1 mL min^{-1}. Water (solvent A) and methanol (solvent B) were used with trifluoroacetic acid (0.5% *v/v*) added if necessary. For analysis of enzyme products of tryptophan and simple indole derivatives, a linear gradient of 20–100% or 40–100% solvent B over 15 min was used. For analysis of products from hydroxynaphthalene derivatives, a linear gradient of 40–100% solvent B over 15 or 20 min was used. The column was then washed with solvent B for 5 min and equilibrated with 20 or 40% solvent B for 5 min. Detection was carried out with a photodiode array detector.

The same HPLC equipment and a larger column (250×10 mm) were used to isolate enzyme products. The flow rate was 2.5 mL min^{-1}. Water (solvent A) and methanol (solvent B) without acid were used as solvents: 40–100 or 65–100% solvent B over different times. The column was then washed with solvent B for 5 min and equilibrated with 40 or 65% solvent B for 5 min.

NMR spectroscopic analysis and high-resolution electrospray ionization mass spectra (HR-EI-MS): The isolated products were analyzed by HR-EI-MS with a AutoSpec (Micromass). Positive EI-MS data are given in Table S3. ^{1}H NMR spectra were recorded on an ECA-500 spectrometer (JEOL). Chemical shifts were referenced to CD_3OD at 3.31 ppm. All spectra were processed with MestReNova 5.2.2 software (see the Supporting Information). The NMR data are given in Tables S4 and S5.

Nucleotide sequence accession numbers: The protein sequences of SAML0654 and Strvi8510 are available at GenBank (accession numbers CAJ89640 and YP_004818099.1).

Acknowledgements

This work was supported by a grant from the Deutsche Forschungsgemeinschaft (Grant Li844/4-1 to S.M.L.). J.W. is partially financed by the LOEWE program of the State of Hessen (SynMikro to S.M.L.). We thank Dr. Edyta Stec for synthesis of GPP and FPP, Lena Ludwig for synthesis of DMAPP, Nina Zitzer and Stefan Newel (all from Philipps-Universität Marburg) for MS and NMR spectra, respectively. We also thank Wolfgang Wohlleben from University of Tübingen for providing S. violaceusniger.

Keywords: dimethylallyltryptophan synthases · enzymes · hydroxynaphthalenes · indole prenyltransferases · natural products · *Streptomyces*

[1] D. J. Newman, G. M. Cragg, *J. Nat. Prod.* **2012**, *75*, 311 – 335.
[2] S.-M. Li, *Nat. Prod. Rep.* **2010**, *27*, 57 – 78.
[3] B. Botta, G. D. Monache, P. Menendez, A. Boffi, *Trends Pharmacol. Sci.* **2005**, *26*, 606 – 608.
[4] R. M. Williams, E. M. Stocking, J. F. Sanz-Cervera, *Top. Curr. Chem.* **2000**, *209*, 97 – 173.
[5] T. Lindel, N. Marsch, S. K. Adla, *Top. Curr. Chem.* **2012**, *309*, 67 – 129.
[6] L. A. Wessjohann, J. Keim, B. Weigel, M. Dippe, *Curr. Opin. Chem. Biol.* **2013**, *17*, 229 – 235.
[7] T. Ozaki, M. Nishiyama, T. Kuzuyama, *J. Biol. Chem.* **2013**, *288*, 9946 – 9956.
[8] X. Yu, S.-M. Li, *Methods Enzymol.* **2012**, *516*, 259 – 278.
[9] S. Takahashi, H. Takagi, A. Toyoda, M. Uramoto, T. Nogawa, M. Ueki, Y. Sakaki, H. Osada, *J. Bacteriol.* **2010**, *192*, 2839 – 2851.
[10] S. Subramanian, X. Shen, Q. Yuan, Y. Yan, *Process Biochem.* **2012**, *47*, 1419 – 1422.
[11] X. Yu, Y. Liu, X. Xie, X.-D. Zheng, S.-M. Li, *J. Biol. Chem.* **2012**, *287*, 1371 – 1380.
[12] A. Kremer, L. Westrich, S.-M. Li, *Microbiology* **2007**, *153*, 3409 – 3416.
[13] I. A. Unsöld, S.-M. Li, *Microbiology* **2005**, *151*, 1499 – 1505.
[14] A. W. Schultz, D.-C. Oh, J. R. Carney, R. T. Williamson, D. W. Udwary, P. R. Jensen, S. J. Gould, W. Fenical, B. S. Moore, *J. Am. Chem. Soc.* **2008**, *130*, 4507 – 4516.
[15] D. Pockrandt, S.-M. Li, *ChemBioChem* **2013**, *14*, 2023 – 2028.
[16] N. Steffan, I. A. Unsöld, S.-M. Li, *ChemBioChem* **2007**, *8*, 1298 – 1307.
[17] A. Kremer, S.-M. Li, *Appl. Microbiol. Biotechnol.* **2008**, *79*, 951 – 961.
[18] X. Yu, X. Xie, S.-M. Li, *Appl. Microbiol. Biotechnol.* **2011**, *92*, 737 – 748.
[19] E. Haug-Schifferdecker, D. Arican, R. Brückner, L. Heide, *J. Biol. Chem.* **2010**, *285*, 16487 – 16494.
[20] T. Kumano, S. B. Richard, J. P. Noel, M. Nishiyama, T. Kuzuyama, *Bioorg. Med. Chem.* **2008**, *16*, 8117 – 8126.
[21] F. Choulet, B. Aigle, A. Gallois, S. Mangenot, C. Gerbaud, C. Truong, F.-X. Francou, C. Fourrier, M. Guérineau, B. Decaris, V. Barbe, J.-L. Pernodet, P. Leblond, *Mol. Biol. Evol.* **2006**, *23*, 2361 – 2369.
[22] J. D. Rudolf, C. D. Poulter, *ACS Chem. Biol.* **2013**, *8*, 2707 – 2714.
[23] U. Metzger, C. Schall, G. Zocher, I. Unsöld, E. Stec, S.-M. Li, L. Heide, T. Stehle, *Proc. Natl. Acad. Sci. USA* **2009**, *106*, 14309 – 14314.
[24] Y. Haagen, I. Unsöld, L. Westrich, B. Gust, S. B. Richard, J. P. Noel, L. Heide, *FEBS Lett.* **2007**, *581*, 2889 – 2893.
[25] M. Liebhold, X. Xie, S.-M. Li, *Org. Lett.* **2012**, *14*, 4882 – 4885.
[26] M. Liebhold, S.-M. Li, *Org. Lett.* **2013**, *15*, 5834 – 5837.
[27] M. Liebhold, X. Xie, S.-M. Li, *Org. Lett.* **2013**, *15*, 3062 – 3065.
[28] T. Kumano, T. Tomita, M. Nishiyama, T. Kuzuyama, *J. Biol. Chem.* **2010**, *285*, 39663 – 39671.
[29] A. B. Woodside, Z. Huang, C. D. Poulter, *Org. Synth.* **1988**, *66*, 211 – 215.
[30] J. M. Jez, J. L. Ferrer, M. E. Bowman, R. A. Dixon, J. P. Noel, *Biochemistry* **2000**, *39*, 890 – 902.
[31] J. Sambrook, D. W. Russell, *Molecular Cloning: A Laboratory Manual*, 3rd ed., Cold Spring Harbor Laboratory Press, New York, **2001**.
[32] T. Kieser, M. J. Bibb, M. J. Buttner, K. F. Chater, D. A. Hopwood, *Practical Streptomyces Genetics*, 2nd ed., John Innes Foundation, Norwich, **2000**.
[33] U. K. Laemmli, *Nature* **1970**, *227*, 680 – 685.

Received: January 18, 2014
Published online on April 1, 2014

CHEMBIOCHEM

Supporting Information

Biochemical Investigations of Two 6-DMATS Enzymes from *Streptomyces* Reveal New Features of L-Tryptophan Prenyltransferases

Julia Winkelblech[a, b] and Shu-Ming Li*[a, b]

cbic_201400046_sm_miscellaneous_information.pdf

Table S1. Enzyme activity of SAML0654 (6-DMATS$_{Sa}$) and Strvi8510 (6-DMATS$_{Sv}$) towards L-tryptophan and derivatives

Substrate	Structure	Prenyl donor	Relative product yield [%]		Substrate	Structure	Prenyl donor	Relative product yield [%]	
			SAML0654	Strvi8510				SAML0654	Strvi8510
L-tryptophan (**1a**)	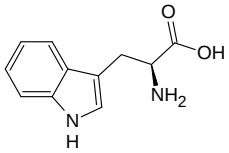	DMAPP	100	100	1-methyl-DL-tryptophan	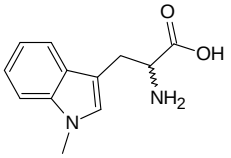	DMAPP	2.2	5.7
		GPP	46.2	3.7			GPP	n.d.	n.d.
L-abrine (**2a**)	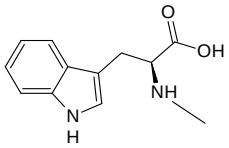	DMAPP	106	121.2	N-acety-DL-tryptophan	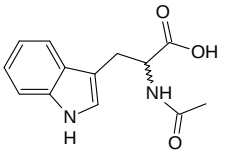	DMAPP	26.9	16.5
		GPP	18.8	-			GPP	n.d.	n.d.
L-ß-homotrypto-phan (**3a**)	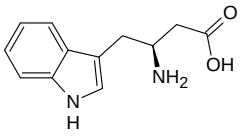	DMAPP	97.2	36.7	DL-indole-3-lactic acid	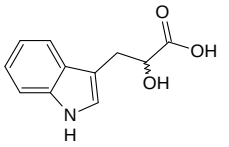	DMAPP	26.9	16.4
		GPP	1.5	-			GPP	n.d.	n.d.
4-methyl-DL-tryptophan (**4a**)	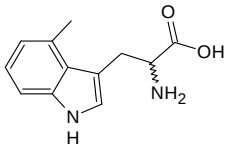	DMAPP	96.4	104.7	indole-3-propionic acid	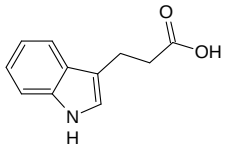	DMAPP	31.1	28.8
		GPP	4	-			GPP	n.d.	n.d.
5-methyl-DL-tryptophan (**5a**)	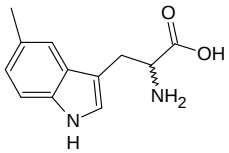	DMAPP	87.9	96	*trans*-indole-3-acrylic-acid	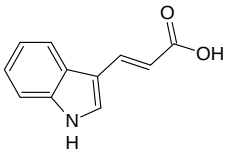	DMAPP	34.5	12.6
		GPP	37.8	6.2			GPP	n.d.	n.d.
6-methyl-DL-tryptophan (**6a**)	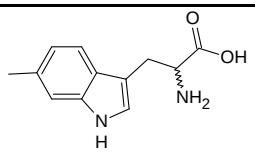	DMAPP	72.2	82	D- tryptophan	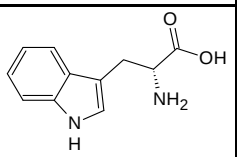	DMAPP	73.5	60.7
		GPP	-	-			GPP	n.d.	n.d.
7-methyl-DL-tryptophan (**7a**)	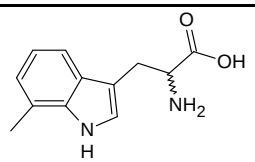	DMAPP	51.3	32.2	6-fluoro-DL-tryptophan	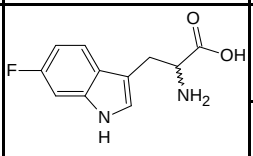	DMAPP	8.2	4.4
		GPP	-	-			GPP	n.d.	n.d.

n.d.: no determined; -: conversion yield <0.5 %

The reaction mixtures contained 1 mM of aromatic substrate and 1 mM DMAPP or GPP and were incubated with 2.3 or 2.4μM of purified protein at 37°C for 16 h. The conversion yield of L-tryptophan with SAML0654 at 59.4 % and with Strvi8510 at 42.2 % were defined as 100% of relative activity.

Table S2. Enzyme activity of SAML0654 (6-DMATS$_{Sa}$) and Strvi8510 (6-DMATS$_{Sv}$) towards all tested naphthalene derivatives

Substrate	Structure	Prenyl donor	Relative product yield [%]		Substrate	Structure	Prenyl donor	Relative product yield [%]	
			SAML0654	Strvi8510				SAML0654	Strvi8510
naphthalene	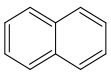	DMAPP	-	-	2,3-dihydroxy naphthalene (**10a**)	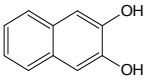	DMAPP	43.8	14
1-naphthol	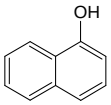	DMAPP	2.9	-			GPP	-	-
2-naphthol	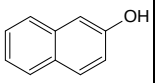	DMAPP	6.0	-	2,6-dihydroxy naphthalene	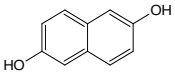	DMAPP	9.6	-
1,3-dihydroxy naphthalene (**8a**)	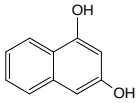	DMAPP	61.5	66					-
		GPP	-	-	2,7-dihydroxy-naphthalene	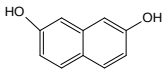	DMAPP	-	42.1
1,4-dihydroxy naphthalene	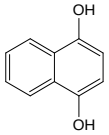	DMAPP	-	-	3,5-dihydroxy-2-naphtoic acid	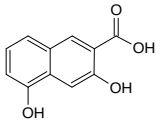	DMAPP	13.1	-
1,5-dihydroxy naphthalene	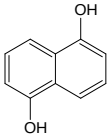	DMAPP	-	-	3,7-dihydroxy-2-naphtoic acid	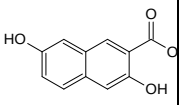	DMAPP	-	-
1,6-dihydroxy naphthalene	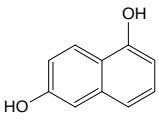	DMAPP	7.8	-	5-amino-2-naphthol	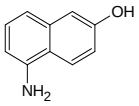	DMAPP	10.4	-
1,7-dihydroxynaphthalene (**9a**)	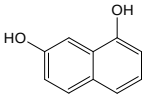	DMAPP	33.7	5.3	alizarine	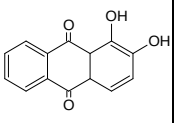	DMAPP	-	-
		GPP	-	-					

-: not detected, conversion rate ≤ 0.2 %

The reaction mixtures of SAML0654 contain 1 mM aromatic substrate, 2 mM DMAPP or GPP and 9.6 μM protein. The reaction mixtures of Strvi8510 contain 1 mM aromatic substrate, 1mM DMAPP and 4.6 μM protein. The reaction mixtures were incubated at 37°C for 16 h. The conversion yield of Strvi8510 towards L-tryptophan at 53 % was defined as 100% of relative activity. Under the conditions used for naphthalene derivatives, L-tryptophan was completely converted by SAML0654.

Table S3. HR-EI-MS data of enzyme products of 6-DMATS$_{Sa}$ for L-tryptophan and derivatives as well as hydroxynaphthalenes

Compound	Chemical formula	HR-EI-MS([M]$^+$)		Deviation (ppm)
		Calculated	Measured	
6-DMA-L-tryptophan (**1b**)	$C_{16}H_{20}N_2O_2$	272.1525	272.1532	-2.6
6-geranyl-L-tryptophan (**1c**)	$C_{21}H_{28}N_2O_2$	340.2151	340.2138	3.8
6-DMA-L-abrine (**2b**)	$C_{17}H_{22}N_2O_2$	286.1681	286.1704	-8
6-geranyl-L-abrine (**2c**)	$C_{22}H_{30}N_2O_2$	354.2307	354.2324	-4.8
6-DMA-L-ß-homotryptophan (**3b**)	$C_{17}H_{22}N_2O_2$	286.1681	286.1714	-11.5
6-geranyl-L-ß-homotryptophan (**3c**)	$C_{22}H_{40}N_2O_2$	354.2307	354.2282	7.1
6-DMA-4-methyl-DL-tryptophan (**4b**)	$C_{17}H_{22}N_2O_2$	286.1681	286.1715	-11.9
6-DMA-5-methyl-DL-tryptophan (**5b**)	$C_{17}H_{22}N_2O_2$	286.1681	286.1704	-8.0
7-DMA-6-methyl-DL-tryptophan (**6b**)	$C_{17}H_{22}N_2O_2$	286.1681	286.1691	-3.5
6-DMA-7-methyl-DL-tryptophan (**7b**)	$C_{17}H_{22}N_2O_2$	286.1681	286.1724	-15
6- or 7-DMA-1,3-dihydroxynaphthalene (**8b**)	$C_{15}H_{16}O_2$	228.1150	228.1145	2.2
4-DMA-1,7-dihydroxynaphthalene (**9b**)	$C_{15}H_{16}O_2$	228.1150	228.1165	-6.6
6-DMA-2,3-dihydroxynaphthalene (**10b**)	$C_{15}H_{16}O_2$	228.1150	228.1139	4.8

DMA: dimethylallyl

Table S4.1 ^{1}H-NMR data of prenylated enzyme products (6-DMATS$_{Sa}$) for L-tryptophan and derivatives with the prenyl donor DMAPP obtained in CD_3OD

	6-DMA-L-Trp (1b) 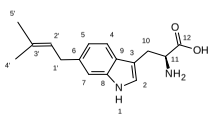	**6-DMA-L-abrine (2b)** 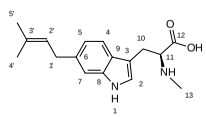	**6-DMA-L-ß-homo-Trp (3b)** 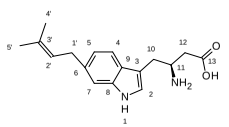	**6-DMA-4-methyl-DL-Trp (4b)** 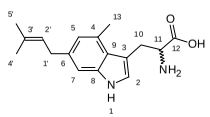	**7-DMA-4-methyl-DL-Trp (4c)** 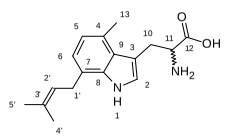	**6-DMA-5-methyl-DL-Trp (5b)** 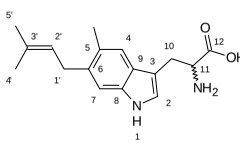	**7-DMA-6-methyl-DL-Trp (6b)** 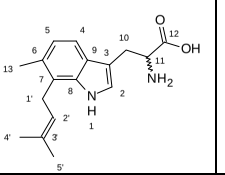	**6-DMA-7-DL-methyl-Trp (7b)** 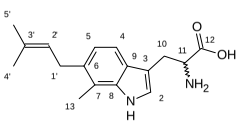
Pos	δ_H, multi., *J*	δ_H, multi., *J*	δ_H, multi., *J*	δ_H, multi., *J*	δ_H, multi., *J*	δ_H, multi., *J*	δ_H, multi., *J*	δ_H, multi., *J*
2	7.12, s	7.15, s	7.09,s	7.08, s	7.16, s	7.08,s	7.13,s	7.14,s
4	7.58, d, 8.2	7.58 ,d, 8.2	7.47, d, 8.2	-	-	7.47,s	7.43, d ,8.1	7.44, d, 8.1
5	6,89, dd, 8.2,1.4	6.89, dd, 8.2, 1.5	6.89, dd ,8.2, 1.2	6.97, s	6.77, d, 7.2	-	6.89, d, 8.1	6.88, d, 8.1
6	-	-	-	-	6.71, d, 7.2	-	-	-
7	7.15, d, 1.4	7.15, br s	7.15, s	6.61, s	-	7.13, s	-	-
10a	3.49, dd, 15.3, 4.0, 0.8	3.45, ddd, 15.5, 4.6, 0.8	2.52, dd, 16.9, 3.8	3.79,overlapping	3.85, m	3.48,dd,15.1, 3.7	3.49, dd, 15.3, 4.0	3.49, dd, 15.2, 4.0
10b	3.12,dd,15.3,9.5	3.25,dd,15.5,8.0	2.34,dd,16.9,8.9	3.09, dd,15.3,11.5	3.12, overlapping	3.08,dd, 15.1, 9.6	3.09, dd, 15.3, 9.4	3.11, dd,15.2,9.5
11	3,84, dd, 9.5, 4.0	3.76, dd, 8.0, 4.6	3.33, m	3.79, overlapping	3.83, overlapping	3.84, dd, 9.6, 3.7	3.85, dd, 9.4, 4.0	3.84, dd, 9.5,4.0
12	-	-	3.05,d,7.04	-	-	-	-	-
13	-	2.56, s	-	2.69, s	2.65, s	2.36, s	2.32, s	2.4, s
1’	3.41,d,7.4	3.41,d,7.4	3.41,d,7.3	3.49,d, 7.3	3.48, overlapping	3.37,d,7.1	3.56,d,6.7	3.42,d,7.1
2’	5.34, tsept, 7.4, 1.5	5.34, tsept, 7.4, 1.5	5.35, tsept, 7.3, 1.5	5.33, tsept, 7.3,1.5	5.40, t sept, 7.3, 1.5	5.25, tsept, 7.1, 1.5	5.09, tsept, 6.7, 1.5	5.20, tsept, 7.1, 1.5
4’	1.74, brs	1.74 s	1.75, s	1.74, brs	1.74, overlapping	1.75, s	1.83, s	1.77, s
5‘	1.74, br s	1.74 s	1.75, s	1.74, brs	1.74, overlapping	1.74,s	1.68, d, 1.2	1.71, d, 1.1

Chemical shifts (δ) are given in ppm and coupling constants (*J*) in Hz

Table S4.2 ^{1}H-NMR data of enzyme products (6-DMATS$_{Sa}$) for L-tryptophan (**1a**), L-abrine (**2a**) and 5-methyl-DL-tryptophan (**5a**) with the prenyl donor GPP in CD_3OD

	6-Geranyl-L-Trp (1c) 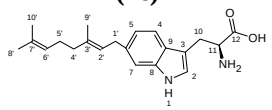	**6-Geranyl-L-abrine (2c)** 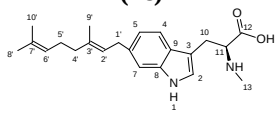	**6-Geranyl-5-methyl-DL-Trp (5c)** 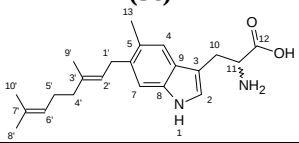
Pos.	δ_H, multi., *J*	δ_H, multi., *J*	δ_H, multi., *J*
2	7.12, s	7.14, s	7.07, s
4	7.59, d, 8.2	7.58, d, 8.2	7.48, s
5	6,89, dd, 8.2, 1.4	6.90, dd, 8.2, 1.4	-
7	7.16, dd, 1.4, 0.7	7.15, dd, 1.4, 0.7	7.14, s
10	3.49, dd, 15.0, 4.0 3.10, dd, 15.0, 9.4	3.44, dd, 15.5, 4.6 3.23, dd, 15.5, 8.0	3.46, dd, 15.2, 4.0 3.06, dd, 15.2, 9.6
11	3,82, dd, 9.4, 4.0	3.73, dd, 8.0, 4.6	3.82, dd, 9.6, 4.0
13	-	2.55, s	2.36, s
1’	3.42, d, 7.4	3.42, d, 7.4	3.38, d, 6.8
2’	5.34, tsept, 7.4, 1.4	5.35, tsept, 7.4, 1.4	5.24, m
4’	2.12, m	2.11, m	2,12, m
5’	2.04, m	2.04, m	2.04, m
6’	5.11, tsept, 6.9, 1.4	5.11, tsept, 6.9, 1.4	5.10, m
8’	1.74, s	1.74, s	1.74, s
9’	1.66, s	1.66, s	1.65, s
10’	1.59, s	1.59, s	1.59, s

Chemical shifts (δ) are given in ppm and coupling constants (*J*) in Hz

Table S5. ^{1}H-NMR data of enzyme products (6-DMATS$_{Sa}$) for selected dihydroxynaphthalenes obtained in CD_3OD

	7 or 6-DMA-1,3-dihydroxynaphthalene (8b)	**4-DMA-1,7-dihydroxynaphthalene (9b)**	**6-DMA-2,3-dihydroxynaphthalene (10b)**
	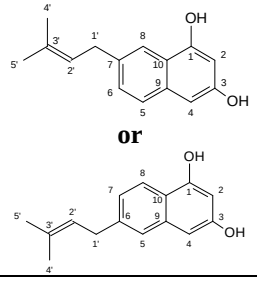 **or**	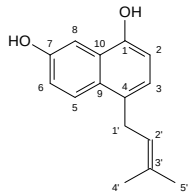	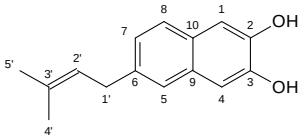
Pos.	δ_H, multi., *J*	δ_H, multi., *J*	δ_H, multi., *J*
1	-	-	7.04, s
2	6.56, d, 2.1	6.63, d, 7.6	-
3	-	6.87, d, 7.6	-
4	6.43, d, 2.1	-	7.01, s
5	7.44, d, 8.4 7.15, dd, 8.4, 1.8 7.80, br s	7.77, d, 9.1	7.29, br s
6		7.04, dd, 9.1, 2.6	-
7		-	7.02, dd, 8.4, 1.8
8		7.48, d, 2.6	7.45, d, 8.4
1‘	3.42, d, 7.4,	3.59, d, 6.9	3.40, d, 7.4
2‘	5,37, tsept, 7.4, 1.4	5.31, tsept, 6.9, 1.4	5.36, tsept, 7.4, 1.4
4‘	1.76, s	1.78, s	1,76, s
5‘	1.76, s	1.73, s	1.76, s

Chemical shifts (δ) are given in ppm and coupling constants (*J*) in Hz.

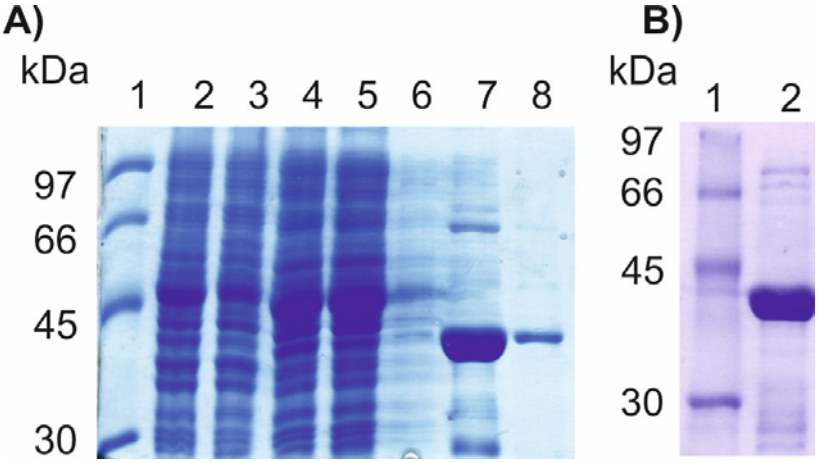

Figure S1. SDS-PAGE analysis of the recombinant proteins SAML0654 (**A)** and of Strvi8510 (**B).** A) Lane 1: molecular mass standard; lane 2: total protein before induction; lane 3: total protein after IPTG induction, lane 4: soluble protein fraction, lane 5: flow through fraction, lane 6: wash fraction of Ni-NTA-agarose; lanes 7 and 8: purified SAML0654-His_6. B) Lane 1: molecular mass standard, lane 2: purified His_8- Strvi8510.

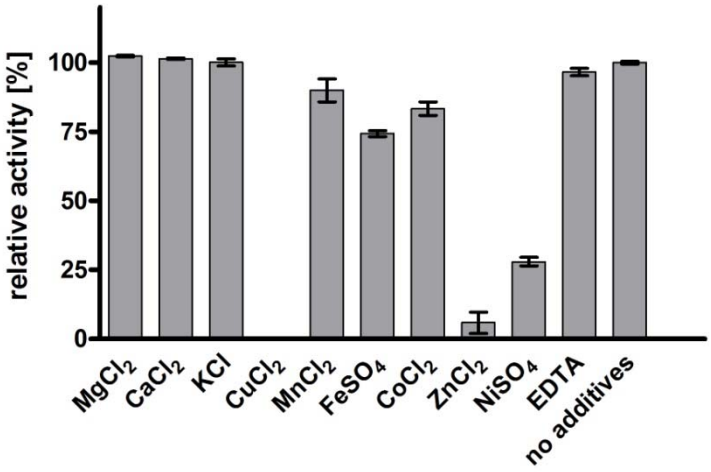

Figure S2. Ion dependency of the 6-$DMATS_{Sa}$ reaction
The enzyme assays containing 1 mM L-tryptophan, 1 mM DMAPP, 5 mM metal ions and were incubated with 1.2 µM protein for 2 h. The enzyme activity without additives was defined as 100 %.

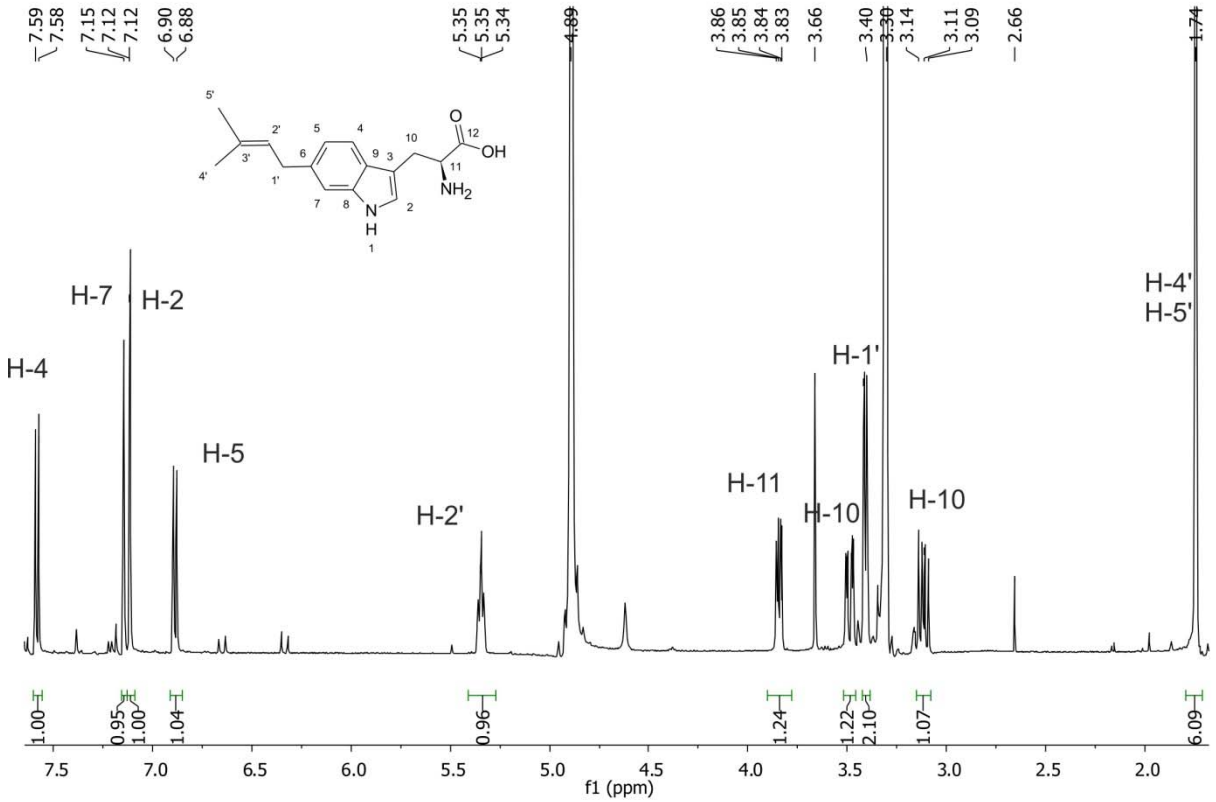

Figure S3.1. [1]H-NMR spectrum of **1b** in CD_3OD (500 MHz)

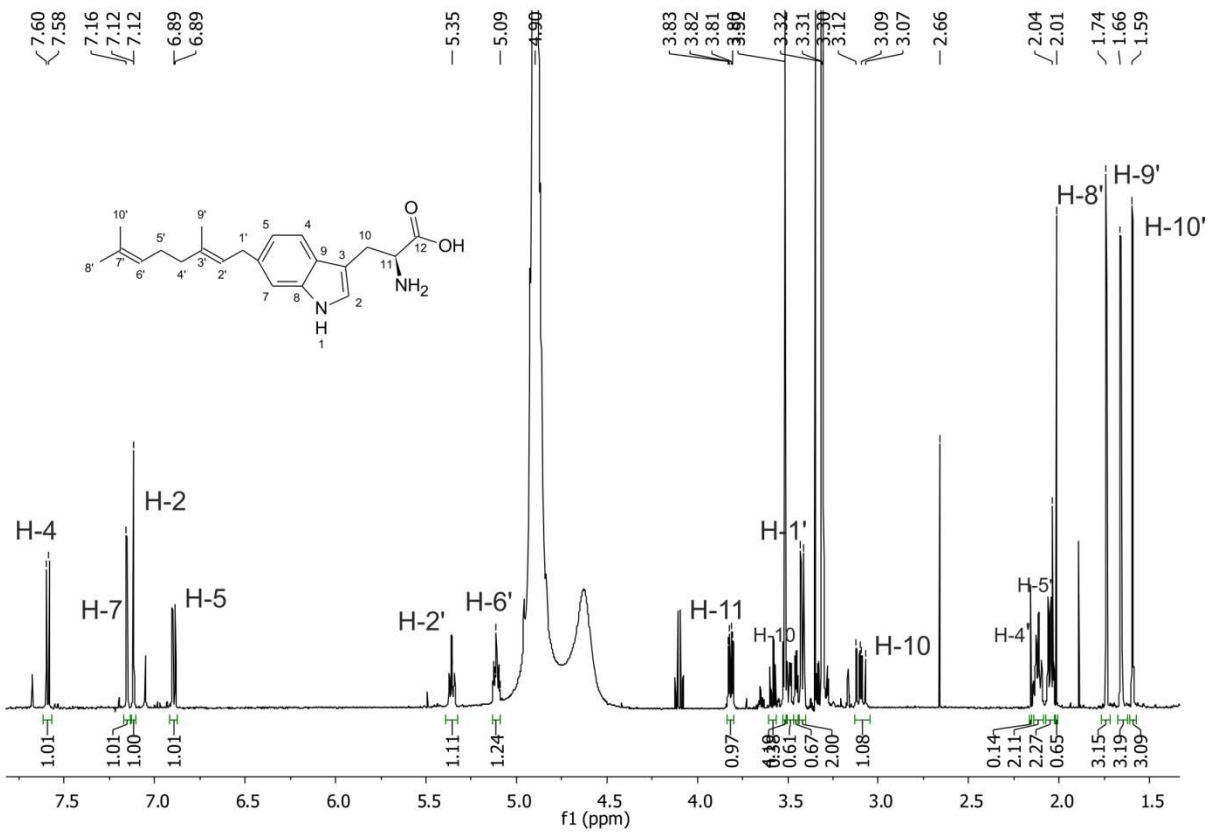

Figure S3.2. [1]H-NMR spectrum of **1c** in CD_3OD (500 MHz)

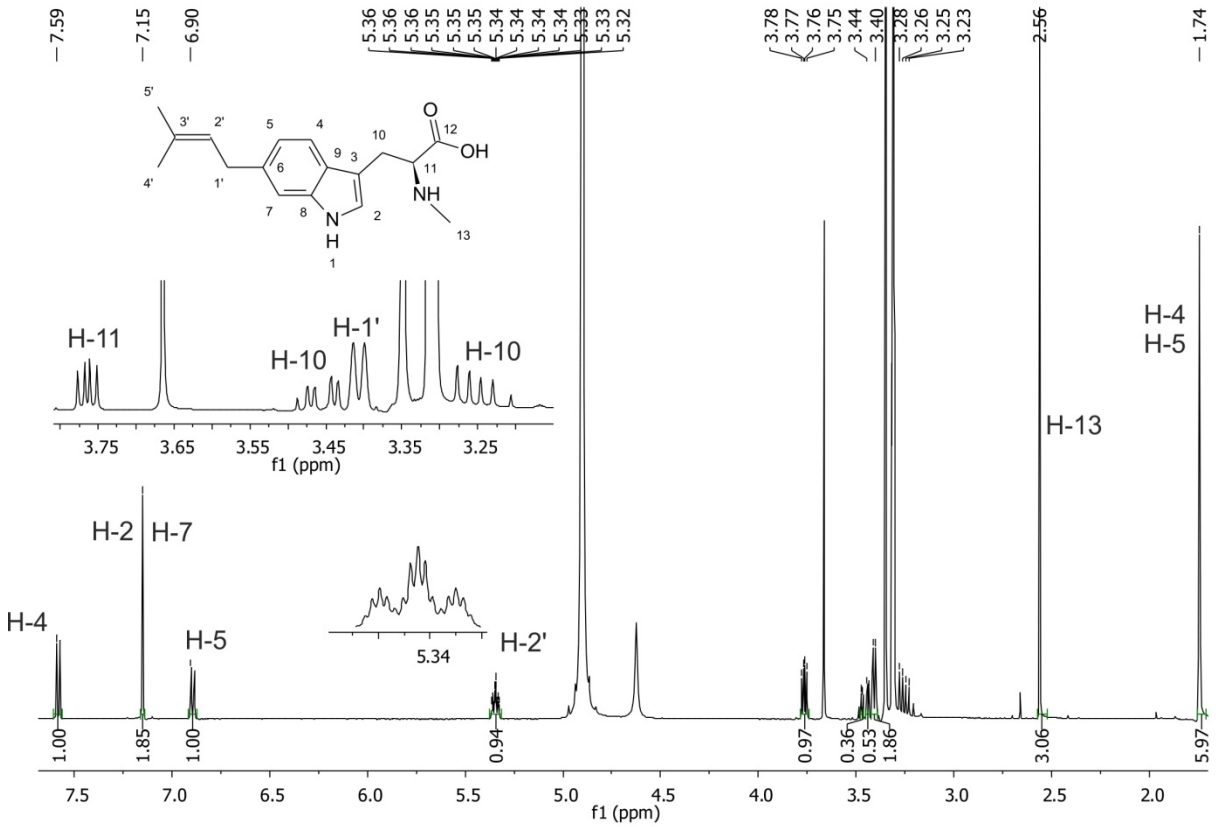

Figure S3.3. ^{1}H-NMR spectrum of **2b** in CD_3OD (500 MHz)

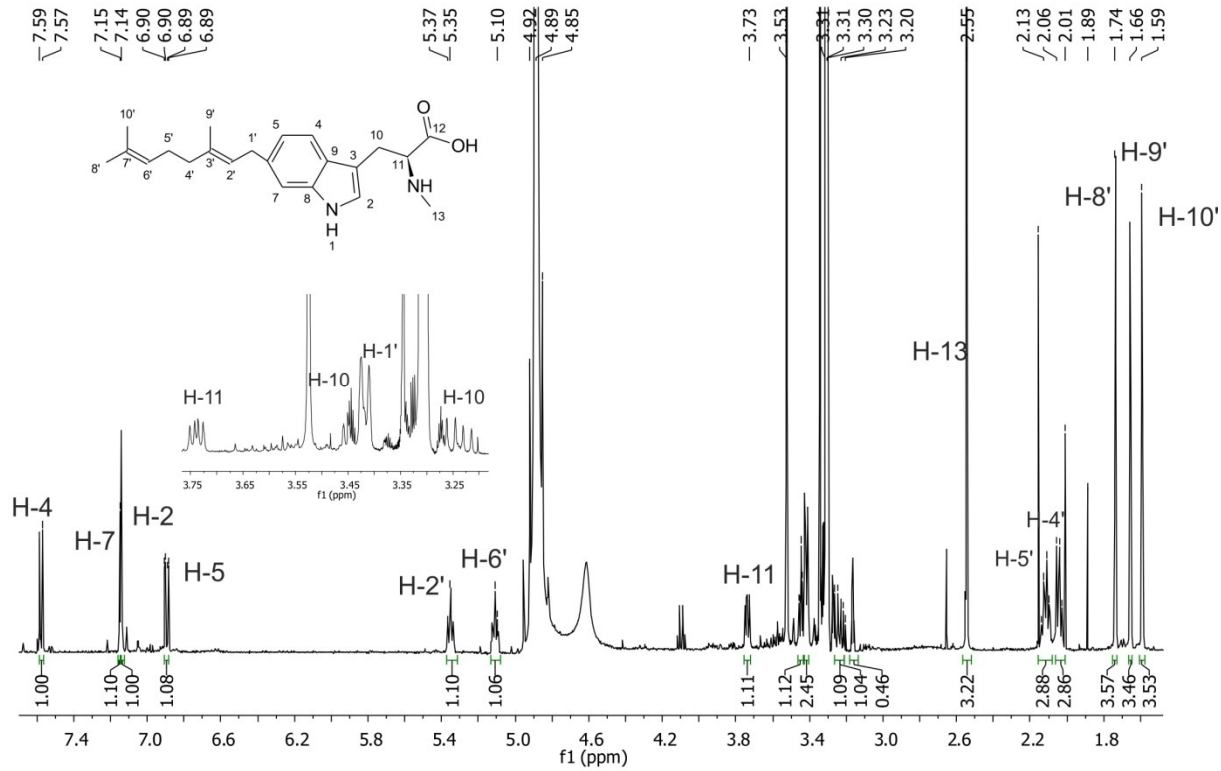

Figure S3.4. ^{1}H-NMR spectrum of **2c** in CD_3OD (500 MHz)

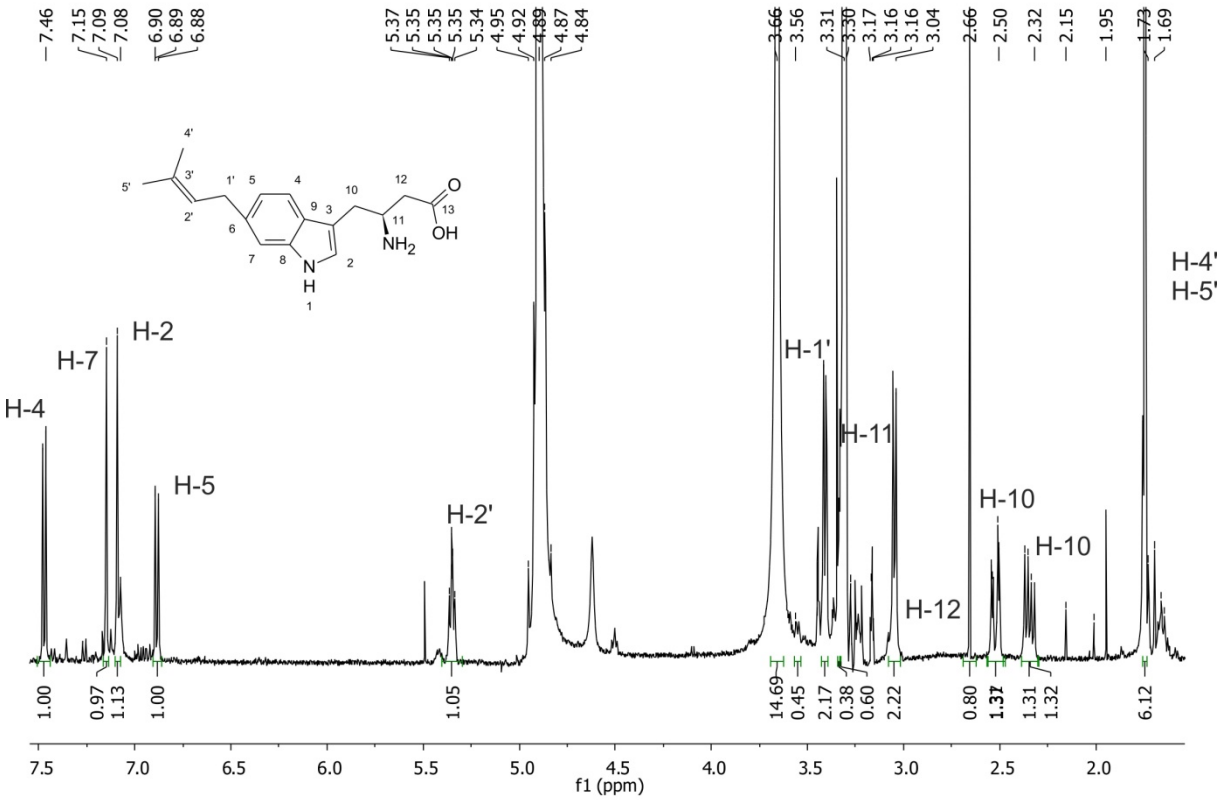

Figure S3.5. ^{1}H-NMR spectrum of **3b** in CD_3OD (500 MHz)

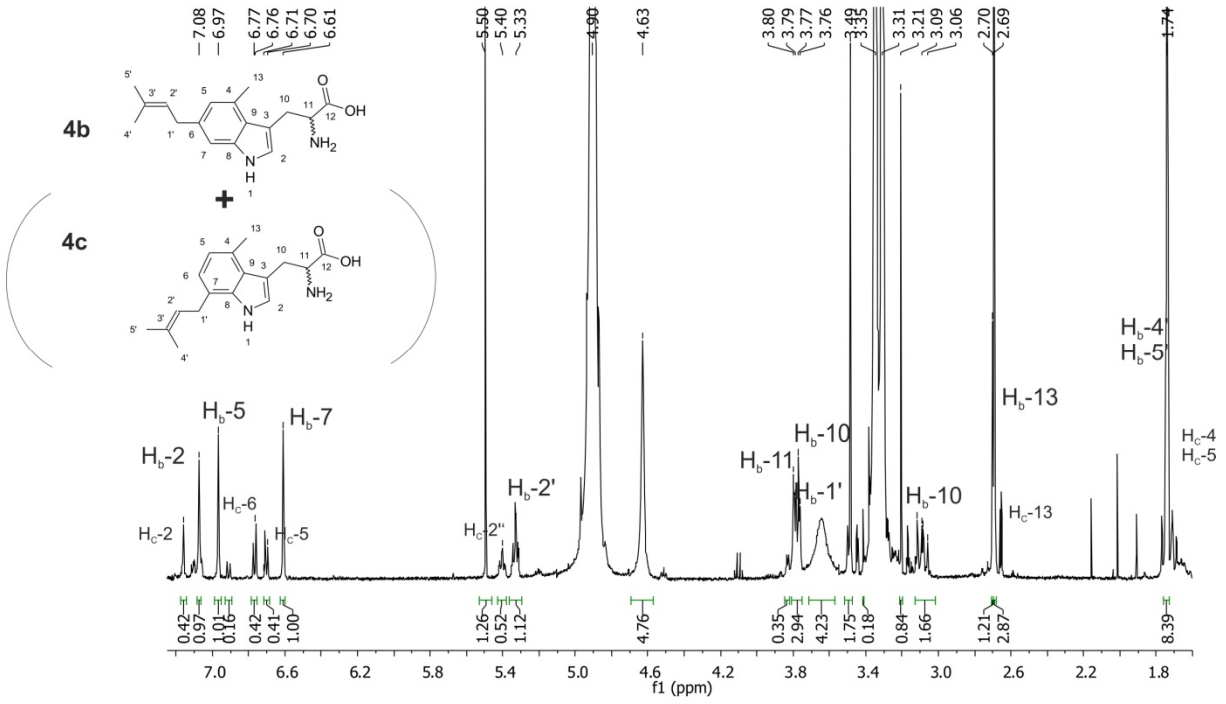

Figure S3.6. ^{1}H-NMR spectrum of **4b** and **4c** in CD_3OD (500 MHz)

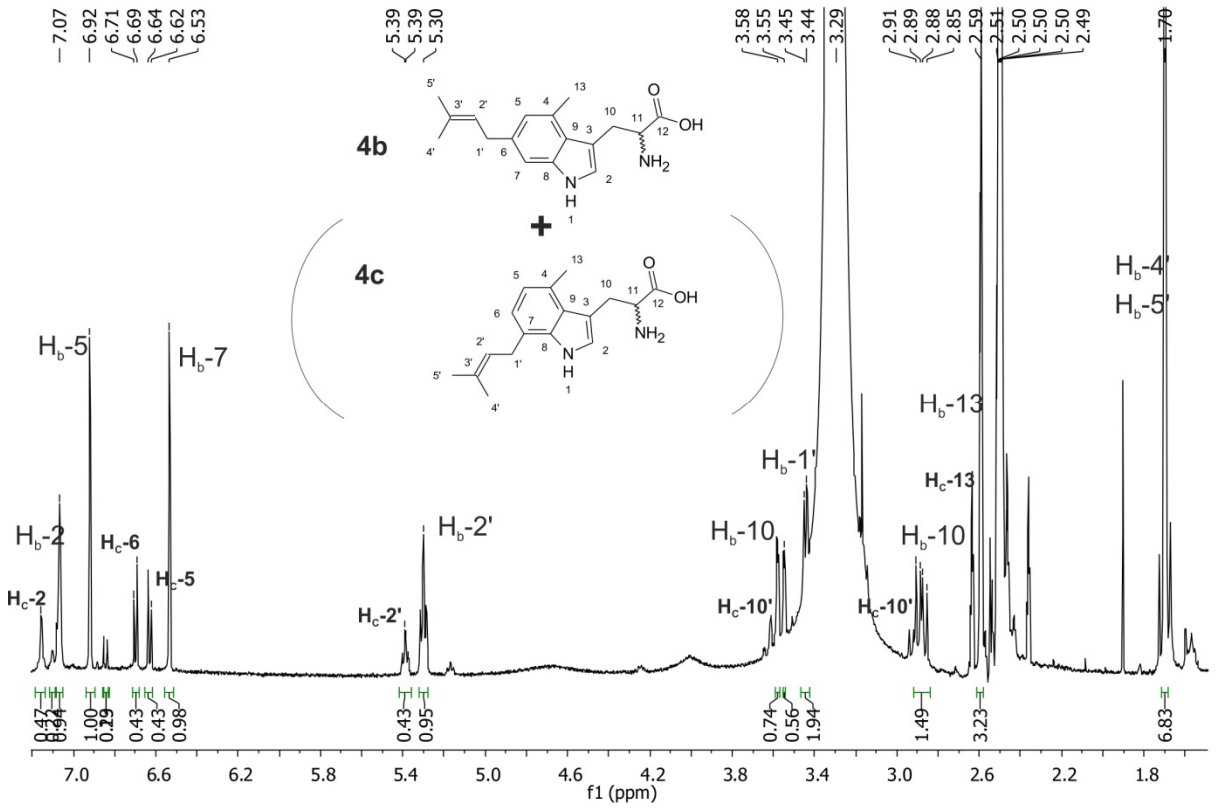

Figure S3.7. [1]H-NMR spectrum of **4b** and **4c** in DMSO-d_6 (500 MHz)

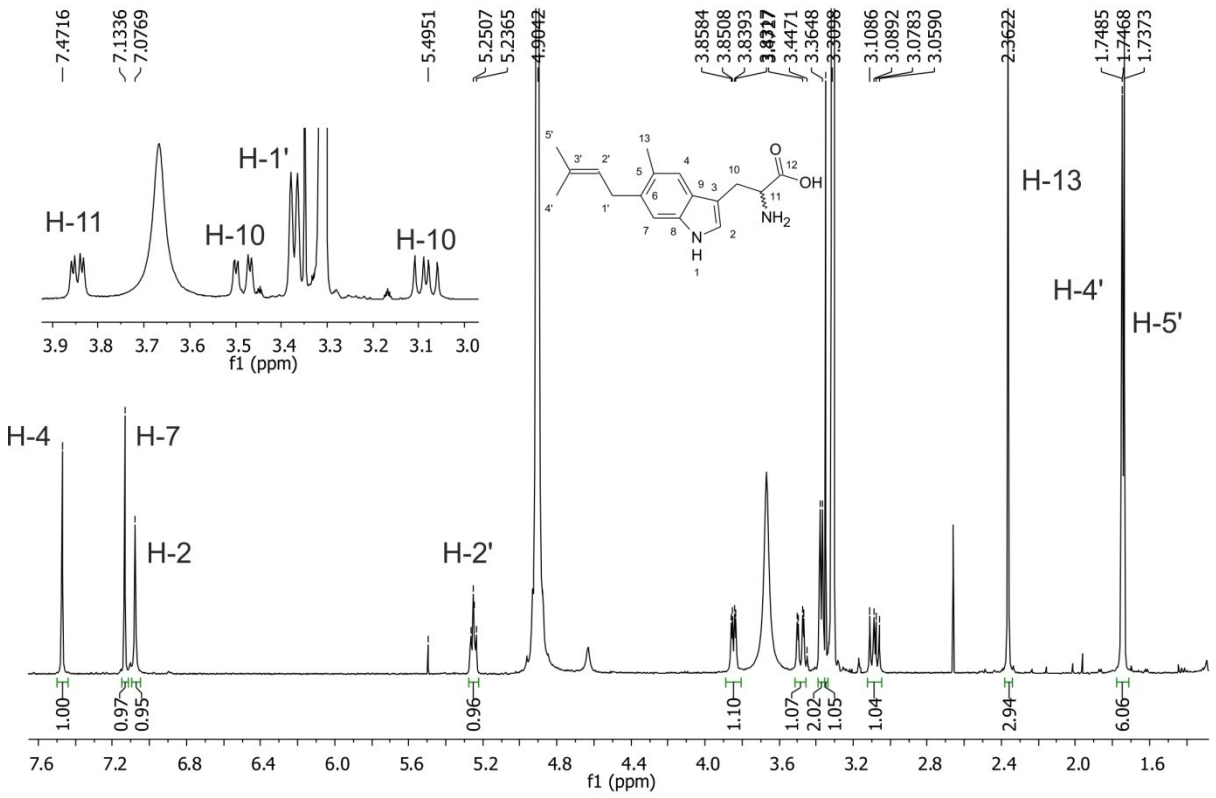

Figure S3.8. [1]H-NMR spectrum of **5b** in CD_3OD (500 MHz)

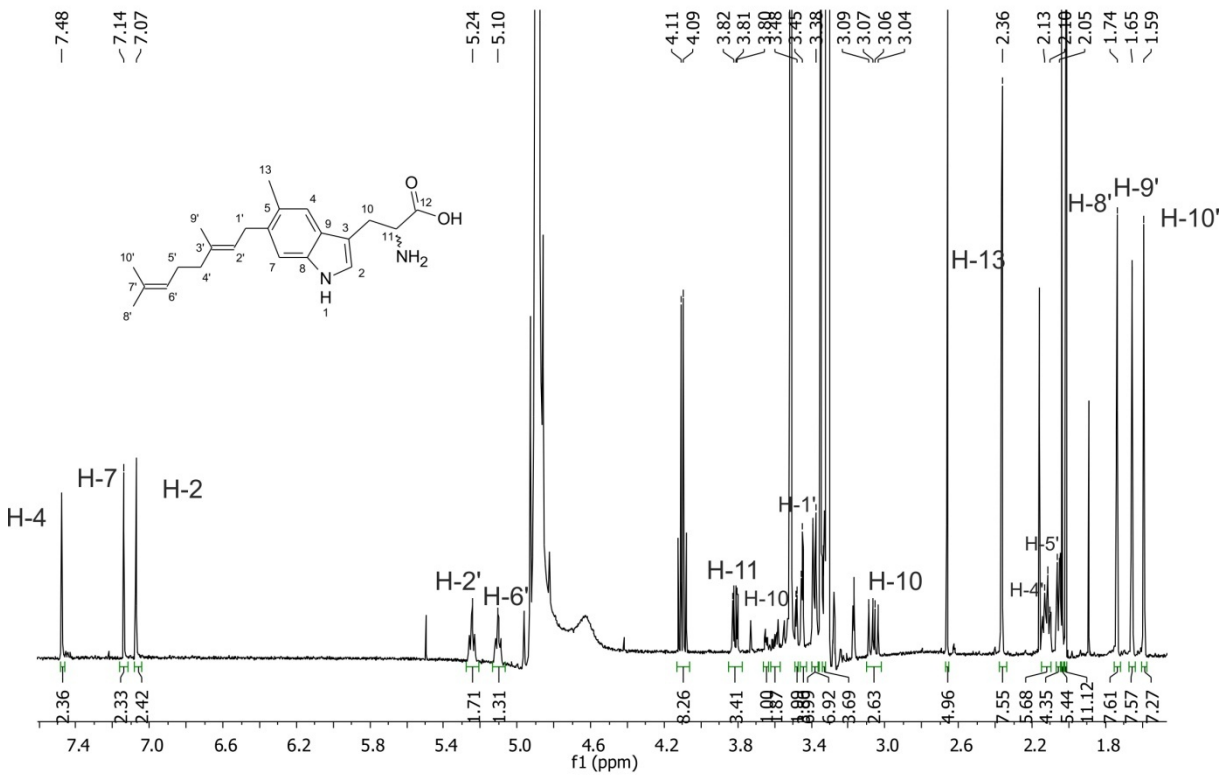

Figure S3.9. [1]H-NMR spectrum of **5c** in CD_3OD (500 MHz)

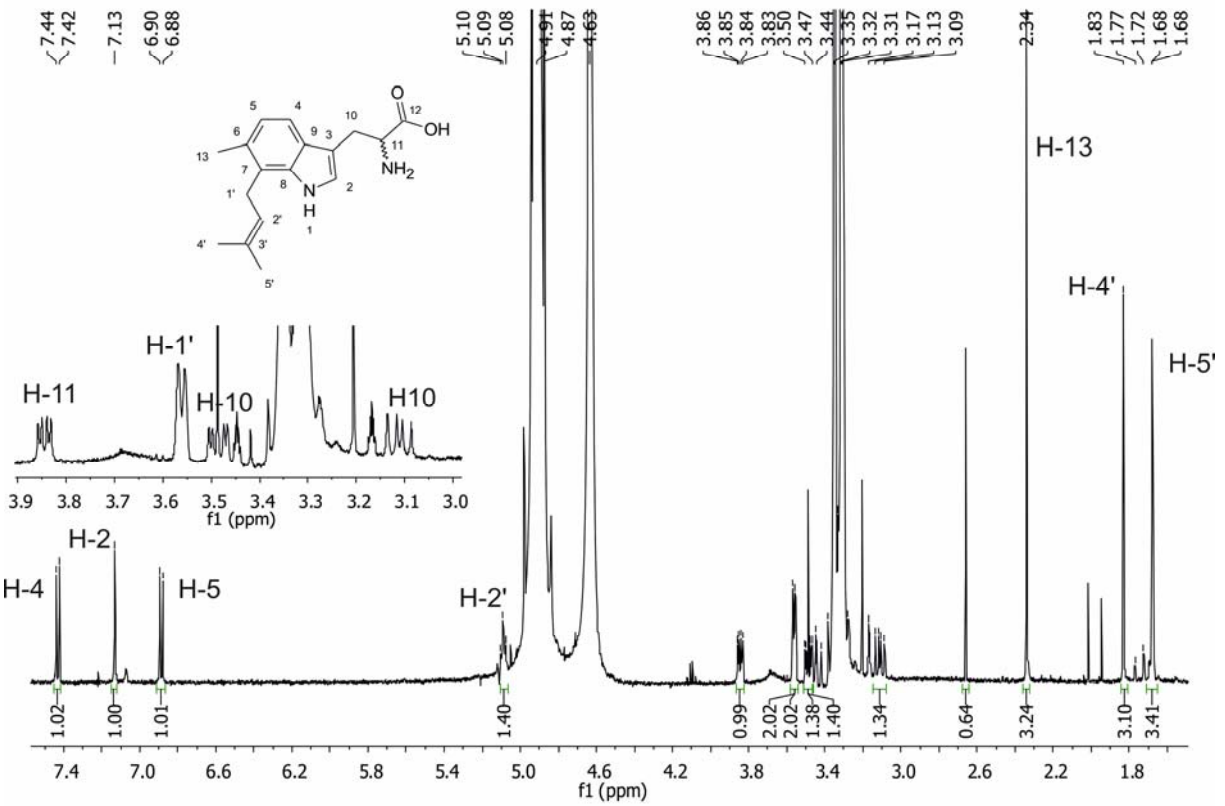

Figure S3.10. [1]H-NMR spectrum of **6b** in CD_3OD (500 MHz)

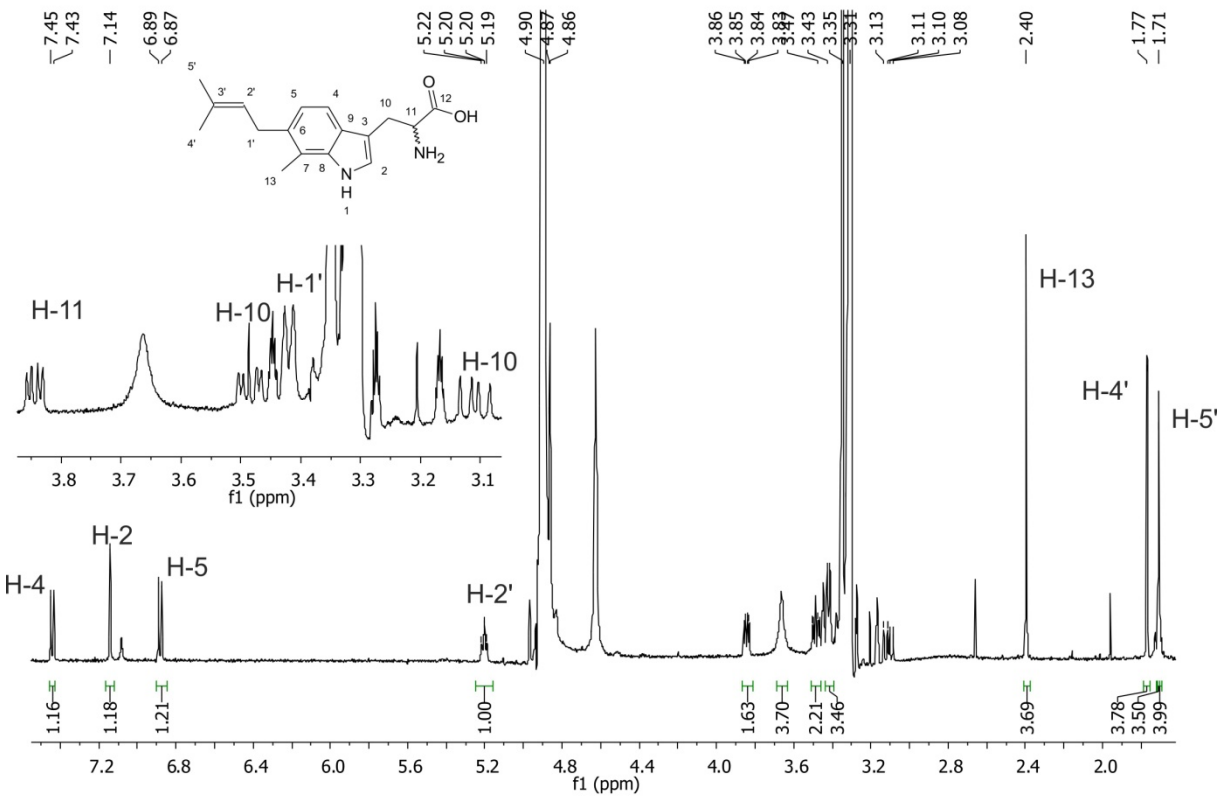

Figure S3.11. [1]H-NMR spectrum of **7b** in CD_3OD (500 MHz)

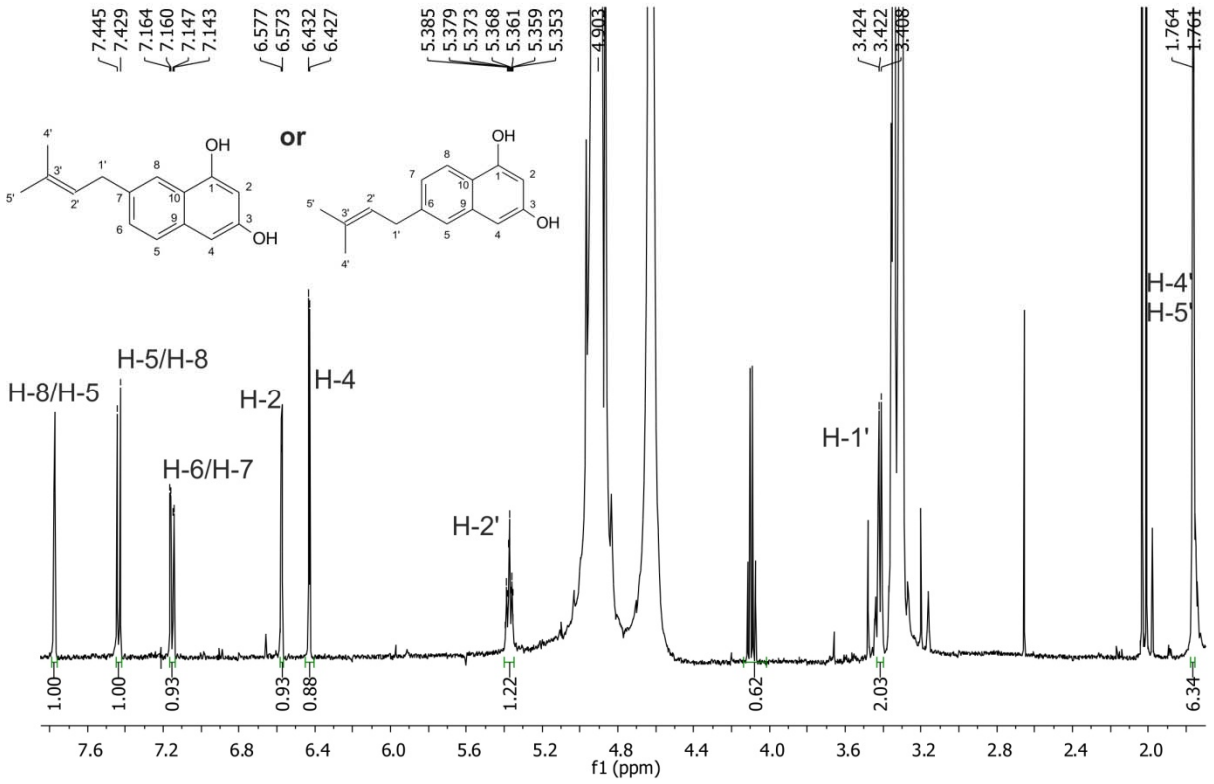

Figure S3.12. [1]H-NMR spectrum of **8b** in CD_3OD (500 MHz)

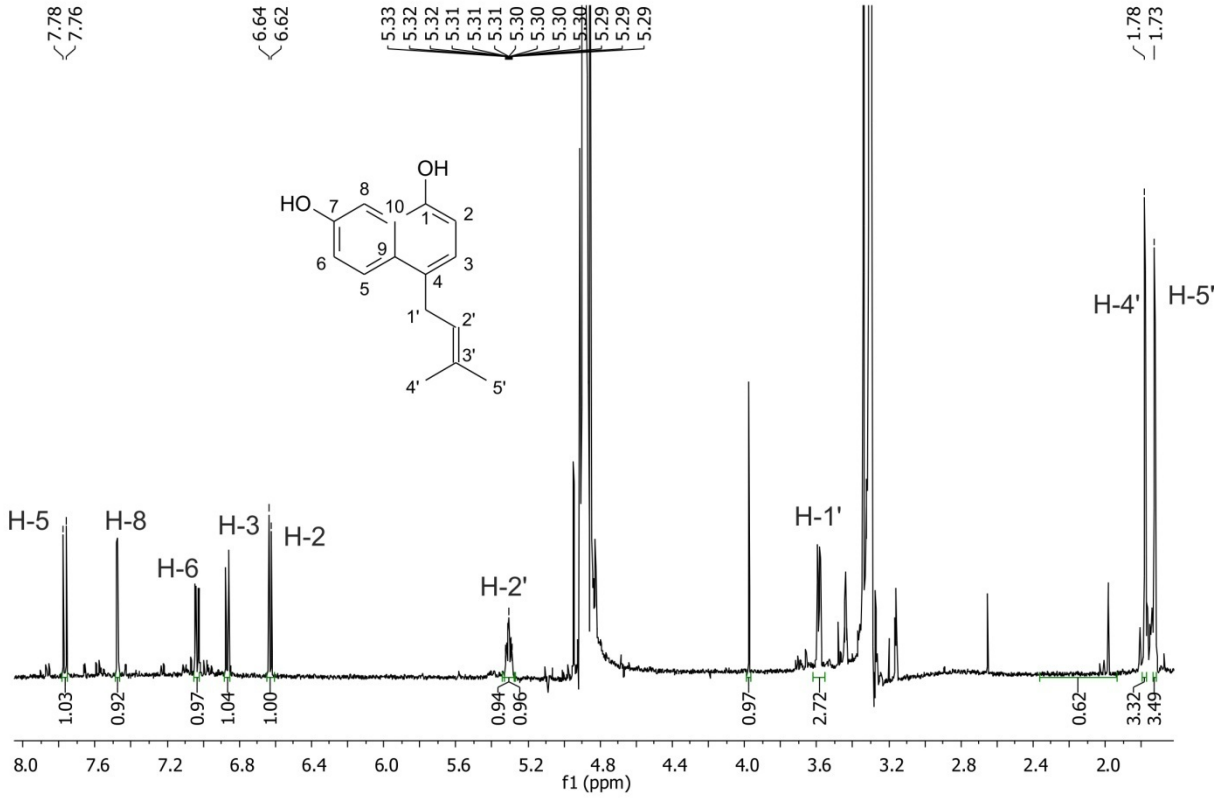

Figure S3.13. [1]H-NMR spectrum of **9b** in CD_3OD (500 MHz)

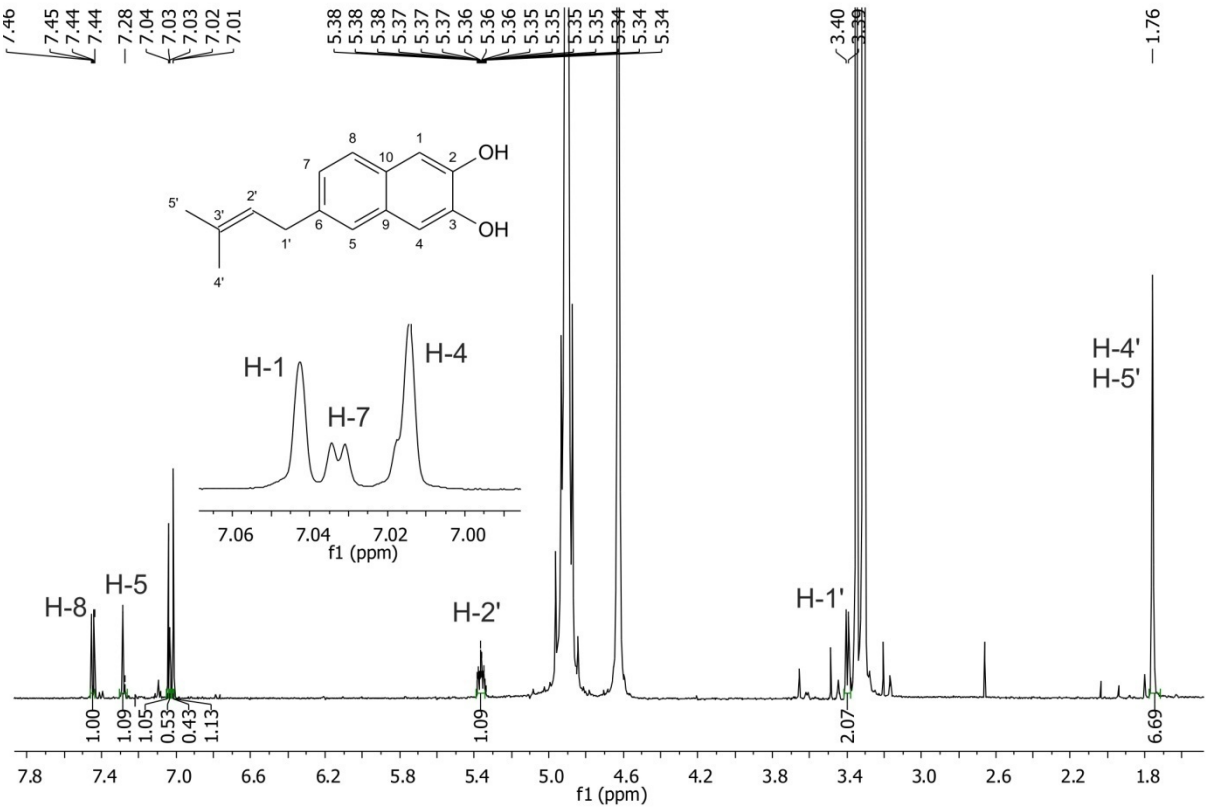

Figure S3.14. [1]H-NMR spectrum of **10b** in CD_3OD (500 MHz)

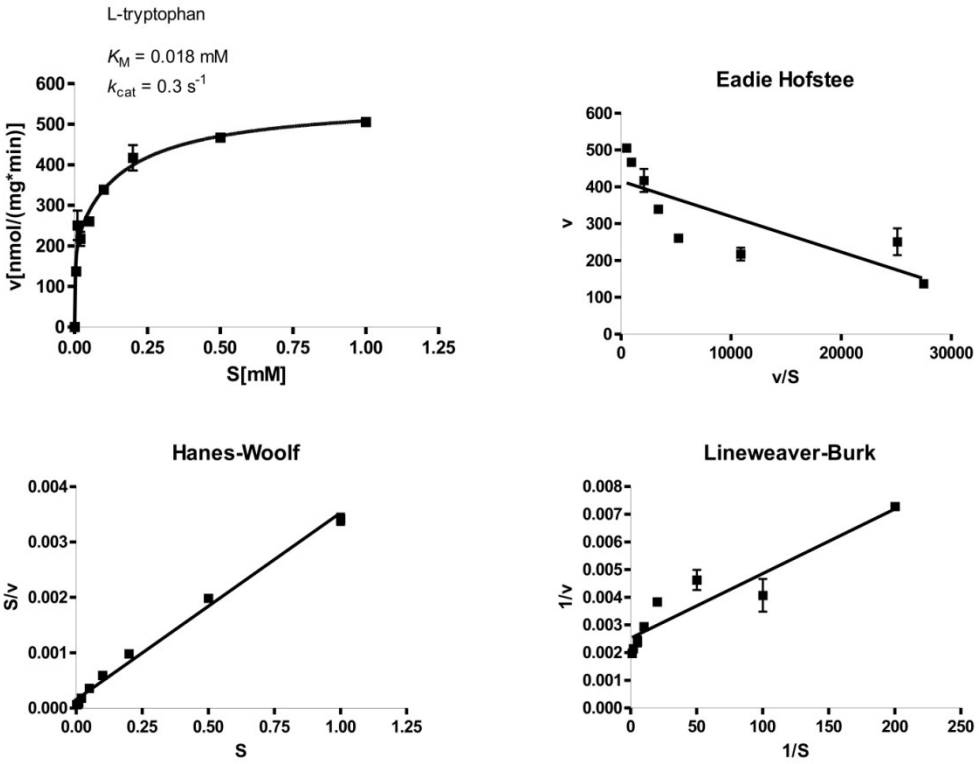

Figure S4.1. Dependence of product formation on L-tryptophan (**1a**) concentrations

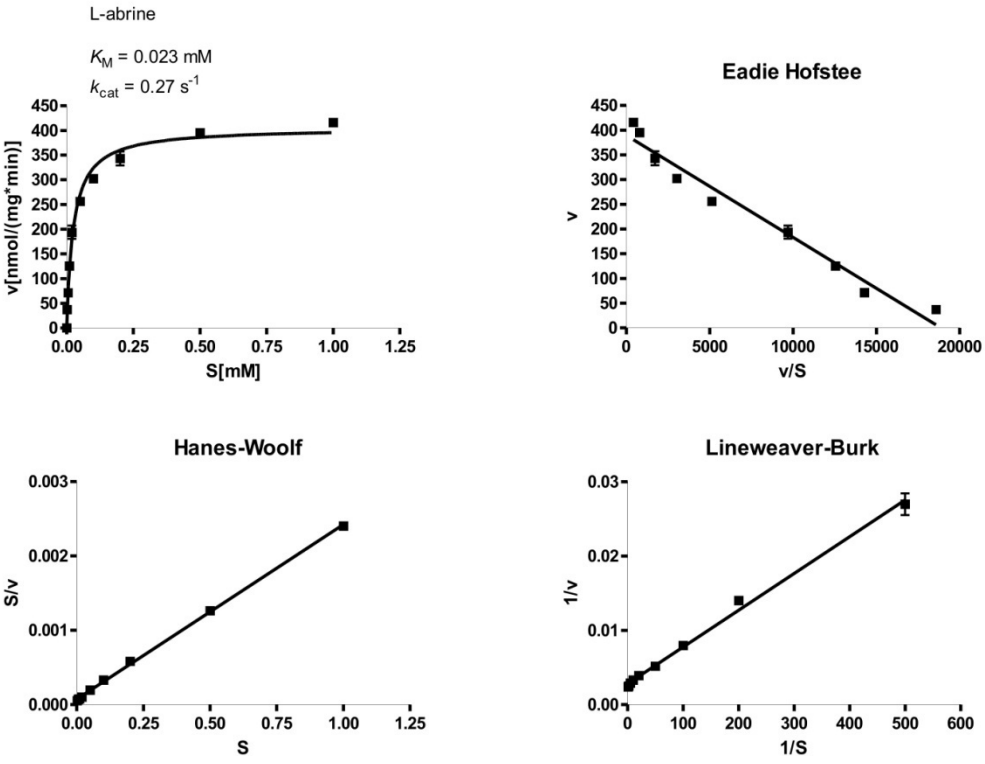

Figure S4.2. Dependence of product formation on L-abrine (**2a**) concentrations

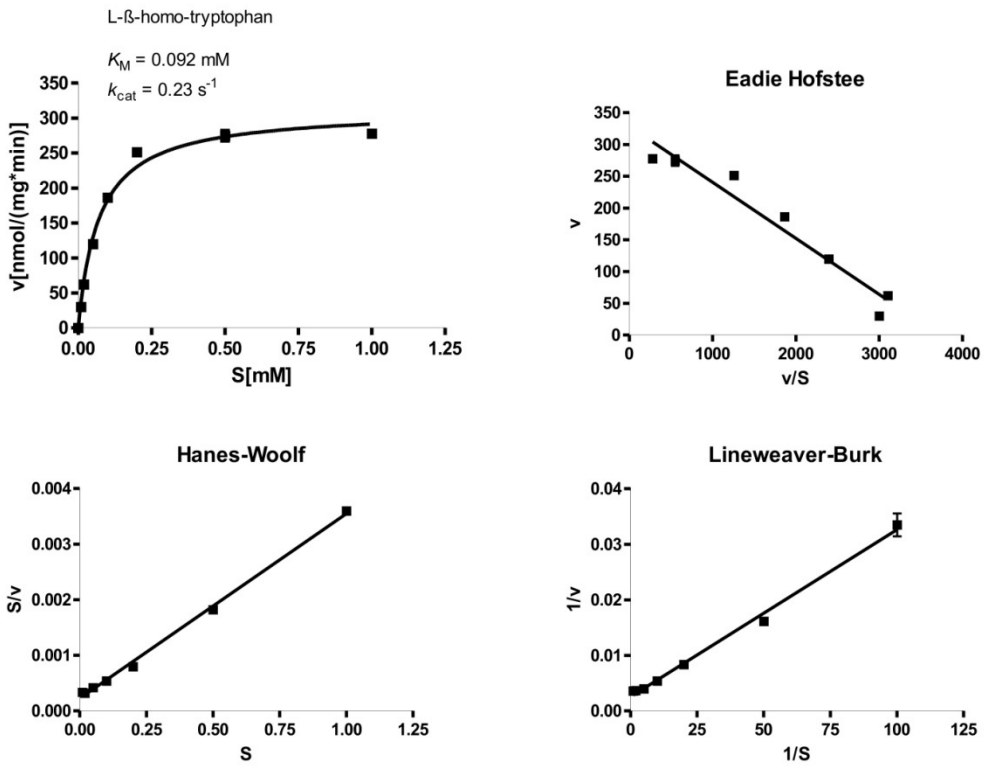

Figure S4.3. Dependence of product formation on L-ß-homotryptophan (**3a)** concentrations

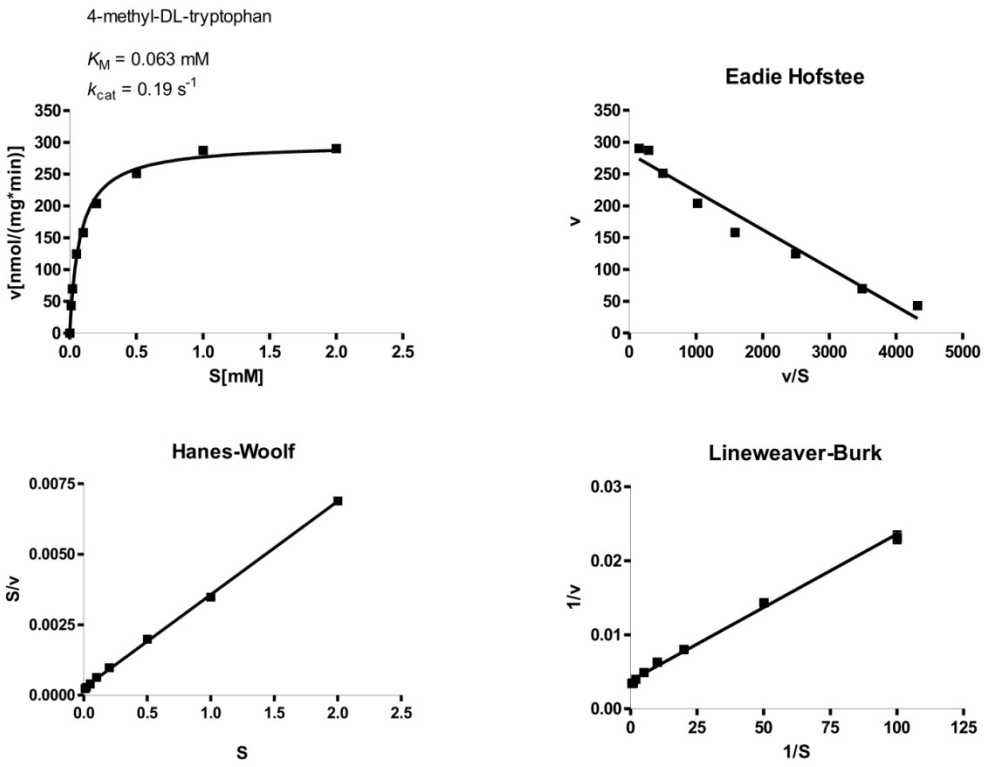

Figure S4.4. Dependence of product formation on 4-methyl-DL-tryptophan (**4a**) concentrations

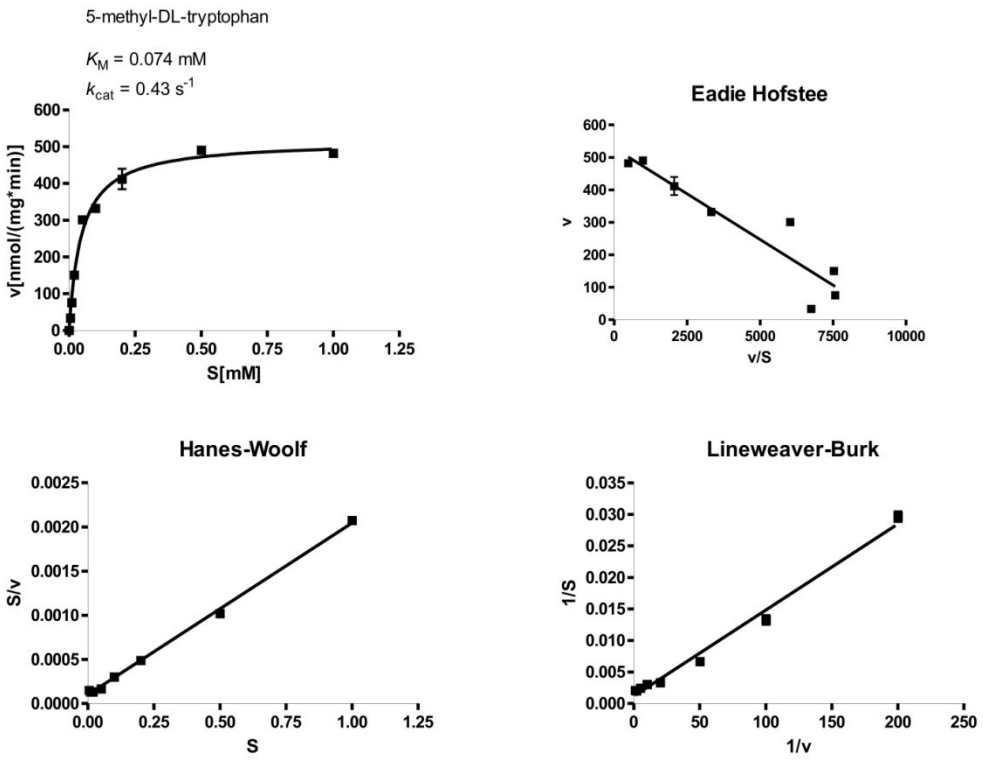

Figure S4.5. Dependence of product formation on 5-methyl-DL-tryptophan (**5a**) concentrations

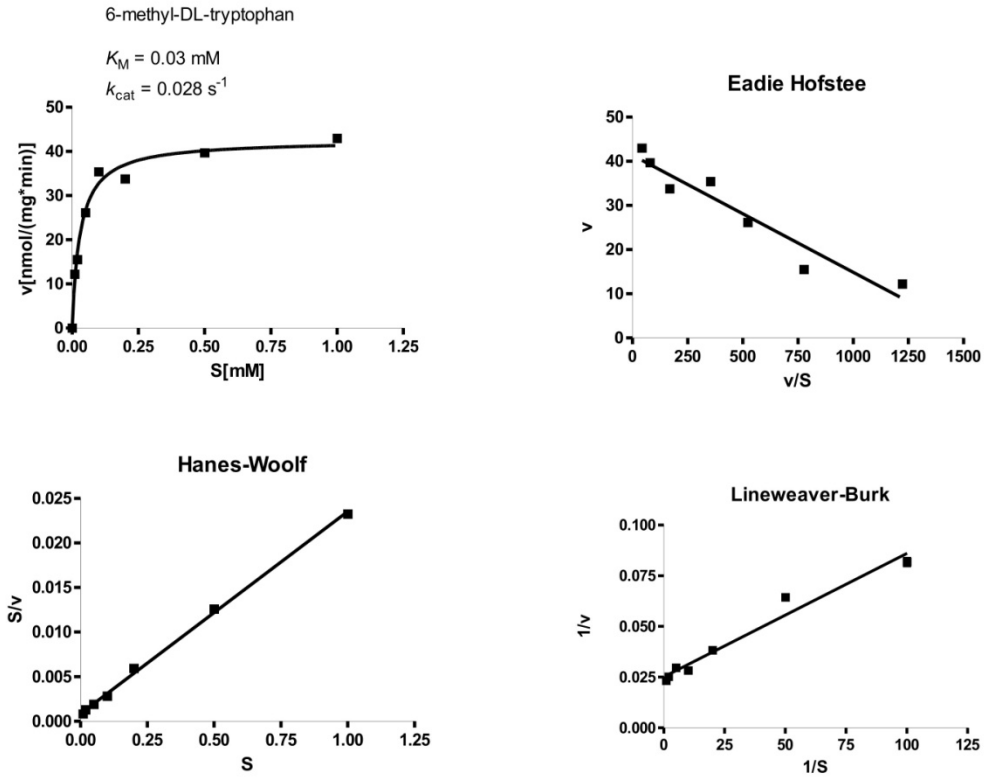

Figure S4.6. Dependence of product formation on 6-methyl-DL-tryptophan (**6a**) concentrations

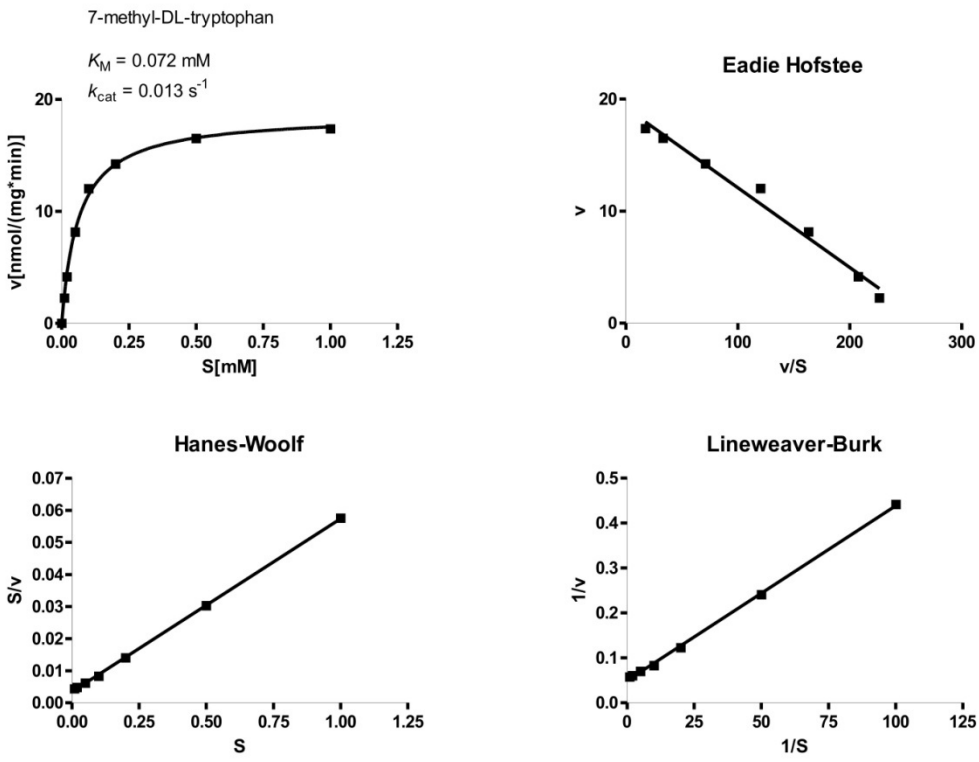

Figure S4.7. Dependence of product formation on 7-methyl-DL-tryptophan (**7a**) concentrations

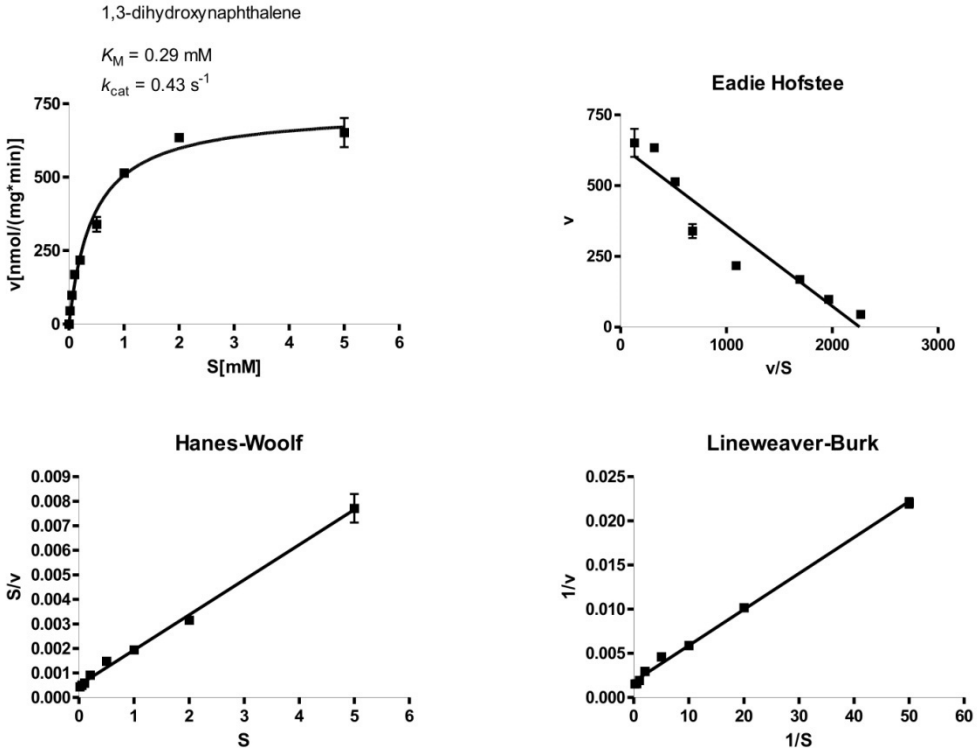

Figure S4.8. Dependence of product formation on 1,3-dihydroxynaphthalene (**8a**) concentrations

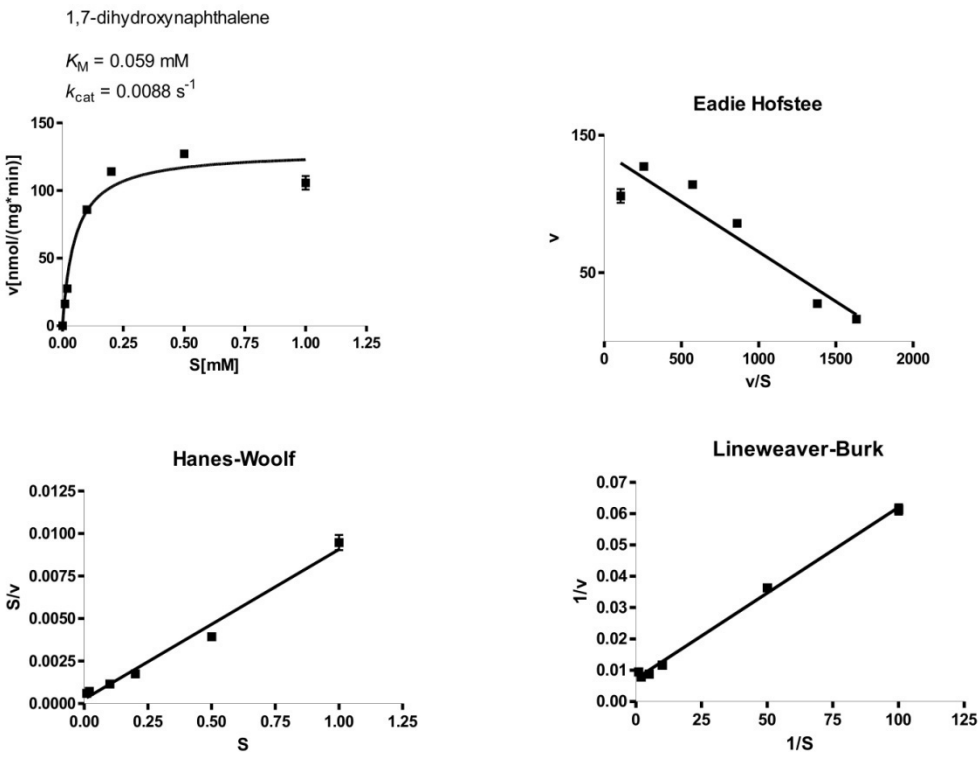

Figure S4.9. Dependence of product formation on 1,7-dihydroxynaphthalene (**9a**) concentrations

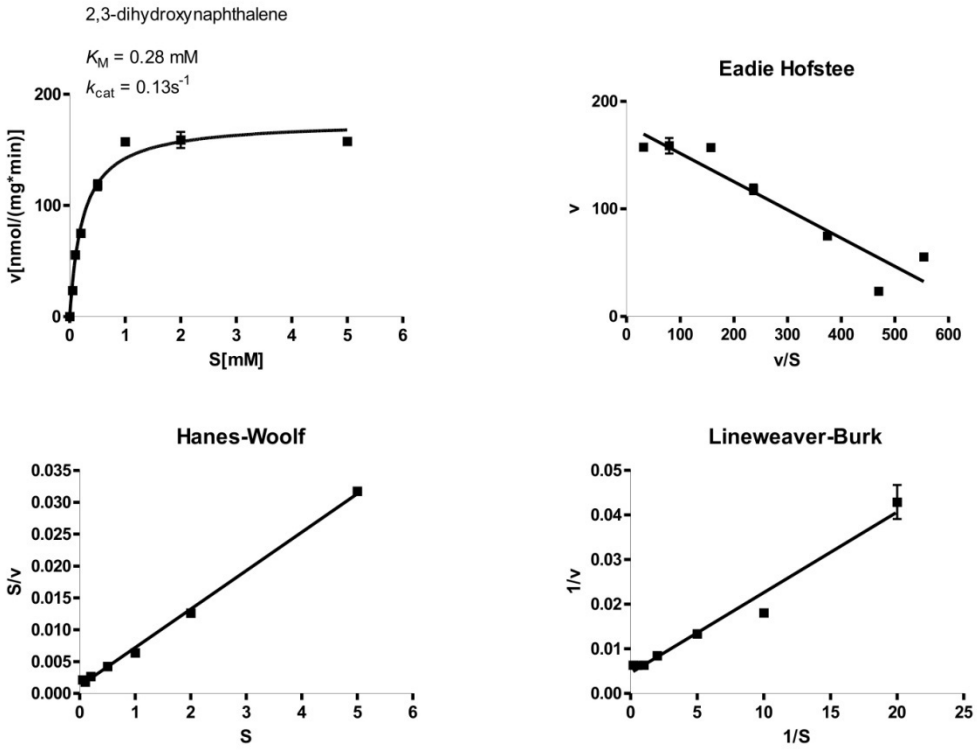

Figure S4.10. Dependence of product formation on 2,3-dihydroxynaphthalene (**10a**) concentrations

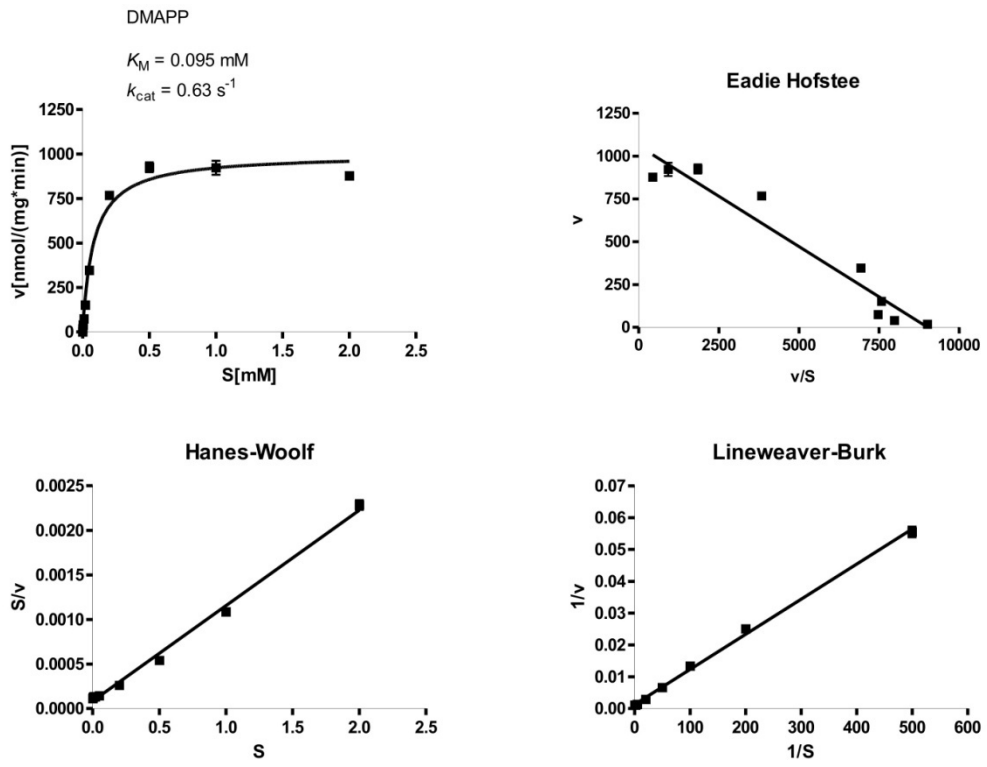

Figure S4.11. Dependence of product formation on DMAPP concentrations in the presence of L-tryptophan (**1a**)

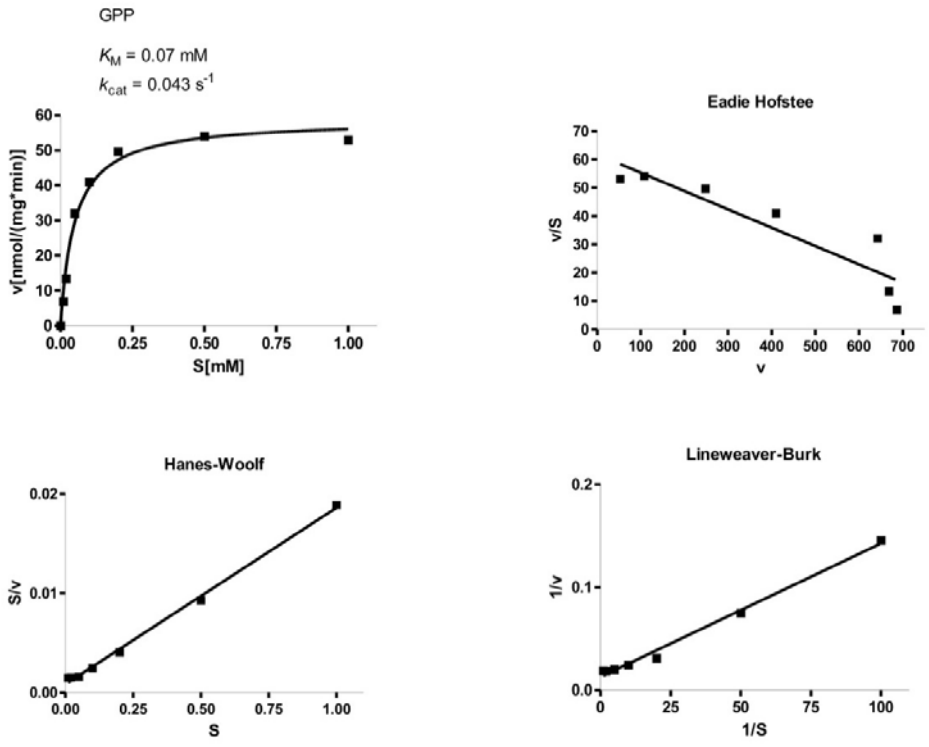

Figure S4.12. Dependence of product formation on GPP concentrations in the presence of L-tryptophan (**1a**)

4.2. Tryptophan *C5*-, *C6*- and *C7*-prenylating enzymes displaying a preference for C-6 of the indole ring in the presence of unnatural dimethylallyl diphosphate analogues

Advanced Synthesis & Catalysis

DOI: 10.1002/adsc.201400958

Tryptophan *C5*-, *C6*- and *C7*-Prenylating Enzymes Displaying a Preference for C-6 of the Indole Ring in the Presence of Unnatural Dimethylallyl Diphosphate Analogues

Julia Winkelblech,[+a,b] Mike Liebhold,[+a] Jakub Gunera,[b,c] Xiulan Xie,[d] Peter Kolb,[b,c] and Shu-Ming Li[a,b,*]

[a] Philipps-Universität Marburg, Institut für Pharmazeutische Biologie und Biotechnologie, Deutschhausstrasse 17A, 35037 Marburg, Germany
Fax: (+49)-6421-282-5365; phone: (+49)-6421-282-2461; e-mail: shuming.li@staff.uni-marburg.de
[b] Philipps-Universität Marburg, Zentrum für Synthetische Mikrobiologie, 35032 Marburg, Germany
[c] Philipps-Universität Marburg, Institut für Pharmazeutische Chemie, Marbacher Weg 6, 35032 Marburg, Germany
[d] Philipps-Universität Marburg, Fachbereich Chemie, Hans-Meerwein-Strasse, 35032 Marburg, Germany
[+] These authors contributed equally to this work.

Received: October 2, 2014; Revised: December 28, 2014; Published online: March 13, 2015

Supporting information for this article is available on the WWW under http://dx.doi.org/10.1002/adsc.201400958.

Abstract: The behavior of four dimethylallyltryptophan synthases (DMATSs) (5-DMATS and 5-$DMATS_{Sc}$ as tryptophan *C5*-prenyltransferases, and 6-$DMATS_{Sa}$ and 6-$DMATS_{Sv}$ as *C6*-prenyltransferases) and one L-tyrosine prenyltransferase with a tryptophan *C7*-prenyltransferase activity was investigated in the presence of two unnatural alkyl donors (methylallyl and 2-pentenyl diphosphate) and one benzyl donor (benzyl diphosphate). Detailed biochemical investigations revealed the acceptance of these dimethylallyl diphosphate (DMAPP) analogues by all tested enzymes with different relative activities. Enzyme products with the allyl or benzyl moiety attached to different positions were identified in the reaction mixtures, whereby C-6 alkylated or benzylated L-tryptophan was found as one of the main products. This observation demonstrates a preference of the five prenyltransferases toward C-6 of the indole ring in the presence of unnatural DMAPP derivatives. Molecular dynamics simulation experiments with a homologous model of 5-DMATS explained well its reactions with methylallyl and 2-pentenyl diphosphate. Furthermore this study expands significantly the potential usage of tryptophan prenylating enzymes as biocatalysts for Friedel–Crafts alkylation.

Keywords: dimethylallyltryptophan synthase; enzyme catalysis; Friedel–Crafts alkylation; prenyltransferase; regioselectivity

Introduction

Secondary metabolites with biological activities represent an important source for medicinal research and drug development.[1,2] They are widely distributed in nature, especially in plants and microorganisms.[1–3] Among microorganisms, fungi of Ascomycetes and bacteria of Actinomycetes are important producers of biologically active compounds.[3,4] Due to significant progress in genome sequencing and genome mining, a number of gene clusters involved in the biosynthesis of such metabolites have been identified in recent years.[4–8] A large group of natural products comprises the prenylated aromatic substances derived from prenyl diphosphate and an aromatic scaffold from different pathways.[9,10] Prenyltransferases catalyze the linkage of these two residues and play an important role in the structural diversity of these compounds. Indole prenyltransferases belong to the ***d****i****m***ethyl***a***llyl-***t***ryptophan ***s***ynthase (DMATS) superfamily, which catalyze the underlying prenylation reaction of indole derivatives in nature, and represent one of the most investigated class of prenyltransferases.[11] In the presence of the natural prenyl donor dimethylallyl diphosphate (DMAPP), most members of this superfamily usually show remarkable flexibility toward their aromatic substrates, but high regioselectivity of the prenylation position on the indole ring.[12–15] These characteristics were observed for fungal tryptophan prenyltransferases, e.g., FgaPT2, 5-DMATS and 7-

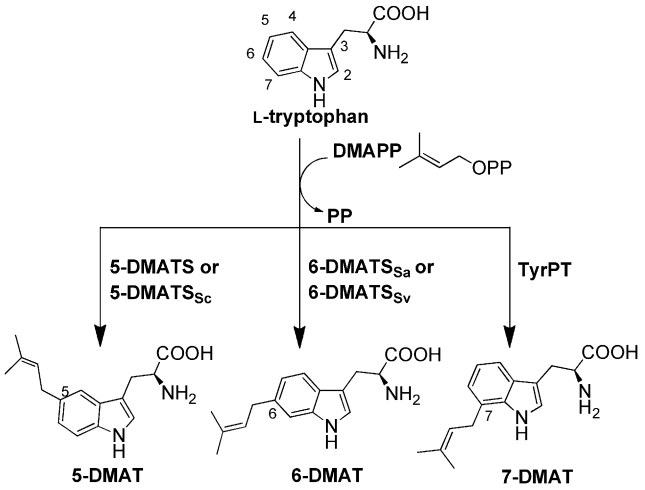

Scheme 1. Regiospecific prenylation of tryptophan by the five prenyltransferases used in this study in the presence of their natural prenyl donor DMAPP. Origin of the enzymes: 6-DMATS$_{Sa}$ from *Streptomyces ambofaciens*, 6-DMATS$_{Sv}$ from *Streptomyces violaceusniger*, 5-DMATS from *Aspergillus clavatus*, 5-DMATS$_{Sc}$ from *Streptomyces coelicolor* and TyrPT from *Aspergillus niger*.

DMATS from different *Aspergillus* spp., which catalyze tryptophan *C4*-, *C5*- and *C7*-prenylations, respectively (Scheme 1). Two bacterial enzymes, SCO7467 from *Streptomyces coelicolor* A3(2) and IptA from *Streptomyces* sp. SN-593, are tryptophan *C5*- and *C6*-prenyltransferases, respectively.[12,16] IptA is involved in the biosynthesis of 6-dimethylallylindole-3-carbaldehyde.[12,17] Recently, two further 6-DMATS enzymes, 6-DMATS$_{Sa}$ (SAML0654) from *Streptomyces ambofaciens* (*S. ambofaciens*) ATCC238 and 6-DMATS$_{Sv}$ (Strvi8510) from *Streptomyces violaceusniger (S. violaceusniger)* Tü4113 were identified and characterized biochemically.[18] These two 6-DMATS enzymes showed high flexibility toward their prenyl donor and acceptor. In contrast to other indole prenyltransferases, both DMAPP and geranyl diphosphate (GPP) were used by both enzymes.[18] Consequently, this flexibility makes them interesting candidates for further investigations on the acceptance of unnatural alkyl or benzyl donors.

Biochemical investigations on the tryptophan prenyltransferases FgaPT2 and 5-DMATS with methylallyl (MAPP) and 2-pentenyl diphosphate (2-pentenyl-PP) showed that these enzymes also accepted such unnatural alkyl donors. The alkylation positions were shifted partially or completely to the neighboring position.[19] The tryptophan *C4*-prenyltransferase FgaPT2 even accepted benzyl diphosphate (benzyl-PP) as substrate and catalyzed the regiospecific benzylation of L-tryptophan at position C-5.[20] Our previous data on the reactions of tryptophan prenyltransferases with unnatural alkyl and benzyl donors were limited to enzymes which catalyzed the transfer reactions of the dimethylallyl moiety onto position C-4 and C-5 of the indole ring.[19,20] In a previous study, the behavior of the 7-DMATS from *A. fumigatus* could not be investigated in detail, due to its low activity in the presence of unnatural DMAPP analogues.[19]

Fortunately, the recently identified L-tyrosine prenyltransferase TyrPT from *Aspergillus niger* showed a remarkable tryptophan *C7*-prenyltransferase activity[21] and can be considered as a tryptophan *C7*-prenylating enzyme in this study. As shown in Scheme 1, the five enzymes 5-DMATS,[13] 5-DMATS$_{Sc}$,[17] 6-DMATS$_{Sa}$,[18] 6-DMATS$_{Sv}$[18] and TyrPT[21] used in this study share the same substrates (tryptophan and DMAPP), but catalyze regiospecific prenylations at different positions of the indole ring. After having the availability of the two tryptophan *C6*-prenyltransferases 6-DMATS$_{Sa}$ and 6-DMATS$_{Sv}$ as well as of TyrPT in our laboratory, we initiated a study to prove their behavior toward MAPP, 2-pentenyl-PP and benzyl-PP.

Results and Discussion

C-6 Alkylated/Benzylated Derivatives as Unique Enzyme Products of the Two *C6*-Prenyltransferases

The purified recombinant proteins 6-DMATS$_{Sa}$ and 6-DMATS$_{Sv}$ were firstly incubated with L-tryptophan in the presence of one of the three unnatural DMAPP analogues MAPP (**I**), 2-pentenyl-PP (**II**), and benzyl-PP (**III**). HPLC analysis of the enzyme assays showed clear product formation in all of these reaction mixtures, with the highest conversions of $91.2 \pm 0.07\%$ and $89.3 \pm 0.6\%$ observed in the presence of 2-pentenyl-PP for 6-DMATS$_{Sa}$ and 6-DMATS$_{Sv}$, respectively (Figure 1, Scheme 2, see the Supporting Information, Table S1). Lower conversion yields of $51.1 \pm 0.5\%$ and $37.6 \pm 0.3\%$ were observed in the incubation mixtures with MAPP, and $13.9 \pm 0.3\%$ and $8.2 \pm 0.3\%$ with benzyl-PP (Figure 1, Scheme 2, see the Supporting Information, Table S1). To determine the alkylation position, enzyme assays were prepared on a large scale. The enzyme products **Ia–IIIa** were isolated from both assays of 6-DMATS$_{Sa}$ and 6-DMATS$_{Sv}$ on HPLC and their structures were elucidated by MS and NMR analyses. For better understanding, we named the products by a combination of **I** (product from MAPP), **II** (2-pentenyl-PP) or **III** (benzyl-PP) with **a** (regular alkyl or benzyl at C-6), **b1** (regular alkyl at C-7), **b2** (reverse alkyl at C-7), **b** (benzyl at C-7) or **c** (regular alkyl or benzyl at C-5). MS data confirmed the monoalkylation or benzylation of the isolated products. ^{1}H NMR analysis (for structural elucidation see the Supporting Information) proved the regular attachment of the alkyl or benzyl residue onto posi-

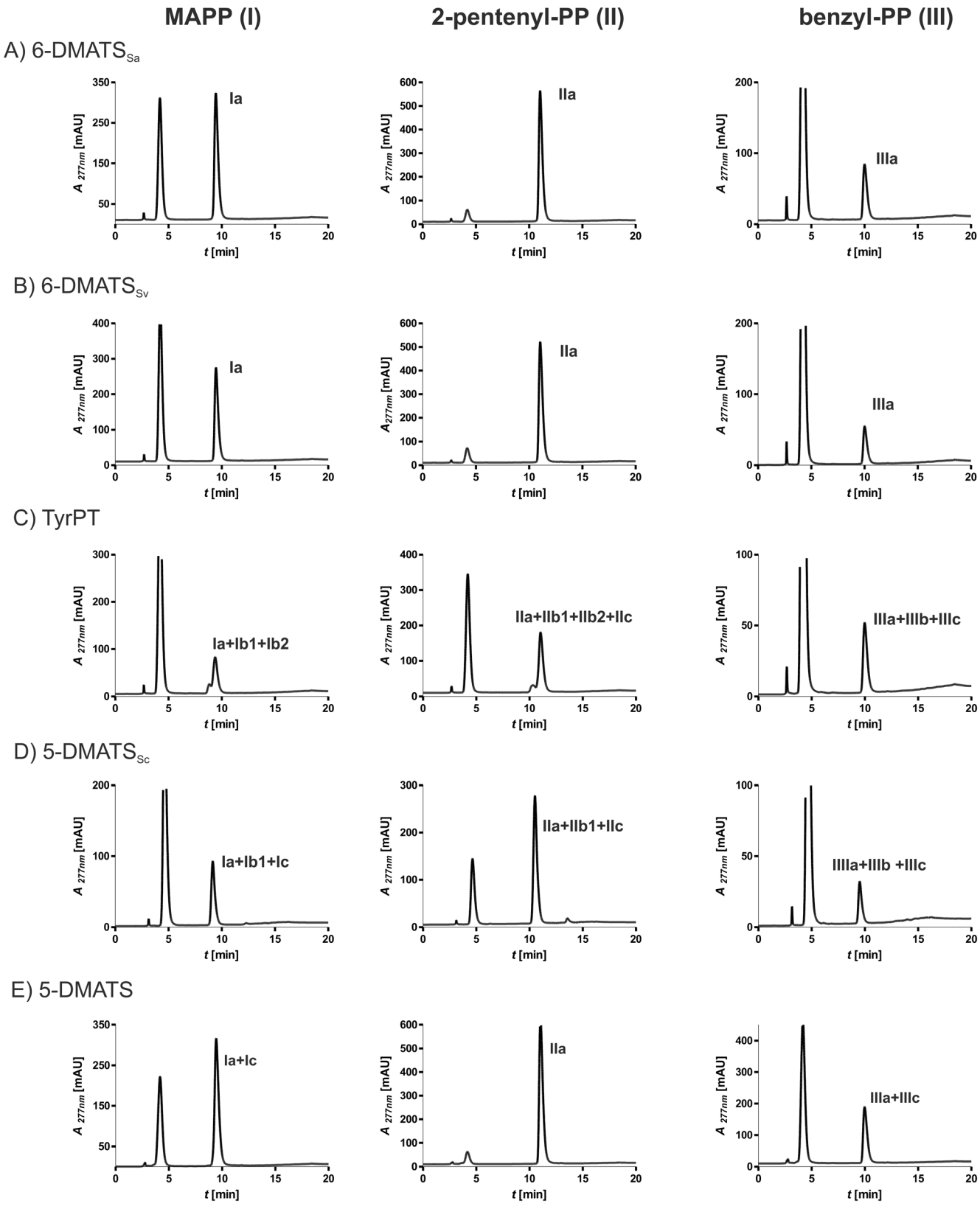

Figure 1. HPLC analysis of the reaction mixtures of L-tryptophan with unnatural DMAPP analogues.

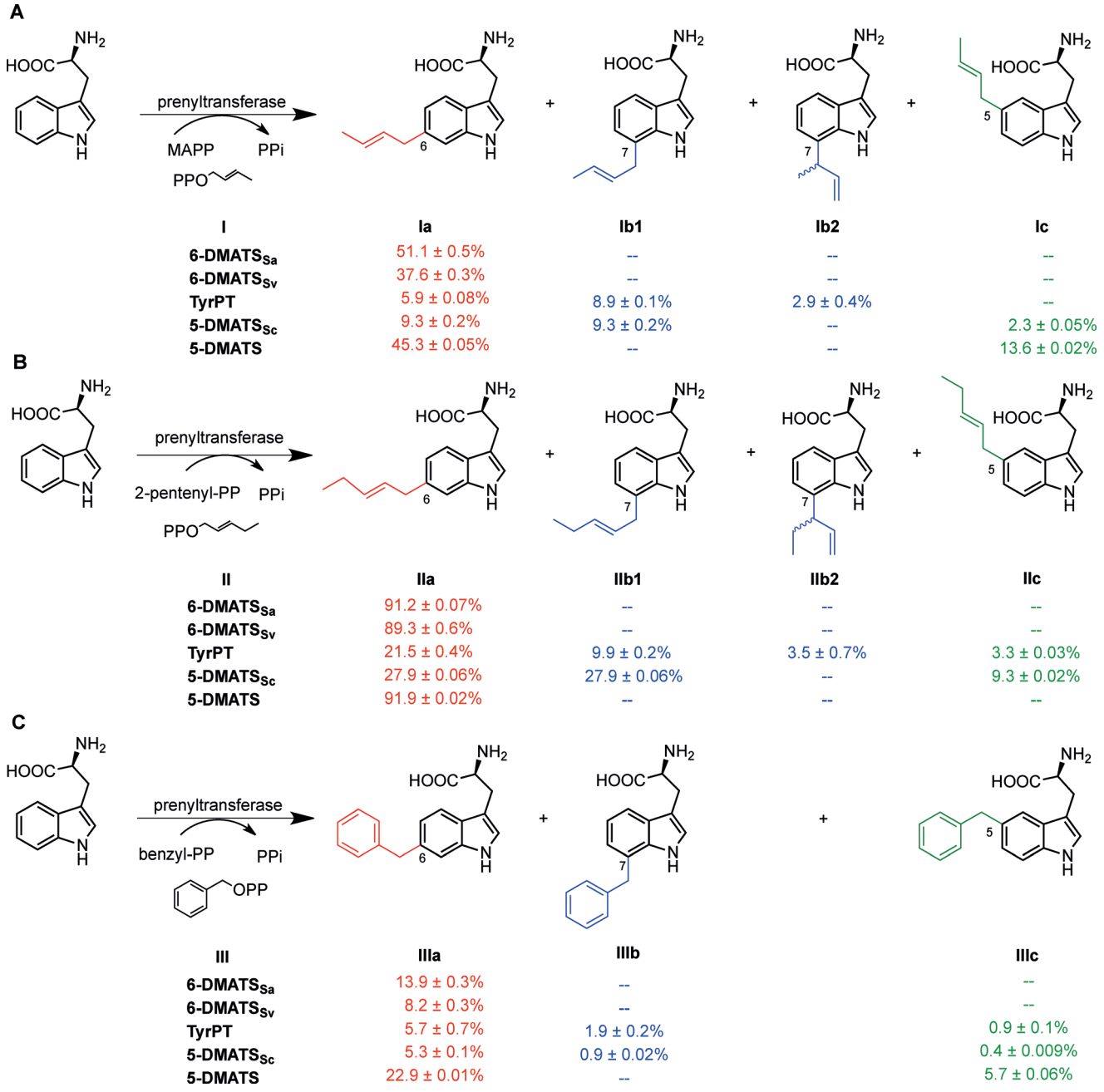

Scheme 2. Alkylation/benzylation of L-tryptophan catalyzed by *C5*-, *C6*- and *C7*-prenylating enzymes in the presences of three DMAPP analogues. –: product yields <0.3%. The mean of the total conversion yields were measured in duplicate by HPLC and the percentages for different products were calculated by using the corresponding NMR data.

tion C-6 of the indole ring in all of these cases (see the Supporting Information, Figures S9–S11). This conclusion was drawn by comparison of the coupling patterns of the signals for aromatic protons with those of the published data for C-6 alkylated L-tryptophan.[18–20] In the presence of the natural prenyl donors DMAPP or GPP, 6-DMATS$_{Sa}$ and 6-DMATS$_{Sv}$ also catalyze a C-6 prenylation.[18] Therefore, the alkylation position for both enzymes was proven to be independent of the used alkyl or benzyl donor.

C-6 Alkylated/Benzylated derivatives were Main Products of TyrPT Reactions with DMAPP Analogues

Taking the data on 6-DMATS$_{Sa}$ and 6-DMATS$_{Sv}$ with the previous published results on FgaPT2 and 5-DMATS[19,20,22] together, we have shown the behavior of tryptophan *C4*-, *C5*- and *C6*-prenyltransferases toward unnatural DMAPP analogues. It would be interesting to complete this series with *C7*-prenylating

enzymes. A previous study showed that the tryptophan *C7*-prenyltransferase 7-DMATS from *A. fumigatus*[23] accepted very poorly MAPP and 2-pentenyl-PP.[19] Recently, CAK41583 from *A. niger* was identified as a tyrosine prenyltransferase (TyrPT), catalyzing an *O*-prenylation at the phenolic hydroxy group of L-tyrosine.[21] As in the case of SirD from *Leptosphaeria maculans*,[24] TyrPT also catalyzed the transfer reaction of a dimethylallyl moiety from DMAPP to C-7 of L-tryptophan and several derivatives thereof.[21] The broad substrate specificity of TyrPT led us to test its activity for DMAPP analogues in the presence of L-tryptophan. In analogy to 6-DMATS$_{Sa}$ and 6-DMATS$_{Sv}$, TyrPT was incubated with L-tryptophan in the presence of MAPP, 2-pentenyl-PP and benzyl-PP. Product formation was detected in all three incubation mixtures (Figure 1). However, the observed enzyme activities were much lower than those of the two 6-DMATS enzymes. Total product yields of 38.3 ± 0.6, 17.7 ± 0.2 and $8.5 \pm 1.0\%$ were calculated for 2-pentenyl-PP, MAPP and benzyl-PP, respectively (Figure 1, Scheme 2, see the Supporting Information, Table S1). This is justified by the fact that L-tyrosine, but not L-tryptophan is the best accepted aromatic substrate by TyrPT, also in the presence of DMAPP. Interestingly, the ratio of the relative activities toward the three DMAPP analogues was similar to those of the two 6-DMATS enzymes. In contrast to the unique C-7 prenylation of L-tryptophan by TyrPT in the presence of DMAPP, interpretation of the individual peaks of the ^{1}H NMR spectra indicated the presence of more than one product each in the incubation mixtures with DMAPP analogues. Optimization of the HPLC conditions and the application of a Chiralpak Zwix (+) column (see the Supporting Information, Figure S1) allowed a partial separation of these product mixtures. Although the compounds to be separated differ from each other by alkylation positions rather than by stereochemistry, they showed different behavior on the Chiralpak Zwix (+) column. It seems that the indole derivatives had different interactions with the column material.

HPLC analysis of the incubation mixture with 2-pentenyl-PP and interpretation of the NMR data led to the identification of three substances with a regular alkyl moiety attached to C-6 (**IIa**), C-7 (**IIb1**) and C-5 (**IIc**), respectively. Product yields of 21.5 ± 0.4, 9.9 ± 0.2 and $3.3 \pm 0.03\%$ were calculated for these products (Scheme 2, see also the Supporting Information). In addition, a reversely C-7 alkylated L-tryptophan (**IIb2**) was isolated with a product yield of $3.5 \pm 0.7\%$ (Scheme 2, see the Supporting Information, Figure S21). With MAPP as alkyl donor, regularly C-6 (**Ia**) and C-7 alkylated (**Ib1**) as well as reversely C-7 alkylated derivatives (**Ib2**) were identified by interpretation of their NMR spectra (see the Supporting Information). Product yields of 5.9 ± 0.08, 8.9 ± 0.1 and $2.9 \pm 0.4\%$ were calculated for **Ia**, **Ib1** and **Ib2**, respectively. Regularly C-6, C-7 and C-5 benzylated products (**IIIa**, **IIIb**, **IIIc**) with product yields of 5.7 ± 0.7, 1.9 ± 0.2 and $0.9 \pm 0.1\%$ were identified in the reaction mixture of L-tryptophan with benzyl-PP. These results demonstrated clearly that C-6 alkylated or benzylated derivatives were main or one of two predominant products of TyrPT reactions in the presence of the unnatural donors (Scheme 2) and differed clearly from that of L-tryptophan with DMAPP.[21]

Comparison of Bacterial and Fungal Alkylation/Benzylation Reactions by Investigations on 5-DMATS and 5-DMATS$_{Sc}$

As described above, the two 6-DMATS enzymes from bacteria catalyzed the regiospecific alkylation and only one product with the same position, i.e, C-6, was identified, independent of DMAPP, GPP[18] or the DMAPP analogues MAPP, 2-pentenyl-PP or benzyl-PP. In comparison, the fungal prenyltransferases FgaPT2 and 5-DMATS catalyzed the regiospecific C-4 and C-5 prenylation in the presence of DMAPP, respectively.[13,14] But in the presence of the unnatural DMAPP analogues, the regioselectivity was partially or completely shifted.[19,20] In the presence of L-tryptophan, the fungal L-tyrosine *O*-prenyltransferase TyrPT also accepted DMAPP analogues as substrates. In the case of 2-pentenyl-PP and benzyl-PP, C-6 alkylated or benzylated L-tryptophan was the predominant product. In the presence of methylally-PP, the C-6 alkylated derivative was one of the two dominant products. It seems that in the presence of DMAPP analogues, C-6 is the preferable alkylation position for enzymes which usually catalyzed the prenylation of L-tryptophan at C-5 (like 5-DMATS), C-6 (6-DMATS enzymes) and C-7 (TyrPT).

These results pose an important question on the possible reason for the decreasing regioselectivity of 5-DMATS and TyrPT. One plausible explanation could be the orientation of the DMAPP analogues in the binding sites of the enzymes, which make C-6 to be the preferable alkylation position. However, it cannot be excluded that the observed regiospecific alkylation or benzylation of L-tryptophan at the same position by 6-DMATS$_{Sa}$ and 6-DMATS$_{Sv}$ in the presence of DMAPP, GPP and DMAPP analogues is based on their bacterial origin. It could be speculated that bacterial prenyltransferases retain their regioselectivities independent of the used donors, while fungal enzymes exhibit relaxed selectivity in the presence of different alkyl donors. 5-DMATS and TyrPT are fungal enzymes and therefore showed different behavior regarding regioselectivity compared with 6-DMATS enzymes. The latter hypothesis would also be supported by the fact that FgaPT2 catalyzed tryp-

tophan alkylation and benzylation in the presence of these unnatural alkyl and benzyl donors with partial or complete shift of the attachment positions.[19,20]

To clarify the possible reason for this difference, we investigated the regioselectivity of the tryptophan *C5*-prenyltransferase SCO7467 (5-DMATS$_{Sc}$) from the bacterium *Streptomyces coelicolor* A3(2) in the biosynthesis of 5-dimethylallylindole-3-acetonitrile.[16,17] SCO7467 was overproduced in *E. coli* as reported by Ozaki,[17] purified and investigated in the presence of MAPP, 2-pentenyl-PP and benzyl-PP. For comparison, the behavior of the fungal 5-DMATS from *A. clavatus*,[13] toward MAPP and 2-pentenyl-PP[19] was reproduced in this study. In addition, this enzyme was assayed with benzyl-PP in the presence of L-tryptophan.

The previously reported data for 5-DMATS[19] were reproduced in this study by identification of C-5 and C-6 alkylated products with MAPP, with products yields of 13.6 ± 0.02 and $45.3 \pm 0.05\%$, respectively. In the presence of 2-pentenyl-PP, the alkylation position was completely shifted from C-5 to C-6. Similar to those of MAPP, C-5 and C-6 benzylated products with yields of 5.7 ± 0.06 and $22.9 \pm 0.01\%$ were detected in the assay with benzyl-PP (Figure 1, Scheme 2). Again, C-6 alkylated or benzylated L-tryptophan represented the predominant product.

HPLC analysis clearly revealed product formation in the reaction mixtures of L-tryptophan with the recombinant 5-DMATS$_{Sc}$ in the presence of all three DMAPP analogues (Figure 1). HR-MS data confirmed the attachment of one alkyl or benzyl residue on the substrate for all of the obtained products (see the Experimental Section). Structure elucidation by NMR indicated that the isolated product peaks consisted of more than one substance. C-6, C-7 and C-5 alkylated derivatives were identified with ratios of 3:3:1 for 2-pentenyl-PP and of 4:4:1 for MAPP. By using a Chiralpak Zwix (+) column, the C-7 alkylated products were purified from these mixtures (Scheme 2, see the Supporting Information, Figure S1). With 2-pentenyl-PP as alkyl donor, a product yield of $9.3 \pm 0.02\%$ was calculated for C-5 (**IIc**) and $27.9 \pm 0.06\%$ each for C-6 (**IIa**) and C-7 alkylated (**IIb1**) L-tryptophan (Scheme 2). In the case of MAPP, product yields of 9.3 ± 0.2, 9.3 ± 0.2 and $2.3 \pm 0.05\%$ were determined for **Ia**, **Ib1** and **Ic**, respectively. Inspection of the NMR spectra of the products obtained with benzyl-PP revealed the presence of 6-benzyl-L-tryptophan (**IIIa**) with a product yield of $5.3 \pm 0.1\%$ and 7-benzyl-L-tryptophan (**IIIb**) of $0.9 \pm 0.02\%$ (see the Supporting Information, Figures S11 and S22). In addition, signals of a C-5 benzylated L-tryptophan (**IIIc**) with a product yield of $0.4 \pm 0.009\%$ could also be observed (together with **IIIa** as a mixture, see the Supporting Information, Figure S2).

The results obtained with the bacterial 5-DMATS$_{Sc}$ were distinguishable not only from those with the fungal 5-DMATS, but also from those of the two bacterial 6-DMATS enzymes. Formation of three different alkylated or benzylated products by 5-DMATS$_{Sc}$ in all of the three incubations disproved the bacterial origin of the observed high regiospecificity for the two 6-DMATS enzymes. These results confirmed the preference of the enzymes investigated in this study for C-6 of the indole ring in the presence of the three unnatural DMAPP analogues.

Kinetic Parameters

Determination of the kinetic parameters of the enzymes with the DMAPP analogues indicated that the observed reactions were consistent with Michaelis–Menten kinetics (Table 1). K_M values in the range of 0.011 to 0.13 mM proved their relatively high affinity toward the tested DMAPP analogues. In contrast, the turnover numbers of the reactions with these DMAPP analogues were much lower than those with DMAPP. As observed in Figure 1 and given in Scheme 2, 2-pentenyl-PP was accepted in most cases as the best unnatural alkyl donor. This was also confirmed by the kinetic parameters with an exception for TyrPT. Here the efficiencies toward MAPP and 2-pentenyl-PP are almost identical, although higher relative activities toward 2-pentenyl-PP were observed. The unnatural donor MAPP was also well accepted but to a lesser degree. Benzyl-PP is a poor substrate for all enzymes, as verified by kinetic parameters.

Homology Modelling of 5-DMATS

To get insights into the reduced regioselectivity of the tested enzymes in the presence of DMAPP analogues and to assess how the protein might be able to discriminate between the different analogues, we homology modelled 5-DMATS. Four enzymes from the DMATS superfamily, FgaPT2,[25] FtmPT1,[26] CdpNPT[27] and AnaPT[28] could principally serve as templates. As expected, the structure of the tryptophan *C4*-prenyltransferase FgaPT2 is the most suitable for this purpose, owing to the sequence identity of 52% with the target. As shown in Figure 2 A and Figure S26 in the Supporting Information, our model of 5-DMATS consists of five $\alpha\beta\beta\alpha$ units, being similar to those of the known structures of the DMATS enzymes. Due to the low homology of only about 26% or less on the amino acid level to proteins with known structures, no model with a sufficient level of detail for the approaches used in this study could be obtained for 5-DMATS$_{Sc}$, 6-DMATS$_{Sa}$, 6-DMATS$_{Sv}$, or TyrPT.

Table 1. Kinetic parameters of the tested prenyltransferases toward DMAPP and analogues thereof (MAPP, 2-pentenyl-PP and benzyl-PP).

	DMAPP		2-pentenyl-PP		MAPP		benzyl-PP	
	K_M [mM]	k_{cat} [min^{-1}]	K_M [mM]	k_{cat} [min^{-1}]	K_M [mM]	k_{cat} [min^{-1}]	K_M [mM]	k_{cat} [min^{-1}]
6-DMATS$_{Sa}$	0.095[a] ± 0.011[a]	37.8[a] ± 4.1	0.011 ± 0.000094	0.18 ± 0.0043	0.025 ± 0.0019	0.066 ± 0.00088	0.036 ± 0.00049	0.074 ± 0.00065
6-DMATS$_{Sv}$	0.025 ± 0.0008	9.9 ± 0.13	0.049 ± 0.0021	0.24 ± 0.0018	0.040 ± 0.0018	0.064 ± 0.00036	0.081 ± 0.0021	0.047 ± 0.0027
5-DMATS$_{Sc}$	0.05[b] ± 0.002	24[b] ± 6	0.028 ± 0.0011	0.082 ± 0.0035	0.054 ± 0.0004	0.029 ± 0.00014	0.11 ± 0.019	0.017 ± 0.0022
TyrPT	0.39[c] ± 0.018	0.22[c] ± 0.023	0.033 ± 0.00078	0.056 ± 0.0003	0.026 ± 0.00024	0.067 ± 0.00077	0.02 ± 0.00042	0.029 ± 0.00058
5-DMATS	0.076[d]	78[d]	0.13[e] ± 0.021	1.38[e] ± 0.12	0.04[e] ± 0.003	0.3[e] ± 0.024	0.12 ± 0.0014	0.092 ± 0.00054

[a]–[e] Data were adapted from previous publications for 6-DMATS$_{Sa}$,[18] 5-DMATS$_{Sc}$,[17] TyrPT[21], 5-DMATS.[13,19] Data for DMAPP analogues are mean values with difference range obtained from two independent measurements.

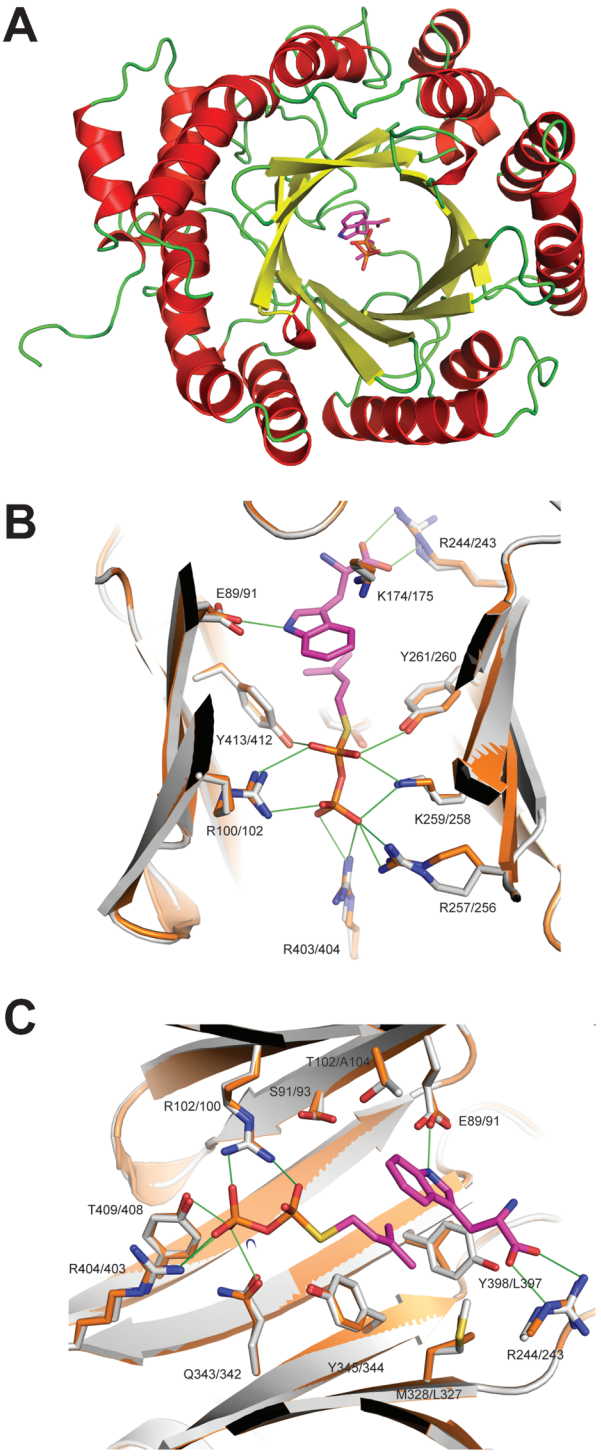

Figure 2. Homology model of 5-DMATS (**A**). α-helices are colored in red, β-sheets in yellow and turns and loops in green, respectively. The ABBA motif of dimethylallyltryptophan synthases is reproduced in the model, the Cα-RMSD between model and template being 0.1 Å. Active site residues of the model (orange) and template (white) are shown (**B** and **C**). The corresponding amino acids are labelled as pairs (FgaPT2/5-DMATS). **C** is rotated by 90° with respect to **B**.

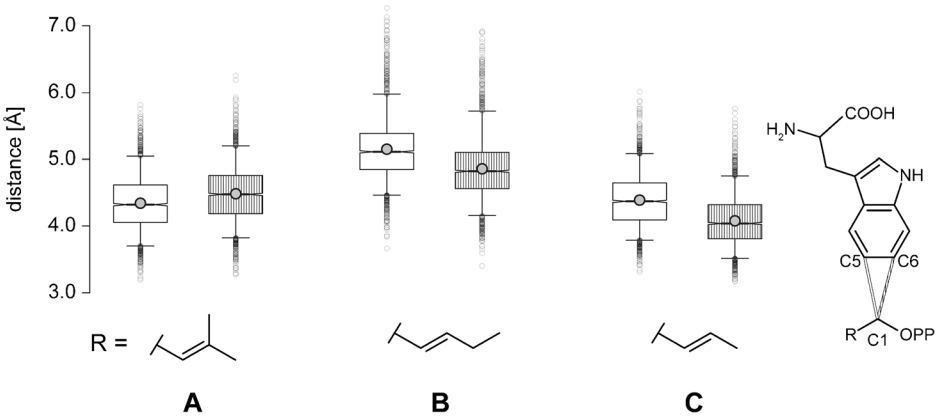

Figure 3. For each donor molecule the distances between the C-1 atom of the donor and the C-5 and C-6 atoms of tryptophan were measured over 2500 generated snapshots. Distance distributions are shown as box plots: Grey circles represent mean values, white circles measurements outside the 95th percentile. Boxes span 50% of the measurements, whiskers 95%. White boxes correspond to distances between the C-1 and C-5 atom, while shaded boxes show distances between the C-1 and C-6 atom, respectively.

Docking Experiments with DMAPP and Analogues

Initial docking experiments led to acceptor and donor poses consistent with the interactions observed for the respective molecules in the template X-ray structure. In particular, contacts with the conserved basic residues interacting with the pyrophosphate tail of the donor molecules are preserved. Yet, this static picture of protein acceptor–donor interactions did not allow us to formulate a hypothesis that was consistent with the experimental findings. Thus, we carried out molecular dynamics (MD) calculations to assess how the interactions might change over time.

These MD studies (Supporting Information, Figure S27) showed that DMAPP resides in the cavity with a mean distance of 4.32 Å between its C-1 and the C-5 of the indole ring (Figure 3A). In contrast, the average distance between C-1 and C-6 on L-tryptophan is significantly larger, thus providing a possible explanation for the formation of solely C-5 prenylated tryptophan in the presence of DMAPP. In comparison, C-1 of 2-pentenyl-PP is predominantly close to C-6 of the indole ring with a distance of 4.82 Å (compared to 5.11 Å between C-1 and C-5; Figure 3B), so that an exclusive C-6 alkylation is plausible. As shown in Figure 3C, C-1 of MAPP is located at a shorter distance to C-6 of the indole ring, which is also consistent with the formation of the predominantly C-6 alkylated derivative for this donor. All these simulations were remarkably stable over the simulation time, as evidenced by the RMSD and RMSF plots in Figure S28 and S29 of the Supporting Information and the overlay of the starting structure and the final snapshot (Supporting Information, Figure S27). In contrast, the MD simulations with benzyl-PP became unstable shortly after the start of the unrestrained equilibration step (despite several repetitions), with an unusual edge-to-face orientation of benzyl-PP with respect to L-tryptophan (Supporting Information, Figure S27). We were thus unable to use these data within the present study. We speculate that the reason for this behavior of the simulations could be that the binding sites for the prenyl donors in the structures of the DMATS enzymes were determined with linear DMAPP analogues, which have significantly different sizes and electron densities than benzyl-PP.

It also seems intuitive that the donor–acceptor distance is a major factor determining the regioselectivity of alkylations: As evidenced by the experiments, the reactivitoies of both C-5 and C-6 can be considered as equal. Thus, the preference for prenylation at a certain position can be a direct effect of the number of times donor and acceptor come so close to each other that an activated complex can be formed.

Conclusions

In conclusion, all the tested enzymes used MAPP, 2-pentenyl-PP and benzyl-PP as substrates and catalyzed Friedel–Crafts alkylation or benzylation reactions on the indole ring. The observed reactions differ from each other in relative activities and regioselectivity of the attached position. One to four alkylated or benzylated derivatives have been identified as enzyme products (Scheme 2). From Scheme 2, it is obvious that in the presence of unnatural DMAPP analogues, C-6 of tryptophan was the preferable alkylation and benzylation position for tryptophan *C5*-, *C6*- and *C7*-prenylating enzymes. C-6 Alkylated or benzylated derivatives were identified in all the reaction mixtures. It was found as a unique product in the cases of the both 6-DMATS enzymes with all of the

three DMAPP analogues or as one of two main products in the reaction mixtures of 5-DMATS$_{Sc}$ with MAPP and 2-pentenyl-PP. Such derivatives were predominant products in all other reaction mixtures. From Scheme 2, it is also clear that the tryptophan *C5*-prenyltransferases 5-DMATS and 5-DMATS$_{Sc}$ as well as TyrPT with a tryptophan *C7*-prenyltransferase activity also produced C-5 or/and C-7 alkylated or benzylated derivatives, indicating a shift of the alkylation or benzylation position from C-5 to C-7 and *vice versa*. By using the program MODELLER, a structural model was constructed for 5-DMATS from *A. clavatus* and used for docking and MD studies with DMAPP, MAPP and 2-pentenyl-PP, leading to a distance-based explanation of their observed reaction preferences. Unfortunately, the MD simulations with benzyl-PP became unstable. It seems that the available structure information is still too limited for a universal interpretation or prediction of all possible enzyme reactions. Therefore, it will be interesting to have more protein structures elucidated in the near future, most importantly also as complexes with different acceptors and donors including unnatural DMAPP analogues.

Experimental Section

Chemicals

Syntheses of methylallyl-PP (MAPP), 2-pentenyl-PP and benzyl-PP were carried out as described previously.[19,29] L-Tryptophan was purchased from Roth (Karlsruhe, Germany).

Overproduction and Purification of the Recombinant Proteins

Gene expression and subsequent protein purification of the recombinant 6-DMATS$_{Sa}$-His$_6$, His$_8$-6-DMATS$_{Sv}$, His$_6$-TyrPT and 5-DMATS-His$_6$ were carried out as described previously.[13,18,21]

Cloning and Expression of *5-DMATS$_{Sc}$* (*SCO7467*)

PCR amplification of *SCO7467* from *Streptomyces coelicolor* A3(2) was carried out as described by Ozaki et al.[30] The expression vector pHis$_8$ containing the coding sequence was termed pML10. *E. coli* BL21 [DE3] cells harboring pML10 were cultivated in 1 L liquid lysogeny broth (LB) medium supplemented with kanamycin (50 μg mL^{-1}) until an absorption at 600 nm of 0.6. For induction of gene expression, IPTG was added to a final concentration of 0.5 mM. After further incubation at 30 °C and 220 rpm for 6 h, the recombinant protein was purified as routinely on Ni-NTA agarose.

Enzyme Assays for Determination of the Activities and Kinetic Parameters

The reaction mixtures (100 μL) for determination of the enzyme activities contained 1 mM L-tryptophan, 5 mM $CaCl_2$, 2 mM alkyl diphosphate [DMAPP, MAPP (**I**), 2-pentenyl-PP (**II**)] or benzyl-PP (**III**), 1.0–1.5% (v/v) glycerol, 50 mM Tris-HCl (pH 7.5) and 7.5 μM of purified recombinant protein. The reaction mixtures were incubated at 37 °C for 16 h. For HPLC analysis, the reactions were terminated with 100 μL MeOH. Protein was then removed by centrifugation at 17,000 × *g* for 15 min. HPLC measurements were carried out in duplicate on a RP-18 and a Chiralpak Zwix column (+).

Enzyme assays for determination of the kinetic parameters for DMAPP and its analogues MAPP, 2-pentenyl-PP and benzyl-PP contained 1 mM L-tryptophan, 5 mM $CaCl_2$ for fungal or $MgCl_2$ for bacterial prenyltransferases, 0.15% (v/v) glycerol, 50 mM Tris-HCl (pH 7.5) and the respective alkyl or benzyl diphosphate in final concentrations of up to 0.5 mM or 1 mM in the case of 5-DMATS with benzyl-PP were incubated at 37 °C in duplicates. For 6-DMATS$_{Sa}$, a protein amount of 5 μg and an incubation time of 30 min were used in the presence of 2-pentenyl-PP. For incubation with MAPP or benzyl-PP, the protein amount and incubation time were 10 μg and 60 min. 1 μg 6-DMATS$_{Sv}$ was assayed with DMAPP for 5 min and 10 μg with DMAPP analogues for 60 min. The assays for TyrPT contained 15 μg protein and were incubated for 60 min with 2-pentenyl-PP and 90 min with MAPP or benzyl-PP. 10 μg 5-DMATS$_{Sc}$ and an incubation time of 60 min were used for 2-pentenyl-PP, 20 μg and 90 min for MAPP. For the reactions with benzyl-PP, 25 μg 5-DMATS$_{Sc}$ and an incubation time of 90 min were used. Kinetic parameters of 5-DMATS were obtained from enzyme assays with 20 μg of purified protein and incubation time of 60 min. The reactions were terminated with 100 μL MeOH and the protein was removed by centrifugation at 17.000 × *g* for 15 min. Parameters of Michaelis–Menten kinetics such as K_M and turnover number (k_{cat}) were determined by Lineweaver–Burk, Hanes–Woolf and Eadie–Hofstee plots.

Enzyme Assays for Isolation and Structure Elucidation

Assays for isolation of the enzyme products were carried out in large scales (10 mL) containing 1 mM L-tryptophan, 2 mM MAPP, 2-pentenyl-PP or benzyl-PP, 5 mM $CaCl_2$, 0.0–1.5% (v/v) glycerol, 50 mM Tris-HCl (pH 7.5) and with 2 to 4 mg of purified recombinant protein. After incubation for 16 h at 37 °C, the reaction mixtures were terminated with 10 mL MeOH and precipitated protein was removed by centrifugation at 4.750 × *g* for 15 min. The obtained supernatant was then concentrated on a rotating vacuum evaporator to 1 mL for injection in HPLC.

HPLC Analysis and Isolation of the Enzyme Products for Structure Elucidation

The enzyme products were analyzed on an Agilent series 1200 HPLC (Agilent Technologies Deutschland GmbH, Böblingen, Germany) with a Multospher 120 RP-18 column (250 × 4 mm, 5 μm, C+S-Chromatography Service, Langer-

wehe, Germany) at a flow rate of 1 mL min^{-1}. Water (solvent A) and methanol (solvent B) were used as solvents for analysis and isolation of the enzyme products. For analysis of the alkylated tryptophan, a linear gradient of 40–100% (v/v) solvent B over 15 min was used. The column was then washed with 100% solvent B for 5 min and equilibrated with 40% solvent B for 5 min. Detection was carried out on a photo diode array detector.

By using the same HPLC equipment and a semipreparative Multospher 120 RP-18 column (250×10 mm, 5 μm, C+S-Chromatographie Service, Langerwehe, Germany), the enzyme products were isolated at a flow rate of 2.5 mL min^{-1} and a gradient of 60–100% solvent B in 20–25 min. If necessary, an isocratic step with solvent B before the gradient was included for 5 min. After each run the column was washed with 100% solvent B and equilibrated with 60% solvent B for 5 min.

A much better separation of the L-tryptophan derivatives with different alkylation positions on the indole ring was achieved by using a Chiralpak Zwix column (+) (150×3 mm, 3 μm, Chiral technologies Europe, Daicel Group, Illkirch Cedex, France). This column was used for detailed investigations on the enzyme products in the incubation mixtures (Figure S1, Supporting Information) and for separation of the product mixtures that were not separated by using the semipreparative Multospher 120 RP-18 column mentioned above. Analysis of the enzyme assays and isolation of the products were carried out at a flow rate of 0.5 mL min^{-1} with water (solvent A) and methanol (solvent B) as solvents. An isocratic run with 50% solvent B was used.

NMR and MS Analyses as well as Structure Elucidation

NMR including two-dimensional HSQC and HMBC spectra were recorded on JEOL ECA-500 (JEOL Germany GmbH, Munich, Germany) or Bruker Avance-600 (Bruker Corporation, Billerica, USA) spectrometers, respectively. The spectra were processed with MestReNova 6.0.2. Chemical shifts were referred to the signals of CD_3OD at $\delta_H = 3.31$ and $\delta_C = 49.2$ ppm. The isolated compounds were also analyzed by electrospray ionization (ESI-MS) or electron impact mass spectrometry (EI-MS) on a Q-Trap 2000 (Life Technologies Ltd, Paisley, United Kingdom) and by high resolution electrospray ionization (HR-ESI-MS) or electron impact mass spectrometry (HR-EI-MS) on an Auto SPEC (Waters MS Technology Centre, Manchester, United Kingdom).

Compound Ia: ^{1}H NMR (MeOH-d_4, 500 MHz): δ = 7.60 (dd, J = 8.1, 0.4 Hz, H-4), 7.15 (d, 0.7, H-7), 7.12 (s, H-2), 6.89 (dd, J = 8.1, 1.4 Hz, H-5), 5.60 (dtq, J = 15.1, 6.6, 1.4 Hz, H-2′), 5.51 (dqt, J = 15.1, 6.3, 1.3 Hz, H-3′), 3.84 (dd, J = 9.5, 4.0 Hz, H-11), 3.49 (ddd, J = 15.2, 4.0, 0.6 Hz, H-10), 3.37 (d, J = 6.7 Hz, H_2-1′), 3.11 (dd, J = 15.2, 9.5 Hz, H-10), 1.67 (dd, J = 6.2, 1.4 Hz, H_3-4′); ESI-MS: m/z (intensity) = 517.30 $[2M+H]^+$ (100), 539.3 $[2M+Na]^+$ (58), 297.10 $[M+K]^+$ (47), 259.10 $[M+H]^+$ (31), 281.10 $[M+Na]^+$(24); HR-EI-MS: m/z = 258.1322, calcd. for $C_{15}H_{18}N_2O_2$ $[M]^+$: 258.1368.

Compound IIa: ^{1}H NMR (MeOH-d_4, 500 MHz): δ = 7.60 (d, J = 8.2 Hz, H-4), 7.16 (d, J = 0.6 Hz, H-7), 7.13 (s, H-2), 6.90 (dd, J = 8.2, 1.4 Hz, H-5), 5.63–5.50 (m, H-2′/H-3′), 3.84 (dd, J = 9.5, 4.0 Hz, H-11), 3.49 (ddd, J = 15.1, 4.0, 0.6 Hz, H-10), 3.38 (d, J = 6.0 Hz, H_2-1′), 3.12 (dd, J = 15.2, 9.5 Hz, H-10), 2.04 (m, H_2-4′), 0.99 (t, J = 7.5 Hz, H_3-5′); ESI-MS: m/z (intensity) = 273.25 $[M+H]^+$ (100), 295.14 $[M+Na]^+$ (87), HR-EI-MS: m/z = 272.1557, calcd. for $C_{16}H_{20}N_2O_2$ $[M]^+$: 272.1525.

Compound IIIa: ^{1}H NMR (MeOH-d_4, 500 MHz): δ = 7.60 (dd, J = 8.2, 0.6 Hz, H-4), 7.25–7.17 (m, H-2′/H-6′, H-3′/H-5′), 7.18 (s, H-7, overlaid with H-2′/H-6’, H-3′/H-5′), 7.15–7.11 (m, H-4′), 7.13 (s, H-2’ overlaid with H-4′), 6.93 (dd, J = 8.2, 1.5 Hz, H-5), 4.04 (s, H_2-1′), 3.82 (dd, J = 9.4, 4.0 Hz, H-11), 3.48 (ddd, J = 15.2, 4.0, 0.7 Hz, H-10), 3.11 (dd, J = 15.2, 9.4 Hz, H-10); ESI-MS: m/z (intensity) = 295.20 $[M+H]^+$ (100), 589.70 $[2M+H]^+$ (50), 316.92 $[M+Na]^+$ (11); HR-EI-MS: m/z = 294.1368, calcd. for $C_{18}H_{18}N_2O_2$ $[M]^+$: 294.1362.

Compound Ib1: ^{1}H NMR (MeOH-d_4, 500 MHz): δ = 7.56 (dd, J = 7.9, 1.0 Hz, H-4), 7.19 (s, H-2), 7.00 (dd, J = 7.9, 7.1 Hz, H-5), 6.93 (dd, J = 7.1, 0.6 Hz, H-6), 5.65 (dtq, J = 15.1, 6.4, 1.4 Hz, H-2′), 5.57 (dqt, J = 15.1, 6.2, 1.2 Hz, H-3′), 3.85 (dd, J = 9.5, 4.0 Hz, H-11), 3.53 (d, J = 5.2 Hz, H_2-1′), 3.51 (m, H-10, overlaid with H-1′), 3.14 (dd, J = 15.4, 9.5 Hz, H-10), 1.66 (ddt, J = 6.0, 1.4, 1.3 Hz, H_3-4′); ESI-MS: m/z (intensity) = 259.30 $[M+H]^+$ (100), 281.10 $[M+Na]^+$ (55.8), 539.23 $[2M+Na]^+$ (14), 517.32 $[2M+H]^+$ (8), 297.00 $[M+K]^+$ (6); HR-ESI-MS: m/z = 281.1266, calcd. for $C_{15}H_{18}N_2O_2$ $[M+Na]^+$: 281.1288.

Compound IIb1: ^{1}H NMR (MeOH-d_4, 600 MHz): 7.55 (d, J = 7.8 Hz, H-4), 7.19 (s, H-2), 7.00 (t, J = 7.5 Hz, H-5), 6.93, (d, J = 7.0 Hz, H-6), 5.67–5.58 (m, H-2′/H-3′), 3.84 (dd, J = 9.3, 3.8 Hz, H-11), 3.54 (d, J = 3.3 Hz, H_2-1′), 3.50 (dd, J = 15.1, 3.8 Hz, H-10), 3.13 (dd, J = 15.1, 9.3 Hz, H-10), 2.03 (m, H_2-4′), 0.97 (t, J = 7.5 Hz, H_3-5′); ^{13}C NMR (MeOH-d_4, 150 MHz, deduced from HSQC/HMBC): δ = 136.8, 134.1, 128.4, 127.9, 125.1, 124.7, 122.2, 120.2, 117.1, 109.9, 56.5, 35.0, 28.4, 26.1, 13.8; ESI-MS: m/z (intensity) = 295.10 $[M+Na]^+$ (100), 273.14 $[M+H]^+$ (29), 545.35 $[2M+H]^+$ (6), 567.39 $[2M+Na]^+$ (6), 311.10 $[M+K]^+$ (3); HR-ESI-MS: m/z = 295.1395, calcd. for $C_{16}H_{20}N_2O_2$ $[M+Na]^+$: 295.1422.

Compound IIIb: ^{1}H NMR (MeOH-d_4, 500 MHz): δ = 7.58 (dd, J = 8.1, 0.8 Hz, H-4), 7.26–7.20 (m, H-2′/H-6′, H-3′/H-5′), 7.18 (s, H-2), 7.14 (m, H-4′), 7.01 (t, J = 7.6 Hz, H-5), 6.92 (dd, J = 7.2, 0.4 Hz, H-6), 4.20 (s, H_2-1′), 3.83 (dd, J = 9.4, 4.0 Hz, H-11), 3.50 (dd, J = 15.1. 4.0 Hz, H-10), 3.13 (dd, J = 15.1, 9.4 Hz, H-10); ESI-MS: m/z (intensity) = 316.90 $[M+Na]^+$ (100), 295.2 $[M+H]^+$ (11.4). HR-EI-MS: m/z = 294.1368, calcd. for $C_{18}H_{18}N_2O_2$ $[M]^+$: 294.1339 (as a mixture with **IIIa**).

Compound Ib2: ^{1}H NMR (MeOH-d_4, 500 MHz): δ = 7.56 (dd, J = 7.8, 1.1 Hz, H-4), 7.20 (s, H-2), 7.03 (t, J = 7.6 Hz, H-5), 6.98 (d, J = 7.1 Hz, H-6), 6.12 (ddd, J = 17.2, 10.3, 6.3 Hz, H-2′), 5.12 (dt, J = 17.2, 1.6 Hz, H-1′), 5.04 (dt, J = 10.3, 1.6 Hz, H-1′), 3.89 (m, H-3′), 3.85 (dd, J = 9.3, 4.1 Hz, H-11), 3.51 (ddd, J = 15.1, 4.1, 0.9 Hz, H-10), 3.15 (dd, J = 15.1, 9.3 Hz, H-10), 1.44 (d, J = 7.0 Hz, H_3-4′); ESI-MS: m/z (intensity) = 281.30 $[M+Na]^+$ (100), 259.16 $[M+H]^+$ (63), 539.40 $[2M+Na]^+$ (12), 517.40 $[2M+H]^+$ (8), HR-ESI-MS: m/z = 281.1255, calcd. for $C_{15}H_{18}N_2O_2$ $[M+Na]^+$: 281.1266.

Compound IIb2: ^{1}H NMR (MeOH-d_4, 500 MHz): δ = 7.55 (dd, J = 7.8, 1.1 Hz, H-4), 7.16 (s, H-2), 7.01 (t, J = 7.5 Hz, H-5), 6.96 (d, J = 7.5 Hz, H-6), 6.06 (ddd, J = 17.2, 10.2, 7.6 Hz, H-2′), 5.08 (dt, J = 17.2, 1.5 Hz, H-1′), 4.99 (ddd, J = 10.2, 1.9, 1.0 Hz, H-1′), 3.71 (m, H-11), 3.59 (m, H-3′), 3.41 (m, H-10), 3.04 (dd, J = 14.9, 8.5 Hz, H-10), 1.86 (m, H_2-4′), 0.89 (t, J =

7.4 Hz, H_3-5′), coupling constants of signals observed for H-11, H-3' and H-10 were not determinable, due to low signal intensity; ESI-MS: *m/z* (intensity) = 295.30 $[M+Na]^+$ (100), 273.34 $[M+H]^+$ (18), 568.10 $[2M+Na]^+$ (5), 318.10 $[M+2Na]^+$ (2); HR-ESI-MS: *m/z* = 295.1437, calcd. for $C_{16}H_{20}N_2O_2$ $[M+Na]^+$: 295.1422.

Compound Ic: ^{1}H NMR (MeOH-d_4, 500 MHz): δ = 7.50 (s, H-4), 7.27 (dd, *J* = 8.4, 0.6 Hz, H-7), 6.96, (dd, *J* = 8.5, 1.7 Hz, H-6), signals at approx. 7.17–7.15 (H-2), 5.67–5.61 (H-2′), 5.54–5.47 (H-3′), 3.86–3.82 (H-11), 3.52–3.48 (H-10), 3,41–3.38 (H-1′) 3.12–3.06 (H-10) and 1.69–1.66 (H-4′) are overlaid with those of **Ia**; ESI-MS: *m/z* (intensity) = 281.04 $[M+Na]^+$ (100), 259.11 $[M+H]^+$ (10), 517.26 $[2M+H]^+$ (6), HR-EI-MS: *m/z* = 258.1366, calcd. for $C_{15}H_{18}N_2O_2$ $[M]^+$: 258.1368 (in a mixture with **Ia**).

Compound IIc: ^{1}H NMR (MeOH-d_4, 500 MHz): δ = 7.50 (s H-4), 7.27 (d, *J* = 8.2 Hz, H-7), 7.15 (s, H-2), 6.97 (dd, *J* = 8.3, 1.6 Hz, H-6), 3,48 (dd, *J* = 15.0, 4.6 Hz, H-10), 3.40 (d, *J* = 6.6 Hz, H-1′), signals at approx. 5.66–5.50 (H-2′ and H-3′), 3.85–3.82 (H-11), 3.11–3.05 (H-10), 2.07–2.00 (H-4′) and 1.00–0.96 (H-5′) are overlaid with those of **IIa**; ESI-MS: *m/z* (intensity) = 295.08 $[M+Na]^+$ (100), 273.20 $[M+H]^+$ (7), 567.58 $[2M+Na]^+$ (6), 545.39 $[M+H]^+$(3); HR-ESI-MS: *m/z* = 295.1433, calcd. for $C_{16}H_{20}N_2O_2$ $[M+Na]^+$: 295.1422 (in a mixture with **IIa**).

Compound IIIc: ^{1}H NMR (MeOH-d_4, 500 MHz): δ = 7.60 (dd, *J* = 1.5, 0.7 Hz, H-4), 7.27 (dd, *J* = 8.3, 0.5 Hz, H-7), 7.16 (s, H-2), 6.97 (dd, *J* = 8.3, 1.6 Hz, H-6), 4.05 (s, H_2-1′), 3.84 (m, H-11), 3.51 (m, H-10), signals at approx. 7.25–7.17 (H-2′/H-6′, H-3′/H-5′), 7.14–7.10 (H-4′), 3.12–3.06 (H-10), are overlaid with those of **IIIa**; ESI-MS: *m/z* (intensity) = 295.14 $[M+H]^+$ (100), 589.19 $[2M+H]^+$ (31), 317.37 $[M+Na]^+$ (6); HR-EI-MS: *m/z* = 294.1368, calcd. for $C_{18}H_{18}N_2O_2$ $[M]^+$: 294.1339 (as a mixture with **IIIa**).

Homology Model of 5-DMATS

The 3D structure of the 5-DMATS from *A. clavatus* was generated with the software MODELLER[31] using the X-ray structure of the *C4*-prenyltransferase FgaPT2[25] as template. The overall sequence identity between the two proteins is 52%, and the sequences were aligned with Uni*Prot*. Since the FgaPT2 structure was solved with L-tryptophan and DMSPP within the active site, these molecules were included during 5-DMATS model building to obtain a model with an active site conformation close to the one of the FgaPT2 X-ray structure. Furthermore, and in contrast to FgaPT2, raw initial models showed two pairs of cysteine residues within disulfide bonding distance. These cysteine pairs, Cys63–Cys127 and Cys96–Cys363, were then explicitly modelled as disulfide bridges in the final model.

Due to the stochastic component in conformational sampling during homology modelling, five models were constructed using the same alignment. The most accurate model was selected according to the DOPE (Discrete Optimized Protein Energy) atomic distance-dependent statistical potential function,[32] which is implemented in MODELLER. The best-scored model was visually inspected in order to ascertain sensible structural motifs. Criteria in this visual inspection were the absence of obvious steric clashes between side chains themselves or with the ligand used; orientation of the tryptophan substrate away from Arg243 and Glu91; correct conformation of charged and polar residues in the pyrophosphate sub-pocket responsible for fixation of the diphosphate moiety of the donor molecule. Model refinement was carried out within the active site by minimizing amino acids directly interacting with either the substrate or donor molecule using CHARMM.[33]

Docking Studies

All calculations were carried out using FRED[34] and conformations of tryptophan and the four donor molecules were generated with OMEGA (OMEGA 2.5.1.4: OpenEye Scientific Software, Santa Fe, NM; http://www.eyesopen.com; P.C.D. Hawkins, A.G. Skillman, G.L. Warren, B.A. Ellingson, M. T. Stahl). For receptor preparation, the homology model of 5-DMATS was processed with the apopdb2receptor-tool (part of the FRED docking suite) in order to determine the docking volume. The five molecules, i.e., tryptophan and the four donor molecules DMAPP, MAPP 2-pentenyl-PP and benzyl-PP, were docked independently, storing the best 10,000 poses of each for further processing.

The first percentile of the stored poses was selected for visual inspection. Among these poses, the most reasonable ones by physicochemical criteria were selected as starting points for molecular dynamics (MD) calculations.

Molecular Dynamics Studies

The three-dimensional model structure of 5-DMATS used for docking and the selected docking poses of pairs of substrate and donor were processed further using MOE [Molecular Operating Environment (MOE) 2010.10. Quebec: Chemical Computing Group; 2010]. Protonation states were calculated with the Protonate3D routine within MOE and visually inspected for plausibility. AMBER atom types were assigned to protein, substrate and donor atoms.

The MD simulations were run with the Amber14 software suite (University of California, San Francisco). The force field parameters were determined using the antechamber program (within the Amber14 suite). Amber coordinate, parameter and topology files were generated by xleap and an octahedral explicit water box (based on the TIP3P water model)[35] was constructed 10 Å away from the protein. The resulting systems were minimized, heated from 100 K to 300 K over 20 ps at constant number of particles, volume and temperature (NVT) and equilibrated at 300 K for 100 ps at constant pressure (NPT) with unrestrained water molecules and restrained protein, substrate and donor molecules. One more minimization step and subsequent heating from 100 K to 300 K for 20 ps (NVT) followed by five separate equilibration steps [four steps of 100 ps each and a final step of 2 ns at 300 K (NPT)] were performed while lowering the restraints applied to protein, substrate and donor with each step (unrestrained system at the final equilibration step). The productive simulation was carried out for 5 ns at 300 K (NVT) and 2 fs time step, storing the coordinates every picosecond. All simulations were carried out with the pmemd.cuda module of the Amber14 suite on four GPUs.

The simulations were visualized with VMD.[36] Dynamic trajectory analysis and geometric data extraction was performed with cpptraj (Amber14 suite). Graphical representations of the simulated complexes were prepared using

PyMOL (The PyMOL Molecular Graphics System, Version 1.5.0.4 Schrödinger, LLC.).

Acknowledgements

This work was supported by a grant from the Deutsche Forschungsgemeinschaft (Grant Li844/4-1 to S.-M. Li). Julia Winkelblech and Jakub Gunera are financially supported by the LOEWE program of the State of Hessen (SynMikro to S.-M. Li and P. Kolb). We thank Dr. Laufenberg and Lena Ludwig (Philipps-Universität Marburg) for acquiring mass spectra and for the synthesis of DMAPP, respectively.

References

[1] J. Clardy, C. Walsh, *Nature* **2004**, *432*, 829–837.
[2] D. J. Newman, G. M. Cragg, *J. Nat. Prod.* **2012**, *75*, 311–335.
[3] C. T. Walsh, M. A. Fischbach, *J. Am. Chem. Soc.* **2010**, *132*, 2469–2493.
[4] P. Wiemann, N. P. Keller, *J. Ind. Microbiol. Biotechnol.* **2014**, *41*, 301–313.
[5] S. D. Bentley, K. F. Chater, A. M. Cerdeno-Tarraga, G. L. Challis, N. R. Thomson, K. D. James, D. E. Harris, M. A. Quail, H. Kieser, D. Harper, A. Bateman, S. Brown, G. Chandra, C. W. Chen, M. Collins, A. Cronin, A. Fraser, A. Goble, J. Hidalgo, T. Hornsby, S. Howarth, C. H. Huang, T. Kieser, L. Larke, L. Murphy, K. Oliver, S. O'Neil, E. Rabbinowitsch, M. A. Rajandream, K. Rutherford, S. Rutter, K. Seeger, D. Saunders, S. Sharp, R. Squares, S. Squares, K. Taylor, T. Warren, A. Wietzorrek, J. Woodward, B. G. Barrell, J. Parkhill, D. A. Hopwood, *Nature* **2002**, *417*, 141–147.
[6] H. Ikeda, J. Ishikawa, A. Hanamoto, M. Shinose, H. Kikuchi, T. Shiba, Y. Sakaki, M. Hattori, S. Omura, *Nat. Biotechnol.* **2003**, *21*, 526–531.
[7] Y. Ohnishi, J. Ishikawa, H. Hara, H. Suzuki, M. Ikenoya, H. Ikeda, A. Yamashita, M. Hattori, S. Horinouchi, *J. Bacteriol.* **2008**, *190*, 4050–4060.
[8] A. A. Brakhage, *Nat. Rev. Microbiol.* **2013**, *11*, 21–32.
[9] L. Heide, *Curr. Opin. Chem. Biol.* **2009**, *13*, 171–179.
[10] S.-M. Li, *Nat. Prod. Rep.* **2010**, *27*, 57–78.
[11] X. Yu, S.-M. Li, *Methods Enzymol.* **2012**, *516*, 259–278.
[12] S. Takahashi, H. Takagi, A. Toyoda, M. Uramoto, T. Nogawa, M. Ueki, Y. Sakaki, H. Osada, *J. Bacteriol.* **2010**, *192*, 2839–2851.
[13] X. Yu, Y. Liu, X. Xie, X.-D. Zheng, S.-M. Li, *J. Biol. Chem.* **2012**, *287*, 1371–1380.
[14] N. Steffan, I. A. Unsöld, S.-M. Li, *Chembiochem* **2007**, *8*, 1298–1307.
[15] A. Kremer, S.-M. Li, *Appl. Microbiol. Biotechnol.* **2008**, *79*, 951–961.
[16] S. Subramanian, X. Shen, Q. Yuan, Y. Yan, *Process Biochem.* **2012**, *47*, 1419–1422.
[17] T. Ozaki, M. Nishiyama, T. Kuzuyama, *J. Biol. Chem.* **2013**, *288*, 9946–9956.
[18] J. Winkelblech, S.-M. Li, *Chembiochem* **2014**, *15*, 1030–1039.
[19] M. Liebhold, X. Xie, S.-M. Li, *Org. Lett.* **2012**, *14*, 4884–4885.
[20] M. Liebhold, S.-M. Li, *Org. Lett.* **2013**, *15*, 5834–5837.
[21] A. Fan, H. Chen, R. Wu, H. Xu, S.-M. Li, *Appl. Microbiol. Biotechnol.* **2014**, *98*, 10119–10129.
[22] M. Liebhold, X. Xie, S.-M. Li, *Org. Lett.* **2013**, *15*, 3062–3065.
[23] A. Kremer, L. Westrich, S.-M. Li, *Microbiology* **2007**, *153*, 3409–3416.
[24] A. Kremer, S.-M. Li, *Microbiology* **2010**, *156*, 278–286.
[25] U. Metzger, C. Schall, G. Zocher, I. Unsöld, E. Stec, S.-M. Li, L. Heide, T. Stehle, *Proc. Natl. Acad. Sci. USA* **2009**, *106*, 14309–14314.
[26] M. Jost, G. Zocher, S. Tarcz, M. Matuschek, X. Xie, S.-M. Li, T. Stehle, *J. Am. Chem. Soc.* **2010**, *132*, 17849–17858.
[27] J. M. Schuller, G. Zocher, M. Liebhold, X. Xie, M. Stahl, S.-M. Li, T. Stehle, *J. Mol. Biol.* **2012**, *422*, 87–99.
[28] X. Yu, G. Zocher, X. Xie, M. Liebhold, S. Schütz, T. Stehle, S.-M. Li, *Chem. Biol.* **2013**, *20*, 1492–1501.
[29] A. B. Woodside, Z. Huang, C. D. Poulter, *Org. Synth.* **1988**, *66*, 211–215.
[30] T. Ozaki, M. Nishiyama, T. Kuzuyama, *J. Biol. Chem.* **2013**, *288*, 9946–9956.
[31] A. Šali, T. L. Blundell, *J. Mol. Biol.* **1993**, *234*, 779–815.
[32] M. Y. Shen, A. Sali, *Protein Sci.* **2006**, *15*, 2507–2524.
[33] B. R. Brooks, C. L. Brooks III, A. D. Mackerell Jr., L. Nilsson, R. J. Petrella, B. Roux, Y. Won, G. Archontis, C. Bartels, S. Boresch, A. Caflisch, L. Caves, Q. Cui, A. R. Dinner, M. Feig, S. Fischer, J. Gao, M. Hodoscek, W. Im, K. Kuczera, T. Lazaridis, J. Ma, V. Ovchinnikov, E. Paci, R. W. Pastor, C. B. Post, J. Z. Pu, M. Schaefer, B. Tidor, R. M. Venable, H. L. Woodcock, X. Wu, W. Yang, D. M. York, M. Karplus, *J. Comput. Chem.* **2009**, *30*, 1545–1614.
[34] M. McGann, *J. Chem. Inf. Model.* **2011**, *51*, 578–596.
[35] W. L. Jorgensen, J. Chandrasekhar, J. D. Madura, R. W. Impey, M. L. Klein, *J. Chem. Phys.* **1983**, *79*, 926–935.
[36] W. Humphrey, A. Dalke, K. Schulten, *J. Mol. Graph.* **1996**, *14*, 33–38.

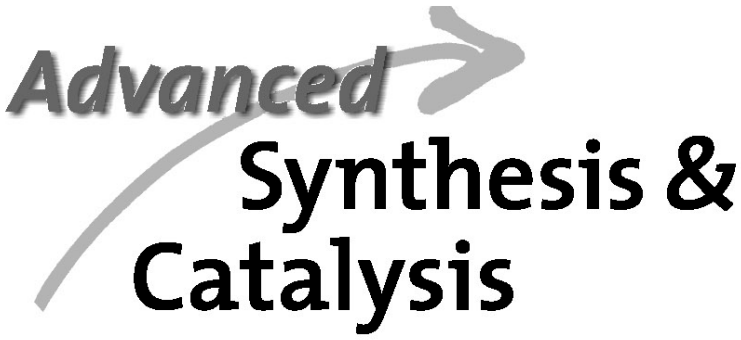

Supporting Information

Tryptophan *C5*-, *C6*- and *C7*-Prenylating Enzymes Displaying a Preference for C-6 of the Indole Ring in the Presence of Unnatural Dimethylallyl Diphosphate Analogues

Supporting Information

Julia Winkelblech[a,b,‡], Mike Liebhold[a,‡], Jakub Gunera[b,c], Xiulan Xie[d], Peter Kolb[b,c] Shu-Ming Li[a,b,*]

a Philipps-Universität Marburg, Institut für Pharmazeutische Biologie und Biotechnologie, Deutschhausstrasse 17A, 35037 Marburg, Germany
Fax: (+49)-6421-282-5365; phone: (+49)-6421-282-2461; e-mail: shuming.li@staff.uni-marburg.de
b Philipps-Universität Marburg, Zentrum für Synthetische Mikrobiologie, D-35032 Marburg, Germany
c Philipps-Universität Marburg, Institut für Pharmazeutische Chemie, Marbacher Weg 6, 35032 Marburg, Germany
d Philipps-Universität Marburg, Fachbereich Chemie, Hans-Meerwein-Strasse, 35032 Marburg, Germany
‡ These authors contributed equally to this work

Structure elucidation

In the ^{1}H-NMR spectra of **Ia**, signals of the indole moiety at 7.60 (1H, dd, 8.1, 0.4), 7.15 (1H, d, 0.7), 7.12 (1H, s) and 6.89 ppm (1H, dd, 8.1, 1.4) superimposed with those for H-4, H-7, H-2 and H-5 of 6-methylallyl-L-tryptophan, respectively.[1] The signals of H-10 and H-11 as well as H-1' and H-4' of **Ia** were also overlapping almost completely (maximum shift 0.03 ppm) with those of 6-methylallyl-L-tryptophan.[1] This proved unequivocally the regular *C6*-alkylation of L-tryptophan with MAPP as alkyl donor in the presence of the tested prenyltransferases (6-DMATS$_{Sa}$, 6-DMATS$_{Sv}$, TyrPT, 5-DMATS$_{Sc}$ and 5-DMATS). Comparing the ^{1}H-NMR spectrum of **IIa** with that of C6-(2-pentenyl)-L-tryptophan[1] showed nearly identical chemical shifts and coupling patterns for all of the protons. This verified the regular alkylation of L-tryptophan at position C-6 of the indole ring by using 2-pentenyl-PP as alkyl donor. The aromatic protons of **IIIa** at 7.60 (1H, dd, 8.2, 0.6), 7.18 (1H, s), 7.12 (1H, s) and 6.93 ppm (1H, dd, 8.2, 1.5) showed the same coupling pattern and chemical shifts as observed for **Ia** and **IIa**. These signals also corresponded to those of *C6*-alkylated L-tryptophan derivatives[1] and therefore proved the *C6*-benzylation of L-tryptophan. The chemical shifts observed for H-10 and H-11 at 3.48, 3.11 and 3.82 ppm, also overlapped very well with those of the other C6-alkylated L-tryptophan derivatives. The five additional aromatic protons and two additional aliphatic protons observed in the ^{1}H-NMR spectra of **IIIa** confirmed the presence of the benzyl moiety.

From the incubation mixtures of TyrPT and 5-DMATS$_{Sc,}$ the regular alkylated products **Ib1** and **IIb1** as well as the regular benzylated product **IIIb** were isolated. The ^{1}H-NMR spectrum of **IIb1** showed one singlet at 7.19, two doublets at 7.55 and 6.93 and one triplet at 7.00 ppm for one proton each. This indicated an alkylation at position C-4 or C-7 of the indole ring. In the HMBC spectrum of **IIb1** (Figure S16-S19), correlations between H-10 at 3.13 and C-2 at 124.7 ppm, C-11 at 56.5 ppm with two quaternary carbon atoms at 109.9 and 128.4 ppm were observed. Correlations between the proton at 7.00 ppm, which is either H-5 or H-6, and two quaternary carbon atoms at 128.4 and at 125.1 ppm but not with that at 109.9 ppm were detected. Consequently, the quaternary carbons at 109.9 and 128.4 ppm were assigned to C-3 and C-9, respectively. Therefore, the signal at 7.00 ppm was assigned to H-5. Further correlations were found between the doublet at 7.56 ppm and the quaternary carbons C-3, C-9 and another one at 136.8 ppm. These correlations are only possible, if the proton at 7.56 ppm is for H-4 and the carbons at 136.8 and 125.1 ppm are for C-8 and C-7, respectively. Thus, an alkylation at position C-7 was proven. This was further confirmed by correlations between H-1' at 3.54 ppm and the quaternary carbons at 125.1 and 136.8 ppm, but not with that at 128.4

ppm (C-9). In addition, the doublet at 6.93 ppm also correlated with the quaternary carbons at 125.1 and 136.8 ppm as well as the signal for H-1'. The signals at 125.1, 136.8 and 6.93 ppm were assigned to C-7, C-8 and H-6, accordingly.

The chemical shifts of the protons in the tryptophan moiety of **Ib1** at 7.56 (H-4), 7.19 (H-2), 7.00 (H-5), 6.93 (H-6), 3.85 (H-11), 3.51 (H-10) and 3.14 ppm (H-10) almost completely overlapped with those of **IIb1**. Similar spectrum was obtained for **IIIb**. Therefore, the alkylation position in **Ib1** and benzylation position in **IIIb** were assigned unequivocally to C-7 of the indole ring.

In the presence of TyrPT, the additional products **Ib2** and **IIb2** were detected by using MAPP and 2-pentenyl-PP as alkyl donor, respectively. The coupling patterns and chemical shifts of the aromatic protons of both compounds corresponded very well to those of **Ib1** and **IIb1**, confirming a *C7*-alkylation of L-tryptophan (Slight shifts of approximate 0.05 ppm were observed). However, the signals of the alkyl residues of **Ib2** and **IIb2**, displayed distinct chemical shifts and coupling patterns in comparison to those of **Ib1** and **IIb1**. The coupling pattern for H-1' at 5.12 (1H, dt, 17.3, 1.7) and 5.04 ppm (1H, dt, 10.3, 1.7) as well as for H-2' at 6.12 ppm (1H, ddd, 17.3, 10.3, 6.3) in the spectrum of **Ib2** showed clearly a reverse alkylation.[2] The same was true for H-1' at 5.08 (1H, dt, 17.2, 1.5) and 4.99 ppm (1H, ddd, 10.2, 1.9, 1.0) as well as for H-2' at 6.06 ppm (1H, ddd, 17.2, 10.2, 7.6) in the spectrum of **IIb2**. This proved the reverse orientation of the alkyl residues of both compounds. Consequently, **Ib2** and **IIb2** were identified as 7-(3'-methylallyl-)-L-tryptophan and 7-(3'-pentenyl-)-L-tryptophan, respectively. From the ^{1}H NMR spectra of **Ib2** and **IIb2**, it was evident that only one of the two possible diastereomers was isolated. Unfortunately, the stereochemistry of these compounds at position C-3' could not be determined in this study.

Due to low conversion and unsuccessful separation on HPLC, **Ic**, **IIc** and **IIIc** were elucidated from the mixture with **Ia**, **IIa** and **IIIa**, respectively. The aliphatic signals of the indole moiety and those of the alkyl or benzyl residue for **Ic** were overlapped by those of **Ia**. The aromatic signals of the indole moiety were distinct from those of **Ia**, and could be used to identify the alkylation position. Comparison of the NMR data obtained in this study with those published previously [1,3] confirmed that **Ic**, **IIc** and **IIIc** to be 5-methylallyl-L-tryptophan, 5-(2-pentenyl)-L-tryptophan and 5-benzyl-L-tryptophan [3], respectively.

Reference List

1. Liebhold, M.; Xie, X.; Li, S.-M. *Org. Lett.* **2012,** *14*, 4884-4885.
2. Liebhold, M.; Xie, X.; Li, S.-M. *Org. Lett.* **2013,** *15*, 3062-3065.
3. Liebhold, M.; Li, S.-M. *Org. Lett.* **2013,** *15*, 5834-5837.

Table S1. Enzyme activities of several prenyltransferases toward L-tryptophan in the presence of DMAPP and its analogues MAPP, 2-pentenyl-PP and benzyl-PP.

	DMAPP [%]	2-pentenyl-PP [%]	MAPP [%]	benzyl-PP [%]
6-DMATS$_{Sa}$	99.9±0.2	91.2±0.07	51.1±0.5	13.9±0.3
6-DMATS$_{Sv}$	99.4±0.9	89.3±0.6	37.6±0.3	8.2±0.3
TyrPT	68.5±0.2	38.3±0.6	17.7±0.2	8.5±1.0
5-DMATS$_{Sc}$	81.4±2.4	65.0±0.1	21.0±0.4	6.6±0.1
5-DMATS	99.8±0.35	91.9±0.1	58.9±0.07	28.6±0.07

The reaction mixtures contained 1 mM L-tryptophan and 2mM DMAPP, 2-pentenyl-PP, MAPP or benzyl-PP and were incubated with 7.5 μM of purified protein at 37°C for 16 h. Conversion yields are given as mean of two independent measurements.

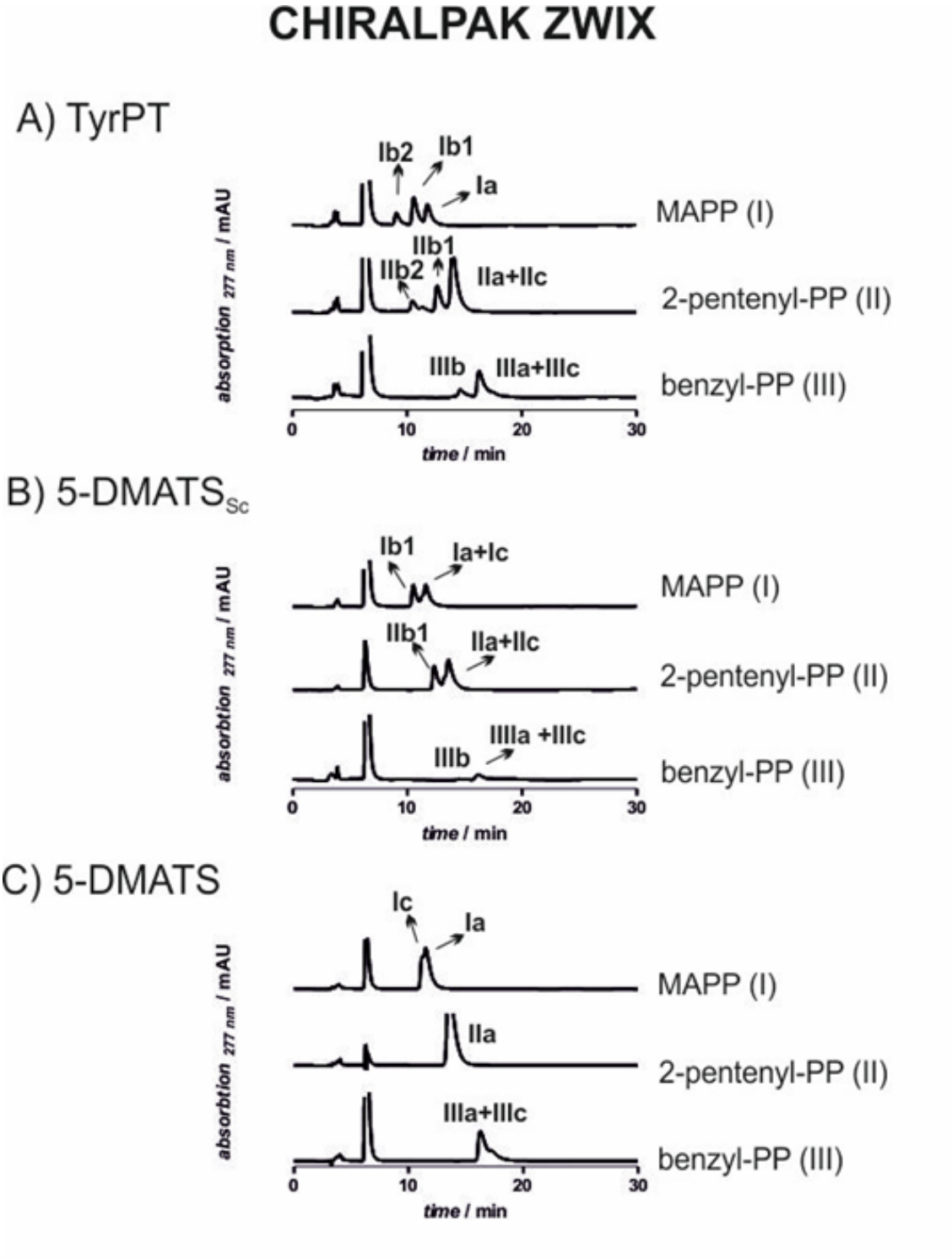

Figure S1. HPLC analysis of the reaction mixtures of L-tryptophan with MAPP (**I**), 2-pentenyl-PP (**II**) and benzyl-PP (**III**) on a Chiralpak Zwix (+) column. The enzyme assays of 100 µL contained 1 mM L-tryptophan, 2 mM alkyl or benzyl diphosphate, 5 mM $CaCl_2$ and 7.5 µM of purified protein were incubated at 37°C for 16 h.

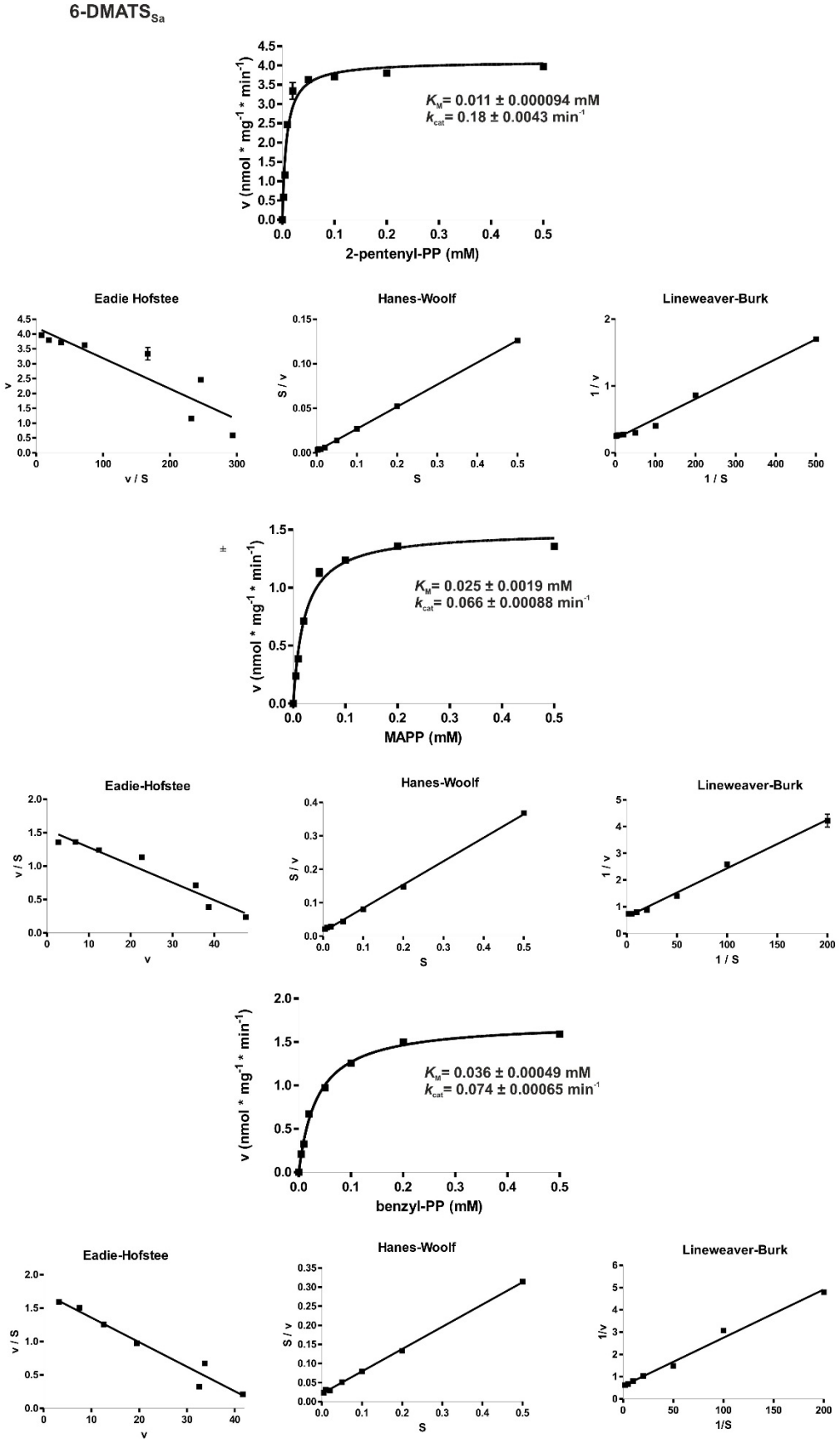

Figure S2. Dependence of the product formation of the 6-DMATS$_{Sa}$ reaction on the presence of 2-pentenyl-PP, methylallyl-PP (MAPP) or benzyl-PP with L-tryptophan.

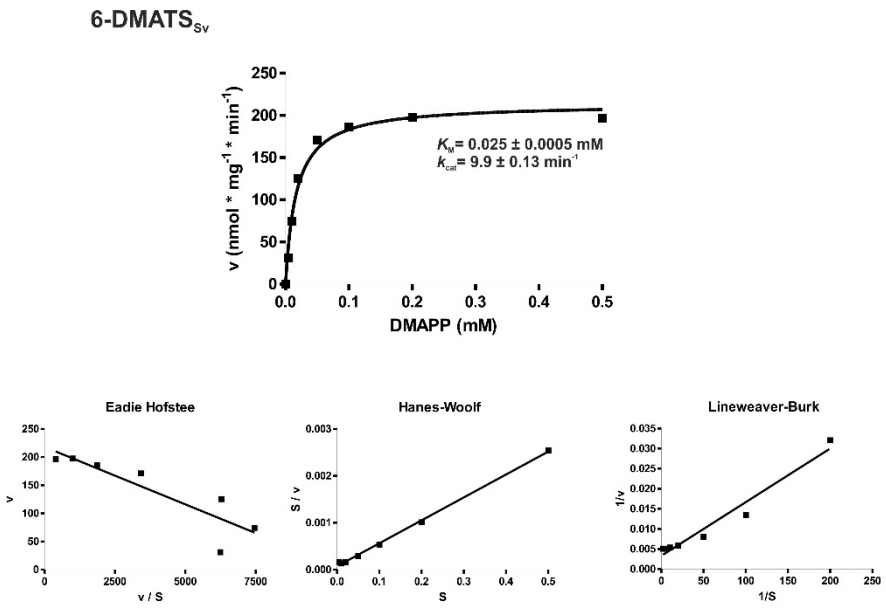

Figure S3. Dependence of the product formation of the 6-DMATS$_{Sv}$ reaction on the presence of DMAPP with L-tryptophan.

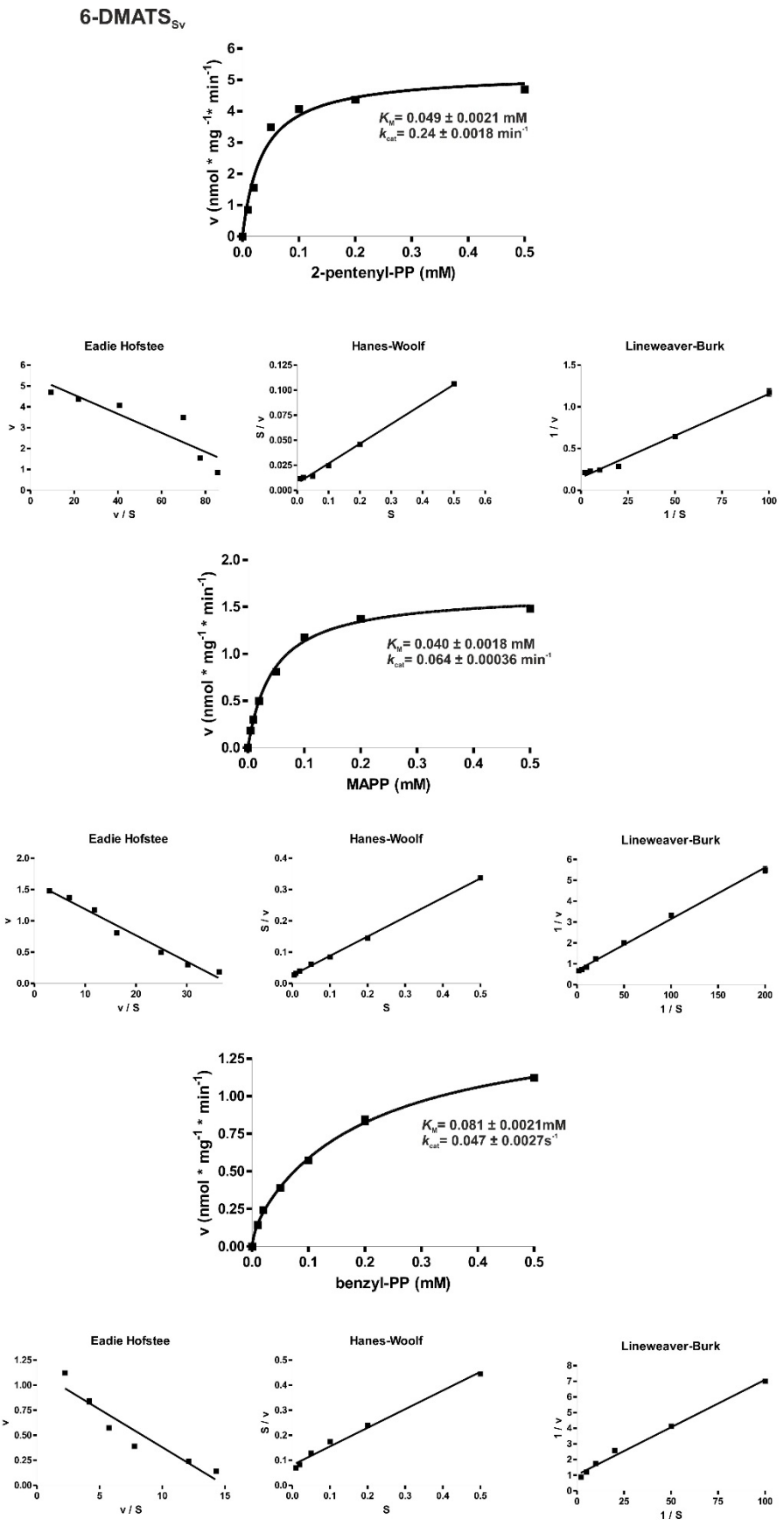

Figure S4. Dependence of the product formation of the 6-DMATS$_{Sv}$ reaction on the presence of 2-pentenyl-PP, methylallyl-PP (MAPP) or benzyl-PP with L-tryptophan.

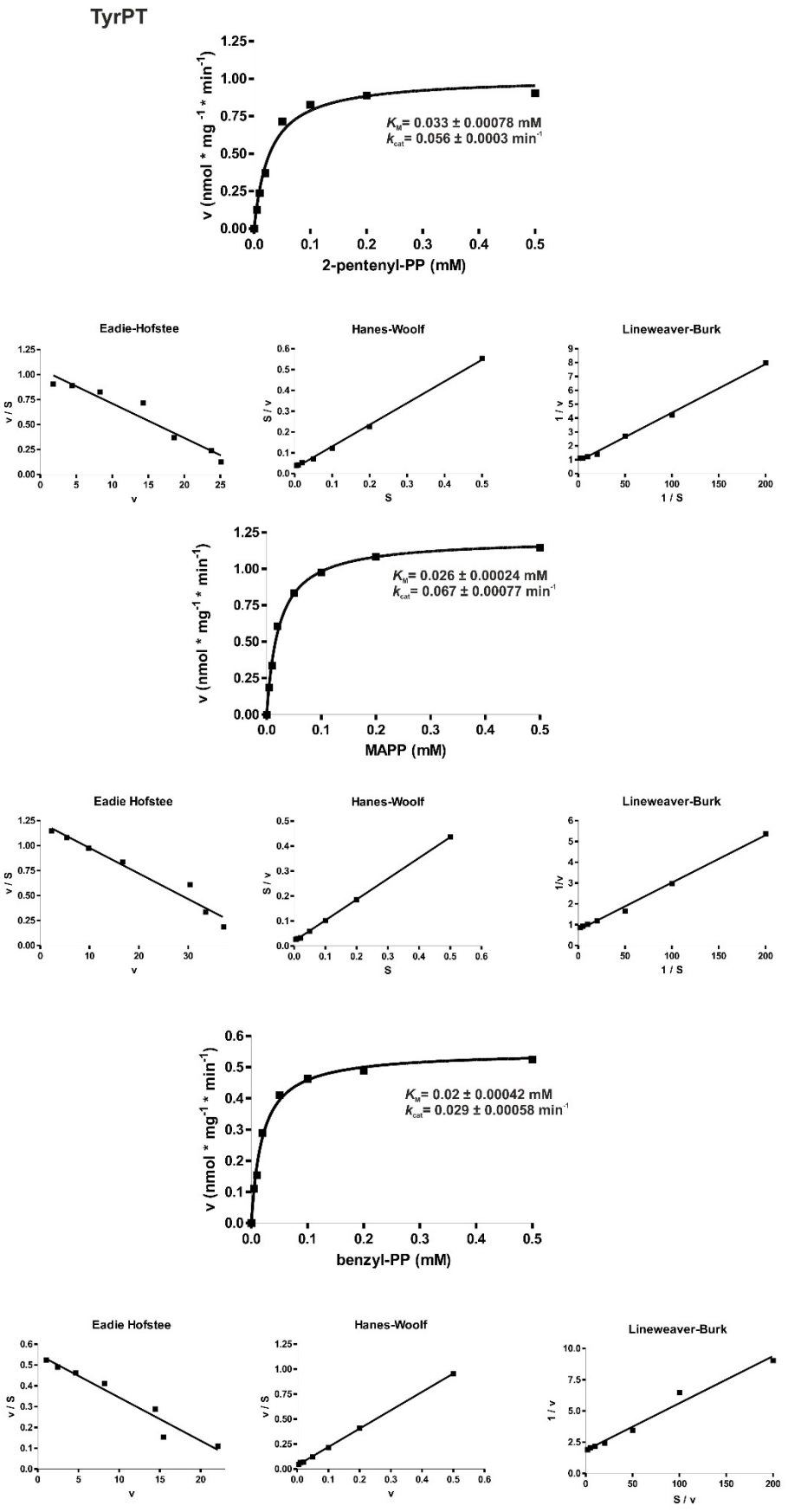

Figure S5. Dependence of the product formation of the TyrPT reaction on the presence of 2-pentenyl-PP, methylallyl-PP (MAPP) or benzyl-PP with L-tryptophan.

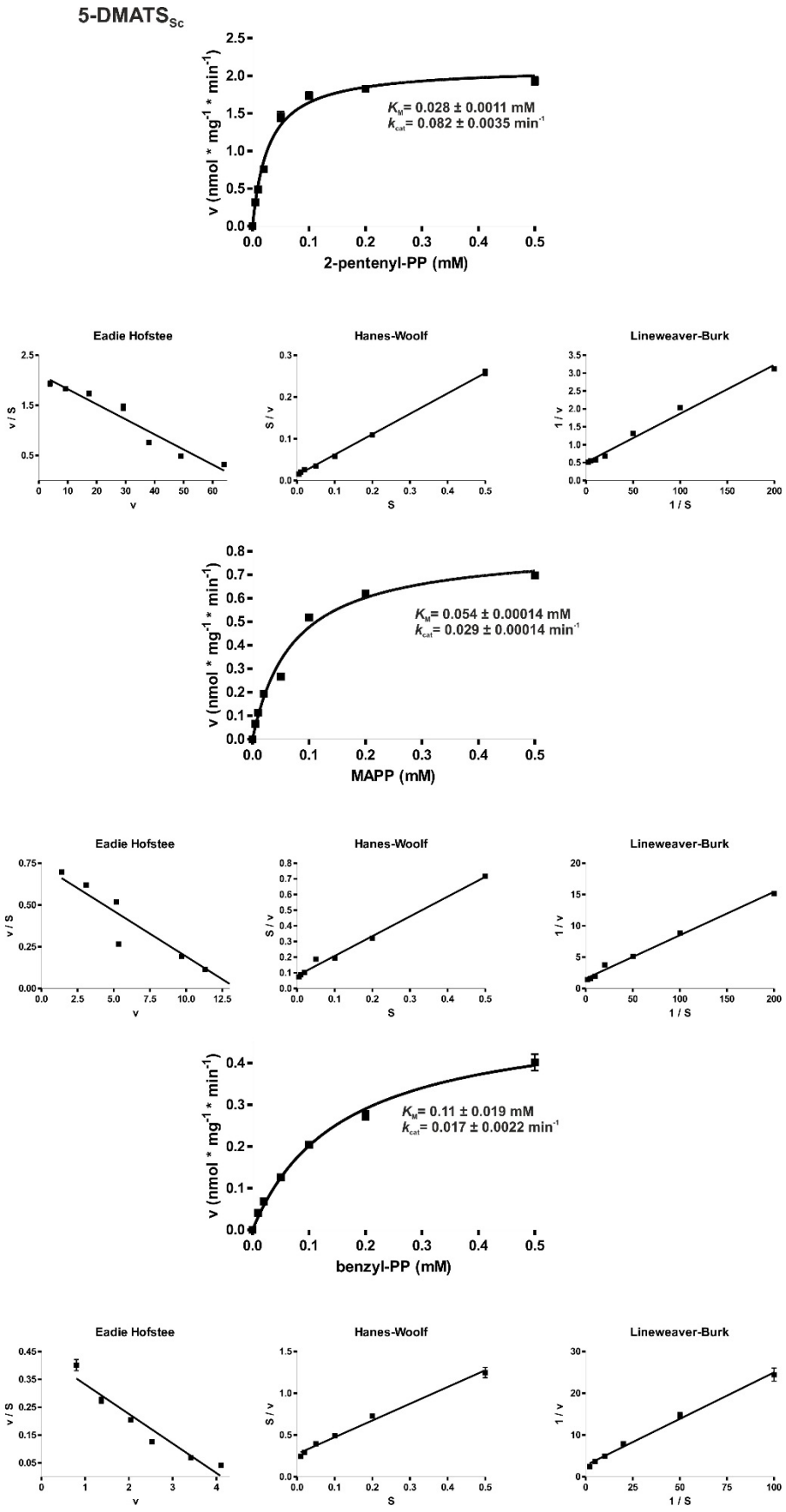

Figure S6. Dependence of the product formation of the 5-DMATS$_{Sc}$ reaction on the presence of 2-pentenyl-PP, methylallyl-PP (MAPP) or benzyl-PP with L-tryptophan.

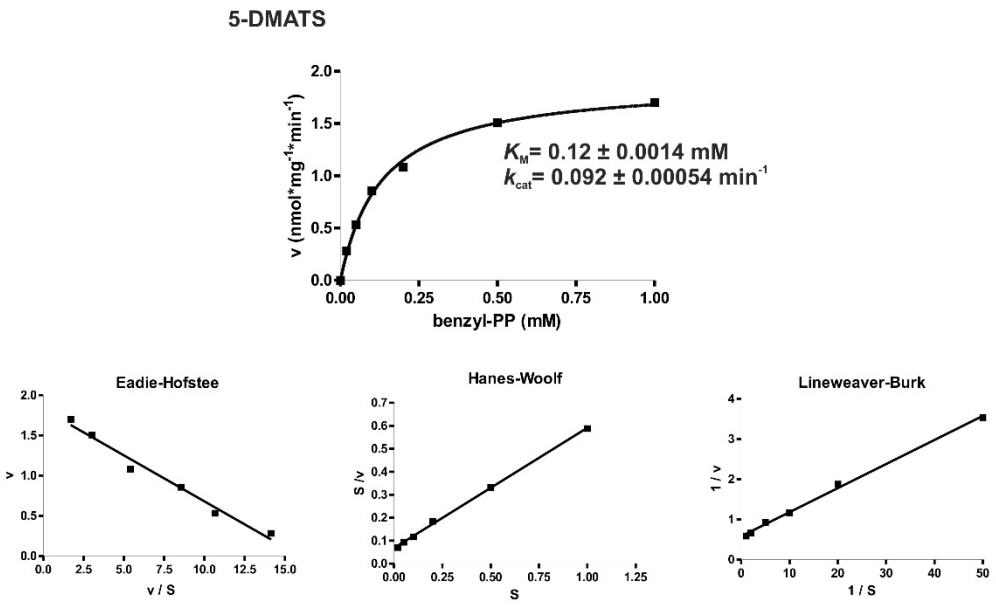

Figure S7. Dependence of the product formation of the 5-DMATS reaction on the presence of benzyl-PP with L-tryptophan.

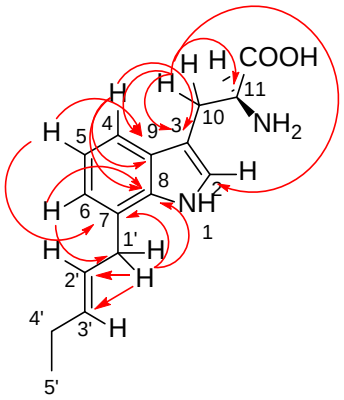

Figure S8. HMBC connectivities of 7-(2-pentenyl-)-L-tryptophan (**IIb1**).

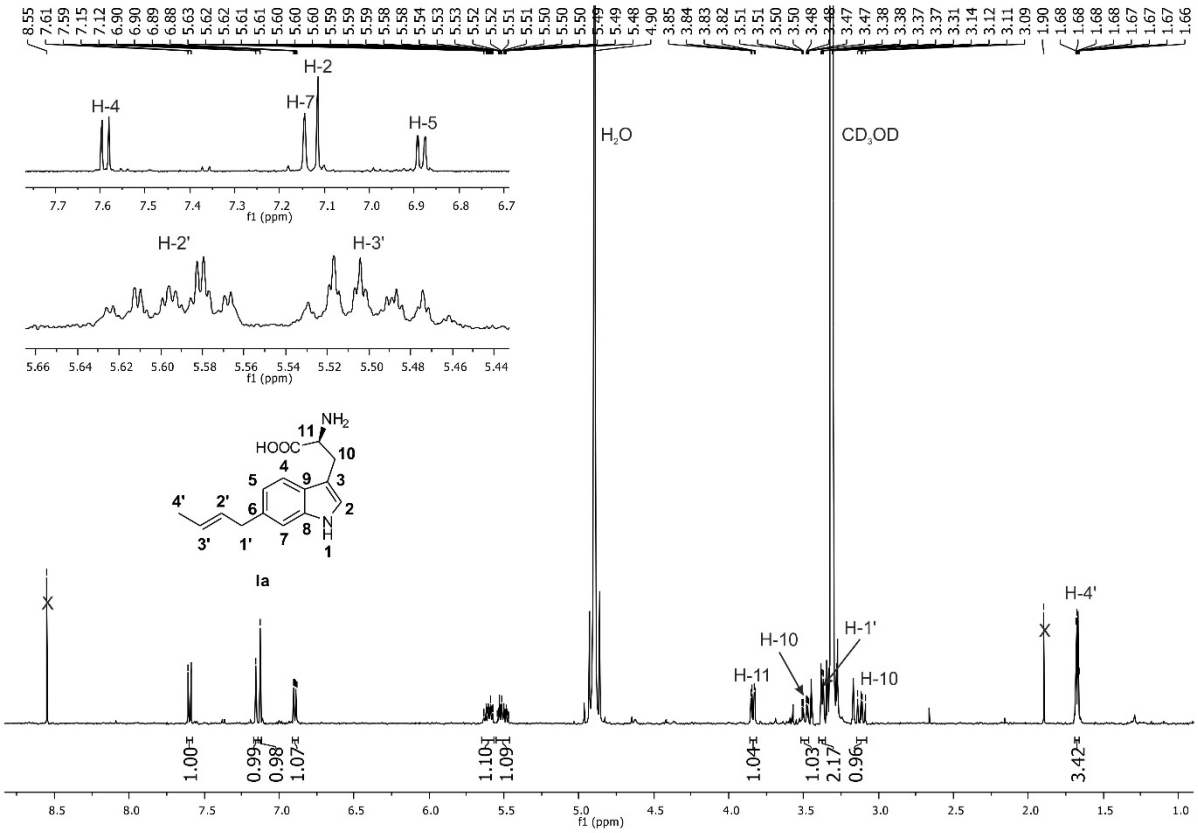

Figure S9. ^{1}H-NMR spectrum of 6-methylallyl-L-tryptophan (**Ia**) in CD_3OD.

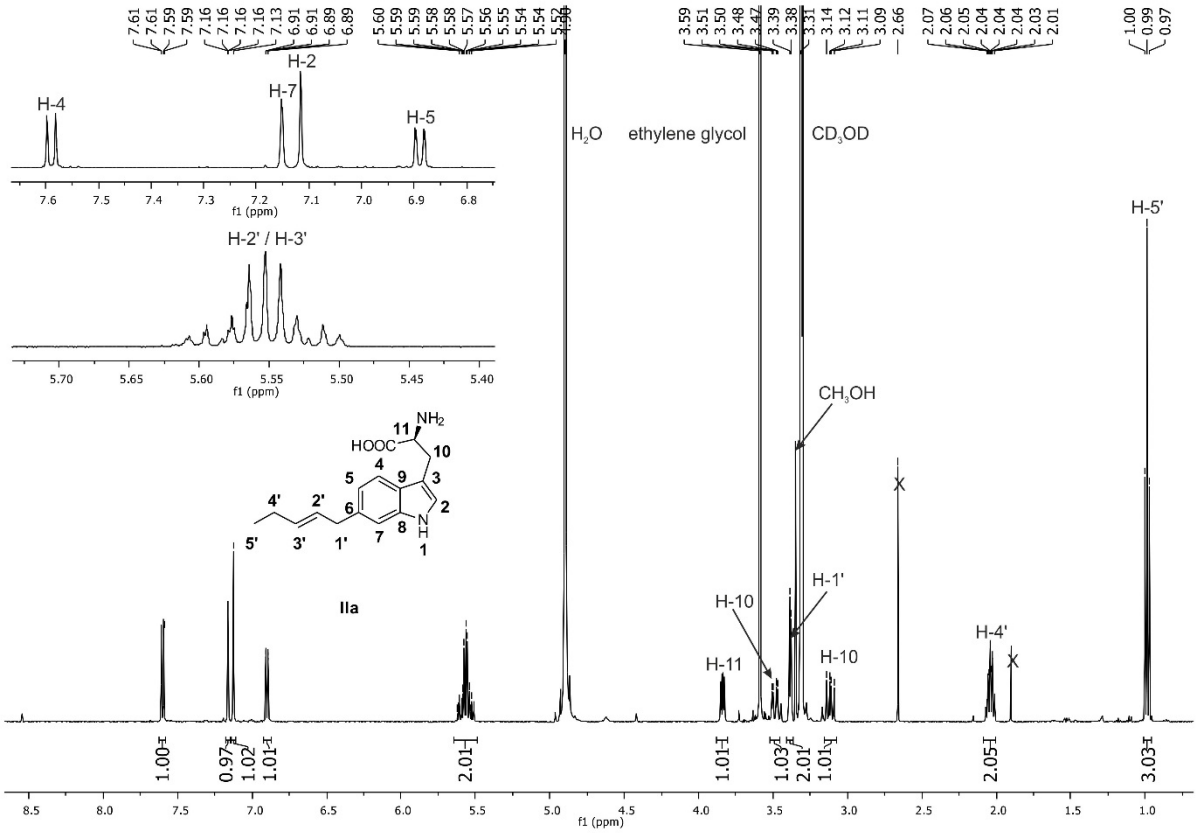

Figure S10. ^{1}H-NMR spectrum of 6-(2-pentenyl-)-L-tryptophan (**IIa**) in CD_3OD.

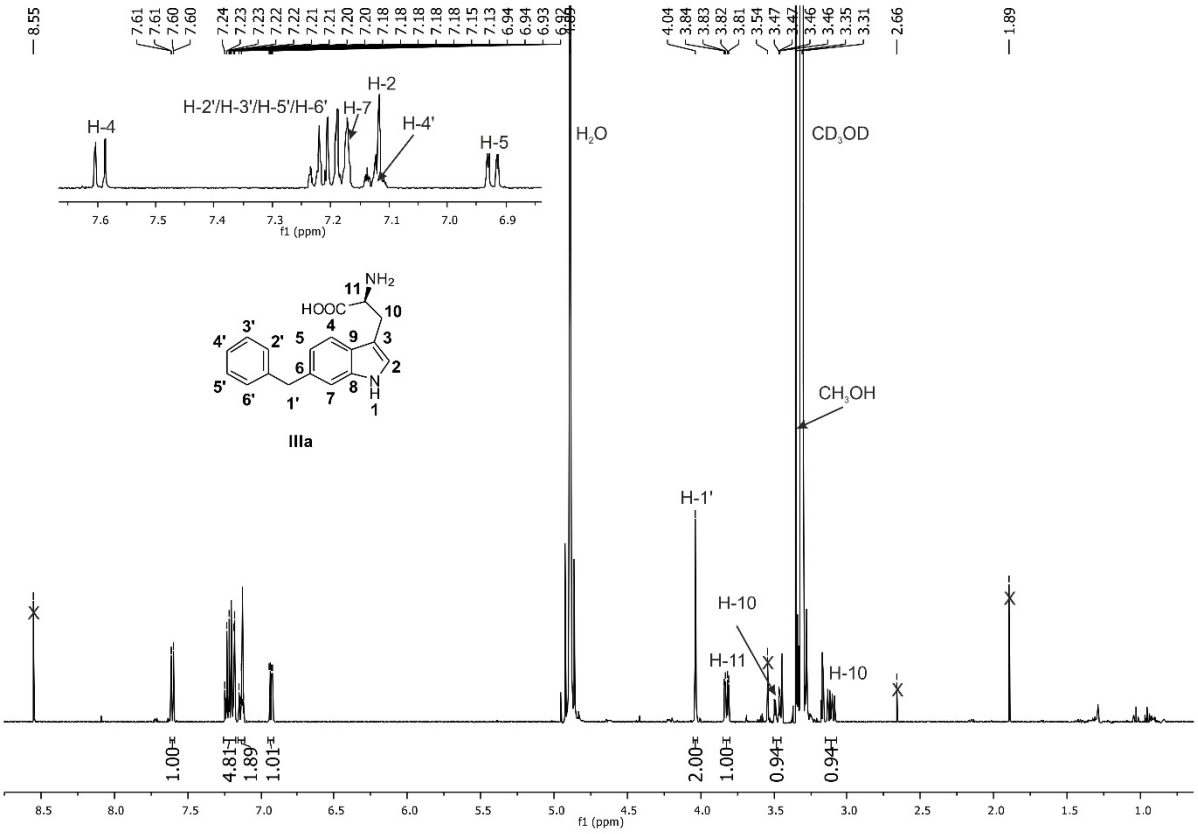

Figure S11. ^{1}H-NMR spectrum of 6-benzyl-L-tryptophan (**IIIa**) in CD_3OD.

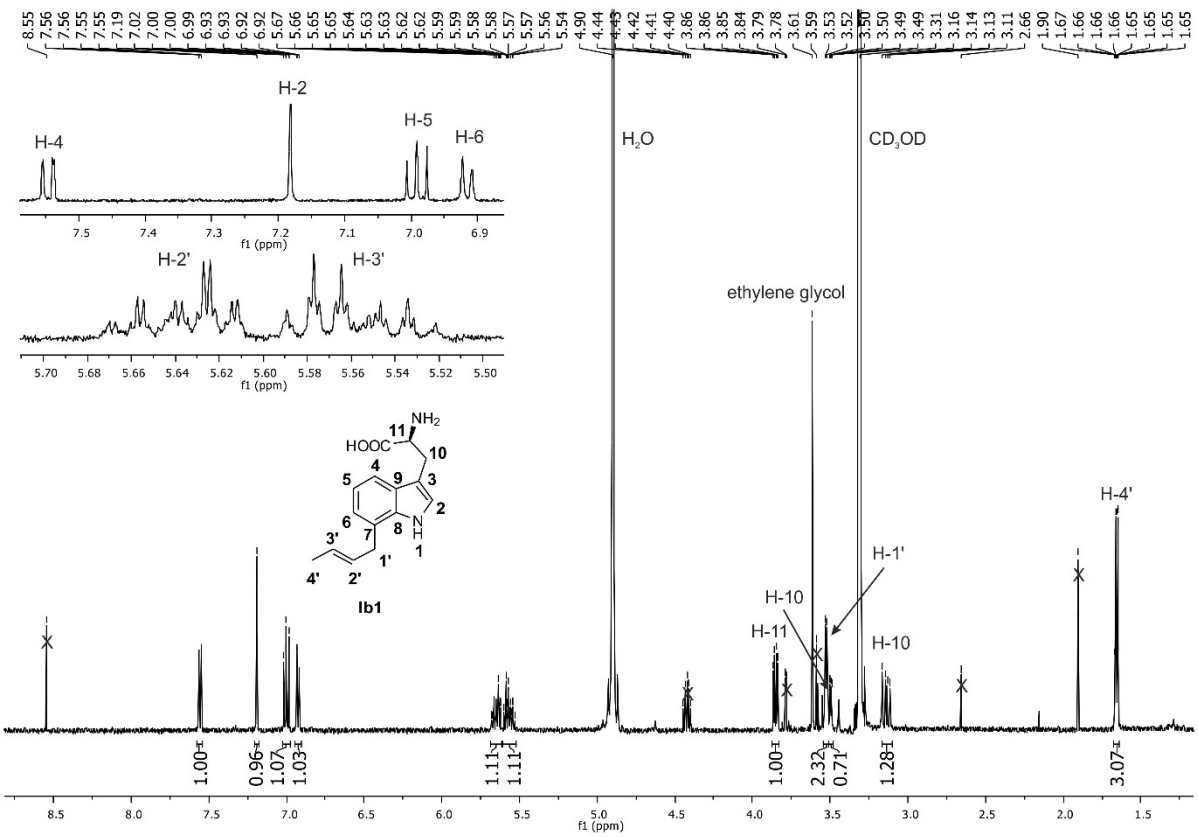

Figure S12. ^{1}H-NMR spectrum of 7-methylallyl-L-tryptophan (**Ib1**) in CD_3OD.

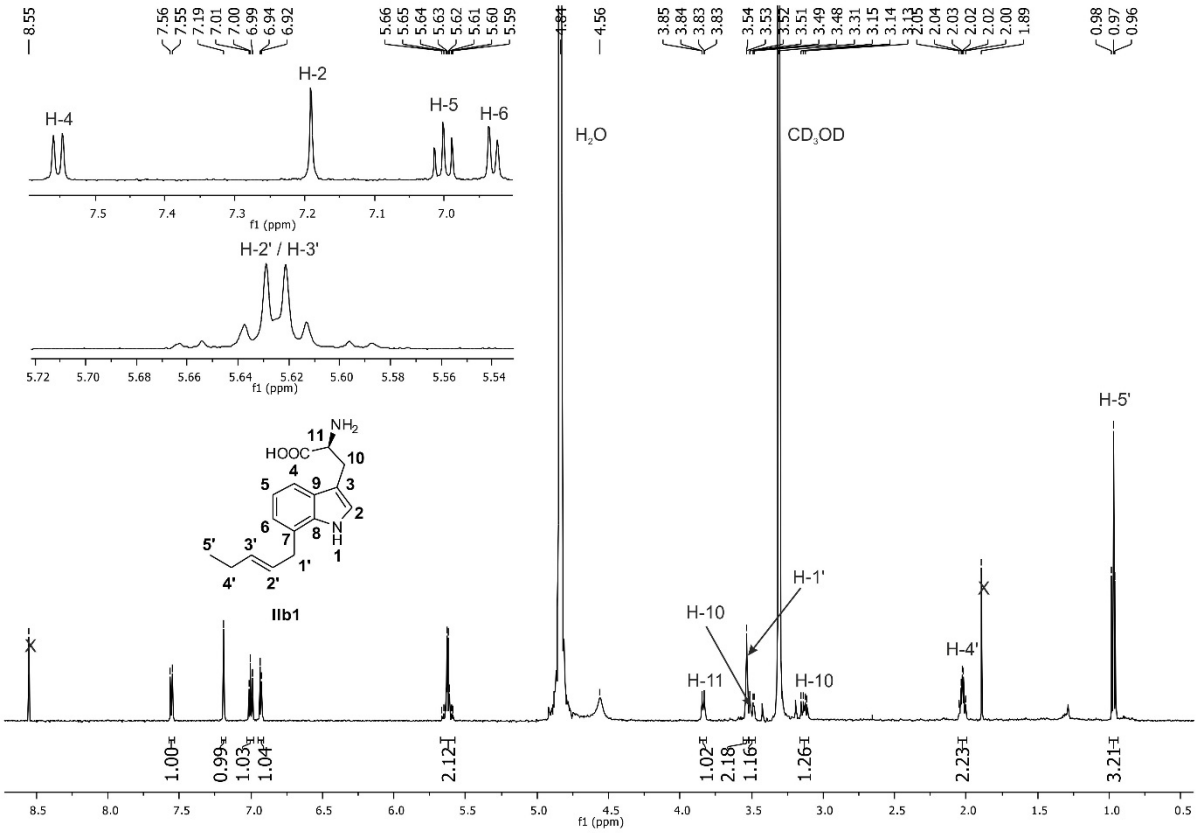

Figure S13. ^{1}H-NMR spectrum of 7-(2-pentenyl-)-L-tryptophan (**IIb1**) in CD_3OD.

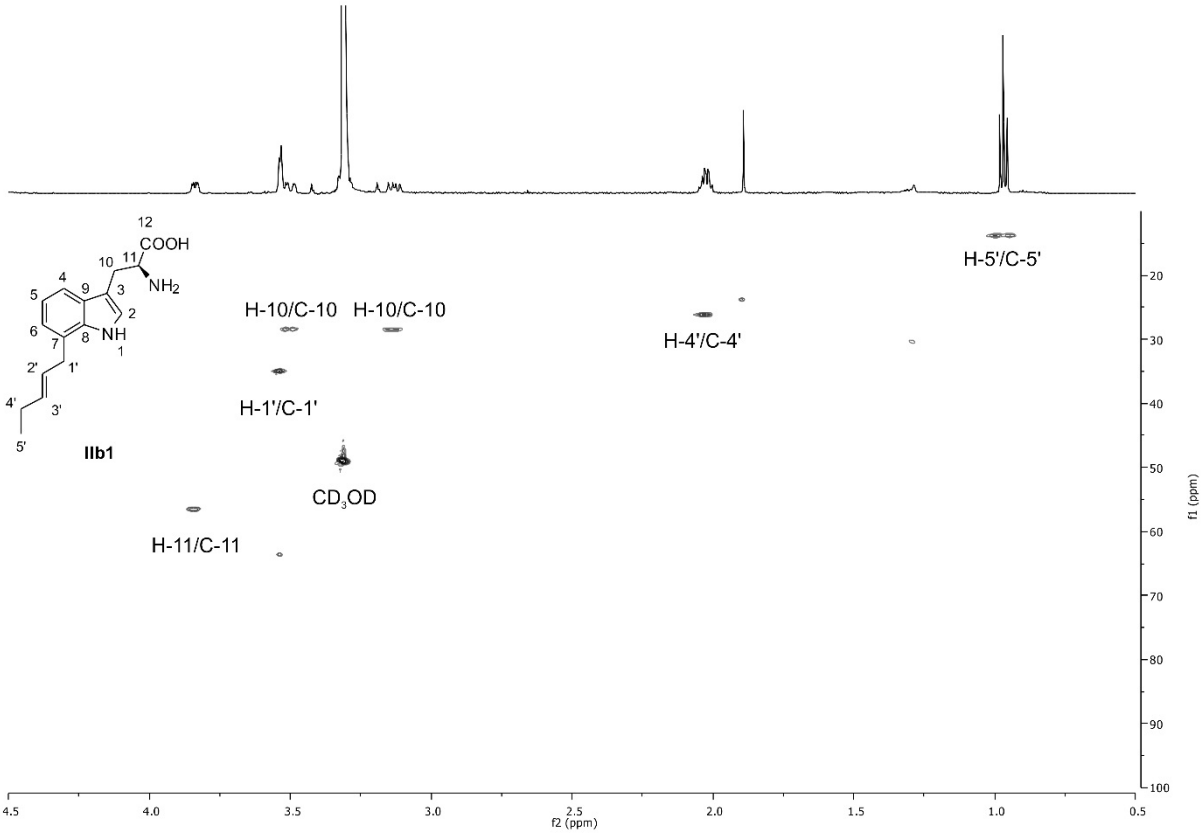

Figure S14. HSQC spectrum of 7-(2-pentenyl-)-L-tryptophan (**IIb1**) in CD_3OD.

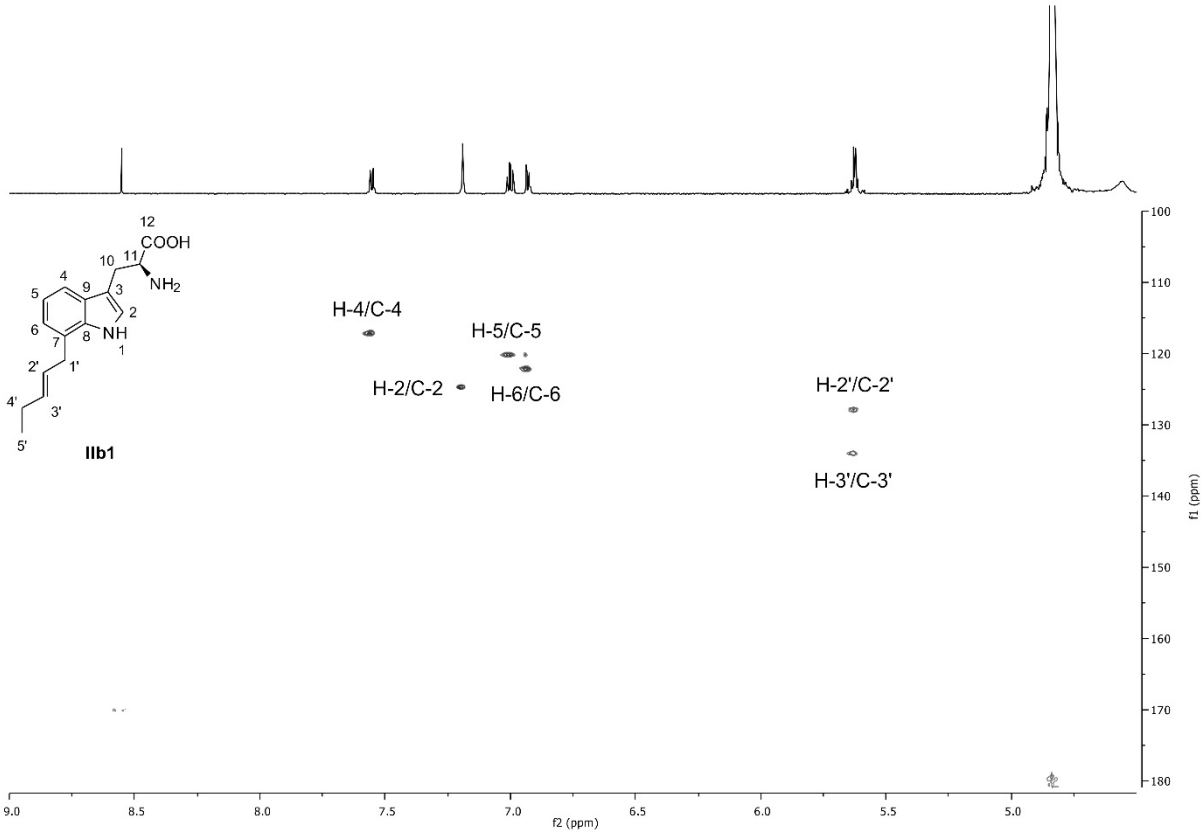

Figure S15. HSQC spectrum of 7-(2-pentenyl-)-L-tryptophan (**IIb1**) in CD_3OD.

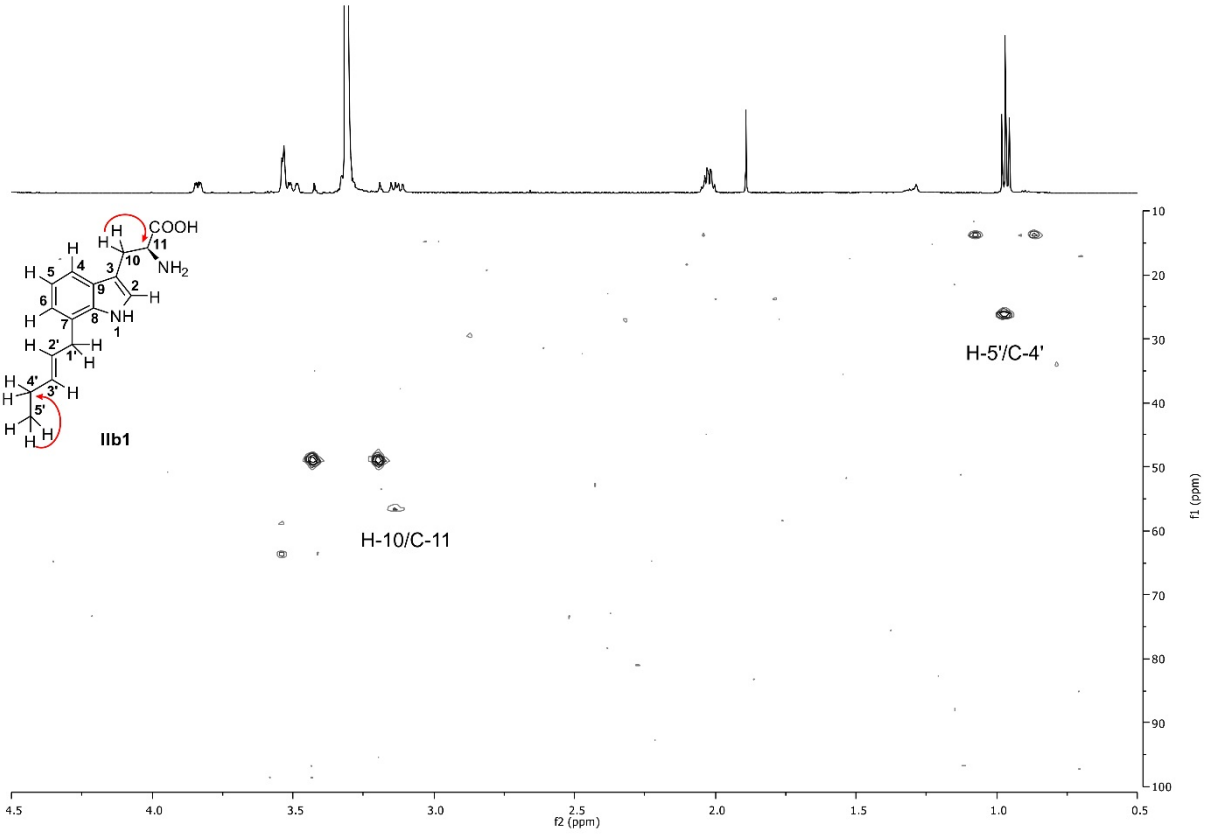

Figure S16. HMBC spectrum of 7-(2-pentenyl-)-L-tryptophan (**IIb1**) in CD_3OD.

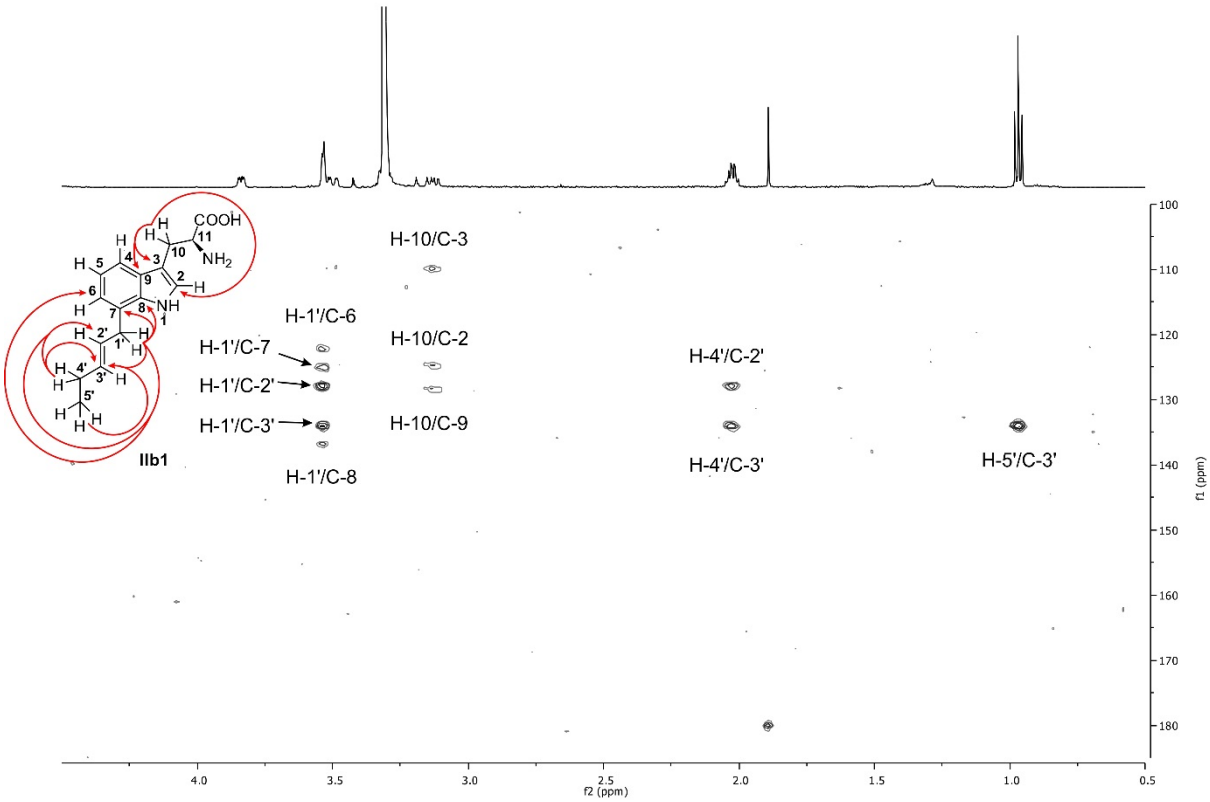

Figure S17. HMBC spectrum of 7-(2-pentenyl-)-L-tryptophan (**IIb1**) in CD_3OD.

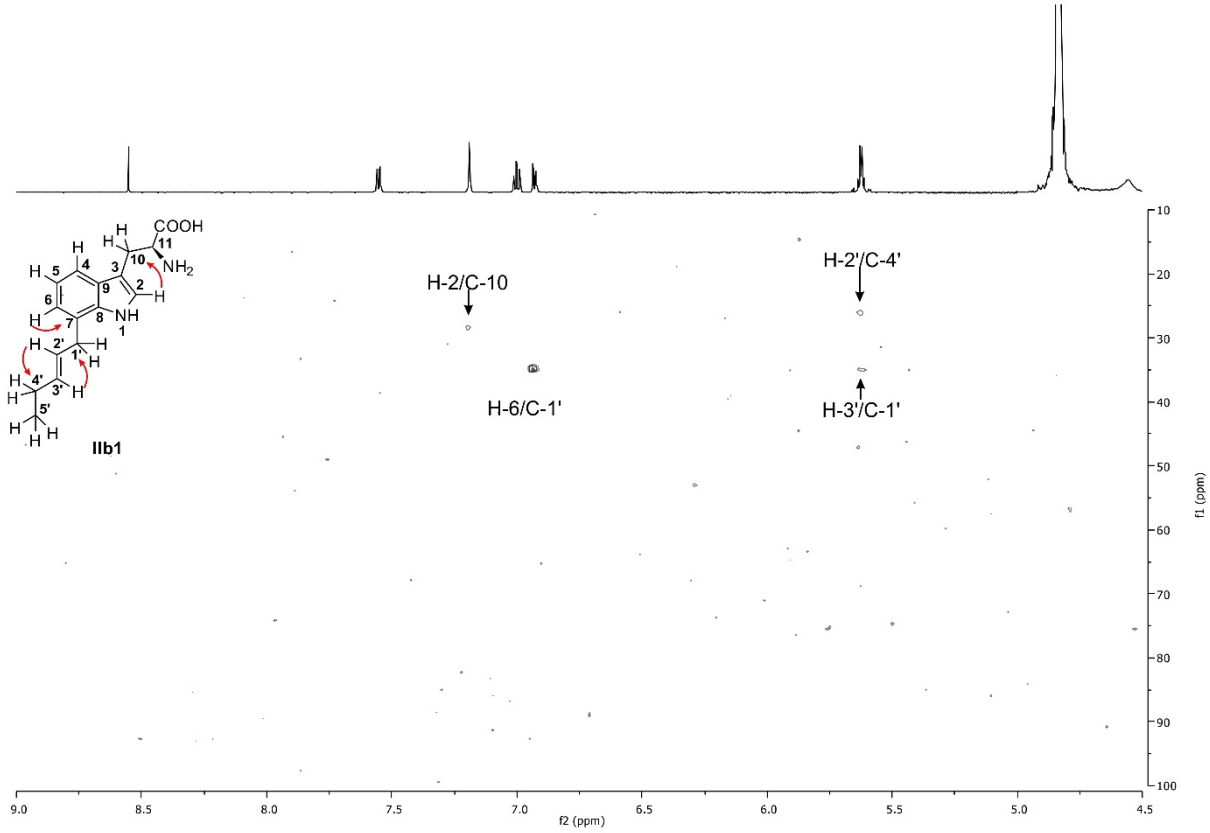

Figure S18. HMBC spectrum of 7-(2-pentenyl-)-L-tryptophan (**IIb1**) in CD_3OD.

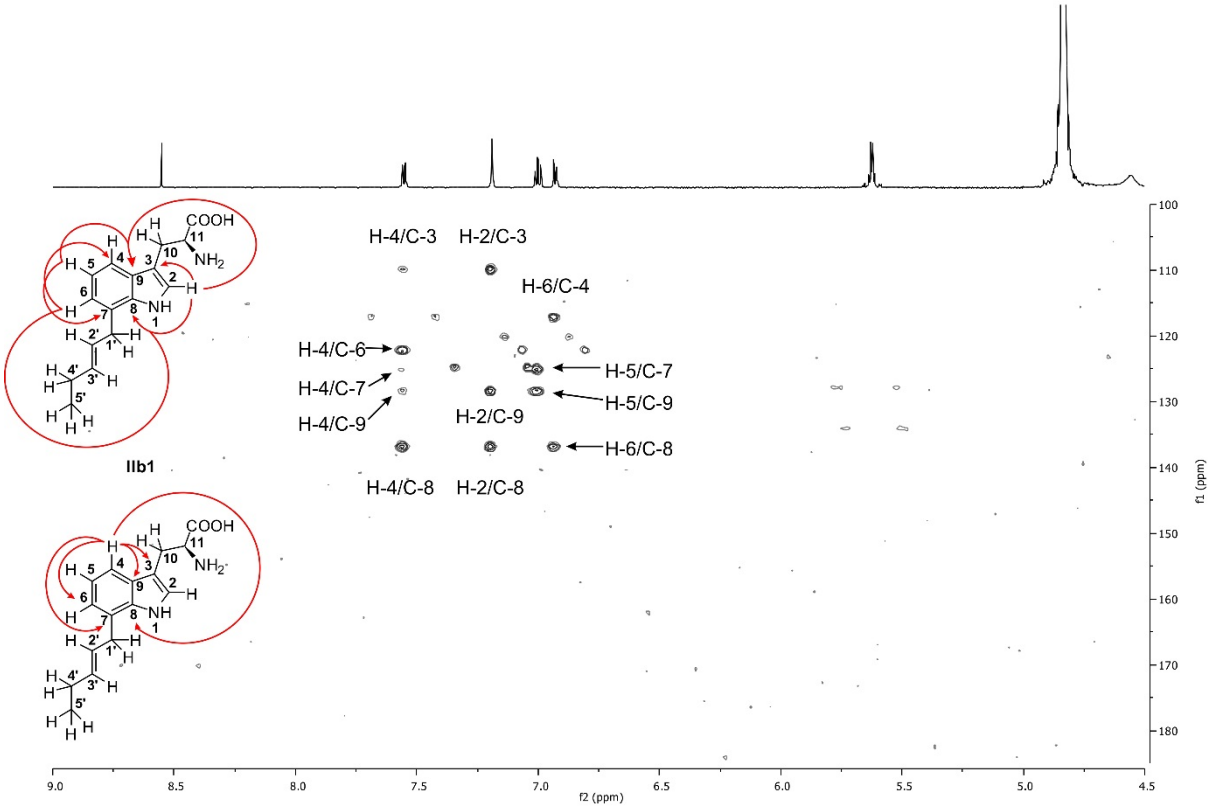

Figure S19. HMBC spectrum of 7-(2-pentenyl-)-L-tryptophan (**IIb1**) in CD_3OD.

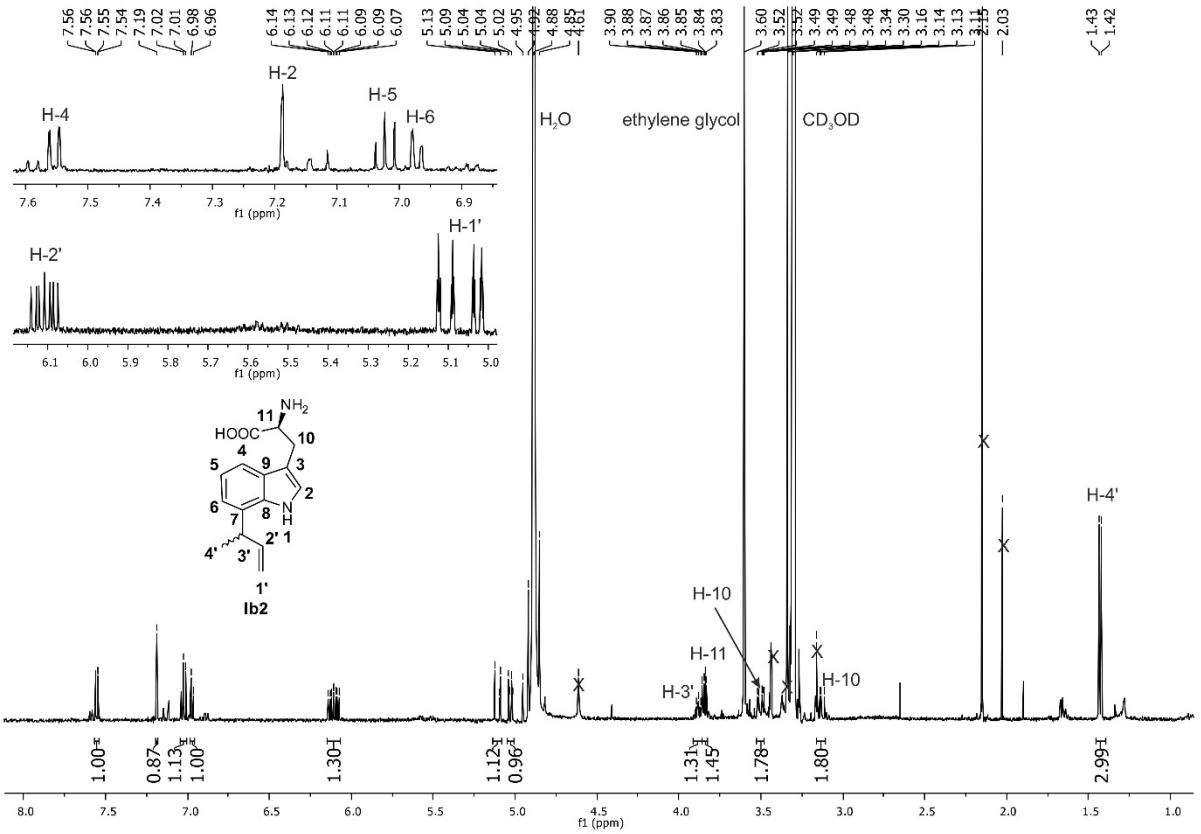

Figure S20. ^{1}H-NMR spectrum of 7-(3'*S* or 3'*R*-but-1-enyl)-L-tryptophan (**Ib2**) in CD_3OD.

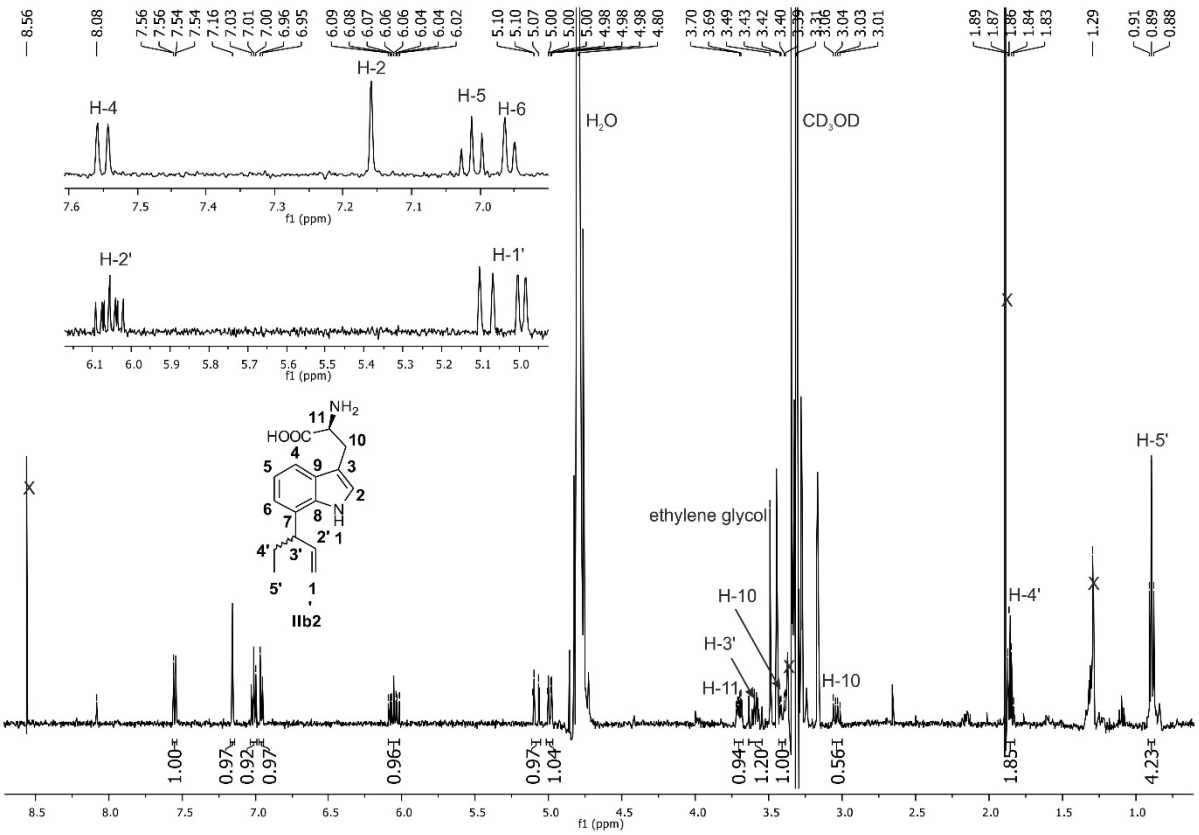

Figure S21. ^{1}H-NMR spectrum of 7-(3'*S* or 3'*R*-pent-1-enyl -)-L-tryptophan (**IIb2**) in CD_3OD.

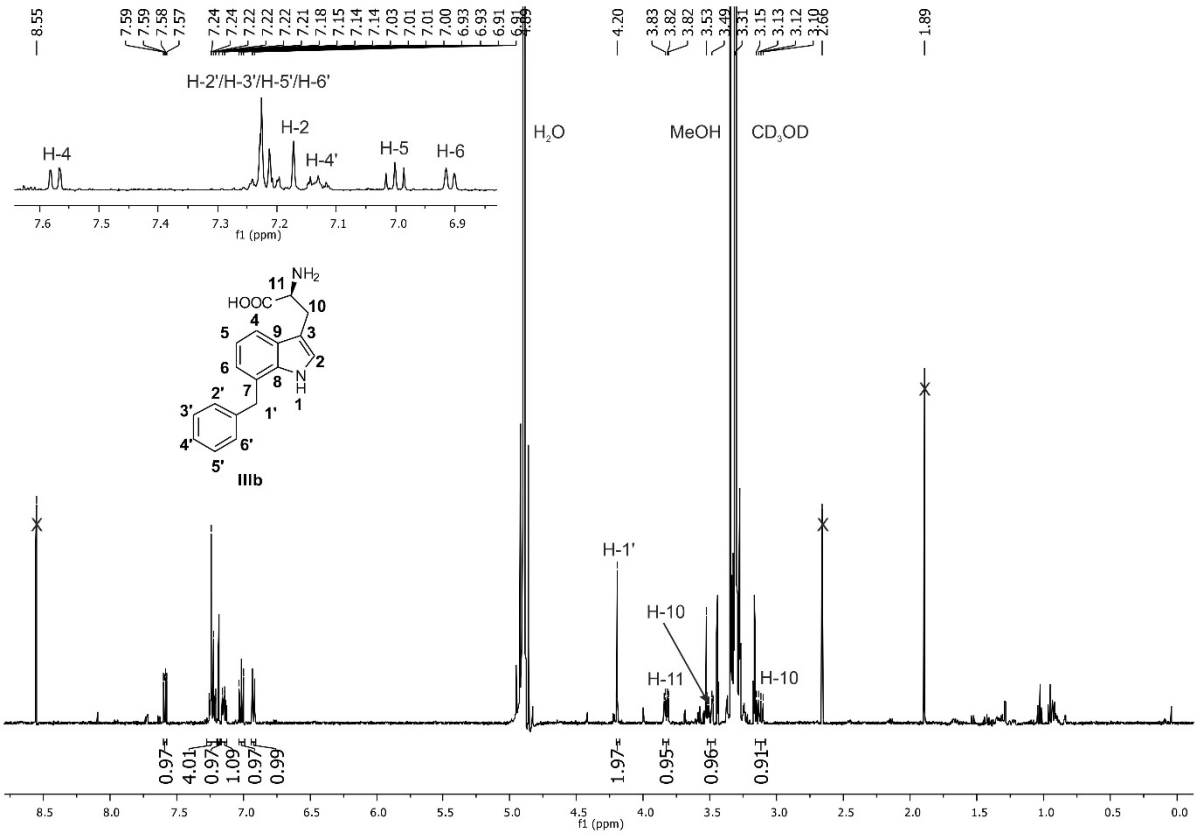

Figure S22. ^{1}H-NMR spectrum of 7-benzyl-L-tryptophan (**IIIb**) in CD_3OD.

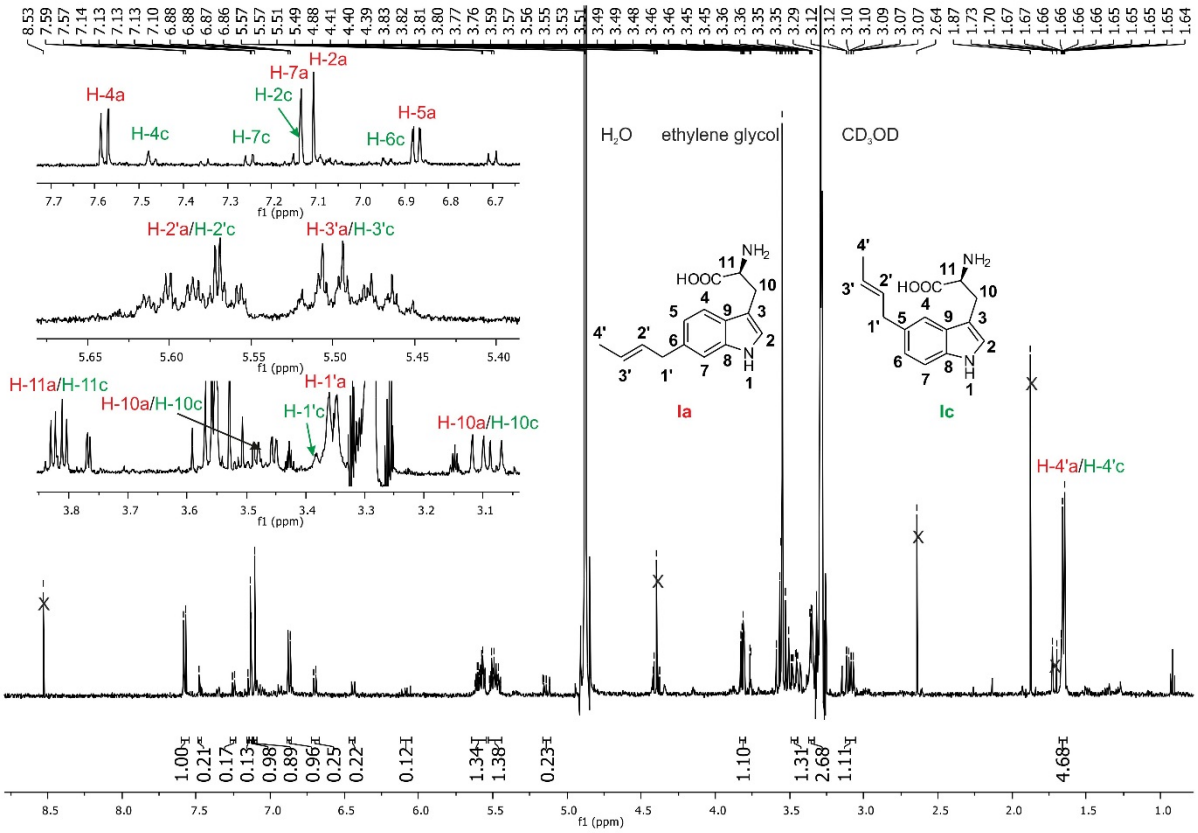

Figure S23. ^{1}H-NMR spectrum of 6-methylallyl-L-tryptophan (**Ia**) and 5-methylallyl-L-tryptophan (**Ic**) in CD_3OD.

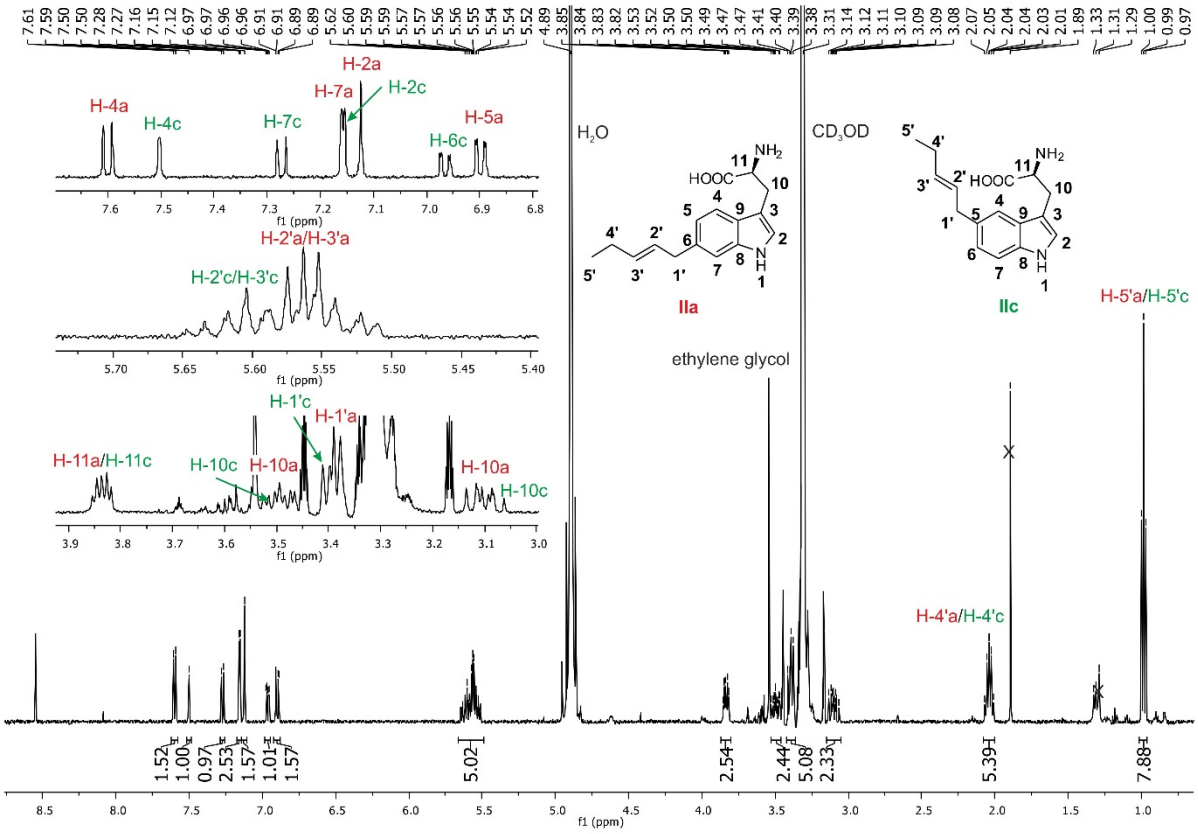

Figure S24. ^{1}H-NMR spectrum of 6-(2-pentenyl-)-L-tryptophan (**IIa**) and 5-(2-pentenyl-)-L-tryptophan (**IIc**) in CD_3OD.

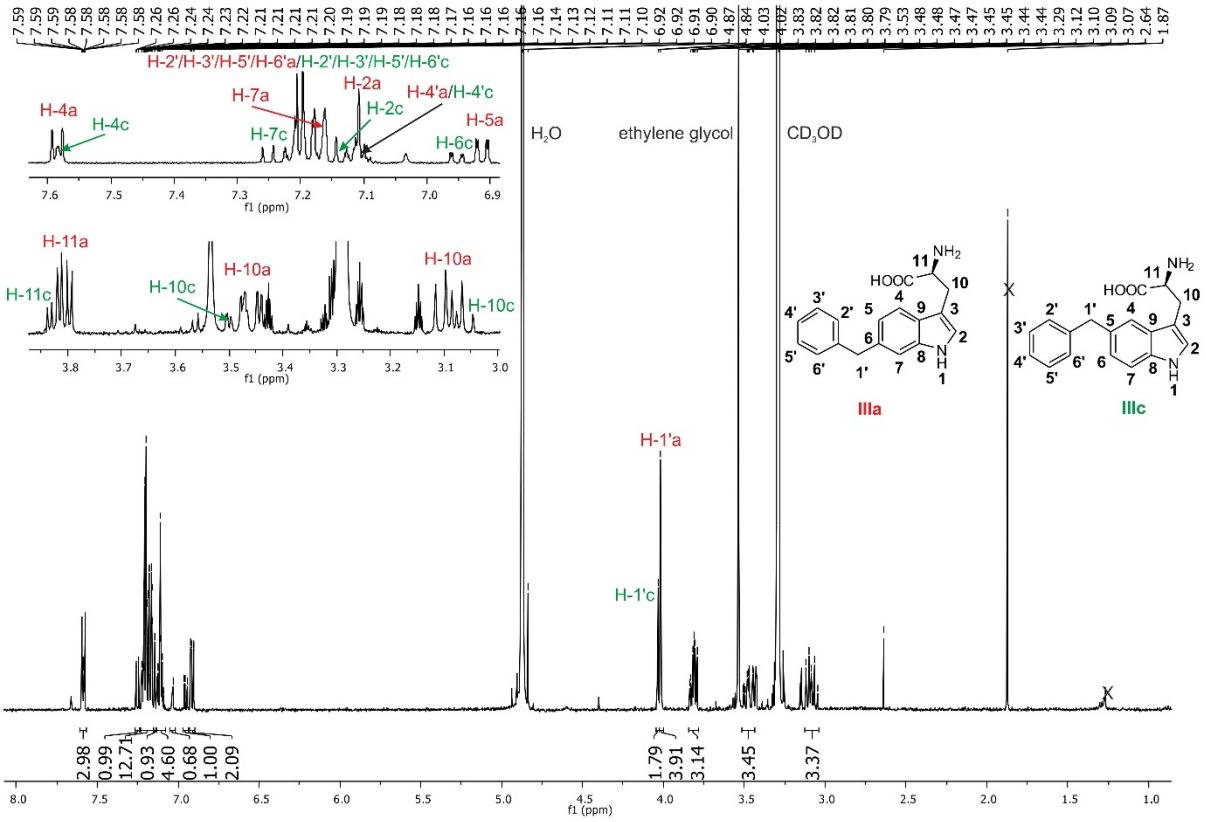

Figure S25. ^{1}H-NMR spectrum of 6-benzyl-L-tryptophan (**IIIa**) and 5-benzyl-L-tryptophan (**IIIc**) in CD_3OD.

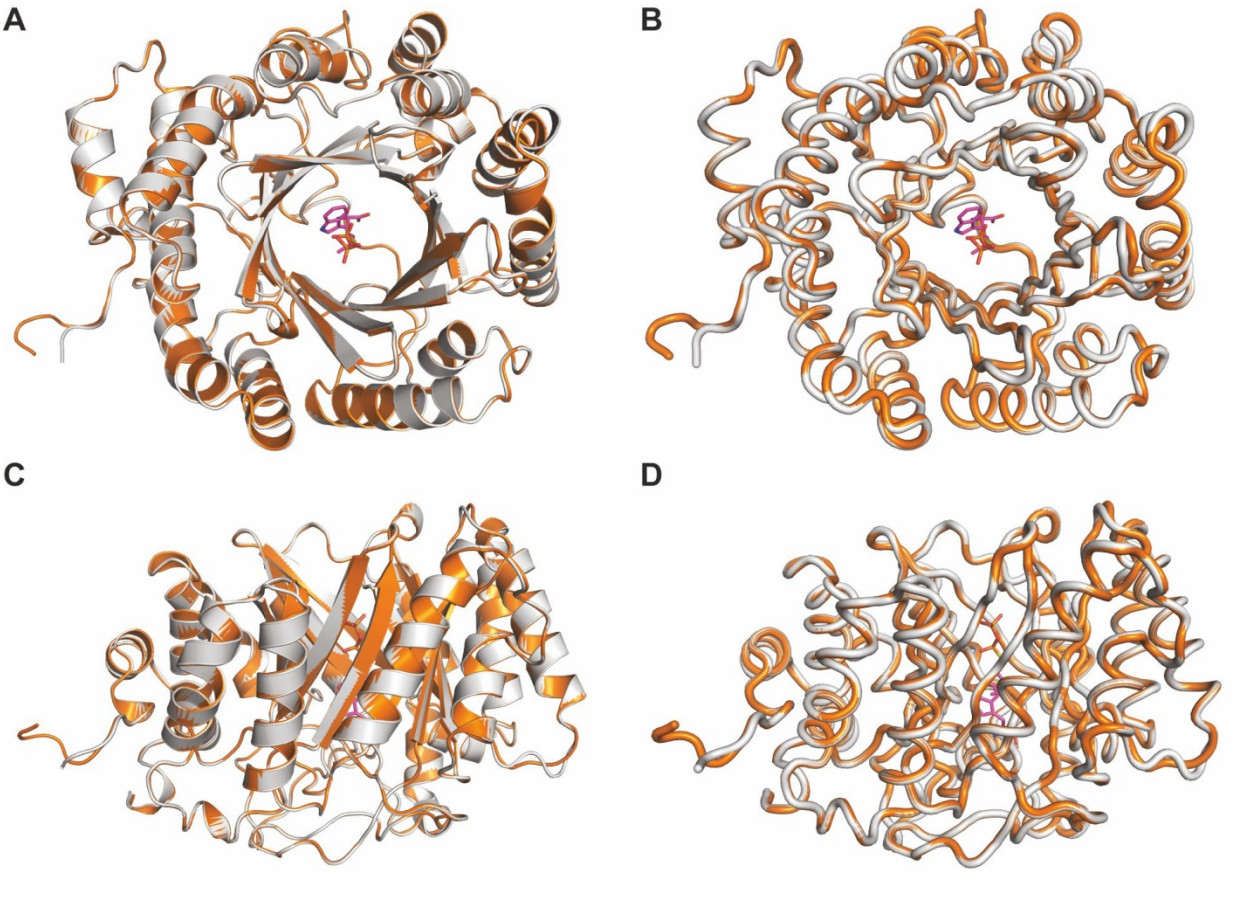

Figure S26. Homology model of 5-DMATS (orange) superimposed on the X-ray structure of FgaPT2 (white). L-tryptophan and DMAPP are shown in magenta. **A** and **C**: Cartoon representations, **B** and **D**: Cα-trace representations of template and model, respectively.

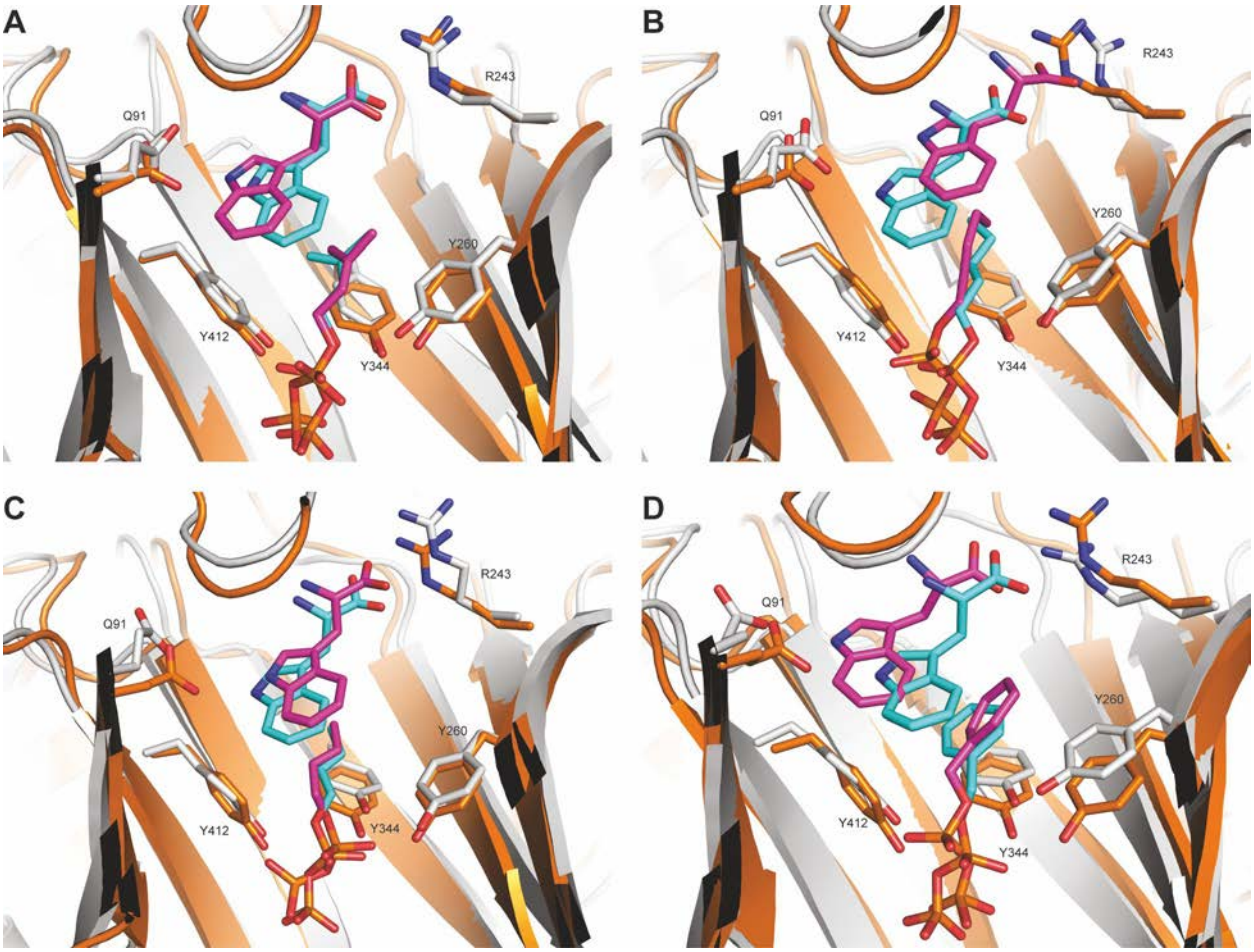

Figure S27. Shown are complexes of 5-DMATS, L-tryptophan and **A**: DMAPP, **B**: 2-pentenyl-PP, **C**: MAPP and **D**: benzyl-PP, respectively. Colored in orange and cyan is the equilibrated complex before the productive molecular dynamics run. Colored in white and magenta are complexes after 5 ns productive simulation run.

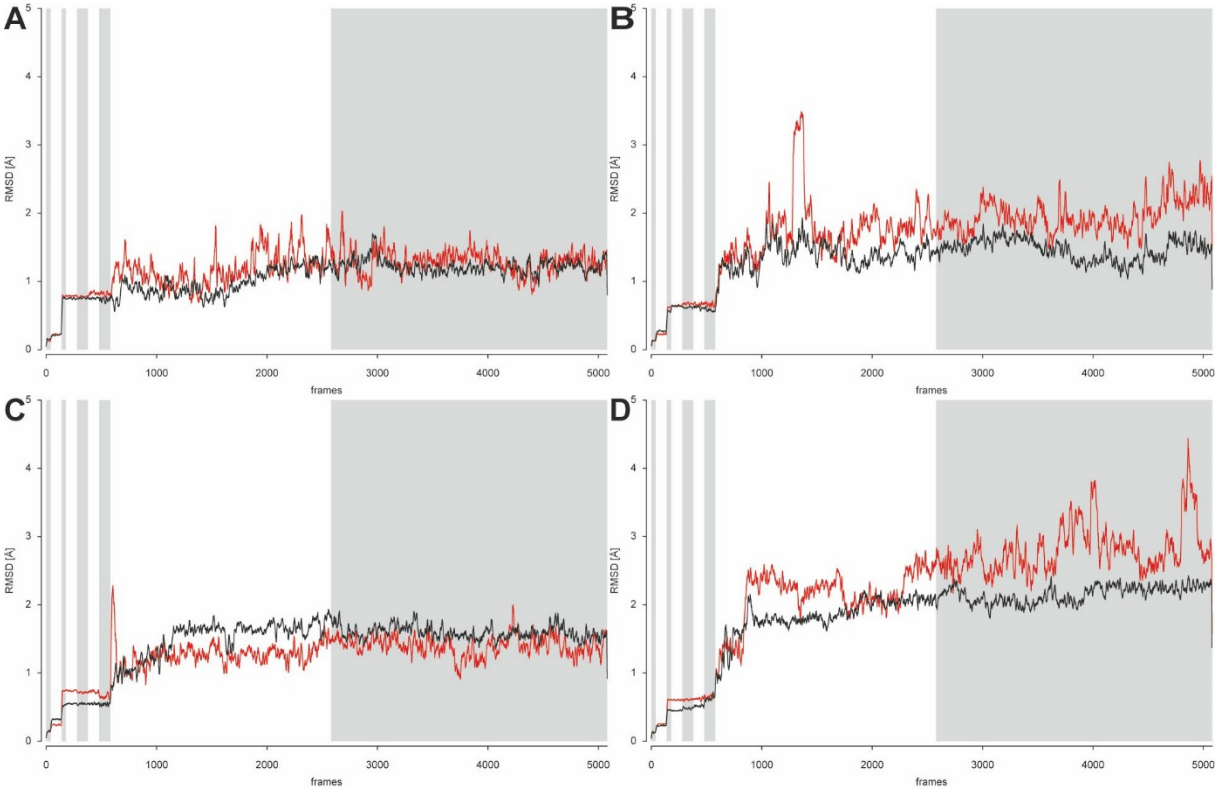

Figure S28. Shown are running averages of the RMSD of pairs of L-tryptophan (red) and a donor molecule (black) during each step of the simulations indicated by white and grey background, respectively. Tryptophan with **A**: DMAPP, **B**: 2-pentenyl-PP, **C**: MAPP and **D**: benzyl-PP.

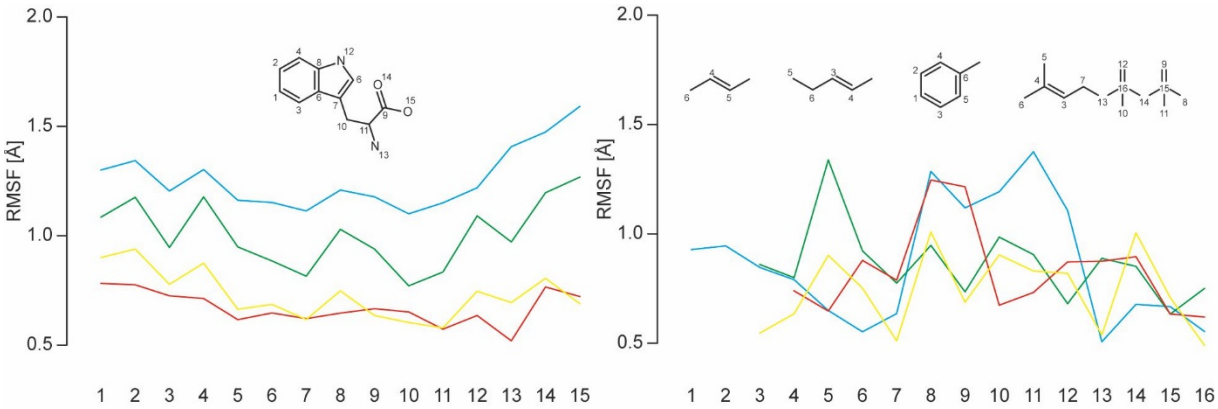

Figure S29. Shown are root-mean-square-fluctuations RMSF of L-tryptophan (TRP) (left) and donor molecules (right) during the complete simulation runs. Color-code: blue: TRP and benzyl-PP complex, green: TRP and 2-pentenyl-PP complex, yellow: TRP and DMAPP complex and red: TRP and MAPP complex.

4.3 Characterisation of 6-DMATS$_{Mo}$ from *Micromonospora olivasterospora* leading to identification of divergence in enantioselectivity, regioselectivity and multiple prenylation of tryptophan prenyltransferases

Organic & Biomolecular Chemistry

PAPER

View Article Online
View Journal

Cite this: DOI: 10.1039/c6ob01803c

Characterisation of 6-DMATS$_{Mo}$ from *Micromonospora olivasterospora* leading to identification of the divergence in enantioselectivity, regioselectivity and multiple prenylation of tryptophan prenyltransferases†

Julia Winkelblech,[a,b] Xiulan Xie[c] and Shu-Ming Li*[a,b]

Prenylated secondary metabolites including indole derivatives usually demonstrate improved biological and pharmacological activities, which make them promising candidates for drug discovery and development. The transfer reactions of a prenyl moiety from a prenyl donor, *e.g.* dimethylallyl diphosphate (DMAPP), to an acceptor is catalysed by prenyltransferases. One special group of such enzymes uses DMAPP and tryptophan as substrates with dimethylallyltryptophans as reaction products and functions therefore as dimethylallyltryptophan synthases (DMATSs). Sequence homology search with known tryptophan prenyltransferases from *Streptomyces* led to identification of a putative prenyltransferase gene *Moll14.36* in *Micromonospora olivasterospora*. Expression and biochemical investigations revealed that Moll14.36 acts as a tryptophan *C*6-prenyltransferase (6-DMATS$_{Mo}$). Study on substrate specificity of 6-DMATS$_{Mo}$ displayed a significantly high activity towards D-tryptophan, which prompted us to carry out comparative studies on enantioselectivity, regioselectivity and multiple prenylation ability of additional DMATSs including FgaPT2, 5-DMATS, 5-DMATS$_{Sc}$, 6-DMATS$_{Sv}$, 6-DMATS$_{Sa}$ and 7-DMATS towards L- and D-isomers of tryptophan and their analogues. The relative activities of the tested enzymes towards D-tryptophan differ clearly from each other. Incubation of L-, D-isomers or the racemates of 5-, 6- and 7-methyltryptophan revealed distinctly different preferences of the DMATS enzymes. Interestingly, 6-DMATS$_{Mo}$ and 5-DMATS$_{Sc}$ accepted 5-methyl-D-tryptophan much better than the L-enantiomer. Furthermore, the conversion yields of the D-isomers were strongly inhibited in the reactions with racemates. More interestingly, the regioselectivities of FgaPT2, 5-DMATS$_{Sc}$ and 7-DMATS towards D-tryptophan and its *C*5-methylated derivative differed clearly from those of the L-forms. In addition, both mono- and diprenylated products were clearly detected for 5-DMATS$_{Sc}$ with L- and D-enantiomers of tryptophan and their methylated derivatives.

Received 18th August 2016,
Accepted 19th September 2016

DOI: 10.1039/c6ob01803c

www.rsc.org/obc

Introduction

Chiral molecules such as D- and L-amino acids play an important role in biological and chemical processes of life.[1] Moreover, the chirality of small molecules is of high importance for their application as drugs. The biological and pharmacological activities of D- and L-isomers as well as toxicity and metabolism could strongly differ from each other.[2] The natural occurrence of α-amino acids is clearly predominated by the L-form, but also the D-form is widely distributed in nature, fulfilling essential roles in biological systems.[3] For example, D-amino acids are found in the cell walls of bacteria to provide protease resistance or as neurotransmitters in the nervous system of animals.[4–6] Moreover, D-amino acids are of great interest for pharmaceutical application. Peptides containing D-amino acids are used as antibiotics or considered as potential agents for treatment of Alzheimer's disease, HIV and cancers.[3,7–9] Amino acids like tryptophan are also key precursors for a number of secondary metabolites including prenylated indole derivatives.[10] These isoprenoid-derived natural products are widely distributed in nature,

[a]*Philipps-Universität Marburg, Institut für Pharmazeutische Biologie und Biotechnologie, Robert-Koch-Straße 4, 35037 Marburg, Germany. E-mail: shuming.li@staff.uni-marburg.de*
[b]*Zentrum für Synthetische Mikrobiologie, Philipps-Universität Marburg, Hans-Meerwein-Straße, D-35032 Marburg, Germany*
[c]*Philipps-Universität Marburg, Fachbereich Chemie, Hans-Meerwein-Straße, 35032 Marburg, Germany*

†Electronic supplementary information (ESI) available. See DOI: 10.1039/c6ob01803c

e.g. in the fungi of ascomycetes and bacteria of actinomycetes.[10] The connection of the indole and isoprenoid moieties is usually catalysed by prenyltransferases.[11] Prenylation of aromatic compounds could improve their biological activity.[10,12–15] For instance, studies on the antifungal activity of substituted indole analogues revealed the importance of the allyl side chain of 6-prenylindole for its bioactivity.[16]

One special group of prenyltransferases uses dimethylallyl diphosphate (DMAPP) as the donor and L-tryptophan as the acceptor and functions thus as dimethylallyltryptophan synthase (DMATS). For example, FgaPT2 from the ascomycetous fungus *Aspergillus fumigatus* (*A. fumigatus*) catalyses the transfer of a dimethylallyl moiety from DMAPP to C-4 of L-tryptophan and is involved in the biosynthesis of ergot alkaloids.[17] Later on, at least six additional fungal DMATSs were identified, which act as *C*4-, *C*5-, and *C*7-prenylating enzymes.[11] In contrast with DMATSs from fungi, a few members of the bacterial tryptophan prenyltransferases were only recently characterised biochemically. Therefore, biochemical characterisation of new DMATSs from bacteria will contribute to our understanding on the catalytic features of these enzymes from different origins. The known bacterial DMATSs are from actinomycetes, catalyse the transfer of the dimethylallyl moiety to C-5, C-6 or C-7 of the indole ring, and are involved in the biosynthesis of prenylated indole derivatives.[11] For example, IptA from *Streptomyces* sp. SN-593 functions as a 6-DMATS and is involved in the biosynthesis of 6-dimethylallylindole-3-carbaldehyde.[18] Three IptA orthologues, $IptA_{Am}$ from *Actinoplanes missouriensis*,[19] 6-$DMATS_{Sa}$ from *Streptomyces ambofaciens* (*S. ambofaciens*), and 6-$DMATS_{Sv}$ from *S. violaceusniger* have been recently identified and characterised.[20] *SCO7467* from *S. coelicolor* A3(2) belongs to a gene cluster being responsible for the biosynthesis of 5-dimethylallylindole-3-acetonitrile and the encoded protein acts as a 5-DMATS (5-$DMATS_{Sc}$).[21,22] Recently, Wu *et al.* have identified a biosynthetic gene cluster for a new antibiotic 7-prenylisatin in *Streptomyces* MBT28-91. Thereby, the prenyltransferase IsaA catalyses the prenylation of L-tryptophan at C-7.[23]

In the present study, we continue to expand our knowledge on DMATSs from bacteria by cloning, expression and biochemical investigations on a putative prenyltransferase MolI14.36 from *Micromonospora olivasterospora* (*M. olivasterospora*). Biochemical investigations revealed that MolI14.36 acts as a tryptophan *C*6-prenyltransferase (6-$DMATS_{Mo}$). Previous studies on DMATSs revealed that L-tryptophan was much better accepted than D-tryptophan.[24] In comparison, D-tryptophan was very well accepted by 6-$DMATS_{Mo}$. This finding promoted us to carry out systematic investigation on the acceptance and enzyme products of L- and D-tryptophan and their methylated derivatives including 5-, 6-, and 7-methyltryptophan by DMATSs from bacteria and fungi. These include three fungal (FgaPT2, 5-DMATS, and 7-DMATS) and four bacterial DMATSs (5-$DMATS_{Sc}$, 6-$DMATS_{Sa}$, 6-$DMATS_{Sv}$, and 6-$DMATS_{Mo}$). Evaluation of the enzyme products demonstrated a clear difference in substrate specificity, regioselectivity of the prenyl transfer reactions as well as the ability for multiple prenylation.

Results and discussion

Identification and characterisation of a new 6-DMATS from *M. olivasterospora*

BLAST search by using known bacterial tryptophan prenyltransferases led to the identification of a putative prenyltransferase from *M. olivasterospora*. MolI14.36 comprises 376 amino acids and has a predicted molecular mass of 40.6 kDa. MolI14.36 shares clearly different sequence identities with known tryptophan *C*6-prenyltransferases on the amino acid level, *e.g.* 68% with $IptA_{Am}$ from *A. missouriensis*,[19] 44% with IptA from *Streptomyces* sp. SN-593,[18] 42% with 6-$DMATS_{Sv}$ from *S. violaceusniger*,[20] and 38% with 6-$DMATS_{Sa}$ from *S. ambofaciens*.[20] The differences of the sequence identities raised the question about the function of MolI14.36.

MolI14.36 was then cloned from genomic DNA into the expression vector $pHIS_8$ and overexpressed in *E. coli*. The recombinant His_8-tagged protein with a molecular mass of 43.5 kDa was purified to near homogeneity with a yield of 16 mg per litre culture (Fig. S1, ESI†). Size exclusion chromatography revealed that the enzyme acts as a monomer.

To prove its function and substrate specificity, the purified recombinant MolI14.36 (1 μM) was incubated with 0.5 mM of L-tryptophan (**1a**), D-tryptophan (**1b**), and eight analogues thereof (**2a**, **3a**, **4–8**, and **9a**) in the presence of 1 mM DMAPP. To show the relationships of the enantiomers, we use Arabic numbers for racemates, numbers with **a** for L-isomers and with **b** for D-isomers. After incubation at 37 °C for 1 h, the reaction mixtures were analysed on HPLC under the conditions listed in Table S1 in the ESI.† As shown in Table 1 and the ESI (Fig. S2 and S3†), eight of them, **1a**, **1b**, **2a**, **3a**, **4**, **5**, **8**, and **9a**, were well accepted by this enzyme, with **1a** as the best substrate. In the presence of L-tryptophan (**1a**), MolI14.36 also used geranyl diphosphate as the prenyl donor, but with a significantly lower product yield than with DMAPP (about 10% of that of DMAPP). Farnesyl diphosphate was not accepted by MolI14.36 (Table S2, ESI†). HPLC analysis of the reaction mixtures of MolI14.36 with seven tryptophan-containing cyclic dipeptides showed product formation, but with much lower conversion yields than with tryptophan and its analogues (less than 8% of that of **1a**) (Table S3, ESI†). These results provided evidence for the function of MolI14.36 as a dimethylallyl diphosphate:L-tryptophan transferase.

To confirm the prenylation in their structures and particularly the prenylation positions, the enzyme products of tryptophan and its analogues were isolated from large-scale incubation mixtures on preparative HPLC and subsequently analysed by MS and NMR including homonuclear correlation spectroscopy (^1H–^1H COSY) for **5-C5–5-C7**, **6-C6** and **6-C7** (Tables S4–S7 and Fig. S4–S22, ESI†). For better understanding, the enzyme products were termed by addition of the prenylation position like *C*4, *C*5, *C*6 or *C*7 to the number of the substrate. Inspection of the NMR spectra of the isolated peaks confirmed the unique *C*6-prenylated products **1a-C6**, **1b-C6**, **2a-C6**, **3a-C6**, **4-C6**, **8-C6**, and **9a-C6** from the reaction mixtures of **1a**, **1b**, **2a**, **3a**, **4**, **8**, and **9a**, whereas three products with the

Table 1 Prenyl transfer reactions catalysed by 6-DMATS$_{Mo}$

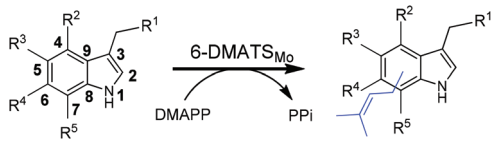

	Substrate	Product (relative product yield in %)
1a	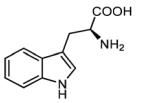	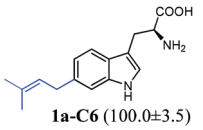 **1a-C6** (100.0±3.5)
1b	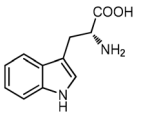	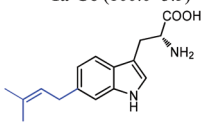 **1b-C6** (54.1±5.2)
2a	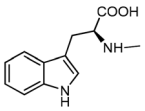	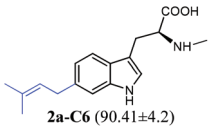 **2a-C6** (90.41±4.2)
3a	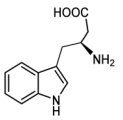	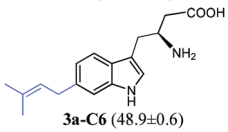 **3a-C6** (48.9±0.6)
4	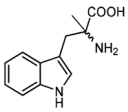	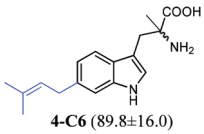 **4-C6** (89.8±16.0)
5	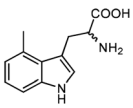	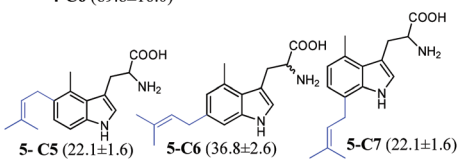 **5- C5** (22.1±1.6) **5-C6** (36.8±2.6) **5-C7** (22.1±1.6)
6	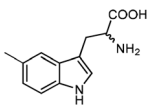	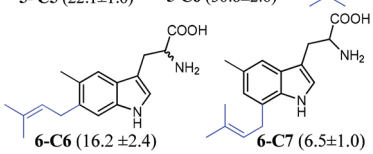 **6-C6** (16.2 ±2.4) **6-C7** (6.5±1.0)
7	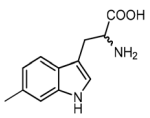	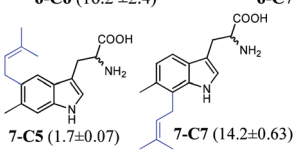 **7-C5** (1.7±0.07) **7-C7** (14.2±0.63)
8	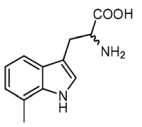	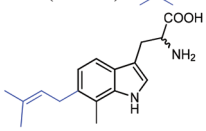 **8-C6** (58.2±6.2)
9a	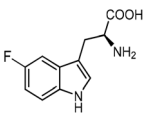	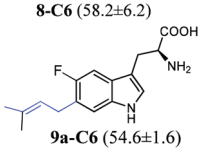 **9a-C6** (54.6±1.6)

The enzyme assays contained 0.5 mM aromatic substrate, 5 mM $MgCl_2$, and 1 mM DMAPP were incubated with 1 μM of the purified protein at 37 °C for 1 h. The product yield of L-tryptophan at 37.8% was defined as 100%. NMR data of the prenylated products were used for structure elucidation and also for calculation of the ratio of different products.

prenyl moiety attached to C-5 (**5-C5**), C-6 (**5-C6**) and C-7 (**5-C7**) in a ratio of 0.6 : 1 : 0.6 were identified in the reaction mixture of **5**. Two products either **6-C6** and **6-C7** or **7-C5** and **7-C6** were detected in those of **6** and **7** (see the ESI† for detailed structure elucidation, Tables S5–S7, Fig. S4–S22†).

In conclusion, MS and NMR analyses of the isolated enzyme products prove that MolI14.36 acts as a L-tryptophan *C*6-prenyltransferase and is termed 6-DMATS$_{Mo}$, in analogy to the notation of 6-DMATS$_{Sa}$ and 6-DMATS$_{Sv}$.[20] 6-DMATS$_{Mo}$ catalyses a unique or predominant *C*6-prenylation at the indole ring of tryptophan and its analogues (Table 1). If the position 6 is blocked by a methyl group as in the case of **7**, a switch of the prenylation site to C-7 was detected, as observed for IptA and 6-DMATS$_{Sa}$, previously.[18,20]

Additional biochemical characterisation revealed that metal ions are not essential for the enzyme activity as observed for other members of the DMATS superfamily (Fig. S23, ESI†).[18,20,25] Furthermore, the function of 6-DMATS$_{Mo}$ as a tryptophan prenyltransferase was justified by kinetic studies. The K_M value of 0.014 ± 0.002 mM and a turnover number k_{cat} of 0.07 ± 0.002 s^{-1} were determined for **1a**. The kinetic parameters for the prenyl donor DMAPP were found to be 0.037 ± 0.007 mM and 0.08 ± 0.004 s^{-1}, respectively (Fig. S24, ESI†). For comparison of the substrate preferences of 6-DMATS$_{Mo}$ and its orthologues 6-DMATS$_{Sa}$ and 6-DMATS$_{Sv}$, enzyme assays of **1a**, **1b**, **2a**, **3a**, **4–8** and **9a** were carried out for the three 6-DMATSs under similar conditions and the relative enzyme activities to **1a** were compared with each other (Fig. S3, ESI†). In summary, with the exception for **3a**, 6-DMATS$_{Sa}$ and 6-DMATS$_{Sv}$ seem to share similar substrate preferences towards the tested tryptophan analogues, whereas 6-DMATS$_{Mo}$ shows more distinct preferences from those of the two other 6-DMATSs. **1b**, **4**, **5**, and **8** were better accepted by 6-DMATS$_{Mo}$, whereas **6**, **7**, and **9a** were better substrates for the other two 6-DMATS enzymes. The most remarkable feature is the high acceptance of **1b** by 6-DMATS$_{Mo}$, with a relative activity of approximately 50% of that of **1a** (Table 1 and Fig. S3, ESI†). To the best of our knowledge, such high conversion of **1b** has not been reported for other prenyltransferases prior to this study. In comparison, less than 25% relative activities of that of **1a** were detected for 6-DMATS$_{Sa}$ and 6-DMATS$_{Sv}$ with **1b** under these conditions. These results prompted us to have detailed insights into the enantioselectivity of the DMATS enzymes towards tryptophan.

DMATSs showed different preferences towards D-tryptophan

To gain deeper insights into the substrate preferences of DMATSs towards the stereoisomers of tryptophan, FgaPT2, 5-DMATS, 5-DMATS$_{Sc}$, 6-DMATS$_{Sa}$, 6-DMATS$_{Sv}$, 6-DMATS$_{Mo}$, and 7-DMATS were overproduced in *E. coli* and purified to near homogeneity as reported previously.[20,25–28] As aforementioned, these enzymes use the same substrates **1a** and DMAPP, but catalyse prenylations at different positions of the indole ring. By size exclusion chromatography, these enzymes were determined to have different quaternary structures. The native forms of FgaPT2 and 5-DMATS were found to be homodimer, whereas 5-DMATS$_{Sc}$ and 7-DMATS were reported to be active as monomers.[17,25,28] In this study, the molecular mass of 6-DMATS$_{Sa}$ was determined to be 36.9 kDa and the other two enzymes 6-DMATS$_{Sv}$ and 6-DMATS$_{Mo}$ to be 46.0 kDa. This proved that they are active as monomers, being consistent with their orthologue IptA.[18] Crystal structure analysis of several fungal prenyltransferases including FgaPT2 revealed that each single subunit contains one active centre and forms one catalytic unit.[29–32] To ensure adequate comparability, the following analyses on substrate specificity and kinetic parameters of the recombinant proteins all refer to a unique protein subunit.

For investigations on substrate preferences, the seven DMATSs were incubated with the prenyl donor DMAPP and **1a**, **1b**, or their racemate **1**. The relative activities to **1a** were determined by HPLC analysis on the CHIRALPAK® Zwix(+) column. The prenylation of the enzyme products was proven by LC-MS analysis (Table 2 and Fig. 1, S25–S48, ESI†). As given in Table 2, clearly different enantioselectivities were observed for the tested DMATSs. 5-DMATS and 6-DMATS$_{Mo}$ accepted **1b** much better than other enzymes, with relative activities of 34.7 and 45.7% of those of L-tryptophan (**1a**), respectively. In contrast, **1b** was a very poor substrate for FgaPT2 and 7-DMATS with relative conversion yields of approximately 5 and 6%, respectively, corresponding well to the data reported previously.[17,27,28,33] In the reaction mixtures of racemates, the conversion of **1b** was strongly reduced, indicating an inhibition. For better understanding of the observed acceptance of **1a** and **1b** by the tested DMATSs, kinetic parameters were determined by nonlinear regression using GraphPad Prism 4.0 (Fig. S49–S55, ESI†). All investigated reactions apparently followed the Michaelis–Menten kinetics. The calculated K_M values of the seven DMATSs for **1a** varied from 0.012 mM to 0.055 mM, whereas those for **1b** were found in the range of 0.10 to 1.76 mM (Table 3). The significantly higher affinity of the enzymes to the L-form is justified by their native functions as L-tryptophan prenyltransferases and also explained in parts the very low conversion of **1b** in the reaction with the racemate. It is plausible that in the initial phase of the reactions with racemates, only **1a** was used as substrate by the enzymes. However, the higher affinity and turnover numbers of the tested enzymes towards **1a** than **1b** could not explain the observed very low conversion of **1b**. Under the conditions used for the conversion yields given in Table 2, **1a** was almost completely converted. Therefore, we speculated that the products of **1a** should also contribute to the inhibition of **1b** reactions.

The calculated turnover numbers (k_{cat}) for **1a** from 0.07 to 0.67 s^{-1} are in almost all cases much higher than those for **1b** between 0.012 and 0.066 s^{-1}. In comparison to **1b** reactions with other enzymes, relative high affinity and turnover numbers were determined for those with 5-DMATS and 6-DMATS$_{Mo}$. The turnover numbers of 6-DMATS$_{Mo}$ towards **1a** and **1b** are nearly identical at approximately 0.07 s^{-1}. These data supported the high conversion yields of **1b** by 5-DMATS and 6-DMATS$_{Mo}$ given in Table 2.

Table 2 Relative activities of DMATSs towards D- and L-isomers of tryptophan and their analogues

Substrate		Relative conversion yields [%]						
		FgaPT2	5-DMATS	5-DMATS$_{Sc}$	6-DMATS$_{Sa}$	6-DMATS$_{Sv}$	6-DMATS$_{Mo}$	7-DMATS
L-Tryptophan	**1a**	100.0 ± 2.5	100.0 ± 0.7	100.0 ± 0.04[a]	100.0 ± 2.7	100.0 ± 0.9	100.0 ± 12.2	100.0 ± 4.3
D-Tryptophan	**1b**	5.2 ± 0.9	34.7 ± 4.4	20.2 ± 2.6[b]	10.4 ± 0.02	16.8 ± 1.1	45.7 ± 2.9	6.4 ± 0.2
DL-Tryptophan	**1a**	96.3 ± 2.1	96.7 ± 4.8	103.5 ± 4.7	99.4 ± 8.2	87.1 ± 2.6	99.9 ± 1.0	98.9 ± 1.5
	1b	≤0.5	12.6 ± 2.2	≤0.5	1.6 ± 0.3	2.5 ± 0.01	1.3 ± 0.1	≤0.5
5-Methyl-L-tryptophan	**6a**	43.0 ± 1.8	2.5 ± 0.1	2.3 ± 0.2	102.5 ± 0.2	100.5 ± 0.7	12.9 ± 0.2	84.9 ± 3.8
5-Methyl-D-tryptophan	**6b**	≤0.5	≤0.5	57.3 ± 1.8	11.4 ± 0.6	22.4 ± 0.4	66.6 ± 0.5	2.5 ± 0.6
5-Methyl-DL-tryptophan	**6a**	22.4 ± 4.0	3.1 ± 1.1	3.8 ± 0.6	76.2 ± 6.5	100.7 ± 4.1	13.0 ± 0.6	97.9 ± 4.3
	6b	≤0.5	≤0.5	≤0.5	2.4 ± 1.1	4.7 ± 0.1	≤0.5	≤0.5
6-Methyl-L-tryptophan	**7a**	84.0 ± 1.2	85.5 ± 5.7	15.0 ± 1.7	9.1 ± 1.7	35.4 ± 2.3	5.5 ± 0.2	17.5 ± 1.1
6-Methyl-D-tryptophan	**7b**	≤0.5	≤0.5	1.1 ± 0.1	≤0.5	≤0.5	1.2 ± 0.2	≤0.5
6-Methyl-DL-tryptophan	**7a**	61.2 ± 0.8	82.5 ± 5.1	15.1 ± 0.2	8.2 ± 0.4	33.2 ± 0.6	5.0 ± 0.6	16.6 ± 0.9
	7b	≤0.5	≤0.5	≤0.5	≤0.5	≤0.5	≤0.5	≤0.5
7-Methyl-L-tryptophan	**8a**	97.8 ± 1.7	75.7 ± 0.5	8.2 ± 2.3	4.3 ± 0.2	7.4 ± 1.6	72.4 ± 8.5	≤0.5
7-Methyl-D-tryptophan	**8b**	≤0.5	3.7 ± 1.4	1.9 ± 0.2	≤0.5	≤0.5	13.8 ± 3.8	≤0.5
7-Methyl-DL-tryptophan	**8a**	68.2 ± 5.0	70.6 ± 4.2	5.9 ± 0.2	3.8 ± 0.4	7.5 ± 0.7	72.5 ± 13.1	≤0.5
	8b	≤0.5	≤0.5	≤0.5	≤0.5	≤0.5	≤0.5	≤0.5

The enzyme assays contained 0.5 mM of the L- or D-isomers or 1 mM of the racemates and 1 mM DMAPP were incubated at 37 °C for 1.5 h with 1 μM purified protein. The conversion yields of L-tryptophan (**1a**) with FgaPT2 at 97.3%, 5-DMATS at 98.4%, 5-DMATS$_{Sc}$ at 96%, 6-DMATS$_{Mo}$ at 82.7%, 6-DMATS$_{Sv}$ at 96.1%, 6-DMATS$_{Sa}$ at 97.0%, and with 7-DMATS at 88.9% were defined as 100% relative activity, respectively. The conversion yields of D- or L-enantiomers in the reaction mixtures with racemates were calculated separately by considering the respective enantiomer as the substrate. [a] Diprenylated products, with a ratio of 0.6 : 1 to the monoprenylated product, were detected. [b] Diprenylated products, with a ratio of 0.1 : 1 to the monoprenylated product, were detected.

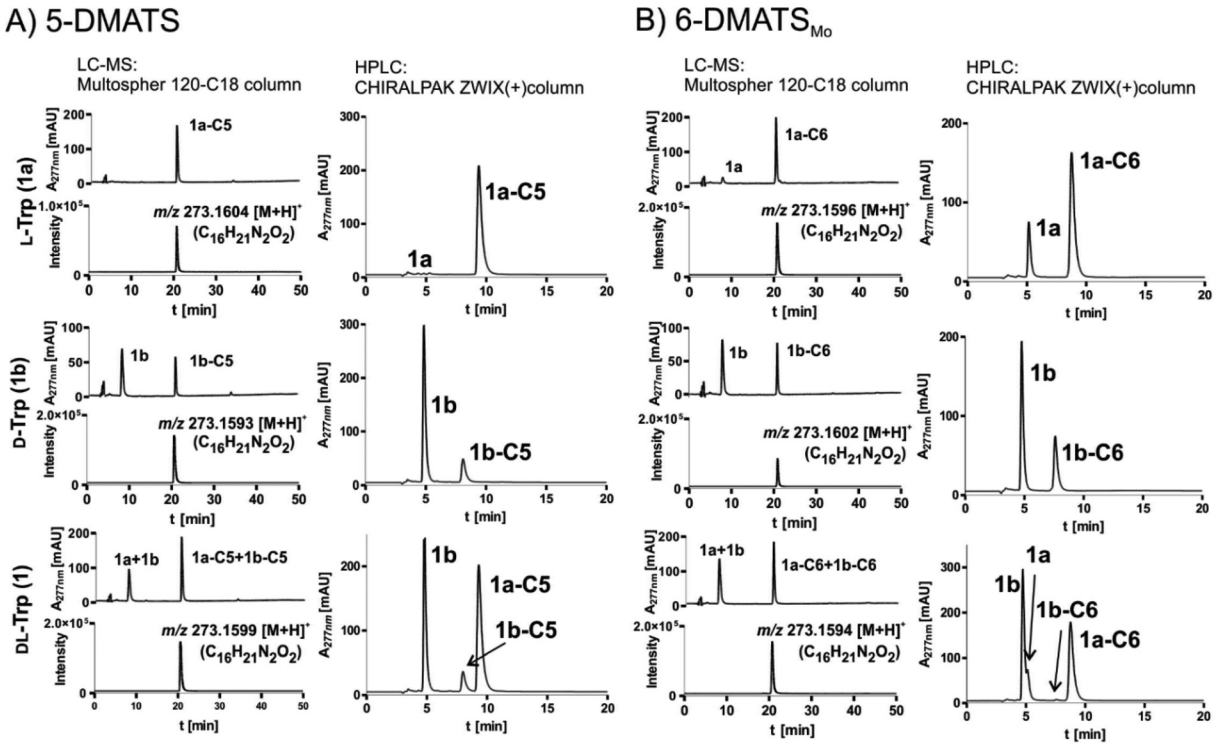

Fig. 1 Evaluation of the enantioselectivity of (A) 5-DMATS and (B) 6-DMATS$_{Mo}$. The enzymes were incubated with 1 mM DMAPP and 0.5 mM of L-tryptophan, D-tryptophan or a combination of both (1 mM) and the reaction products were profiled by LC-MS and HPLC. 1 μM of the indicated enzyme was incubated with the indicated substrate(s). UV detection was carried out with a diode array detector and illustrated for absorption at 277 nm. Additional chromatograms and MS analyses for all tested enzymes and substrates are provided as Fig. S25–S48 in the ESI.†

Table 3 Kinetic parameters of DMATSs towards L- and D-forms of tryptophan and 5-methyltryptophan

	L-Tryptophan		D-Tryptophan		5-Methyl-L-tryptophan		5-Methyl-D-tryptophan	
	1a		**1b**		**6a**		**6b**	
DMATS	K_M [mM]	k_{cat} [s^{-1}]	K_M [mM]	k_{cat} [s^{-1}]	K_M [mM]	k_{cat} [s^{-1}]	K_M [mM]	k_{cat} [s^{-1}]
FgaPT2	0.034 ± 0.003	0.67 ± 0.01	0.10 ± 0.007	0.012 ± 0.0002	—	—	—	—
5-DMATS	0.055 ± 0.002	0.39 ± 0.001	0.62 ± 0.08	0.066 ± 0.004	—	—	—	—
5-$DMATS_{Sc}$	0.020 ± 0.002	0.19 ± 0.004	1.47 ± 0.08	0.046 ± 0.001	0.009 ± 0.001	0.005 ± 0.0001	0.03 ± 0.01	0.035 ± 0.005
6-$DMATS_{Sa}$	0.012 ± 0.001	0.10 ± 0.002	1.02 ± 0.07	0.021 ± 0.001	—	—	—	—
6-$DMATS_{Sv}$	0.022 ± 0.002	0.19 ± 0.004	0.77 ± 0.08	0.021 ± 0.001	—	—	—	—
6-$DMATS_{Mo}$	0.014 ± 0.002	0.07 ± 0.002	0.47 ± 0.04	0.066 ± 0.002	0.008 ± 0.001	0.012 ± 0.0002	0.30 ± 0.05	0.042 ± 0.003
7-DMATS	0.043 ± 0.004	0.12 ± 0.002	1.76 ± 0.19	0.013 ± 0.001	—	—	—	—

—, Not determined.

Different regioselectivities of DMATSs towards 1a and 1b

Previous investigations have shown that the characterised DMATSs are highly regiospecific for **1a**, *i.e.* *C*4-prenylation by FgaPT2,[17] *C*5-prenylation by 5-DMATS and 5-$DMATS_{Sc}$,[22,25,26] *C*6-prenylation by IptA, 6-$DMATS_{Sa}$, 6-$DMATS_{Sv}$ and 6-$DMATS_{Mo}$[18,20] and *C*7-prenylation by 7-DMATS and 7-$DMATS^{Neo}$.[28,34] In the course of the biochemical characterisation, the enzyme activities of DMATSs towards **1b** were usually demonstrated by HPLC analysis using achiral columns.[18,20,25,27,28,34–36] No product of **1b** has been isolated and characterised. As mentioned above, isolation and structure elucidation of the enzyme products confirmed the same *C*6-prenylation of 6-$DMATS_{Mo}$ for **1a** and **1b** (Tables 4, S5 and Fig. S4, S5, ESI†). In contrast, inspection of the NMR spectrum of the enzyme products of 5-$DMATS_{Sc}$ with **1b** revealed the presence of a mixture of three compounds (Table 4, Fig. 2 and Table S8 and Fig. S56, ESI†). Comparison of the chemical shifts and coupling patterns with the previously published data of the prenylated derivatives of **1a** led to the identification of these compounds to be *C*5-prenylated **1b-C5**, *C*6-prenylated **1b-C6**, and *C*7-prenylated **1b-C7** in a ratio of 0.4 : 1 : 0.4. In comparison, the *C*5-monoprenylated derivative **1a-C5** is the unique product in the reaction mixture of **1a** with 5-$DMATS_{Sc}$.

To prove the prenylation positions, the seven DMATSs were incubated with **1a** and **1b** and analysed on an achiral XDB-C18 column under the improved HPLC condition 4 (Fig. 2 and Tables S1, S9, ESI†). Under this condition, the enantiomeric pairs **1a** and **1b** have the same retention times, which is also true for their derivatives with the same prenylation positions.

Table 4 Prenylation sites of the enzyme products of L- and D-enantiomers of tryptophan and 5-methyltryptophan

		Enzyme products and their ratios						
	Substrate structures	FgaPT2	5-DMATS	5-$DMATS_{Sc}$	6-$DMATS_{Sa}$	6-$DMATS_{Sv}$	6-$DMATS_{Mo}$	7-DMATS
1a	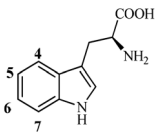	*C*4	*C*5	*C*5	*C*6	*C*6	*C*6	*C*7
1b	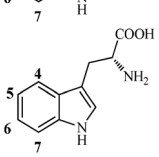	*C*4 : *C*5 : *C*7 0.2 : 1 : 0.04	*C*5	*C*5 : *C*6 : *C*7 0.4 : 1 : 0.4[a]	*C*6	*C*6	*C*6	*C*6 : *C*7 0.05 : 1
6a	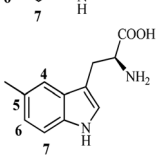	*C*4	[b]	*C*6 : *C*7 1 : 1	*C*6	*C*6	*C*6 : *C*7 1 : 0.05	*C*7
6b	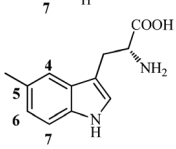	*C*4 : *C*6/*C*7 1 : 0.4	[b]	*C*6 : *C*7 1 : 0.2[a]	*C*6	*C*6	*C*6 : *C*7 1 : 0.1[a]	*C*6 : *C*7 1 : 0.2

The ratio of the enzyme products was evaluated from HPLC chromatograms. [a] The ratio of the enzyme products was evaluated from ^{1}H NMR spectra. [b] Product formation was detected by LC-MS analysis.

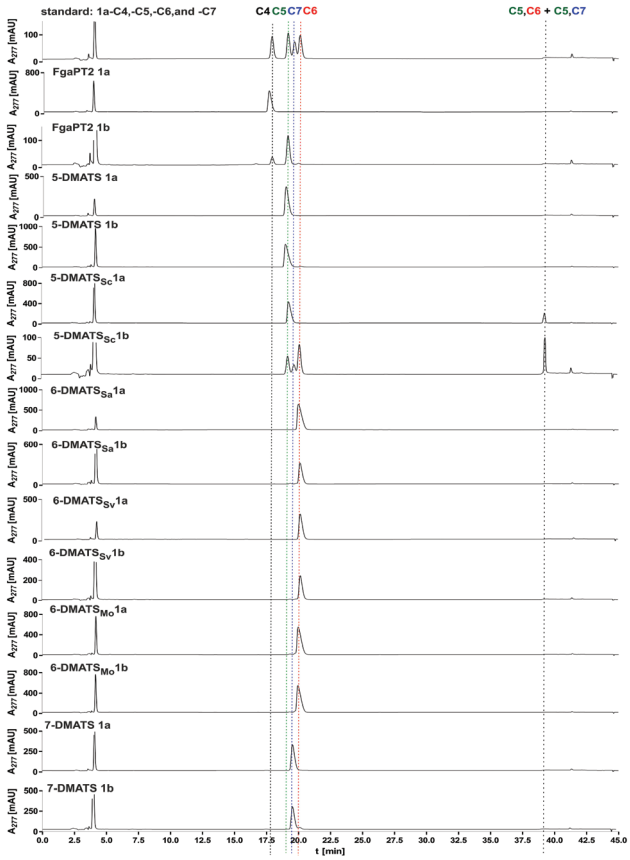

Fig. 2 HPLC identification of the enzyme products of DMATSs and **1a** or **1b**. The enzymes were incubated with 1 mM DMAPP and 1 mM of L-tryptophan (**1a**) or D-tryptophan (**1b**). Detailed conditions of the enzyme assays are given in Table S9 in the ESI.† For HPLC analysis, an Eclipse XDB-C18 column was used (condition 4 in Table S1†). Detection was carried out on a diode array detector and illustrated for absorption at 277 nm.

More importantly, *C*4-, *C*5-, *C*6-, and *C*7-prenylated tryptophan were well separated from each other. The results in Fig. 2 confirmed the previously published regiospecific prenylation of **1a** by the tested DMATSs. The enzyme products of **1b** with 5-DMATS and the three *C*6-prenyltransferases 6-DMATS$_{Sa}$, 6-DMATS$_{Sv}$ and 6-DMATS$_{Mo}$ had the same prenylation positions as those of **1a**. Interestingly, the main product of **1b** with FgaPT2 was prenylated at position C-5 instead of C-4. *C*4- and likely *C*7-prenylated derivatives were detected as minor products (Table 4 and Fig. 2). As aforementioned, three products **1b-C5**, **1b-C6**, and **1b-C7** with a ratio of 0.4 : 1.0 : 0.4 were detected in the reaction mixture of **1b** with 5-DMATS$_{Sc}$ (Fig. 2, Tables 4, S8 and Fig. S56, ESI†).[20,25,37] HPLC analysis of the reaction mixture of **1b** with 7-DMATS proved the main product to be 7-DMA-D-tryptophan (**1b-C7**) and the minor product the *C*6-prenylated derivative **1b-C6** in a ratio of 1 : 0.05 (Fig. 2 and Table 4). The observed changes in regioselectivity could indicate different orientations of the two enantiomers in the active sites. Crystal structures of such bacterial tryptophan prenyltransferases could provide detailed insights into their reaction chambers.

DMATSs also catalyse the diprenylation of 1a and 1b with different activities

HPLC analysis on a chiral column of the reaction mixture of **1a** with 5-DMATS$_{Sc}$ revealed the presence of two product peaks with retention times at 9.2 and 18.5 min in a ratio of 1 : 0.6 (Fig. S32, ESI†). The main peak was identified as *C*5-monoprenylated tryptophan by Ozaki *et al.*,[21] and also confirmed in this study, whereas the second peak was not mentioned in the previous study. LC-MS analysis led to the identification of the second product peak as diprenylated derivative(s). Isolation and structure elucidation with the help of ^{1}H NMR confirmed the diprenylation of **1a** and provided evidence for the presence of a mixture of two products (Table S8 and Fig. S57, ESI†). Detailed interpretation of the spectra and comparison of the coupling patterns with those of the previously published data led to identification of 5,6- and 5,7-di-dimethylallyl-L-tryptophan (**1a-C5,C6**, **1a-C5,C7**) in a ratio of approximately 1 : 1.[20,25,37] The characteristic singlets for H-4, H-7 and H-2 of **1a-C5,C6** were observed at 7.45, 7.14 and 7.08 ppm, respectively. For **1a-C5,C7**, the signals of H-4 and H-6 were detected as broad singlets. The two products were well separated from each other under an improved HPLC condition (Fig. 3). In the HPLC chromatogram of the reaction mixture of **1b** with 5-DMATS$_{Sc}$ (Fig. 2), four product peaks were detected. As mentioned above, three monoprenylated derivatives were identified as *C*5-, *C*6-, and *C*7-prenylated D-tryptophan. LC-MS confirmed the additional product peak to be diprenylated D-tryptophan. An improved HPLC condition (condition 6) allowed the separation of this peak into one predominant peak and one minor product peak (Fig. 3), with similar retention times to those observed for the diprenylated products of **1a**.

Structure elucidation of the isolated diprenylated peak by NMR analysis confirmed the *C*5,*C*6-diprenylation in the main product **1b-C5,C6** (Table S8 and Fig. S58, ESI†) with three singlets at 7.45, 7.15 and 7.10 ppm for H-4, H-7 and H-2, respectively. In this spectrum, signals of aromatic protons for *C*5,*C*7-diprenylated derivatives **1b-C5,C7** were also detected, with a low intensity of 5% of that of **1b-C5,C6**. To the best of our knowledge, this is the first report on diprenylation of tryptophan by a tryptophan prenyltransferase. By UV detection mentioned above, diprenylated products of **1a**, **1b** and **1** were only observed for 5-DMATS$_{Sc}$ after incubation for 1.5 h. By using the extracted ion chromatogram (EIC) mode, diprenylated products were also detected for almost all the DMATSs with **1a**, with an exception for FgaPT2 (Fig. S25–S48, ESI†). However, the product yields were less than 0.5% of those of monoprenylated derivatives.

Separation and identification of L- and D-enantiomers of 5-, 6-, and 7-methyltryptophan

To expand our knowledge on the enantioselectivity and regioselectivity of DMATSs, we initiated to investigate their behaviours towards enantiomer pairs of methylated tryptophan derivatives. Unfortunately, these compounds are commercially

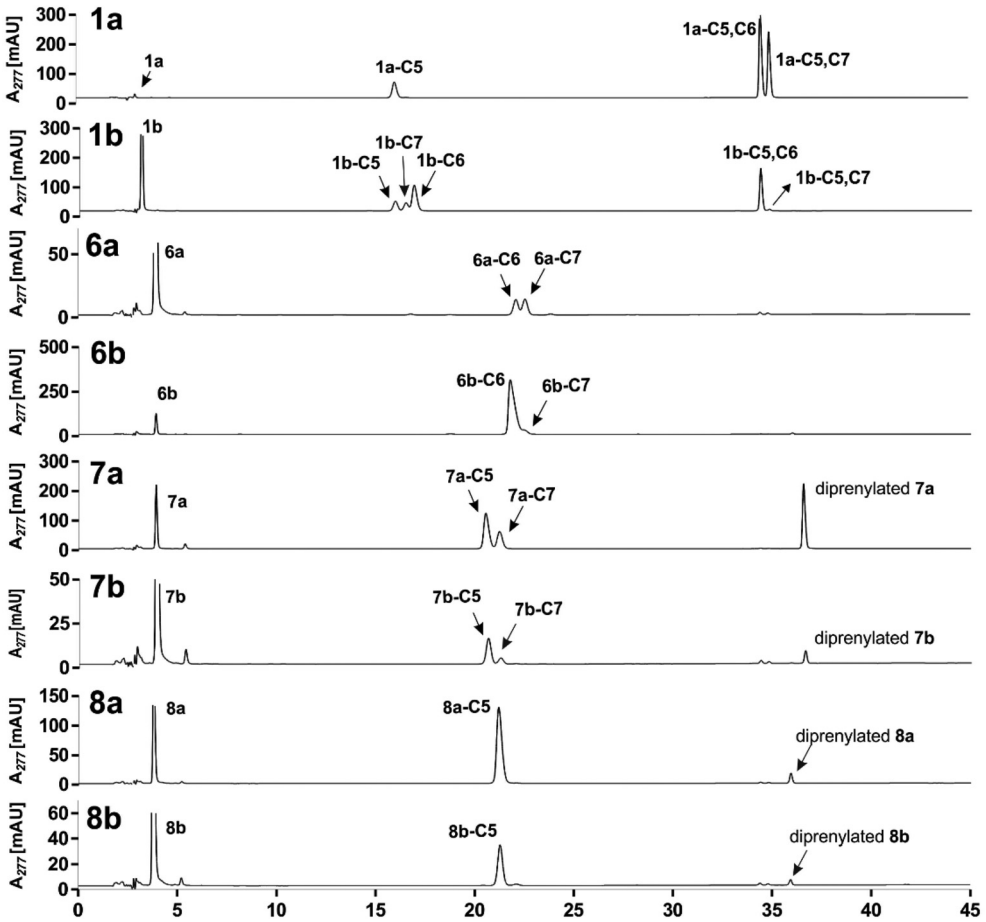

Fig. 3 HPLC analysis of the reaction mixtures of 5-DMATS$_{Sc}$ with L- and D-enantiomers of tryptophan and methylated derivatives. 1 μM of the enzyme was incubated with 1 mM DMAPP and 0.5 mM of the indicated substrate(s) at 37 °C for 16 h. The reaction mixtures were analysed on an Eclipse Plus-C18 column (condition 6, Table S1, ESI†). The structures of the enzyme products of **1a**, **1b**, and **6b** have been elucidated by NMR and MS analyses. The main products of **7a**, **7b**, **8a**, and **8b** are expected to be *C*5-prenylated derivatives. Detection was carried out with a diode array detector and illustrated for absorption at 277 nm.

not available, or available but very expensive. Therefore, we separated L- and D-enantiomers from the racemates 5-methyl-DL-tryptophan (**6**), 6-methyl-DL-tryptophan (**7**) and 7-methyl-DL-tryptophan (**8**) on HPLC by using the CHIRALPAK® Zwix(+) column (Fig. S59, ESI†). Inspection of the HPLC chromatograms of **1a**, **1b** and their racemate (**1**) revealed that the D-enantiomer **1b** was eluted from the column prior to the L-enantiomer **1a**. This elution order is also true for *C*5-, *C*6-, and *C*7-methylated tryptophan, which was proven by determination of their CD-spectra. Two opposite cotton effects were observed for the isolated enantiomers, which corresponded very well to those of **1a** and **1b** (Fig. S59, ESI†), respectively. The enantiomers in the racemate 4-methyl-DL-tryptophan (**5**) (Fig. S60, ESI†) could not be separated in this study.

Substrate preferences of DMATSs for L- and D-enantiomers of methylated tryptophan

The isolated L- and D-enantiomers of *C*5-, *C*6- and *C*7-methylated tryptophan (**6a**, **6b**, **7a**, **7b**, **8a**, **8b**) and their racemates (**6**, **7**, **8**) were incubated with the seven DMATSs under similar conditions (Fig. 4 and S25–S48, ESI†). The observed substrate preferences of the DMATSs differed clearly from each other (Table 2). As reported previously[20,25,26,28] and demonstrated in this study, **6** was a poor substrate for the *C*5-prenyltransferases 5-DMATS and 5-DMATS$_{Sc}$ and the *C*6-methylated derivative **7** was accepted by the *C*6-prenyltransferases 6-DMATS$_{Sa}$ and 6-DMATS$_{Mo}$ with low conversion yields. Higher conversion yields were found for their orthologue 6-DMATS$_{Sv}$ (Table 2). **8** was not accepted by 7-DMATS. The low acceptance of tryptophan analogues, which were blocked at the prenylation position for **1a** by a methyl group, was also demonstrated by using the pure L-enantiomers (Table 2). For methylated tryptophan analogues, L-enantiomers were in general better or in most cases much better accepted by DMATSs than D-enantiomers as in the case of tryptophan.

It seems that FgaPT2 had a much higher enantioselectivity than other tested enzymes and accepted no D-enantiomers **6b**, **7b**, or **8b**. **7b** and **8b** were no substrates for 6-DMATS$_{Sa}$, 6-DMATS$_{Sv}$, and 7-DMATS. No product formation was detected in the reaction mixture of **7b** with 5-DMATS. From Table 2, it is

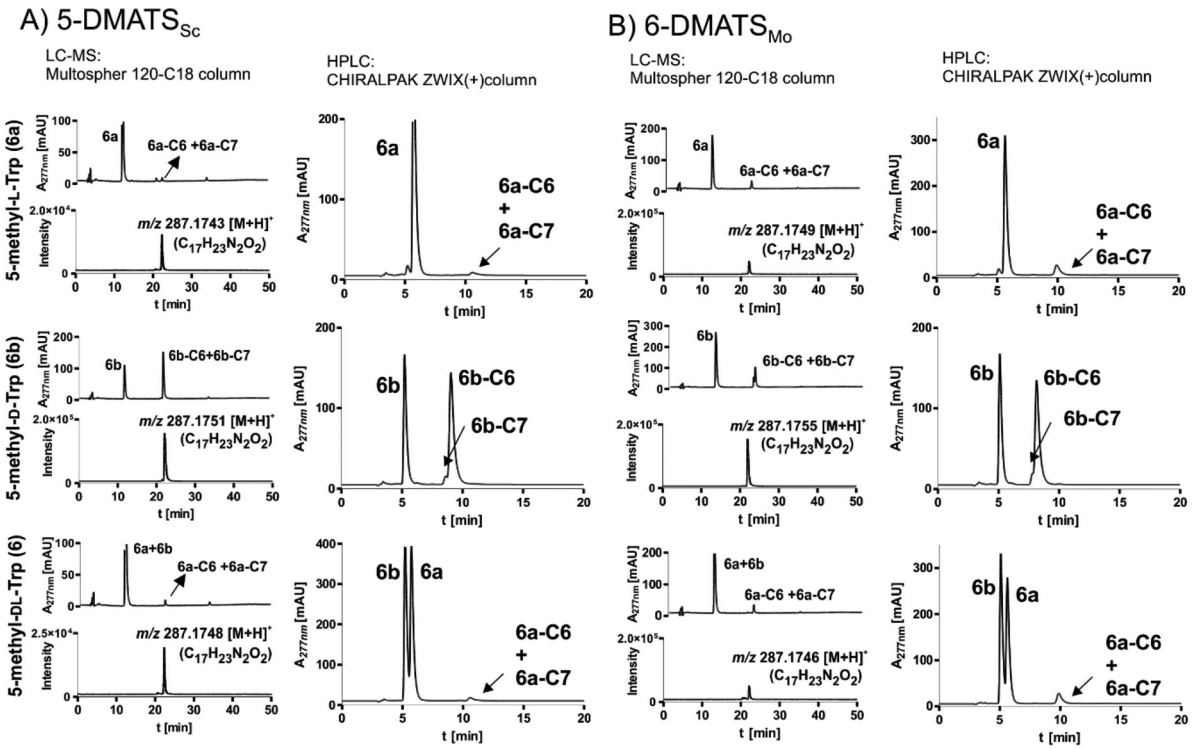

Fig. 4 Evaluation of the enantioselectivity of (A) 5-DMATS$_{Sc}$ and (B) 6-DMATS$_{Mo}$. The enzymes were incubated with 1 mM DMAPP and 0.5 mM of the L-enantiomer, D-enantiomer of 5-methyltryptophan or a combination of both (1 mM) and the reaction products were profiled by LC-MS and HPLC. 1 μM of the indicated enzyme was incubated with the indicated substrate(s) prior to chemical profiling. UV detection was carried out with a diode array detector and illustrated for absorption at 277 nm.

obvious that the reactions of L-enantiomers were almost not inhibited by D-enantiomers and nearly the same activities were detected for the L-enantiomers in the racemates. Interestingly, **6b** was a much better substrate for 5-DMATS$_{Sc}$ and 6-DMATS$_{Mo}$ than **6a**. Relative conversion yields of 57.3 ± 1.8 and 66.6 ± 0.5% of that of **1a** were calculated for the reactions of **6b** with 5-DMATS$_{Sc}$ and 6-DMATS$_{Mo}$, respectively, whereas the values for **6a** are 2.3 ± 0.2 and 12.9 ± 0.2%, respectively (Table 2 and Fig. 4).

More interestingly, **6b** in the racemate **6** was not converted by these two enzymes, while similar conversion yields for **6a** were observed. This indicated an inhibition of the **6b** reactions in the presence of **6a**, which could be explained by determination of their kinetic parameters. Kinetic parameters of 6-DMATS$_{Mo}$ and 5-DMATS$_{Sc}$ were then determined for **6a** and **6b** (Table 3 and Fig. S61–S62, ESI†). Substrate inhibition was observed for the 5-DMATS$_{Sc}$ reaction with **6b** at concentrations higher than 0.05 mM. Therefore, the K_M value was determined from graphical nonlinear evaluation for concentrations less than 0.05 mM. For calculation of k_{cat}, the maximal velocity v_{max} at 0.05 mM **6b** was used (Fig. S61, ESI†). For other reactions, kinetic parameters were calculated from nonlinear regression (Fig. S61 and S62, ESI†) and are given in Table 3. K_M values of 0.009 ± 0.001 and 0.03 ± 0.01 mM and k_{cat} values of 0.005 ± 0.0001 and 0.035 ± 0.005 s^{-1} were calculated for 5-DMATS$_{Sc}$ reactions with L- and D-isomers, respectively. For the 6-DMATS$_{Mo}$ reaction with **6a**, a K_M value of 0.008 ± 0.001 mM and a k_{cat} of 0.012 ± 0.0002 s^{-1} were determined. In comparison, a significantly higher K_M value of 0.30 ± 0.05 mM and larger k_{cat} of 0.042 ± 0.003 s^{-1} were calculated for the 6-DMATS$_{Mo}$ reaction with **6b**. In summary, 5-DMATS$_{Sc}$ and 6-DMATS$_{Mo}$ also display higher affinities to the L- than the D-enantiomer. The turnover numbers for the D-enantiomer are, however, clearly higher than those of the L-enantiomer, confirming the observed conversion yields of the reactions with pure enantiomers and the inhibition of the **6b** reactions in the presence of **6a** in the racemates. Due to the high affinity of the DMATSs towards the L-form, the active site of the enzyme will be occupied by the L-enantiomer, so that no or very low prenylation of **6b** is observed in the reaction with the racemate.

Regioselectivity of DMATSs towards L- and D-enantiomers of methylated tryptophan derivatives

For determination of the prenylation positions, DMATS enzymes, which accepted D-enantiomers (Table 2), were incubated with **6a** and **6b**, **7a** and **7b** as well as **8a** and **8b**. As shown in Fig. S63 in the ESI† and given in Table 4, the three *C*6-prenyltransferases 6-DMATS$_{Sa}$, 6-DMATS$_{Sv}$ and 6-DMATS$_{Mo}$ catalysed the same unique or predominant *C*6-prenylation of **6a** and **6b**. In the reaction mixtures of 6-DMATS$_{Mo}$ with **6a** and **6b**, *C*7-prenylated derivatives were identified as

minor products (Tables 4 and S10, Fig. S63 and S66, ESI†). Different regioselectivities were observed for the reactions of **6a** and **6b** with FgaPT2, 5-DMATS$_{Sc}$ and 7-DMATS. *C*4-prenylated **6a** was detected as the unique product of the FgaPT2 reaction, while an additional product (*C*6- or *C*7-prenylated) was detected for the **6b** reaction with FgaPT2 by LC-MS (Fig. S26, ESI†). In comparison, 5-DMATS$_{Sc}$ displayed a low regioselectivity towards **6a**, with *C*6- and *C*7-prenylated derivatives **6a-C6** and **6a-C7** in a ratio of approximately 1 : 1 as enzyme products. For the 5-DMATS$_{Sc}$ reaction with **6b**, **6b-C6** was detected as the main and **6b-C7** as a minor product in a ratio of 1 : 0.2 (Table S10 and Fig. S63, ESI†). ^{1}H NMR spectra of the product mixture confirmed these results (Fig. S66, ESI†). For the 7-DMATS reaction, a switch from a unique *C*7-prenylation with the L-isomer to a predominant *C*6-prenylation with the D-isomer of 5-methyltryptophan was observed. **6b-C7** was detected as a minor product with a relative product yield of 20% to that of **6b-C6** (Fig. S63, ESI†). These results demonstrated again that stereochemistry of the substrates has influence on the regioselectivity of the used enzymes, at least in several cases. For 6-methyl- (**7a** and **7b**) and 7-methyltryptophan (**8a** and **8b**), accurate determination of the prenylation positions of the enzyme products was not always possible, because the products could not be separated completely from each other under the HPLC conditions used in this study (Fig. S64 and S65, ESI†). *C*5- and *C*7-prenylations of **7a** and **7b** with 6-DMATS$_{Mo}$ confirmed the previous results (Table S1†). Two product peaks each of the 5-DMATS$_{Sc}$ reactions with **7a** and **7b** indicate *C*5- and *C*7-prenylations. In the HPLC chromatograms of the reaction mixtures of **8a** and **8b** with 5-DMATS, 5-DMATS$_{Sc}$, and 6-DMATS$_{Mo}$, one monoprenylated product peak with similar retention times could also be observed.

Diprenylation of methylated tryptophan derivatives by DMATSs

As mentioned above, diprenylation of tryptophan was observed for most of the tested DMATSs by the EIC mode in LC-MS. With exceptions for 5-DMATS$_{Sc}$, the product yields of less than 0.5% were so low that UV detection was almost not possible for 1.5 h incubation mixtures. Even after extension of the incubation time to 16 h, UV detection of the diprenylated derivatives of **1a** and **1b** was only observed for 5-DMATS$_{Sc}$ (data not shown). HPLC analysis of the 16 h reaction mixture of **7a** with 5-DMATS$_{Sc}$ revealed the presence of two mono- and one diprenylated product peaks (Fig. 3). Low product formation was observed in the reaction mixtures of 5-DMATS$_{Sc}$ with **7b**, **8a** and **8b**. Similar retention times of the products of the D-form with those of the L-form suggest identical diprenylated products for both enantiomers. The diprenylated features of these products were confirmed by LC-MS analysis. These results highlight the increased capability of 5-DMATS$_{Sc}$ for diprenylation of tryptophan and its derivatives. Diprenylation of tryptophan and its analogues by tandem reactions of two DMATSs has been described for FgaPT2 and 7-DMATS.[38] However, diprenylation by one single tryptophan prenyltransferase has not been reported previously.

Conclusion

This study deals with comparative investigation on the divergence of microbial dimethylallyltryptophan synthases regarding their enantio- and regioselectivities. Different preferences were clearly observed for the seven tested DMATSs towards D- and L-enantiomers of tryptophan and methylated derivatives. High flexible enantioselectivity was found for 5-DMATS, 5-DMATS$_{Sc}$, and 6-DMATS$_{Mo}$. Remarkably high conversion yields were detected for D-tryptophan with 6-DMATS$_{Mo}$ and 5-DMATS. 5-Methyl-D-tryptophan was even better accepted by 5-DMATS$_{Sc}$ and 6-DMATS$_{Mo}$ than the L-enantiomer. In other cases, the L-forms were the best accepted substrates. Interestingly, lower or in most cases, no product formation was observed for D-enantiomers in the presence of L-enantiomers in the racemates. Kinetic studies of 5-DMATS$_{Sc}$ and 6-DMATS$_{Mo}$ suggest that the very high affinities towards the L-enantiomers led, in most cases, to the repression of the D-enantiomer reaction under the used conditions.

In contrast with the highly regiospecific prenylation on the L-tryptophan of the tested enzymes, the L-tryptophan *C*4-prenyltransferase FgaPT2 and *C*5-prenyltransferase 5-DMATS$_{Sc}$ displayed a reduced regioselectivity towards D-tryptophan with *C*5- and *C*6-prenylated derivatives as the main products, respectively. Clearly different regioselectivities were also identified for the enantiomers of 5-methyltryptophan with FgaPT2, 5-DMATS$_{Sc}$ and 7-DMATS. Furthermore, diprenylation of tryptophan by 5-DMATS$_{Sc}$ was the first example that a tryptophan prenyltransferase catalyses two successive prenylation steps. These results expand our knowledge on the similarity and differences in the biochemical features of the tryptophan prenyltransferases. Moreover, the presented biochemical properties of these enzymes make them potential biocatalysts in chemical synthesis for prenylated indole derivatives, which represent promising candidates for drug discovery and development in the pharmaceutical industry. As mentioned in the Introduction, D-amino acids and their derivatives are interesting drug candidates and could be used for treatment of different diseases.[3,39–44] Testing the bioactivity of these compounds is intended in the near future.

Experimental section

Chemicals

DMAPP, GPP, and FPP were synthesised according to the method described for GPP reported elsewhere.[45] Aromatic substrates used for the enzyme assays were purchased from TCI, Sigma-Aldrich, Bachem, Roth, and Fluka and were of the highest available purity.

Bacterial strains and plasmids

pGEM-T Easy was obtained from Promega (Mannheim, Germany). pHIS$_8$ was kindly provided by Prof. Joseph P. Noel (Salk Institute for Biological Studies). *Escherichia coli* strains XL1 Blue MRF' (Stratagene, Amsterdam, the Netherlands),

M15 (pREP4) (Qiagen), and BL21 (DE3) pLysS (AMS Biotechnology, Abingdon, UK) were used for cloning and expression experiments. *Micromonospora olivasterospora* DSM 43868 was purchased from the Deutsche Sammlung von Mikroorganismen und Zellkulturen (Braunschweig, Germany).

Cloning and expression of *MolI14.36*

For genomic DNA isolation by phenol-chloroform extraction,[46] cultivation of *M. olivasterospora* was carried out in a 300 ml cylindrical flask containing 50 ml liquid YMG medium (0.4% (w/v) yeast extract, 1% (w/v) malt extract, and 0.4% (w/v) glucose) at 160 rpm on a rotary shaker at 28 °C for three days. Standard procedures for DNA manipulation in *E. coli* were performed as described previously.[47]

With the isolated genomic DNA as the template, a PCR fragment of 1143 bp containing the coding sequence of MolI14.36 was amplified by using the Expand high fidelity kit (Roche Diagnostic, Mannheim, Germany) and the primers Mol_SacI_fw: (5′-**GAGCTC**ATGGCCGGCTTGTCCG-3′) and Mol_HindIII_Rev: 5′-**AAGCTT**TCAGGGTCGGGTACGGC-3′). Bold underlined letters represent the restriction sites for SacI and HindIII, located immediately before the predicted start and at the stop codon in the primer sequences. PCR amplification was performed on an iCycler from Bio-Rad. The PCR product was cloned *via* the pGEM-T Easy vector into $pHIS_8$ [48] resulting in the expression construct pJW32. *E. coli* BL21 [DE3] cells harbouring pJW32 were cultivated in 1 L liquid lysogeny broth (LB) medium supplemented with kanamycin (50 μg ml^{-1}) until an OD_{600} of 0.6. For induction of gene expression, IPTG was added to a final concentration of 1 mM. After further incubation at 30 °C and 220 rpm for 16 h, the recombinant His_8-tagged protein was purified on Ni-NTA agarose according to the manufacturer's protocol.

Overproduction and purification of the recombinant DMATS enzymes

Escherichia coli (*E. coli*) M15 [pREP4] (Qiagen) and BL21 (DE3) pLysS (AMS Biotechnology, Abingdon, UK) were used for expression. Culture conditions for gene expression and purification of FgaPT2, 5-DMATS, 5-$DMATS_{Sc}$, 6-$DMATS_{Sa}$, 6-$DMATS_{Sv}$ and 7-DMATS were carried out as described previously.[20,21,25,27,28]

Protein analyses

The purified proteins were analysed on 12% (w/v) SDS-PAGE[49] and stained with Coomassie Brilliant Blue G-250 (Fig. S1, ESI†). The protein content was determined on a NanoDrop 2000c (Thermo Scientific) at an absorption of 280 nm. The molecular masses of the native recombinant His_8-6-$DMATS_{Mo}$, His_8-6-$DMAT_{Sv}$ and 6-$DMAT_{Sa}$-His_6 were determined by size exclusion chromatography on a HiLoad 16/60 Superdex 200 column (GE Healthcare). 50 mM Tris-HCl buffer (pH 7.5) containing 150 mM NaCl was used to equilibrate the column and elute proteins. The column was calibrated with blue dextran 2000 (2000 kDa), aldolase (158 kDa), conalbumin (75 kDa), chymotrypsinogen A (25 kDa) and ribonuclease A (13.7 kDa) (GE Healthcare).

Enzyme assays

All reaction mixtures contained 50 mM Tris-HCl (pH 7.5) and were incubated at 37 °C. The conditions of the reaction mixtures for identification of the prenylated products are described in Table S9 in the ESI.†

Kinetic parameters of 6-$DMATS_{Mo}$ toward DMAPP were determined with 1 mM of **1a** as the prenyl acceptor. Assays containing 229.9 nM 6-$DMATS_{Mo}$ and DMAPP at final concentrations of 0.002 to 0.5 mM were incubated for 30 min. For determination of the kinetic parameters of different DMATSs towards **1a**, DMAPP at 1 mM and **1a** at final concentrations of up to 1 mM were used. Assays with 36.2 nM FgaPT2, 99.2 nM 5-DMATS, 118.5 nM 5-$DMATS_{Sc}$, 121.7 nM 6-$DMATS_{Sa}$, 231.0 nM 6-$DMATS_{Sv}$, 229.9 nM 6-$DMATS_{Mo}$, and 228.8 nM 7-DMATS were incubated for 15 min or in the case of 6-$DMATS_{Mo}$ for 30 min. For determination of the kinetic parameters of **1b**, the maximal substrate concentration was increased to 2 mM or even 4 mM in the case of 5-$DMATS_{Sc}$. The assays contained 905.8 nM FgaPT2, 396.8 nM 5-DMATS, 473.9 nM 5-$DMATS_{Sc}$, 486.6 nM 6-$DMATS_{Sa}$, 461.9 nM 6-$DMATS_{Sv}$, 459.8 nM 6-$DMATS_{Mo}$, or 1.4 μM 7-DMATS and were incubated for 30 min, or in the case of 5-$DMATS_{Sc}$ for 15 min. The assays for determination of the kinetic parameters of 6-$DMATS_{Mo}$ for **6a** and **6b** contained 1 mM DMAPP, 459.8 nM of the recombinant protein, **6a** from 0.002 to 0.5 mM or **6b** from 0.01 to 1 mM. The reaction mixtures were incubated for 30 min. For the 5-$DMATS_{Sc}$ reactions with **6a** and **6b**, the assays contained 7.1 μM and 473.9 nM of the recombinant protein and 0.002 to 0.5 mM of **6a** or **6b**, which were incubated for 15 min. The conditions for all other enzyme assays are given in the legends of respective figures or tables.

Assays for isolation of the enzyme products of 6-$DMATS_{Mo}$ were prepared in large scales (10 ml) containing 50 mM Tris-HCl (pH 7.5), 5 mM $MgCl_2$, 1 mM L-tryptophan or its analogues, 2 mM DMAPP, and recombinant protein in an adequate quantity (2.3–6.9 μM). Enzyme products of 6-$DMATS_{Mo}$ with 5-methyl-D-tryptophan as well as 5-$DMATS_{Sc}$ with D-tryptophan and 5-methyl-D-tryptophan were isolated from up-scaled assays (5 ml) containing 50 mM Tris-HCl (pH 7.5), 5 mM $MgCl_2$, 1 mM D-tryptophan or 0.5 mM 5-methyl-D-tryptophan, 2 mM DMAPP and the recombinant protein in an adequate quantity (4.7–11.9 μM 5-$DMATS_{Sc}$ or 4.6–11.5 μM 6-$DMATS_{Mo}$). Assays were incubated for 16 h.

All enzyme reactions were terminated by addition of one volume of methanol. Assays of up to 100 μl were centrifuged at 17 000*g* for 20 min before further analysis on HPLC. Isolation assays of 5–10 ml were centrifuged at 4500*g* for 30 min and the obtained supernatants were concentrated on a rotating vacuum evaporator at 35 °C to a volume of 1 ml for isolation on HPLC.

HPLC and LC-MS analyses

The methods and the column used for HPLC measurements are listed as conditions 1–9 in Table S1 in the ESI.† For all ana-

lyses with the exception of condition 4, an Agilent HPLC 1200 (Böblingen, Germany) was used. Reaction mixtures for comparison of the substrate specificities of 6-DMATS$_{Sa}$, 6-DMATS$_{Sv}$, and 6-DMATS$_{Mo}$ were analysed under condition 1. For investigation of the substrate preferences of DMATSs towards L- und D-isomers of tryptophan and analogues thereof, the incubation mixtures were analysed with a CHIRALPAK® Zwix(+) column (150 × 3 mm, 3 μm, Chiral Technologies Europe, Daicel Group, Illkirch Cedex, France) and an isocratic run (condition 2, Table S1, ESI†). Condition 2 was also used to determine the kinetic parameters of 5-methyl-L-tryptophan and 5-methyl-D-tryptophan. Incubation mixtures for kinetic studies on tryptophan were analysed under condition 1.

To detect prenylation, the assays were analysed on an Agilent HPLC 1260 equipped with a Bruker microTOF QIII mass spectrometer. The applied method is illustrated as condition 3. Chromatograms with UV detection and the extracted ion chromatograms (EIC) are given in Fig. 1 and 4 as well as in Fig. S25–S48 (ESI†).

Reaction mixtures for better separation of the enzyme products with prenylations at different positions were analysed under condition 4 for L- and D-tryptophan or under condition 5 for the L- and D-forms of 5-, 6-, and 7-methyltryptophan as substrates. Enzyme assays with 5-DMATS$_{Sc}$, illustrated in Fig. 3, were measured under condition 6. The enantiomeric substrates were separated isocratically with the same chiral column by using methanol as the elution solvent (condition 7).

For isolation of the prenylated products, the same HPLC equipment under condition 8 or 9 was used. Detection was carried out with a photodiode array detector and illustrated at 277 nm in this paper.

Structure elucidation by NMR analysis

NMR spectra of the enzyme products were recorded on a JEOL ECA-500 MHz (**1a-C6**, **1b-C6**, **1a-C5,C6**, and **1a-C5,C7**), a JEOL ECX-400 MHz (**1b-C5**, **1b-C6**, **1b-C7**, **2a-C6**, **3a-C6**, **4-C6**, **7-C6**, and **9a-C6**) (JEOL Germany GmbH, Munich, Germany) or a Bruker Avance III HD 500 (Bruker Biospin GmbH, Rheinstetten, Germany) (**5-C5**, **5-C6**, **5-C7**, **6-C6**, **6-C7**, **8-C6**, and **1b-C5,C6**) spectrometer. All spectra were processed with MestReNova 6.0.2-5475 and ^{1}H chemical shifts were referenced to those of the solvent signals at 3.31 ppm for methanol. The NMR data are given in the ESI† (Tables S5–S8, S10, and Fig. S4–S22, S57–58, S66†).

Circular dichroism (CD) spectroscopy of the isolated substrates

For determination of the configuration, CD spectra of the L- and D-forms of tryptophan and its methylated derivatives were taken on a Jasco J-810 CD spectrometer. The samples were dissolved in water and measured in the range of 180–350 nm by using a 1 mm path length quartz cuvette.

Accession numbers

The nucleotide sequence of *MolI14.36* is available in the GenBank database under accession number AJ628421.2 and the corresponding protein sequence under accession number CAF31565.1.

Acknowledgements

We thank Lena Ludwig for synthesis of DMAPP, Stefan Newel and Rixa Kraut for taking NMR and mass spectra, respectively. J. W. was partially financed by the LOEWE program of the State of Hessen (SynMikro to S. M. L.). S. M. L. also acknowledges the Deutsche Forschungsgemeinschaft for funding the Bruker microTOF QIII mass spectrometer. (INST 160/620-1)

References

1 A. Shimada and H. Ozaki, *Life*, 2012, **2**, 215–228.
2 L. A. Nguyen, H. He and C. Pham-Huy, *Int. J. Biomed. Sci.*, 2006, **2**, 85–100.
3 X. Gao, Q. Ma and H. Zhu, *Appl. Microbiol. Biotechnol.*, 2015, **99**, 3341–3349.
4 S. D'Aniello, I. Somorjai, J. Garcia-Fernandez, E. Topo and A. D'Aniello, *FASEB J.*, 2011, **25**, 1014–1027.
5 F. Cava, H. Lam, M. A. de Pedro and M. K. Waldor, *Cell. Mol. Life Sci.*, 2011, **68**, 817–831.
6 R. C. Strauch, E. Svedin, B. Dilkes, C. Chapple and X. Li, *Proc. Natl. Acad. Sci. U. S. A.*, 2015, **112**, 11726–11731.
7 D. M. Veine, H. Yao, D. R. Stafford, K. S. Fay and D. L. Livant, *Clin. Exp. Metastasis*, 2014, **31**, 379–393.
8 B. D. Welch, A. P. VanDemark, A. Heroux, C. P. Hill and M. S. Kay, *Proc. Natl. Acad. Sci. U. S. A.*, 2007, **104**, 16828–16833.
9 J. Kumar and V. Sim, *Prion*, 2014, **8**, 119–124.
10 S.-M. Li, *Nat. Prod. Rep.*, 2010, **27**, 57–78.
11 J. Winkelblech, A. Fan and S.-M. Li, *Appl. Microbiol. Biotechnol.*, 2015, **99**, 7379–7397.
12 B. Wollinsky, L. Ludwig, A. Hamacher, X. Yu, M. U. Kassack and S.-M. Li, *Bioorg. Med. Chem. Lett.*, 2012, **22**, 3866–3869.
13 B. Botta, A. Vitali, P. Menendez, D. Misiti and M. G. Delle, *Curr. Med. Chem.*, 2005, **12**, 717–739.
14 A. H. Liu, D. Q. Liu, T. J. Liang, X. Q. Yu, M. T. Feng, L. G. Yao, Y. Fang, B. Wang, L. H. Feng, M. X. Zhang and S. C. Mao, *Bioorg. Med. Chem. Lett.*, 2013, **23**, 2491–2494.
15 A. Oya, N. Tanaka, T. Kusama, S. Y. Kim, S. Hayashi, M. Kojoma, A. Hishida, N. Kawahara, K. Sakai, T. Gonoi and J. Kobayashi, *J. Nat. Prod.*, 2015, **78**, 258–264.
16 T. Sasaki, Y. Igarashi, M. Ogawa and T. Furumai, *J. Antibiot.*, 2002, **55**, 1009–1012.
17 I. A. Unsöld and S.-M. Li, *Microbiology*, 2005, **151**, 1499–1505.

18 S. Takahashi, H. Takagi, A. Toyoda, M. Uramoto, T. Nogawa, M. Ueki, Y. Sakaki and H. Osada, *J. Bacteriol.*, 2010, **192**, 2839–2851.
19 R. Satou, M. Izumikawa, Y. Katsuyama, M. Matsui, M. Takagi, K. Shin-ya and Y. Ohnishi, *J. Antibiot.*, 2014, **67**, 231–236.
20 J. Winkelblech and S.-M. Li, *ChemBioChem*, 2014, **15**, 1030–1039.
21 T. Ozaki, M. Nishiyama and T. Kuzuyama, *J. Biol. Chem.*, 2013, **288**, 9946–9956.
22 S. Subramanian, X. Shen, Q. Yuan and Y. Yan, *Process Biochem.*, 2012, **47**, 1419–1422.
23 C. Wu, C. Du, J. Gubbens, Y. H. Choi and G. P. van Wezel, *J. Nat. Prod.*, 2015, **78**, 2355–2363.
24 A. Fan, J. Winkelblech and S.-M. Li, *Appl. Microbiol. Biotechnol.*, 2015, **99**, 7399–7415.
25 X. Yu, Y. Liu, X. Xie, X.-D. Zheng and S.-M. Li, *J. Biol. Chem.*, 2012, **287**, 1371–1380.
26 J. Winkelblech, M. Liebhold, J. Gunera, X. Xie, P. Kolb and S.-M. Li, *Adv. Synth. Catal.*, 2015, **357**, 975–986.
27 N. Steffan, I. A. Unsöld and S.-M. Li, *ChemBioChem*, 2007, **8**, 1298–1307.
28 A. Kremer, L. Westrich and S.-M. Li, *Microbiology*, 2007, **153**, 3409–3416.
29 X. Yu, G. Zocher, X. Xie, M. Liebhold, S. Schütz, T. Stehle and S.-M. Li, *Chem. Biol.*, 2013, **20**, 1492–1501.
30 J. M. Schuller, G. Zocher, M. Liebhold, X. Xie, M. Stahl, S.-M. Li and T. Stehle, *J. Mol. Biol.*, 2012, **422**, 87–99.
31 M. Jost, G. Zocher, S. Tarcz, M. Matuschek, X. Xie, S.-M. Li and T. Stehle, *J. Am. Chem. Soc.*, 2010, **132**, 17849–17858.
32 U. Metzger, C. Schall, G. Zocher, I. Unsöld, E. Stec, S.-M. Li, L. Heide and T. Stehle, *Proc. Natl. Acad. Sci. U. S. A.*, 2009, **106**, 14309–14314.
33 A. Kremer and S.-M. Li, *Appl. Microbiol. Biotechnol.*, 2008, **79**, 951–961.
34 K. Miyamoto, F. Ishikawa, S. Nakamura, Y. Hayashi, I. Nakanishi and H. Kakeya, *Bioorg. Med. Chem.*, 2014, **22**, 2517–2528.
35 Y. Ding, R. M. Williams and D. H. Sherman, *J. Biol. Chem.*, 2008, **283**, 16068–16076.
36 A. Markert, N. Steffan, K. Ploss, S. Hellwig, U. Steiner, C. Drewke, S.-M. Li, W. Boland and E. Leistner, *Plant Physiol.*, 2008, **147**, 296–305.
37 A. Fan, H. Chen, R. Wu, H. Xu and S.-M. Li, *Appl. Microbiol. Biotechnol.*, 2014, **98**, 10119–10129.
38 H.-L. Ruan, E. Stec and S.-M. Li, *Arch. Microbiol.*, 2009, **191**, 791–795.
39 L. Jia, K. Schweikart, J. Tomaszewski, J. G. Page, P. E. Noker, S. A. Buhrow, J. M. Reid, M. M. Ames and D. H. Munn, *Food Chem. Toxicol.*, 2008, **46**, 203–211.
40 M. Tanaka, X. Li, H. Hikawa, T. Suzuki, K. Tsutsumi, M. Sato, O. Takikawa, H. Suzuki and Y. Yokoyama, *Bioorg. Med. Chem.*, 2013, **21**, 1159–1165.
41 P. T. Di, S. Danese, C. R. De and S. Rutella, *Expert Opin. Ther. Pat.*, 2010, **20**, 229–250.
42 K. Saito, C. Y. Chen, M. Masana, J. S. Crowley, S. P. Markey and M. P. Heyes, *Biochem. J.*, 1993, **291**(Pt 1), 11–14.
43 B. Heller, D-Phenylalanine Treatment, *US Pat.*, 4355044, 1982.
44 T. Fukushima, A. Sugiura, I. Furuta, S. Iwasa, H. Iizuka, H. Ichiba, M. Onozato, H. Hikawa and Y. Yokoyama, *Int. J. Tryptophan Res.*, 2015, **8**, 1–5.
45 A. B. Woodside, Z. Huang and C. D. Poulter, *Org. Synth.*, 1988, **66**, 211–215.
46 T. Kieser, M. J. Bibb, M. J. Buttner, K. F. Chater and D. A. Hopwood, *Practical Streptomyces Genetics*, John Innes Foundation, Norwich, UK, 2000.
47 J. Sambrook and D. W. Russell, *Molecular Cloning: a Laboratory Manual*, Cold Spring Harbor Laboratory Press, Cold Spring Harbor, New York, 2001.
48 J. M. Jez, J. L. Ferrer, M. E. Bowman, R. A. Dixon and J. P. Noel, *Biochemistry*, 2000, **39**, 890–902.
49 U. K. Laemmli, *Nature*, 1970, **227**, 680–685.

Electronic supplementary material for:

Characterisation of 6-DMATS$_{Mo}$ from *Micromonospora olivasterospora* leading to identification of divergence in enantioselectivity, regioselectivity and multiple prenylation of tryptophan prenyltransferases

Julia Winkelblech[a,b], Xiulan Xie[c], Shu-Ming Li [a,b]*

[a] Institut für Pharmazeutische Biologie und Biotechnologie, Philipps-Universität Marburg, Robert-Koch-Straße 4, 35037 Marburg, Germany

[b] Zentrum für Synthetische Mikrobiologie, Philipps-Universität Marburg, Hans-Meerwein-Straße, D-35032 Marburg, Germany.

[c] Philipps-Universität Marburg, Fachbereich Chemie, Hans-Meerwein-Straße, 35032 Marburg, Germany

*Correspondence to Shu-Ming Li: shuming.li@staff.uni-marburg.de;

Telefon: 49(0) 6421 282-2461; Fax: 49(0)6421 282-

Structure elucidation of enzyme products of 6-DMATS$_{Mo}$ by NMR analysis

Inspection of the NMR spectra of the isolated peaks revealed the presence of a unique product each from the reaction mixtures of **1a**, **1b**, **2a**, **3a**, **4**, **5**, **8**, and **9a**, whereas three products **5-C5**, **-C6,** and **-C7** were found from that of **5** and two products each **6-C6** and **6-C7** or **7-C5** and **7-C6** from those of **6** and **7** (Table S5-S7, Fig. S4-S22). The presence of the signals for dimethylallyl moieties at δ_H 3.30 - 3.56 (d/ or m, 2H-1'), 5.09 - 5.41 (t sept or m, H-2'), 1.74 - 1.83 (s, 3H-4'), 1.68 - 1.75 ppm (s, 3H-5') verified a regular *C*-prenylation in all the structures (Table S5-S7).[2,3,5-7] In comparison to the respective substrates, signals for one aromatic proton was absent in the spectra of the enzyme products. The presence of the singlet in the range of δ_H 7.06 - 7.17 ppm for H-2 implies the prenylation at the benzene ring.

Comparison of the spectra of **1a**, **1b**, **2a**, **3a**, and **4** with each other (Table S5, Fig. S4-S8) showed similar chemical shifts of the three coupling aromatic protons at δ_H 7.49 - 7.59, 6.89 - 6.91, and 7.14 - 7.15 ppm. The two coupling constants of 8.2 and 1.4 - 1.5 Hz indicates *C5*- or *C6*-prenylation in their structures. Considering the relative positions of the signals of the aromatic protons and comparison of the spectra with those of *C5*- and *C6*-prenylated tryptophan and analogues [6,8] led to identification of **1a-C6,** **1b-C6**, **2a-C6**, **3a-C6**, and **4-C6** to be *C6*-prenylated derivatives. **1a-C6**, **2a-C6,** and **3a-C6** have been identified as enzyme products of **1a**, **2a**, and **3a** with 6-DMATS$_{Sa}$.[6]

Signals for three products **5-C5**, **-C6**, and **-C7** with a ratio of 0.6:1:0.6 were detected in the ^{1}H NMR spectrum of the isolated peak from the enzyme assay of **5**. Due to different coupling pattern, it was possible to determine the prenylation positions in their structures. The three singlets at δ_H 7.06, 6.96, and 6.60 ppm of the main product **5-C6** verified a *C6*-prenylation in its structure (Table S6, Fig S9). The correlations in ^{1}H-^{1}H

COSY confirmed this conclusion and facilitated the assignment of the protons (Fig S10-S14). **5-C5** and **5-C7** were identified as *C5*- and *C7*-prenylated products by interpretation of the ^{1}H-^{1}H COSY correlations and by comparison of their coupling pattern with those published previously.[4,6,8]

Two products **6-C6** and **6-C7** with a ratio of 1:0.4 were identified as products in the reaction mixture of **6** (Table S6, Fig. S15). The chemical shifts and the coupling pattern of the main product **6-C6** were nearly the same as those of 6-DMA-5-methyl-DL-tryptophan, the product of 6-DMATS$_{Sa}$ with **6**.[6] This result was further confirmed by the interpretation of correlations in ^{1}H-^{1}H COSY (Fig S16-S19). Three singlets at δ_H 7.15, 7.35, and 6.76 ppm for three aromatic protons were observed for **6-C7**, which are distinct from those of **6-C6** and correspond very well to those of the *C7*-prenylated product reported previously for TyrPT.[1] Thus, MolI14.36 catalyses mainly a *C6*-prenylation of **6** rather than a *C7*-prenylation. From the reaction mixture of MolI14.36 with **7**, two products **7-C5** and **7-C7** with a ratio of 0.12:1 were isolated as a mixture. The ^{1}H NMR data of the main product **7-C7** correspond very well to those observed for the *C7*-prenylated product of **7** reported for 6-DMATS$_{Sa.}$[6] Signals of **7-C5** had a very low intensity. The observed three singlets of the indole moiety at δ_H 7.14, 7.45, and 7.07 ppm indicates a *C4*- or *C5*-prenylation of **7** (Table S7, Fig S20). Comparison of these data with those of the *C5*-prenylated derivative proved unequivocally the *C5*-prenylation in **7-C5**.[8] Interpretation of the ^{1}H NMR spectra of **8-C6** and **9a-C6** revealed the attachment of the dimethylallyl moiety at position C-6 of the indole ring (Table S7, Fig. S21 – S22)

Reference List

1 A. Fan, H. Chen, R. Wu, H. Xu, and S.-M. Li, *Appl. Microbiol. Biotechnol.*, 2014, **98**, 10119-10129.

2 A. Fan and S.-M. Li, *Tetrahedron Lett*, 2014, **55**, 5199-5202.

3 A. Kremer and S.-M. Li, *Appl. Microbiol. Biotechnol.*, 2008, **79**, 951-961.

4 J. D. Rudolf and C. D. Poulter, *ACS Chem. Biol.*, 2013, **8**, 2707-2714.

5 S. Takahashi, H. Takagi, A. Toyoda, M. Uramoto, T. Nogawa, M. Ueki, Y. Sakaki, and H. Osada, *J. Bacteriol.*, 2010, **192**, 2839-2851.

6 J. Winkelblech and S.-M. Li, *Chembiochem.*, 2014, **15**, 1030-1039.

7 X. Yu and S.-M. Li, *Methods Enzymol.*, 2012, **516**, 259-278.

8 X. Yu, Y. Liu, X. Xie, X.-D. Zheng, and S.-M. Li, *J. Biol. Chem.*, 2012, **287**, 1371-1380.

Table S1 HPLC conditions for analyses of enzyme assays.

Condition 1		
Column	Multospher 120 RP-18 column (250×4 mm, 5 µm, C+S Chromatography Service, Langerwehe, Germany)	
Flow rate	1 ml*min^{-1}	
Solvent A	water	
Solvent B	methanol	
Elution profile	solvent B in A [v/v]	duration [min]
	from 40 % to 100 %	15 min
	100 %	5 min
	40 %	5 min
Condition 2		
Column	CHIRALPAK®Zwix(+) column (150 × 3 mm, 3 µm, Chiral technologies Europe, Daicel Group, Illkirch Cedex, France)	
Flow rate	0.5 ml*min^{-1}	
Solvent A	water:methanol (1:1), 25 mM diethylamine, 50 mM formic acid	
Solvent B	methanol, 25 mM diethylamine, 50 mM formic acid	
Elution profile	solvent B in A [v/v]	duration [min]
	0%	25 min
	100 %	5 min
	0 %	5 min
Condition 3		
Column	Multospher 120-C18 column (250 x 2 mm, 5 µm; C+S Chromatography Service, Langenfeld, Germany))	
Flow rate	0.5 ml*min^{-1}	
Solvent A	water, 0.1 % (v/v) formic acid	
Solvent B	acetonitrile, 0.1 % (v/v) formic acid	
Elution profile	solvent B in A [v/v]	duration [min]
	from 5 % to 100 %	40 min
	100 %	10 min
	5 %	5 min
Condition 4		
Column	Eclipse XDB-C18 column (5 µm, 4.6 x 150 mm, Agilent)	
Flow rate	0.5 ml*min^{-1}	
Solvent A	water, 0.5 % (v/v) trifluoroacetic acid	
Solvent B	acetonitrile, 0.5 % (v/v) trifluoroacetic acid	
Elution profile	solvent B in A [v/v]	duration [min]
	30 %	5 min
	from 30 % to 45 %	30 min
	100 %	5 min
	30 %	5 min
Condition 5		
Column	Eclipse Plus-C18 column (3.5 µm, 4.6 x 150 mm, Agilent)	
Flow rate	0.5 ml*min^{-1}	
Solvent A	water, 0.5 % (v/v) trifluoroacetic acid	
Solvent B	acetonitrile, 0.5 % (v/v) trifluoroacetic acid	
Elution profile	solvent B in A [v/v]	duration [min]
	30 %	5 min
	From 30 % to 35 %	30 min
	100 %	5 min
	30 %	5 min
Condition 6		
Column	Eclipse Plus-C18 column (3.5 µm, 4.6 x 150 mm, Agilent)	
Flow rate	0.5 ml*min^{-1}	
Solvent A	water, 0.5 % (v/v) trifluoroacetic acid	
Solvent B	acetonitrile, 0.5 % (v/v) trifluoroacetic acid	
Elution profile	solvent B in A [v/v]	duration [min]
	30 %	5 min

	from 30 % to 35 %	15 min
	from 35 % to 70 %	25 min
	100 %	5 min
	30 %	5 min
Condition 7		
Column	CHIRALPAK®Zwix(+) column (150 × 3 mm, 3 µm, Chiral technologies Europe, Daicel Group, Illkirch Cedex, France)	
Flow rate	0.5 ml*min^{-1}	
Solvent A	methanol	
Elution profile	solvent A	duration [min]
	100 %	25 min
Condition 8		
Column	Multospher 120 RP-18 column (250×10 mm, 5 µm, C+S Chromatography Service, Langerwehe, Germany)	
Flow rate	2.5 ml*min^{-1}	
Solvent A	water	
Solvent B	methanol	
Elution profile	solvent B in A [v/v]	duration [min]
	60 %	5 min
	from 60 % to 100 %	25 min
	100 %	5 min
	60 %	5 min
Condition 9		
Column	Multospher 120 RP-18 column (250×10 mm, 5 µm, C+S Chromatography Service, Langerwehe, Germany)	
Flow rate	2.5 ml*min^{-1}	
Solvent A	water	
Solvent B	methanol	
Elution profile	solvent B in A [v/v]	duration [min]
	from 70 % to 100 %	20 min
	100 %	5 min
	70 %	5 min

Table S2 Enzyme activities of 6-DMATS$_{Mo}$ towards different prenyl donors.

prenyl donor	relative conversion yield [%]	
	(4 µM, 4 h, 1 mM donor)	(6 µM, 6 h, 2 mM donor)
DMAPP	100	100
GPP	7.8	11.7
FPP	≤0.5	≤0.5

The enzyme assays were analyzed on HPLC under condition 1. The conversion yields of L-tryptophan in the presence of DMAPP at 51.2 % (1 mM DMAPP) or 98.3 % (2 mM DMAPP) were defined as 100 % relative activity.

Table S3 Comparison of enzyme activities of 6-DMATS$_{Mo}$, 6-DMATS$_{Sa}$ and 6-DMATS$_{Sv}$ towards tryptophan-containing cyclic dipeptides.

substrate	relative conversion yield [%]		
	6-DMATS$_{Mo}$	**6-DMATS$_{Sv}$**	**6-DMATS$_{Sa}$**
cyclo-L-Trp-Gly	7.1±0.5	0.8±0.2	1.8±0.3
cyclo-L-Trp-L-Leu	1.3±0.2	1.3±0.1	9.1±1.2
cyclo-L-Trp-L-Trp	2.7±0.3	2.5±0.1	13.3±0.01
cyclo-L-Trp-L-Phe	2.0±0.01	2.3±0.4	6.9±0.8
cyclo-L-Trp-L-Ala	4.4±0.1	0.8±0.01	1.7±0.1
cyclo-L-Trp-L-His	≤0.5	≤0.5	≤0.5
cyclo-L-Trp-L-Tyr	0.9±0.1	1.6±0.1	17.8±14.8
L-Trp	100.0±5.00	100.0±0.1	100.0±10.1

The enzyme assays contained 0.5 mM aromatic substrate and 1 mM DMAPP were incubated at 37 °C for 2 h with 1 µM of the purified protein of 6-DMATS$_{Mo}$, 6-DMATS$_{Sa}$ and 6-DMATS$_{Sv}$, respectively. Relative product yields were measured in duplicate on HPLC with Multospher 120 RP-18 column. The conversion yields of 6-DMATS$_{Mo}$, 6-DMATS$_{Sv}$ and 6-DMATS$_{Sa}$ with L-tryptophan at 86.6, 99.5 and 90.3 % were defined as 100 % of relative activity, respectively.

Table S4 HR-ESI-MS analysis of the enzyme products of MolI14.36 (6-DMATS$_{Mo}$).

Product	HR-ESI-MS of the prenylated products ([M+H$^+$])		
	Calculated	Measured	Deviation [ppm]
1a-C6	273.1598	273.1601	-1.1
1b-C6	273.1598	273.1590	2.9
2a-C6	287.1754	287.1775	-7.3
3a-C6	287.1754	287.1757	-1.0
4-C6	287.1754	287.1757	-1.0
5-C5, 5-C6, 5-C7	287.1754	287.1768*	-4.9
6-C6, 6-C7	287.1754	287.1766*	-4.2
7-C5, 7-C7	287.1754	287.1768*	-4.9
8-C6	287.1754	287.1762	-2.8
9a-C6	291.1503	291.1519	-5.5

*Mass obtained from a product mixture.

Table S5 ^{1}H NMR data of the enzyme products of 6-DMATS$_{Mo}$ **1a-C6**, **1b-C6**, **2a-C6**, **3a-C6**, and **4-C6** in CD_3OD

Comp	6-DMA-L-Trp (**1a-C6**)	6-DMA-D-Trp (**1b-C6**)	6-DMA-L-abrine (**2a-C6**)	6-DMA-L-β-homo-Trp (**3a-C6**)	6-DMA-α-methyl-DL–Trp (**4-C6**)
	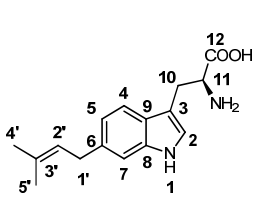	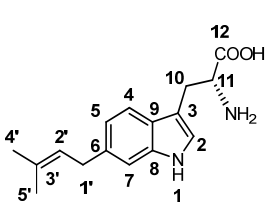	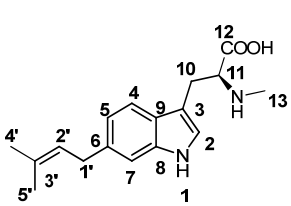	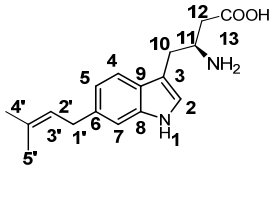	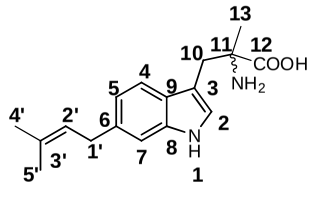
Pos.	δ_H, *multi*, *J*	δ_H, *multi*, *J*	δ_H, *multi*, *J*	δ_H, *multi*, *J*	δ_H, *multi*, *J*
2	7.12, s	7.13, s	7.14, br s	7.09, s	7.12, s
4	7.59, d, 8.2	7.57, d, 8.1	7.58, dd, 8.2, 0.8	7.49, dd, 8.2, 0.6	7.56, d, 8.2
5	6.89, dd, 8.2, 1.4	6.90, dd, 8.1	6.89, dd, 8.2, 1.5	6.89, dd ,8.2, 1.5	6.88, dd ,8.2, 1.5
7	7.15, d, 1.4	7.16, s	7.14, br s	7.15, dd, 1.5, 0.6	7.14, s
10	3.49, dd, 15.2, 4.0, 0.8	3.49, dd, 15.2, 4.8	3.42, ddd, 15.4, 4.8, 0.8	2.51, dd, 16.7, 4.0	3.12, d, 15.0
	3.12, dd, 15.2, 9.4	3.17, dd, 15.2, 9.0	3.23, ddd, 15.4, 7.8, 0.6	2.34, dd , 16.7, 8.9	3.31-3.36, m*
11	3.84, dd, 9.4, 4.0	3.95, m	3.71, dd, 7.8, 4.8	3.46-3.50, m	-
12	-	-	-	3.02, d, 7.1	-
13	-	-	2.66, s	-	1.51, s
1′	3.41, d, 7.3	3.41, d, 7.3	3.41, d, 7.4	3.42, d, 7.3	3.41, d, 7.4
2′	5.35, tsept, 7.3, 1.4	5.35, tsept, 7.3, 1.4	5.34, tsept, 7.4, 1.5	5.36, tsept, 7.3, 1.5	5.36, tsept, 7.4, 1.5
4′	1.74, br s	1.75, br s	1.74, s	1.75, s	1.75, br s
5′	1.74, br s	1.75, br s	1.74, s	1.75, s	1.75, br s

Chemical shifts (δ) are given in ppm and coupling constants (*J*) in Hz. *Signals are overlaying with solvent signal.

Table S6 ^{1}H NMR data of the enzyme products of 6-DMATS$_{Mo}$ **5-C5** - **5-C7**, **6-C6** and **6-C7** in CD_3OD

Comp.	5-DMA-4-methyl-DL-Trp (**5-C5**)	6-DMA-4-methyl-DL-Trp (**5-C6**)	7-DMA-4-methyl-DL-Trp (**5-C7**)	6-DMA-5-methyl-DL-Trp (**6-C6**)	7-DMA-5-methyl-DL-Trp (**6-C7**)
	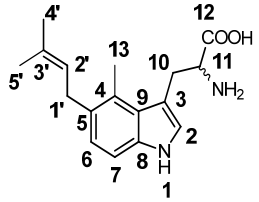	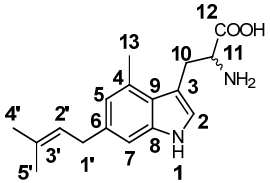	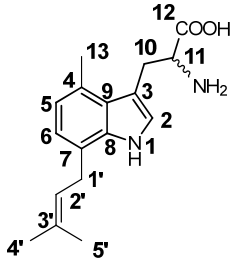	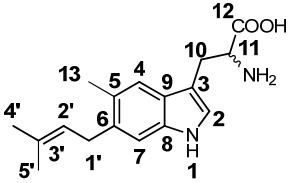	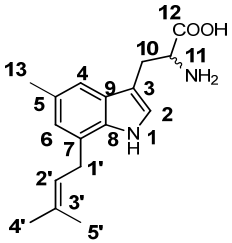
Pos.	δ_H, *multi*, *J*	δ_H, *multi*, *J*	δ_H, *multi*, *J*	δ_H, *multi*, *J*	δ_H, *multi*, *J*
2	7.09, s	7.06, s	7.15, s	7.08, s	7.15, s
4	-	-	-	7.47, s	7.35, s
5	-	6.96, s	6.76, d, 7.3	-	-
6	6.90, d, 8.2	-	6.69, d, 7.3	-	6.76, s
7	7.10, d, 8.2	6.60, s	-	7.14, s	-
10	3.53-3.61, m	3.73, m	3.53-3.61, m	3.47, dd, 15.1, 3.8	3.56-3.59, m
	3.02-3.12, m	3.05, dd, 16.0, 11.1	3.02-3.12, m	3.07, dd, 15.1, 9.6	3.07, m
11	3.74-3.82, m	3.73, m	3.74-3.82, m	3.83, dd, 9.6, 3.8	3.5-3.54, m
13	2.58, s	2.69, s	2.70, s	2.36, s	2.40, s
1´	3.30-3.36*	3.34, d, 7.4	3.39, d, 7.1	3.37, d, 7.1	3.35-3.37, m
2´	5.20, tsept, 7.0, 1.5	5.33, tsept, 7.4, 1.5	5.40, tsept, 7.1, 1.5	5.25, tsept, 7.1, 1.6	5.41, m
4´	1.74, br s	1.74, br s	1.74, br s	1.75, s	1.75, s
5´	1.74, br s	1.74, br s	1.74, br s	1.74, s	1.74, s

Chemical shifts (δ) are given in ppm and coupling constants (*J*) in Hz.*Signals are overlaying with solvent signal.

Table S7 ^{1}H NMR data of the enzyme products of 6-DMATS$_{Mo}$ **7-C5**, **7-C7**, **8-C6** and **9a-C6** in CD_3OD.

Comp	5-DMA-6-methyl-DL-Trp (**7-C5**) 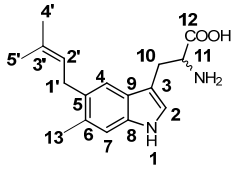	7-DMA-6-methyl-DL-Trp (**7-C7**) 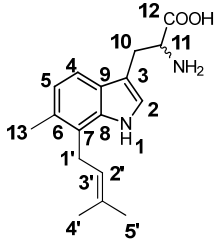	6-DMA-7-methyl-DL-Trp (**8-C6**) 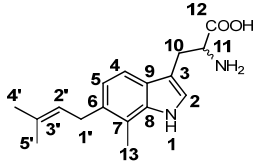	6-DMA-5-Fluoro-L-Trp (**9a-C6**) 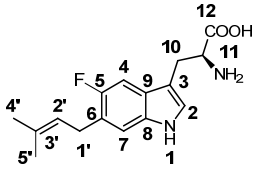
Pos.	$\delta_{H,}$ *multi,* J	$\delta_{H,}$ *multi,* J	$\delta_{H,}$ *multi,* J	$\delta_{H,}$ *multi,* J
2	7.14, s	7.13, s	7.14, s	7.17, s
4	7.45, s	7.43, d ,8.2	7.44, d, 8.0	7.36, d, 11.0
5	-	6.89, d, 8.2	6.88, d, 8.0	-
6	-	-	-	-
7	7.07, s	-	-	7.15, d, 6.4
10	3.48-3.52, m	3.48, dd, 15.3, 4.0	3.46-3.64, m	3.39-3.43, m
	3.03-3.09, m	3.10, dd, 15.3, 9.5	3.09, dd, 15.3, 9.4	3.12, dd, 15.3, 9.1
11	3.83, dd, 9.8, 3.9	3.83, dd, 9.5, 4.0	3.81, dd, 9.4, 4.0	3.81, dd, 9.1, 3.9
13	2.34, s	2.34, s	2.39, s	-
1′	3.42, d,7.1	3.56, d, 6.7	3.42, d, 7.2	3.40, d, 7.5
2′	5.24, m	5.09, tsept, 6.7, 1.4	5.20, m	5.32, m
4′	1.78, s	1.83, s	1.77, s	1,74, s
5′	1.73, s	1.68, s	1.71, s	1.73, s

Chemical shifts (δ) are given in ppm and coupling constants (J) in Hz

Table S8 ^{1}H NMR data of the enzyme products of 5-DMATS$_{Sc}$ **1b-C5**, **1b-C7**, **1a-C5,C6**, **1a-C5,C7**, and **1b-C5,C6** in CD_3OD

Comp	5-DMA-D-Trp (**1b-C5**)	7-DMA-D-Trp (**1b-C7**)	5,6-di-DMA-L-Trp (**1a-C5,C6**)	5,7-di-DMA-L-Trp (**1a-C5,C7**)	5,6-di-DMA-D-Trp (**1b-C5,C6**)
Pos.	δ_H, *multi*, *J*	δ_H, *multi*, *J*	δ_H, *multi*, *J*	δ_H, *multi*, *J*	δ_H, *multi*, *J*
2	7.14, br s	7.19, s	7.08, s	7.15, s	7.10, s
4	7.49, s	7.53, d, 7.1	7.45, s	7.33, br s	7.45, s
5	-	6.98, t, 7.8	-	-	-
6	6.95, dd, 8.5, 1.7	6.91, dd, 7.3	-	6.75, br s	-
7	7.26, d, 8.5	-	7.14, s	-	7.15, s
10	3.50, dd, 15.3, 4.2	3.56, m	3.48, m[a]	3.48, m [a]	3.49, dd, 15.2, 3.9
	3.08, m	3.13, m	3.06, dd, 15.3, 9.6 [b]	3.07, dd, 15.3, 9.6 [b]	3.09, dd, 15.2, 9.6
11	3.84, m	3.81-3.86, m	3.82, dd, 9.6, 4.4	3.82, dd, 9.6, 4.4	3.86, dd, 9.6, 3.9
1′	3.42, m	3.54, d, 7.3	3.42, d, 6.8 [c]	3.39, m [c]	3.42, d, 6.7 [g]
2′	5.38, m	5.42, m	5.25, t, 6.8 [d]	5.36, t, 7.3 [f]	5.24, t, 6.7 [h]
4′	1.73-1.76, m	1.73-1.76, m	1.74, s [e]	1.75, s [e]	1.74, s [i]
5′	1.73-1.76, m	1.73-1.76, m	1.71, s [e]	1.75, s [e]	1.71, s [i]
1”	-	-	3.39, m [c]	3.39, m [c]	3.38, d, 6.8 [g]
2”	-	-	5.27, t, 7.0 [d]	5.41, t, 7.0 [f]	5.25, t, 6.8 [h]
4”	-	-	1.75, s [e]	1.75, s [e]	1.74, s [i]
5”	-	-	1.73, s [e]	1.75, s [e]	1.72, s [i]

Chemical shifts (δ) are given in ppm and coupling constants (*J*) in Hz. Signals with the same letters are interchangeable.

Table S9 Conditions for enzyme assays to identify enzyme products of DMATSs.

Substrate	Protein amount of DMATS	Incubation time
1 mM **1a**	0.5 μM FgaPT2 8.5 μM 5-DMATS 1.4 μM 5-DMATS$_{Sc}$ 1.2 μM 6-DMATS$_{Sa}$ 3.1 μM 6-DMATS$_{Sv}$ 4.0 μM 6-DMATS$_{Mo}$ 0.6 μM 7-DMATS	2 h
1 mM **1b**	2.0 μM FgaPT2, 5-DMATS, 5-DMATS$_{Sc}$, 6-DMATS$_{Sa}$, 6-DMATS$_{Sv}$, 6-DMATS$_{Mo}$, 7-DMATS	4 h
0.5 mM **6a**	2.7 μM FgaPT2 3.0 μM 5-DMATS 3.5 μM 5-DMATS$_{Sc}$ 3.7 μM 6-DMATS$_{Sa}$ 3.5 μM 6-DMATS$_{Sv}$ 3.5 μM 6-DMATS$_{Mo}$ 2.8 μM 7-DMATS	16 h
0.5 mM **6b**	3.5 μM 5-DMATS$_{Sc}$ 3.7 μM 6-DMATS$_{Sa}$ 3.5 μM 6-DMATS$_{Sv}$ 3.5 μM 6-DMATS$_{Mo}$ 2.8 μM 7-DMATS	
0.5 mM, **7a**	2.7 μM FgaPT2 3.0 μM 5-DMATS 3.5 μM 5-DMATS$_{Sc}$ 3.5 μM 6-DMATS$_{Sv}$ 3.5 μM 6-DMATS$_{Mo}$ 2.8 μM 7-DMATS	
0.5 mM, **7b**	3.0 μM 5-DMATS 3.5 μM 5-DMATS$_{Sc}$ 3.5 μM 6-DMATS$_{Mo}$	
0.5 mM, **8a**	2.7 μM FgaPT2 3.0 μM 5-DMATS 3.5 μM 5-DMATS$_{Sc}$ 3.5 μM 6-DMATS$_{Sv}$ 3.5 μM 6-DMATS$_{Mo}$	
0.5 mM, **8b**	3.0 μM 5-DMATS 3.5 μM 5-DMATS$_{Sc}$ 3.5 μM 6-DMATS$_{Mo}$	

Enzyme assays of 100μl contained 1 mM DMAPP and 5 mM $CaCl_2$.

Table S10 ^{1}H NMR data of the enzyme products of 5-DMATS$_{Sc}$ **6b-C6** and **6b-C7** in CD_3OD.

Comp	6-DMA-5-methyl-D-Trp (**6b-C6**)	7-DMA-5-methyl-D-Trp (**6b-C7**)
	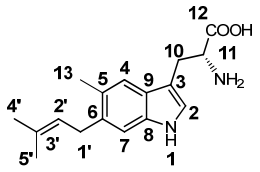	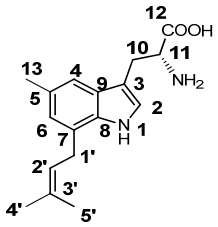
Pos.	δ_H, *multi*, *J*	δ_H, *multi*, *J*
2	7.07, s	7.14, s
4	7.47, s	7.34, s
5	-	-
6	-	6.75, s
7	7.13, s	-
10	3.4, dd, 14.9, 3.3 3.08, dd, 14.9, 9.7	3.47-3.52, m 3.08, m
11	3.83, dd, 9.7, 3.3	3.51-3.54, m
13	2.36, s	2.39, s
1′	3.36, d, 7.2	3.38, m
2′	5.25, tsept, 7.2, 1.6	5.34, m
4′	1.74, s	1.74, s
5′	1.73, s	1.73, s

Chemical shifts (δ) are given in ppm and coupling constants (*J*) in Hz.

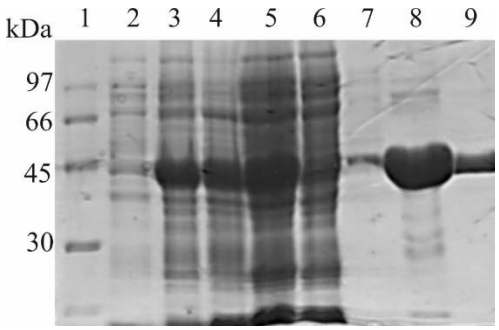

Fig. S1: SDS-PAGE analysis of 6-DMATS$_{Mo}$ from *M. olivasterospora*. Proteins were separated on a 12 % SDS gel and stained with Coomassie Brilliant Blue G-250. Lane 1: molecular mass standard; Lane 2: total protein before IPTG induction; lane 3: total protein after IPTG induction; lane 4: insoluble protein fraction; lane 5: soluble protein fraction; lane 6: flow through fraction; lane 7: wash fraction of Ni-NTA-agarose; lanes 8 and 9: purified His$_8$-tagged recombinant protein.

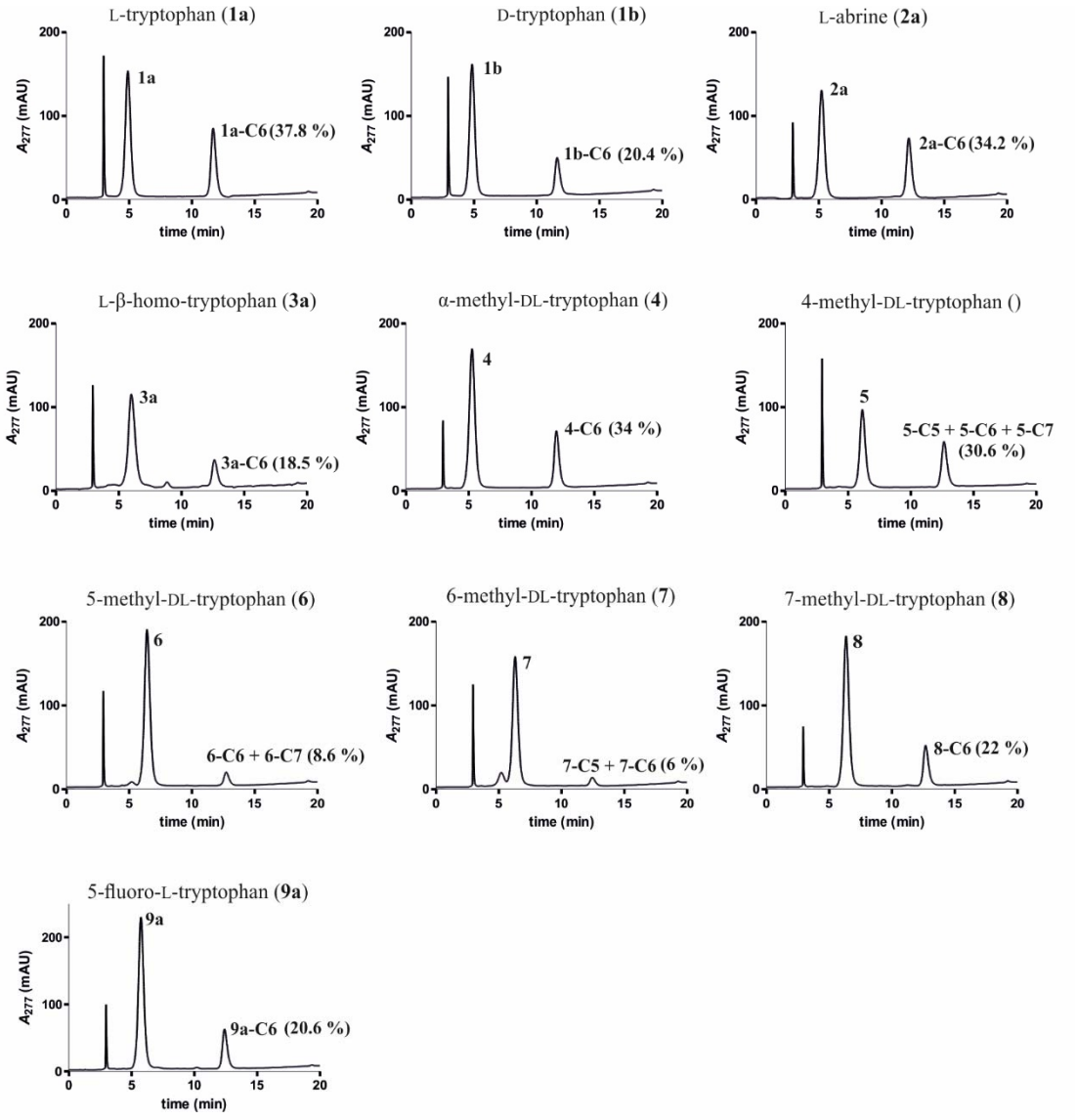

Fig. S2: HPLC analysis of the reaction mixtures of 6-DMATS$_{Mo}$ with L-tryptophan and analogs. For conditions see legends of Table S2. A Multospher 120 RP-18 column was used and an absorption at 277 nm was illustrated. Product yields are given in parentheses after product numbers.

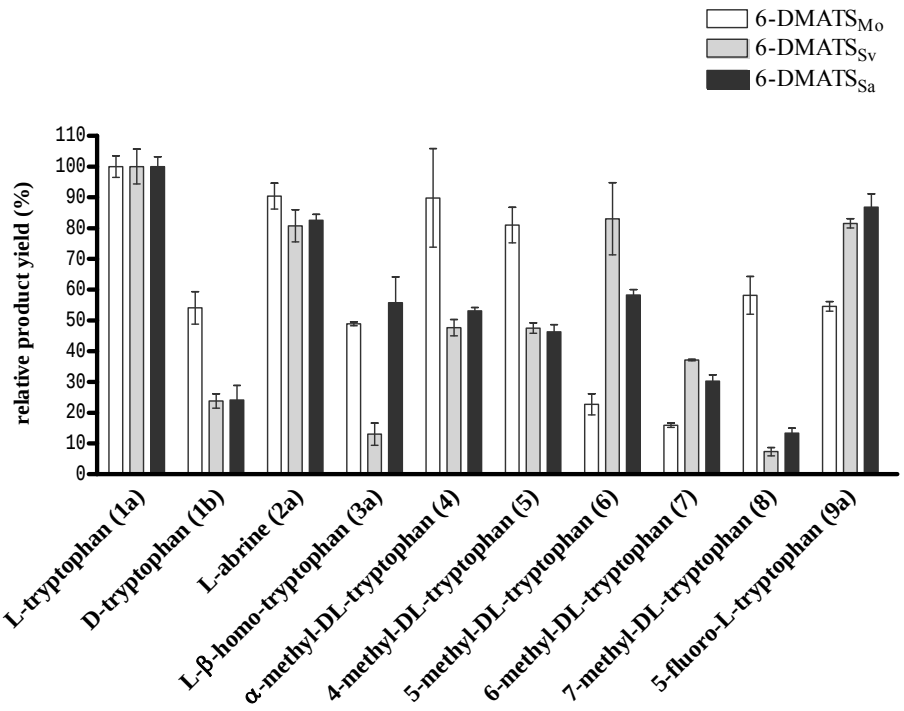

Fig. S3: Comparison of the substrate preferences of 6-DMATS$_{Mo}$, 6-DMATS$_{Sa}$, and 6-DMATS$_{Sv}$ towards tryptophan and analogs. The reaction mixtures contained 0.5 mM aromatic substrate and 1 mM DMAPP were incubated with 1 µM 6-DMATS$_{Mo}$, 6-DMATS$_{Sa}$, or 6-DMATS$_{Sv}$ at 37 °C for 1 h. Relative product yields were measured in duplicate on HPLC with Multospher 120 RP-18 column.

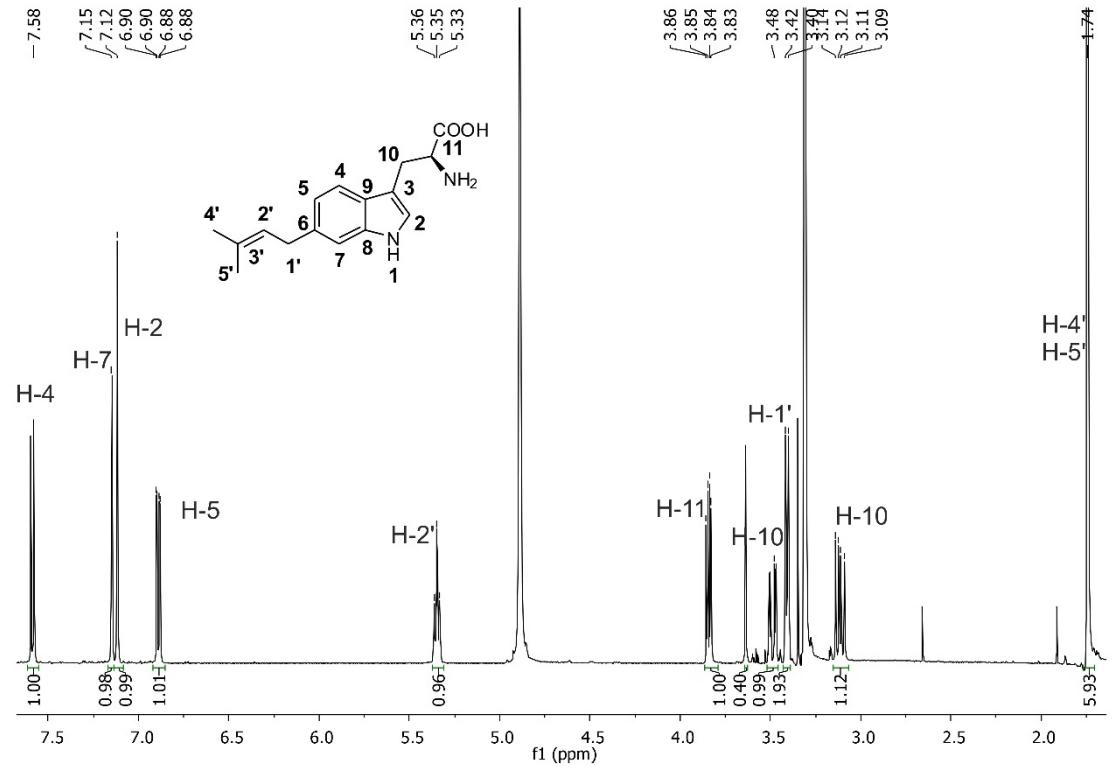

Fig. S4 ^{1}H NMR spectrum of **1a-C6** in CD_3OD (500MHz)

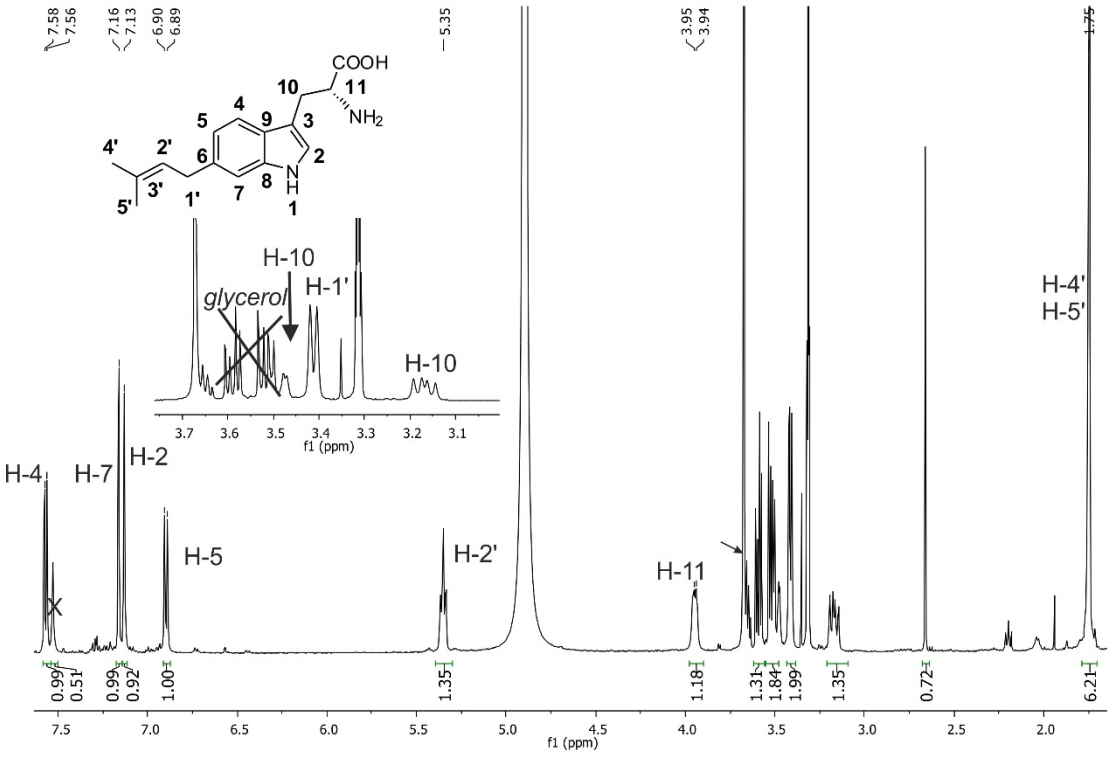

Fig. S5 ^{1}H NMR spectrum of **1b-C6** in CD_3OD (500MHz)

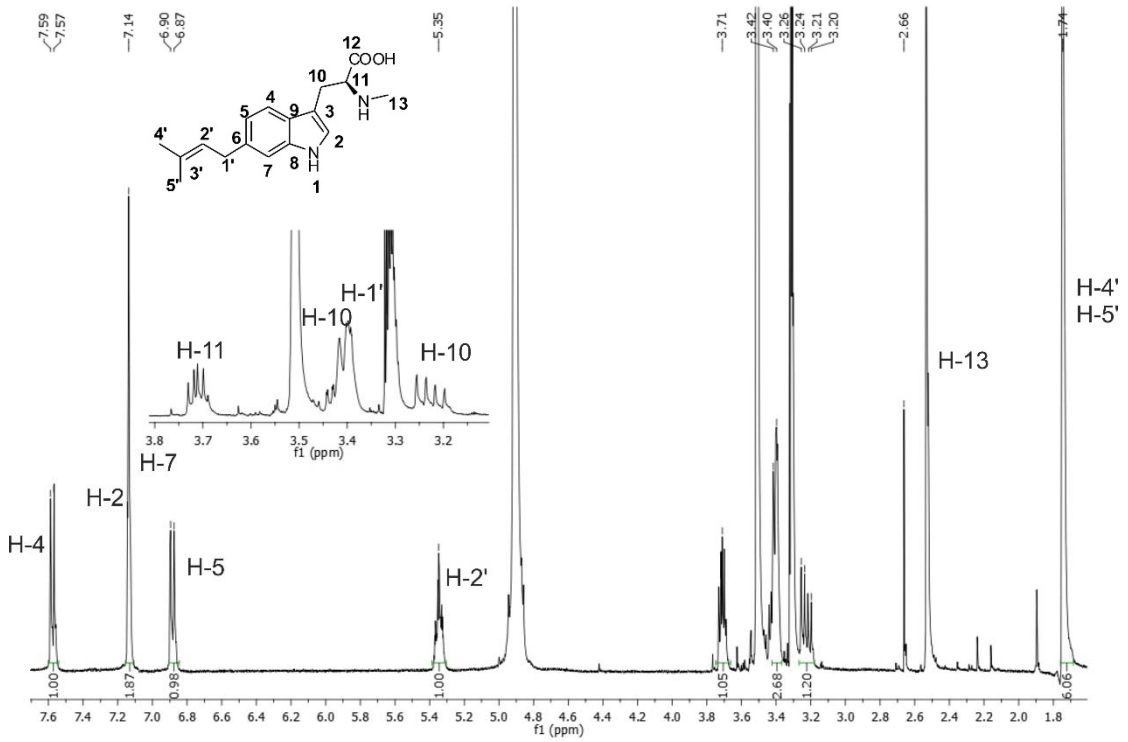

Fig. S6 ^{1}H NMR spectrum of **2a-C6** in CD_3OD (400MHz)

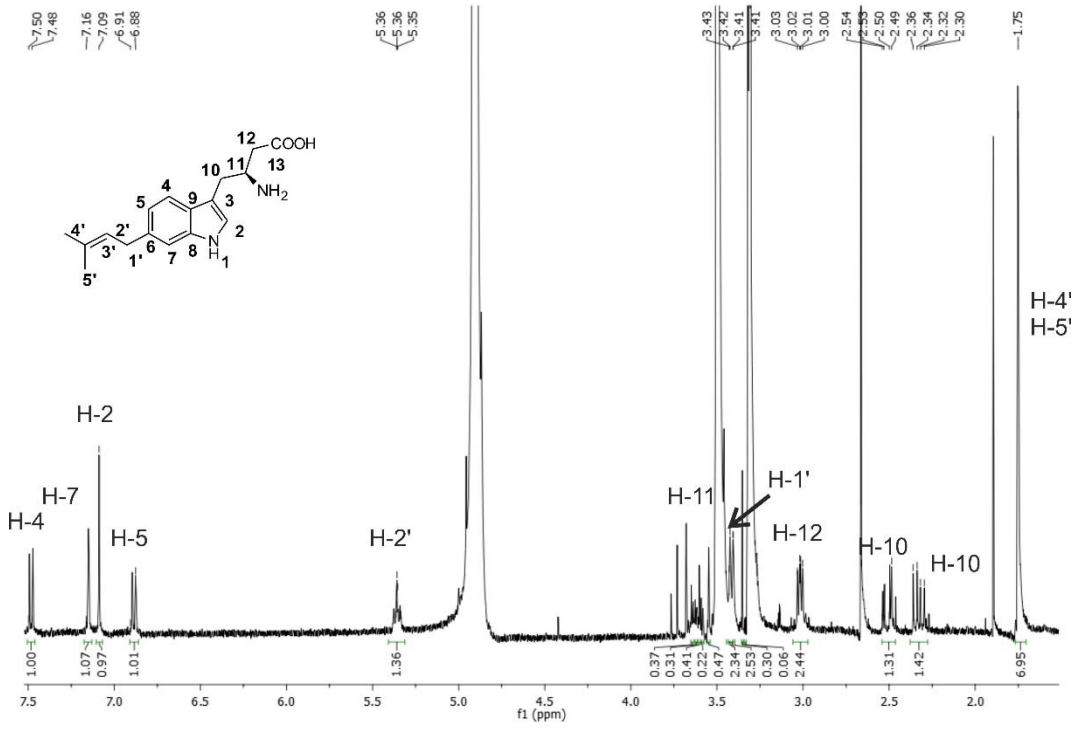

Fig. S7 ^{1}H NMR spectrum of **3a-C6** in CD_3OD (400MHz)

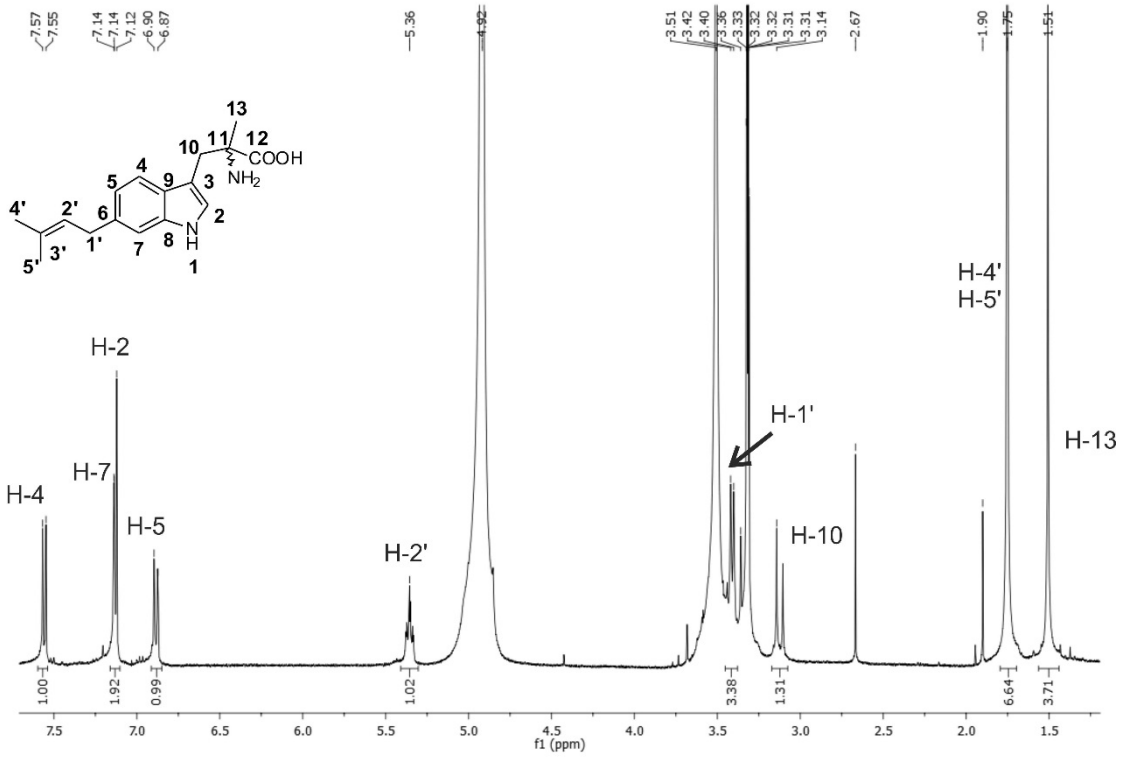

Fig. S8 ^{1}H NMR spectrum of **4-C6** in CD_3OD (400MHz)

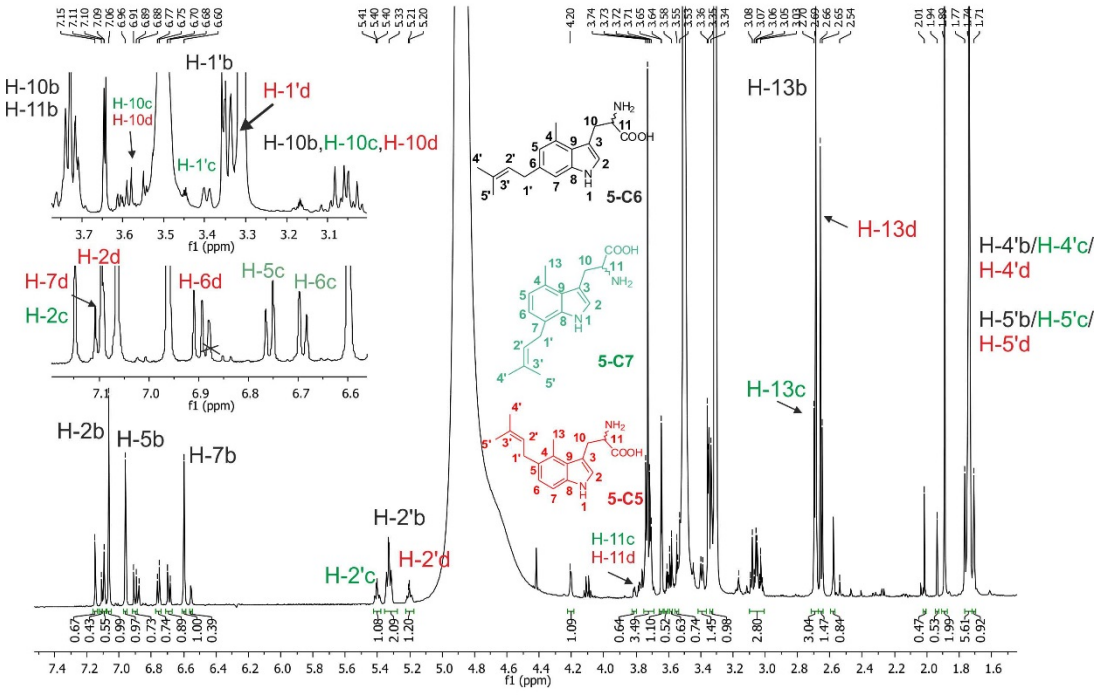

Fig. S9 ^{1}H NMR spectrum of **5-C5**, **5-C6**, and **5-C7** as a mixture in CD_3OD (500MHz)

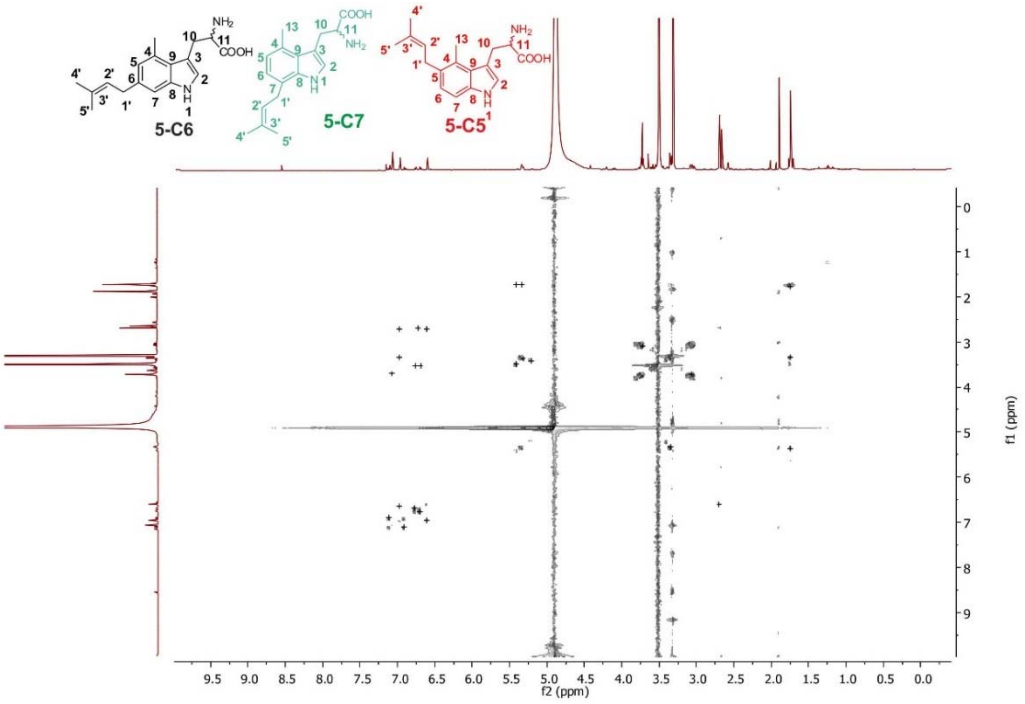

Fig. S10 ^{1}H-^{1}H COSY spectrum of **5-C5, 5-C6,** and **5-C7** as a mixture in CD_3OD (500MHz) (1)

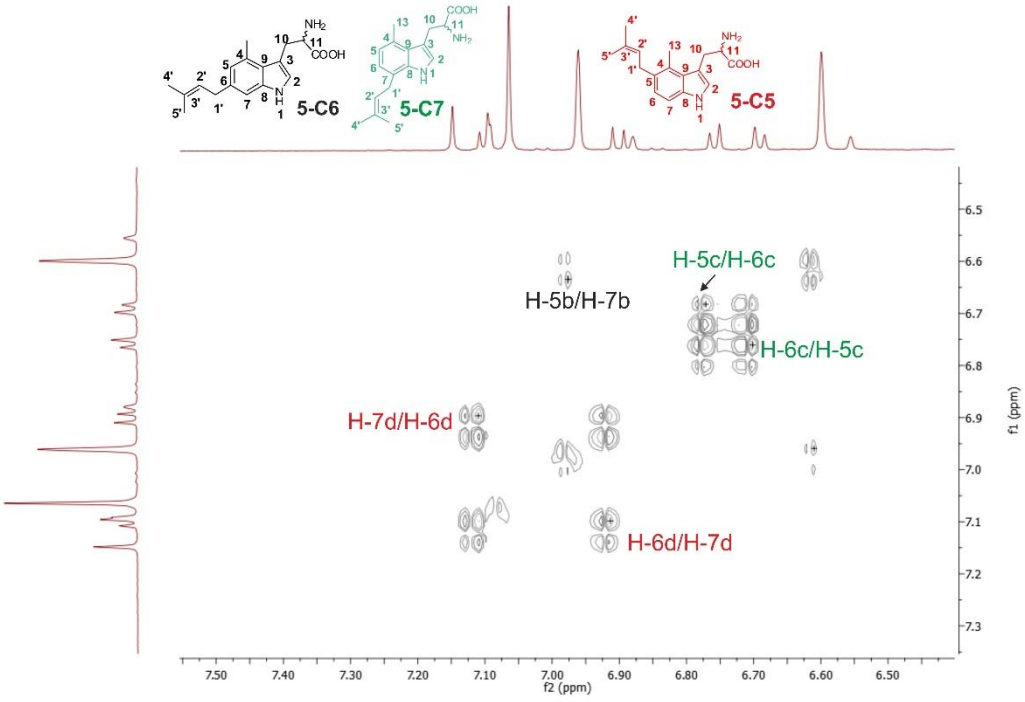

Fig. S11 ^{1}H-^{1}H COSY spectrum of **5-C5, 5-C6,** and **5-C7** as a mixture in CD_3OD (500MHz) (2)

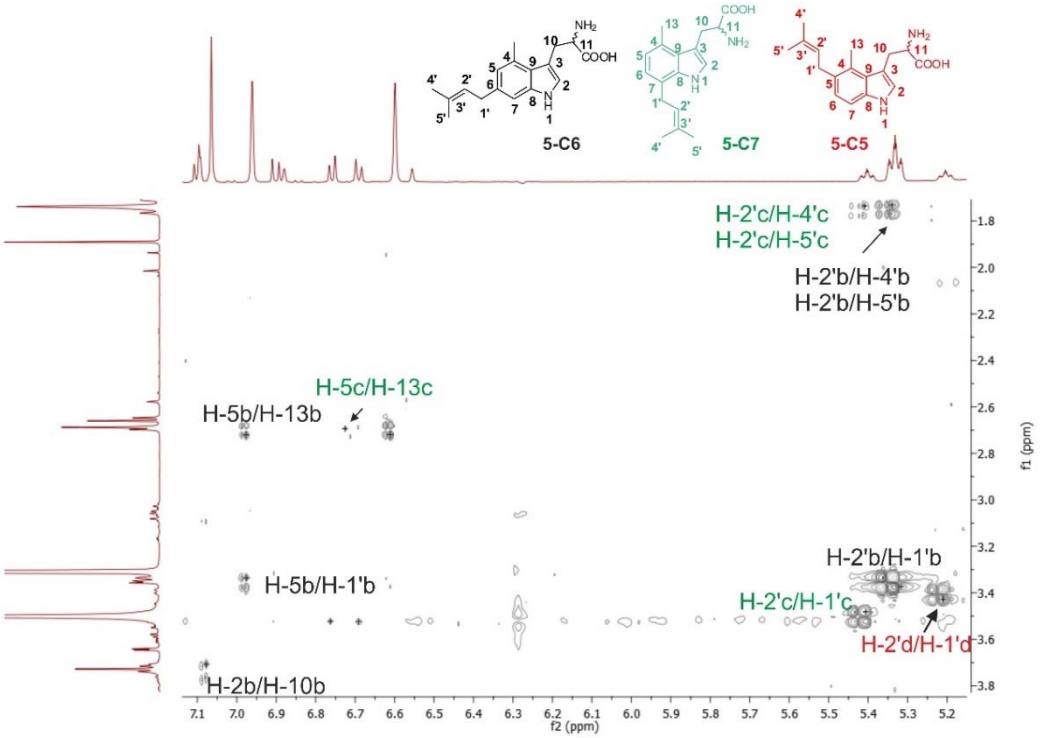

Fig. S12 ^{1}H-^{1}H COSY spectrum of **5-C5**, **5-C6**, and **5-C7** as a mixture in CD_3OD (500MHz) (3)

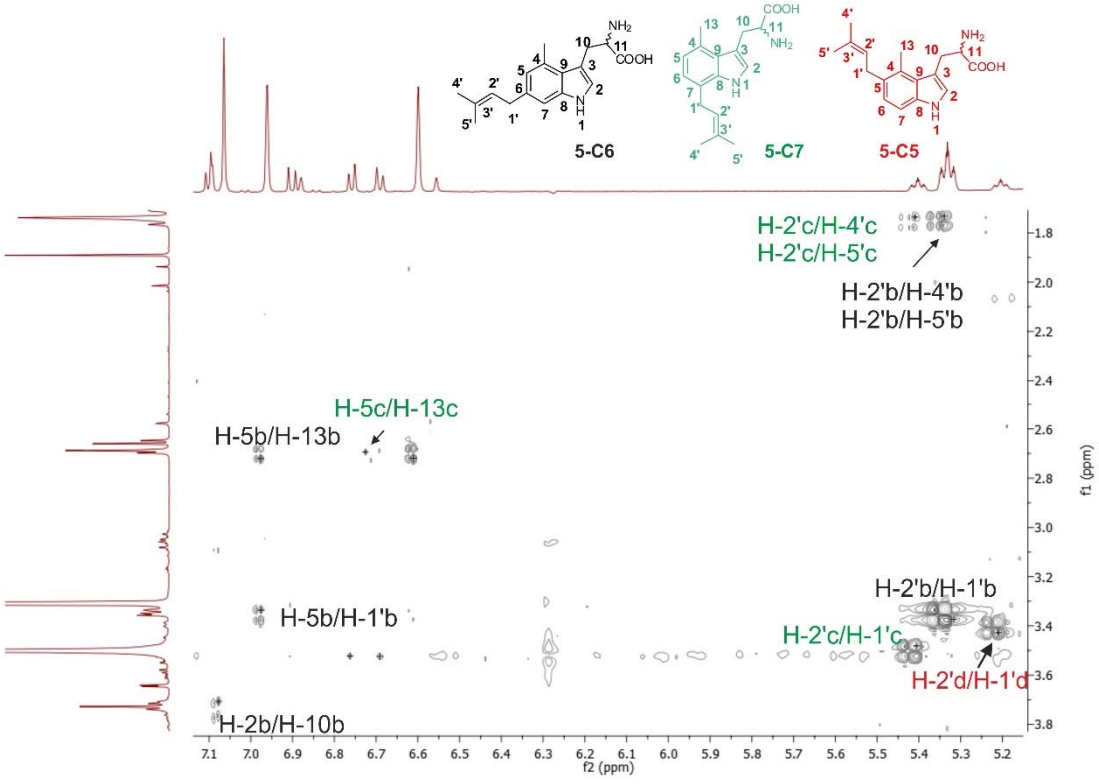

Fig. S13 ^{1}H-^{1}H COSY spectrum of **5-C5, 5-C6,** and **5-C7** as a mixture in CD_3OD (500MHz) (4)

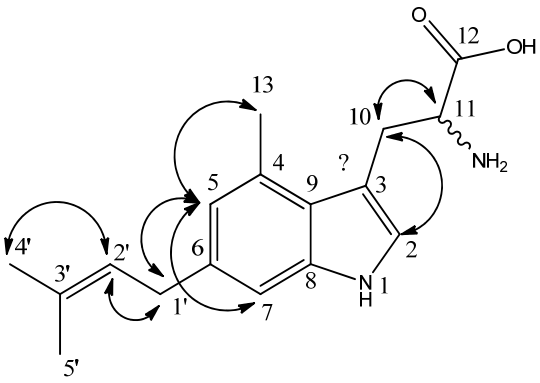

Fig. S14 Selected ^{1}H-^{1}H COSY connectivities of **5-C6**

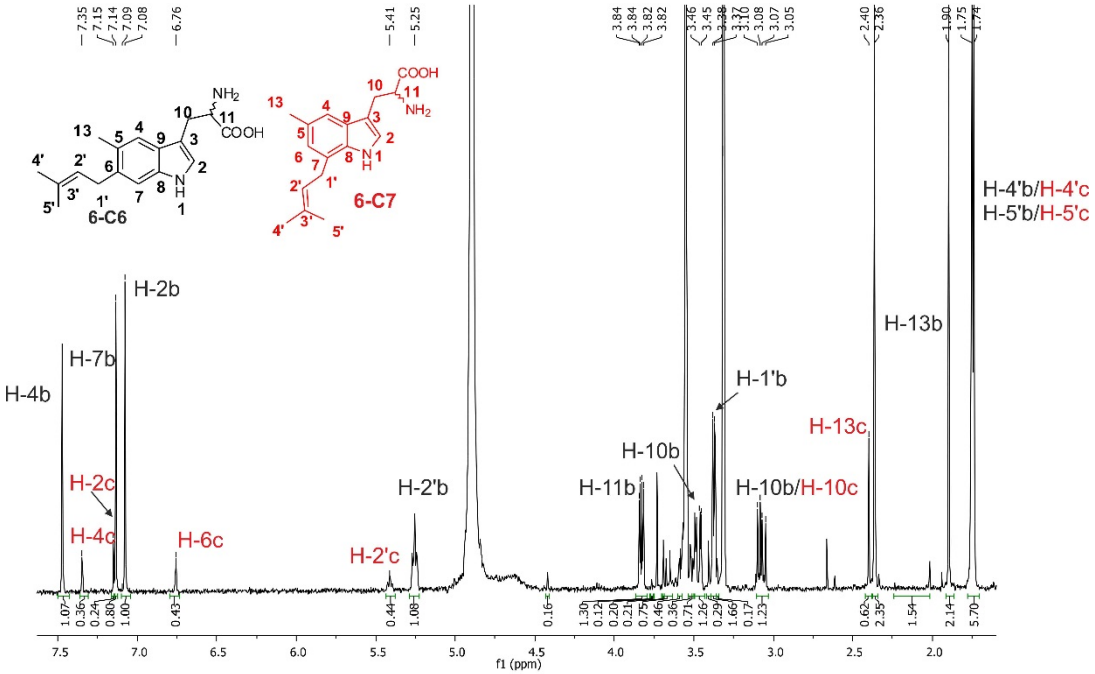

Fig. S15 ^{1}H NMR spectrum of the mixture of **6-C6** and **6-C7** in CD_3OD (500MHz)

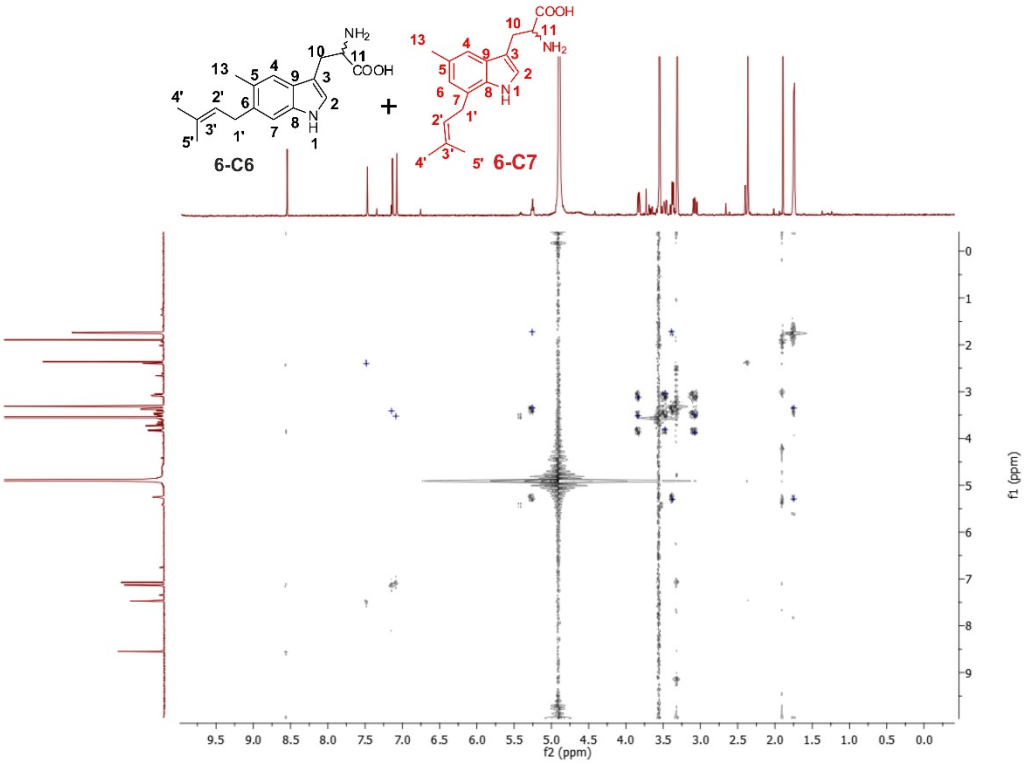

Fig. S16 ^{1}H-^{1}H COSY spectrum of the mixture of **6-C6** and **6-C7** in CD_3OD (500MHz) (1)

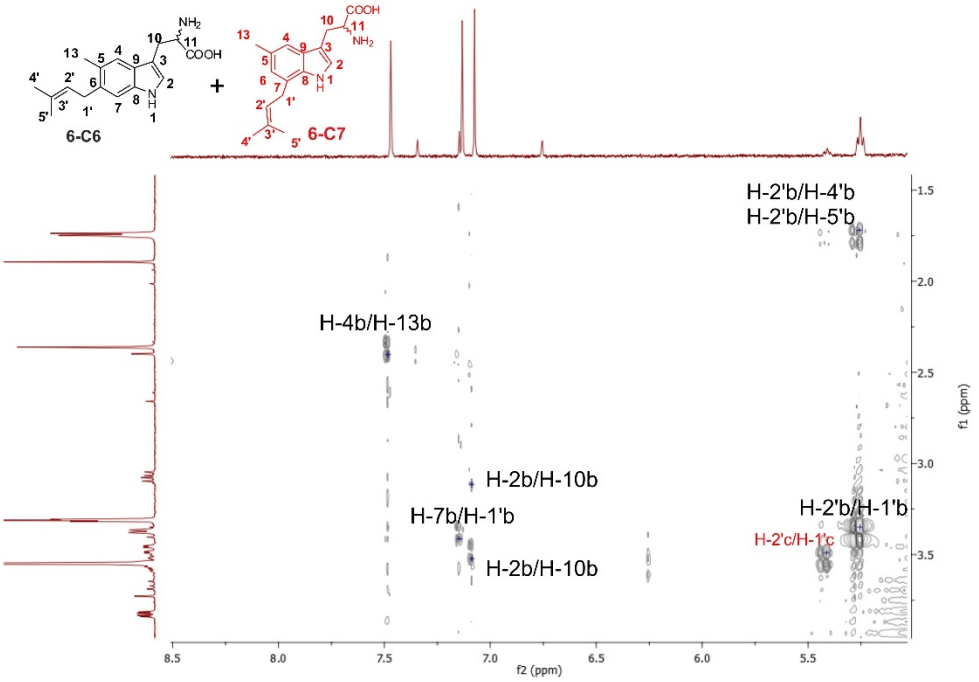

Fig. S17 ^{1}H-^{1}H COSY spectrum of the mixture of **6-C6** and **6-C7** in CD_3OD (500MHz) (2)

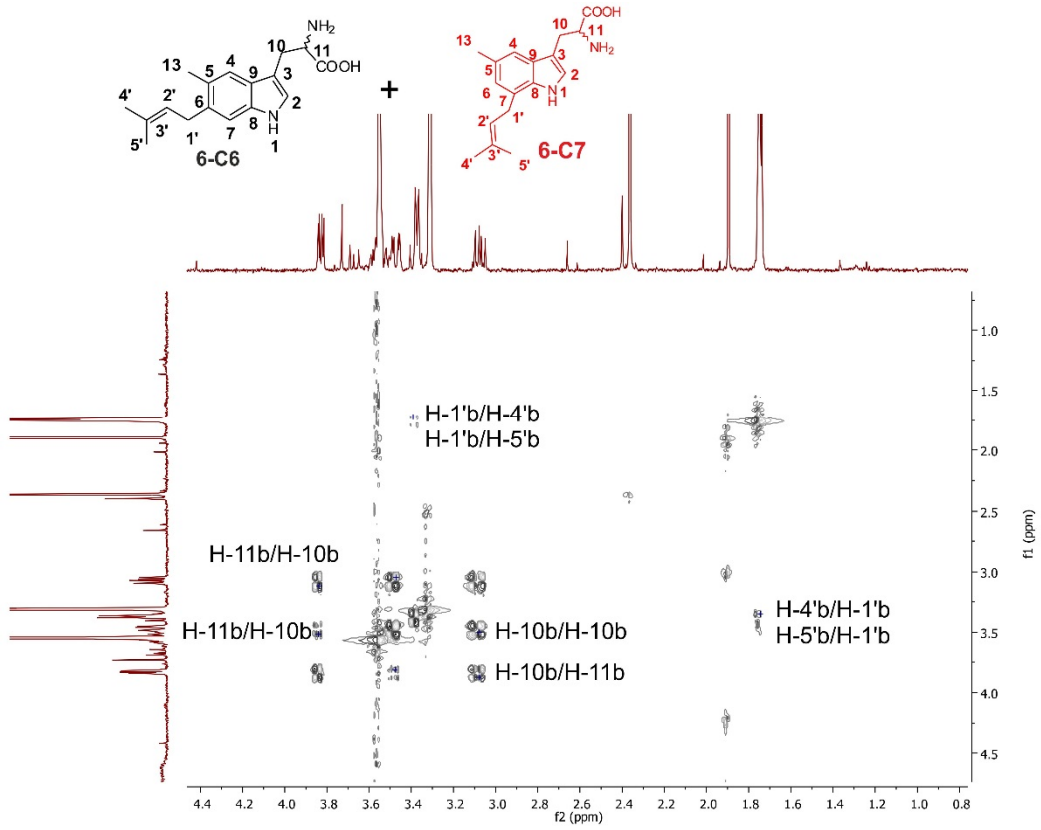

Fig. S18 ^{1}H-^{1}H COSY spectrum of the mixture of **6-C6** and **6-C7** in CD_3OD (500MHz) (3)

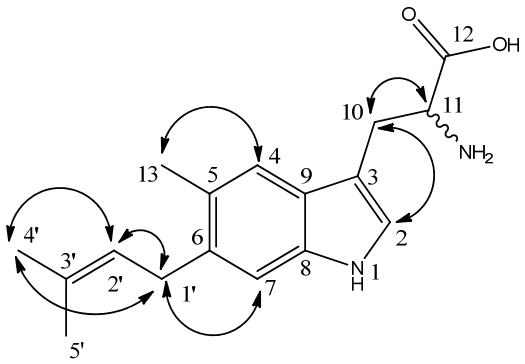

Fig. S19 Selected ^{1}H-^{1}H COSY connectivities of **6-C6**

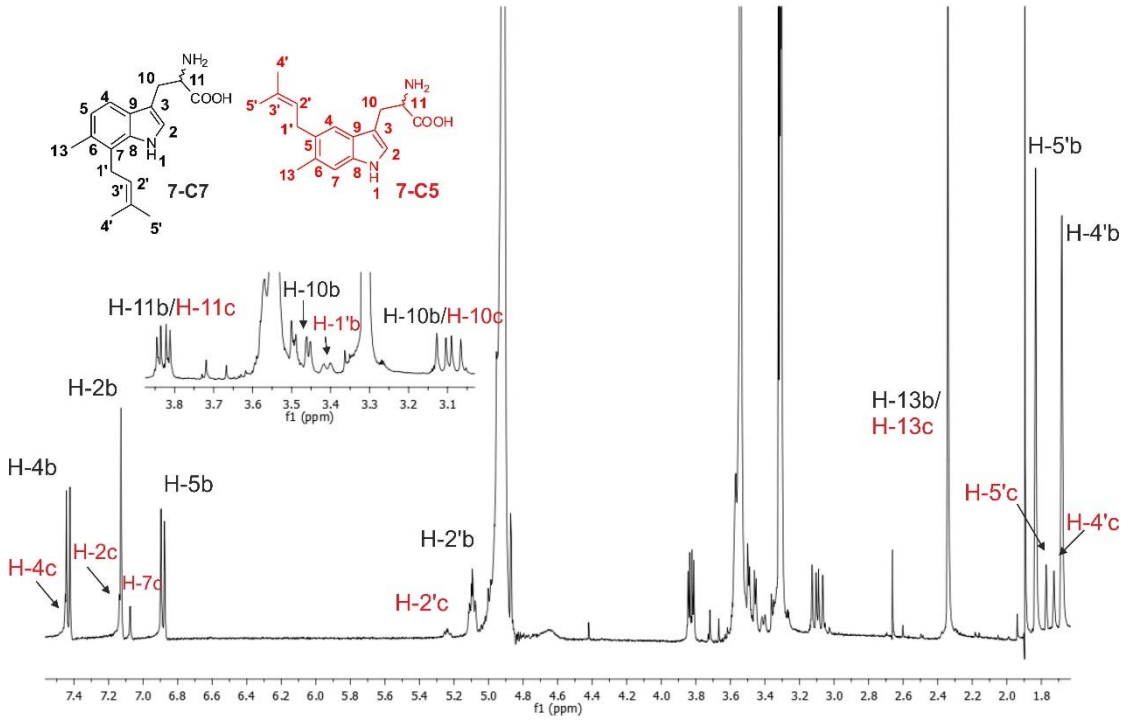

Fig. S20 ^{1}H NMR spectrum of the mixture of **7-C5** and **7-C7** in CD_3OD (400MHz)

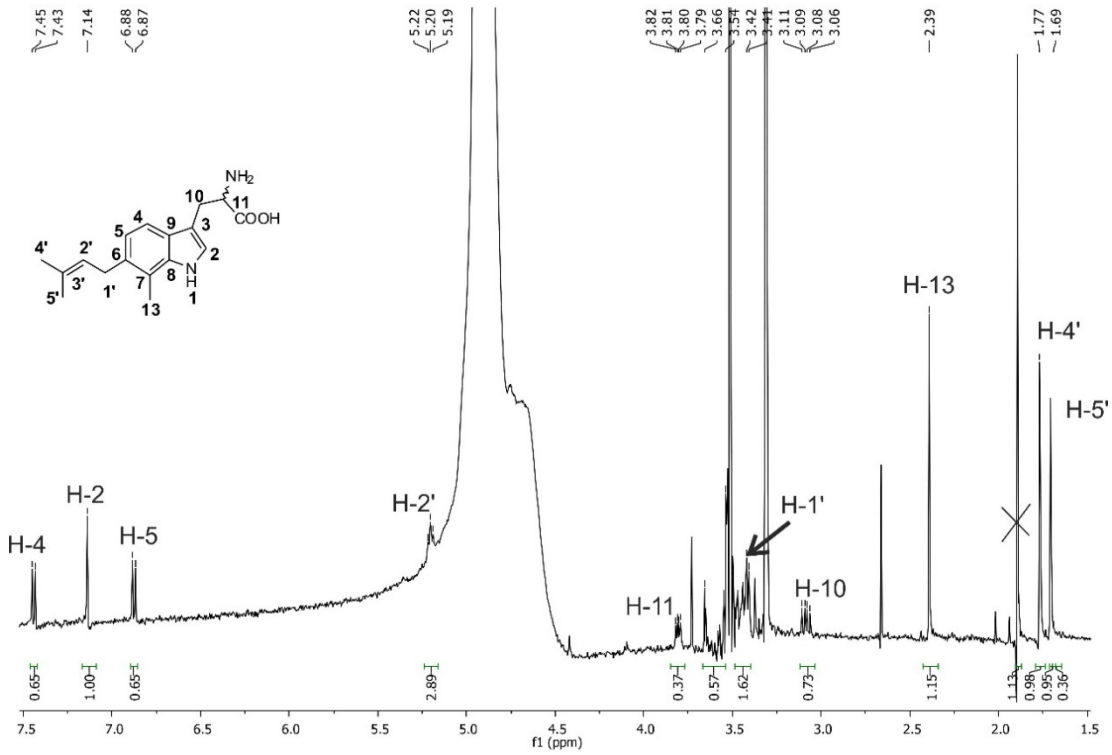

Fig. S21 ^{1}H NMR spectrum of **8-C6** in CD_3OD (500MHz)

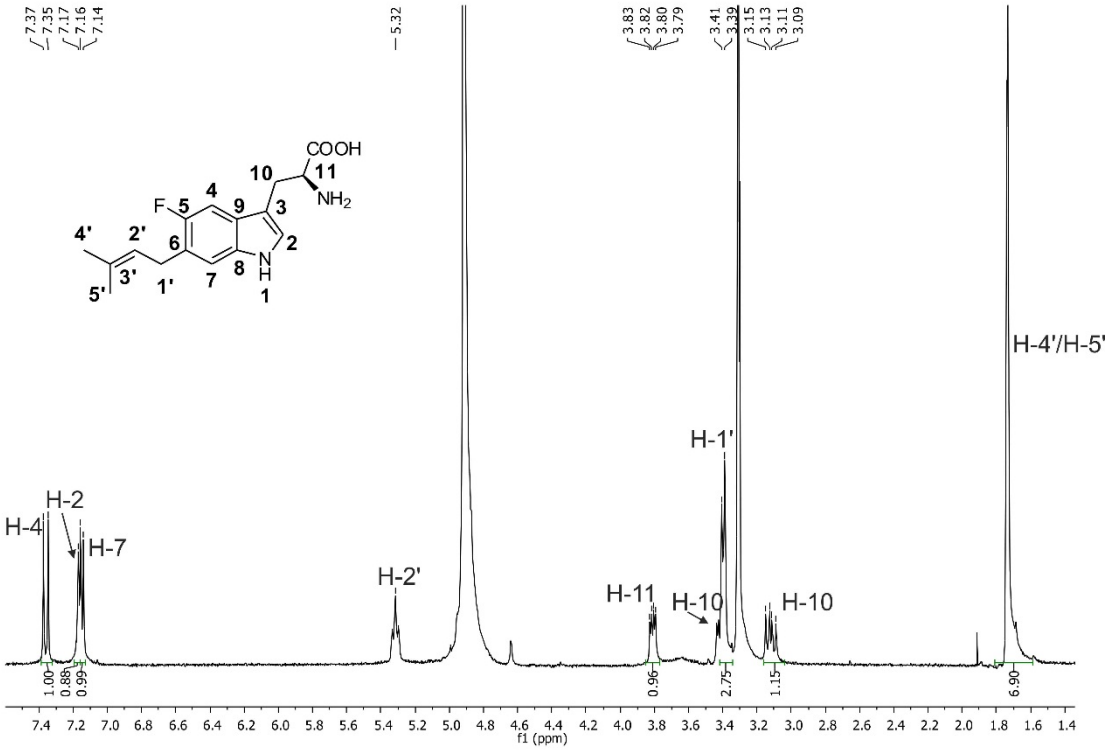

Fig. S22 ^{1}H NMR spectrum of **9a-C6** in CD_3OD (400MHz)

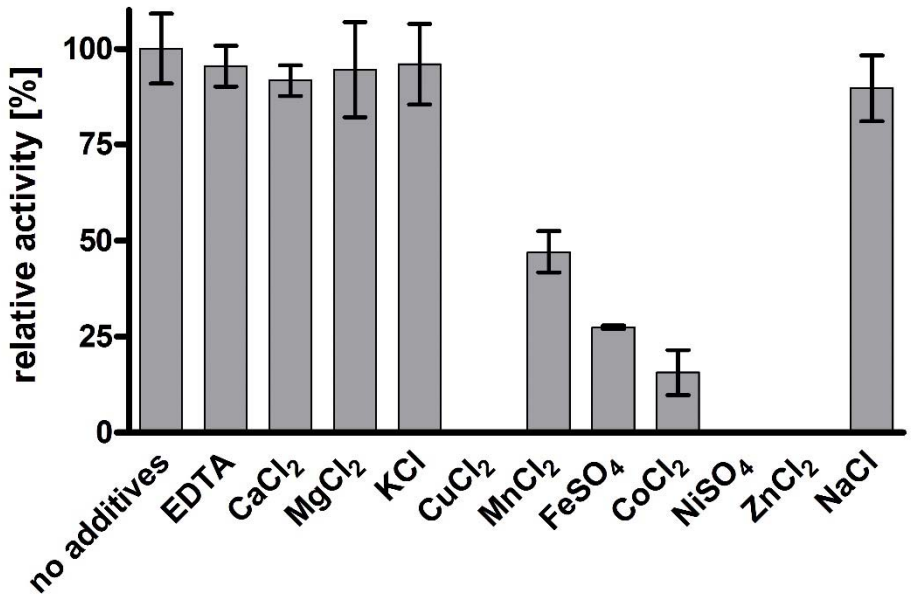

Fig. S23 Ion dependency of the 6-DMATS$_{Mo}$ reaction.
The enzyme assays containing 1 mM L-tryptophan, 1 mM DMAPP, 5 mM metal ions and were incubated with 1 µM of the recombinant protein for 1.5 h. The enzyme activity without additives was defined as 100 %.

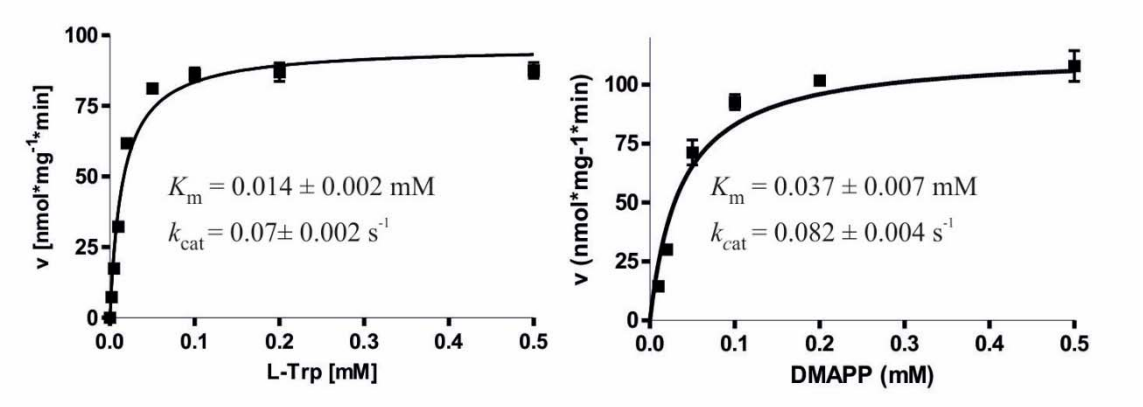

Fig. S24 Determination of the kinetic parameters of 6-DMATS$_{Mo}$ towards L-tryptophan and DMAPP. Reaction mixtures contained 229.9 nM 6-DMATS$_{Mo}$, 5 mM $MgCl_2$ and were incubated for 30 min at 37 °C. 1 mM L-tryptophan and 1 mM DMAPP were used for determination of the kinetic parameters of DMAPP and L-tryptophan, respectively.

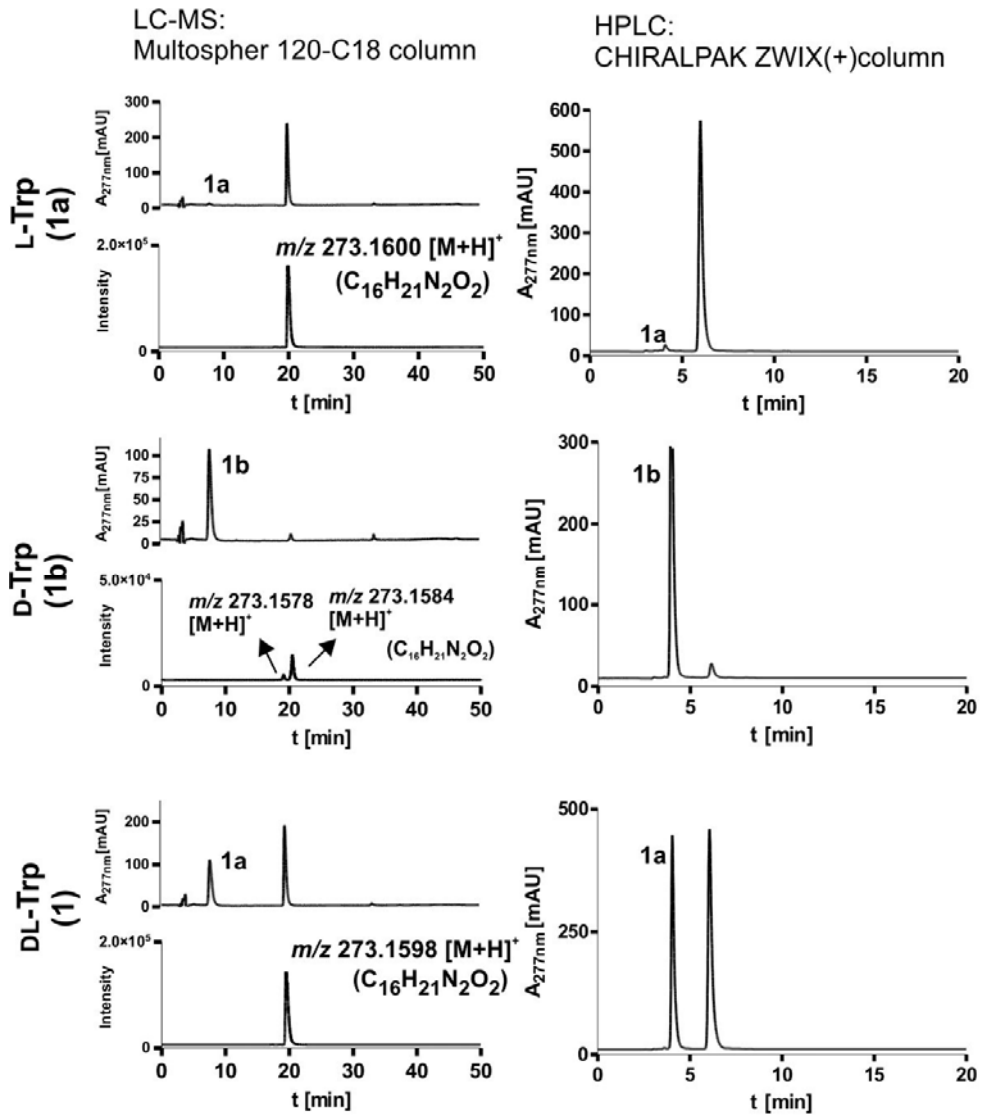

Fig. S25 LC-MS and HPLC analyses of the enzyme assays of tryptophan with FgaPT2. The enzyme assays contained 1 mM DMAPP, 1 µM purified protein, and 0.5 mM of L- or D-isomer, or 1 mM of their racemate and were incubated at 37 °C for 1.5 h. UV-detection was carried out on a Diode Array detector and illustrated for absorption at 277 nm.

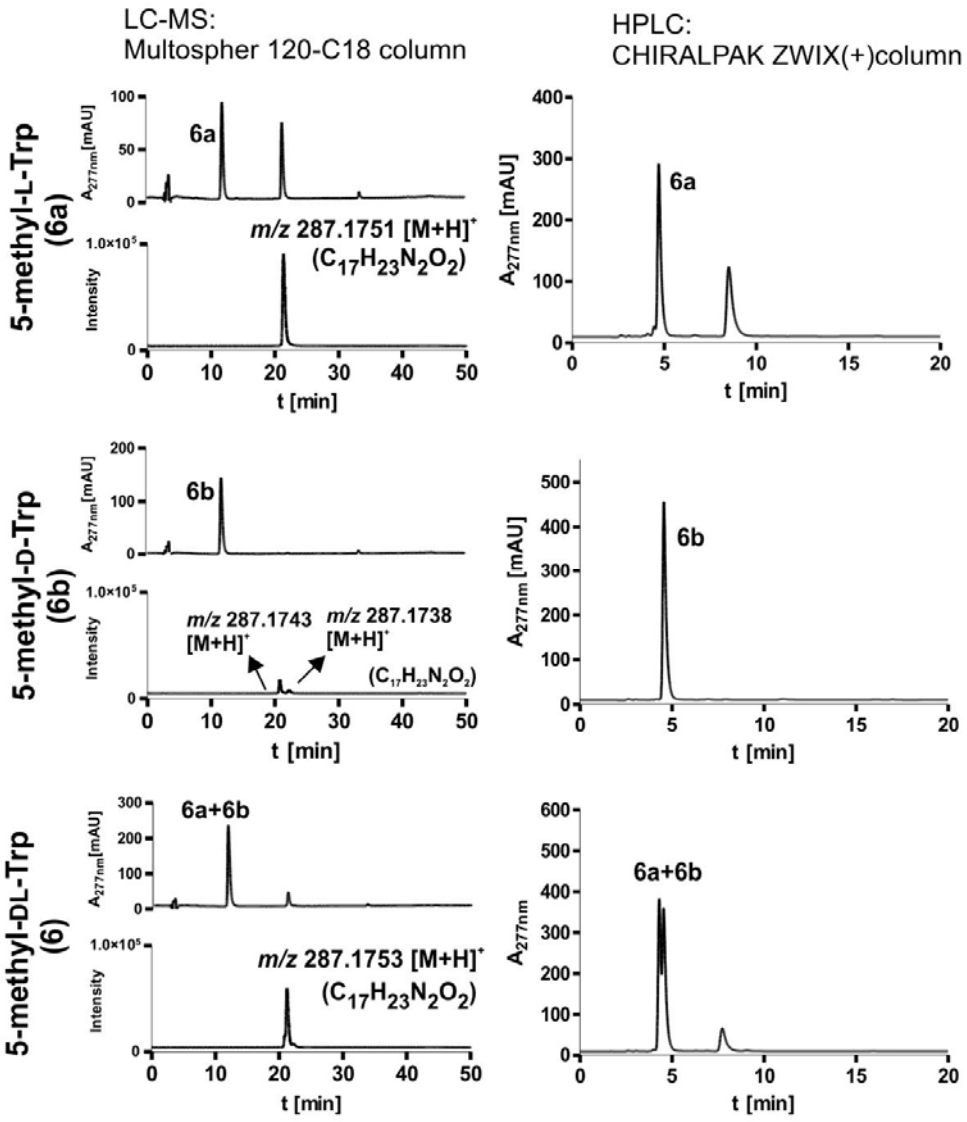

Fig. S26 LC-MS and HPLC analyses of the enzyme assays of 5-methyltryptophan with FgaPT2. The enzyme assays contained 1 mM DMAPP, 1 μM purified protein, and 0.5 mM of L- or D-isomer, or 1 mM of their racemate were incubated at 37 °C for 1.5 h. UV-detection was carried out on a Diode Array detector and illustrated for absorption at 277 nm.

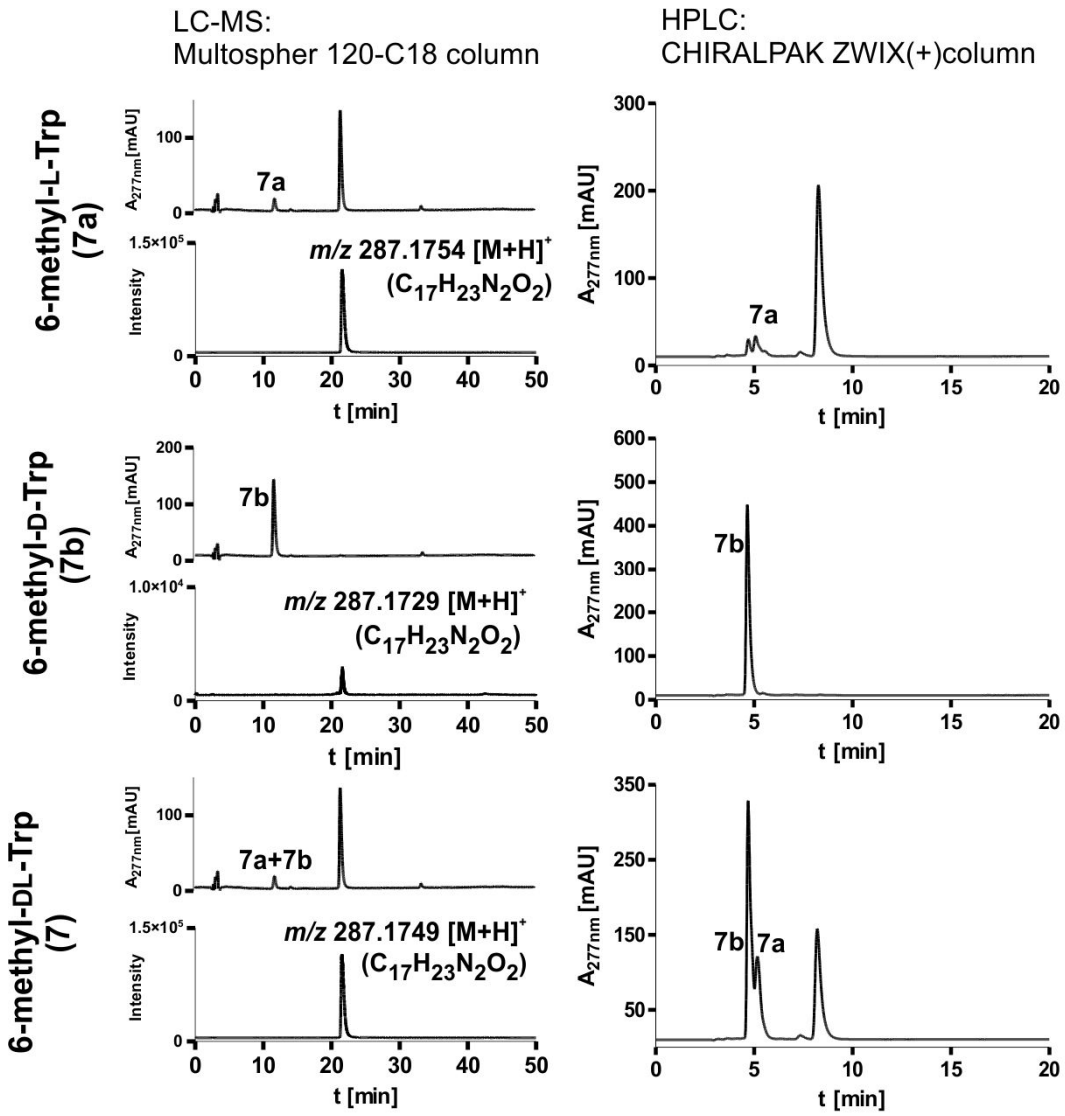

Fig. S27 LC-MS and HPLC analyses of the enzyme assays of 6-methyltryptophan with FgaPT2. The enzyme assays contained 1 mM DMAPP, 1 μM purified protein, and 0.5 mM of L- or D-isomer, or 1 mM of their racemate were incubated at 37 °C for 1.5 h. UV-detection was carried out on a Diode Array detector and illustrated for absorption at 277 nm.

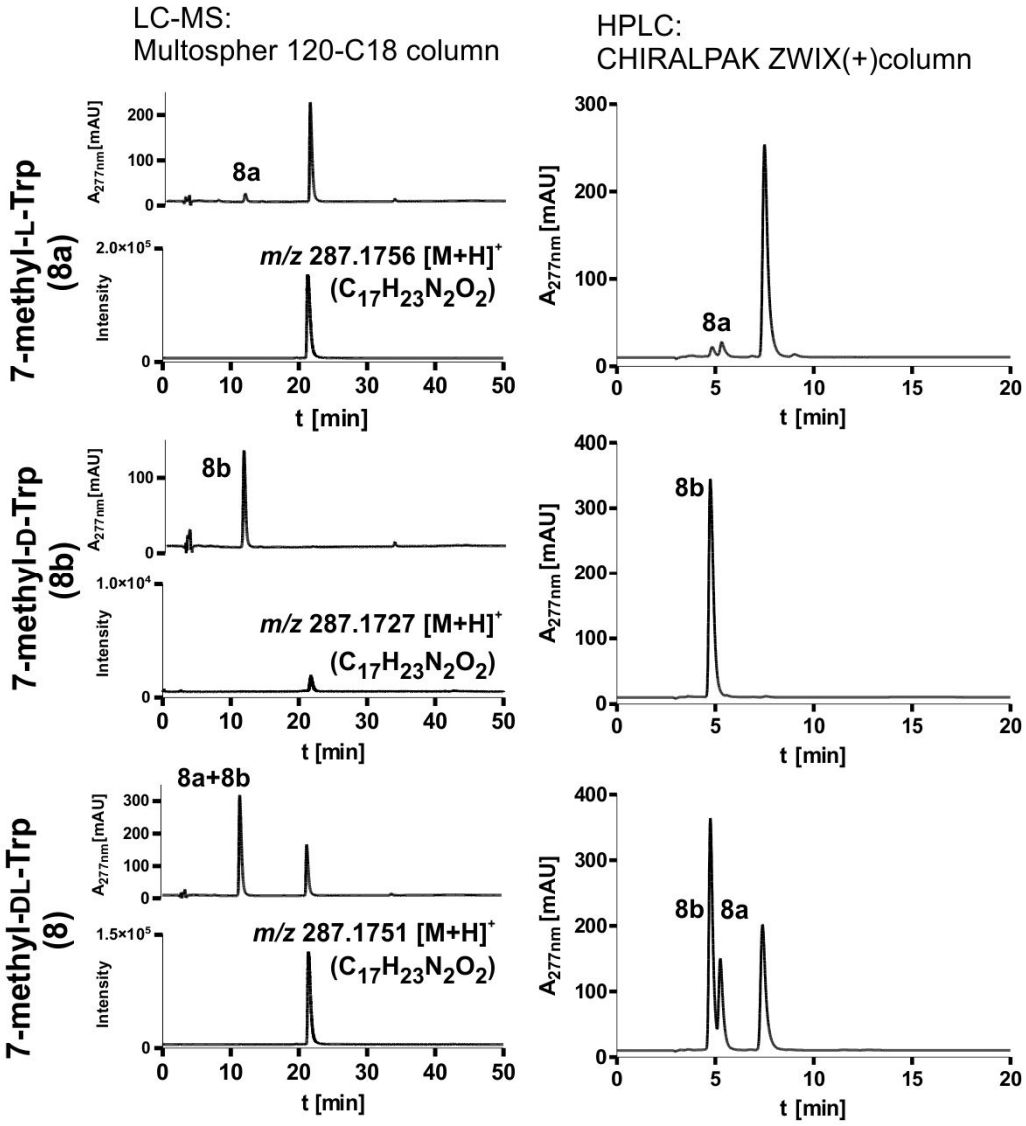

Fig. S28 LC-MS and HPLC analyses of the enzyme assays of 7-methyltryptophan with FgaPT2. The enzyme assays contained 1 mM DMAPP, 1 µM purified protein, and 0.5 mM of L- or D-isomer, or 1 mM of their racemate were incubated at 37 °C for 1.5 h. UV-detection was carried out on a Diode Array detector and illustrated for absorption at 277 nm.

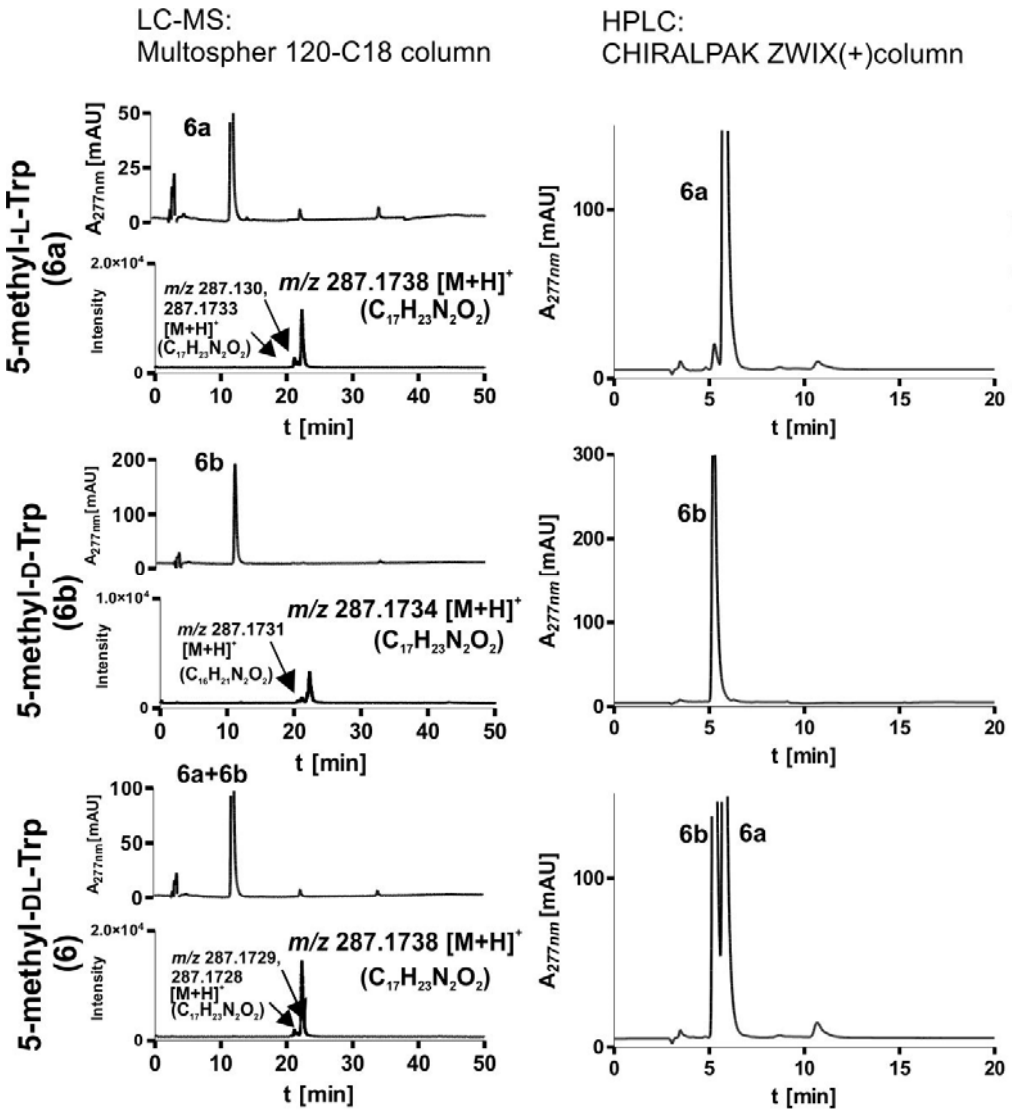

Fig. S29 LC-MS and HPLC analyses of the enzyme assays of 5-methyltryptophan with 5-DMATS. The enzyme assays contained 1 mM DMAPP, 1 µM purified protein, and 0.5 mM of L- or D-isomer, or 1 mM of their racemate were incubated at 37 °C for 1.5 h. UV-detection was carried out on a Diode Array detector and illustrated for absorption at 277 nm.

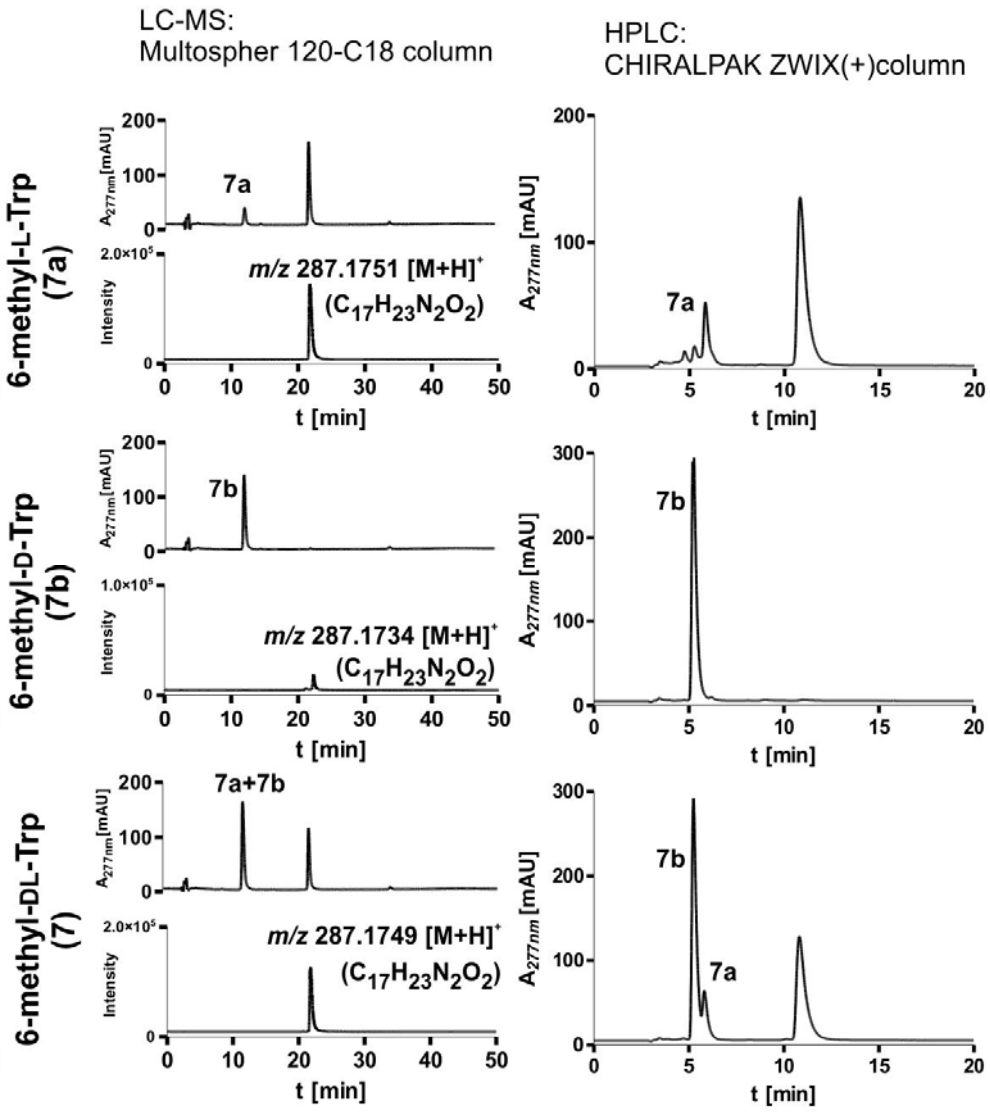

Fig. S30 LC-MS and HPLC analyses of the enzyme assays of 6-methyltryptophan with 5-DMATS. The enzyme assays contained 1 mM DMAPP, 1 μM purified protein, and 0.5 mM of L- or D-isomer, or 1 mM of their racemate were incubated at 37 °C for 1.5 h. UV-detection was carried out on a Diode Array detector and illustrated for absorption at 277 nm.

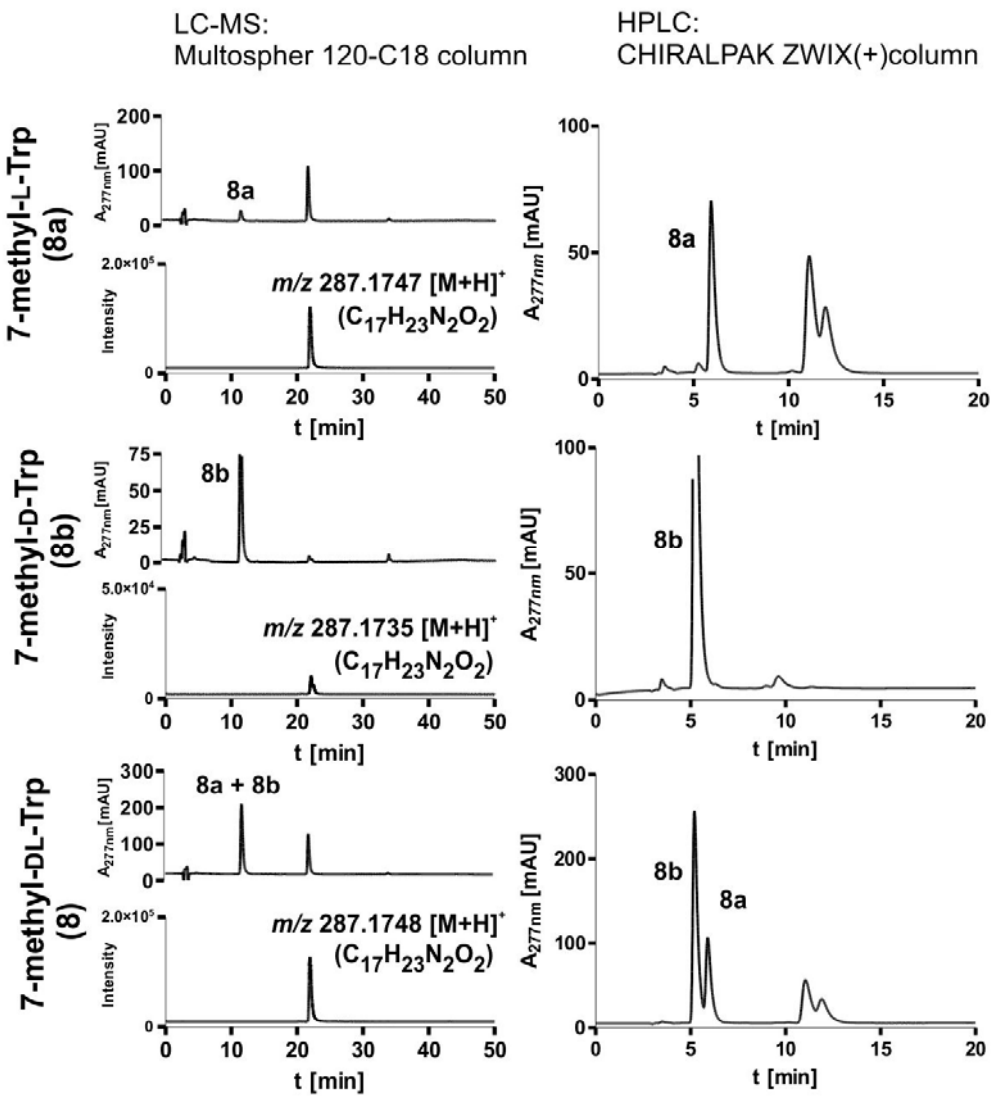

Fig. S31 LC-MS and HPLC analyses of the enzyme assays of 7-methyltryptophan with 5-DMATS. The enzyme assays contained 1 mM DMAPP, 1 µM purified protein, and 0.5 mM of L- or D-isomer, or 1 mM of their racemate were incubated at 37 °C for 1.5 h. UV-detection was carried out on a Diode Array detector and illustrated for absorption at 277 nm.

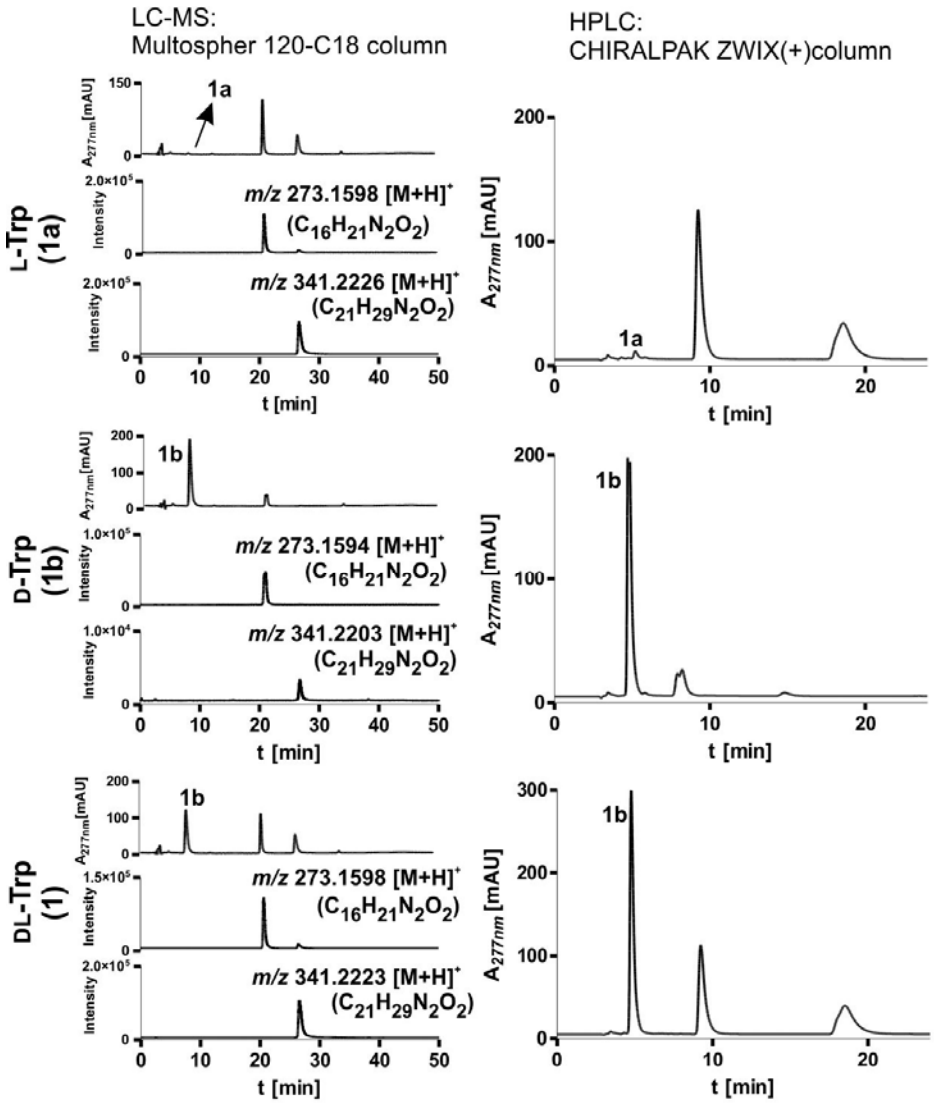

Fig. S32 LC-MS and HPLC analyses of the enzyme assays of tryptophan with 5-DMATS$_{Sc}$. The enzyme assays contained 1 mM DMAPP, 1 µM purified protein, and 0.5 mM of L- or D-isomer, or 1 mM of their racemate were incubated at 37 °C for 1.5 h. UV-detection was carried out on a Diode Array detector and illustrated for absorption at 277 nm.

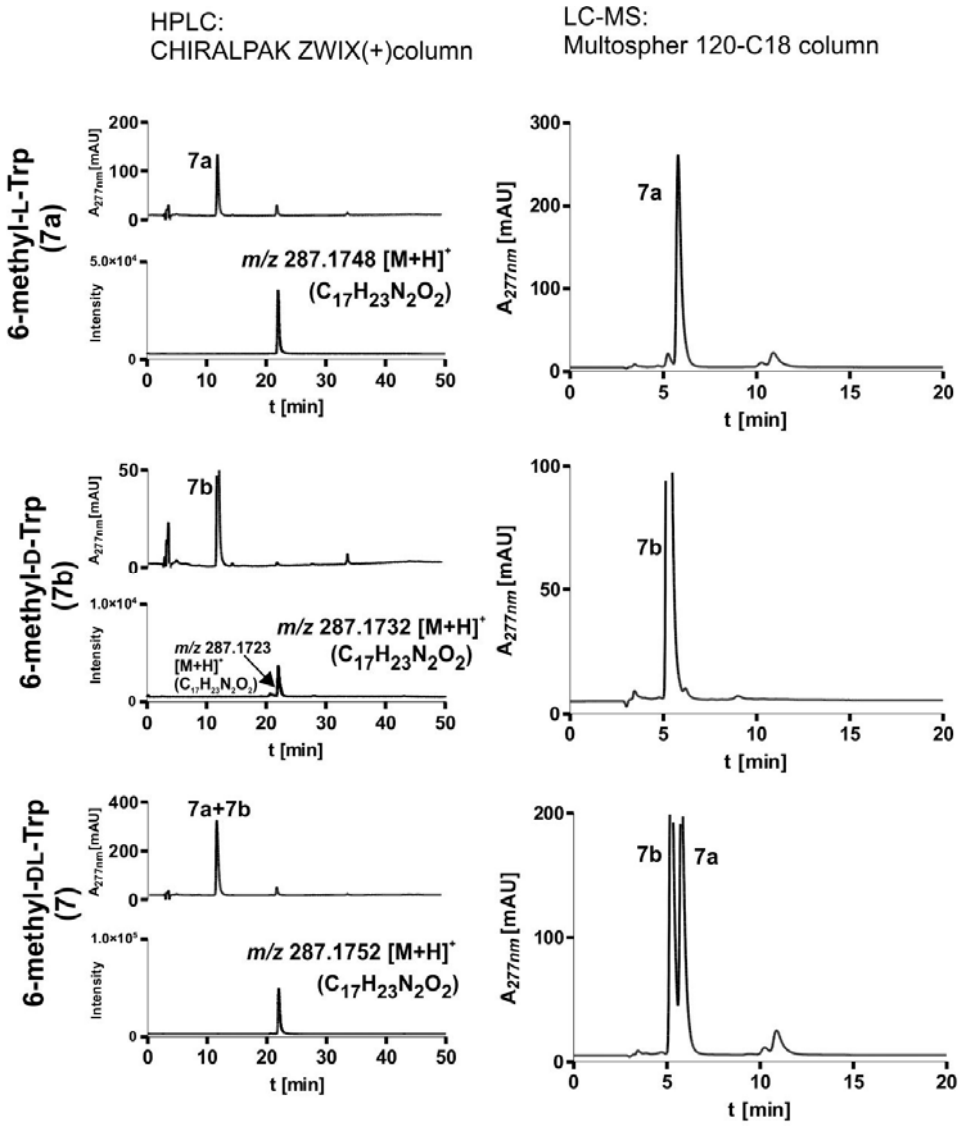

Fig. S33 LC-MS and HPLC analyses of the enzyme assays of 6-methyltryptophan with 5-DMATS$_{Sc}$. The enzyme assays contained 1 mM DMAPP, 1 µM purified protein, and 0.5 mM of L- or D-isomer, or 1 mM of their racemate were incubated at 37 °C for 1.5 h. UV-detection was carried out on a Diode Array detector and illustrated for absorption at 277 nm.

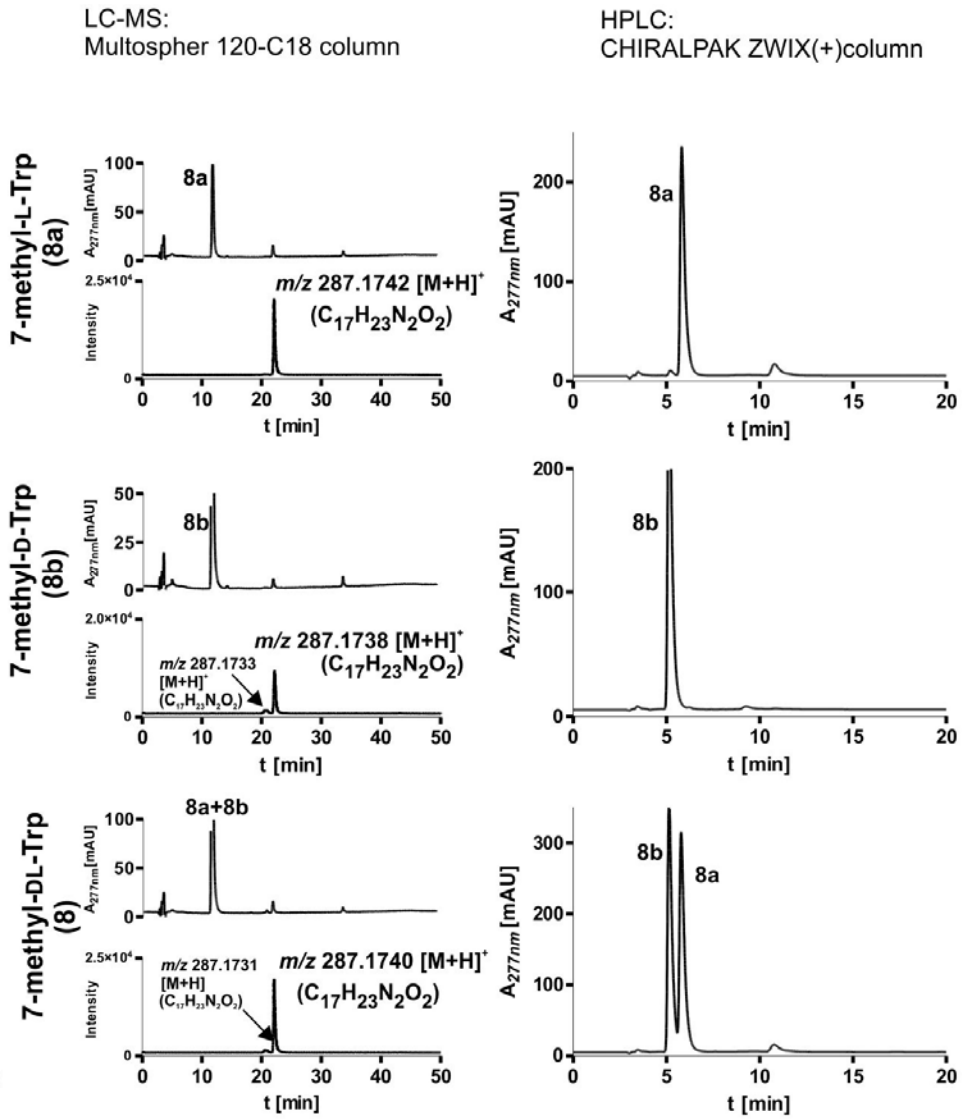

Fig. S34 LC-MS and HPLC analyses of the enzyme assays of 7-methyltryptophan with 5-DMATS$_{Sc}$. The enzyme assays contained 1 mM DMAPP, 1 µM purified protein, and 0.5 mM of L- or D-isomer, or 1 mM of their racemate were incubated at 37 °C for 1.5 h. UV-detection was carried out on a Diode Array detector and illustrated for absorption at 277 nm.

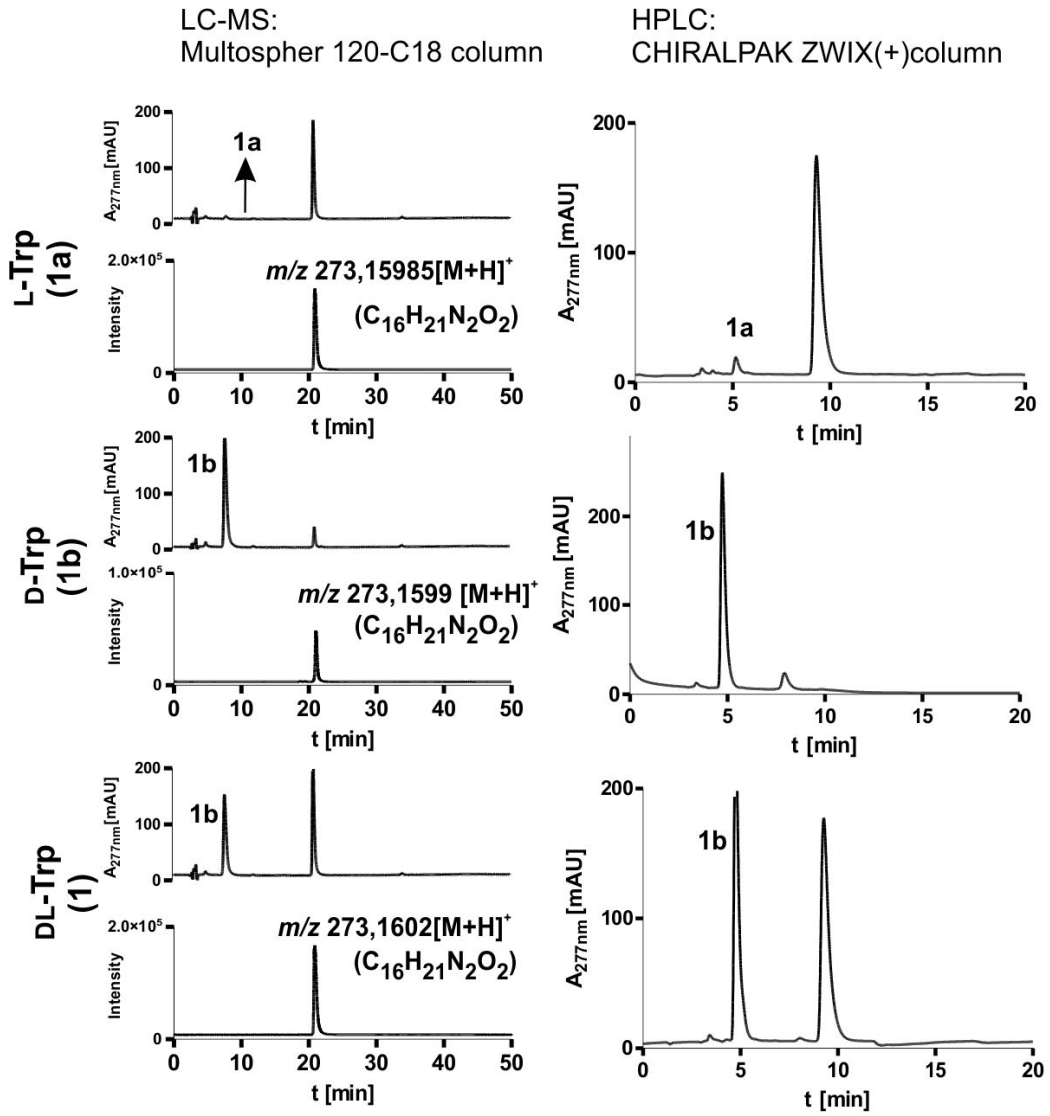

Fig. S35 LC-MS and HPLC analyses of the enzyme assays of tryptophan with 6-DMATS$_{Sa}$. The enzyme assays contained 1 mM DMAPP, 1 μM purified protein, and 0.5 mM of L- or D-isomer, or 1 mM of their racemate were incubated at 37 °C for 1.5 h. UV-detection was carried out on a Diode Array detector and illustrated for absorption at 277 nm.

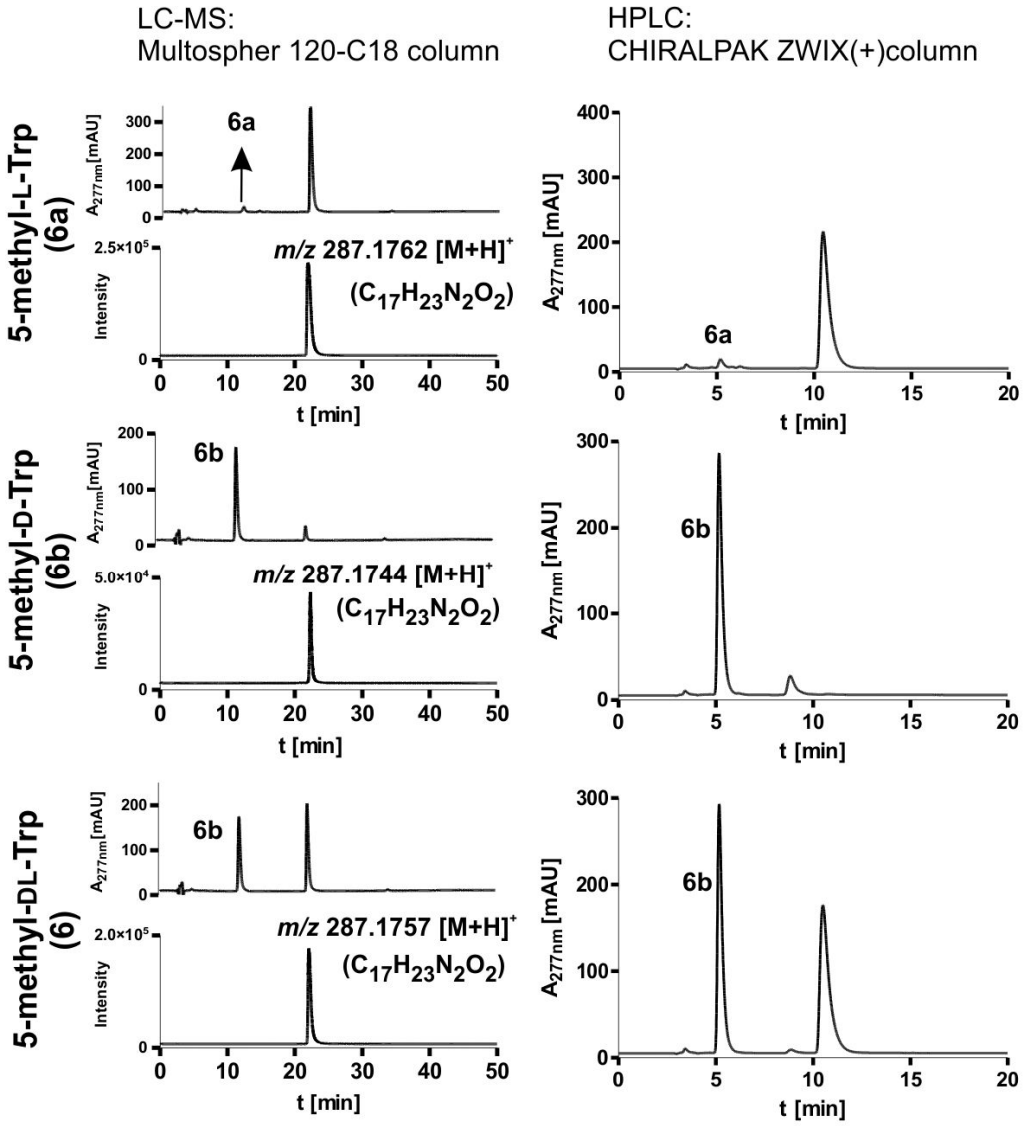

Fig. S36 LC-MS and HPLC analyses of the enzyme assays of 5-methyltryptophan with 6-DMATS$_{Sa}$. The enzyme assays contained 1 mM DMAPP, 1 µM purified protein, and 0.5 mM of L- or D-isomer, or 1 mM of their racemate were incubated at 37 °C for 1.5 h. UV-detection was carried out on a Diode Array detector and illustrated for absorption at 277 nm.

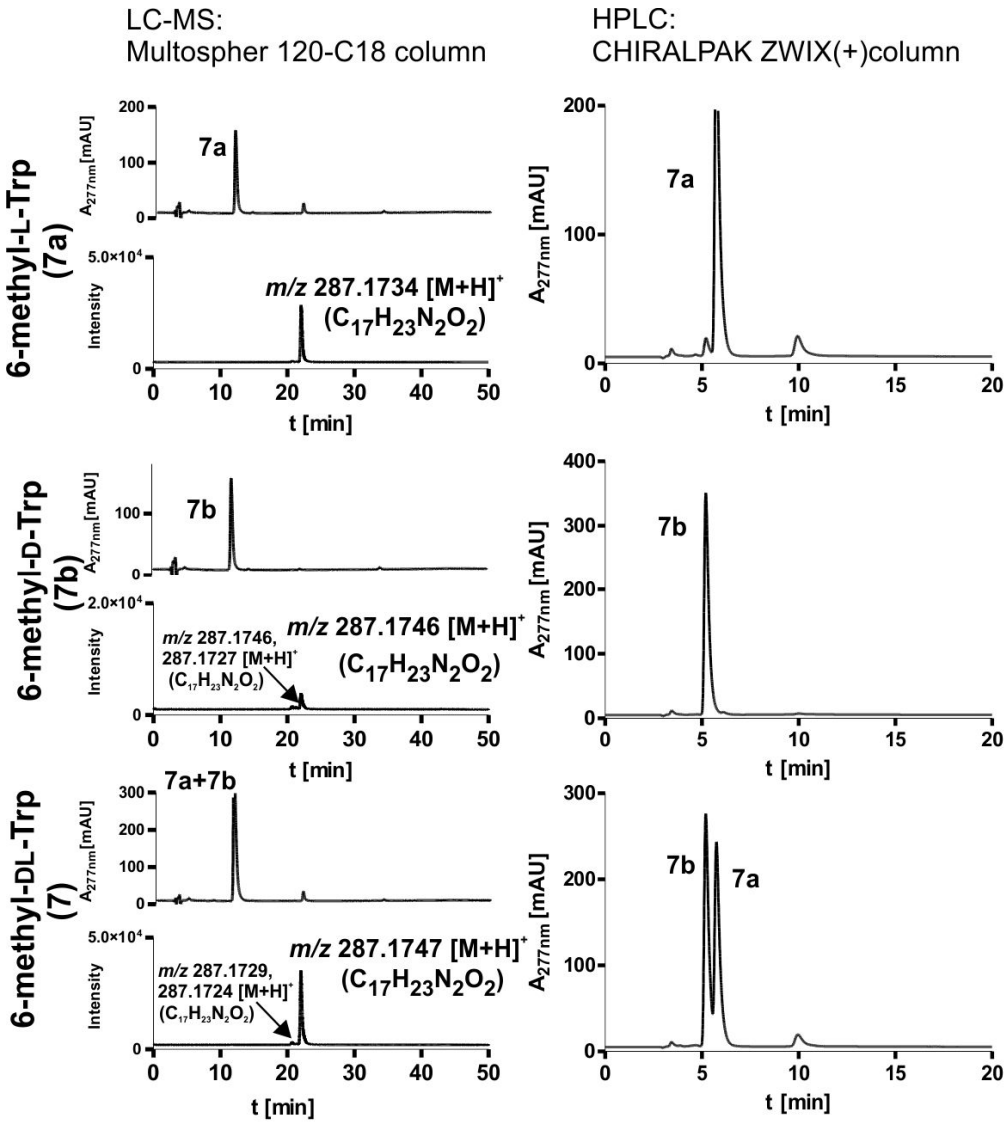

Fig. S37 LC-MS and HPLC analyses of the enzyme assays of 6-methyltryptophan with 6-DMATS$_{Sa}$. The enzyme assays contained 1 mM DMAPP, 1 µM purified protein, and 0.5 mM of L- or D-isomer, or 1 mM of their racemate were incubated at 37 °C for 1.5 h. UV-detection was carried out on a Diode Array detector and illustrated for absorption at 277 nm.

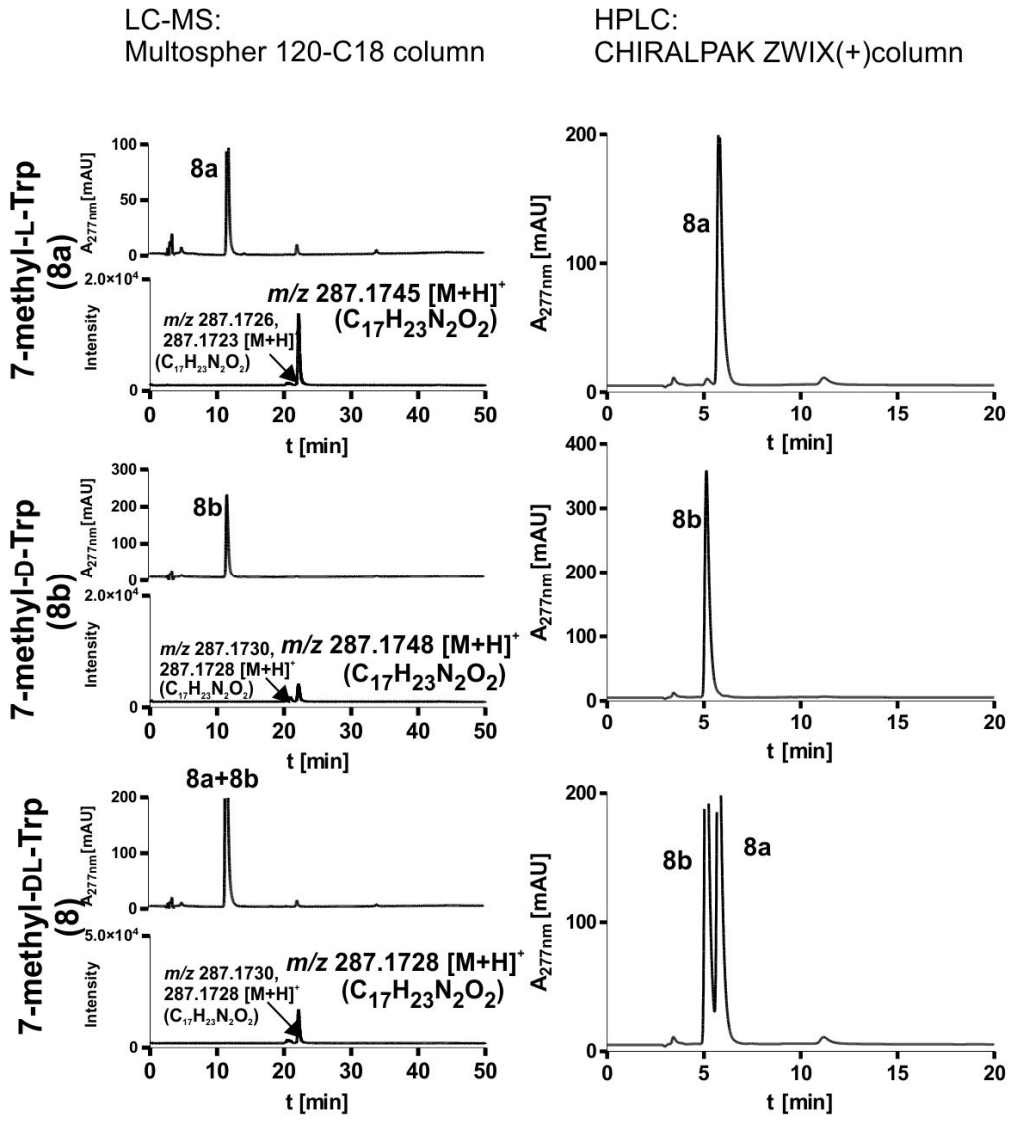

Fig. S38 LC-MS and HPLC analyses of the enzyme assays of 7-methyltryptophan with 6-DMATS$_{Sa}$. The enzyme assays contained 1 mM DMAPP, 1 µM purified protein, and 0.5 mM of L- or D-isomer, or 1 mM of their racemate were incubated at 37 °C for 1.5 h. UV-detection was carried out on a Diode Array detector and illustrated for absorption at 277 nm.

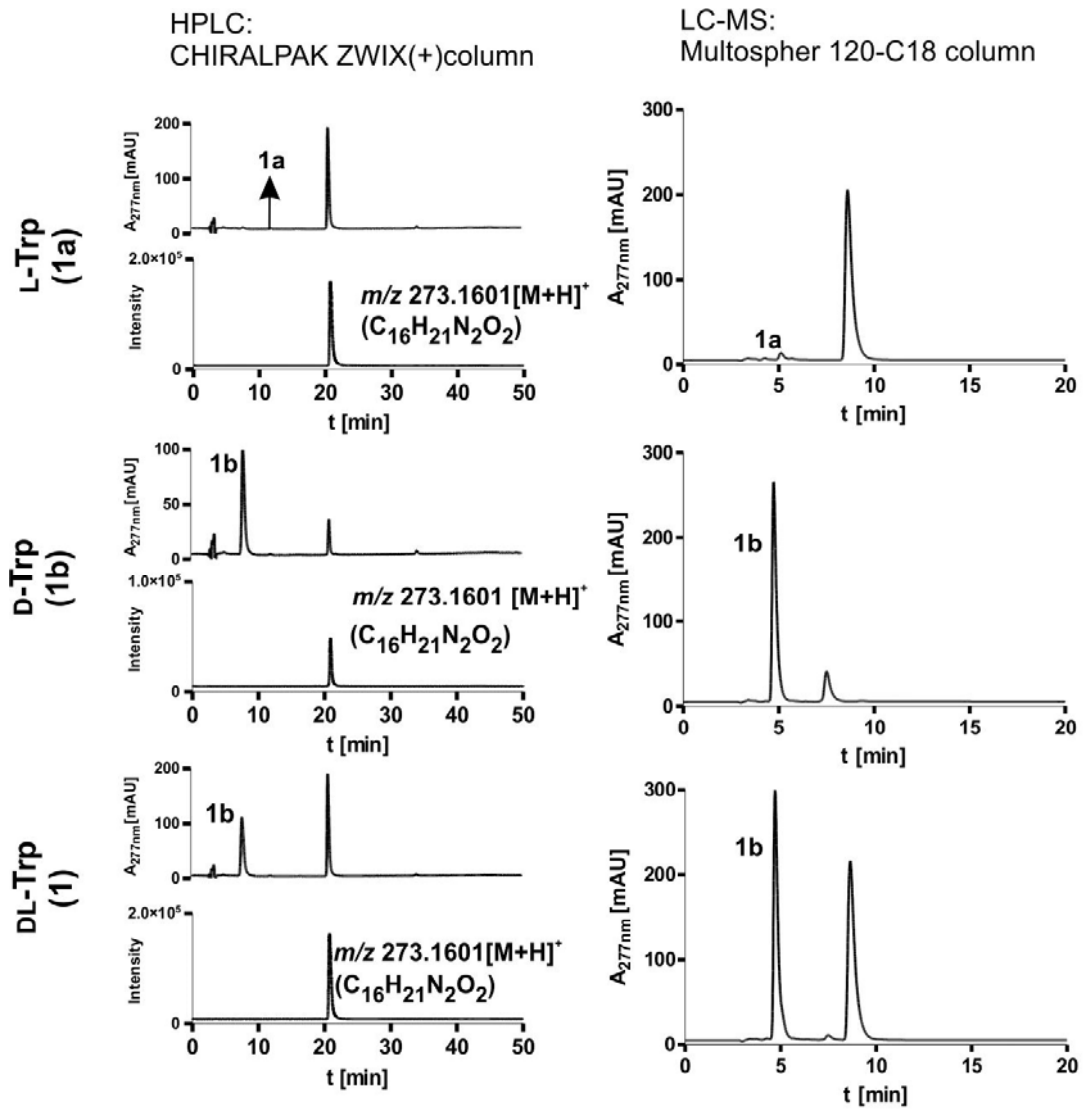

Fig. S39 LC-MS and HPLC analyses of the enzyme assays of tryptophan with 6-DMATS$_{Sv}$. The enzyme assays contained 1 mM DMAPP, 1 µM purified protein, and 0.5 mM of L- or D-isomer, or 1 mM of their racemate were incubated at 37 °C for 1.5 h. UV-detection was carried out on a Diode Array detector and illustrated for absorption at 277 nm.

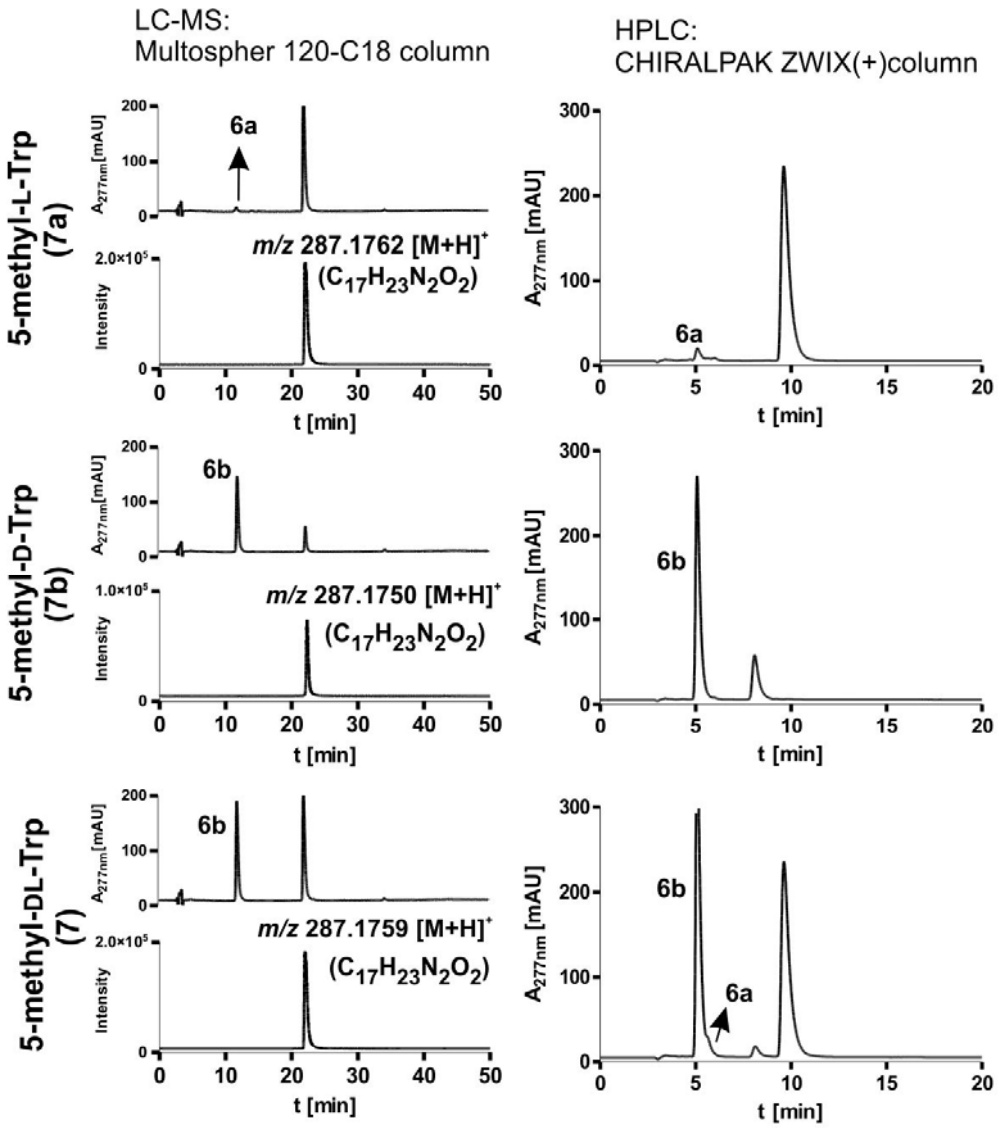

Fig. S40 LC-MS and HPLC analyses of the enzyme assays of 5-methyltryptophan with 6-DMATS$_{Sv}$. The enzyme assays contained 1 mM DMAPP, 1 µM purified protein, and 0.5 mM of L- or D-isomer, or 1 mM of their racemate were incubated at 37 °C for 1.5 h. UV-detection was carried out on a Diode Array detector and illustrated for absorption at 277 nm.

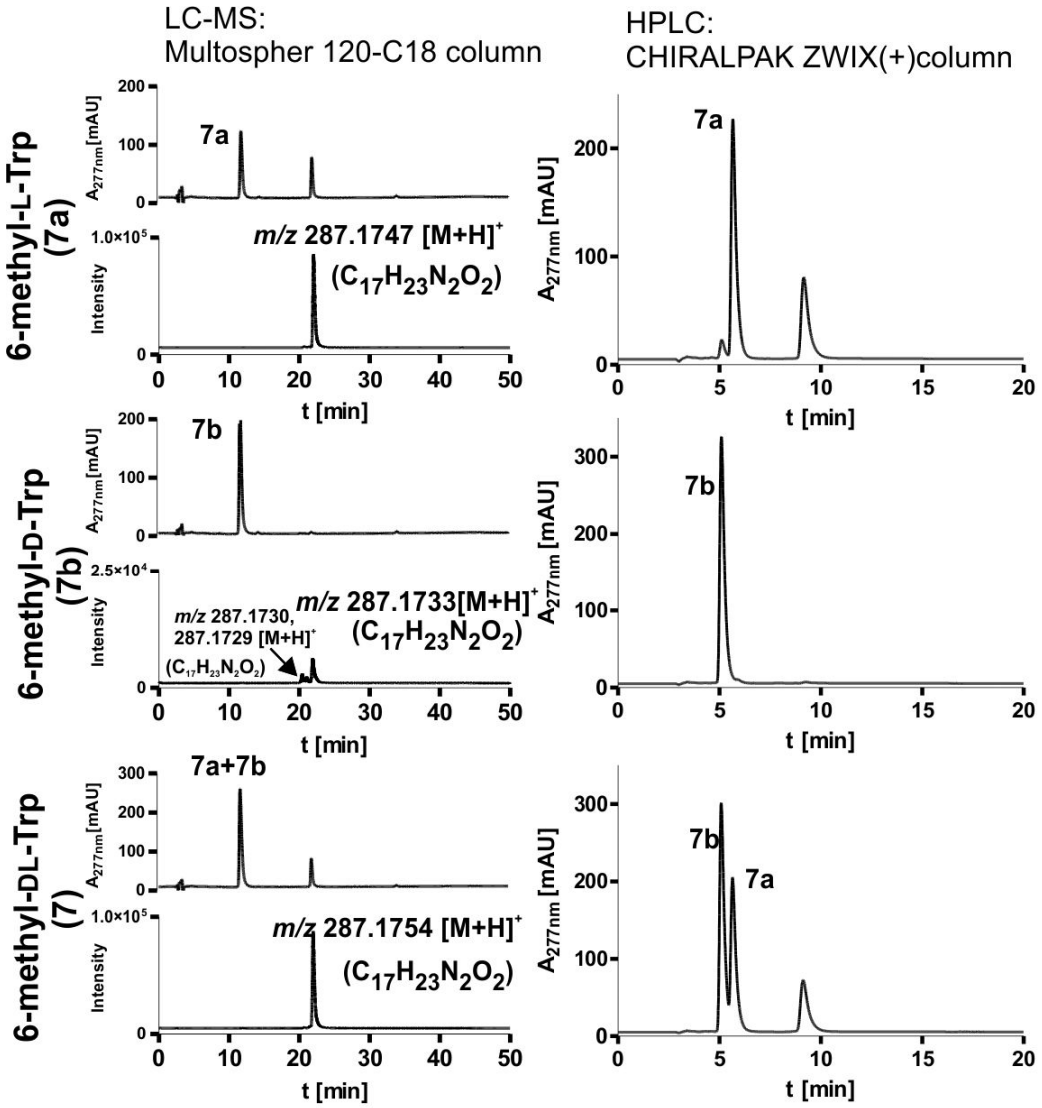

Fig. S41 LC-MS and HPLC analyses of the enzyme assays of 6-methyltryptophan with 6-DMATS$_{Sv}$. The enzyme assays contained 1 mM DMAPP, 1 µM purified protein, and 0.5 mM of L- or D-isomer, or 1 mM of their racemate were incubated at 37 °C for 1.5 h. UV-detection was carried out on a Diode Array detector and illustrated for absorption at 277 nm.

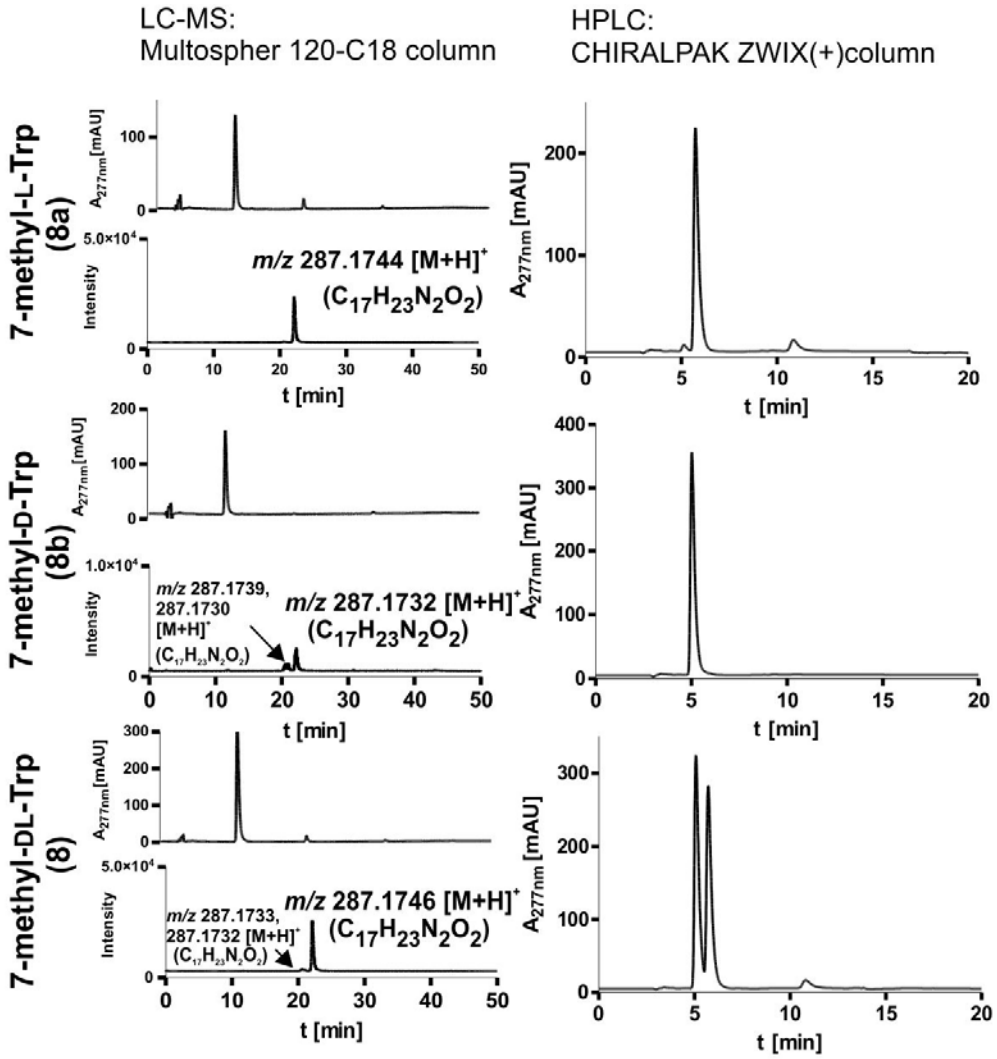

Fig. S42 LC-MS and HPLC analyses of the enzyme assays of 7-methyltryptophan with 6-DMATS$_{Sv}$. The enzyme assays contained 1 mM DMAPP, 1 µM purified protein, and 0.5 mM of L- or D-isomer, or 1 mM of their racemate were incubated at 37 °C for 1.5 h. UV-detection was carried out on a Diode Array detector and illustrated for absorption at 277 nm.

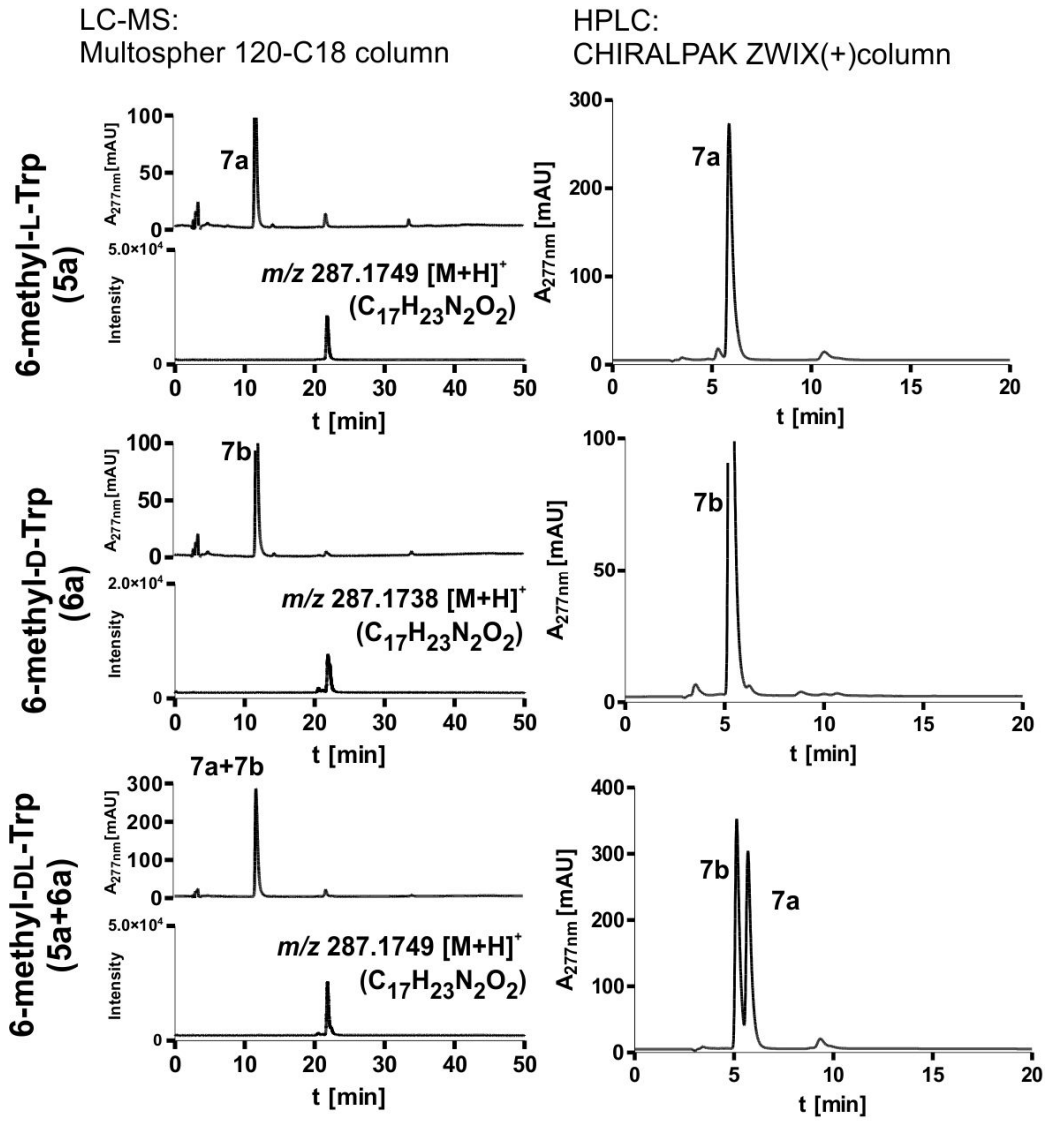

Fig. S43 LC-MS and HPLC analyses of the enzyme assays of 6-methyltryptophan with 6-DMATS$_{Mo}$. The enzyme assays contained 1 mM DMAPP, 1 µM purified protein, and 0.5 mM of L- or D-isomer, or 1 mM of their racemate were incubated at 37 °C for 1.5 h. UV-detection was carried out on a Diode Array detector and illustrated for absorption at 277 nm.

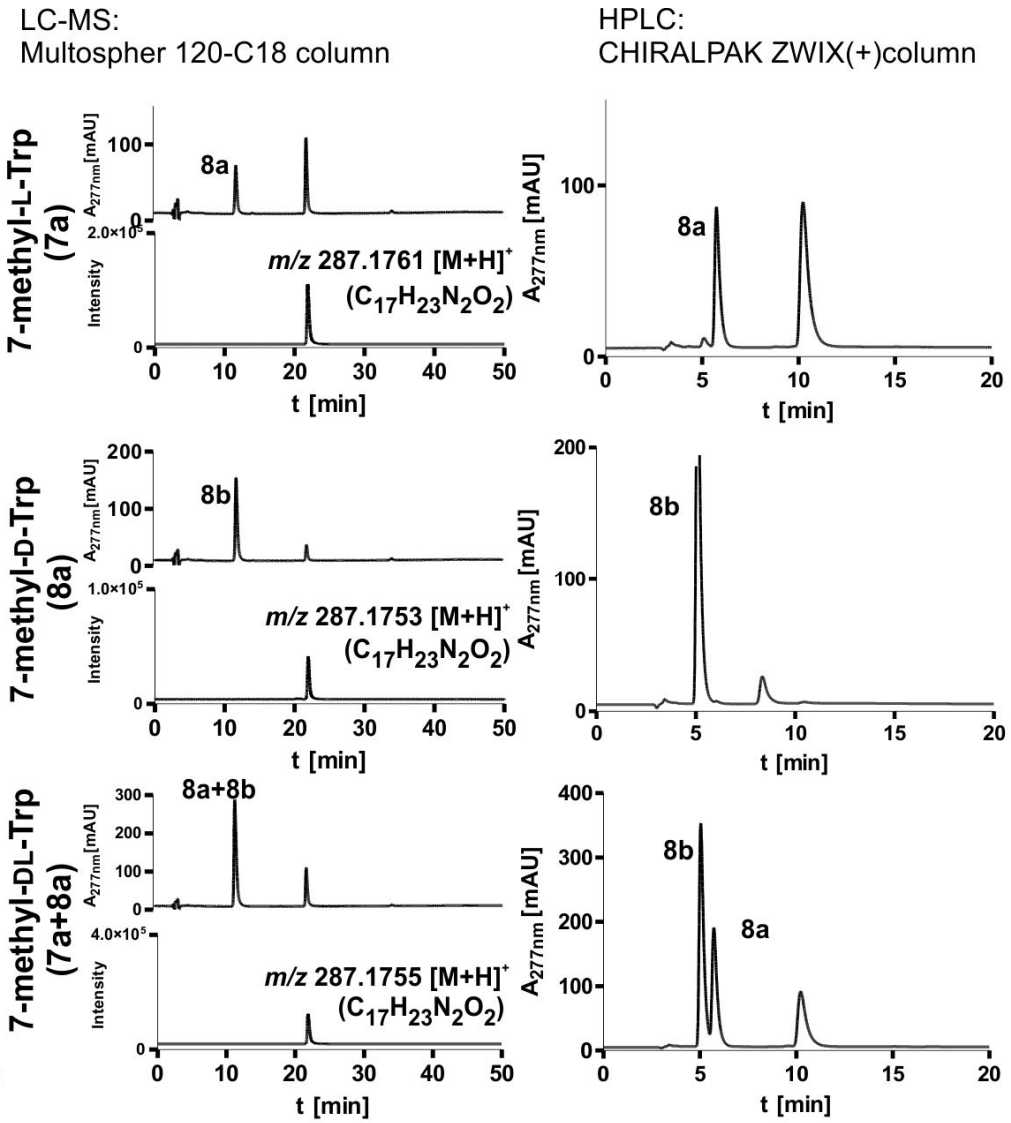

Fig. S44 LC-MS and HPLC analyses of the enzyme assays of 7-methyltryptophan with 6-DMATS$_{Mo}$. The enzyme assays contained 1 mM DMAPP, 1 µM purified protein, and 0.5 mM of L- or D-isomer, or 1 mM of their racemate were incubated at 37 °C for 1.5 h. UV-detection was carried out on a Diode Array detector and illustrated for absorption at 277 nm.

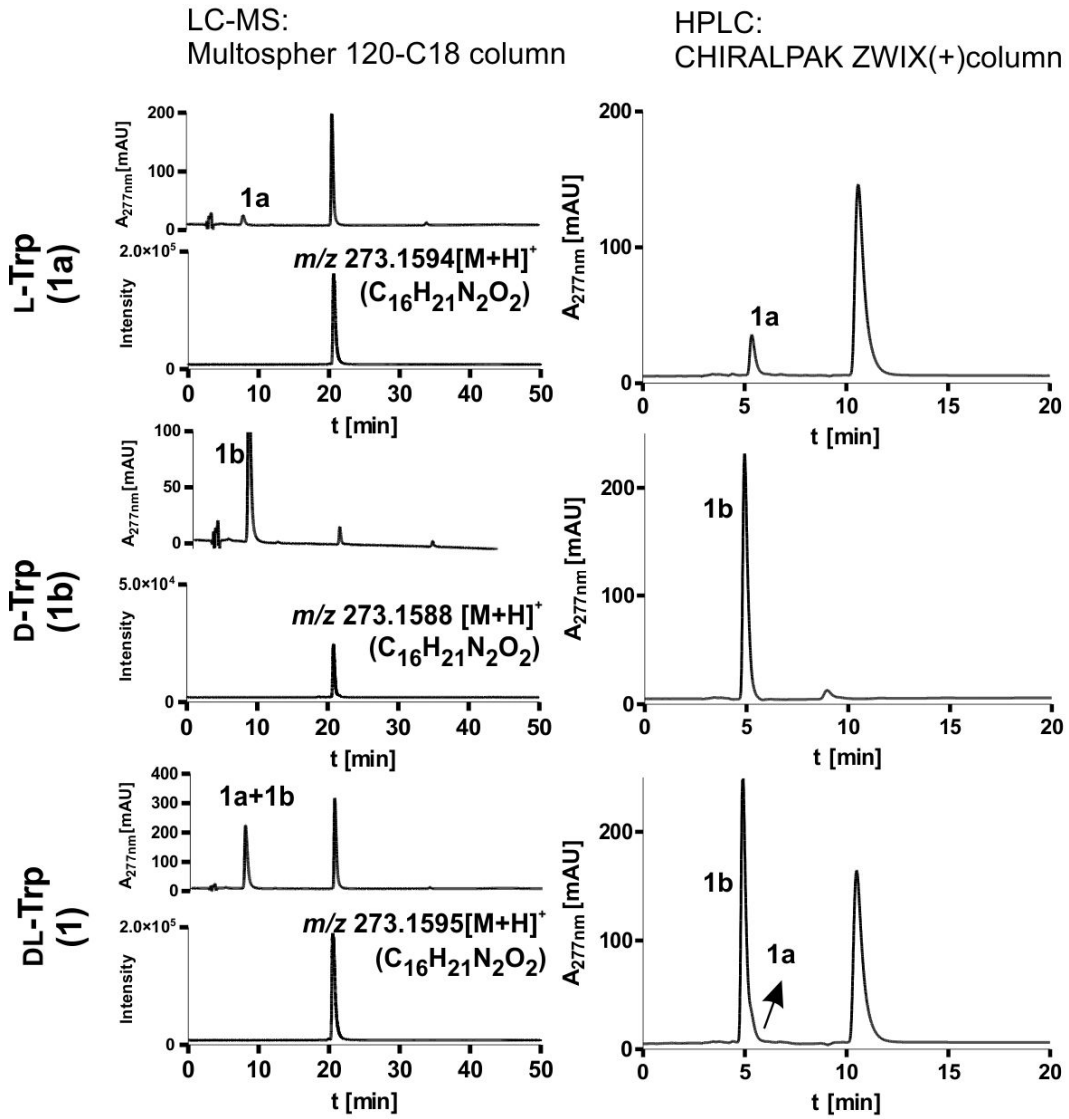

Fig. S45 LC-MS and HPLC analyses of the enzyme assays of tryptophan with 7-DMATS. The enzyme assays contained 1 mM DMAPP, 1 µM purified protein, and 0.5 mM of L- or D-isomer, or 1 mM of their racemate were incubated at 37 °C for 1.5 h. UV-detection was carried out on a Diode Array detector and illustrated for absorption at 277 nm.

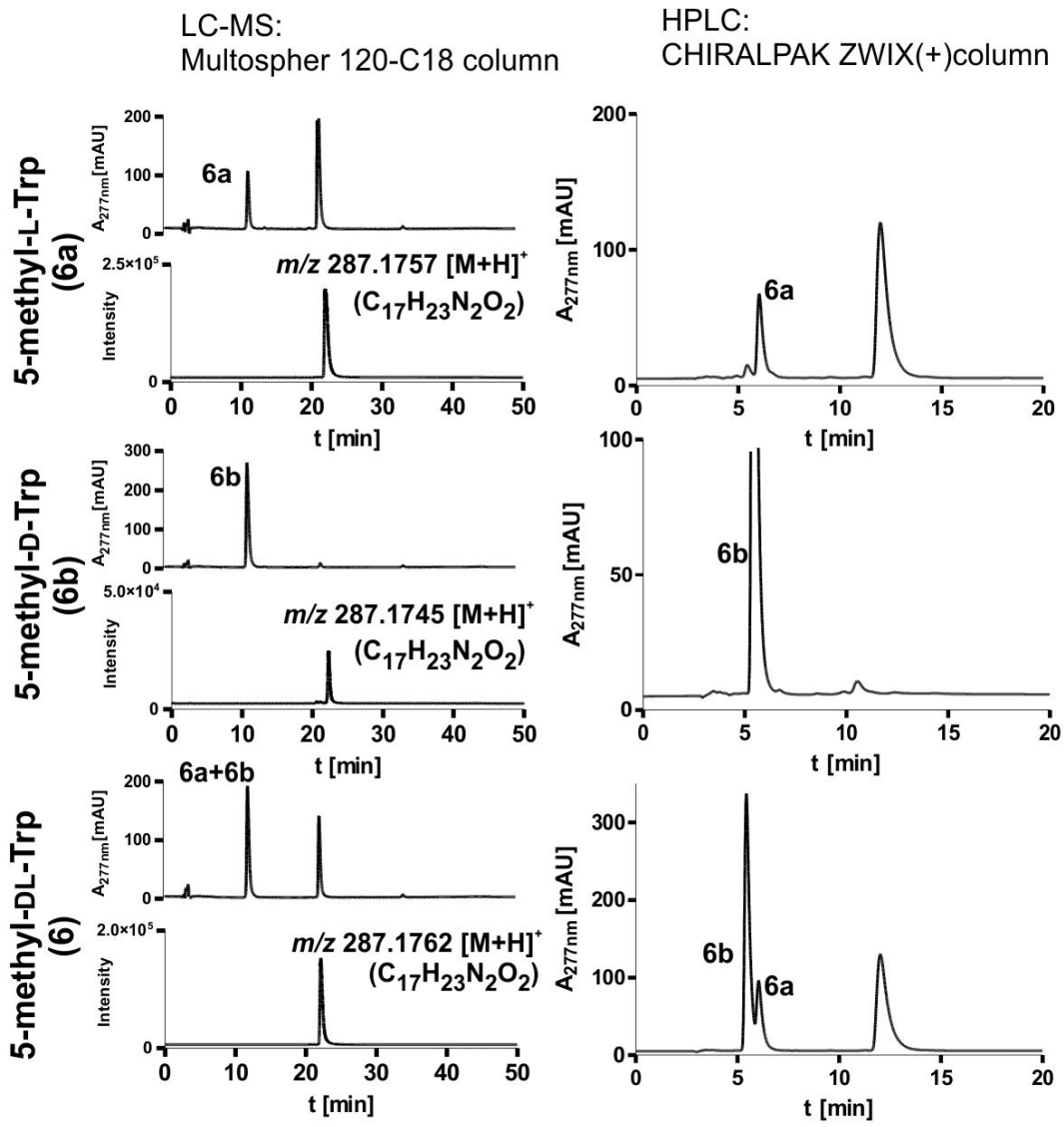

Fig. S46 LC-MS and HPLC analyses of the enzyme assays of 5-methyltryptophan with 7-DMATS. The enzyme assays contained 1 mM DMAPP, 1 μM purified protein, and 0.5 mM of L- or D-isomer, or 1 mM of their racemate were incubated at 37 °C for 1.5 h. UV-detection was carried out on a Diode Array detector and illustrated for absorption at 277 nm.

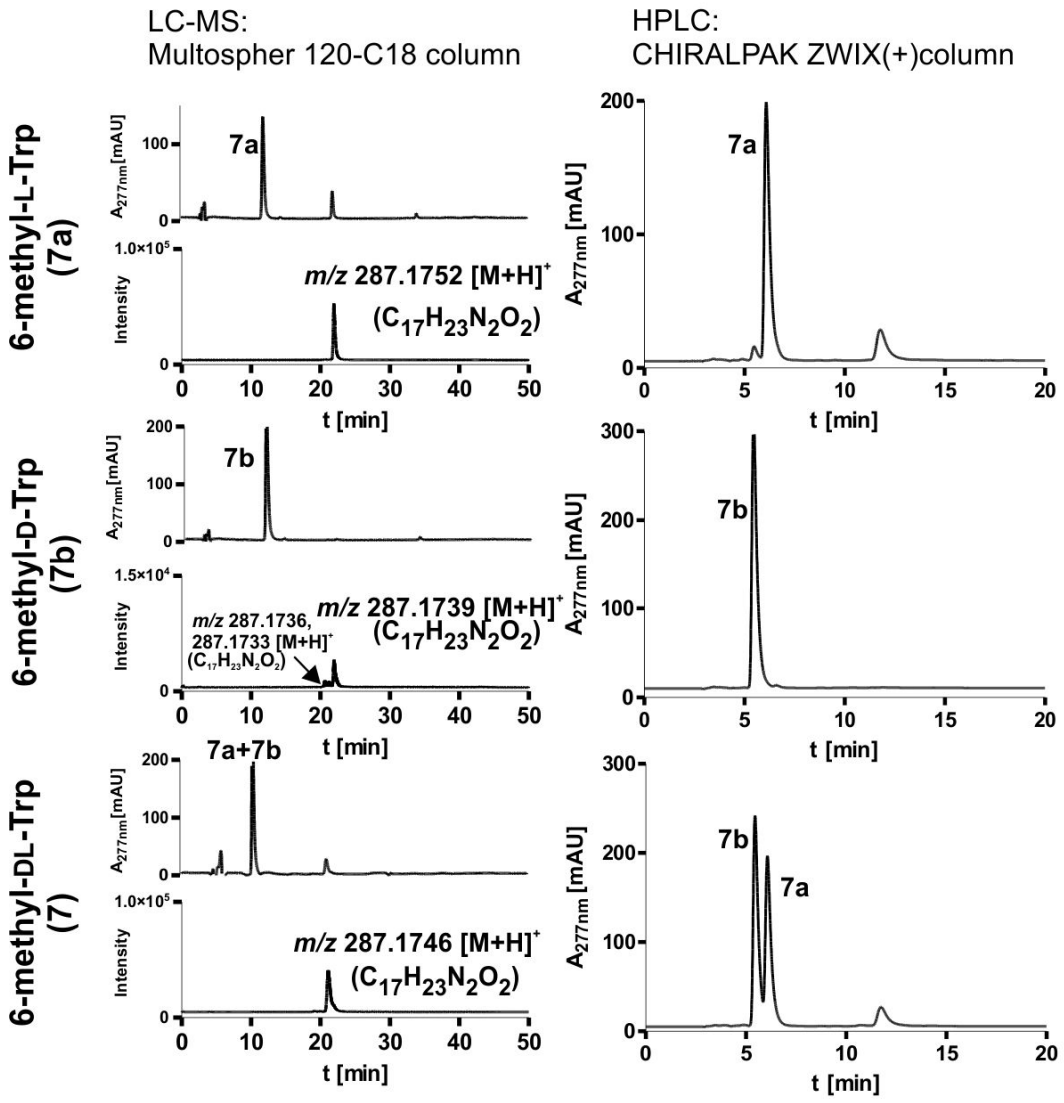

Fig. S47 LC-MS and HPLC analyses of the enzyme assays of 6-methyltryptophan with 7-DMATS. The enzyme assays contained 1 mM DMAPP, 1 µM purified protein, and 0.5 mM of L- or D-isomer, or 1 mM of their racemate were incubated at 37 °C for 1.5 h. UV-detection was carried out on a Diode Array detector and illustrated for absorption at 277 nm.

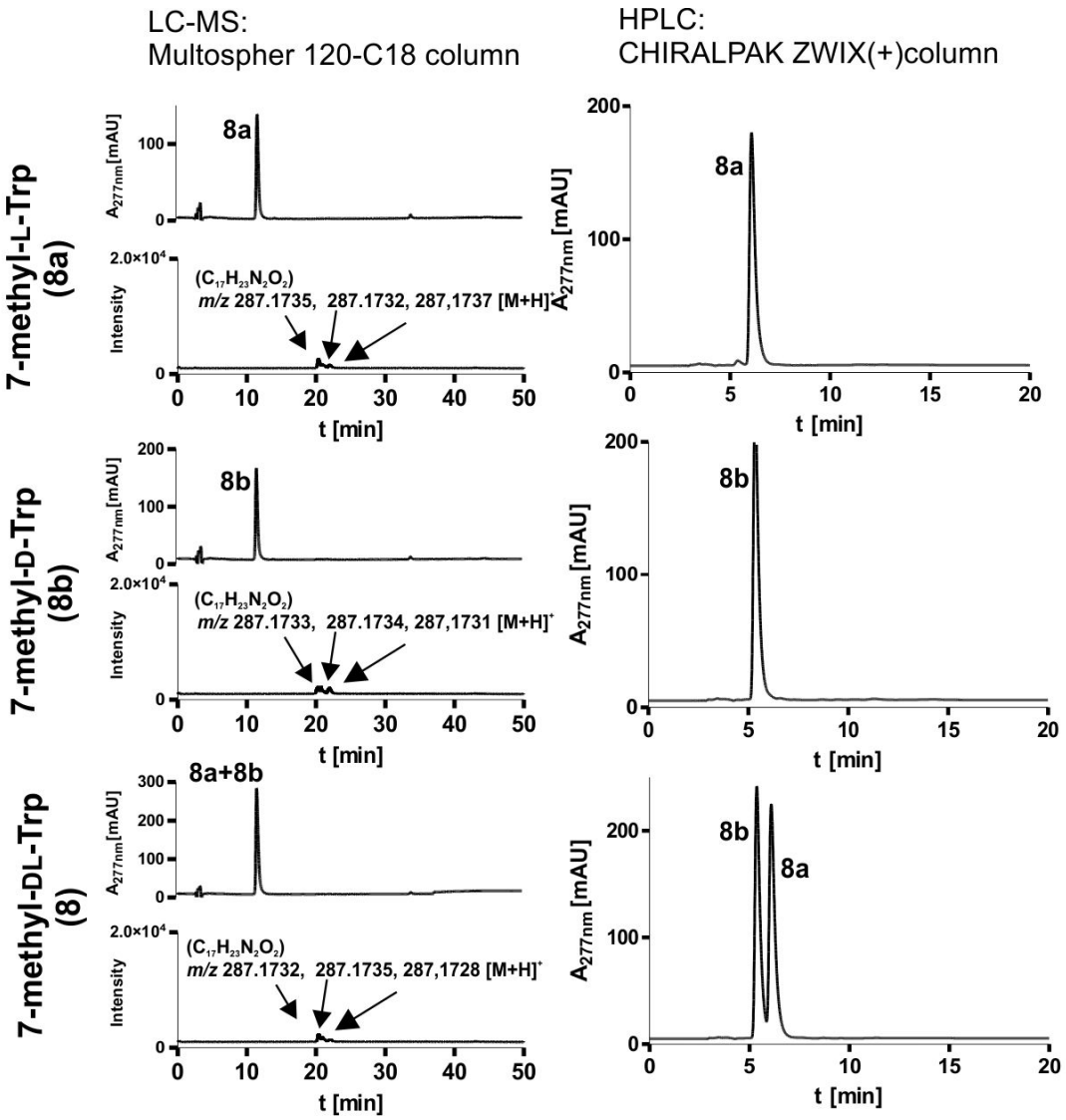

Fig. S48 LC-MS and HPLC analyses of the enzyme assays of 7-methyltryptophan with 7-DMATS. The enzyme assays contained 1 mM DMAPP, 1 µM purified protein, and 0.5 mM of L- or D-isomer, or 1 mM of their racemate were incubated at 37 °C for 1.5 h. UV-detection was carried out on a Diode Array detector and illustrated for absorption at 277 nm.

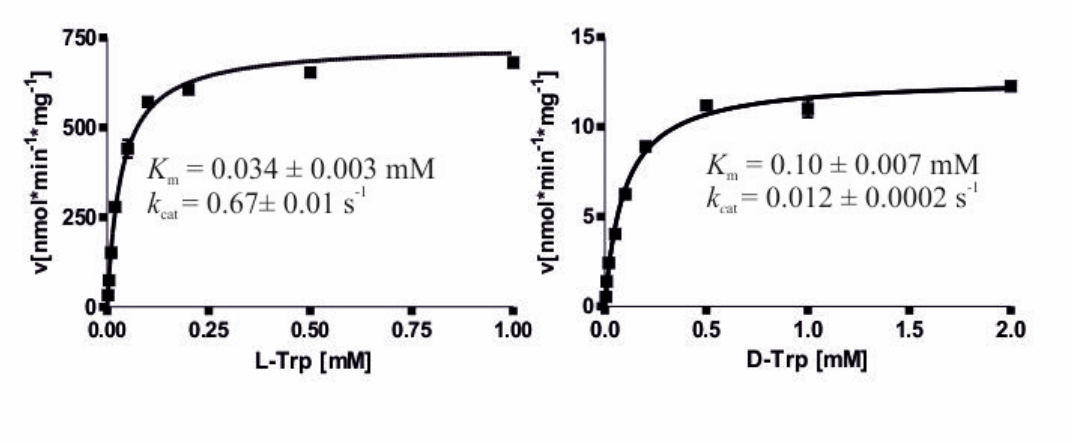

Fig. S49 Determination of the kinetic parameters of FgaPT2 towards L- and D-tryptophan. The reaction mixtures with L-tryptophan contained 1 mM DMAPP, 5 mM $CaCl_2$, and 36.2 nM of the purified protein and were incubated at 37 °C for 15 min. The reaction mixtures with D-tryptophan contained 1 mM DMAPP, 5 mM $CaCl_2$, and 905.8 nM of the purified protein and were incubated at 37 °C for 30 min.

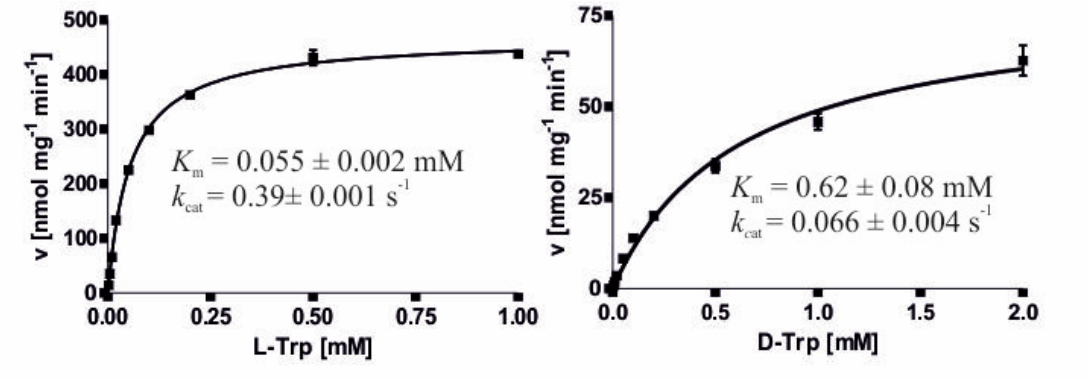

Fig. S50 Determination of the kinetic parameters of 5-DMATS towards L- and D-tryptophan. The reaction mixtures with L -tryptophan contained 1 mM DMAPP, 5 mM $CaCl_2$, and 99.2 nM of the purified protein and were incubated at 37 °C for 15 min. The reaction mixtures with D-tryptophan contained 1 mM DMAPP, 5 mM $CaCl_2$, and 396.8 nM of the purified protein and were incubated at 37 °C for 30 min.

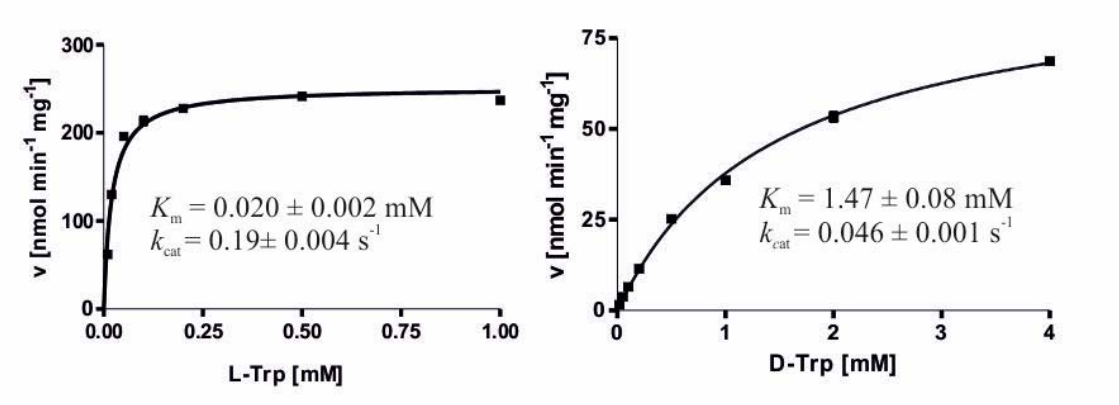

Fig. S51 Determination of the kinetic parameters of 5-DMATS$_{Sc}$ towards L- and D-tryptophan. The reaction mixtures with L-tryptophan contained 1 mM DMAPP, 5 mM $MgCl_2$, and 118.5 nM of the purified protein and were incubated at 37 °C for 15 min. The reaction mixtures with D-tryptophan contained 1 mM DMAPP, 5 mM $MgCl_2$, and 473.9 nM of the purified protein and were incubated at 37 °C for 15 min.

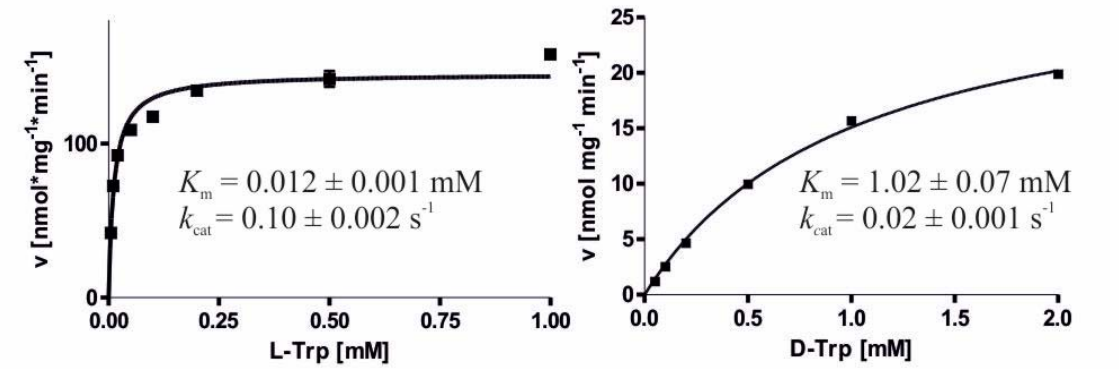

Fig. S52 Determination of the kinetic parameters of 6-DMATS$_{Sa}$ towards L- and D-tryptophan. The reaction mixtures with L-tryptophan contained 1 mM DMAPP, 5 mM $MgCl_2$, and 121.7 nM of the purified protein and were incubated at 37 °C for 15 min. The reaction mixtures with D-tryptophan contained 1 mM DMAPP, 5 mM $MgCl_2$, and 486.6 nM of the purified protein and were incubated at 37 °C for 30 min.

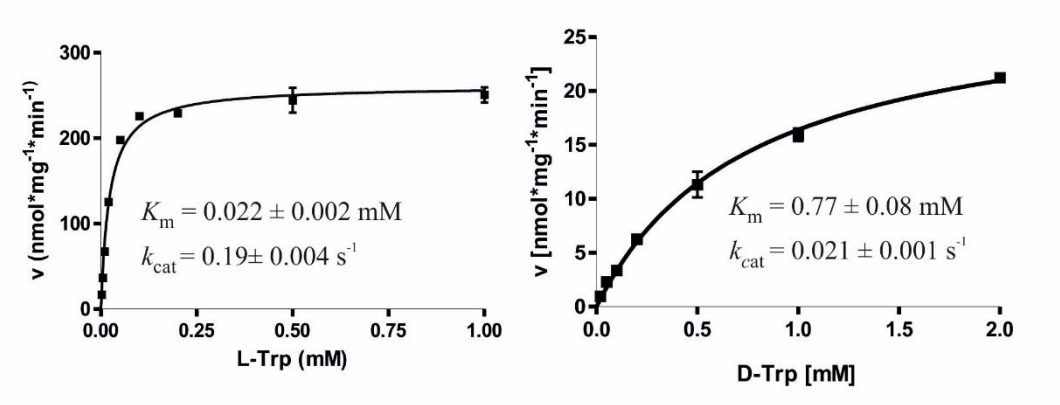

Fig. S53 Determination of the kinetic parameters of 6-DMATS$_{Sv}$ towards L- and D-tryptophan. The reaction mixtures with L-tryptophan contained 1 mM DMAPP, 5 mM $MgCl_2$, and 231.0 nM of the purified protein and were incubated at 37 °C for 15 min. The reaction mixtures with D-tryptophan contained 1 mM DMAPP, 5 mM $MgCl_2$, and 461.9 nM of the purified protein and were incubated at 37 °C for 30 min.

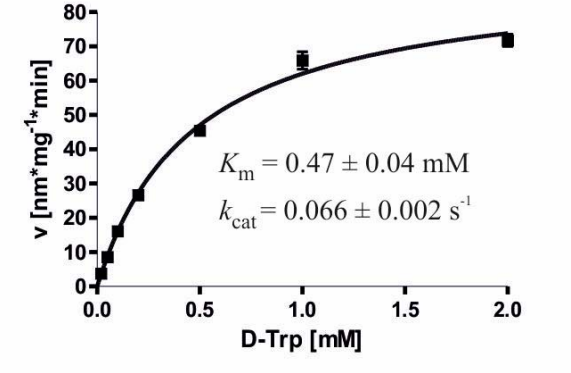

Fig. S54 Determination of the kinetic parameters of 6-DMATS$_{Mo}$ towards D-tryptophan.
The reaction mixtures contained 1 mM DMAPP, 5 mM $MgCl_2$, and 459.8 nM of the purified protein and were incubated at 37 °C for 30 min.

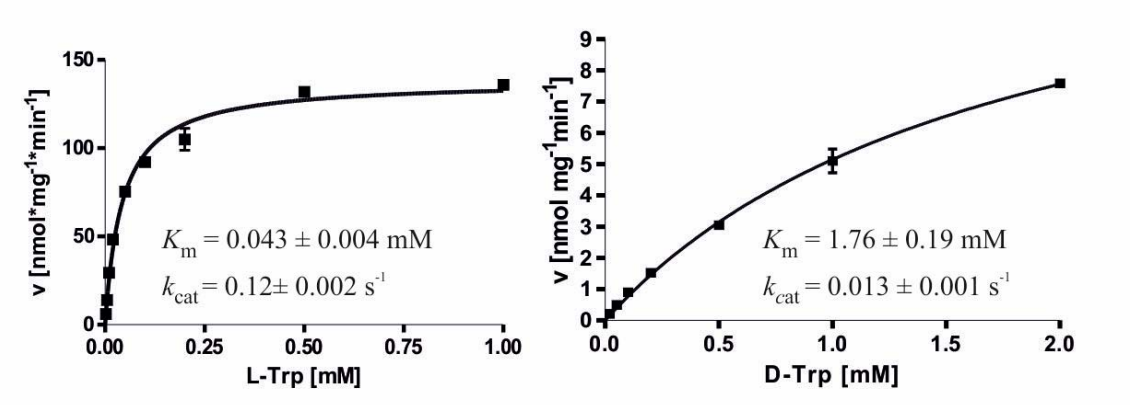

Fig. S55 Determination of the kinetic parameters of 7-DMATS towards L- and D-tryptophan. The reaction mixtures with L-tryptophan contained 1 mM DMAPP, 5 mM $CaCl_2$, and 228.8 nM of the purified protein and were incubated at 37 °C for 15 min. The reaction mixtures with D-tryptophan contained 1 mM DMAPP, 5 mM $CaCl_2$, and 1.4 µM of the purified protein and were incubated at 37 °C for 30 min.

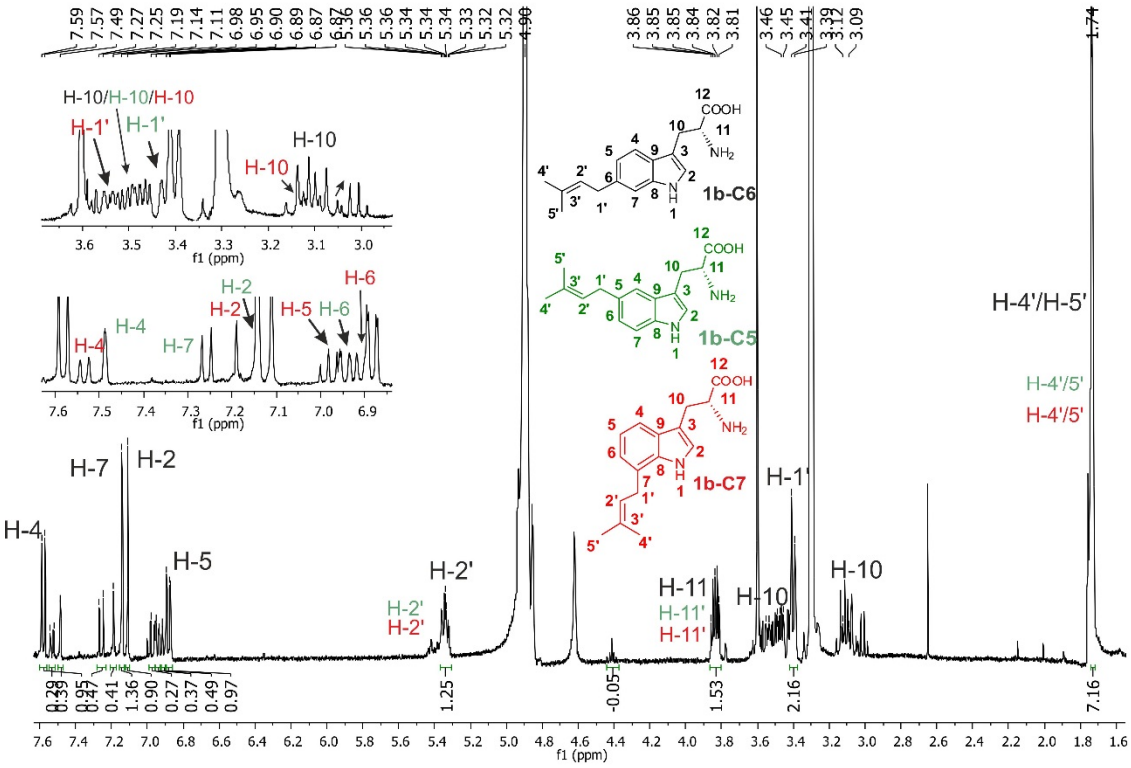

Fig. S56 ^{1}H NMR spectrum of the isolated enzyme product mixture of **1b-C5**, **1b-C6**, and -**1b-C7** of 5-DMATS$_{Sc}$ in CD_3OD (400MHz).

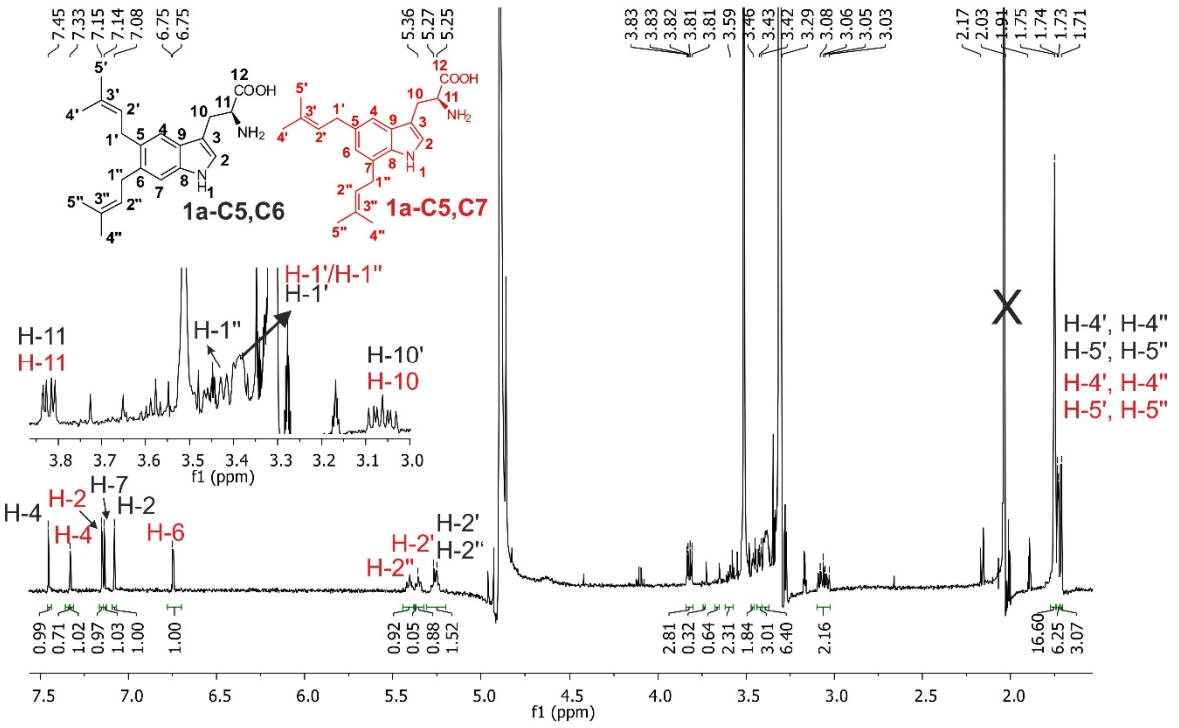

Fig. S57 ^{1}H NMR spectrum of the mixture of **1a-C5,C6** and **1a-C5,C7** in CD_3OD (500MHz)

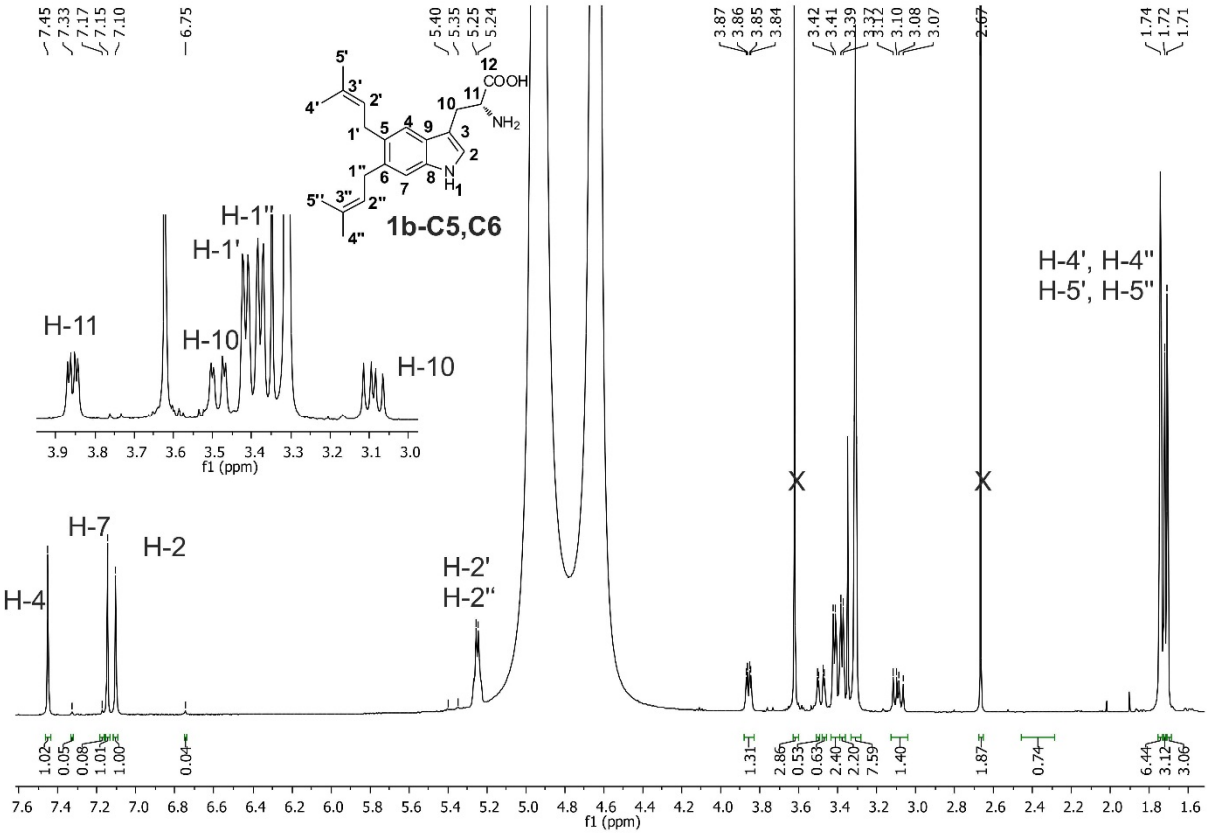

Fig. S58 ^{1}H NMR spectrum of **1b-C5,C6** in CD_3OD (500MHz)

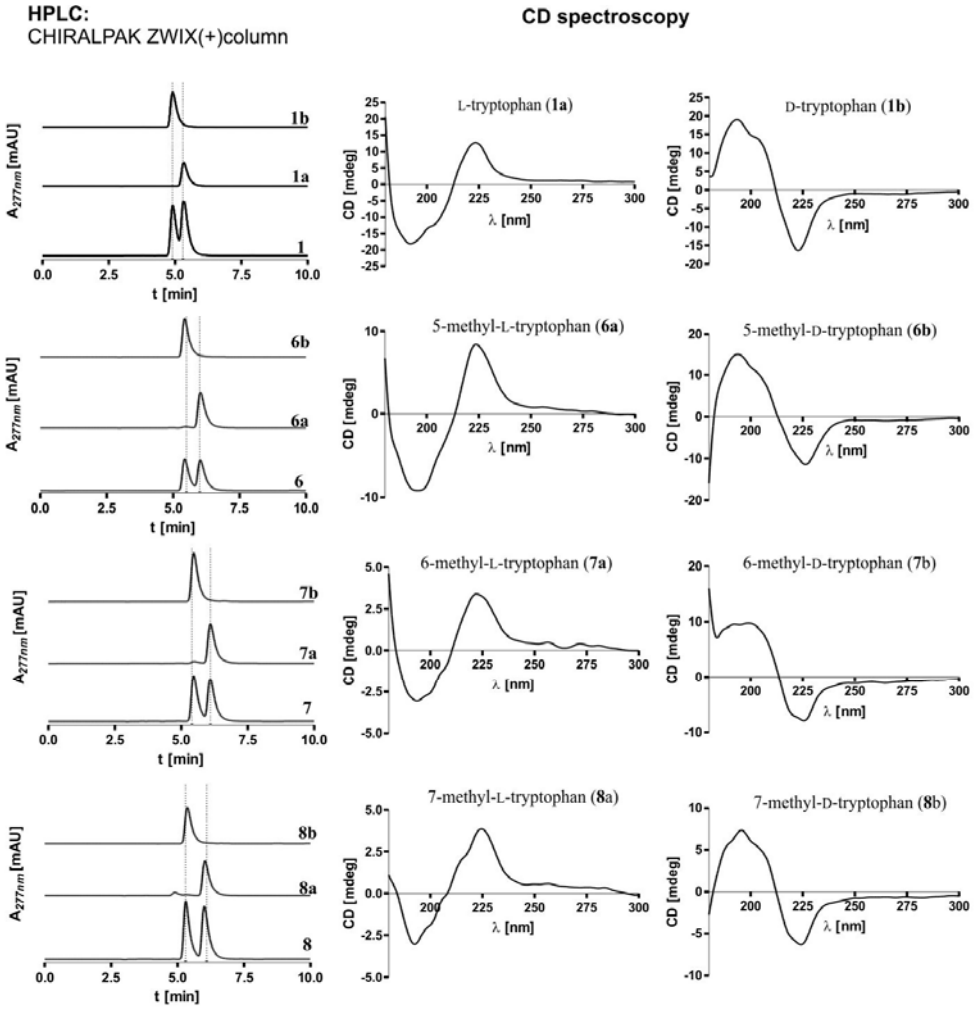

Fig. S59 CD spectra of the isolated L- and D-enantiomers. The enantiomers were isolated from racemate on a CHIRALPAK®Zwix(+) column and dissolved in water. CD spectra were recorded on a Jasco J-810 CD spectrometer in the wavelength range of 180-350 nm.

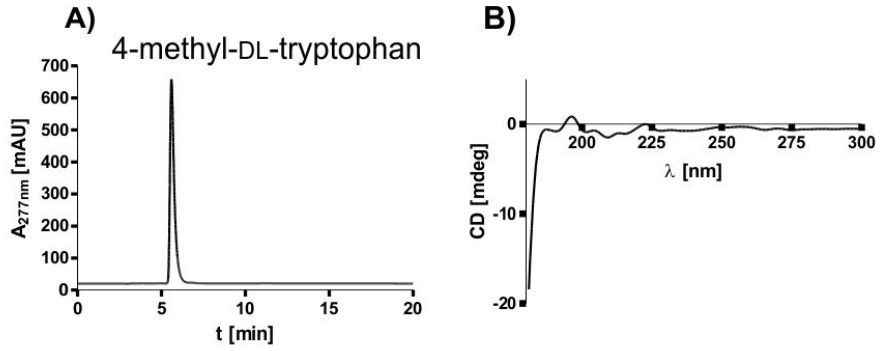

Fig. S60 HPLC chromatogram with CHIRALPAK®Zwix(+) column A) and CD-spectrum B) of 4-methyl-DL-tryptophan (**5**).

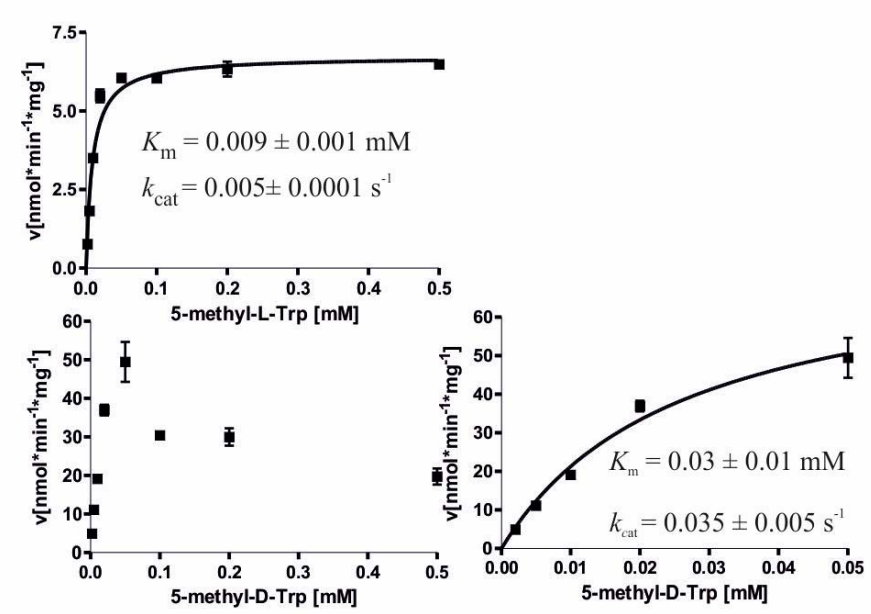

Fig. S61 Determination of the kinetic parameters of 5-DMATS$_{Sc}$ towards 5-methyl-L-tryptophan and 5-methyl-D-tryptophan. The reaction mixtures with 5-methyl-L-tryptophan contained 1 mM DMAPP, 5 mM $MgCl_2$ and 7.1 µM of the purified protein and were incubated at 37 °C for 15 min. The reaction mixtures with 5-methyl-D-tryptophan contained 1 mM DMAPP, 5 mM $MgCl_2$ and 473.9 nM of the purified protein and were incubated at 37 °C for 15 min.

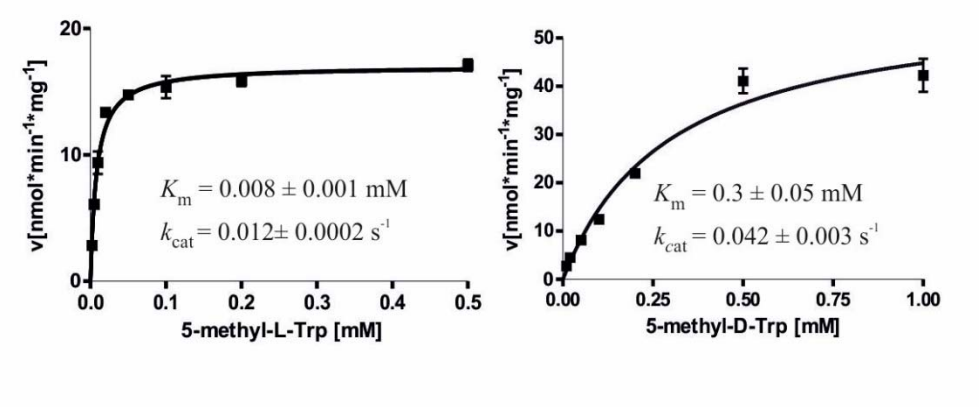

Fig. S62 Determination of the kinetic parameters for 6-DMATS$_{Mo}$ towards 5-methyl-L-tryptophan and 5-methyl-D-tryptophan. The reaction mixtures contained 1 mM DMAPP, 5 mM $MgCl_2$ and 459.8 nM of the purified protein and were incubated at 37 °C for 30 min.

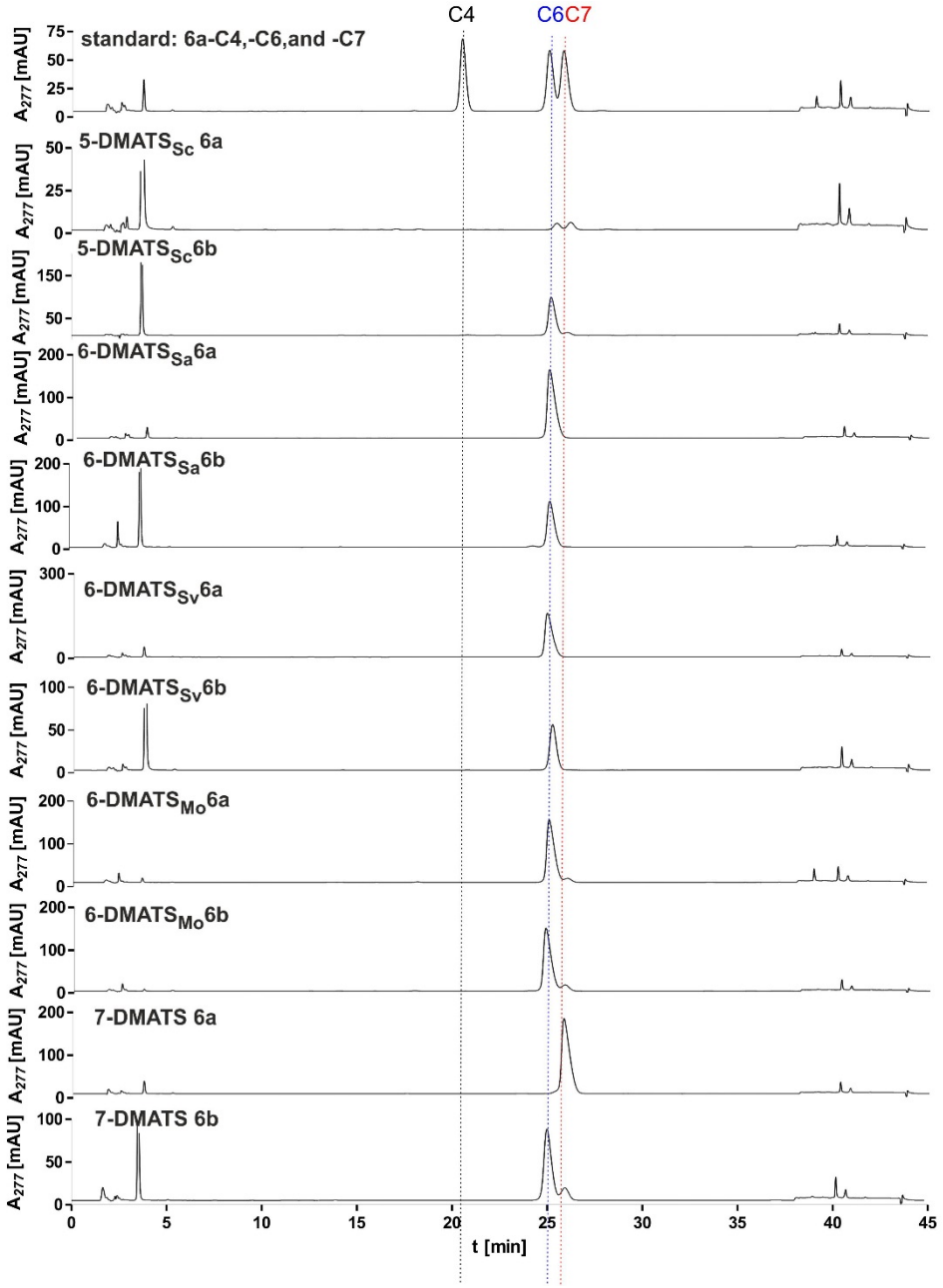

Fig. S63 HPLC analysis for identification of the enzyme products of 5-methyltryptophan. The enzyme assays contained 1 mM DMAPP and 0.5 mM of 5-methyl-L-tryptophan (**6a**) and 5-methyl-D-tryptophan (**6b**). Detailed conditions for the incubation mixtures are given in Table S9. For HPLC analysis, an Eclipse XDB-C18 column was used (condition 5 in Table S1). Detection was carried out with a Diode Array detector and illustrated for absorption at 277 nm.

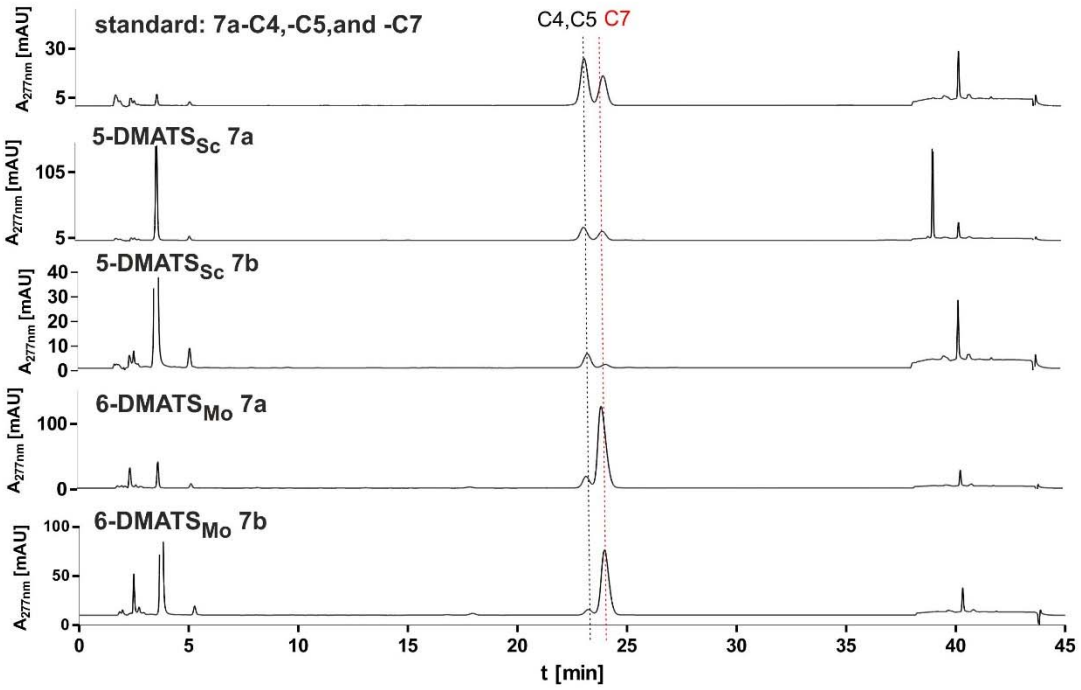

Fig. S64 HPLC analysis for identification of the enzyme products of 6-methyltryptophan. The enzyme assays contained 1 mM DMAPP and 0.5 mM of 6-methyl-L-tryptophan (**7a**) and 6-methyl-D-tryptophan (**7b**). Detailed conditions for the incubation mixtures are given in Table S9. For HPLC analysis, an Eclipse Plus-C18 column was used (condition 5 in Table S1). Detection was carried out with a Diode Array detector and illustrated for absorption at 277 nm.

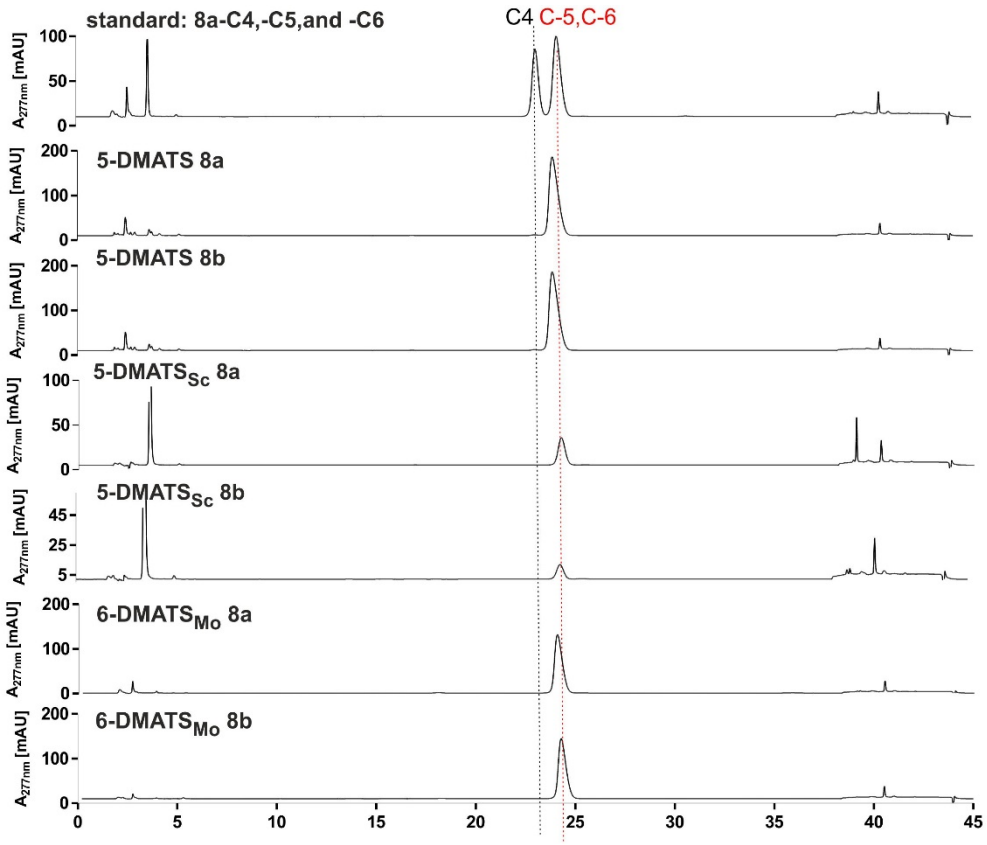

Fig. S65 HPLC analysis for identification of the enzyme products of 7-methyltryptophan. The enzyme assays contain 1 mM DMAPP and 0.5 mM of 7-methyl-L-tryptophan (**8a**) and 7-methyl-D-tryptophan (**8b**). Detailed conditions for the incubation mixtures are given in Table S9. For HPLC analysis, an Eclipse Plus-C18 column was used (condition 5 in Table S1). Detection was carried out with a Diode Array detector and illustrated for absorption at 277 nm.

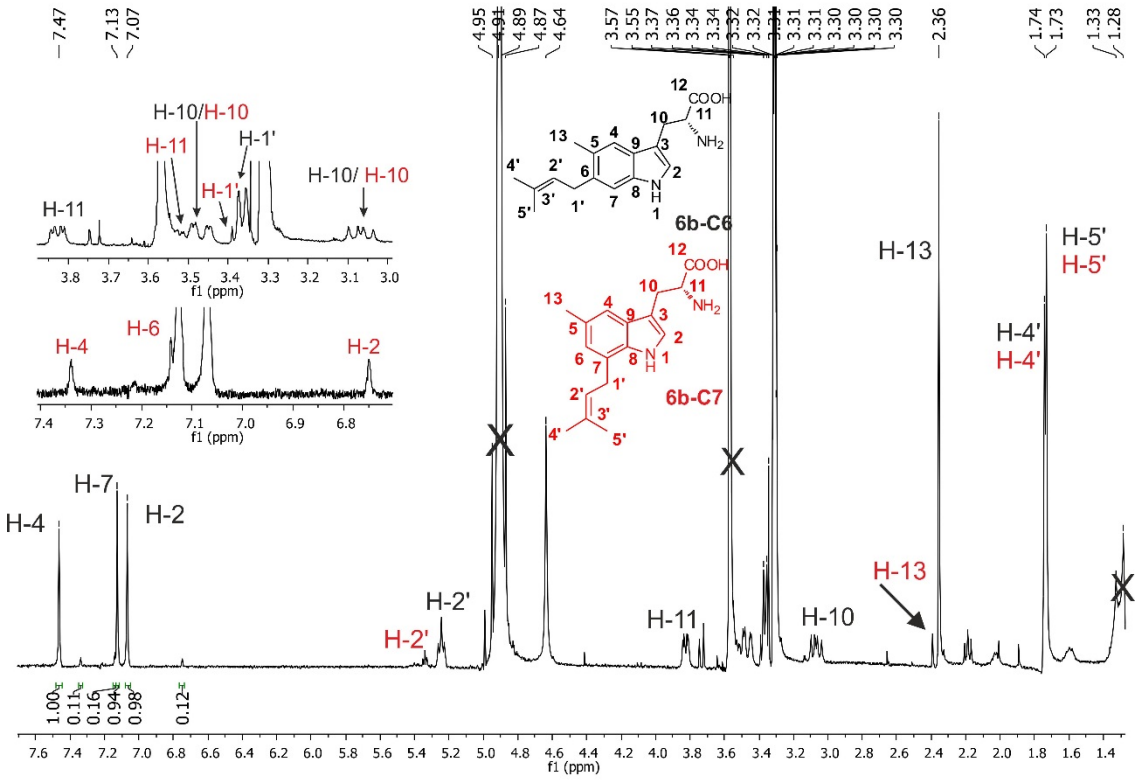

Fig. S66 ^{1}H NMR spectrum of the isolated enzyme product mixture of **6b-C6** and **6b-C7** of 5-DMATS$_{Sc}$ in CD_3OD (400MHz).

4.4. Prenyltransferases as key enzymes in primary and secondary metabolism

Appl Microbiol Biotechnol (2015) 99:7379–7397
DOI 10.1007/s00253-015-6811-y

MINI-REVIEW

Prenyltransferases as key enzymes in primary and secondary metabolism

Julia Winkelblech[1,2] · **Aili Fan**[1] · **Shu-Ming Li**[1,2]

Received: 4 May 2015 / Revised: 29 June 2015 / Accepted: 1 July 2015 / Published online: 28 July 2015

Abstract Attachment of isoprene units to various acceptors by prenylation plays an important role in primary and secondary metabolism of living organisms. Protein prenylation belongs to posttranslational modification and is involved in cellular regulation process. Prenylated secondary metabolites usually demonstrate promising biological and pharmacological activities. Prenyl transfer reactions catalyzed by prenyltransferases represent the key steps in the biosynthesis and contribute significantly to the structural and biological diversity of these compounds. In the last decade, remarkable progress has been achieved in the biochemical, molecular, and structural biological investigations of prenyltransferases, especially on those of the members of the dimethylallyltryptophan synthase (DMATS) superfamily. Until now, more than 40 of such soluble enzymes are identified and characterized biochemically. They catalyze usually regioselective and stereoselective prenylations of a series of aromatic substances including tryptophan, tryptophan-containing peptides, and other indole derivatives as well as tyrosine or even nitrogen-free substrates. Crystal structures of a number of prenyltransferases have been solved in the past 10 years and provide a solid basis for understanding the mechanism of prenyl transfer reactions.

✉ Shu-Ming Li
shuming.li@staff.uni-marburg.de

[1] Institut für Pharmazeutische Biologie und Biotechnologie, Philipps-Universität Marburg, Deutschhausstrasse 17A, D-35037 Marburg, Germany

[2] Zentrum für Synthetische Mikrobiologie, Philipps-Universität Marburg, D-35032 Marburg, Germany

Keywords Aromatic prenyltransferase · Dimethylallyltryptophan synthase · Peptide prenyltransferase · Phylogenetic relationships · Prenyl diphosphate synthase · Protein prenyltransferase · tRNA prenyltransferase

Introduction

Prenyltransferases catalyze the transfer reactions of prenyl moieties from different prenyl donors, e.g., dimethylallyl (DMAPP with a branched C_5-chain), geranyl (GPP, C_{10}), farnesyl (FPP, C_{15}), or geranylgeranyl (GGPP, C_{20}) diphosphate, to various aliphatic or aromatic acceptors of both low and high molecular substances including proteins and nucleic acids (Dumelin et al. 2012; Heide 2009a; Li 2009a; Oldfield and Lin 2012; Palsuledesai and Distefano 2015; Xie et al. 2007; Yazaki et al. 2009). The prenylation reactions can take place in regular manner (regular prenylation) by connection of the prenyl moieties via their C-1 to an acceptor or reverse manner (reverse prenylation) via their C-3 atoms (Heide 2009a; Yu and Li 2012).

Prenylated secondary metabolites including indole alkaloids, flavonoids, coumarins, xanthones, quinones, and naphthalenes are widely distributed in terrestrial and marine organisms (Fig. 1). They exhibit a wide range of biological activities such as cytotoxicity, antioxidant (Sunassee and Davies-Coleman 2012), and antimicrobial activities (Liu et al. 2013a; Oya et al. 2015), which are often distinct from their non-prenylated precursors. Prenyl transfer reactions usually represent the key steps in the biosynthesis of such compounds. Furthermore, the prenylated products can be further modified by cyclization, hydroxylation, oxidation, and so on (Raju et al. 2011; Tagami et al. 2013). Therefore, prenyltransferases

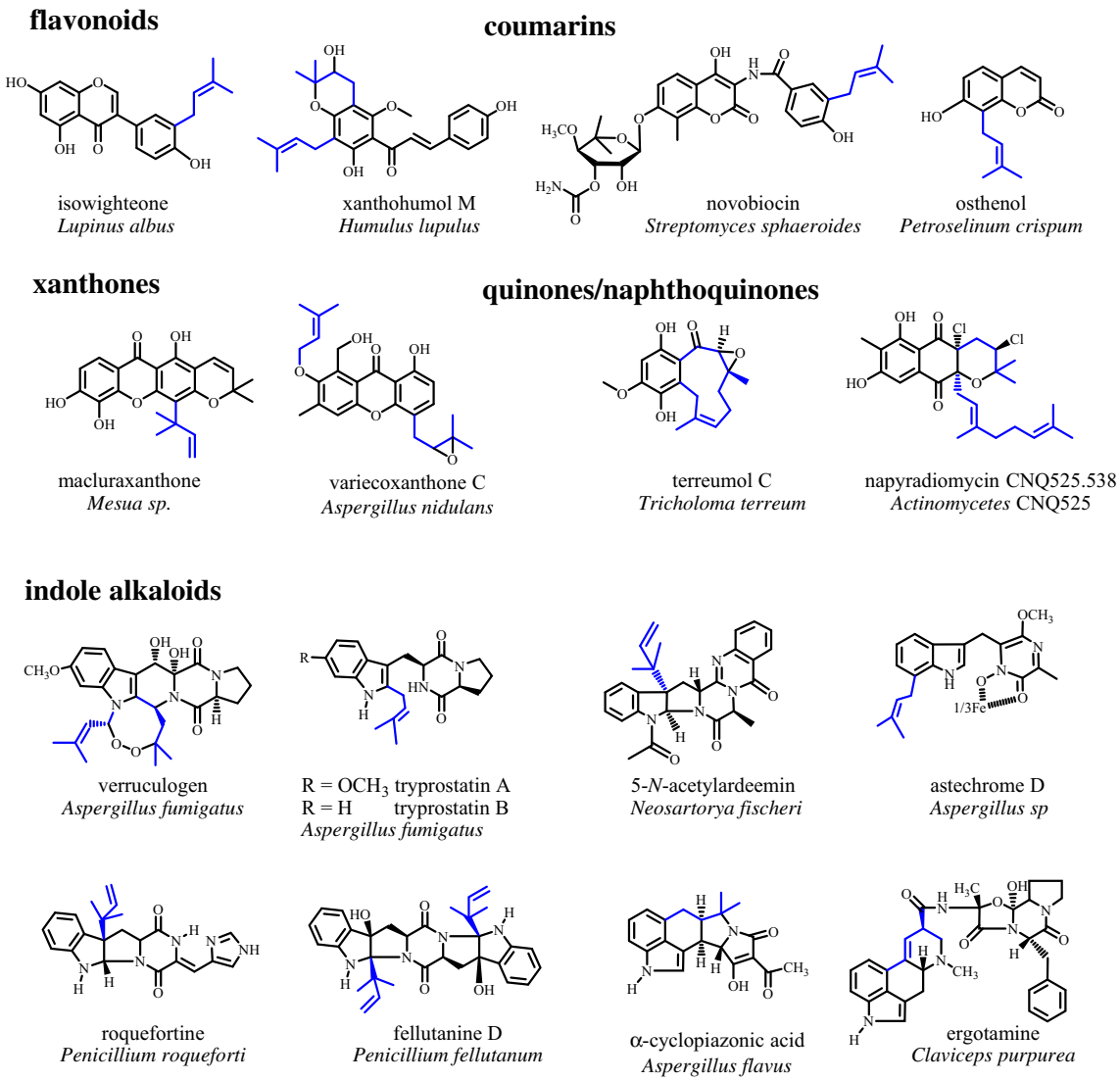

Fig. 1 Examples of prenylated natural products

contribute significantly to structural and biological diversity of natural products.

Based on their primary amino acid sequences, biochemical and structural characteristics, prenyltransferases are categorized into different subgroups (Table 1). Prenyl diphosphate synthases use prenyl diphosphate as donor and isopentenyl diphosphate (IPP) as acceptor (Oldfield and Lin 2012), while protein prenyltransferases catalyze the transfer reactions of C_{15} chain from FPP or C_{20} chain from GGPP to cysteine residues of proteins (Palsuledesai and Distefano 2015). Peptide prenyltransferases of the TruF family catalyze *O*-prenylations of tyrosyl residues of cyclic peptides in the presence of DMAPP. DMAPP and GPP serve as prenyl donors for tRNA prenyltransferases from bacteria (Dumelin et al. 2012; McIntosh et al. 2011, 2013; Xie et al. 2007). A large prenyltransferase group uses diverse nitrogen-containing and nitrogen-free aromatic compounds as substrates, and among them, the dimethylallyltryptophan synthase (DMATS) superfamily is one of the most investigated subgroup. The name of this superfamily was given due to their sequence similarity to DMATS involved in the biosynthesis of ergot alkaloids of *Claviceps* sp. (Tsai et al. 1995).

Since the first reviews on the DMATS enzymes in 2009 (Li 2009a, b; Steffan et al. 2009), significant progress has been achieved for this enzyme group. Thirty-two new enzymes have been characterized biochemically. The natural substrates of the DMATS enzymes were found to be much broader than just indole derivatives known at that time. Tyrosine, xanthones, tricyclic or tetracyclic aromatic or even nonaromatic compounds also serve as natural substrates of enzymes with sequence similarity to DMATS. In contrast, the spectrum of the natural prenyl donors of these enzymes is relatively narrow, and most of the members of the DMATS superfamily use DMAPP for prenylation. In addition, crystal structures of four DMATS enzymes were solved and used as basis for understanding

Table 1 Classification of prenyltransferases with their natural functions

Enzyme type	Donor	Acceptor (examples)	Function/biosynthesis
prenyl diphosphate synthases			
trans-prenyltransferases	prenyl diphosphate	isopentenyl diphosphate	all-*trans*-isoprenoids, terpenoids, steroids
cis-prenyltransferases	prenyl diphosphate	isopentenyl diphosphate	*trans*-/*cis*-isoprenoids, membrane components
peptide prenyltransferases	dimethylallyl, geranyl diphosphate	(cyclic) oligopeptides	pheromones/secondary metabolites
protein prenyltransferases	farnesyl or geranylgeranyl diphosphate	cysteine residue of proteins	posttranslational modification of proteins, cellular localization, protein-protein interaction
tRNA prenyltransferases	dimethylallyl and geranyl diphosphate	adenine or 5-methylaminomethyl-2-thiouridine	translational regulation
aromatic prenyltransferases			
membrane-bound prenyltransferases	prenyl diphosphate	benzoic & naphthoic acids, flavonoids	primary & secondary metabolites
soluble aromatic prenyltransferases			
NphB/CloQ group	dimethylallyl, geranyl and farnesyl diphosphate,	naphthalenes, quinones, phenols, phenazines	secondary metabolites
DMATS family	dimethylallyl, geranyl and farnesyl diphosphate	indole derivatives, tyrosine, naphthalenes, xanthones	secondary metabolites,

of the reaction mechanism. Since 2009, several reviews on different aspects of the DMATS superfamily, mainly on indole prenyltransferases, have appeared (Tanner 2014; Walsh 2014; Yu and Li 2012). A systematic summary covering classification, occurrence, natural function, biochemical properties, crystal structures, and reaction mechanism of this intriguing enzyme group is now necessary. For a better understanding of prenyltransferases as nxC_5 transferring enzymes onto diverse acceptors and their natural roles, we begin in this review with a brief overview on different classes of prenyltransferases and then focus on the members of the DMATS superfamily. In another mini-review in this issue, we will discuss the potential usage of DMATS prenyltransferases in biotechnology, which has been demonstrated by a large number of studies in the last years.

Classification of prenyltransferases

IPP and DMAPP, derived from the acetate-mevalonate or methylerythritol phosphate pathway (Boronat and Rodriguez-Concepcion 2015; Chang et al. 2013; Zhao et al. 2013), serve as precursors for prenyl diphosphate (nxC_5) biosynthesis (Oldfield and Lin 2012). The prenyl diphosphates can be used for the biosynthesis of different terpenoids by cyclization and oxidation or as prenyl donors for peptide, protein and tRNA prenyltransferases, or aromatic prenyltransferases. The donors, acceptors, products, and functions of different prenyltransferases are summarized in Table 1.

Prenyl diphosphate synthases

Over 63,000 isoprenoid natural products have been identified to date, which bear numerous important biological functions and show an enormous structural diversity based on their different carbon skeletons and substitutions (Liang et al. 2002; Ramamoorthy et al. 2015). In the biosynthesis of isoprenoids, prenyl diphosphate synthases catalyze the formation of the carbon backbone with defined chain length by sequential condensation of DMAPP or other prenyl diphosphates with a given number of IPP. According to the formed double bond configuration in the prenyl units, these chain elongating enzymes can be classified into two major groups, i.e., *trans*- and *cis*-prenyltransferases (Fig. 2).

FPP synthases (FPPase) belong to the first group and catalyze the formation of all-*trans* C_{15} precursor FPP by utilizing IPP as acceptor for the sequential condensations with DMAPP and GPP (Poulter 2006). FPP could serve as a precursor for a number of essential or important metabolites, e.g., sesquiterpenoids, triterpenoids, sterols, dolichols, and ubiquinones (Anderson et al. 1989).

GGPP synthases also belong to *trans*-prenyltransferases and catalyze, similar to FPPases, the formation of all-*trans* configured geranylgeranyl diphosphate. They are involved in the biosynthesis of plant secondary metabolites like diterpenoids or carotenoids (Liu et al. 2014b). Furthermore, octaprenyl diphosphate synthase (OPPS) catalyzes successive condensation reactions of FPP with five IPP to generate C_{40} products with *trans*-configured double bonds (Fig. 2). The resulted prenyl diphosphate can be used as donor for quinone

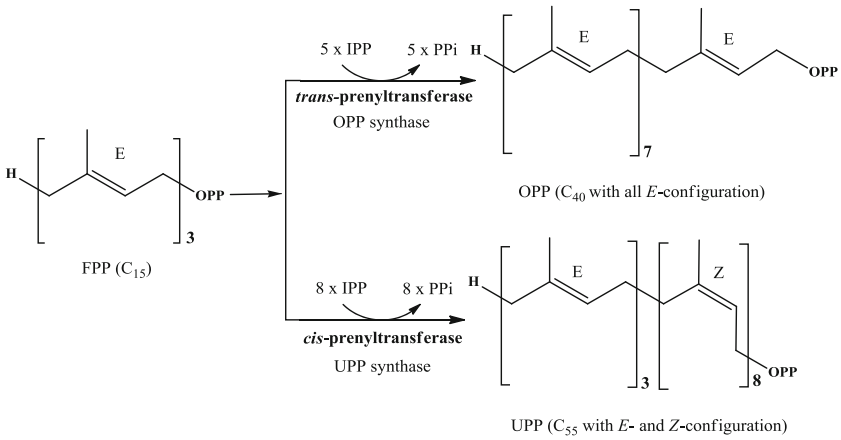

Fig. 2 Examples of prenyl diphosphate synthase reactions

prenylation in the biosynthesis of ubiquinone, menaquinone, or plastoquinones (Soballe and Poole 1999). The homodimeric enzymes of *trans*-prenyltransferases consist of α-helices with two conserved aspartate-rich DDxxD motifs, which allowed the binding of the substrates in complex with Mg^{2+} (Guo et al. 2004).

In contrast, *cis*-prenyltransferases produce prenyl diphosphates containing both *Z*- and *E*-configured double bonds, although they use the same substrates and their catalyzed reactions are Mg^{2+} dependent (Fig. 2). Their amino acid sequences and three-dimensional structures completely differ from those of *trans*-prenyltransferases. Instead of the DDxxD motif, an aspartate in the conserved P-loop of *cis*-prenyltransferases is involved in the chelating of Mg^{2+} (Guo et al. 2005). According to the length of their products, they are further classified into short- (C_{15}), medium- (C_{50}–C_{55}), and long-chain (C_{70}–C_{120}) *cis*-prenyltransferases (Lu et al. 2009; Takahashi and Koyama 2006). Undecaprenyl diphosphate synthase for example catalyzes the condensation of FPP with eight IPPs, resulting in the formation of a C_{55} product (Fig. 2). Undecaprenyl monophosphate acts as a lipid carrier in the peptidoglycan biosynthesis of bacterial cell wall and therefore serves as a target for antibacterial drugs (Danley et al. 2015).

Prenylated lipids are also found in membranes of archaeal bacteria. The geranylgeranylglyceryl phosphate synthase (GGGP synthase) from *Methanobacterium thermoautotrophicum*, which shows practically no homology to other prenyltransferases, catalyzes the alkylation of glyceryl phosphate in the presence of GGPP (Soderberg et al. 2001).

Peptide, protein, and tRNA prenyltransferases

The ComX pheromone identified in *Bacillus subtilis* is a hexapeptide containing a regularly *C3*-geranylated tryptophan residue. The responsible prenyltransferase ComQ was identified by overproduction in *Escherichia coli* (*E. coli*) and incubation with an oligopeptide comprising 58 amino acids in the presence of GPP. The C-terminal geranylated hexapeptide corresponding to the mature ComX pheromone was identified as a minor and a C-terminal geranylated heptapeptide as the main product (Tsuji et al. 2012).

Cyanobactins from *Lyngbya aestuarii* are cyclic heptapeptides containing regularly *C3*-prenylated tyrosyl residues. The prenyltransferase LynF uses cyclic heptapeptides as substrates and catalyzes regular and reverse *O*-prenylations of tyrosyl residues. The reversely prenylated enzyme products then undergo a Claisen rearrangement resulting in *C*-prenylated derivatives (McIntosh et al. 2011, 2013).

Protein prenyltransferases use polypeptides as substrates. They play an important role in the posttranslational modification of proteins in eukaryotes and represent interesting drug targets (Palsuledesai and Distefano 2015). They transfer either a farnesyl (C_{15}) or a geranylgeranyl (C_{20}) moiety to a conserved cysteine residue in a CaaX motif at the C-terminus of the targeted proteins or peptides (Palsuledesai and Distefano 2015; Perez-Sala 2007). These modifications are responsible for correct cellular localization and activity of several proteins including those from the Ras family. The primary sequences as well as the crystal structures of protein prenyltransferases clearly differ from that of the prenyl diphosphate synthases. For the Ras farnesyltransferase reaction, the formation of Zn^{2+}-activated thiolate by the cysteine residue of the CaaX box is necessary (Long et al. 2002). Due to the role of farnesylated proteins in oncogenic processes or several diseases including progeria, aging, parasitic diseases, and bacterial or viral infections, the underlying prenylation reaction and its inhibition by potential therapeutics have been extensively investigated (Abuhaie et al. 2013; Palsuledesai and Distefano 2015; Sousa et al. 2009; Zhu et al. 2014).

Modifications by prenylations are not only found in proteins, but also in nucleic acids, e.g., tRNAs. Two dimethylallyltransferases (DMATase) from *Pseudomonas aeruginosa* (*P. aeruginosa*) and *E. coli* were proven to prenylate the amino group of adenosine-37 (A37) of all tRNAs with uridine at the beginning (Xie et al. 2007).

Recently, SelU from *E. coli* was reported to catalyze *S*-geranylation of 5-methylaminomethyl-2-thiouridyl residue in tRNA in the presence of GPP (Dumelin et al. 2012).

Aromatic prenyltransferases

Aromatic prenyltransferases catalyze the transfer reactions of prenyl moieties onto aromatic acceptors such as phenols, phenolic acids, flavonoids, coumarins, naphthalenes, phenazines, or indole derivatives. These enzymes contribute substantially to the large diversity of prenylated secondary metabolites in plants, fungi, and bacteria (Heide 2009b; Li 2009b; Yazaki et al. 2009). They usually catalyze the formation of C–C, C–O, or C–N bonds between the carbon of the prenyl and carbon or functional groups of the aromatic substrates. Membrane-bound and soluble aromatic prenyltransferases were found to exhibit distinct characteristics such as structural fold, substrate binding motifs, or metal ion dependency.

Membrane-bound prenyltransferases for aromatic substrates

Members of this enzyme group are involved in the biosynthesis of both primary metabolites such as ubiquinones and menaquinones (Boronat and Rodriguez-Concepcion 2015; Meganathan and Kwon 2009) and secondary metabolites like microbial and plant natural products (Holm et al. 2014; Wang et al. 2014; Yazaki et al. 2009; Zeyhle et al. 2014a, b).

Ubiquinones and menaquinones function as electron and proton carrier in photosynthesis and cellular respiration and also as antioxidants for prevention of cell damage. Membrane-bound prenyltransferases contain, similar to the aforementioned FPPs, characteristic aspartate-rich motifs, e.g., NDxxDxxxD, and require metal ions such as Mg^{2+} for their catalytic activity. The underlying prenyl transfer reactions were observed for various aromatic substrates like 4-hydroxybenzoate (4HB), homogentisic acid, coumarines, flavonoids, 1,4-dihydroxy-2-naphthoate, or phenazines (Heide 2009a; Karamat et al. 2014; Yazaki et al. 2009; Zeyhle et al. 2014a, b). Several examples of membrane-bound prenyltransferases and their catalyzed reactions are summarized in Table 2. UbiA from *E. coli* as a prototype of this family plays an important role in the biosynthesis of ubiquinones and catalyzes the attachment of an all-*trans* octaprenyl moiety onto 4HB (Melzer and Heide 1994). UbiA shows a broad substrate specificity toward prenyl donors and is able to generate ubiquinones CoQ_6 to CoQ_{10} in different species (Cheng and Li 2014). Recently, the crystal structure of an archeal UbiA was reported (Cheng and Li 2014), which provides new insights into the substrate binding sites and mechanism of the enzyme catalysis. Very recently, a prenyltransferase UbiX from *P. aeruginosa* involved in the biosynthesis of ubiquinones was demonstrated to use flavin as a prenyl acceptor. In contrast to prenyl diphosphates for other known prenyltransferases, dimethylallyl monophosphate (DMAP) serves as prenyl donor for UbiX reaction (White et al. 2015).

In human cells, COQ2 is involved in the biosynthesis of ubiquinone for mitochondrial respiration, while UBIAD1 in the biosynthesis of vitamin K for maintaining vascular homeostasis (Hegarty et al. 2013; Nakagawa et al. 2010). UbiA homologs, e.g., AtPPT1 from *Arabidopsis thaliana* (*A. thaliana*) and OsPPT1 from *Oryza sativa*, were found to be involved in primary metabolism of plants (Okada et al. 2004; Ohara et al. 2006). In plants, membrane-bound aromatic prenyltransferases are also involved in the biosynthesis of secondary metabolites. The 4HB geranyltransferases LePGT-1 and LePGT-2 from *Lithospermum erythrorhizon* are involved in the biosynthesis of the naphthoquinone shikonin (Yazaki et al. 2002). In contrast to the 4HB prenyltransferases for ubiquinone biosynthesis, these enzymes are localized in the endoplasmatic reticulum rather than in mitochondria. They show strict substrate specificity for GPP as prenyl donor. Several members of the membrane-bound prenyltransferases are involved in the biosynthesis of prenylated flavonoids and isoflavonoids in plants. N8DT, G6DT, and SfiLDT from *Sophora flavescens* catalyze the prenylations of naringenin, genistein, and isoliquiritigenin, respectively (Chen et al. 2013; Sasaki et al. 2011). Furthermore, the formation of *C3′*-prenylated genistein was detected in vitro with LaPT1 from *Lupinus albus* (Shen et al. 2012). Pterocarpan 4-dimethylallytransferase (G4DT) catalyzes the transfer of a dimethylallyl moiety onto pterocarpan skeleton and is therefore responsible for the formation of the soybean phytoalexin glyceollin (Akashi et al. 2009). In plants, three kinds of homogentisic acid prenyltransferases use solanesyl (C_{45}), geranylgeranyl (C_{20}), and phytyl (C_{20}, partially saturated) diphosphate for their prenylation reactions in the biosynthesis of plastoquinones, tocotrienols, and tocopherols, respectively (Heide 2009a). The last two compounds are also known as vitamin E. Moreover, 1,4-dihydroxy-2-naphthoate serves as substrate for the octaprenyltransferase MenA in *E. coli* and for the phytyltransferase ABC4 in phylloquinone biosynthesis in *A. thaliana* (Shimada et al. 2005; Suvarna et al. 1998). In addition, chlorophyllide and protoheme IX were used by chlorophyll synthase ATG4 (Eckhardt et al. 2004) and protoheme IX farnesyltransferase COX10, both from *A. thaliana*, respectively (Saiki et al. 1993). Furthermore, two membrane-bound prenyltransferases were found to catalyze three sequential prenylation steps in the biosynthesis of bitter acid in hop (Li et al. 2015). PcPT from parsley was found to be a key enzyme in the biosynthesis of linear and angular furanocoumarins and to catalyze prenylations of umbelliferon at both C-6 and C-8 positions (Karamat et al. 2014).

Membrane-bound aromatic prenyltransferases were also identified for the secondary metabolism in bacteria. One

Table 2 Examples of membrane-bound prenyltransferases and their catalyzed reactions

Enzyme (accession number)	Organism	Substrate	Product	Biosynthetic pathway	Reference
UbiA (WP_000455227)	*E. coli*	 4-hydroxybenzoic acid	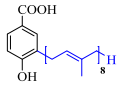 3-octaprenyl-4-hydroxybenzoic acid	ubiquinones	(Melzer and Heide 1994)
LePGT-1 (BAB84122)	*L. erythrorhizon*	 4-hydroxybenzoic acid	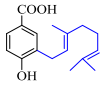 3-geranyl-4-hydroxybenzoic acid	shikonin	(Yazaki et al. 2002)
G4DT (BAH22520)	*Glycine max*	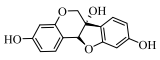 (-)-glycinol	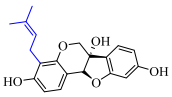 4-dimethylallylglycinol	glyceollin	(Akashi et al. 2009)
AuaA (CCA65701)	*Stigmatella aurantiaca*	 2-methyl-4-hydroxy-quinoline	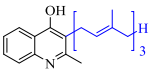 aurachin D	aurachin A	(Stec et al. 2011)
HlPT-1 (BAJ61049)	*H. lupulus*	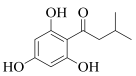 phlorisovalerophenone	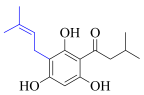 prenyl phlorisovalerophenone	bitter acid	(Tsurumaru et al. 2012)
PcPT (BAO31627)	*P. crispum*	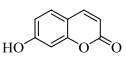 umbelliferone	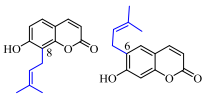 osthenol + demethylsuberosin (DMS)	furanocoumarin	(Karamat et al. 2014)
CnqPT1 (AIT42139)	*Streptomyces sp. CNQ-509*	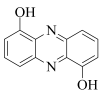 1,6-dihydroxy phenazine	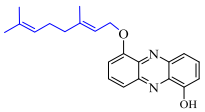 marinophenazine B	marinophenazine	(Zeyhle et al. 2014b)

E. Escherichia, *L. Lithospermum*, *P. Petroselinum*, *H. Humulus*

example is the farnesyltransferase AuaA from the myxobacterium *Stigmatella aurantiaca* in the biosynthesis of aurachins, which catalyzes the farnesylation of 2-methyl-4-hydroxyquinoline (Stec et al. 2011). Very recently, two membrane-bound aromatic prenyltransferases were identified in *Streptomyces* and found to be responsible for phenazine prenylations (Zeyhle et al. 2014a, b).

Soluble prenyltransferases with PT barrel mostly for aromatic substrates

The large enzyme group for prenylation of aromatic substrates comprises the CloQ/NphB group and the extensively investigated DMATS superfamily, which are soluble proteins from bacteria and fungi. One common structural feature of these enzymes is their *aßßa*-fold (ABBA), termed PT-barrel and firstly observed for the naphthalene geranyltransferase NphB (Kumano et al. 2008; Kuzuyama et al. 2005).

Enzymes of the CloQ/NphB subgroup

Known prenyltransferases of the CloQ/NphB group use only aromatic compounds as substrates and catalyze prenylations of naphthalenes, phenazines, quinones, and phenolic compounds (Table 3) (Heide 2009a). They were found in both bacteria and fungi and differ strongly from the aforementioned membrane-bound prenyltransferases (Haug-Schifferdecker et al. 2010). They do not contain the aspartate-rich NDxxD motif, and their reactions are with the exception of that for NphB independent of divalent metal ions (Bonitz et al. 2011; Heide 2009a). The notation of the subgroup referred to the first identified enzyme CloQ from *Streptomyces roseochromogenes* and the 2 years later

reported NphB from *Streptomyces* sp. (Kuzuyama et al. 2005; Pojer et al. 2003). CloQ and its ortholog NovQ from *Streptomyces spheroides* catalyze the prenylation of 4-hydroxyphenylpyruvic acid in the biosynthesis of clorobiocin (Pojer et al. 2003) and novobiocin (Steffensky et al. 2000) (Fig. 1). NphB is involved in the biosynthesis of the geranylated derivative naphterpin (Kuzuyama et al. 2005). The crystal structures of NphB, CloQ, and EpzP share an ABBA barrel in common (Kuzuyama et al. 2005; Metzger et al. 2010; Wierenga et al. 2010; Zocher et al. 2012). These structures can serve as basis for molecular modeling studies and therefore provide valuable contributions to our knowledge on mechanisms of the prenyl transfer reactions (Bayse and Merz 2014; Yang et al. 2012). Furthermore, NphB shows a broad substrate specificity toward several phenolic compounds, e.g., resveratrol, flavonoids, and 4-HPP (Heide 2009a; Kumano et al. 2008; Kuzuyama et al. 2005). In the last years, several additional prenyltransferases of the CloQ/NphB group have been identified. SCO7190, a homolog of NphB from *Streptomyces coelicolor* A3(2), catalyzes the attachment of the dimethylallyl from DMAPP, but not geranyl moiety from GPP onto 1,6-dihydroxynaphthalene (Kumano et al. 2008; Kuzuyama et al. 2005). SCO7190 and NovQ were successfully used for production of novel prenylated polyphenols in transgenic plants (Sugiyama et al. 2011). Fnq26 from *Streptomyces cinnamonensis* DSM 1042 shares a sequence identity of 40 % with NphB and catalyzes reverse and regular *C*- as well as regular *O*-prenylations of several phenolic substrates (Haagen et al. 2007). Recently, McI23 from *Streptomyces* sp. CNH-189 was found to catalyze the formation of a prenylated precursor of merochlorin by utilizing a diphosphate of an unusual branched C_{15} unit as prenyl donor, which was formed by addition of a dimethylallyl moiety to GPP in a reverse manner catalyzed by Mcl22 (Teufel et al. 2014). In the secondary metabolism of *Streptomyces cinnamonensis* and *Streptomyces anulatus*, EpzP and PpzP catalyze the regiospecific *C9*-prenylation of 5,10-dihydrophenazine-1-carboxylic acid (Saleh et al. 2009; Seeger et al. 2011). As aforementioned, prenylation of phenazine derivatives can also be catalyzed by membrane-bound prenyltransferases (Table 3) (Zeyhle et al. 2014a, b). DzmP from *Micromonospora* sp. RV115 is the first member of this subgroup which utilize FPP instead of DMAPP and GPP as prenyl donor and catalyzes the unusual *N*-farnesylation of dibenzodiazepinone (Bonitz et al. 2013).

Enzymes of the DMATS superfamily

The DMATS superfamily is the most investigated subgroup among the prenyltransferases. In the last years, enormous advances have been achieved on the biochemical, molecular, and structural biological investigations of these soluble enzymes. So far, more than 40 such enzymes from fungi and bacteria have been identified mostly by genome mining and characterized biochemically by using the recombinant proteins (Fan et al. 2014; Pockrandt et al. 2014; Winkelblech and Li 2014; Wunsch et al. 2015; Yu et al. 2012; Yu and Li 2012). They mainly catalyze the prenylation of indole derivatives including tryptophan and tryptophan-containing cyclic dipeptides. DMATS prenyltransferases carry no aspartate-rich motifs and their catalysis is independent of the presence of metal ions, although Ca^{2+}, Mg^{2+}, or other metal ions strongly enhance their activities in several cases (Li 2009a; Pockrandt et al. 2012; Yu and Li 2012).

The first member of the DMATS superfamily was the tryptophan *C4*-prenyltransferase DmaW involved in the biosynthesis of ergot alkaloids in *Claviceps fusiformis*, reported as *Claviceps purpurea* (*C. purpurea*) (Gebler and Poulter 1992; Tsai et al. 1995). Its ortholog FgaPT2 from *Aspergillus fumigatus* (*A. fumigatus*) was identified in 2005 by genome mining using the DmaW sequence from *C. purpurea* (Tudzynski et al. 1999; Unsöld and Li 2005). Until now, 12 enzymes were identified, which catalyze different prenylations of tryptophan at N-1 and C-4 to C-7 (Table 4) (Li 2010; Yu and Li 2012). Cyclic (di)peptide or related prenyltransferases with 14 members build the largest group, which catalyze the prenylations at N-1, C-2, C-3, and C-7 of the indole ring (Table 5). In addition, a large number of indole derivatives were identified as substrates of these enzymes (Table 6). Two members of the DMATS superfamily, SirD and TyrPT, use tyrosine as substrate and catalyze *O*-prenylation (Table 6) (Fan et al. 2014; Kremer and Li 2010). Since 2010, nitrogen-free or nonaromatic compounds were identified as substrates of additional 16 prenyltransferases of the DMATS superfamily (Table 6). In total, 19 such enzymes have been characterized biochemically so far.

Tryptophan prenyltransferases

As summarized in Table 4, 12 tryptophan prenyltransferases, five from bacteria and seven from fungi, were identified and characterized biochemically. These enzymes catalyze the formation of dimethylallyltryptophan and therefore also termed DMATSs. As aforementioned, DmaW from *C. fusiformis* was identified as the first enzyme from the DMATS superfamily and catalyzes the first pathway-specific step in the biosynthesis of ergot alkaloids, i.e., the prenylation of tryptophan at C-4 of the indole ring (Gerhards et al. 2014; Tsai et al. 1995). With the identification and characterization of its ortholog, FgaPT2 from *A. fumigatus* in 2005 began the systematic study on the enzymes of the DMATS superfamily by genome mining and biochemical investigation (Unsöld and Li 2005).

Table 3 Examples of prenyltransferases of the CloQ/NphB subgroup and their catalyzed reactions

Enzyme (accession number)	Organism	Substrate	Product	Biosynthetic pathway	References
CloQ/NovQ (AAN65239)/(AAF67510)	*Streptomyces roseochromogenes*/ *Streptomyces spheroids*	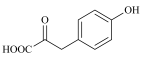 4-hydroxyphenylpyruvic acid	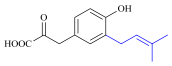 3-dimethylallyl-4-hydroxyphenylpyruvic acid	clorobiocin/ novobiocin	(Pojer et al. 2003)/(Ozaki et al. 2009)
NphB (1ZB6_A)	*Streptomyces sp.*	 1,6-dihydroxynaphthalene	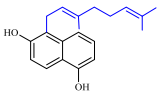 5-geranyl-1,6-dihydroxynaphthalene	naphterpin	(Kuzuyama et al. 2005)
SCO7190 (NP_631248)	*Streptomyces coelicolor* A3(2)	 1,6-dihydroxynaphthalene	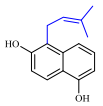 5-dimethylallyl-1,6-dihydroxynaphthalene	unknown	(Kumano et al. 2008)
Fnq26 (CAL34104)	*Streptomyces cinnamonensis*	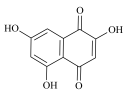 flaviolin	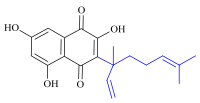 3-geranyl-flaviolin	furano-naphthoquinone	(Haagen et al. 2007)
McI23 (AGH68908)	*Streptomyces sp* CNH-189	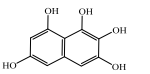 1,3,6,8-tetrahydroxynaphthalene	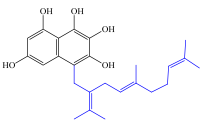 pre-merochlorin	merochlorin A & B	(Teufel et al. 2014)
EpzP/PpzP (ADQ43372)/(CAX48655)	*Streptomyces cinnamonensis*/ *Streptomyces anulatus*	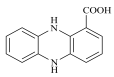 5,10-dihydrophenazine-1-carboxylic acid	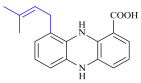 5,10-dihydrophenazine A	endophenazine	(Seeger et al. 2011)/(Saleh et al. 2009)
DzmP (AHG27152)	*Micromonospora sp.*	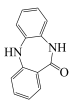 dibenzodiazepinone	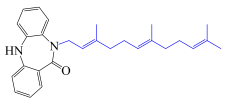 *N10*-farnesyl-dibenzodiazepinone	diazepinomicin	(Bonitz et al. 2013).

Later, two additional fungal 4-DMATS, i.e., DmaW-Cs from *Periglandula* (Markert et al. 2008; Steiner et al. 2011) and *Malbranchea* (Ding et al. 2008), were also identified. Identification of 7-DMATS from *A. fumigatus* as a tryptophan *C7*-prenylating enzyme obligated to donate the position of the prenyl moiety at the indole ring of tryptophan for prenyltransferase names. 7-DMATS was proven to be involved in the biosynthesis of hexadehydroastechrome (Yin et al. 2013c). Identification of 5-DMATS from *A. clavatus* filled the last gap of prenylation positions of fungal tryptophan and tryptophan-containing cyclic dipeptide prenyltransferases (Yu et al. 2012).

The first bacterial tryptophan prenyltransferase CymD was identified in *Salinispora arenicola* and catalyzes the *N1*-prenylation at the indole ring in the biosynthesis of the anti-inflammatory cyclomarin A and the antibacterial cyclomarazine A (Schultz et al. 2010). Later, four further bacterial DMATSs catalyzing the prenylations at *C-5* and *C-6* of the indole ring were identified from different *Streptomyces* strains (Subramanian et al. 2012; Takahashi et al. 2010; Winkelblech and Li 2014). Heterologous expression of the 5-DMATS gene *SCO7467* with the flavin-dependent monooxygenase gene *SCO7468* from *Streptomyces coelicolor* in *Streptomyces lividans* resulted in the formation of 5-dimethylallylindole-3-acetonitrile (Ozaki et al. 2013). IptA from *Streptomyces* sp. SN-593 was found to prenylate tryptophan at C-6 in the biosynthesis of 6-DMAI-3-carbaldehyde (Takahashi et al. 2010). 6-$DMATS_{Sa}$ from *Streptomyces ambofaciens* and 6-$DMATS_{Sv}$ from *Streptomyces violaceusniger* were identified as homologs of IptA. 6-$DMATS_{Sa}$ and 6-$DMATS_{Sv}$ can also utilize GPP as a prenyl donor and catalyze

Table 4 Tryptophan prenyltransferases and their catalyzed reactions

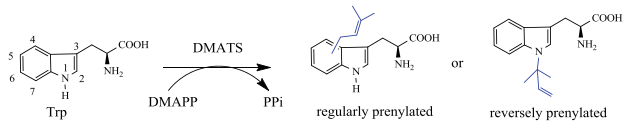

Enzyme (accession number)	Organism	Prenylation	Biosynthetic pathway	Reference
CymD (ABW00334)	*Sa. arenicola*	*N1*-reverse	cyclomarin/cyclomarazine	(Schultz et al. 2010)
DmaW (AAC18893)	*C. fusiformis*	*C4*-regular	ergot alkaloids	(Tsai et al. 1995)
FgaPT2 (AAX08549)	*A. fumigatus*	*C4*-regular	fumigaclavine C	(Unsöld and Li 2005)
DmaW-Cs (AAZ29613)	*Periglandula*	*C4*-regular	ergot alkaloids	(Markert et al. 2008; Steiner et al. 2011)
MaPT (EU4200091)	*M. aurantiaca*	*C4*-regular	unknown	(Ding et al. 2008)
5-DMATS (EAW08391)	*A. clavatus*	*C5*-regular	unknown	(Yu et al. 2012)
5-DMATS$_{Sc}$ (NP_631515)	*S. coelicolor*	*C5*-regular	5-DMAI-3-acetonitrile	(Subramanian et al. 2012)
IptA (BAJ07990)	*Streptomyces sp*	*C6*-regular	6-DMAI-3-carbaldehyde	(Takahashi et al. 2010)
6-DMATS$_{Sa}$ (CAJ89640)	*S. ambofaciens*	*C6*-regular	unknown	(Winkelblech and Li 2014)
6-DMATS$_{Sv}$ (AEM87819)	*S.violaceusniger*	*C6*-regular	unknown	(Winkelblech and Li 2014)
7-DMATS (ABS89001)	*A. fumigatus*	*C7*-regular	astechrome	(Kremer et al. 2007)
7-DMATS^{Neo} (not available)	*Neosartorya sp.*	*C7*-regular	unknown	(Miyamoto et al. 2014)

A. Aspergillus, *C. Claviceps*, *M. Malbranchea*, *S. Streptomyces*, *Sa. Salinispora*

prenylations at the same position as for DMAPP, which had not been reported for tryptophan prenyltransferases before (Winkelblech and Li 2014).

Tryptophan-containing cyclic dipeptide and related prenyltransferases

Tryptophan-containing cyclic dipeptide prenyltransferases catalyze regiospecific prenylations at different positions of the indole ring, especially at N-1, C-2, C-3, and C-7 (Grundmann and Li 2005; Wunsch et al. 2015; Yin et al. 2009, 2010, 2013a; Zou et al. 2010). Some peptide-related substances like *cyclo*-acetoacetyl-L-tryptophan (cAATrp) or ardeemin FQ, a derivative of the cyclic tripeptide of anthranilic acid, alanine, and tryptophan, were also identified as substrates of this subgroup (Haynes et al. 2013; Liu and Walsh 2009). Until now, 14 enzymes from this group have been characterized biochemically (Table 5). With the exception of the two geranyltransferases, LtxC from the cyanobacterium *Lyngbya majuscule* and TleC from the actinomycetes *Streptomyces blastmyceticus*, all other 12 enzymes are identified in fungi of *Aspergillus* and *Neosartorya* species.

The first identified cyclic dipeptide prenyltransferase was FtmPT1 from *A. fumigatus*, which catalyzes a regular *C2*-prenylation of brevianamide F (*cyclo*-L-Trp-L-Pro) in the biosynthesis of verruculogen/fumitremorgins (Grundmann and Li 2005; Li 2011). Three cyclic dipeptide reverse *C2*-prenyltransferases, NotF from an *Aspergillus* sp. and BrePT from *Aspergillus versicolor* involved in the biosynthesis of notoamides as well as CdpC2PT from *Neosartorya fischeri* (*N. fischeri*), were identified 5 years later (Table 5) (Ding et al. 2010; Mundt and Li 2013; Yin et al. 2013a). CdpC2PT was speculated to be involved in the biosynthesis of fellutanine (Mundt and Li 2013). Recently, a regular cyclic dipeptide *C7*-prenyltransferase CdpC7PT was identified in *Aspergillus terreus* (*A. terreus*) (Wunsch et al. 2015), with much higher regioselectivity and substrate flexibility toward cyclic dipeptides than CTrpPT, an *N1*- and *C7*-prenyltransferase from *Aspergillus oryzae* (*A. oryzae*) (Zou et al. 2010). CdpC7PT also accepted *cyclo*-L-Tyr-L-Tyr as substrate and catalyzed an *O*-prenylation at the tyrosyl residue, providing the first example from the DMATS superfamily with an *O*-prenyltransferase activity toward tyrosine-containing dipeptides (Wunsch et al. 2015). CdpNPT from *A. fumigatus* was reported to catalyze an *N1*-prenylation of cyclic dipeptides (Yin et al. 2007). The prenylation position was later revised to C-3 of the indoline ring (Schuller et al. 2012; Yu et al. 2013).

The DMATS enzymes catalyze not only regiospecific, but also stereospecific prenylations. For example, AnaPT from *N. fischeri* is involved in the biosynthesis of acetylaszonalenin and catalyzes a reverse *C3α*-prenylation of (R)-benzodiazepinedinone, while CdpNPT from *A. fumigatus* and CdpC3PT from *N. fischeri* the reverse *C3ß*-prenylations of cyclic dipeptides (Schuller

Table 5 Tryptophan-containing peptide or peptide-related prenyltransferases and their catalyzed reactions

Enzyme (accession number, pdb code)	Organism	Aromatic substrate[a]	Prenylation	Biosynthetic pathway	Reference
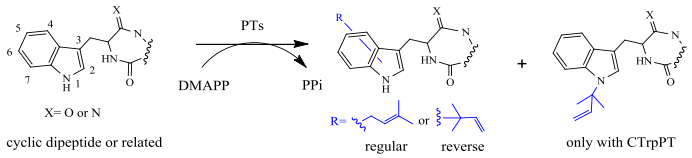 cyclic dipeptide or related				only with CTrpPT	
CTrpPT (GU722589)	*A. oryzae*	c-L-Trp-L-Trp	*N1*-reverse, *C7*-regular	unknown	(Zou et al. 2010)
FtmPT1 (AAX56314/3O2K)	*A. fumigatus*	c-L-Trp-L-Pro	*C2*-regular	fumitremorgin/ verruculogen	(Grundmann and Li 2005)
NotF (ADM34132)	*Aspergillus* sp.	c-L-Trp-L-Pro	*C2*-reverse	notoamide	(Ding et al. 2010)
BrePT (AFM09725)	*A. versicolor*	c-L-Trp-L-Pro	*C2*-reverse	brevianamide	(Yin et al. 2013a)
CdpC2PT (EAW25546)	*N. fischeri*	c-L-Trp-L-Trp	*C2*-reverse	fellutanine	(Mundt and Li 2013)
CpaD-Af (EED51182)	*A. flavus*	c-AA-L-Trp	*C4*-regular	cyclopiazonic acid	(Liu and Walsh 2009)
CpaD-Ao (BAE59503)	*A. oryzae*	c-AA-L-Trp	*C4*-regular	cyclopiazonic acid	(Liu and Walsh 2009)
CdpC7PT (EAU36020)	*A. terreus*	c-D-Trp-Ant	*C7*-regular	unknown	(Wunsch et al. 2015)
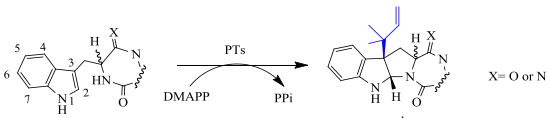 cyclic dipeptide or related; reversely prenylated					
AnaPT (EAW16181/4LD7)	*N. fischeri*	c-D-Trp-Ant	*anti-cis C3*-reverse	acetylaszo-nalenin	(Yin et al. 2009)
CdpNPT (ABR14712/4E0U)	*A. fumigatus*	c-L -Trp-Ant	*syn-cis -C3*-reverse	unknown	(Schuller et al. 2012)
CdpC3PT (EAW17508)	*N. fischeri*	c-L-Trp-L-Leu	*syn-cis-C3*-reverse	roquefortine (?)	(Yin et al. 2010)
ArdB (n.a.)	*A. fischeri*	ardeemin FQ	*syn-cis-C3*-reverse	ardeemin	(Haynes et al. 2013)
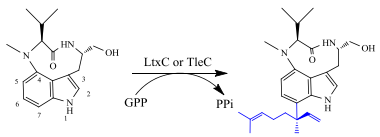 (-)-indolactam V; lyngbyatoxin A					
LtxC (AAT12285)	*L. majuscula*	(-)-indolactam V	*C7*-reverse	lyngbyatoxins	(Edwards and Gerwick 2004)
TleC (BAP27943)	*S. blastmyceticus*	(-)-indolactam V	*C7*-reverse	teleocidin B	(Awakawa et al. 2014)

A. Aspergillus, *N. Neosartorya*, *L. Lyngbya*, *Ant anthranilate*, *AA* acetoacetyl, *n.a.* not available

[a] Natural or if unknown the best accepted substrate was given

et al. 2012; Yin et al. 2009, 2010). ArdB from *Aspergillus fischeri* catalyzes *C3ß*-prenylation of ardeemin FQ at the indole ring (Haynes et al. 2013). Investigation with stereoisomers of cyclic dipeptides of tryptophan with proline or alanine revealed that AnaPT and CdpC3PT catalyze reverse *anti-cis* and *syn-cis C3*-prenylation, respectively. In contrast, CdpNPT produced both *anti-cis* and *syn-cis C3*-prenylated derivatives (Yu et al. 2013).

The product of a NRPS-PKS hybrid cAATrp was found to be the substrate of CpaD in the biosynthesis of the fungal neurotoxin α-cyclopiazonic acid in *Aspergillus flavus* (*A. flavus*) and *A. oryzae* (Liu and Walsh 2009). CpaD catalyzes the regiospecific *C4*-prenylation of cAATrp (Table 6) (Liu and Walsh 2009).

Several cyclic dipeptide prenyltransferases from bacteria use indolactams as substrates and catalyze prenylations at C-7 of the indole ring. In addition to LtxC mentioned above (Edwards and Gerwick 2004), the function of TleC in the biosynthetic pathway of teleocidin B in *Streptomyces blastmyceticus* was also characterized

Table 6 DMATS prenyltransferases of other substrates and their catalyzed reactions

Enzyme (accession number)	Organism	Substrate	Product	Biosynthetic pathway	Reference
Prenyltransferases of other indole and quinolinone derivatives					
FtmPT2 (EU622826)	*A. fumigatus*	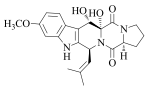 12,13-dihydroxyfumtremorgin C	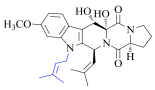 fumitremorgin B	fumitremorgin/ verruculogen	(Grundmann et al. 2008)
NotC (BAH24002)	*Aspergillus* sp.	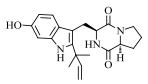 6-hydroxy-deoxybrevianamide E	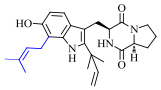 notamide S	stephacidin/ notoamide	(Ding et al. 2010)
FgaPT1 (XP_756136)	*A. fumigatus*	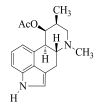 fumigaclavine A	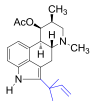 fumigaclavine C	fumigaclavine C	(Unsöld and Li 2006)
TdiB (ABU51603)	*A. nidulans*	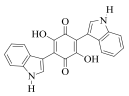 didemethylasterriquinone D	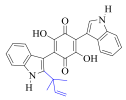 asterriquinone C-1	terrequinone A	(Schneider et al. 2008)
AstPT (EAU29429)	*A. terreus*	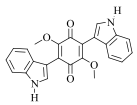 asterriquinone D	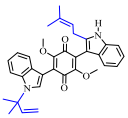 *N1′*-reversely,*C2′′*-regularly diprenylated didemethyl-asterriqinnone D	unknown	(Tarcz et al. 2014)
AtmD (BAN67270)	*A. flavus*	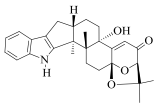 paspalinine	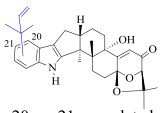 20- or 21-prenylated aflatrem or *β*-aflatrem	(ß-)aflatrem	(Liu et al. 2013b)
PaxD (AAK11526)	*P. paxilli*	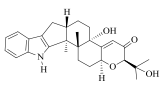 paxilline	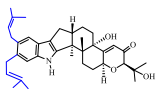 21-,22- diprenylated paxillin	diprenylated paxillin, paspalitrem	(Liu et al. 2014a)

biochemically (Awakawa et al. 2014). Gene deletion experiments revealed the involvement of MpnD in the biosynthesis of methylpendolmycin in *Marinactinospora thermotolerans* (Ma et al. 2012).

Prenyltransferases utilizing other indole or quinolinone derivatives as prenyl acceptor

In addition to tryptophan and tryptophan-containing cyclic dipeptide prenyltransferases listed in Tables 4 and 5, eight members of the DMATS superfamily, which use other indole derivatives as prenylation substrates, are identified in different fungal strains (Table 6). These include FtmPT2 and FtmPT3 in the biosynthesis of verruculogen and fumitremorgin A in *A. fumigatus* and *N. fischeri* (Grundmann et al. 2008; Mundt et al. 2012). FgaPT1 from *A. fumigatus* catalyzes a reverse *C2*-prenylation, the last step in the biosynthesis of the ergot alkaloid fumigaclavine C (Unsöld and Li 2006). In addition to the cyclic dipeptide prenyltransferase NotF, NotC is also involved in the biosynthesis of stephacidin/notoamides (Ding et al. 2010). TdiB from *Aspergillus nidulans* (*A. nidulans*) and AstPT from *A. terreus* are involved in the biosynthesis of prenylated bisindolyl benzoquinones (Balibar et al. 2007; Schneider et al. 2008; Tarcz et al. 2014). AtmD from *A. flavus* and PaxD from *Penicillium paxilli* use indole diterpene derivatives as prenylation substrates (Liu et al. 2013b,

Table 6 (continued)

FtmPT3 (EAW19377)	*N. fischeri*	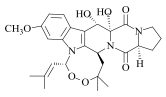 verruculogen	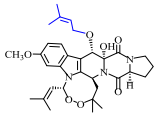 fumitremorgin A	fumitremorgin	(Mundt et al. 2012)
PenI (n.a.)	*P. thymicola*	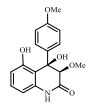 quinolinone B	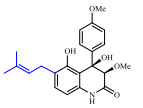 7-dimethylallylquinolone	penigequinolones	(Zou et al. 2015)
PenG (n.a.)	*P. thymicola*	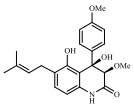 7-dimethylallylquinolone	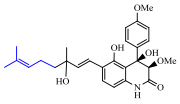 styrenyl quinolone	penigequinolones	(Zou et al. 2015)
Tyrosine prenyltransferases					
SirD (AAS92554)	*L. maculans*	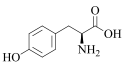 L-tyrosine	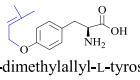 4-*O*-dimethylallyl-L-tyrosine	sirodesmin PL	(Kremer and Li 2010)
TyrPT (CAK41583)	*A. niger*			unknown	(Fan et al. 2014)
Prenyltransferases of miscellaneous substrates					
XptB (BN001302)	*A. nidulans*	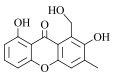 1,7-dihydroxy-6-methyl-8-hydroxymethylxanthone	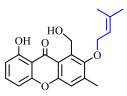 variecoxythone	shamixanthone/ epishamixanthone	(Pockrandt et al. 2012)
PAPT (BAL68129)	*Phomopsis amygdali*	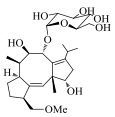 fusioccin P	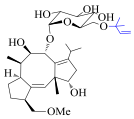 fusicoccin J	fusicoccin J	(Noike et al. 2012)
BAE61387 (AP007162)	*A. oryzae*	 R=H: 1-naphthol R=OH: 1,7-dihydroxy-naphthalene	 R=H: 4-dimethylallyl-1-naphthol R=OH: 4-dimethylallyl-1,7-dihydroxynaphthalene	unknown	(Pockrandt et al. 2014)
NscD (EAW20699)	*N. fischeri*				(Chooi et al. 2013)
Mc03599 (EEQ30780)	*Microsporum canis*	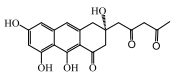	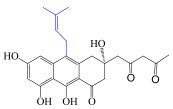	neosartoricins	(Chooi et al. 2012)
Tt06703 (EGD99349)	*T. tonsurans*				(Yin et al. 2013b)
VrtC (ADI24928)	*P. aethiopicum*	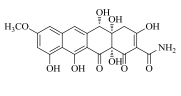 naphtacenedione	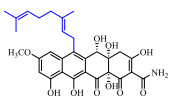 6-geranyl-naphtacenedione	viridicatumtoxin	(Chooi et al. 2012)

A. Aspergillus, *L. Leptosphaeria*, *N. Neosartorya*, *P. Penicillium*, *T. Trichophyton*, *n.a.* not available

2014a). With the exception of FtmPT3, which catalyzes an *O*-prenylation of a secondary alcohol, all other enzymes from this group carry out reverse or regular prenylations at the indole ring (Table 6).

Very recently, two members of the DMATS superfamily, PenI and PenG, have been identified in *Penicillium thymicola* and proven to be involved in the biosynthesis of penigequinolone I. Both enzymes use DMAPP as prenyl donor. PenI catalyzes the prenylation of the quinolinone core at C-7, whereas PenG transfers a C_5 unit to the dimethylallyl moiety of the product of PenI, i.e., the elongation of the prenyl moiety by addition of a second dimethylallyl unit (Zou et al. 2015).

Prenyltransferases of tyrosine and other aromatic or nonaromatic substrates

The tyrosine *O*-prenyltransferase SirD in the biosynthesis of sirodesmin PL in *Leptosphaeria maculans* was identified in 2010 as the first member of the DMATS superfamily, which use nonindole derivatives as prenylation substrates (Kremer and Li 2010). The second tyrosine *O*-prenyltransferase TyrPT of an unknown cluster was identified in *Aspergillus niger* (Fan et al. 2014). Both enzymes share relatively high sequence similarity with 7-DMATS from *A. fumigatus* and also catalyze the *C7*-prenylation of tryptophan (Fan et al. 2014; Kremer and Li 2010).

Since 2010, several enzymes of the DMATS superfamily were proven to use even polyketide products, e.g., xanthones by XptB from *A. nidulans* (Pockrandt et al. 2012), hydroxynaphthalenes by BAE61387 from *A. oryzae* (Pockrandt et al. 2014), or naphtacenedione by VrtC from *Penicillium aethiapicum* (Chooi et al. 2010). VrtC utilizes GPP instead of DMAPP as prenyl donor to generate a viridicatumtoxin precursor (Chooi et al. 2010). Interestingly, its homologs from *N. fischeri*, *Microsporum canis*, and *Trichophyton tonsurans* accepted DMAPP as prenyl donor and were proven to be involved in the biosynthesis of neosatoricin (Chooi et al. 2012, 2013; Yin et al. 2013b). More interestingly, PAPT from *Phomopsis amygdali* catalyzes an *O*-prenylation of the glucose moiety in the biosynthesis of fusicoccin A (Noike et al. 2012). It should be mentioned that all of the enzymes described here were identified in fungi.

Crystal structures of DMATS prenyltransferases providing basic knowledge for understanding the prenylation reactions

Determination of the crystal structure of the first indole prenyltransferase FgaPT2 was a fundamental step in the advanced understanding of prenyltransferases of the DMATS superfamily and their reaction mechanisms (Metzger et al. 2009). FgaPT2 revealed an unusual PT-barrel fold, formed by ten antiparallel *β*-strands surrounded by ten *α*-helices (Fig. 3). The active site is located in the center of the barrel, and the absence of any metal ion in this area is consistent with the independency of divalent metals for enzyme activity. Interestingly, this architecture has been already observed for the bacterial hydroxynaphthalene prenyltransferase NphB (Kuzuyama et al. 2005), although its primary amino acid sequence and active site differ substantially from that of FgaPT2. The structural information, gained from this work, allowed the first understanding of the enzymatic catalysis and also supported the hypothesis of a common evolutionary origin of the bacterial and the fungal prenyltransferases of the ABBA-family (Luk and Tanner 2009; Metzger et al. 2009). In 2010, the crystal structure of the cyclic dipeptide *C2*-prenyltransferase FtmPT1 was solved (Jost et al. 2010),

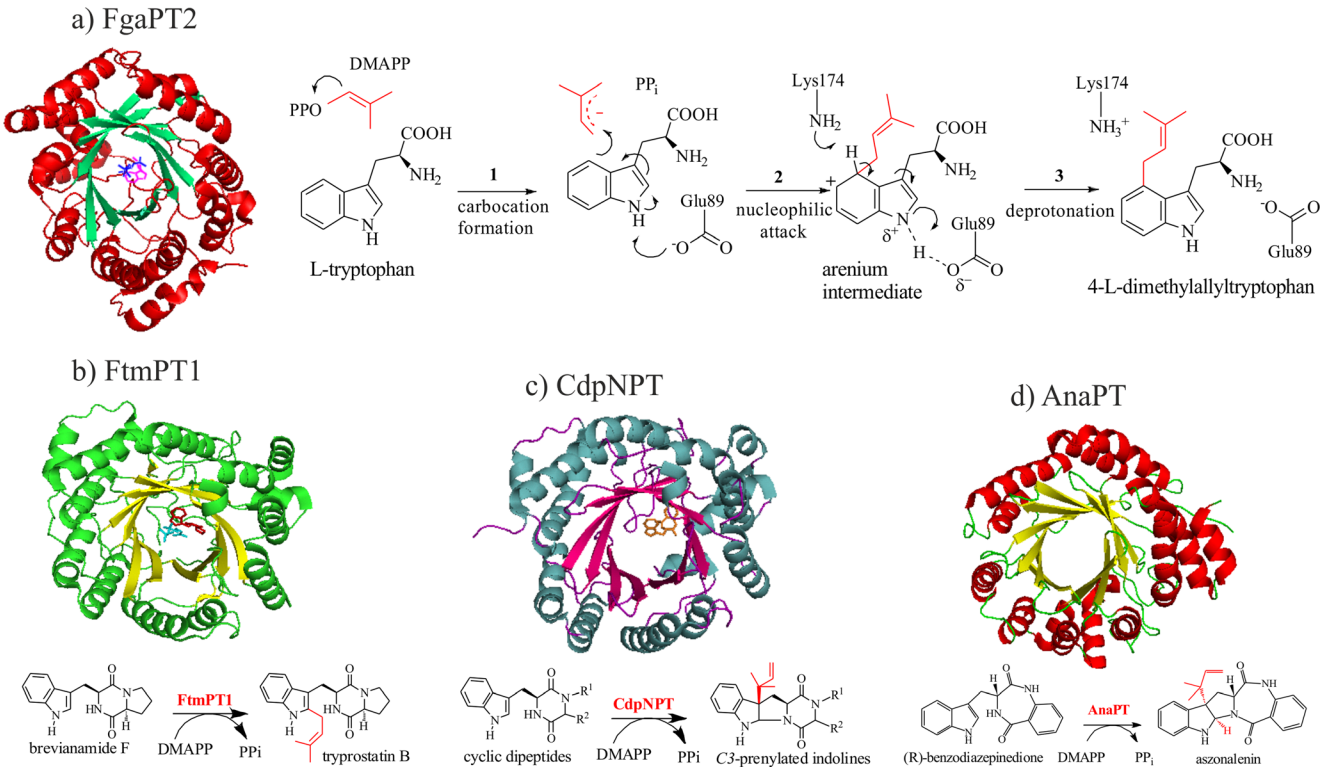

Fig. 3 Structures and enzyme reactions of FgaPT2 (**a**), FtmPT1 (**b**), CdpNPT (**c**), and AnaPT (**d**)

followed by the structures of two tryptophan-containing cyclic dipeptide *C3*-prenyltransferases CdpNPT and AnaPT in 2012 and 2013 (Schuller et al. 2012; Yu et al. 2013). Currently, the crystal structures of FgaPT2, FtmPT1, CdpNPT, and AnaPT are available in their unbound states. In addition, three of them (FgaPT2, FtmPT1, CdpNPT) were crystallized together with their aromatic substrates and an unreactive analog of DMAPP DMSPP (dimethylallyl S-thiolodiphosphate) or SPP (S-thiolodiphosphate). Comparison of the crystal structures revealed that they share a similar secondary core structure with the already described PT-barrel fold (Fig. 3). The amino acids in the DMAPP binding site seem to be strictly conserved in these four structures, whereas the binding sites of the aromatic substrates differ from each other. This feature makes molecular modeling with unknown structures more difficult. Therefore, additional enzyme structures from this superfamily are required. Nevertheless, the detailed structure analysis of the liganded and unliganded structures provides important insight into the catalyzed reaction mechanisms (Jost et al. 2010). Prenylations catalyzed by the enzymes of the DMATS superfamily were proposed as three-step reactions. They begin with the formation of a dimethylallyl cation by removal of the pyrophosphate group, which was proven by a positional isotope exchange with O^{18}-labeled DMAPP (Luk and Tanner

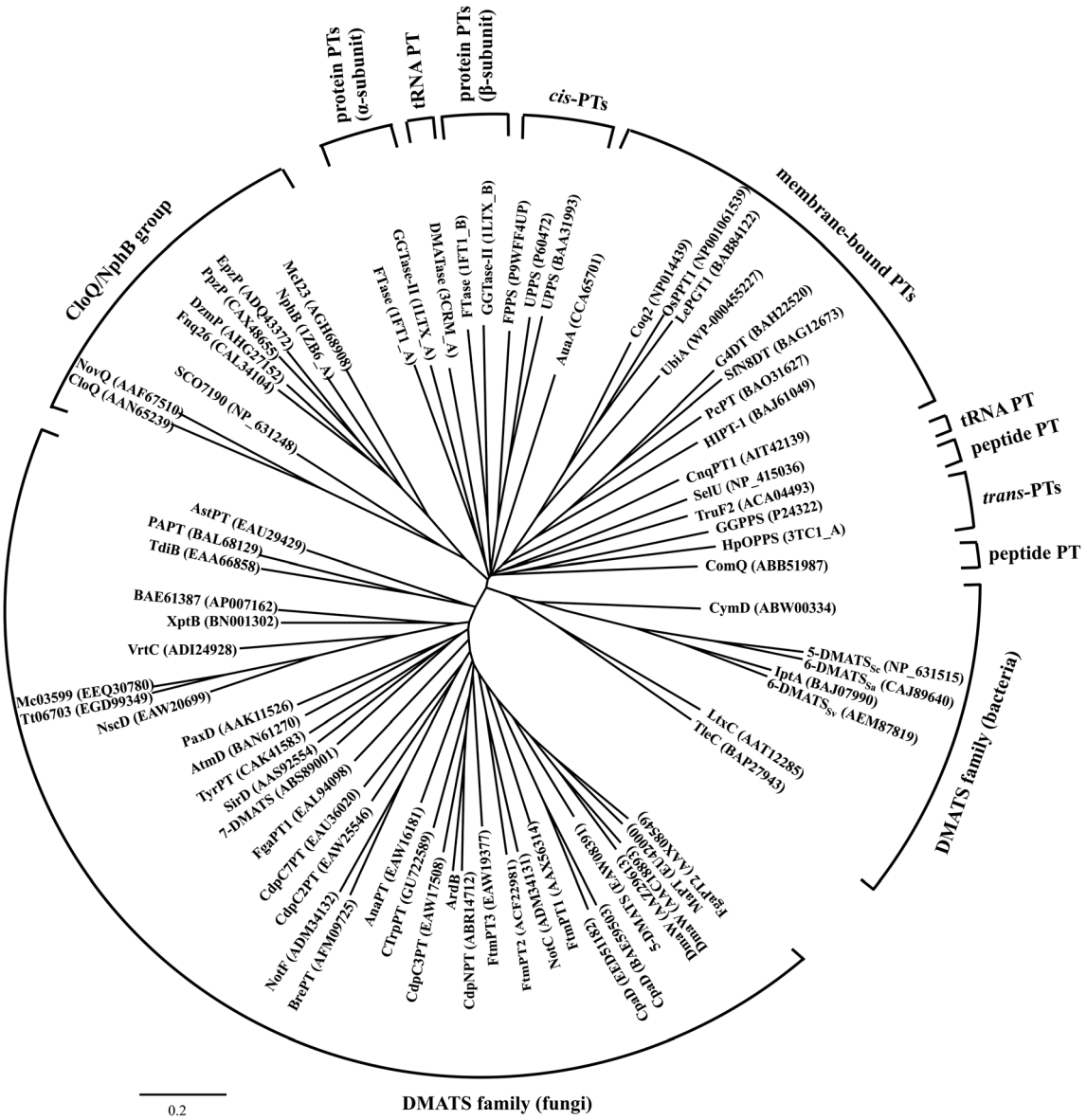

Fig. 4 Phylogenetic relationships of different prenyltransferases (PTs). The phylogenetic tree was created by using the programs ClustalX2 (http://www.clustal.org/) and Treedyn (www.phylogeny.fr). In addition to enzymes listed in Tables 2, 3, 4, 5 and 6, *cis*- and *trans*-PTs, peptide and tRNA PTs as well as α- and β-subunits of protein PTs are also included. The accession numbers or pdb codes of the enzymes are given in *parenthesis*

2009). The subsequent nucleophilic attack of this cation by the indole nucleus or other electron-rich atoms to form the σ-complex defined the second step. Then, the resulting arenium intermediate was deprotonated to generate the final product (Fig. 3a). The most controversial issue of this mechanism focused on the second step, whether an electrophilic aromatic substitution mechanism occurs directly at the site of substitution or as results of rearrangements after initial prenylation at C-3 of the indole ring to generate the final product (Luk et al. 2011; Mahmoodi et al. 2013; Mahmoodi and Tanner 2013; Tanner 2014). Furthermore, these results could be applied for generation of modified prenyltransferases by modeling and site-directed mutagenesis experiments. For example, the enzymatic reaction of FtmPT1 was modified by a single point mutation to perform a reverse prenylation at C-3 of the indole nucleus instead of a regular *C2*-prenylation.

Phylogenic relationships of different prenyltransferases

To get insights into the phylogenetic relationships of prenyltransferases, enzymes listed in Tables 2, 3, 4, 5, and 6 and examples of prenyl diphosphate synthases as well as peptide, protein, and tRNA prenyltransferases were analyzed and illustrated as a phylogenetic tree in Fig. 4. The phylogenetic analysis confirmed the diversity of prenyltransferases, which are located in different clades. The membrane-bound prenyltransferases from different sources are grouped together, while the enzymes of the CloQ/NphB group build a defined clade. The members of the DMATS family are found in two clades, one with fungal and another with bacterial origin. The *cis*- and *trans*-prenyltransferases of prenyl diphosphate synthases are clearly separated from each other. The relationships among peptide prenyltransferases appear to be very far. This is also observed for tRNA prenyltransferases.

Conclusion and outlook

In this review, we demonstrated the sequence, biochemical, and structural diversities of prenyltransferases, which catalyze the transfer of nxC_5 units to different acceptors such as prenyl moieties, peptides, proteins, tRNAs, and aliphatic or aromatic small molecules (Dumelin et al. 2012; McIntosh et al. 2013; Palsuledesai and Distefano 2015). As given in Fig. 4, enzyme groups mentioned in this review can be found in different clades.

Prenyltransferases play important roles in primary and secondary metabolism as well as in the cellular regulation (Heide 2009a; Palsuledesai and Distefano 2015; Yazaki et al. 2009; Yu and Li 2012). The most intensively studied prenyltransferases belong to the DMATS superfamily, which are mainly identified in fungi, but also in bacteria. They are of great importance for the biosynthesis of secondary metabolites in microorganisms. Until now, no example from this group was known from plants and animals. To date, over 40 members of the DMATS superfamily have been identified and characterized biochemically, and crystal structures of four members are available. Members of this family do not require metal ions for their transfer reactions. Most of these enzymes utilize DMAPP as prenyl donor and an aromatic scaffold as prenyl acceptor, e.g., tryptophan, tyrosine, tryptophan-containing cyclic dipeptides, or other indole derivatives. With the first solved crystal structure of the 4-DMATS and its unexpected PT-barrel, new insights into reaction mechanism, substrate binding, and evolutionary origin were gained.

As demonstrated in the last years, mining of available genome sequences has proven to be a convenient approach for identification of putative prenyltransferase genes. It can be expected that additional prenyltransferases with new features will be identified in the next years. Prenyltransferases, especially the members of the DMATS superfamily, show a high potential for production of biologically active low molecular weight compounds by in vitro catalysis or by synthetic biology. This has already been demonstrated by a large number of studies on their substrate and catalytic promiscuity in the last years. This aspect will be discussed in another mini-review in the same issue in detail. Moreover, elucidation of further prenyltransferase structures would provide new chance and challenge for a better understanding of their functionality. This in turn will enable us to create modified enzymes with special features, e.g., changes in substrate specificity, regioselectivity, and stereoselectivity.

Acknowledgments The works in the authors' laboratory were supported in part by a grant from Deutsche Forschungsgemeinschaft (Li844/4-1 to S.-M. Li). Julia Winkelblech is partially financed by the LOEWE program of the State of Hessen (SynMikro to S.-M. Li). Aili Fan is a recipient of a scholarship from China scholarship council.

Conflict of interest The authors declare that there are no conflicts of interest.

References

Abuhaie CM, Ghinet A, Farce A, Dubois J, Rigo B, Bîcu E (2013) Synthesis and biological evaluation of a new series of *N*-ylides as protein farnesyltransferase inhibitors. Bioorg Med Chem Lett 23: 5887–5892

Anderson MS, Yarger JG, Burck CL, Poulter CD (1989) Farnesyl diphosphate synthetase. Molecular cloning, sequence, and expression of an essential gene from *Saccharomyces cerevisiae*. J Biol Chem 264: 19176–19184

Akashi T, Sasaki K, Aoki T, Ayabe S, Yazaki K (2009) Molecular cloning and characterization of a cDNA for pterocarpan 4-dimethylallyltransferase catalyzing the key prenylation step in the biosynthesis of glyceollin, a soybean phytoalexin. Plant Physiol 149:683–693

Awakawa T, Zhang L, Wakimoto T, Hoshino S, Mori T, Ito T, Ishikawa J, Tanner ME, Abe I (2014) A methyltransferase initiates terpene cyclization in teleocidin B biosynthesis. J Am Chem Soc 136:9910–9913

Balibar CJ, Howard-Jones AR, Walsh CT (2007) Terrequinone A biosynthesis through L-tryptophan oxidation, dimerization and bisprenylation. Nat Chem Biol 3:584–592

Bayse CA, Merz KM (2014) Mechanistic insights into Mg^{2+}-independent prenylation by CloQ from classical molecular mechanics and hybrid quantum mechanics/molecular mechanics molecular dynamics simulations. Biochemistry 53:5034–5041

Bonitz T, Alva V, Saleh O, Lupas AN, Heide L (2011) Evolutionary relationships of microbial aromatic prenyltransferases. PLoS One 6, e27336

Bonitz T, Zubeil F, Grond S, Heide L (2013) Unusual *N*-prenylation in diazepinomicin biosynthesis: The farnesylation of a benzodiazepine substrate is catalyzed by a new member of the ABBA prenyltransferase superfamily. PLoS One 8, e85707

Boronat A, Rodriguez-Concepcion M (2015) Terpenoid biosynthesis in prokaryotes. Adv Biochem Eng Biotechnol 148:3–18

Chang WC, Song H, Liu HW, Liu P (2013) Current development in isoprenoid precursor biosynthesis and regulation. Curr Opin Chem Biol 17:571–579

Chen R, Liu X, Zou J, Yin Y, Ou C, Li J, Wang R, Xie D, Zhang P, Dai J (2013) Regio- and stereospecific prenylation of flavonoids by *Sophora flavescens* prenyltransferases. Adv Synth Catal 355: 1817–1828

Cheng W, Li W (2014) Structural insights into ubiquinone biosynthesis in membranes. Science 343:878–881

Chooi YH, Cacho R, Tang Y (2010) Identification of the viridicatumtoxin and griseofulvin gene clusters from *Penicillium aethiopicum*. Chem Biol 17:483–494

Chooi YH, Wang P, Fang J, Li Y, Wu K, Wang P, Tang Y (2012) Discovery and characterization of a group of fungal polycyclic polyketide prenyltransferases. J Am Chem Soc 134:9428–9437

Chooi YH, Fang J, Liu H, Filler SG, Wang P, Tang Y (2013) Genome mining of a prenylated and immunosuppressive polyketide from pathogenic fungi. Org Lett 15:780–783

Danley DE, Baima ET, Mansour M, Fennell KF, Chrunyk BA, Mueller JP, Liu S, Qiu X (2015) Discovery and structural characterization of an allosteric inhibitor of bacterial cis-prenyltransferase. Protein Sci 24:20–26

Ding Y, Williams RM, Sherman DH (2008) Molecular analysis of a 4-dimethylallyltryptophan synthase from *Malbranchea aurantiaca*. J Biol Chem 283:16068–16076

Ding Y, Wet JR, Cavalcoli J, Li S, Greshock TJ, Miller KA, Finefield JM, Sunderhaus JD, McAfoos TJ, Tsukamoto S, Williams RM, Sherman DH (2010) Genome-based characterization of two prenylation steps in the assembly of the stephacidin and notoamide anticancer agents in a marine-derived *Aspergillus* sp. J Am Chem Soc 132:12733–12740

Dumelin CE, Chen Y, Leconte AM, Chen YG, Liu DR (2012) Discovery and biological characterization of geranylated RNA in bacteria. Nat Chem Biol 8:913–919

Eckhardt U, Grimm B, Hortensteiner S (2004) Recent advances in chlorophyll biosynthesis and breakdown in higher plants. Plant Mol Biol 56:1–14

Edwards DJ, Gerwick WH (2004) Lyngbyatoxin biosynthesis: sequence of biosynthetic gene cluster and identification of a novel aromatic prenyltransferase. J Am Chem Soc 126:11432–11433

Fan A, Chen H, Wu R, Xu H, Li S-M (2014) A new member of the DMATS superfamily from *Aspergillus niger* catalyzes prenylations of both tyrosine and tryptophan derivatives. Appl Microbiol Biotechnol 98:10119–10129

Gebler JC, Poulter CD (1992) Purification and characterization of dimethylallyl tryptophan synthase from *Claviceps purpurea*. Arch Biochem Biophys 296:308–313

Gerhards N, Neubauer L, Tudzynski P, Li S-M (2014) Biosynthetic pathways of ergot alkaloids. Toxins (Basel) 6:3281–3295

Grundmann A, Li S-M (2005) Overproduction, purification and characterization of FtmPT1, a brevianamide F prenyltransferase from *Aspergillus fumigatus*. Microbiology 151:2199–2207

Grundmann A, Kuznetsova T, Afiyatullov SS, Li S-M (2008) FtmPT2, an *N*-prenyltransferase from *Aspergillus fumigatus*, catalyses the last step in the biosynthesis of fumitremorgin B. Chembiochem 9: 2059–2063

Guo RT, Kuo CJ, Chou CC, Ko TP, Shr HL, Liang PH, Wang AH (2004) Crystal structure of octaprenyl pyrophosphate synthase from hyperthermophilic *Thermotoga maritima* and mechanism of product chain length determination. J Biol Chem 279:4903–4912

Guo RT, Ko TP, Chen AP, Kuo CJ, Wang AH, Liang PH (2005) Crystal structures of undecaprenyl pyrophosphate synthase in complex with magnesium, isopentenyl pyrophosphate, and farnesyl thiopyrophosphate: roles of the metal ion and conserved residues in catalysis. J Biol Chem 280:20762–20774

Haagen Y, Unsöld I, Westrich L, Gust B, Richard SB, Noel JP, Heide L (2007) A soluble, magnesium-independent prenyltransferase catalyzes reverse and regular *C*-prenylations and *O*-prenylations of aromatic substrates. FEBS Lett 581:2889–2893

Haug-Schifferdecker E, Arican D, Brueckner R, Heide L (2010) A new group of aromatic prenyltransferases in fungi, catalyzing a 2,7-dihydroxynaphthalene dimethylallyltransferase reaction. J Biol Chem 285:16487–16494

Haynes SW, Gao X, Tang Y, Walsh CT (2013) Complexity generation in fungal peptidyl alkaloid biosynthesis: A two-enzyme pathway to the hexacyclic MDR export pump inhibitor ardeemin. ACS Chem Biol 8:741–748

Hegarty JM, Yang H, Chi NC (2013) UBIAD1-mediated vitamin K2 synthesis is required for vascular endothelial cell survival and development. Development 140:1713–1719

Heide L (2009a) Prenyl transfer to aromatic substrates: genetics and enzymology. Curr Opin Chem Biol 13:171–179

Heide L (2009b) The aminocoumarins: biosynthesis and biology. Nat Prod Rep 26:1241–1250

Holm DK, Petersen LM, Klitgaard A, Knudsen PB, Jarczynska ZD, Nielsen KF, Gotfredsen CH, Larsen TO, Mortensen UH (2014) Molecular and chemical characterization of the biosynthesis of the 6-MSA-derived meroterpenoid yanuthone D in *Aspergillus niger*. Chem Biol 21:519–529

Jost M, Zocher G, Tarcz S, Matuschek M, Xie X, Li S-M, Stehle T (2010) Structure-function analysis of an enzymatic prenyl transfer reaction identifies a reaction chamber with modifiable specificity. J Am Chem Soc 132:17849–17858

Karamat F, Olry A, Munakata R, Koeduka T, Sugiyama A, Paris C, Hehn A, Bourgaud F, Yazaki K (2014) A coumarin-specific prenyltransferase catalyzes the crucial biosynthetic reaction for furanocoumarin formation in parsley. Plant J 77:627–638

Kremer A, Li S-M (2010) A tyrosine *O*-prenyltransferase catalyses the first pathway-specific step in the biosynthesis of sirodesmin PL. Microbiology 156:278–286

Kremer A, Westrich L, Li S-M (2007) A 7-dimethylallyltryptophan synthase from *Aspergillus fumigatus*: overproduction, purification and biochemical characterization. Microbiology 153:3409–3416

Kumano T, Richard SB, Noel JP, Nishiyama M, Kuzuyama T (2008) Chemoenzymatic syntheses of prenylated aromatic small molecules using *Streptomyces* prenyltransferases with relaxed substrate specificities. Bioorg Med Chem 16:8117–8126

Kuzuyama T, Noel JP, Richard SB (2005) Structural basis for the promiscuous biosynthetic prenylation of aromatic natural products. Nature 435:983–987

Li S-M (2009a) Applications of dimethylallyltryptophan synthases and other indole prenyltransferases for structural modification of natural products. Appl Microbiol Biotechnol 84:631–639

Li S-M (2009b) Evolution of aromatic prenyltransferases in the biosynthesis of indole derivatives. Phytochemistry 70:1746–1757

Li S-M (2010) Prenylated indole derivatives from fungi: structure diversity, biological activities, biosynthesis and chemoenzymatic synthesis. Nat Prod Rep 27:57–78

Li S-M (2011) Genome mining and biosynthesis of fumitremorgin-type alkaloids in ascomycetes. J Antibiot 64:45–49

Li H, Ban Z, Qin H, Ma L, King AJ, Wang G (2015) A heteromeric membrane-bound prenyltransferase complex from hop catalyzes three sequential aromatic prenylations in the bitter acid pathway. Plant Physiol 167:650–659

Liang PH, Ko TP, Wang AH (2002) Structure, mechanism and function of prenyltransferases. Eur J Biochem 269:3339–3354

Liu X, Walsh CT (2009) Characterization of cyclo-acetoacetyl-L-tryptophan dimethylallyltransferase in cyclopiazonic acid biosynthesis: substrate promiscuity and site directed mutagenesis studies. Biochemistry 48:11032–11044

Liu AH, Liu DQ, Liang TJ, Yu XQ, Feng MT, Yao LG, Fang Y, Wang B, Feng LH, Zhang MX, Mao SC (2013a) Caulerprenylols A and B, two rare antifungal prenylated *para*-xylenes from the green alga *Caulerpa racemosa*. Bioorg Med Chem Lett 23:2491–2494

Liu C, Minami A, Noike M, Toshima H, Oikawa H, Dairi T (2013b) Regiospecificities and prenylation mode specificities of the fungal indole diterpene prenyltransferases AtmD and PaxD. Appl Environ Microbiol 79:7298–7304

Liu C, Noike M, Minami A, Oikawa H, Dairi T (2014a) Functional analysis of a prenyltransferase gene (paxD) in the paxilline biosynthetic gene cluster. Appl Microbiol Biotechnol 98:199–206

Liu C, Sun Z, Shen S, Lin L, Li T, Tian B, Hua Y (2014b) Identification and characterization of the geranylgeranyl diphosphate synthase in *Deinococcus radiodurans*. Lett Appl Microbiol 58:219–224

Long SB, Casey PJ, Beese LS (2002) Reaction path of protein farnesyltransferase at atomic resolution. Nature 419:645–650

Lu YP, Liu HG, Liang PH (2009) Different reaction mechanisms for *cis*- and *trans*-prenyltransferases. Biochem Biophys Res Commun 379: 351–355

Luk LYP, Tanner ME (2009) Mechanism of dimethylallyltryptophan synthase: evidence for a dimethylallyl cation intermediate in an aromatic prenyltransferase reaction. J Am Chem Soc 131:13932–13933

Luk LY, Qian Q, Tanner ME (2011) A cope rearrangement in the reaction catalyzed by dimethylallyltryptophan synthase? J Am Chem Soc 133:12342–12345

Ma J, Zuo D, Song Y, Wang B, Huang H, Yao Y, Li W, Zhang S, Zhang C, Ju J (2012) Characterization of a single gene cluster responsible for methylpendolmycin and pendolmycin biosynthesis in the deep sea bacterium *Marinactinospora thermotolerans*. Chembiochem 13: 547–552

Mahmoodi N, Tanner ME (2013) Potential rearrangements in the reaction catalyzed by the indole prenyltransferase FtmPT1. Chembiochem 14:2029–2037

Mahmoodi N, Qian Q, Luk LYP, Tanner ME (2013) Rearrangements in the mechanisms of the indole alkaloid prenyltransferases. Pure Appl Chem 85:1935–1948

Markert A, Steffan N, Ploss K, Hellwig S, Steiner U, Drewke C, Li S-M, Boland W, Leistner E (2008) Biosynthesis and accumulation of ergoline alkaloids in a mutualistic association between *Ipomoea asarifolia* (*Convolvulaceae*) and a clavicipitalean fungus. Plant Physiol 147:296–305

McIntosh JA, Donia MS, Nair SK, Schmidt EW (2011) Enzymatic basis of ribosomal peptide prenylation in cyanobacteria. J Am Chem Soc 133:13698–13705

McIntosh JA, Lin Z, Tianero MD, Schmidt EW (2013) Aestuaramides, a natural library of cyanobactin cyclic peptides resulting from isoprene-derived Claisen rearrangements. ACS Chem Biol 8:877–883

Meganathan R, Kwon O (2009) Biosynthesis of menaquinone (vitamin K) and ubiquinone (coenzyme Q). Ecosal Plus 3:DOI: 10.1128/ecosalplus.3.6.3.3

Melzer M, Heide L (1994) Characterization of polyprenyldiphosphate: 4-hydroxybenzoate polyprenyltransferase from *Escherichia coli*. Biochim Biophys Acta 1212:93–102

Metzger U, Schall C, Zocher G, Unsöld I, Stec E, Li S-M, Heide L, Stehle T (2009) The structure of dimethylallyl tryptophan synthase reveals a common architecture of aromatic prenyltransferases in fungi and bacteria. Proc Natl Acad Sci U S A 106:14309–14314

Metzger U, Keller S, Stevenson CE, Heide L, Lawson DM (2010) Structure and mechanism of the magnesium-independent aromatic prenyltransferase CloQ from the clorobiocin biosynthetic pathway. J Mol Biol 404:611–626

Miyamoto K, Ishikawa F, Nakamura S, Hayashi Y, Nakanishi I, Kakeya H (2014) A 7-dimethylallyl tryptophan synthase from a fungal *Neosartorya* sp.: Biochemical characterization and structural insight into the regioselective prenylation. Bioorg Med Chem 22:2517–2528

Mundt K, Li S-M (2013) CdpC2PT, a reverse prenyltransferase from *Neosartorya fischeri* with distinct substrate preference from known *C2*-prenyltransferases. Microbiology 159:2169–2179

Mundt K, Wollinsky B, Ruan HL, Zhu T, Li S-M (2012) Identification of the verruculogen prenyltransferase FtmPT3 by a combination of chemical, bioinformatic and biochemical approaches. Chembiochem 13:2583–2592

Nakagawa K, Hirota Y, Sawada N, Yuge N, Watanabe M, Uchino Y, Okuda N, Shimomura Y, Suhara Y, Okano T (2010) Identification of UBIAD1 as a novel human menaquinone-4 biosynthetic enzyme. Nature 468:117–121

Noike M, Liu C, Ono Y, Hamano Y, Toyomasu T, Sassa T, Kato N, Dairi T (2012) An enzyme catalyzing *O*-prenylation of the glucose moiety of fusicoccin A, a diterpene glucoside produced by the fungus *Phomopsis amygdali*. Chembiochem 13:566–573

Ohara K, Yamamoto K, Hamamoto M, Sasaki K, Yazaki K (2006) Functional characterization of OsPPT1, which encodes p-hydroxybenzoate polyprenyltransferase involved in ubiquinone biosynthesis in *Oryza sativa*. Plant Cell Physiol 47:581–590

Okada K, Ohara K, Yazaki K, Nozaki K, Uchida N, Kawamukai M, Nojiri H, Yamane H (2004) The AtPPT1 gene encoding 4-hydroxybenzoate polyprenyl diphosphate transferase in ubiquinone biosynthesis is required for embryo development in *Arabidopsis thaliana*. Plant Mol Biol 55:567-577

Oldfield E, Lin FY (2012) Terpene biosynthesis: modularity rules. Angew Chem Int Ed Engl 51:1124–1137

Oya A, Tanaka N, Kusama T, Kim SY, Hayashi S, Kojoma M, Hishida A, Kawahara N, Sakai K, Gonoi T, Kobayashi J (2015) Prenylated benzophenones from *Triadenum japonicum*. J Nat Prod 78:258–264

Ozaki T, Mishima S, Nishiyama M, Kuzuyama T (2009) NovQ is a prenyltransferase capable of catalyzing the addition of a dimethylallyl group to both phenylpropanoids and flavonoids. J Antibiot 62:385–392

Ozaki T, Nishiyama M, Kuzuyama T (2013) Novel tryptophan metabolism by a potential gene cluster that is widely distributed among actinomycetes. J Biol Chem 288:9946–9956

Palsuledesai CC, Distefano MD (2015) Protein prenylation: enzymes, therapeutics, and biotechnology applications. ACS Chem Biol 10: 51–62

Perez-Sala D (2007) Protein isoprenylation in biology and disease: general overview and perspectives from studies with genetically engineered animals. Front Biosci 12:4456–4472

Pockrandt D, Ludwig L, Fan A, König GM, Li S-M (2012) New insights into the biosynthesis of prenylated xanthones: XptB from *Aspergillus nidulans* catalyses an *O*-prenylation of xanthones. Chembiochem 13:2764–2771

Pockrandt D, Sack C, Kosiol T, Li S-M (2014) A promiscuous prenyltransferase from *Aspergillus oryzae* catalyses *C*-prenylations of hydroxynaphthalenes in the presence of different prenyl donors. Appl Microbiol Biotechnol 98:4987–4994

Pojer F, Wemakor E, Kammerer B, Chen H, Walsh CT, Li S-M, Heide L (2003) CloQ, a prenyltransferase involved in clorobiocin biosynthesis. Proc Natl Acad Sci U S A 100:2316–2321

Poulter CD (2006) Farnesyl diphosphate synthase. A paradigm for understanding structure and function relationships in E-polyprenyl diphosphate synthases. Phytochem Rev 5:17–26

Raju R, Piggott AM, Huang XC, Capon RJ (2011) Nocardioazines: a novel bridged diketopiperazine scaffold from a marine-derived bacterium inhibits p-glycoprotein. Org Lett 13:2770–2773

Ramamoorthy G, Pugh ML, Tian BX, Phan RM, Perez LB, Jacobson MP, Poulter CD (2015) Synthesis and enzymatic studies of bisubstrate analogs for farnesyl diphosphate synthase. J Org Chem 80:3902–3913

Saiki K, Mogi T, Ogura K, Anraku Y (1993) *In vitro* heme O synthesis by the *cyoE* gene product from *Escherichia coli*. J Biol Chem 268: 26041–26044

Saleh O, Gust B, Boll B, Fiedler H-P, Heide L (2009) Aromatic prenylation in phenazine biosynthesis: dihydrophenazine-1-carboxylate dimethylallyltransferase from *Streptomyces anulatus*. J Biol Chem 284:14439–14447

Sasaki K, Tsurumaru Y, Yamamoto H, Yazaki K (2011) Molecular characterization of a membrane-bound prenyltransferase specific for isoflavone from *Sophora flavescens*. J Biol Chem 286:24125–24134

Schneider P, Weber M, Hoffmeister D (2008) The *Aspergillus nidulans* enzyme TdiB catalyzes prenyltransfer to the precursor of bioactive asterriquinones. Fungal Genet Biol 45:302–309

Schuller JM, Zocher G, Liebhold M, Xie X, Stahl M, Li S-M, Stehle T (2012) Structure and catalytic mechanism of a cyclic dipeptide prenyltransferase with broad substrate promiscuity. J Mol Biol 422:87–99

Schultz AW, Lewis CA, Luzung MR, Baran PS, Moore BS (2010) Functional characterization of the cyclomarin/cyclomarazine prenyltransferase CymD directs the biosynthesis of unnatural cyclic peptides. J Nat Prod 73:373–377

Seeger K, Flinspach K, Haug-Schifferdecker E, Kulik A, Gust B, Fiedler HP, Heide L (2011) The biosynthetic genes for prenylated phenazines are located at two different chromosomal loci of *Streptomyces cinnamonensis* DSM 1042. Microb Biotechnol 4:252–262

Shen G, Huhman D, Lei Z, Snyder J, Sumner LW, Dixon RA (2012) Characterization of an isoflavonoid-specific prenyltransferase from *Lupinus albus*. Plant Physiol 159:70–80

Shimada H, Ohno R, Shibata M, Ikegami I, Onai K, Ohto MA, Takamiya K (2005) Inactivation and deficiency of core proteins of photosystems I and II caused by genetical phylloquinone and plastoquinone deficiency but retained lamellar structure in a T-DNA mutant of *Arabidopsis*. Plant J 41:627–637

Soballe B, Poole RK (1999) Microbial ubiquinones: multiple roles in respiration, gene regulation and oxidative stress management. Microbiology 145(Pt 8):1817–1830

Soderberg T, Chen A, Poulter CD (2001) Geranylgeranylglyceryl phosphate synthase. Characterization of the recombinant enzyme from *Methanobacterium thermoautotrophicum*. Biochemistry 40:14847–14854

Sousa SF, Fernandes PA, Ramos MJ (2009) Molecular dynamics simulations on the critical states of the farnesyltransferase enzyme. Bioorg Med Chem 17:3369–3378

Stec E, Pistorius D, Müller R, Li S-M (2011) AuaA, a membrane-bound farnesyltransferase from *Stigmatella aurantiaca*, catalyzes the prenylation of 2-methyl-4-hydroxyquinoline in the biosynthesis of aurachins. Chembiochem 12:1724–1730

Steffan N, Grundmann A, Yin W-B, Kremer A, Li S-M (2009) Indole prenyltransferases from fungi: a new enzyme group with high potential for the production of prenylated indole derivatives. Curr Med Chem 16:218–231

Steffensky M, Mühlenweg A, Wang Z-X, Li S-M, Heide L (2000) Identification of the novobiocin biosynthetic gene cluster of *Streptomyces spheroides* NCIB 11891. Antimicrob Agents Chemother 44:1214–1222

Steiner U, Leibner S, Schardl CL, Leuchtmann A, Leistner E (2011) *Periglandula*, a new fungal genus within the *Clavicipitaceae* and its association with *Convolvulaceae*. Mycologia 103:1133–1145

Subramanian S, Shen X, Yuan Q, Yan Y (2012) Identification and biochemical characterization of a 5-dimethylallyltryptophan synthase in *Streptomyces coelicolor* A3(2). Process Biochem 47:1419–1422

Sugiyama A, Linley PJ, Sasaki K, Kumano T, Yamamoto H, Shitan N, Ohara K, Takanashi K, Harada E, Hasegawa H, Terakawa T, Kuzuyama T, Yazaki K (2011) Metabolic engineering for the production of prenylated polyphenols in transgenic legume plants using bacterial and plant prenyltransferases. Metab Eng 13:629–637

Sunassee SN, Davies-Coleman MT (2012) Cytotoxic and antioxidant marine prenylated quinones and hydroquinones. Nat Prod Rep 29: 513–535

Suvarna K, Stevenson D, Meganathan R, Hudspeth ME (1998) Menaquinone (vitamin K2) biosynthesis: localization and characterization of the menA gene from *Escherichia coli*. J Bacteriol 180: 2782–2787

Tagami K, Liu C, Minami A, Noike M, Isaka T, Fueki S, Shichijo Y, Toshima H, Gomi K, Dairi T, Oikawa H (2013) Reconstitution of biosynthetic machinery for indole-diterpene paxilline in *Aspergillus oryzae*. J Am Chem Soc 135:1260–1263

Takahashi S, Koyama T (2006) Structure and function of cis-prenyl chain elongating enzymes. Chem Rec 6:194–205

Takahashi S, Takagi H, Toyoda A, Uramoto M, Nogawa T, Ueki M, Sakaki Y, Osada H (2010) Biochemical characterization of a novel indole prenyltransferase from *Streptomyces* sp. SN-593. J Bacteriol 192:2839–2851

Tanner ME (2014) Mechanistic studies on the indole prenyltransferases. Nat Prod Rep 32:88–101

Tarcz S, Ludwig L, Li S-M (2014) AstPT catalyses both reverse *N1*- and regular *C2*-prenylation of a methylated bisindolyl benzoquinone. Chembiochem 15:108–116

Teufel R, Kaysser L, Villaume MT, Diethelm S, Carbullido MK, Baran PS, Moore BS (2014) One-pot enzymatic synthesis of merochlorin A and B. Angew Chem Int Ed 53:11019–11022

Tsai HF, Wang H, Gebler JC, Poulter CD, Schardl CL (1995) The *Claviceps purpurea* gene encoding dimethylallyltryptophan synthase, the committed step for ergot alkaloid biosynthesis. Biochem Biophys Res Commun 216:119–125

Tsuji F, Ishihara A, Kurata K, Nakagawa A, Okada M, Kitamura S, Kanamaru K, Masuda Y, Murakami K, Irie K, Sakagami Y (2012) Geranyl modification on the tryptophan residue of $ComX_{RO-E-2}$ pheromone by a cell-free system. FEBS Lett 586:174–179

Tsurumaru Y, Sasaki K, Miyawaki T, Uto Y, Momma T, Umemoto N, Momose M, Yazaki K (2012) HlPT-1, a membrane-bound prenyltransferase responsible for the biosynthesis of bitter acids in hops. Biochem Biophys Res Commun 417:393–398

Tudzynski P, Holter K, Correia T, Arntz C, Grammel N, Keller U (1999) Evidence for an ergot alkaloid gene cluster in *Claviceps purpurea*. Mol Gen Genet 261:133–141

Unsöld IA, Li S-M (2005) Overproduction, purification and characterization of FgaPT2, a dimethylallyltryptophan synthase from *Aspergillus fumigatus*. Microbiology 151:1499–1505

Unsöld IA, Li S-M (2006) Reverse prenyltransferase in the biosynthesis of fumigaclavine C in *Aspergillus fumigatus*: gene expression, purification and characterization of fumigaclavine C synthase FgaPT1. Chembiochem 7:158–164

Walsh CT (2014) Biological matching of chemical reactivity: pairing indole nucleophilicity with electrophilic isoprenoids. ACS Chem Biol 9:2718–2728

Wang R, Chen R, Li J, Liu X, Xie K, Chen D, Yin Y, Tao X, Xie D, Zou J, Yang L, Dai J (2014) Molecular characterization and phylogenetic analysis of two novel regio-specific flavonoid prenyltransferases from *Morus alba* and *Cudrania tricuspidata*. J Biol Chem 289:35815–35825

White MD, Payne KA, Fisher K, Marshall SA, Parker D, Rattray NJ, Trivedi DK, Goodacre R, Rigby SE, Scrutton NS, Hay S, Leys D (2015) UbiX is a flavin prenyltransferase required for bacterial ubiquinone biosynthesis. Nature 522:502–506. doi:10.1038/nature14559

Wierenga RK, Kapetaniou EG, Venkatesan R (2010) Triosephosphate isomerase: a highly evolved biocatalyst. Cell Mol Life Sci 67:3961–3982

Winkelblech J, Li S-M (2014) Biochemical investigations of two 6-DMATS enzymes from *Streptomyces* revealing novel features of L-tryptophan prenyltransferases. Chembiochem 15:1030–1039

Wunsch C, Zou HX, Linne U, Li S-M (2015) *C7*-prenylation of tryptophanyl and *O*-prenylation of tyrosyl residues in dipeptides by an *Aspergillus terreus* prenyltransferase. Appl Microbiol Biotechnol 99:1719–1730

Xie W, Zhou C, Huang RH (2007) Structure of tRNA dimethylallyltransferase: RNA modification through a Channel. J Mol Biol 367:872–881

Yang Y, Miao Y, Wang B, Cui G, Merz KM Jr (2012) Catalytic mechanism of aromatic prenylation by NphB. Biochemistry 51:2606–2618

Yazaki K, Kunihisa M, Fujisaki T, Sato F (2002) Geranyl diphosphate:4-hydroxybenzoate geranyltransferase from *Lithospermum erythrorhizon*. Cloning and characterization of a key enzyme in shikonin biosynthesis. J Biol Chem 277:6240–6246

Yazaki K, Sasaki K, Tsurumaru Y (2009) Prenylation of aromatic compounds, a key diversification of plant secondary metabolites. Phytochemistry 70:1739–1745

Yin W-B, Ruan H-L, Westrich L, Grundmann A, Li S-M (2007) CdpNPT, an *N*-prenyltransferase from *Aspergillus fumigatus*: overproduction, purification and biochemical characterisation. Chembiochem 8:1154–1161

Yin W-B, Grundmann A, Cheng J, Li S-M (2009) Acetylaszonalenin biosynthesis in *Neosartorya fischeri*: Identification of the biosynthetic gene cluster by genomic mining and functional proof of the genes by biochemical investigation. J Biol Chem 284:100–109

Yin W-B, Yu X, Xie X-L, Li S-M (2010) Preparation of pyrrolo[2,3-*b*]indoles carrying a ß-configured reverse *C3*-dimethylallyl moiety by using a recombinant prenyltransferase CdpC3PT. Org Biomol Chem 8:2430–2438

Yin S, Yu X, Wang Q, Liu XQ, Li S-M (2013a) Identification of a brevianamide F reverse prenyltransferase BrePT from *Aspergillus versicolor* with a broad substrate specificity towards tryptophan-containing cyclic dipeptides. Appl Microbiol Biotechnol 97:1649–1660

Yin WB, Chooi YH, Smith AR, Cacho RA, Hu Y, White TC, Tang Y (2013b) Discovery of cryptic polyketide metabolites from dermatophytes using heterologous expression in *Aspergillus nidulans*. ACS Synth Biol 2:629–634

Yin W-B, Baccile JA, Bok JW, Chen Y, Keller NP, Schroeder FC (2013c) A nonribosomal peptide synthetase-derived iron(III) complex from the pathogenic fungus *Aspergillus fumigatus*. J Am Chem Soc 135:2064–2067

Yu X, Li S-M (2012) Prenyltransferases of the dimethylallyltryptophan synthase superfamily. Methods Enzymol 516:259–278

Yu X, Liu Y, Xie X, Zheng X-D, Li S-M (2012) Biochemical characterization of indole prenyltransferases: Filling the last gap of prenylation positions by a 5-dimethylallyltryptophan synthase from *Aspergillus clavatus*. J Biol Chem 287:1371–1380

Yu X, Zocher G, Xie X, Liebhold M, Schütz S, Stehle T, Li S-M (2013) Catalytic mechanism of stereospecific formation of *cis*-configured prenylated pyrroloindoline diketopiperazines by indole prenyltransferases. Chem Biol 20:1492–1501

Zeyhle P, Bauer JS, Kalinowski J, Shin-ya K, Gross H, Heide L (2014a) Genome-based discovery of a novel membrane-bound 1,6-dihydroxyphenazine prenyltransferase from a marine actinomycete. PLoS One 9, e99122

Zeyhle P, Bauer JS, Steimle M, Leipoldt F, Rösch M, Kalinowski J, Gross H, Heide L (2014b) A membrane-bound prenyltransferase catalyzes the *O*-prenylation of 1,6-dihydroxyphenazine in the marine bacterium *Streptomyces* sp. CNQ-509. Chembiochem 15:2385–2392

Zhao L, Chang WC, Xiao Y, Liu HW, Liu P (2013) Methylerythritol phosphate pathway of isoprenoid biosynthesis. Annu Rev Biochem 82:497–530

Zhu HY, Desai J, Cooper AB, Wang J, Rane DF, Kirschmeier P, Strickland C, Liu M, Nomeir AA, Girijavallabhan VM (2014) New class of azaheptapyridine FPT inhibitors as potential cancer therapy agents. Bioorg Med Chem Lett 24:1228–1231

Zocher G, Saleh O, Heim JB, Herbst DA, Heide L, Stehle T (2012) Structure-based engineering increased the catalytic turnover rate of a novel phenazine prenyltransferase. PLoS One 7, e48427

Zou H-X, Xie X-L, Linne U, Zheng X-D, Li S-M (2010) Simultaneous *C7*- and *N1*-prenylation of cyclo-L-Trp-L-Trp catalyzed by a prenyltransferase from *Aspergillus oryzae*. Org Biomol Chem 8:3037–3044

Zou Y, Zhan Z, Li D, Tang M, Cacho RA, Watanabe K, Tang Y (2015) Tandem prenyltransferases catalyze isoprenoid elongation and complexity generation in biosynthesis of quinolone alkaloids. J Am Chem Soc 137:4980–4983

5. Conclusions and future prospects

In this thesis, we gained new insights into the biochemical properties of enzymes belonging to the DMATS superfamily regarding their substrate specificity toward donor and acceptor, regioselectivity and enantioselectivity. Moreover, the obtained results expand significantly the potential usage of microbial DMATS enzymes in chemoenzymatic synthesis.

At the beginning of this thesis, only limited information about bacterial tryptophan prenyltransferases was available and investigations were focused on enzymes from fungi of ascomycetes. Bioinformatic analyses led to the finding of several putative tryptophan prenyltransferases in bacteria of actinomycetes. Subsequently, three new enzymes were identified as tryptophan *C6*-prenyltransferases 6-DMATS$_{Sa}$, 6-DMATS$_{Sv}$, and 6-DMATS$_{Mo}$. Comprehensive investigations on their biochemical properties revealed several interesting aspects and expanded significantly our knowledge on bacterial tryptophan prenyltransferases. The three 6-DMATSs show a high substrate flexibility toward both prenyl donor and acceptor with a strict regioselectivity toward the prenylation position on the indole ring. In addition to a number of tryptophan derivatives, also cyclic dipeptides and naphthalene derivatives were accepted by these enzymes. Moreover, 6-DMATS$_{Sa}$ and 6-DMATS$_{Sv}$ used as first examples DMAPP and GPP as prenyl donor with same prenylation positions. This high regioselectivity was also observed with unnatural donors demonstrated in the advanced study on the acceptance of MAPP, 2-pentenyl-PP and benzyl-PP by DMATS enzymes.

This study complemented the previous projects by investigations on additional bacterial *C5*-prenyltransferase 5-DMATS$_{Sc}$, two *C6*-prenyltransferases 6-DMATS$_{Sa}$ and 6-DMATS$_{Sv}$ and the *C7*-prenyltransferase TyrPT. The three unnatural DMAPP analogs were accepted by all five enzymes with different enzyme activities and regioselectivities. Thereby, *C6*-alkylation or benzylation was preferred by the tested prenyltransferases. Following these results, the synthesis of new interesting compounds could be facilitated by the mentioned enzymes as biocatalysts. In a further study, the enantioselectivity of seven DMATSs was elucidated, initiated by the high relative activity of 6-DMATS$_{Mo}$ toward D-tryptophan. Different behaviors in regioselectivity and substrate preference toward the L- and D-enantiomers of tryptophan and methylated derivatives were observed. Remarkable results were obtained in several cases including the reduced regioselectivity of FgaPT2, 5-DMATS$_{Sc}$ and 7-DMATS in the presence of D-tryptophan. In addition, the *C5*- and *C6*-prenyltransferases 5-DMATS$_{Sc}$ and 6-DMATS$_{Mo}$ from *Streptomyces* accepted the D-enantiomer of 5-methyltryptophan much better than the L-

enantiomer, although in all other reaction mixtures the L-enantiomer was the better substrate. These findings demonstrate that the stereochemistry of the substrates strongly influence the enzyme activity and that the behavior of the DMATSs toward the enantiomers differ from each other. Furthermore, the enantioselective prenylation of tryptophan and substituted derivatives provides new chances for the synthesis of promising biological active compounds.

The following projects are to be addressed in the future

- Identification and characterization of further indole prenyltransferases from actinomycetes.
- Elucidation of the natural function of different gene clusters containing the prenyltransferase genes by gene deletion experiments or heterologous expression of the whole gene clusters.
- Protein crystallization and subsequent structure analysis, especially for bacterial tryptophan prenyltransferases to clarify the reaction mechanism in detail. Protein structures as complexes with distinct acceptors and donors including natural and unnatural DMAPP analogs would be useful for understanding their biochemical properties such as regioselectivity or substrate specificity.
- Mutational analysis to create enzymes with modified biochemical features *e.g.* substrate specificity. For instance, in order to increase the acceptance to special donors or to increase the relative enzyme activity toward D-enantiomers.
- Testing bioactivity of new unnatural compounds synthesized by DMATSs.

6. References

Achenbach, H., Renner, C. & Waibel, R. (1995). Constituents of tropical medicinal plants, LXIX. The hexalobines, diprenylated indoles from *Hexalobus crispiflorus* and *Hexalobus monopetalus*. *Liebigs Ann.* **1995**, 1327-1337.

Adla, S. K., Sasse, F., Kelter, G., Fiebig, H. H. & Lindel, T. (2013). Doubly prenylated tryptamines: cytotoxicity, antimicrobial activity and cyclisation to the marine natural product flustramine A. *Org. Biomol. Chem.* **11**, 6119-6130.

Alhassan A.M., Abdullahi M.I., Ahmad Uba & Umar A. (2014). Prenylation of Aromatic Secondary Metabolites: A New Frontier for Development of Novel Drugs. *Trop. J. Pharm. Res.* **13**, 307-314.

Allen, J. D., van Loevezijn, A., Lakhai, J. M., van, d., V, van Tellingen, O., Reid, G., Schellens, J. H., Koomen, G. J. & Schinkel, A. H. (2002). Potent and specific inhibition of the breast cancer resistance protein multidrug transporter in vitro and in mouse intestine by a novel analogue of fumitremorgin C. *Mol. Cancer Ther.* **1**, 417-425.

Amaike, S. & Keller, N. P. (2011). *Aspergillus flavus*. *Annu. Rev. Phytopathol.* **49**, 107-133.

Andersen, M. R., Salazar, M. P., Schaap, P. J., van de Vondervoort, P. J. et al. (2011). Comparative genomics of citric-acid-producing *Aspergillus niger* ATCC 1015 versus enzyme-producing CBS 513.88. *Genome Res.* **21**, 885-897.

Awakawa, T., Zhang, L., Wakimoto, T., Hoshino, S., Mori, T., Ito, T., Ishikawa, J., Tanner, M. E. & Abe, I. (2014). A methyltransferase initiates terpene cyclization in teleocidin B biosynthesis. *Journal of the American Chemical Society* **136**, 9910-9913.

Balibar, C. J., Howard-Jones, A. R. & Walsh, C. T. (2007). Terrequinone A biosynthesis through L-tryptophan oxidation, dimerization and bisprenylation. *Nat. Chem. Biol.* **3**, 584-592.

Barron, D. & Ibrahim, R. K. (1996). Isoprenylated flavonoids–a survey. *Phytochemistry* **43**, 921-982.

Barthomeuf, C., Lim, S., Iranshahi, M. & Chollet, P. (2008). Umbelliprenin from *Ferula szowitsiana* inhibits the growth of human M4Beu metastatic pigmented malignant melanoma cells through cell-cycle arrest in G1 and induction of caspase-dependent apoptosis. *Phytomedicine.* **15**, 103-111.

Bentley, S. D., Chater, K. F., Cerdeno-Tarraga, A. M., Challis, G. L. et al. (2002). Complete genome sequence of the model actinomycete *Streptomyces coelicolor* A3(2). *Nature* **417**, 141-147.

Bonitz, T., Alva, V., Saleh, O., Lupas, A. N. & Heide, L. (2011). Evolutionary relationships of microbial aromatic prenyltransferases. *PLoS One* **6**, e27336.

Boronat, A. & Rodriguez-Concepcion, M. (2015). Terpenoid biosynthesis in prokaryotes. *Adv. Biochem. Eng Biotechnol.* **148**, 3-18.

Borthwick, A. D. (2012). 2,5-diketopiperazines: synthesis, reactions, medicinal chemistry, and bioactive natural products. *Chem. Rev.* **112**, 3641-3716.

Botta, B., Delle Monache, F., Delle Monache, G., MariniBettolo, G. B. & Oguakwa, J. U. (1983). 3-Geranyloxy-6-methyl-1,8-dihydroxyanthraquinone and vismiones C, D and E from *Psorospermum febrifugum*. *Phytochemistry* **22**, 539-542.

Botta, B., Monache, G. D., Menendez, P. & Boffi, A. (2005a). Novel prenyltransferase enzymes as a tool for flavonoid prenylation. *Trends Pharmacol. Sci.* **26**, 606-608.

Botta, B., Vitali, A., Menendez, P., Misiti, D. & Delle, M. G. (2005b). Prenylated flavonoids: pharmacology and biotechnology. *Curr. Med. Chem.* **12**, 717-739.

Brakhage, A. A., Sprote, P., Al Abdallah, Q., Gehrke, A., Plattner, H. & Tuncher, A. (2004). Regulation of penicillin biosynthesis in filamentous fungi. *Adv. Biochem. Eng Biotechnol.* **88**, 45-90.

Brown, G. D., Denning, D. W., Gow, N. A., Levitz, S. M., Netea, M. G. & White, T. C. (2012). Hidden killers: human fungal infections. *Sci. Transl. Med.* **4**, 165rv13.

Cava, F., Lam, H., de Pedro, M. A. & Waldor, M. K. (2011). Emerging knowledge of regulatory roles of D-amino acids in bacteria. *Cell Mol. Life Sci.* **68**, 817-831.

Chen, X., Si, L., Liu, D., Proksch, P., Zhang, L., Zhou, D. & Lin, W. (2015). Neoechinulin B and its analogues as potential entry inhibitors of influenza viruses, targeting viral hemagglutinin. *Eur. J. Med. Chem.* **93**, 182-195.

Cheng, W. & Li, W. (2014). Structural insights into ubiquinone biosynthesis in membranes. *Science* **343**, 878-881.

Cherry, J. M., Ball, C., Weng, S., Juvik, G. et al. (1997). Genetic and physical maps of *Saccharomyces cerevisiae*. *Nature* **387**, 67-73.

Choulet, F., Aigle, B., Gallois, A., Mangenot, S. et al. (2006). Evolution of the terminal regions of the *Streptomyces* linear chromosome. *Mol. Biol. Evol.* **23**, 2361-2369.

Clardy, J. & Walsh, C. (2004). Lessons from natural molecules. *Nature* **432**, 829-837.

Cole, R. J., Kirksey, J. W., Weinreb, S. M., Singh, P., Kim, D., Clardy, J. & Eickman, N. (1976). Structures of rugulovasine-A and -B and 8-chlororugulovasine-A and -B. *Tetrahedron Lett.* **17**, 3849-3852.

D'Aniello, S., Somorjai, I., Garcia-Fernandez, J., Topo, E. & D'Aniello, A. (2011). D-Aspartic acid is a novel endogenous neurotransmitter. *FASEB J.* **25**, 1014-1027.

Davis, R. H. & Perkins, D. D. (2002). Timeline: *Neurospora*: a model of model microbes. *Nat. Rev. Genet.* **3**, 397-403.

de los Reyes, C., Zbakh, H., Motilva, V. & Zubia, E. (2013). Antioxidant and anti-inflammatory meroterpenoids from the brown alga Cystoseira usneoides. *J. Nat. Prod.* **76**, 621-629.

Debbab, A., Aly, A. H., Edrada-Ebel, R. A., Muller, W. E. G., Mosaddak, M., Hakiki, A., Ebel, R. & Proksch, P. (2009). Bioactive secondary metabolites from the endophytic fungus Chaetomium sp isolated from Salvia officinalis growing in Morocco. *Biotechn. Agron. Soc. Environ.* **13**, 229-234.

Di, P. T., Danese, S., De, C. R. & Rutella, S. (2010). Inhibitors of indoleamine 2,3-dioxygenase: a review of novel patented lead compounds. *Expert. Opin. Ther. Pat* **20**, 229-250.

Ding, Y., Wet, J. R., Cavalcoli, J., Li, S. et al. (2010). Genome-based characterization of two prenylation steps in the assembly of the stephacidin and notoamide anticancer agents in a marine-derived *Aspergillus* sp. *J. Am. Chem. Soc.* **132**, 12733-12740.

Dittmann, J., Wenger, R. M., Kleinkauf, H. & Lawen, A. (1994). Mechanism of cyclosporin A biosynthesis. Evidence for synthesis via a single linear undecapeptide precursor. *J. Biol. Chem.* **269**, 2841-2846.

Dumelin, C. E., Chen, Y., Leconte, A. M., Chen, Y. G. & Liu, D. R. (2012). Discovery and biological characterization of geranylated RNA in bacteria. *Nat. Chem. Biol.* **8**, 913-919.

Edwards, D. J. & Gerwick, W. H. (2004). Lyngbyatoxin biosynthesis: sequence of biosynthetic gene cluster and identification of a novel aromatic prenyltransferase. *J. Am. Chem. Soc.* **126**, 11432-11433.

El-Seedi, H. R., El-Barbary, M. A., El-Ghorab, D. M. H., Bohlin, L., Borg-Karlson, A. K., Göransson, U. & Verpoorte, R. (2010). Recent insights into the biosynthesis and biological activities of natural xanthones. *Curr. Med. Chem.* **17**, 854-901.

El-Seedi, H. R., El-Ghorab, D. M. H., El-Barbary, M. A., Zayed, M. F., Göransson, U., Larsson, S. & Verpoorte, R. (2009). Naturally occurring xanthones; latest investigations: isolation, structure elucidation and chemosystematic significance. *Curr. Med. Chem.* **16**, 2581-2626.

Fan, A., Chen, H., Wu, R., Xu, H. & Li, S.-M. (2014). A new member of the DMATS superfamily from *Aspergillus niger* catalyzes prenylations of both tyrosine and tryptophan derivatives. *Appl. Microbiol. Biotechnol.* **98**, 10119-10129.

Fan, A. & Li, S.-M. (2013). One substrate - seven products with different prenylation positions in one-step reactions: prenyltransferases make it possible. *Adv. Synth. Catal.* **355**, 2659-2666.

Fan, A. & Li, S.-M. (2014). Prenylation of tyrosine and derivatives by a tryptophan *C*7-prenyltransferase. *Tetrahedron Lett* **55**, 5199-5202.

Fan, A. & Li, S.-M. (2016). Saturation mutagenesis on Arg244 of the tryptophan C4-prenyltransferase FgaPT2 leads to enhanced catalytic ability and different preferences for tryptophan-containing cyclic dipeptides. *Appl. Microbiol. Biotechnol.* **100**, 5389-5399.

Fan, A., Winkelblech, J. & Li, S.-M. (2015a). Impacts and perspectives of prenyltransferases of the DMATS superfamily for use in biotechnology. *Appl. Microbiol. Biotechnol.* **99**, 7399-7415.

Fan, A., Zocher, G., Stec, E., Stehle, T. & Li, S.-M. (2015b). Site-directed mutagenesis switching a dimethylallyl tryptophan synthase to a specific tyrosine *C3*-prenylating enzyme. *J. Biol. Chem.* **290**, 1364-1373.

Flemming, P. (1929). The Medical Aspects of the Mediaeval Monastery in England. *Proc. R. Soc. Med.* **22**, 771-782.

Fredenhagen, A., Petersen, F., Tintelnot-Blomley, M., Rosel, J., Mett, H. & Hug, P. (1997). Semicochliodinol A and B: inhibitors of HIV-1 protease and EGF-R protein tyrosine kinase related to asterriquinones produced by the fungus *Chrysosporium merdarium*. *J. Antibiot.* **50**, 395-401.

Fukushima, T., Sugiura, A., Furuta, I., Iwasa, S., Iizuka, H., Ichiba, H., Onozato, M., Hikawa, H. & Yokoyama, Y. (2015). Enantiomeric separation of monosubstituted tryptophan derivatives and metabolites by HPLC with a cinchona alkaloid-based zwitterionic chiral stationary phase and its application to the evaluation of the optical purity of synthesized 6-chloro-L-tryptophan. *Int. J. Tryptophan. Res.* **8**, 1-5.

Galagan, J. E., Calvo, S. E., Borkovich, K. A., Selker, E. U. et al. (2003). The genome sequence of the filamentous fungus *Neurospora crassa*. *Nature* **422**, 859-868.

Gallagher, R. T. & Latch, G. C. M. (1977). Production of the tremorgenic mycotoxins verruculogen and fumitremorgin B by *Penicillium piscarium* Westling. *Appl. Envir. Microbiol.* **33**, 730-731.

Gallo, C., Dallaglio, K., Bassani, B., Rossi, T., Rossello, A., Noonan, D. M., D'Uva, G., Bruno, A. & Albini, A. (2016). Hop derived flavonoid xanthohumol inhibits endothelial cell functions via AMPK activation. *Oncotarget.* DOI: 10.18632/oncotarget.10990.

Gao, X., Ma, Q. & Zhu, H. (2015). Distribution, industrial applications, and enzymatic synthesis of D-amino acids. *Appl. Microbiol. Biotechnol.* **99**, 3341-3349.

Gebler, J. C. & Poulter, C. D. (1992). Purification and characterization of dimethylallyl tryptophan synthase from *Claviceps purpurea*. *Arch. Biochem. Biophys.* **296**, 308-313.

Gerhards, N., Matuschek, M., Wallwey, C. & Li, S. M. (2015). Genome mining of ascomycetous fungi reveals their genetic potential for ergot alkaloid production. *Arch. Microbiol.* **197**, 701-713.

Gerhards, N., Neubauer, L., Tudzynski, P. & Li, S.-M. (2014). Biosynthetic pathways of ergot alkaloids. *Toxins. (Basel)* **6**, 3281-3295.

Giessen, T. W. & Marahiel, M. A. (2014). The tRNA-dependent biosynthesis of modified cyclic dipeptides. *Int. J. Mol. Sci.* **15**, 14610-14631.

Giessen, T. W. & Marahiel, M. A. (2015). Rational and combinatorial tailoring of bioactive cyclic dipeptides. *Front Microbiol.* **6**, 785.

Gliszczynska, A. & Brodelius, P. E. (2012). Sesquiterpene coumarins. *Phytochemistry Reviews* **11**, 77-96.

Gomez-Escribano, J. P. & Bibb, M. J. (2014). Heterologous expression of natural product biosynthetic gene clusters in *Streptomyces coelicolor*: from genome mining to manipulation of biosynthetic pathways. *J. Ind. Microbiol. Biotechnol.* **41**, 425-431.

Groweiss, A., Cardellina, J. H. & Boyd, M. R. (2000). HIV-Inhibitory prenylated xanthones and flavones from *Maclura tinctoria*. *J. Nat. Prod.* **63**, 1537-1539.

Grundmann, A. & Li, S.-M. (2005). Overproduction, purification and characterization of FtmPT1, a brevianamide F prenyltransferase from *Aspergillus fumigatus*. *Microbiology* **151**, 2199-2207.

Guo, R. T., Ko, T. P., Chen, A. P., Kuo, C. J., Wang, A. H. & Liang, P. H. (2005). Crystal structures of undecaprenyl pyrophosphate synthase in complex with magnesium, isopentenyl pyrophosphate, and farnesyl thiopyrophosphate: roles of the metal ion and conserved residues in catalysis. *J. Biol. Chem.* **280**, 20762-20774.

Guo, R. T., Kuo, C. J., Chou, C. C., Ko, T. P., Shr, H. L., Liang, P. H. & Wang, A. H. (2004). Crystal structure of octaprenyl pyrophosphate synthase from hyperthermophilic *Thermotoga maritima* and mechanism of product chain length determination. *J. Biol. Chem.* **279**, 4903-4912.

Gutierrez-Orozco, F., Chitchumroonchokchai, C., Lesinski, G. B., Suksamrarn, S. & Failla, M. L. (2013). alpha-Mangostin: anti-inflammatory activity and metabolism by human cells. *J. Agric. Food Chem.* **61**, 3891-3900.

Harrison, J. & Studholme, D. J. (2014). Recently published Streptomyces genome sequences. *Microb. Biotechnol.* **7**, 373-380.

Hassan, H. M., Boonlarppradab, C. & Fenical, W. (2016). Actinoquinolines A and B, anti-inflammatory quinoline alkaloids from a marine-derived *Streptomyces* sp., strain CNP975. *J. Antibiot. (Tokyo)* **69**, 511-514.

Hata, Y., Kitamoto, K., Gomi, K., Kumagai, C., Tamura, G. & Hara, S. (1991). The glucoamylase cDNA from Aspergillus oryzae: its cloning, nucleotide sequence, and expression in *Saccharomyces cerevisiae*. *Agric. Biol. Chem.* **55**, 941-949.

Hayashi, H., Takiuchi, K., Murao, S. & Arai, M. (1989). Structure and insecticidal activity of new indole alkaloids, okaramines A and B, from *Penicillium simplicissimum* AK-40. *Agri. Biol. Chem.* **53**, 461-469.

Hayashi, H., Takiuchi, K., Murao, S. & Arai, M. (1991). Identification of the microorganism which produces insecticidal indole alkaloids, okaramines A and B. *Agri. Biol. Chem.* **55**, 2177-2178.

Heide, L. (2009a). Prenyl transfer to aromatic substrates: genetics and enzymology. *Curr. Opin. Chem. Biol.* **13**, 171-179.

Heide, L. (2009b). The aminocoumarins: biosynthesis and biology. *Nat. Prod. Rep.* **26**, 1241-1250.

Heller, B. (1982). D-Phenylalanine treatment. *Unites States Patent 4355044*.

Hisanaga, A., Mukai, R., Sakao, K., Terao, J. & Hou, D. X. (2016). Anti-inflammatory effects and molecular mechanisms of 8-prenyl quercetin. *Mol. Nutr. Food Res.* **60**, 1020-1032.

Holm, D. K., Petersen, L. M., Klitgaard, A., Knudsen, P. B., Jarczynska, Z. D., Nielsen, K. F., Gotfredsen, C. H., Larsen, T. O. & Mortensen, U. H. (2014). Molecular and chemical characterization of the biosynthesis of the 6-MSA-derived meroterpenoid yanuthone D in *Aspergillus niger*. *Chem. Biol.* **21**, 519-529.

Holzapfel, C. W. (1968). The isolation and structure of cyclopiazonic acid, a toxic metabolite of Penicillium cyclopium Westling. *Tetrahedron* **24**, 2101-2119.

Hosek, J., Bartos, M., Chudik, S., Dall'acqua, S. et al. (2011). Natural compound cudraflavone B shows promising anti-inflammatory properties in Vitro. *J Nat. Prod.* **74**, 614-619.

Hussain, H., Krohn, K., Ahmad, V. U., Miana, G. A. & Green, I. R. (2007). Lapachol: An overview. *ARKIVOC (Gainesville,FL,U. S.)* 145-171.

Hussein, A. A., Barberena, I., Capson, T. L., Kursar, T. A., Coley, P. D., Solis, P. N. & Gupta, M. P. (2004). New cytotoxic naphthopyrane derivatives from *Adenaria floribunda*. *J. Nat. Prod.* **67**, 451-453.

Hymery, N., Masson, F., Barbier, G. & Coton, E. (2014). Cytotoxicity and immunotoxicity of cyclopiazonic acid on human cells. *Toxicol. In Vitro* **28**, 940-947.

Iranshahi, M., Arfa, P., Ramezani, M., Jaafari, M. R., Sadeghian, H., Bassarello, C., Piacente, S. & Pizza, C. (2007). Sesquiterpene coumarins from *Ferula szowitsiana* and in vitro antileishmanial activity of 7-prenyloxycoumarins against promastigotes. *Phytochemistry* **68**, 554-561.

James, T. Y., Kauff, F., Schoch, C. L., Matheny, P. B. et al. (2006). Reconstructing the early evolution of fungi using a six-gene phylogeny. *Nature* **443**, 818-822.

Jia, L., Schweikart, K., Tomaszewski, J., Page, J. G., Noker, P. E., Buhrow, S. A., Reid, J. M., Ames, M. M. & Munn, D. H. (2008). Toxicology and pharmacokinetics of 1-methyl-d-tryptophan: absence of toxicity due to saturating absorption. *Food Chem. Toxicol.* **46**, 203-211.

Jost, M., Zocher, G., Tarcz, S., Matuschek, M., Xie, X., Li, S.-M. & Stehle, T. (2010). Structure-function analysis of an enzymatic prenyl transfer reaction identifies a reaction chamber with modifiable specificity. *J. Am. Chem. Soc.* **132**, 17849-17858.

Karamat, F., Olry, A., Munakata, R., Koeduka, T., Sugiyama, A., Paris, C., Hehn, A., Bourgaud, F. & Yazaki, K. (2014). A coumarin-specific prenyltransferase catalyzes the crucial biosynthetic reaction for furanocoumarin formation in parsley. *Plant J.* **77**, 627-638.

Kaysser, L., Bernhardt, P., Nam, S. J., Loesgen, S., Ruby, J. G., Skewes-Cox, P., Jensen, P. R., Fenical, W. & Moore, B. S. (2012). Merochlorins A-D, cyclic meroterpenoid antibiotics biosynthesized in divergent pathways with vanadium-dependent chloroperoxidases. *J. Am. Chem. Soc.* **134**, 11988-11991.

Khaw, K. Y., Choi, S. B., Tan, S. C., Wahab, H. A., Chan, K. L. & Murugaiyah, V. (2014). Prenylated xanthones from mangosteen as promising cholinesterase inhibitors and their molecular docking studies. *Phytomedicine.* **21**, 1303-1309.

Kieser, T., Bibb, M. J., Buttner, M. J., Chater, K. F. & Hopwood, D. A. (2000) *Practical Streptomyces Genetics*. Norwich, UK: John Innes Foundation.

Kim, C. S., Park, S. N., Ahn, S. J., Seo, Y. W., Lee, Y. J., Lim, Y. K., Freire, M. O., Cho, E. & Kook, J. K. (2013). Antimicrobial effect of sophoraflavanone G isolated from *Sophora flavescens* against mutans streptococci. *Anaerobe.* **19**, 17-21.

Kirk, P. M., Cannon, P. F., Minter, D. W. & Stalpers, J. A. (2008) *Dictionary of the Fungi*. Wallingford: UK: CABI Publishing.

Kjeldsen, T. (2000). *Yeast* secretory expression of insulin precursors. *Appl. Microbiol. Biotechnol.* **54**, 277-286.

Koglin, A. & Walsh, C. T. (2009). Structural insights into nonribosomal peptide enzymatic assembly lines. *Nat. Prod. Rep.* **26**, 987-1000.

Kohno, J., Kawahata, T., Otake, T., Morimoto, M. et al. (1996). Boromycin, an anti-HIV antibiotic. *Biosci. Biotechnol. Biochem.* **60**, 1036-1037.

Kosalec, I., Klaric, M. S. & Pepeljnjak, S. (2005). Verruculogen production in airborne and clinical isolates of *Aspergillus fumigatus* Fres. *Acta Pharm.* **55**, 357-364.

Kozlovsky, A. G., Vinokurova, N. G., Adanin, V. M., Burkhardt, G., Dahse, H.-M. & Gräfe, U. (2001). New diketopiperazine alkaloids from *Penicillium fellutanum*. *J. Nat. Prod.* **64**, 553-554.

Kremer, A. & Li, S.-M. (2008). Potential of a 7-dimethylallyltryptophan synthase as a tool for production of prenylated indole derivatives. *Appl. Microbiol. Biotechnol.* **79**, 951-961.

Kremer, A. & Li, S.-M. (2010). A tyrosine *O*-prenyltransferase catalyses the first pathway-specific step in the biosynthesis of sirodesmin PL. *Microbiology* **156**, 278-286.

Kremer, A., Westrich, L. & Li, S.-M. (2007). A 7-dimethylallyltryptophan synthase from *Aspergillus fumigatus*: overproduction, purification and biochemical characterization. *Microbiology* **153**, 3409-3416.

Kumano, T., Richard, S. B., Noel, J. P., Nishiyama, M. & Kuzuyama, T. (2008). Chemoenzymatic syntheses of prenylated aromatic small molecules using *Streptomyces* prenyltransferases with relaxed substrate specificities. *Bioorg. Med. Chem.* **16**, 8117-8126.

Kumar, J. & Sim, V. (2014). D-amino acid-based peptide inhibitors as early or preventative therapy in Alzheimer disease. *Prion.* **8**, 119-124.

Kuzuyama, T., Noel, J. P. & Richard, S. B. (2005). Structural basis for the promiscuous biosynthetic prenylation of aromatic natural products. *Nature* **435**, 983-987.

Kwak, H. H., Kim, I. R., Kim, H. J., Park, B. S. & Yu, S. B. (2016). alpha-Mangostin Induces Apoptosis and Cell Cycle Arrest in Oral Squamous Cell Carcinoma Cell. *Evid. Based. Complement Alternat. Med.* **2016**, 5352412.

Laphookhieo, S., Maneerat, W. & Koysomboon, S. (2009). Antimalarial and cytotoxic phenolic compounds from *Cratoxylum maingayi* and *Cratoxylum cochinchinense*. *Molecules* **14**, 1389-1395.

Latge, J. P. (1999). *Aspergillus fumigatus* and aspergillosis. *Clin. Microbiol. Rev.* **12**, 310-350.

Li, G.-Y., Yang, T., Luo, Y.-G., Chen, X.-Z., Fang, D. M. & Zhang, G.-L. (2009). Brevianamide J, a new Indole alkaloid dimer from fungus *Aspergillus versicolor*. *Org. Lett.* **11**, 3714-3717.

Li, H., Ban, Z., Qin, H., Ma, L., King, A. J. & Wang, G. (2015). A heteromeric membrane-bound prenyltransferase complex from hop catalyzes three sequential aromatic prenylations in the bitter acid pathway. *Plant Physiol* **167**, 650-659.

Li, S.-M. (2009a). Applications of dimethylallyltryptophan synthases and other indole prenyltransferases for structural modification of natural products. *Appl. Microbiol. Biotechnol.* **84**, 631-639.

Li, S.-M. (2009b). Evolution of aromatic prenyltransferases in the biosynthesis of indole derivatives. *Phytochemistry* **70**, 1746-1757.

Li, S.-M. (2010). Prenylated indole derivatives from fungi: structure diversity, biological activities, biosynthesis and chemoenzymatic synthesis. *Nat. Prod. Rep.* **27**, 57-78.

Li, S.-M. (2011). Genome mining and biosynthesis of fumitremorgin-type alkaloids in ascomycetes. *J. Antibiot.* **64**, 45-49.

Liang, P. H., Ko, T. P. & Wang, A. H. (2002). Structure, mechanism and function of prenyltransferases. *Eur. J. Biochem.* **269**, 3339-3354.

Liebhold, M. & Li, S.-M. (2013). Regiospecific benzylation of tryptophan and derivatives catalyzed by a fungal dimethylallyl transferase. *Org. Lett.* **15**, 5834-5837.

Liebhold, M., Xie, X. & Li, S.-M. (2012). Expansion of enzymatic Friedel-Crafts alkylation on indoles: Acceptance of unnatural beta-unsaturated allyl diphospates by dimethylallyl-tryptophan synthases. *Org. Lett.* **14**, 4884-4885.

Liebhold, M., Xie, X. & Li, S.-M. (2013). Breaking cyclic dipeptide prenyltransferase regioselectivity by unnatural alkyl donors. *Org. Lett.* **15**, 3062-3065.

Liu, A. H., Liu, D. Q., Liang, T. J., Yu, X. Q. et al. (2013a). Caulerprenylols A and B, two rare antifungal prenylated *para*-xylenes from the green alga *Caulerpa racemosa*. *Bioorg. Med. Chem. Lett.* **23**, 2491-2494.

Liu, C., Minami, A., Noike, M., Toshima, H., Oikawa, H. & Dairi, T. (2013b). Regiospecificities and prenylation mode specificities of the fungal indole diterpene prenyltransferases AtmD and PaxD. *Appl. Environ. Microbiol.* **79**, 7298-7304.

Liu, C., Noike, M., Minami, A., Oikawa, H. & Dairi, T. (2014). Functional analysis of a prenyltransferase gene (paxD) in the paxilline biosynthetic gene cluster. *Appl. Microbiol. Biotechnol.* **98**, 199-206.

Lou, S., Zheng, Y. M., Liu, S. L., Qiu, J. et al. (2014). Inhibition of hepatitis C virus replication in vitro by xanthohumol, a natural product present in hops. *Planta Med.* **80**, 171-176.

Luk, L. Y., Qian, Q. & Tanner, M. E. (2011). A cope rearrangement in the reaction catalyzed by dimethylallyltryptophan synthase? *J. Am. Chem. Soc.* **133**, 12342-12345.

Luk, L. Y. P. & Tanner, M. E. (2009). Mechanism of dimethylallyltryptophan synthase: evidence for a dimethylallyl cation intermediate in an aromatic prenyltransferase reaction. *J. Am. Chem. Soc.* **131**, 13932-13933.

Ma, J., Zuo, D., Song, Y., Wang, B. et al. (2012). Characterization of a single gene cluster responsible for methylpendolmycin and pendolmycin biosynthesis in the deep sea bacterium *Marinactinospora thermotolerans. Chembiochem* **13**, 547-552.

MacCabe, A. P., Riach, M. B., Unkles, S. E. & Kinghorn, J. R. (1990). The *Aspergillus nidulans* npeA locus consists of three contiguous genes required for penicillin biosynthesis. *EMBO J.* **9**, 279-287.

Mahajan, G. B. & Balachandran, L. (2012). Antibacterial agents from actinomycetes - a review. *Front Biosci. (Elite. Ed)* **4**, 240-253.

Mahmoodi, N., Qian, Q., Luk, L. Y. P. & Tanner, M. E. (2013). Rearrangements in the mechanisms of the indole alkaloid prenyltransferases. *Pure Appl. Chem.* **85**, 1935-1948.

Mahmoodi, N. & Tanner, M. E. (2013). Potential rearrangements in the reaction catalyzed by the indole prenyltransferase FtmPT1. *Chembiochem.* **14**, 2029-2037.

Manzoni, M. & Rollini, M. (2002). Biosynthesis and biotechnological production of statins by filamentous fungi and application of these cholesterol-lowering drugs. *Appl. Microbiol. Biotechnol.* **58**, 555-564.

Meganathan, R. & Kwon, O. (2009). Biosynthesis of menaquinone (vitamin K) and ubiquinone (coenzyme Q). *Ecosal. Plus.* **3**, DOI: 10.1128/ecosalplus.3.6.3.3.

Metzger, U., Schall, C., Zocher, G., Unsöld, I., Stec, E., Li, S.-M., Heide, L. & Stehle, T. (2009). The structure of dimethylallyl tryptophan synthase reveals a common architecture of aromatic prenyltransferases in fungi and bacteria. *Proc. Natl. Acad. Sci. U. S. A* **106**, 14309-14314.

Minetoki, T., Gomi, K., Kitamoto, K., Kumagai, C. & Tamura, G. (1995). Nucleotide sequence and expression of alpha-glucosidase-encoding gene (agdA) from Aspergillus oryzae
2. *Biosci. Biotechnol. Biochem.* **59**, 1516-1521.

Monache, F. D., Botta, B., Monache, G. D. & Bettolo, G. B. M. (1985). Prenylated anthranoids from *Psorospermum* species. *Phytochemistry* **24**, 1855-1856.

Mori, T., Zhang, L., Awakawa, T., Hoshino, S., Okada, M., Morita, H. & Abe, I. (2016). Manipulation of prenylation reactions by structure-based engineering of bacterial indolactam prenyltransferases. *Nat. Commun.* **7**, 10849.

Mundt, K. & Li, S.-M. (2013). CdpC2PT, a reverse prenyltransferase from *Neosartorya fischeri* with distinct substrate preference from known *C2*-prenyltransferases. *Microbiology* **159**, 2169-2179.

Newman, D. J. & Cragg, G. M. (2012). Natural products as sources of new drugs over the 30 years from 1981 to 2010. *J. Nat. Prod.* **75**, 311-335.

Noike, M., Liu, C., Ono, Y., Hamano, Y., Toyomasu, T., Sassa, T., Kato, N. & Dairi, T. (2012). An enzyme catalyzing *O*-prenylation of the glucose moiety of fusicoccin A, a diterpene glucoside produced by the fungus *Phomopsis amygdali*. *Chembiochem* **13**, 566-573.

Oldfield, E. & Lin, F. Y. (2012). Terpene biosynthesis: modularity rules. *Angew. Chem. Int. Ed Engl.* **51**, 1124-1137.

Oya, A., Tanaka, N., Kusama, T., Kim, S. Y. et al. (2015). Prenylated benzophenones from *Triadenum japonicum*. *J. Nat. Prod.* **78**, 258-264.

Ozaki, T., Nishiyama, M. & Kuzuyama, T. (2013). Novel tryptophan metabolism by a potential gene cluster that is widely distributed among actinomycetes. *J. Biol. Chem.* **288**, 9946-9956.

Palsuledesai, C. C. & Distefano, M. D. (2015). Protein prenylation: enzymes, therapeutics, and biotechnology applications. *ACS Chemical Biology* **10**, 51-62.

Pinto, M. M., Sousa, M. E. & Nascimento, M. S. (2005). Xanthone derivatives: new insights in biological activities. *Curr. Med. Chem.* **12**, 2517-2538.

Pockrandt, D. & Li, S.-M. (2013). Geranylation of cyclic dipeptides by the dimethylallyl transferase AnaPT resulting in a shift of prenylation position on the indole ring. *Chembiochem.* **14**, 2023-2028.

Pockrandt, D., Ludwig, L., Fan, A., König, G. M. & Li, S.-M. (2012). New insights into the biosynthesis of prenylated xanthones: XptB from *Aspergillus nidulans* catalyses an *O*-prenylation of xanthones. *Chembiochem* **13**, 2764-2771.

Pockrandt, D., Sack, C., Kosiol, T. & Li, S.-M. (2014). A promiscuous prenyltransferase from *Aspergillus oryzae* catalyses *C*-prenylations of hydroxynaphthalenes in the presence of different prenyl donors. *Appl. Microbiol. Biotechnol.* **98**, 4987-4994.

Pojer, F., Wemakor, E., Kammerer, B., Chen, H., Walsh, C. T., Li, S.-M. & Heide, L. (2003). CloQ, a prenyltransferase involved in clorobiocin biosynthesis. *Proc. Natl. Acad. Sci. U. S. A.* **100**, 2316-2321.

Poulter, C. D. (2006). Farnesyl diphosphate synthase. A paradigm for understanding structure and function relationships in E-polyprenyl diphosphate synthases. *Phytochem. Rev.* **5**, 17-26.

Punt, P. J., van, B. N., Conesa, A., Albers, A., Mangnus, J. & van den Hondel, C. (2002). Filamentous fungi as cell factories for heterologous protein production. *Trends Biotechnol.* **20**, 200-206.

Rabindran, S. K., Ross, D. D., Doyle, L. A., Yang, W. & Greenberger, L. M. (2000). Fumitremorgin C reverses multidrug resistance in cells transfected with the breast cancer resistance protein. *Cancer Res.* **60**, 47-50.

Raju, R., Piggott, A. M., Huang, X. C. & Capon, R. J. (2011). Nocardioazines: a novel bridged diketopiperazine scaffold from a marine-derived bacterium inhibits p-glycoprotein. *Org. Lett.* **13**, 2770-2773.

Ramamoorthy, G., Pugh, M. L., Tian, B. X., Phan, R. M., Perez, L. B., Jacobson, M. P. & Poulter, C. D. (2015). Synthesis and enzymatic studies of bisubstrate analogs for farnesyl diphosphate synthase. *J. Org. Chem.* **80**, 3902-3913.

Ropars, J., Cruaud, C., Lacoste, S. & Dupont, J. (2012). A taxonomic and ecological overview of cheese fungi. *Int. J. Food Microbiol.* **155**, 199-210.

Rosselli, S., Maggio, A., Bellone, G., Formisano, C., Basile, A., Cicala, C., Alfieri, A., Mascolo, N. & Bruno, M. (2007). Antibacterial and anticoagulant activities of coumarins isolated from the flowers of *Magydaris tomentosa*. *Planta Med.* **73**, 116-120.

Ruan, H.-L., Stec, E. & Li, S.-M. (2009). Production of diprenylated indole derivatives by tandem incubation of two recombinant dimethylallyltryptophan synthases. *Arch. Microbiol.* **191**, 791-795.

Saito, K., Chen, C. Y., Masana, M., Crowley, J. S., Markey, S. P. & Heyes, M. P. (1993). 4-Chloro-3-hydroxyanthranilate, 6-chlorotryptophan and norharmane attenuate quinolinic acid formation by interferon-gamma-stimulated monocytes (THP-1 cells). *Biochem. J.* **291 (Pt 1)**, 11-14.

Sasaki, T., Igarashi, Y., Ogawa, M. & Furumai, T. (2002). Identification of 6-prenylindole as an antifungal metabolite of Streptomyces sp. TP-A0595 and synthesis and bioactivity of 6-substituted indoles. *J. Antibiot.* **55**, 1009-1012.

Satou, R., Izumikawa, M., Katsuyama, Y., Matsui, M., Takagi, M., Shin-ya, K. & Ohnishi, Y. (2014). Isolation, structural elucidation and biosynthesis of 3-hydroxy-6-dimethylallylindolin-2-one, a novel prenylated indole derivative from Actinoplanes missouriensis. *J. Antibiot.* **67**, 231-236.

Schneider, P., Weber, M. & Hoffmeister, D. (2008). The *Aspergillus nidulans* enzyme TdiB catalyzes prenyltransfer to the precursor of bioactive asterriquinones. *Fungal. Genet. Biol.* **45**, 302-309.

Schuller, J. M., Zocher, G., Liebhold, M., Xie, X., Stahl, M., Li, S.-M. & Stehle, T. (2012). Structure and catalytic mechanism of a cyclic dipeptide prenyltransferase with broad substrate promiscuity. *J. Mol. Biol.* **422**, 87-99.

Schultz, A. W., Lewis, C. A., Luzung, M. R., Baran, P. S. & Moore, B. S. (2010). Functional characterization of the cyclomarin/cyclomarazine prenyltransferase CymD directs the biosynthesis of unnatural cyclic peptides. *J. Nat. Prod.* **73**, 373-377.

Schultz, A. W., Oh, D. C., Carney, J. R., Williamson, R. T., Udwary, D. W., Jensen, P. R., Gould, S. J., Fenical, W. & Moore, B. S. (2008). Biosynthesis and structures of cyclomarins and cyclomarazines, prenylated cyclic peptides of marine actinobacterial origin. *J Am. Chem Soc.* **130**, 4507-4516.

Scott, P. M. & Kennedy, B. P. C. (1976). Analysis of blue cheese for roquefortine and other alkaloids from *Penicillium roqueforti*. *J. Agric. Food Chem.* **24**, 865-868.

Sedmera, P., PospÍšil, S. & Novák, J. (1991). New furanonaphthoquinone from *Streptomyces cinnamonensis*. *Journal of Natural Products* **54**, 870-872.

Shah, A. M., Wani, A., Qazi, P. H., Rehman, S. U. et al. (2016). Isolation and characterization of alborixin from *Streptomyces scabrisporus*: A potent cytotoxic agent against human colon (HCT-116) cancer cells. *Chem. Biol. Interact.* **256**, 198-208.

Shan, D., Chen, L., Njardarson, J. T., Gaul, C., Ma, X., Danishefsky, S. J. & Huang, X. Y. (2005). Synthetic analogues of migrastatin that inhibit mammary tumor metastasis in mice. *Proc. Natl. Acad. Sci. U. S. A* **102**, 3772-3776.

Shen, G., Huhman, D., Lei, Z., Snyder, J., Sumner, L. W. & Dixon, R. A. (2012). Characterization of an isoflavonoid-specific prenyltransferase from *Lupinus albus*. *Plant Physiol.* **159**, 70-80.

Shibuya, M., Chou, H. M., Fountoulakis, M., Hassam, S. et al. (1990). Stereochemistry of the isoprenylation of tryptophan catalyzed by 4-(g,g-dimethylallyl)tryptophan synthase from *Claviceps*, the first pathway-specific enzyme in ergot alkaloid biosynthesis. *J. Am. Chem. Soc.* **112**, 297-304.

Shimada, A. & Ozaki, H. (2012). Flexible enantioselectivity of tryptophanase attributable to benzene ring in heterocyclic moiety of d-tryptophan. *Life (Basel)* **2**, 215-228.

Shin-Ya, K., Furihata, K., Hayakawa, Y. & Seto, H. (1990a). Biosynthetic studies of naphterpin, a terpenoid metabolite of *Streptomyces*. *Tetrahedron Lett.* **31**, 6025-6026.

Shin-Ya, K., Imai, S., Furihata, K., Hayakawa, Y., Kato, Y., Vanduyne, G. D., Clardy, J. & Seto, H. (1990b). Isolation and structural elucidation of an antioxidative agent, naphterpin. *J. Antibiot.* **43**, 444-447.

Simpson, T. J. (2012). Genetic and biosynthetic studies of the fungal prenylated xanthone shamixanthone and related metabolites in *Aspergillus* spp. revisited. *Chembiochem* **13**, 1680-1688.

Song, F., Liu, X., Guo, H., Ren, B. et al. (2012). Brevianamides with antitubercular potential from a marine-derived isolate of *Aspergillus versicolor*. *Org. Lett.* **14**, 4770-4773.

Stanzani, M., Orciuolo, E., Lewis, R., Kontoyiannis, D. P., Martins, S. L., St John, L. S. & Komanduri, K. V. (2005). *Aspergillus fumigatus* suppresses the human cellular immune response via gliotoxin-mediated apoptosis of monocytes. *Blood* **105**, 2258-2265.

Steffan, N. & Li, S.-M. (2009). Increasing structure diversity of prenylated diketopiperazine derivatives by using a 4-dimethylallyltryptophan synthase. *Arch. Microbiol.* **191**, 461-466.

Steffan, N., Unsöld, I. A. & Li, S.-M. (2007). Chemoenzymatic synthesis of prenylated indole derivatives by using a 4-dimethylallyltryptophan synthase from *Aspergillus fumigatus*. *Chembiochem* **8**, 1298-1307.

Steffensky, M., Mühlenweg, A., Wang, Z.-X., Li, S.-M. & Heide, L. (2000). Identification of the novobiocin biosynthetic gene cluster of *Streptomyces spheroides* NCIB 11891. *Antimicrob. Agents Chemother.* **44**, 1214-1222.

Strauch, R. C., Svedin, E., Dilkes, B., Chapple, C. & Li, X. (2015). Discovery of a novel amino acid racemase through exploration of natural variation in *Arabidopsis thaliana*. *Proc. Natl. Acad. Sci. U. S. A* **112**, 11726-11731.

Subramanian, S., Shen, X., Yuan, Q. & Yan, Y. (2012). Identification and biochemical characterization of a 5-dimethylallyltryptophan synthase in *Streptomyces coelicolor* A3(2). *Process Biochem.* **47**, 1419-1422.

Sunassee, S. N. & Davies-Coleman, M. T. (2012). Cytotoxic and antioxidant marine prenylated quinones and hydroquinones. *Nat. Prod. Rep.* **29**, 513-535.

Suzuki, H., Kubota, T., Takahashi-Nakaguchi, A., Fromont, J., Gonoi, T. & Kobayashi, J. (2014). Nakijiquinone s and nakijinol C, new meroterpenoids from a marine sponge of the family spongiidae. *Chem. Pharm. Bull. (Tokyo)* **62**, 209-212.

Tagami, K., Liu, C., Minami, A., Noike, M. et al. (2013). Reconstitution of biosynthetic machinery for indole-diterpene paxilline in *Aspergillus oryzae*. *J. Am. Chem. Soc.* **135**, 1260-1263.

Takahashi, S., Takagi, H., Toyoda, A., Uramoto, M., Nogawa, T., Ueki, M., Sakaki, Y. & Osada, H. (2010). Biochemical characterization of a novel indole prenyltransferase from *Streptomyces* sp. SN-593. *J. Bacteriol.* **192**, 2839-2851.

Tanaka, M., Li, X., Hikawa, H., Suzuki, T., Tsutsumi, K., Sato, M., Takikawa, O., Suzuki, H. & Yokoyama, Y. (2013). Synthesis and biological evaluation of novel tryptoline derivatives as indoleamine 2,3-dioxygenase (IDO) inhibitors. *Bioorg. Med. Chem.* **21**, 1159-1165.

Tanner, M. E. (2014). Mechanistic studies on the indole prenyltransferases. *Natural Product Reports* **32**, 88-101.

Tarcz, S., Ludwig, L. & Li, S.-M. (2014a). AstPT catalyses both reverse *N1*- and regular *C2*-prenylation of a methylated bisindolyl benzoquinone. *Chembiochem.* **15**, 108-116.

Tarcz, S., Xie, X. & Li, S.-M. (2014b). Substrate and catalytic promiscuity of secondary metabolite enzymes: *O*-prenylation of hydroxyxanthones with different prenyl donors by a bisindolyl benzoquinone *C*- and *N*-prenyltransferase. *RSC Adv.* **4**, 17986-17992.

Thibessard, A., Haas, D., Gerbaud, C., Aigle, B., Lautru, S., Pernodet, J. L. & Leblond, P. (2015). Complete genome sequence of *Streptomyces ambofaciens* ATCC 23877, the spiramycin producer. *J. Biotechnol.* **214**, 117-118.

Tsai, H. F., Wang, H., Gebler, J. C., Poulter, C. D. & Schardl, C. L. (1995). The *Claviceps purpurea* gene encoding dimethylallyltryptophan synthase, the committed step for ergot alkaloid biosynthesis. *Biochem. Biophys. Res. Commun.* **216**, 119-125.

Tsuji, F., Ishihara, A., Kurata, K., Nakagawa, A. et al. (2012). Geranyl modification on the tryptophan residue of $ComX_{RO-E-2}$ pheromone by a cell-free system. *FEBS Lett.* **586**, 174-179.

Tudzynski, P., Holter, K., Correia, T., Arntz, C., Grammel, N. & Keller, U. (1999). Evidence for an ergot alkaloid gene cluster in *Claviceps purpurea*. *Mol. Gen. Genet.* **261**, 133-141.

Unsöld, I. A. & Li, S.-M. (2005). Overproduction, purification and characterization of FgaPT2, a dimethylallyltryptophan synthase from *Aspergillus fumigatus*. *Microbiology* **151**, 1499-1505.

Urmann, C., Oberbauer, E., Couillard-Despres, S., Aigner, L. & Riepl, H. (2015). Neurodifferentiating potential of 8-prenylnaringenin and related compounds in neural precursor cells and correlation with estrogen-like activity. *Planta Med.* **81**, 305-311.

Veine, D. M., Yao, H., Stafford, D. R., Fay, K. S. & Livant, D. L. (2014). A D-amino acid containing peptide as a potent, noncovalent inhibitor of alpha5beta1 integrin in human prostate cancer invasion and lung colonization. *Clin. Exp. Metastasis* **31**, 379-393.

Venugopala, K. N., Rashmi, V. & Odhav, B. (2013). Review on natural coumarin lead compounds for their pharmacological activity. *Biomed. Res. Int.* **2013**, 963248.

Vogel, S., Ohmayer, S., Brunner, G. & Heilmann, J. (2008). Natural and non-natural prenylated chalcones: synthesis, cytotoxicity and anti-oxidative activity. *Bioorg. Med. Chem.* **16**, 4286-4293.

Vougogiannopoulou, K., Fokialakis, N., Aligiannis, N., Cantrell, C. & Skaltsounis, A. L. (2011). Simple indole alkaloids from the neotropical rutaceous tree *Raputia simulans*. *Planta Med.* **77**, 1559-1561.

Wang, R., Chen, R., Li, J., Liu, X. et al. (2014). Molecular characterization and phylogenetic analysis of two novel regio-specific flavonoid prenyltransferases from *Morus alba* and *Cudrania tricuspidata*. *J. Biol. Chem.* **289**, 35815-35825.

Wang, Y., Xia, Z., Xu, J. R., Wang, Y. X., Hou, L. N., Qiu, Y. & Chen, H. Z. (2012). Alpha-mangostin, a polyphenolic xanthone derivative from mangosteen, attenuates beta-amyloid oligomers-induced neurotoxicity by inhibiting amyloid aggregation. *Neuropharmacology* **62**, 871-881.

Webster, J. & Weber, R. (2007) *Introduction to fungi*. Cambridge, UK: Cambridge University Press.

Welch, B. D., VanDemark, A. P., Heroux, A., Hill, C. P. & Kay, M. S. (2007). Potent D-peptide inhibitors of HIV-1 entry. *Proc. Natl. Acad. Sci. U. S. A* **104**, 16828-16833.

Williams, R. M., Stocking, E. M. & Sanz-Cervera, J. F. (2000). Biosynthesis of prenylated alkaloids derived from tryptophan. *Topics Curr. Chem.* **209**, 97-173.

Winkelblech, J., Fan, A. & Li, S.-M. (2015a). Prenyltransferases as key enzymes in primary and secondary metabolism. *Appl. Microbiol. Biotechnol.* **99**, 7379-7397.

Winkelblech, J. & Li, S.-M. (2014). Biochemical investigations of two 6-DMATS enzymes from *Streptomyces* revealing novel features of L-tryptophan prenyltransferases. *Chembiochem.* **15**, 1030-1039.

Winkelblech, J., Liebhold, M., Gunera, J., Xie, X., Kolb, P. & Li, S.-M. (2015b). Tryptophan *C5*-, *C6*- and *C7*-prenylating enzymes displaying a preference for C-6 of the indole ring in the presence of unnatural dimethylallyl diphosphate analogues. *Advanced Synthesis & Catalysis* **357**, 975-986.

Wollinsky, B., Ludwig, L., Hamacher, A., Yu, X., Kassack, M. U. & Li, S.-M. (2012). Prenylation at the indole ring leads to a significant increase of cytotoxicity of tryptophan-containing cyclic dipeptides. *Bioorg. Med. Chem. Lett.* **22**, 3866-3869.

Wu, C., Du, C., Gubbens, J., Choi, Y. H. & van Wezel, G. P. (2015). Metabolomics-driven discovery of a prenylated isatin antibiotic produced by *Streptomyces* species MBT28. *J. Nat. Prod.* **78**, 2355-2363.

Wunsch, C., Zou, H. X., Linne, U. & Li, S.-M. (2015). *C7*-prenylation of tryptophanyl and *O*-prenylation of tyrosyl residues in dipeptides by an *Aspergillus terreus* prenyltransferase. *Appl. Microbiol. Biotechnol.* **99**, 1719-1730.

Xie, W., Zhou, C. & Huang, R. H. (2007). Structure of tRNA dimethylallyltransferase: RNA modification through a Channel. *J. Mol. Biol.* **367**, 872-881.

Xu, Z., Huang, L., Chen, X. H., Zhu, X. F., Qian, X. J., Feng, G. K., Lan, W. J. & Li, H. J. (2014). Cytotoxic prenylated xanthones from the pericarps of *Garcinia mangostana*. *Molecules.* **19**, 1820-1827.

Yamazaki, M., Fujimoto, H. & Kawasaki, T. (1980). Chemistry of tremorogenic metabolites. I. Fumitremorgin A from *Aspergillus fumigatus*. *Chem. Pharm. Bull.* **28**, 245-254.

Yamazaki, M., Sasago, K. & Miyaki, K. (1974). Structure of fumitremorgin B (FTB), a tremorgenic toxin from *Aspergillus fumigatus*. *J. Chem. Soc. , Chem. Commun.* 408-409.

Yamazaki, M. & Suzuki, S. (1986). Toxicology of tremorgenic mycotoxins, fumitremorgin A and B. *Dev. Toxicol. Environ. Sci.* **12**, 273-282.

Yazaki, K., Sasaki, K. & Tsurumaru, Y. (2009). Prenylation of aromatic compounds, a key diversification of plant secondary metabolites. *Phytochemistry* **70**, 1739-1745.

Yin, S., Yu, X., Wang, Q., Liu, X. Q. & Li, S.-M. (2013a). Identification of a brevianamide F reverse prenyltransferase BrePT from *Aspergillus versicolor* with a broad substrate specificity towards tryptophan-containing cyclic dipeptides. *Appl. Microbiol. Biotechnol.* **97**, 1649-1660.

Yin, W.-B., Grundmann, A., Cheng, J. & Li, S.-M. (2009). Acetylaszonalenin biosynthesis in *Neosartorya fischeri*: Identification of the biosynthetic gene cluster by genomic mining and functional proof of the genes by biochemical investigation. *J. Biol. Chem.* **284**, 100-109.

Yin, W.-B., Yu, X., Xie, X.-L. & Li, S.-M. (2010). Preparation of pyrrolo[2,3-*b*]indoles carrying a ß-configured reverse *C3*-dimethylallyl moiety by using a recombinant prenyltransferase CdpC3PT. *Org. Biomol. Chem.* **8**, 2430-2438.

Yin, X., Feng, T., Li, Z. H., Dong, Z. J., Li, Y. & Liu, J. K. (2013b). Highly oxygenated meroterpenoids from fruiting bodies of the mushroom Tricholoma terreum. *J. Nat. Prod.* **76**, 1365-1368.

Yin, Y., Mao, Y., Yin, X., Gao, B. & Wei, D. (2015). Construction of a Shuttle Vector for Heterologous Expression of a Novel Fungal alpha-Amylase Gene in Aspergillus oryzae

1. *J. Microbiol. Biotechnol.* **25**, 988-998.

Yu, H., Liebhold, M., Xie, X. & Li, S.-M. (2015). Tyrosine *O*-prenyltransferases TyrPT and SirD displaying similar behavior toward unnatural alkyl or benzyl diphosphate as their natural prenyl donor dimethylallyl diphosphate. *Appl. Microbiol. Biotechnol.* DOI 10.1007/s00253-015-6452-1.

Yu, X. & Li, S.-M. (2011). Prenylation of flavonoids by using a dimethylallyltryptophan synthase 7-DMATS from *Aspergillus fumigatus*. *Chembiochem* **12**, 2280-2283.

Yu, X. & Li, S.-M. (2012). Prenyltransferases of the dimethylallyltryptophan synthase superfamily. *Methods Enzymol.* **516**, 259-278.

Yu, X., Liu, Y., Xie, X., Zheng, X.-D. & Li, S.-M. (2012). Biochemical characterization of indole prenyltransferases: Filling the last gap of prenylation positions by a 5-dimethylallyltryptophan synthase from *Aspergillus clavatus*. *J. Biol. Chem.* **287**, 1371-1380.

Yu, X., Xie, X. & Li, S.-M. (2011). Substrate promiscuity of secondary metabolite enzymes: prenylation of hydroxynaphthalenes by fungal indole prenyltransferases. *Appl. Microbiol. Biotechnol.* **92**, 737-748.

Yu, X., Zocher, G., Xie, X., Liebhold, M., Schütz, S., Stehle, T. & Li, S.-M. (2013). Catalytic mechanism of stereospecific formation of *cis*-configured prenylated pyrroloindoline diketopiperazines by indole prenyltransferases. *Chem. Biol.* **20**, 1492-1501.

Zamani Taghizadeh, R. S., Iranshahi, M. & Mahmoudi, M. (2016). In vitro anti-inflammatory and immunomodulatory properties of umbelliprenin and methyl galbanate. *J. Immunotoxicol.* **13**, 209-216.

Zeyhle, P., Bauer, J. S., Kalinowski, J., Shin-ya, K., Gross, H. & Heide, L. (2014a). Genome-based discovery of a novel membrane-bound 1,6-dihydroxyphenazine prenyltransferase from a marine actinomycete. *PLoS. One.* **9**, e99122.

Zeyhle, P., Bauer, J. S., Steimle, M., Leipoldt, F., Rösch, M., Kalinowski, J., Gross, H. & Heide, L. (2014b). A membrane-bound prenyltransferase catalyzes the *O*-prenylation of 1,6-dihydroxyphenazine in the marine bacterium *Streptomyces* sp. CNQ-509. *Chembiochem.* **15**, 2385-2392.

Zhang, G., Feng, J., Han, L. & Zhang, X. (2016). Antiviral activity of glycoprotein GP-1 isolated from *Streptomyces kanasensis* ZX01. *Int. J. Biol. Macromol.* **88**, 572-577.

Zhou, K., Yu, X., Xie, X. & Li, S. M. (2015). Complementary Flavonoid Prenylations by Fungal Indole Prenyltransferases. *J. Nat. Prod.* **78**, 2229-2235.

Zou, H.-X., Xie, X.-L., Linne, U., Zheng, X.-D. & Li, S.-M. (2010). Simultaneous *C7*- and *N1*-prenylation of cyclo-L-Trp-L-Trp catalyzed by a prenyltransferase from *Aspergillus oryzae*. *Org. Biomol. Chem.* **8**, 3037-3044.

Zou, X., Li, Y., Zhang, X., Li, Q. et al. (2014). A new prenylated indole diketopiperazine alkaloid from *Eurotium cristatum*. *Molecules.* **19**, 17839-17847.

Statutory Declaration

Ich, Julia Winkelblech, versichere, dass ich meine Dissertation:

„Biochemical investigations on bacterial and fungal dimethylallyltryptophan synthases“

selbständig, ohne unerlaubte Hilfe angefertigt und mich dabei keiner anderen als der von mir ausdrücklich bezeichneten Quellen bedient habe. Alle vollständig oder sinngemäß übernommenen Zitate sind als solche gekennzeichnet.

Die Dissertation wurde in der jetzigen oder einer ähnlichen Form noch bei keiner anderen Hochschule eingereicht und hat noch keinen sonstigen Prüfungszwecken gedient.

Marburg, den …….

…….
Julia Winkelblech

Acknowledgements

Firstly, I would like to express my sincere gratitude to my supervisor Prof. Dr. Shu-Ming Li for his excellent support during my Ph.D. study. His guidance and ambitious motivation helped me in all the time of research and writing of this thesis. He was always open to questions and discussions about new ideas or scientific issues. I learned a lot about protein biochemistry, analytics as well as scientific thinking. My personal and professional development greatly benefit from his supervision. Moreover, I am also grateful for the opportunity to visit china in 2013 in the context of a research stay.

I am grateful to Prof. Dr. Gerhard Klebe and Prof. Dr. Peter Kolb for their good advice in the graduate school of the LOEWE program of the State of Hessen (SynMikro). My sincere thanks go to Prof. Dr. Kolb for acting as second referee and examiner. Furthermore, I thank him for his interesting and helpful introduction in the field of protein modeling and the valuable and successful cooperation within this thesis. In this context, I also give thanks to Jakub Gunera for the successful collaboration. I would also like to thank Dr. Xiulan Xie, Dr. Regina Ortmann and Stefan Newel for taking NMR spectra as well as Dr. Gabriela Laufenberg and Nina Zitzer for taking mass spectra. Many thanks go to Rixa for LC-MS measurements and her helpful assistance. Special thanks go to Lena for her help in analytic questions and the technical support for HPLC. For the great and impressive time in Guangzhou, I would thank Nina.

I would like to express my thanks to all my current and former colleagues including, Beate, Sylwia, Mike, Aili, Xia, Carsten, Kathrin, Alexander, Kirsten, Katja, Nina, Peter, Viola, Huili, Jie, Kang, Elisabeth, Lindsay, Florian, Kristin, Bastian and Jonas for having a nice time. Moreover, I would thank Beate, Soheil and Lennart for enjoying sporting activities. And of course I thank all members of the institute for having a good time with nice meetings for lunch or coffee and cake.

My heartfelt gratitude to Johannes for his motivational support and for enduring this time with me. Thank you that you are always there for me!

Finally, I would deeply thank my family, especially my parents, who always believed in me, for their love and encouragement over all the years.

Curriculum vitae

Julia Winkelblech

Page 228 (Curriculum vitae) contains personal data. It is therefore not part of the onlinepublicationof this thesis.